IAEA-213 VOL. 2

FISSION PRODUCT NUCLEAR DATA (FPND) - 1977

VOL.II

PROCEEDINGS OF THE SECOND ADVISORY GROUP MEETING
ON FISSION PRODUCT NUCLEAR DATA
ORGANIZED BY THE
INTERNATIONAL ATOMIC ENERGY AGENCY
AND HELD AT THE
ENERGY CENTRUM NETHERLANDS, PETTEN
5–9 SEPTEMBER 1977

A TECHNICAL DOCUMENT ISSUED BY THE
INTERNATIONAL ATOMIC ENERGY AGENCY, VIENNA, 1978

FISSION PRODUCT NUCLEAR DATA (FPND) - 1977
IAEA, VIENNA, 1978

Printed by the IAEA in Austria
August 1978

PLEASE BE AWARE THAT
ALL OF THE MISSING PAGES IN THIS DOCUMENT
WERE ORIGINALLY BLANK

The IAEA does not maintain stocks of reports in this series. However, microfiche copies of these reports can be obtained from

INIS Microfiche Clearinghouse
International Atomic Energy Agency
Kärntner Ring 11
P.O. Box 590
A-1011 Vienna, Austria

on prepayment of US $0.65 or against one IAEA microfiche service coupon.

Summary

The Second IAEA Advisory Group Meeting on Fission Product Nuclear Data (FPND) was a follow-up meeting of the first Panel on the same subject which had been organized by IAEA/NDS in Bologna, Italy, in November 1973; the Proceedings of this Panel are published as IAEA-report in three volumes, IAEA-169 (1974).

The main purpose of the Second AGM on FPND was to re-convene users and measurers of FPND in order to review the present state of requirements for FPND as well as the development and progress in FPND research since the Bologna Panel.

Fifteen review papers were presented at this meeting, which covered the full scope of FPND and their applications, and which formed the basis for the subsequent discussions.

The principal results of this meeting were:

- detailed comparisons were performed between the accuracy status and the current requirements for FPND;
- those user areas were clearly delimited which still require an improvement in the status and accuracy of FPND;
- many detailed recommendations for future work on FPND, including coordinating activities to be performed by the IAEA, were formulated.

The meeting was attended by 52 participants from 13 Member States and 3 international organisations. Appendix A contains the list of participants, Appendix B the meeting agenda and Appendix C the working groups which were formed after the presentation of the review papers in order to discuss specific subjects.

Selected contributions to review papers are published separately as INDC(NDS)-87 report.

The scientific secretaries wish to thank the participants of the meeting for their efficient work, and ECN Petten and its staff for the hospitality and the excellent organization.

Table of Contents

Volume 2

Review paper 11

PREDICTION OF UNMEASURED FISSION PRODUCT YIELDS BY NUCLEAR THEORY OR SYSTEMATICS

Hans Otto Denschlag
Institut für Kernchemie
Universität Mainz, Germany

Abstract

Prediction methods for chain yields and (fractional) independent yields from systematics and nuclear theory are referred and discussed. The discussion includes the treatment of pairing effects in various fission systematics, the partition of experimental or predicted yields to particular isomeric states of one isotope and the yields of ternary fission products.

No general rule for the uncertainties of predicted fission product yields is given. Recommendations are made for data compilers in order to facilitate the development and test of systematics.

Introduction

In spite of the efforts made by many experimenters resulting in ca. 20 000 experimental fission-product-yield-values as reviewed in Review Paper 10 of these proceedings there exist still wide blank areas in fission yield compilations. These areas are especially large for fission reactions induced by reactor- and 14 MeV-neutrons and less frequently used fissioning nuclides; but even for the fission of ^{235}U induced by thermal neutrons the lack of reliable data of low-yield products is stringent.

Predictions based on systematics developed from existing experimental yield values or based on theories, developed generally from more complex information, are therefore needed to bridge existing gaps or to allow an extrapolation to unknown areas.

The general principles of the systematics and theories - especially the progress attained since Musgrove's contribution [1] to the last FPND Panel Meeting at Bologna is the topic of the following article.

These proceedings are devoted to the practical uses of nuclear fission. Therefore the basic physical aspects of this process which are necessarily appearing in a discussion of prediction problems will be limited essentially to the points of direct importance for the topic.

Survey of the paper

In the following, at first a few basic considerations on the physics of the fission process will be presented. The effects influencing fission yields will be mentioned and the definitions for various terms will be given.

Specific requirements to data compilations used for the development and test of prediction methods will be presented and a few recommendations will be made. A discussion of the usefulness of partial yield data is included.

The main body of the paper will be devided into two parts. A first part will discuss prediction methods developed from systematics and will deal with different approaches developed to predict mass yields, independent yields, isomeric yields and ternary fission product yields. Single approaches will be presented. A second part will involve prediction methods based on theory. Four main approaches will be discussed involving predictions of mass yields, independent yields, and prompt neutron emission.

The Fission Process

In the practically important case of low energy fission, a particle (or a photon) is captured by the fissioning nucleus providing an excitation

energy which consists of its binding energy plus its kinetic energy in the center of mass system.

The nucleus is subsequently relaxing into a collectively excited compound state oscillating between states of high deformation energy and high internal temperature. Among the many deformation states are a few configurations which allow the nucleus to pass over a barrier (with one or more 'humps') and fission.

A typical plot of the potential energy of a nucleus on a fission path is shown in Fig. 1. The energy of the fission barriers is usually described by the counter balancing surface and coulombic forces derived from the liquid drop model [3] and modulated by shell effects in the deformed nucleus [4]. The maxima 'saddle points' (or one of the maxima) are (is) lying just below the total excitation energy of the compound nucleus in most thermal neutron induced fission reactions.

In consequence, at this point practically the total excitation energy is converted into deformation energy leaving the system cold i.e. in one or a few well defined states which show similarity to the lowest excited states near the ground state ('Intrinsic Channels' in Fig. 1.)[5]. It can, especially, be assumed that all nucleons be paired in even compound nuclei, i.e., that the compound nucleus shows superfluidity.

There is evidence, that in more highly excited fission reactions a deexcitation by neutron emission may take place prior to the fission process (second chance fission, third chance fission).

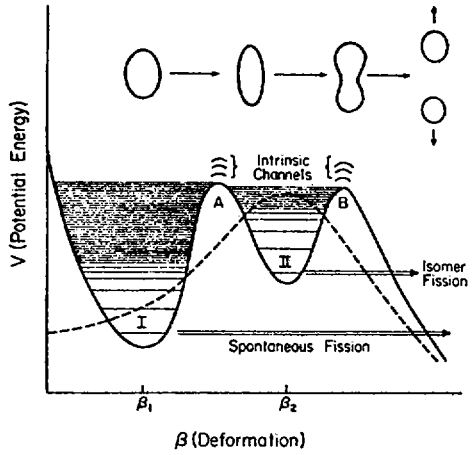

Fig. 1. Schematic illustration of single-humped (-----) and double humped (——) fission barriers. Intrinsic channels at the two barriers are illustrated. The transition in the shape of the nucleus as a function of deformation is schematically represented in the upper part of the figure. Tunnelling processes for spontaneous fission and isomeric fission are indicated. (From /2/).

The most decisive and theoretically important but least understood phase follows in the rapid descent of the fissioning nucleus from the saddle point to scission. This phase is essentially determining the details in the distribution of fission yields.

The differences between most fission theories lie in this point.

In principle the potential energy liberated in the descent may appear in three forms. Two rather extreme situations are shown in Fig. 2 a and b for the case of the spontaneous fission of ^{252}Cf.

The three possibilities are:

(a) The energy is transformed into kinetic energy of the fragments, thus producing fragments of low excitation energy at the scission point preserving superfluidity and leading to a pronounced favoring of even fission products (odd-even effect). This situation is illustrated in Fig. 2a and is treated theoretically in 'adiabatic' models.

(b) The energy is appearing as excitation energy producing fragments of high nuclear temperature in which nucleonic pairs are broken (viscous descent). This situation is illustrated in Fig. 2b and is treated in nonadiabetic models (e.g., the statistical model).

(c) The third possibility is a preservation of potential energy over the scission point in the form of deformation energy of the fragments. In this case nucleonic pairs are remaining unbroken at scission but the fragments becoming highly excited when they return to undeformed states will emit neutrons washing out pairing effects for neutrons subsequently.

It is at this point where the interests of theoreticians, experimentalists and users in the field of fission are mutually overlapping.

In addition to the three possibilities discussed, dynamical effects have to be considered. Shell effects have to be taken into account as a function of deformation. A particular difficulty is the treatment of the discontinuous behavior at the point of scission.

Directly after scission generally two fragments are found close to each other in the mutually repulsive coulombic field of their nuclear

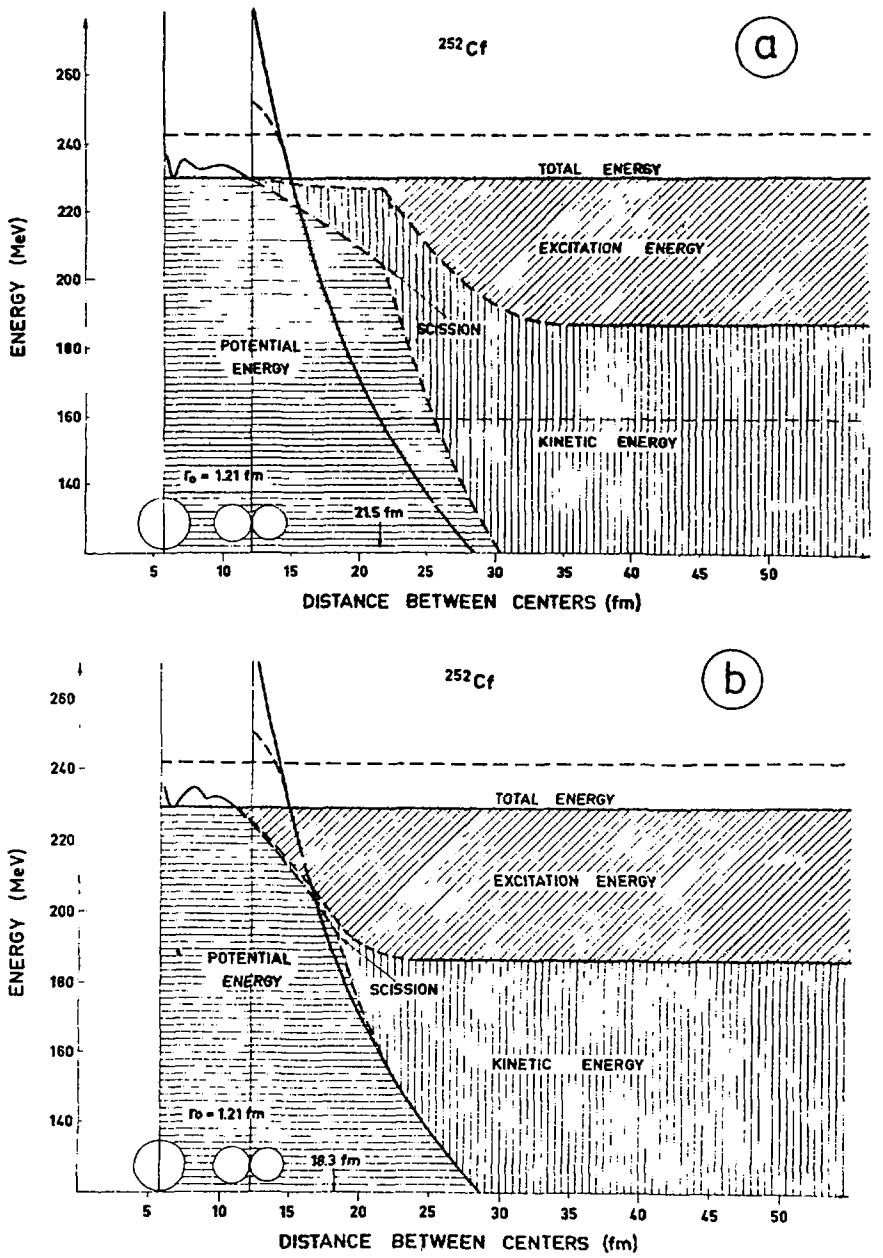

Fig. 2. (a) Illustration of a fission reaction leading to low internal excitation of the fragments and to correspondingly high kinetic (and deformation) energy at the scission point, (adiabatic case).
(b) Illustration of a fission reaction leading to high excitation energy of the fragments and to correspondingly low kinetic (and deformation) energy at the scission point (viscous descent, non-adiabetic models) (From /6/).

charges. The fragments will show varying degrees of deformation and internal excitation and initial kinetic energy as discussed. A light charged particle is emitted in less than 1% of the fission events from the scission configuration prior to coulombic acceleration (ternary fission).

Within $\sim 10^{-20}$s the fragments will be accelerated to their final kinetic energy. Deformation will relax into internal excitation leading to the emission of between 0 and 3 prompt neutrons within a time range of 10^{-15} - 10^{-18}s. The final deexcitation will take place by the emission of prompt γ-rays in less than 10^{-6}s.

The resulting fission products are usually 'short-lived'*(Half-life $>10^{-2}$s) β-unstable nuclei (or isomeric states of such nuclei) decaying into longer-lived daughters which will decay in turn forming a β-decay chain and will eventually reach a stable product. The decay is generally accompanied by the emission of γ-rays. In rare cases ($\sim$1%) neutrons are emitted accompanying the β-decay (β-delayed neutron emission from 'delayed neutron precursors' = d.n.p.). The yields of fission products are the matter of interest of the present paper.

Definitions

The following types of yields will be discussed in this paper :

The independent (direct, primary fission yield, IN) of a fission product (in per cent) is given by the number of atoms of this fission product formed directly (prior to any β-decay) in 100 fission events.

The secondary yield of a fission product (in per cent) is given by the number of atoms of this fission product that are being formed by the β-decay of precursors for 100 fission events. (The secondary yield of a nuclide is equal to the sum of the independent yields of all precursors.)

The cumulative yield (CU) is equal to the sum of the independent and secondary yields.

---

* 'short-lived' is here meant in the time scale of the radiochemist or reactor user and is at least 10 orders of magnitudes slower than the time scale of the fission process.

The chain yield (mass yield) (YA) is the sum of the independent yields of all isobars. It is equal to the cumulative yield of the last member of the chain if all isobars produced are β^--active.

The fractional independent (FI) and fractional cumulative (FC) yields are the respective yields divided by the corresponding chain yields (occasionally fractional yields are also given in per cent).

In addition to the yields of fission products sometimes yields of fission fragments (i.e., prior to prompt neutron emission, see above) will be indicated.

A fragment mass yield will be symbolized by YA', with A' denoting the fragment mass as opposed to A for the product mass.

The number of prompt neutrons emitted will be symbolized by ν. In particular

$\bar{\nu}$ represents the average number of neutrons per fission event (for a particular fission reaction, e.g., the thermal neutron induced fission of ^{235}U);

$\nu_{tot}(A'),\nu_{tot}(A)$ represent the (average) number of neutrons emitted from both fragments of a specific fragment mass pair (e.g., $A'_l = 100$ $A'_h = 136$ for $^{235}U(n_{th},f)$) ν_{tot} depends on the mass chains involved and is described as a function of the mass of either one, light or heavy product (A_l,A_h) or - fragment (A'_l,A'_h).

$\nu(A),\nu(A')$ is the (average) number of neutrons emitted from a fragment with specific mass and is described as a function of either product or fragment mass.

As pointed out in |1| $\nu_{tot}(A')$ and $\nu(A')$ are significantly different from $\nu_{tot}(A)$ and $\nu(A)$ and have to be clearly distinguished.

Fission reactions are symbolized as shown in the following examples:

$^{235}U(n_{th},f)$ for thermal neutron induced fission of ^{235}U

$^{252}Cf(sp.f)$ for the spontaneous fission of ^{252}Cf .

In addition to n_{th} for thermal neutron n_{2MeV}, n_{14MeV} will be used for neutrons of a specific kinetic energy and n_f will be used for fast (reactor) neutrons.

No specific symbol has been introduced for partial yields which are being obtained since recently from the mass-separator LOHENGRIN |8-15| for specific kinetic energies and ionic charge states of the fragments. Since too many parameters would have to be given, these will be made clear in the text.

Data Requirements

Any prediction method has to be developed from and has to be tested by a set of experimental data.

A status report on fission product yields is being presented as Review Paper 10 of these proceedings. There are, however, a few specific requirements to data used to develop prediction methods that will have to be discussed in this paper. Shortcomings of data compilations will have to be pointed out and recommendations shall be made for improvements.

There is no process in nuclear science which has been studied as extensively as nuclear fission. In particular, as mentioned, about 20 000 measurements of yields have been carried out so far for the various fission processes. They have been collected in a number of compilations |16-28|. This bulk of data is, however, by far not yet adequately covering the requirements for a description of the fission of the various nuclei at the variety of energies of interest. Not the fact that there are large gaps where no measurements have been undertaken shall be discussed at this point but the fact that in spite of the continuous efforts of the compilers there is still no complete set of adequately evaluated data: outdated and wrong values have not been removed completely from compilations, even though present-days evidence often allows a clear judgement. Estimated values are appearing as experimental results. Duplicate appearance of values (due to prepublication in progress reports etc.) is biasing the averages.

The elimination of these problems, an immense task due to the number of data, is further complicated by the use of most different experimental methods. Yields at different stages of the fission process have been measured (e.g., before and after prompt neutron emission), delayed neutron emission has been corrected in a few cases in others not. The error responsible for a wrong experimental yield value may be found a few generations of publications back

in a constant influencing indirectly the evaluation of measured data*.

For the further development and for the test of prediction methods it seems, therefore, appropriate to plead for more support to the compilers in order to allow further and more detailed evaluation of data.

This support could be financial, but especially it should consist in a close collaboration of the authors of the corresponding measurements.

It may be allowed to the author of this paper to advance a proposition which will certainly not solve the problem but may allow some definite improvements.

It is proposed that compilers, especially Meek and Rider and Crouch, contact those groups active in the field which can be reached asking for a revision of their entries in the compilation according to specific rules, e.g.,

a) that it be checked whether the value indicated is still the best choice. A value or its error margins may have to be changed due to better knowledge of the method used or of constants influencing the evaluation (half-lives, decay schemes, branching ratios, newly discovered isomeric states, neutron capture cross sections, yields of reference nuclides etc.). (For a change of a value in the compilation a remark should then be added to the corresponding reference stating the changes applied, the reasons, and the date of revision.);

b) that discrepancies to other measurements be commented. Especially, that error margins be reconsidered taking into account the discrepant information, and discussing possible systematic errors. Possibly, the different groups involved could be invited to agree on a common recommended value;

c) that duplicates be removed from the compilation. Duplicates in this sense could be defined as any preliminary value extending over all or a part of the data leading to a final value.

---

* Z. Alfassi, H. Braun, H.O. Denschlag, T. Izak-Biran, Branching ratios and absolute line intensities in chain 133, to be published

Recalculated values, e.g., independent yields obtained from the differences of two experimental cumulative yields (and vice versa) should not be given in the recalculated form.

It should be made certain that estimates (e.g., based on systematics or theory) do not enter into a compilation of experimental yields. Values based partly on estimate should be avoided or a large uncertainty (e.g., 100%) should be attributed to the estimate.

A division of experimental sum yields among single isomeric states according to an estimated formation ratio, e.g., as in [29] and as practiced in [22] should on the basis of these arguments be avoided by both experimenters and compilers;

d) that values which have subsequently (been) shown to be wrong or not trustworthy be taken out (be taken back).

Entries from data groups which cannot be reached or do not respond in time will obviously have to be evaluated essentially in the way used at present.

Partial yield data*

Recently almost complete data sets on light wing fission products in $^{235}U(n_{th},f)$ [8-11] and some results on fission product chains, 132-134 [12-15] have been obtained at the mass separator LOHENGRIN [30]. These data differ in principle from the data obtained up to now as they generally refer to fragments with a specific kinetic energy and a specific ionic charge state. This is due to the particular set up of the separator:

A thin target of UO_2 (40 µg/cm^2 or 400 µg/cm^2, generally) is exposed to a neutron flux of about 10^{15}n/cm^{2}s inside the mass-separator. The fission fragments are recoiling out of the target with nearly their initial kinetic energy (E_{kin}) and with the equilibrium distribution of their ionic charges (q) corresponding to their kinetic energies. The fraction possessing the right angle with respect to the collimator slit of the separator is separated according to $\frac{A}{q}$ and E_{kin}. For a particular energy (e.g., E_{kin} = 80 MeV) and a particular ionic charge state (e.g., q = 23^+) one mass (e.g., A = 134) can be intercepted at the

* The discussions in this chapter are based on the systematics of charge distribution as referred further below.

collector side of the separator. The distribution in Z of the intercepted isobars can be determined by physical [8-11] or γ-spectroscopic methods [12-15]. Fig. 3 shows the fractional independent yields of antinomy, tellurium and iodine-134 determined experimentally for various values of q at E_{kin} = 77 MeV (a) and for various values of the recoil energies at q = 23^+ (b).

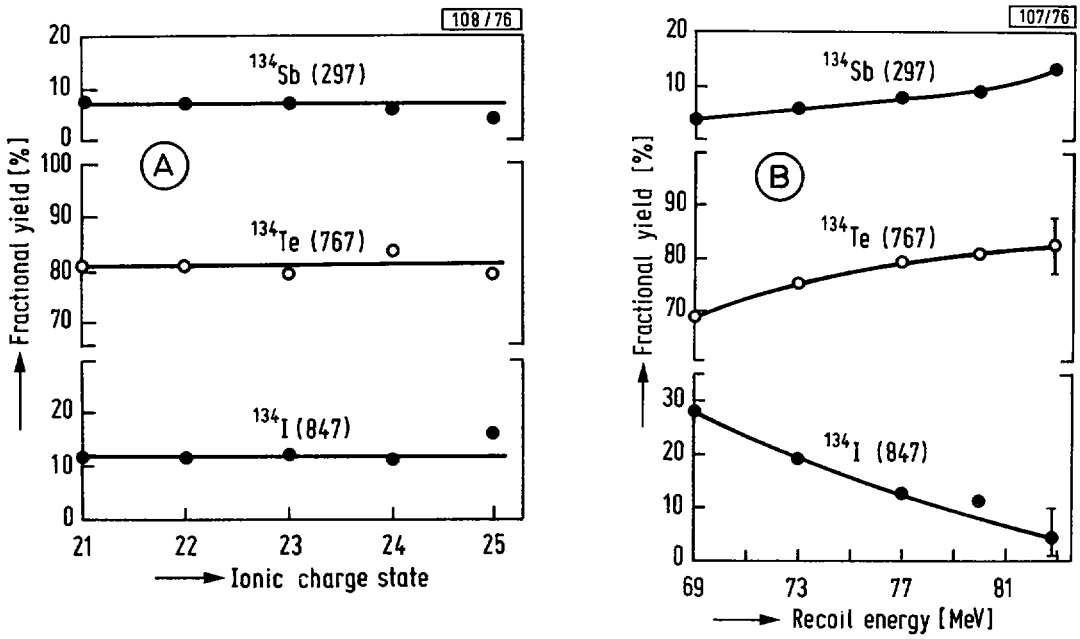

Fig. 3. Fractional independent (Te,I) and cumulative (Sb) yields in chain 134. In parenthesis energy of the γ-ray evaluated (keV). Statistical errors=point size. Part A: various ionic charge states; E_{kin}=77 MeV. Part B: at various recoil energies; q=23^+. The Te and I yields at E_{kin}=85 MeV have been given an increased error because of a discrepancy in the evaluation of alternative γ-rays (I:884 keV). (From /14/).

It appears that in the present case the results are independent of the ionic charge state but that the fractional yields depend strongly on E_{kin}. This is especially apparent for the yield of iodine which varies from FI = 0.28 at E_{kin} = 69 MeV to FI = 0.03 at 85 MeV. It is obvious that the yields measured at these two extreme recoil energies should be prevented from entering a classical yield compilation. The yields at the mean energy do, however, agree within error limits with the radiochemical results given in yield compilations.

Agreement has also been generally found for the light fission products between partial yields at the mean kinetic energy and radiochemical values [31] and partial yields are being used frequently meanwhile to derive systematic trends and to test theoretical predictions (see below and [31]).

In principle, one would expect the distribution of partial yields at the mean kinetic energy to be narrower than the distribution of radiochemical yields because the latter is the sum over the distributions found at all recoil energies.

Therefore, a more fundamental test on the comparability of both sets of yields was made.

Gaussian curves were fitted using the program ORGLS* [32] to the values shown in Fig. 3b correcting for the varying total mass yield at each energy as measured separately. The different curves resulting are shown in Fig. 4a. The corresponding Zp- and σ-values are defined in the chapter Isobaric Charge Distribution further below.

In Fig. 4b the Gaussian charge dispersion curve as obtained for the mean kinetic energy E_{kin} = 77 MeV (Fig. 4a) is given again renormalized to 1. It may be compared with artificial 'radiochemical' data (full points in Fig. 4b) obtained by adding the yield values calculated for the single Gaussians shown in Fig. 4a.

It appears that for fractional independent yields $\geq$ 10% no measurable deviation between radiochemical (total) yields and partial yields at the mean kinetic energy is to be expected if the error margins of $\sim\pm$10% (relative) are taken into account. At lower yield values larger discrepancies have to be expected.

In principle, the situation could be slightly different for other chains depending on the shift of Zp with energy relative to the width of the Gaussians (as shown in Fig. 4) and relative to the width of the distribution function of mass yields versus E_{kin}; but large changes are not expected as the parameters mentioned are fairly constant.

---

* The program was modified in an appropriate way and kindly put at our disposal by Prof. A.C. Wahl (St. Louis).

The yield distribution has been found to be generally nearly independent of the ionic charge state, as shown in Fig. 3a. A few exceptions are the masses 86, 89, 92 and 99. In these cases Clerc et al. [33] are postulating that internal conversion in the deexcitation of specific isotopes is inducing an Auger cascade leading to an increased ionic charge of these isotopes during separation. Special attention has to be paid to these cases.

Concluding, the statement of Wahl [31], based on a more statistical analysis of partial yields at $\overline{E_{kin}}$, is confirmed stating that these values may be used in compilations of total yields with a slightly increased uncertainty of at least the larger of ±0.04 or 15% of a value.

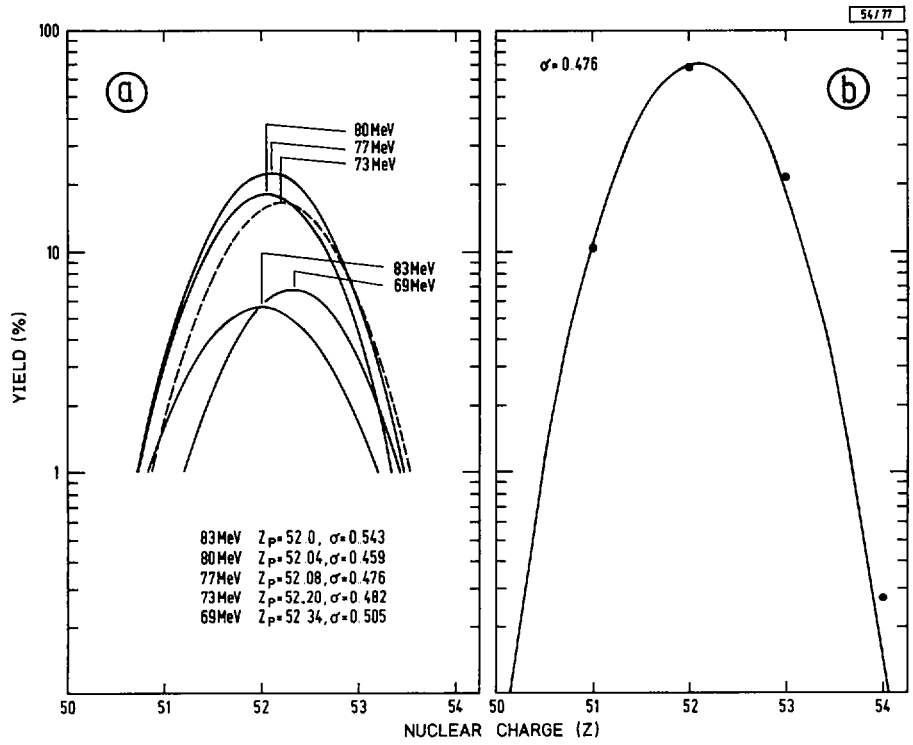

Fig. 4. a) Gaussian charge dispersion curves fitted to absolute yield measurements of ^{134}Sb, ^{134}Te and ^{134}I at the various indicated kinetic energies, Z_p- and σ-values obtained from a fit with a constant odd-even proton factor of 1.25 are also given.
b) Drawn out line: Gaussian charge dispersion curve fitted to the yield values obtained at the mean kinetic energy of the fragments (E_{kin}=77 MeV) (from part a) normalized to 1. Full points: yield values obtained by adding the values of the single Gaussians in a) at Z=51, 52, 53, 54. The points represent an artificial "radiochemical" data set.

Prediction Methods Based on Systematics

Mass yields

The subject of the prediction of mass yields has been covered extensively at the Bologna FPND Panel Meeting by Musgrove, Cook and Trimble [1]. Only recent developments shall be discussed here.

The systematics proposed by Musgrove et al. [1] have been developed further [34,35].

The mass yield data are fitted by a total of five Gaussian curves, one for symmetric fission and two each for light and heavy wing fission products according to:

$$YA = 100 \sum_{i=1}^{5} W_i [(2\pi)^{1/2}\sigma_i]^{-1} \cdot \exp[-(A-A_i)^2/2\sigma_i^2] \qquad (1)$$

where YA(%) is the mass yield of a given chain with mass number A, σ_i the width parameter of the i-th Gaussian, A_i the mass corresponding to the maximum of the i-th Gaussian and W_i the weight of the i-th Gaussian. The situation is illustrated in Fig. 5.

The neglect of ternary fission and the postulate that prompt neutron emission affects light and heavy fragments in much the same way leads to the symmetry conditions

$$\sigma_4 = \sigma_2; \qquad \sigma_3 = \sigma_5$$

and

$$W_4 = W_2; \qquad W_3 = W_5$$

In addition, the positions of the Gaussians follow to be symmetrical around the symmetric mass split (A_1):

$A_4 = 2\,A_1 - A_2$, $A_3 = 2\,A_1 - A_5$. The constraint

$\sum_{i=1}^{3} Wi = 1$ leaves the following parameters to be varied in the fit:

σ_1, σ_2, σ_3, A_1, A_2 (or A_4), A_3 (or A_5), W_1, W_2 (or W_3)

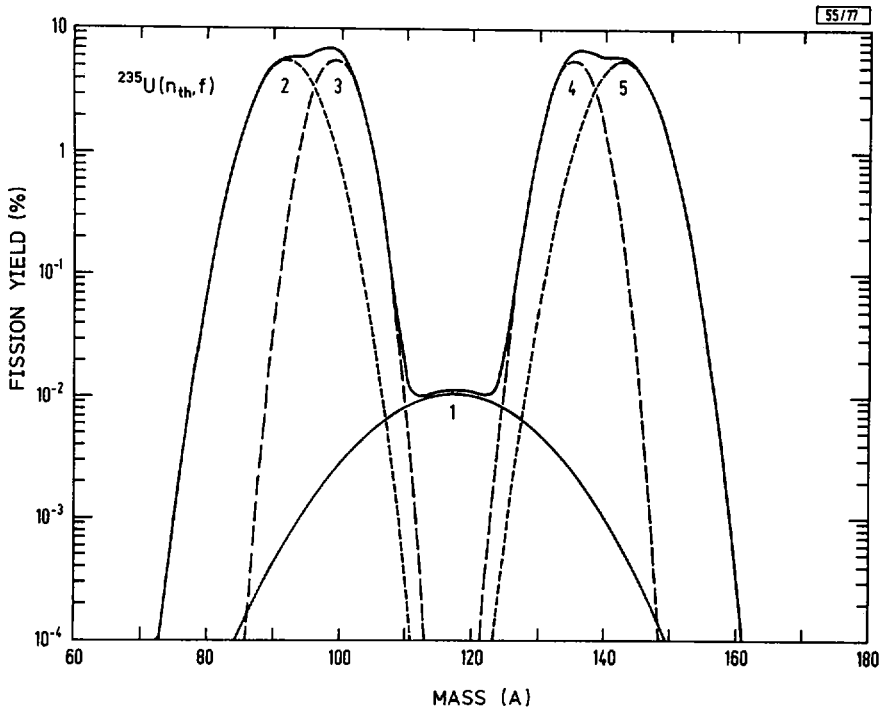

Fig. 5. Illustration of the fit of the mass yield curve for $^{235}U(n_{th},f)$ by five Gaussian curves according to equation (1). The value of index i is assigned to the respective curves.

The parameters W_1, W_2, W_3 are parameterized as*

$$W_1 = \sin^2\theta_1$$
$$W_2 = \cos^2\theta_1 \cdot \cos^2\theta_2 \qquad (2)$$
$$W_3 = \cos^2\theta_1 \cdot \sin^2\theta_2$$

The method has been used to fit 39 fission reactions (spontaneous fission and fission induced by thermal neutrons, 2 MeV- and 14 MeV-neutrons). The agreement between fit and experimental values is defined as

$$\Phi = \sqrt{\frac{1}{N}\sum_{i=1}^{N}\frac{(Y_i^{calc} - Y_i^{exp})^2}{(\delta Y_i)^2}} \qquad (3)$$

* These equations are partly misprinted in [35] and especially in [34]. Another misprint in [34] and the following remarks were communicated by the authors: On p. 136 line 5 $\cos\theta_2$ should be replaced by $\cot\theta_2$. The ^{232}Th fission spectrum average value was taken as 4 MeV rather than 2 MeV. The fits of θ values were carried out for two sets of data. The results of one set (Meek and Rider) are shown in the figures and the results of the other set (Flynn and Glendenin) are appearing in the fitted parameters.

N number of fission yields fitted

Yi chain yield (calc: calculated; exp.: experimental)

δYi experimental error of chain yield (≈ 0.1)

The values of Φ range generally between 1 and 4 indicating a mean deviation from the fit of 10 to 40%. A much better agreement is probably not to be expected as this description does not include odd-even effects and fine structures. Unfortunately, a systematical description of the parameters resulting from the fit in terms of dependence on A_F, the mass number of the compound nucleus or Z_F^2/A_F (Z_F charge number of the compound nucleus) is not possible without considering the dependence of the mass yield curves on excitation energy and fission barrier height. An analysis of the energy dependence of the parameters σ_i, A_i and θ_i [34] for single systems has lead to equations allowing to interpolate chain yield distributions within an overall accuracy of 20%.

The equations are in a general form:

$$\text{a)}\quad \sigma_i = a_i + b_i \sqrt{E - E_f}$$

$$\text{b)}\quad A_i = a_4 + b_4 \cdot E$$

$$\text{c)}\quad A_4 = a_5 + b_5 \sqrt{E - E_f}$$

$$\text{d)}\quad A_5 = a_6 + b_6 \sqrt{E - E_f} \qquad (4)$$

$$\text{e)}\quad \tan\theta_1 = \frac{2}{\Gamma_1}\,(E - E_1)$$

$$\text{f)}\quad \tan\theta_2 = \frac{2}{\Gamma_2}\,(E - E_2)$$

E is the incident neutron energy and a_i, b_i, Γ_i and E_i are constants that can be calculated if a mass yield curve has been determined for at least two different energies.

This approach seems appropriate to calculate the gross structure of fission yield distributions for energies intermediate to measured ones, e.g., for predicting mass yield curves for different reactor neutron spectra from known mass yield distributions in thermal- and 14-MeV neutron-induced fission reactions of the same fissioning nuclide.

An example of an interpolated yield curve for $^{240}Pu(n_{th},f)$ is given in Fig. 6 and is compared there with experimental data which have become available recently |36,37| as well as to a mass yield curve of the same reaction calculated according to the statistical model and to be discussed later. The agreement between the prediction discussed here and the experiment is obviously not good.

Yamamoto and Sugiyama |38| propose a method for obtaining mass yield curves of fission products from a mass yield distribution of fission fragments by correcting for the number of prompt neutrons emitted.

Fission fragment yield distributions [7] are available for some fission reactions for which fission product mass distributions have not been measured.

Unfortunately, the number of neutrons emitted as a function of the fragment mass $\nu(A)$ has been measured only for a few fission reactions [2]. It turns out, however, that the relative shape of the so called 'saw-tooth-neutron-evaporation curve' is not strongly dependent on the fission nucleus [2,39]. Therefore, it can be extended to other fission processes, as will be explained in the chapter Prompt Neutron Emission (Fig. 7).

The results of Yamamoto and Sugiyama for the mass yields of fission products calculated from fragment yields are given in Figs. 8 and 9 and may be compared there with the experimental values taken from the compilation of Crouch [40].

In these calculations the $\nu(A)$ values (saw-tooth prompt-neutron-evaporation curve) of Apalin |41| were used. It is pointed out by Musgrove |1| that these values are most likely in error. Using another set of ν-values from either [42,43] or from [44] - after correction for neutrons emitted backwards from the complementary fragment as explained in [1] - a better agreement in the top part of the heavy mass peak is to be expected.

A third, new approach which could possibly be used to predict mass yields is the "A'_p-method" of Wahl [31]. It has the primary purpose of describing charge distribution but may turn out useful in the description of mass yields. It consists in fitting a Gaussian curve for each element pair of the fission products, (i.e., about 18 Gaussians). The method has the advantage that pairing and shell closures of protons do not distort the shape of the Gaussians but

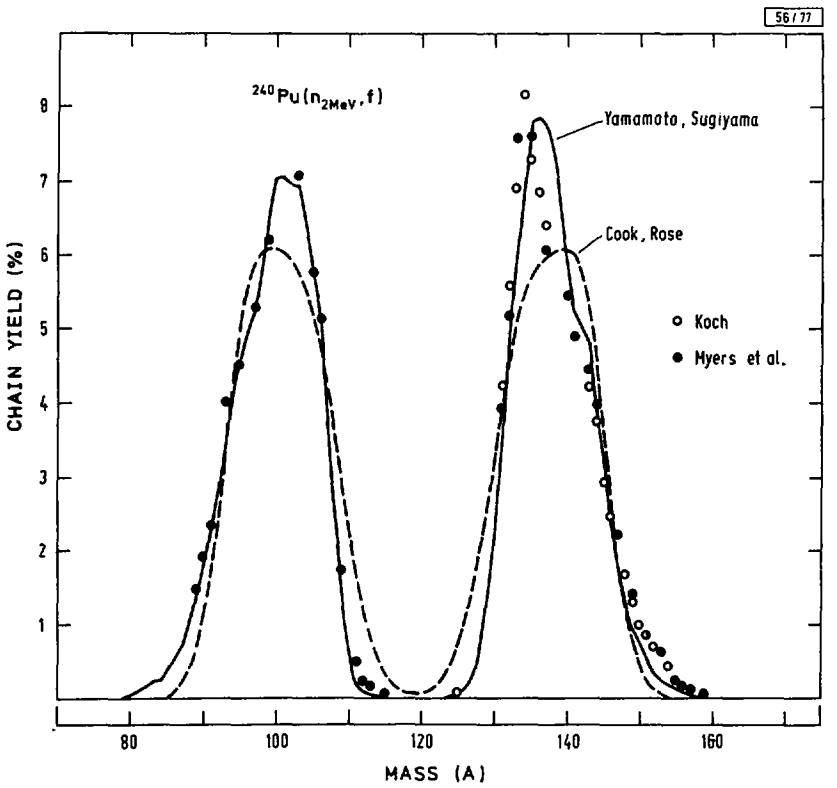

Fig. 6. Mass yield curve for $^{240}Pu(n_{2\ MeV},f)$. Drawn out line: prediction of Yamamoto and Sugiyama /38/; Broken line: prediction of Cook and Rose /35/.
Full points: experimental data from Myers et al. /37/.
Blank points: experimental data from Koch /36/.

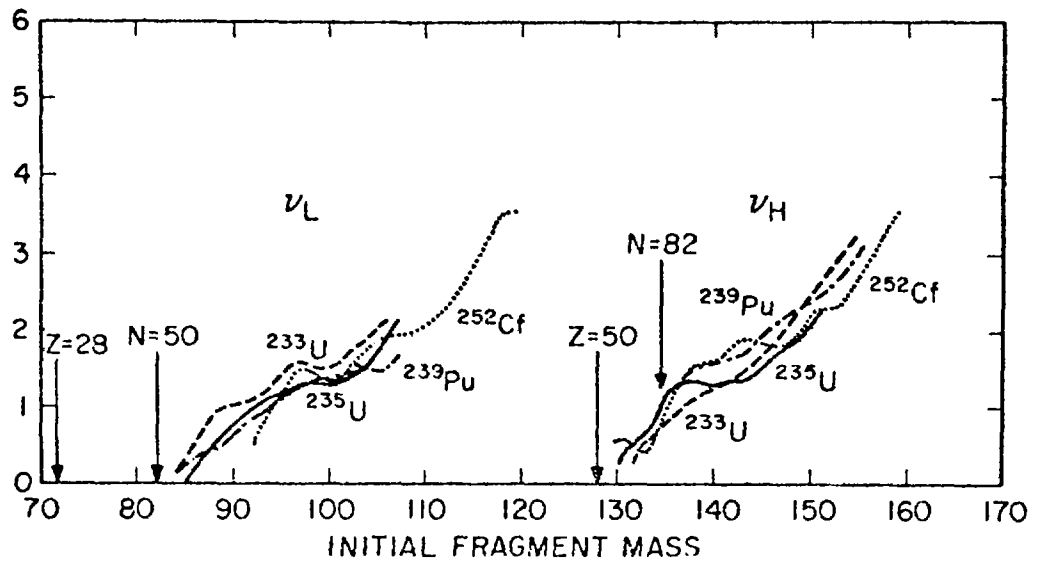

Fig. 7. Neutron yields as a function of fragment mass ($\nu(A')$) for the following fission reactions: $^{233}U(n_{th},f)$, $^{235}U(n_{th},f)$, $^{239}Pu(n_{th},f)$, ^{252}Cf(sp.f.). (From /39/).

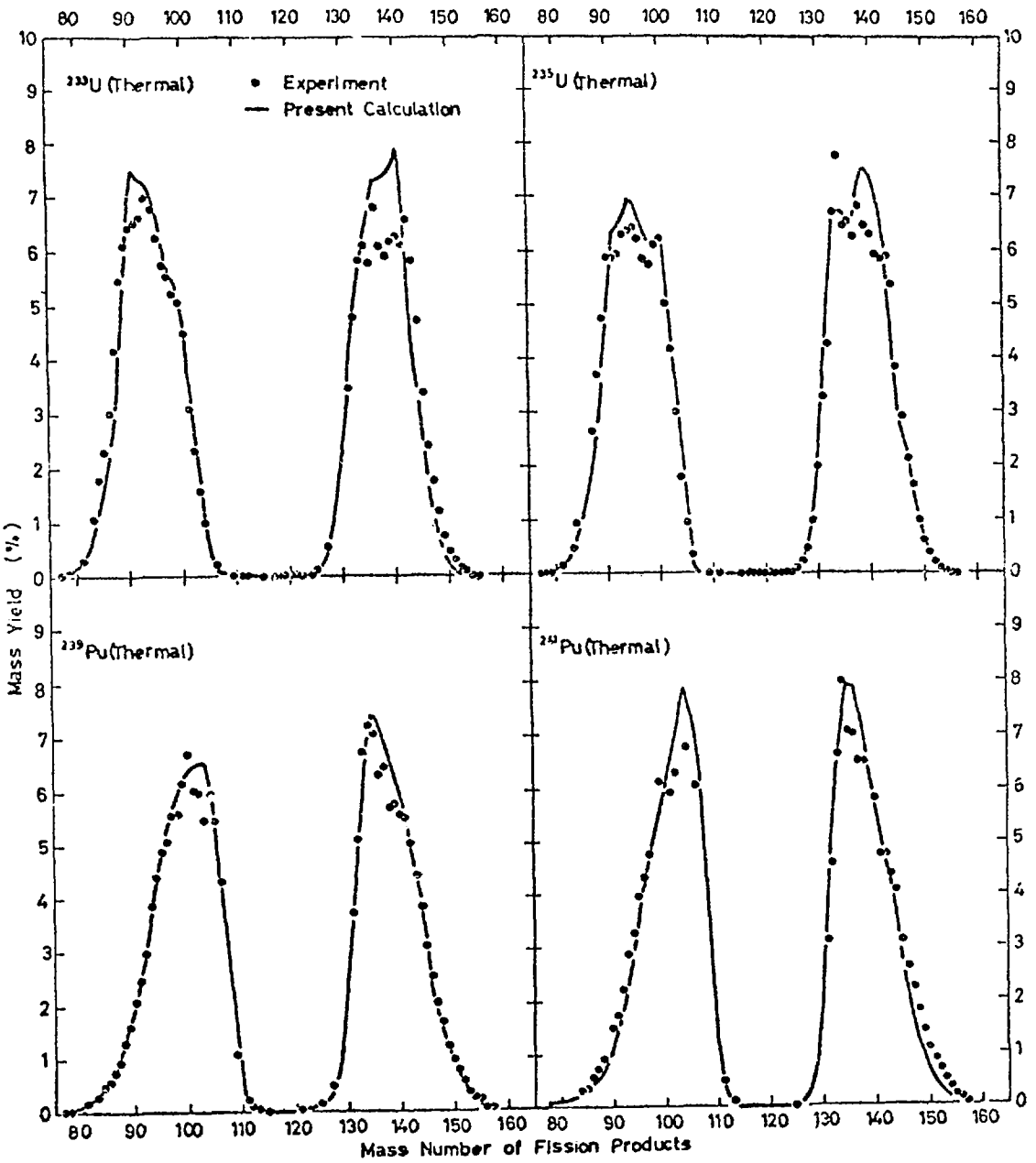

Fig. 8. Mass yields calculated by Yamamoto and Sugiyama for the thermal neutron induced fission reactions indicated. Full points: experimental results taken from Crouch /40/. (From /38/).

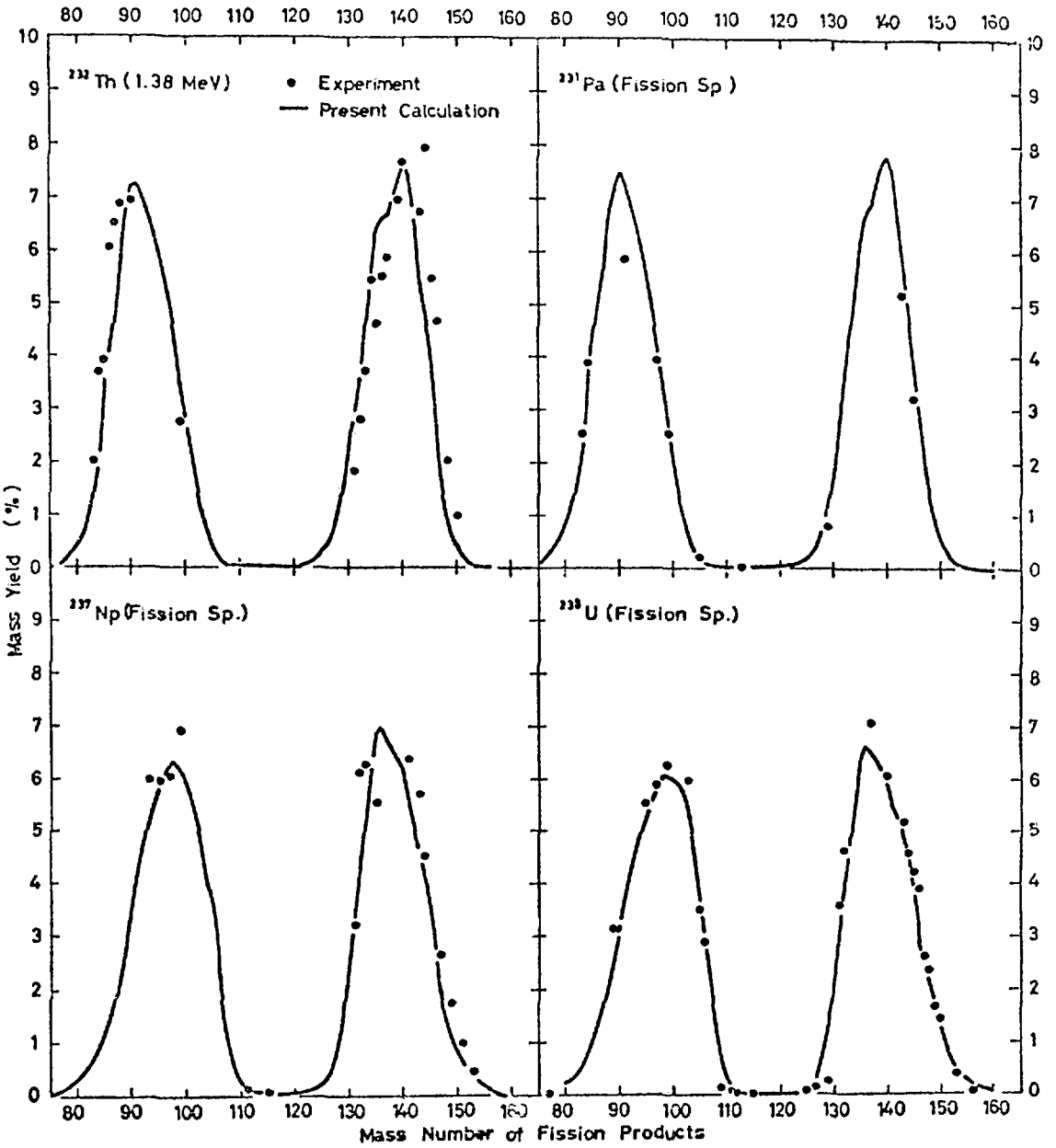

Fig. 9. Mass yields calculated by Yamamoto and Sugiyama for fission reactions indicated. Full points: experimental results taken from Crouch /40/. (From /38/).

are expressed only in their weights. Fine structures due to odd-even or shell effects of protons would, therefore, automatically be included in the description.

The method has the further advantage that the Gaussians used give direct information on the charge distribution. Being based on parameters with a most direct fundamental physical meaning (direct primary yields of nuclides and elements without any normalization), it may turn out to show

systematical trends depending on mass, charge and excitation energy of the compound nucleus more easily than the other description methods.

Unfortunately, the method has severe problems that may make it impractical for the prediction of mass yields: (a) The number of parameters to be fitted is quite high, (b) a fairly detailed knowledge of charge distribution is required. Therefore, at present it has been applied only to U-235(n_{th},f).

Isobaric Charge Distribution

The Terms Used for Describing Charge Distribution

The Charge Dispersion Curve

Almost all sytematics of charge distribution used so far are based on the concept [16] that the fractional independent yields (FI) of fission products along a decay chain are described by P(Z) a Gaussian 'charge distribution curve' (possibly modulated by an odd-even pairing effect to be discussed later). This curve is characterized by its maximum Zp (most probable charge) and a width parameter σ according to the equation

$$P(Z) = (2\pi(\sigma^2 + 1/12))^{-1/2} \exp\left((Z-Zp)^2/2(\sigma^2 + 1/12)\right) \qquad (5)$$

The term 1/12 is a correction accounting for the fact that the Gaussian is applied to a discrete rather than a continuous distribution [16]. In the integrated form of the Gaussian ('error function') describing fractional cumulative yields this correction term is not appearing.
Experimental Zp-values are obtained by solving equation (5) for Zp and identifying the P(Z) with the experimental fractional independent yield. If fractional independent yield values for sufficient isobars are available a mathematical fit may be carried out, determining a weighted average value for Zp* (and possibly also for σ and/or an odd-even factor).

---

* Some authors [8-11] indicate the average nuclear charge $\overline{Z}$ of an isobaric chain rather than the Zp-value. However, this description does not allow to calculate explicit yields from a known $\overline{Z}$ value. It is also likely to produce confusion since the rms width of the charge distribution, called σ by the authors [8-11], will generally differ from the standard deviation of the Gaussian distribution also called σ. (For an exactly Gaussian distribution $\sigma_{gauss} = (\sigma^2_{rms} - 1/12)^{1/2}$, see also [31].

The Charge Displacement ΔZ

The Zp-values obtained from the evaluation of experimental yields are usually compared with Z_{UCD}, a nuclear charge calculated for the chain of mass A assuming Unchanged Charge Distribution (UCD) among the two fragments, i.e.,

$$Z_{UCD} = A' \cdot \frac{ZF}{AF} \quad ; \quad A' = A + \nu(A) \tag{6}$$

$Z_F(A_F)$ being the nuclear charge (and mass number) of the compound nucleus,

A the mass number of a fission product (after prompt neutron emission),

A' the average mass number of fission fragments (giving A by prompt neutron emission), and

$\nu(A)$ the average number of prompt neutrons emitted to form A.

The difference between the most probable charge (Zp) and the charge corresponding to unchanged charge density (Z_{UCD}) may be called charge displacement, ΔZ (or ΔZp as opposed to $\Delta\overline{Z}$).

$$\Delta Z = Zp - Z_{UCD} \tag{6a}$$

ΔZ is representing a polarization in the compound nucleus at scission. In low energy fission reactions the value of ΔZ is normally around +0.5, -0.5 charge units for light and heavy fragments, respectively.

The various fission systematics differ in the treatment of and in the assumptions for the parameters ΔZ and σ and in the inclusion of odd-even factors for protons and possibly for neutrons, as will be discussed.

Prompt Neutron Emission

A critical parameter is also the number of prompt neutrons, $\nu(A)$ or $\nu(A')$, emitted from a fragment of mass A'.

It is actually to be expected that ν, besides its dependence on excitation energy and mass is also dependent on the nuclear charge, Z, of the fragment. But since (almost) no data on the variation of ν with Z have been measured this latter dependence is usually neglected.

The values of $\nu(A')$ have been measured for a few fission reactions and the shape of the so called 'saw-tooth' curve has been found to be largely independent of the fission reaction at low energies (see Fig. 7). In many fission reactions $\nu(A')$ has not been measured directly; but the number of neutrons emitted per fragment pair ($\nu_{tot}(A)$) can be derived from the mass yield data [45] and may be partitioned among the single products according to the ratio found in the direct measurements ('ν_{tot}-method')[25].

For fission reactions with insufficient mass yield data $\nu(A)$ may be obtained by scaling an appropriate experimental saw-tooth curve (e.g., Fig. 7 for spontaneous and thermal- or 2 MeV-neutron induced fission and the corresponding curve for $^{238}U(p_{12MeV},f)$ from [46] for 14 MeV neutron induced fission reactions (see [25])) with $\bar{\nu}$, the average number of prompt neutrons emitted per fission event, ('$\bar{\nu}$-method')[25]. The value of $\bar{\nu}$ is known for most fission reactions or may be extrapolated as a function of nuclear charge and mass number of the fissioning nucleus and the excitation energy at fission [2].

Systematics Based on the 'Normal Fission Yield' Concept

Fission of ^{235}U by Thermal Neutrons

In earlier work, e.g., [16] ΔZ was obtained for $^{235}U(n_{th},f)$ from each experimental value of a fractional independent or cumulative yield according to equations (5,6,6a) using a value of $\sigma=0.59\pm0.06$. A smooth curve was fitted through the values of ΔZ plotted versus A'. Predictions of unmeasured yields could be made by reading the value of ΔZ from the curve and calculating P(Z) using equations (5,6 and 6a). The uncertainty of the predicted yield could be evaluated from the scatter of the single ΔZ-values plotted at the particular fragment mass.

Subsequently [17] a simple mathematical description of ΔZ (A') has been advanced:

$$\begin{aligned} &\text{a)}\quad \Delta Z = -0.45 \pm 0.1 \quad \text{for} \quad A' > 134 \\ &\text{b)}\quad \Delta Z = +0.45 \pm 0.1 \quad \text{for} \quad A' < 102 \\ &\text{c)}\quad \Delta Z = -0.45\,\frac{118-A'}{16} \quad \text{for} \quad 134 > A' > 102 \end{aligned} \tag{7}$$

These ΔZ-values or the Zp-values derived therefrom and a value of $\sigma = 0.56 \pm 0.06$ were used to calculate 'normal' predicted yields (P(Z) equation (5)).

The comparison of calculated and experimental yields shows an odd-even proton effect in the sense that nuclides with odd Z consistently fall under the predictions and nuclides with even Z fall above it. This effect will be discussed later in more detail. Before, the application of the 'normal yield' concept to other fissioning nuclei shall be treated.

Fission Reactions other than $^{235}U(n_{th},f)$

For the application of the method to other fissioning nuclides Wolfsberg [25,47] on the basis of experimental results from various fission reactions postulates that ΔZ is constant with the possible exception of $^{239}Pu(n_{th},f)$ A slightly higher value of ΔZ for $^{239}Pu(n_{th},f)$ as compared to $^{235}U(n_{th},f)$ and $^{233}U(n_{th},f)$ is confirmed in the most recent analysis (Table II in [31]) but due to the sensitivity of ΔZ values to $\nu(A)$ it is not excluded that the higher ΔZ-value in $^{239}Pu(n_{th},f)$ is due to a small systematical error in the number of prompt neutrons assumed. The method used to obtain $\nu(A)$ for the various fission processes is described above (ν_{tot},$\bar{\nu}$ method)(see chapter Prompt Neutron Emission).

Nethaway [48] uses a different approach in taking the Zp(A)-function for $^{235}U(n_{th},f)$ as a reference. This function is obtained from equations (6), (6a) and (7) solved for Zp. The values of Zp(A) for other fissioning systems are obtained by calculating values of DZp* to be used as corrections to the reference Zp(A) function; that is

$$Zp = Zp_{(ref)} + DZp \qquad (7a)$$

for a given mass number and for a particular fissioning system. The values of DZp are obtained from the following equation

$$DZp = a(Z_F-92) + b(A_F-236) + c(E-6.52) \qquad (7b)$$

* In [48] DZp is called ΔZp. The denomination has been changed to prevent confusion with ΔZ defined in equation (6a) of this paper.

where Z_F and A_F are the charge and mass number of the compound nucleus and E is the excitation energy in MeV. The values of the coefficients a, b, and c were obtained by a least-squares fit to the available data of spontaneous and neutron induced fission reactions. The values are found to depend on the fragment mass. The values for a and b are given in Table I.

Table I

Coefficients a and b for equation (7b) as obtained from a least squares fit to experimental data [48].

	light products	valley region	heavy products
a	0.414 ± 0.016	0.50 ± 0.03	0.547 ± 0.01o
b	-0.143 ± 0.007	-0.165 ± 0.02	-0.188 ± 0.004

For c 43 different values ranging from 0.0157 ± 0.0009 (A=98) to 0.0509 ± 0.0031 (A=130) are given.

Zp-values for a total of 35 different fission reactions (spontaneous and induced by thermal, 1.8 MeV- and 14.8 MeV-neutrons) are presented in [48].

Pairing Effects

A quantitative analysis of the odd-even effect was first carried out by Amiel and Feldstein |23,24| leading to a mean value of (22±7)% for protons and a substantially weaker effect for neutrons in the cases of ^{235}U and ^{233}U thermal neutron induced fission.

It was also recognized that the effect is dependent on the excitation energy when a proton pairing effect of (8±4)% was found for the fission of ^{235}U by fission spectrum neutrons [24]. Indication for a very strong proton pairing effect of (30±12)% were found in $^{232}Th(n_f,f)$ by Izak-Biran and Amiel |49,50|. Unfortunately, due to the extreme experimental difficulties, the error margins of this value are too high to draw definite conclusions. The value is, however, in qualitative agreement with a pronounced structure in the mass yield curve of the similar fission reaction $^{229}Th(n_{th},f)$ [7]

interpreted to be due to an unusually strong proton pairing effect. Further measurements should be attempted on $^{232}Th(n_f,f)$ as the odd-even factor of this reaction is of fundamental importance for the systematics of pairing effects for various fissioning nuclides and at various excitation energies [22,51] as will be discussed in the following.

Madland and England [51] have - on the basis of the information available from various fission reactions - made a detailed study of pairing effects. In particular, clearly the four cases listed in Table II are distinguished.

Table II

Modulation factors for the different odd-even combinations of neutrons and protons as proposed in [51]. For the definition of X and Y see text.

case	Number of protons	Number of neutrons	Modulation Factors
1.	even	even	$F_1 = 1 + X + Y$
2.	even	odd	$F_2 = 1 + X - Y$
3.	odd	even	$F_3 = 1 - X + Y$
4.	odd	odd	$F_4 = 1 - X - Y$

In consequence four different 'modulation factors' F_i (i = 1 to 4) are resulting. These factors are determined by the different combinations of two factors X and Y, defined as 'the fractional yield enhancement relative to the normal yield' due to proton (X) and neutron (Y) pairing. X and Y are assumed independent of the fragment mass. The 'normal yields' are those defined above. The assumption of 'normal yields' will have to be discussed later.

The basic modulation equations to the 'normal yield' distribution are

$$\text{a)} \quad IN = F_i \cdot YA \cdot P(Z) \quad \text{and}$$
$$\text{b)} \quad FI = F_i \cdot P(Z) \qquad (8)$$

P(Z) 'normal independent yield' as predicted by equation (5)

F_i see Table II

The factors F_i (i = 1,2,3,4) are determined for the reaction $^{235}U(n_{th},f)$ by comparing the (summed) experimental yields (IN, FI) [21,23,24] with the predictions $(P(Z), Y_A \cdot P(Z))$ according to equations (8a) and (8b). The results according to equation (8a) are more accurate since yields with high absolute values, which are generally known more accurately, are weighted more heavily. Therefore the values of F_i based on this evaluation are used to produce recommended values of X = 0.228 $\pm$ 0.034 and Y = 0.044 $\pm$ 0.034 for $^{235}U(n_{th},f)$. These values have been adopted for the predictions in the latest edition of Meek and Riders compilation /22/.Four remarks shall be made concerning these systematics.

a) It should be checked wether an improved description could be obtained when the constant factors X and Y are replaced by values showing the functional dependence on A as found by Clerc et al. /10/ (Figs. 10 and 11).
The results shown in Figs. 10 and 11 refer to partial yields of fission products at the most probable energy. On the basis of the arguments made above (see Partial Yield Data, especially Fig. 4) and according to the discussion carried in /31/ these partial yields seem to be comparable to total yields.

b) A normalization factor should probably be introduced into equations 8a and 8b assuring that the sum over all (fractional) independent yields remains equal to the chain yield (Eq. 8a) or equal to unity (Eq. 8b) after application of the odd-even factors to the single chain members.

c) The following definition of odd-even factors used by other groups /25,31/ seems preferable to the author:

$$F_1=\overline{EOZ}\cdot\overline{EON};\ F_2=\overline{EOZ}/\overline{EON};\ F_3=\overline{EON}/\overline{EOZ};\ F_4=1/(\overline{EOZ}\cdot\overline{EON})$$

with EOZ≈1+X and EON≈1+Y. This definition has the advantages that the odd-even factors are not affected by a renormalization according to (b) and that very large odd-even factors (X+Y≥1) could be handled.

d) The fourth point is the choice of 'normal' yields /17/ calculated according to a procedure developed when not much was known about odd-even effects. Calculations carried out by Musgrove /1/ and Wahl /31/ and discussed later show that the parameters σ and ΔZ are changed with respect to the assumptions made in the calculation of 'normal yields' when odd-even factors are introduced into the fit program as a varying parameter.

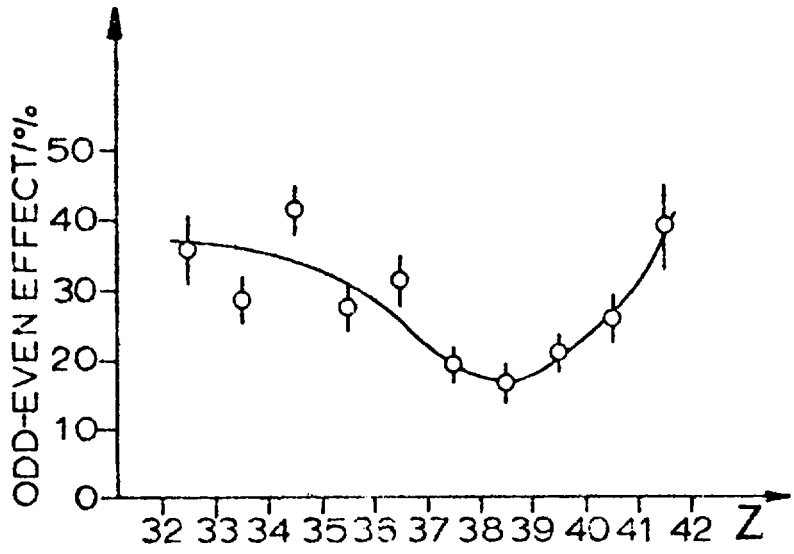

Fig. 10. Odd-even proton effect as a function of Z (from /10/).

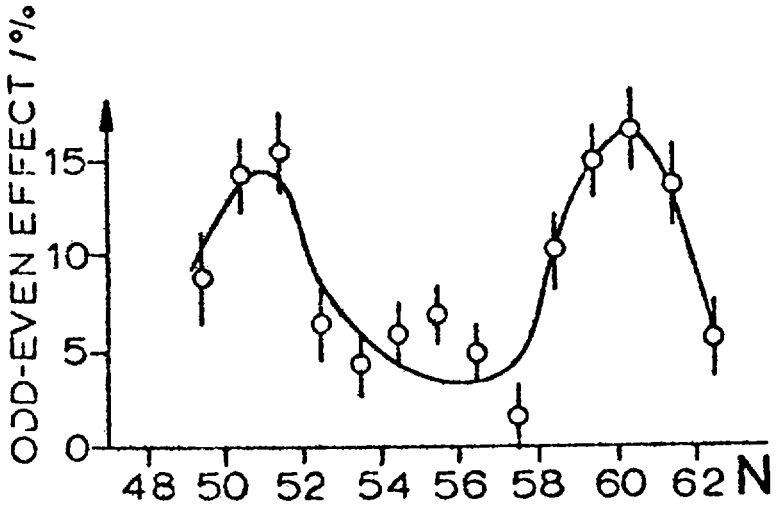

Fig. 11. Odd-even neutron effect as a function of N, the number of neutrons in the fragments (from /10/).

The odd-even Factors in 'other' Fission Reactions

For the extrapolation of odd-even factors to other less known fissioning nuclides and/or other fission energies the procedure described in the following has been proposed /51/ and is being used at present /22/. The procedure involves the following assumptions:

a) the neutron pairing factor Y is directly proportional to the proton pairing factor

$$Y = \alpha X \qquad (9)$$

The value of α is resulting from the values for X and Y in $^{235}U(n_{th},f)$

$$\alpha = \frac{Y}{X} = \frac{0.044 \pm 0.034}{0.228 \pm 0.034} = 0.193 \pm 0.152$$

It is in agreement with a value of $\alpha < 1$ obtained in $^{233}U(n_{th},f)$.

b) X depends directly on the excitation energy of the compound nucleus at the outer fission barrier (ε_b)

$$X = k/(\varepsilon_b + c) \qquad (10)$$

where ε_b is the excitation energy of the compound nucleus compared to the outer fission barrier

$$\varepsilon_b = E^* + E_n - E_b$$

E^* Excitation energy due to capture of a thermal neutron (from a mass table /101/).

E_n Incident neutron energy

E_b Outer fission barrier height in the double humped barrier model /52/. Averages of experimental values /53-55/.

k and c are two parameters which are determined empirically from the values of X

for $^{235}U(n_{th},f)$ $X = 0.228 \pm 0.034$ and

for $^{235}U(n_{1.9\ MeV},f)$ $X = 0.078 \pm 0.063$

to be

$k = 0.225 \pm 0.259$ and

$c = 0.182 \pm 0.789$

It is evident from the large errors of the different parameters calculated that more and more accurate experimental data are needed.

Besides, a few remarks should be made about the parameterization of odd-even effects.

The assumption of a constant α (Equation (9)) is probably a reasonable choice as long as no further data are available. It should, however, be stressed that more data are needed since a constant value of a α is not expected from theoretical arguments /56/.

The choice of the hyperbolic form of equation (10) was made mainly to fit an experimental value of $X \simeq \pm 0.35$ for $^{232}Th(n_f,f)$ determined by S. Amiel and referred in /51/. This value has actually to be replaced by $X=0.30\pm0.12$ (or by $X=0.38\pm0.13$ if it is accepted that the experimental value has to be corrected for the particle-hole excitation at the saddle due to the energetic part of the neutron spectrum /50/) on the basis of later results of the same group /49,50/*. Due to the large errors in the experimental results the decision in favour of the hyperbolic form and against an exponential one discussed also is not compelling. Fortunately, the results are not influenced very much by the choice of either one of the equations.

The choice of the excitation energy above the outer fission barrier ε_b seems appropriate for the energy parameter. However, more information on the descent from saddle to scission may be expected from theoretical studies.

---

*see also S. Amiel et al. Contributed paper (this meeting).

Concluding this discussion on the systematics of odd-even effects, it should be stated that the obvious shortcomings found are due to lack of data and can be overcome only by more experimental work.

Global Fitting Procedures

In the systematics described above the parameters (ΔZ, σ, EOZ) were determined essentially chain by chain and either averaged subsequently or described as a function of A or A'.

In the following approaches the total body of fractional yield data of a fission reaction considered appropriate is fitted at once delivering a number of parameters describing the whole system. Musgrove /1/ fitted all experimental fractional yield data of /19/ for $132 \leq A \leq 104$ for $^{235}U(n_{th},f)$, $^{233}U(n_{th},f)$ and $^{239}Pu(n_{th},f)$ to Gaussian charge distribution curves modulated by the proton pairing effect X (C in /1/) and renormalized by a factor N(A) assuring that the sum over Z for a given A be equal to unity.

The equation used may be written

$$Pm(Z) = P(Z) \cdot \frac{1+X}{N(A)} \qquad (12)$$

Pm(Z)	modulated yield prediction (or experimental yield value used in the fit)	
P(Z)	unmodulated yield prediction according to eq. (5)	
X	proton pairing factor	positive for even Z nuclides negative for odd Z nuclides
N(A)	renormalization factor	

The pairing effect and σ, the width parameter of the Gaussian, were assumed independent of the fragment mass (A). ΔZ was assumed to vary linearly with A according to

a) $\Delta Z(A'_h) = -(\Delta Z_{(132)} + \beta(A'_h - 132))$ or (13)

b) $\Delta Z(A'_l) = \Delta Z_{(132)} + \beta(A'_l - A_F - 132)$

$A'_h(A'_l, A_F)$ mass number of primary heavy fragment (primary light fragment, compound nucleus).

A good fit was obtained for the two reactions listed in Table III together with the corresponding results.

Table III

Results of the fit of results from [19] by Musgrove [1] according to equations (5), (12) and (13).

parameter	$^{235}U(n_{th},f)$	$^{233}U(n_{th},f)$
$\Delta Z_{(132)}$	0.517	0.578
β	$-6.0 \cdot 10^{-3}$	$-9.0 \cdot 10^{-3}$
σ	0.569	0.582
X	0.206	0.158

It appears, that the parameter ΔZ in both fission reactions differs appreciably from the value of ± 0.45 used for the 'normal' yield distribution on which the odd-even systematics described above are based. The odd-even factor is, however, practically identical to the one recommended by Madland (0.228 ± 0.034). It must be said that three different data compilations are involved in the comparison. Data from [17] were used for deriving 'normal' yields. The development of the odd-even factor by Madland was essentially based on values from [23,24] and the global fit was applied to the data from [19].

Finally, the attention shall be drawn here to the contribution of A.C. Wahl to these proceedings [31] where in the frame of a more general discussion of different models a reevaluation of the updated set of the four better known fission reactions $^{235}U(n_{th},f)$ $^{233}U(n_{th},f)$, $^{239}Pu(n_{th},f)$

and ^{252}Cf(sp.f) is undertaken taking into account the existence of odd-even effects and deriving a best fit of the data using the following parameters, which are kept constant throughout the fragment mass numbers (104>A>130):

$\Delta Z(=0.51\pm0.01)$, $\sigma(=0.53\pm0.01)$, $\overline{EOZ}(=1.26\pm0.02)$, $\overline{EON}(=1.07\pm0.02)$

The results obtained for $^{235}U(n_{th},f)$ are given in parenthesis.

In the mass region A=105-107 and A=126-129 a sharp structure in ΔZ was noted for $^{235}U(n_{th},f)$ as was already pointed out in [19] on the basis of weaker evidence. This mass region was therefore fitted separately as discussed in [31] (see dotted line in Fig. 1 [31]).

The reevaluation of the classical model [17] using the global fit procedure is compared with two new approaches:

a) the model of oscillating ΔZ and σ functions (OSC-Model) developed on the basis of observations of Siegert et al. [8,9] and Clerc et al. [10]. In this approach a sine function is fitted to the experimental values of $\bar{Z}-Z_{UCD}$ and to σ describing the odd-even effect influencing both parameters in a periodical way depending on whether the element produced with dominant yield is odd or even.

b) the 'A_p'-Model' discussed in the following paragraph.

The Isotopic Mass Distribution

The A_p'-model as proposed by Wahl [31] replaces the classical description of independent yields using mass yields and isobaric charge distribution by a new approach in which the distribution of isotopic yields for each element is described by a Gaussian curve. The maximum of this curve is called the 'most probable mass' (A_p') of the particular element. A_p', analogous to Zp, is not necessarily an integer number. The 'prime' indicates that(average) mass numbers prior to prompt neutron emission are used. Mass distribution curves have been used before, e.g., by Yaffe and coworkers [57,58] to describe the formation cross sections of the isotopes of an element as a function of their mass. In [31] the advantages and disadvantages of a systematic description on the basis of this concept are discussed.

The A_p'-model is certainly most directly related to the physics of the fission process in that nuclear charge distribution and mass yields are considered together to give directly the independent yields of fission products. The model has the disadvantage, however, of requiring large data sets for the determination of the many parameters involved.

Isomeric Yield Ratios

The evolution of radioactivity with time in the fission process is not only determined by the distribution of independent yields along a β-decay chain and the β^--half-lives of the chain members. The existence of isomeric states in a number of nuclei with widely varying half-lives has to be taken into account.

An attempt to describe the distribution of independent fission-product yields to isomeric states has been developed by Madland and England [29]. It shall be discussed briefly in the following.

The approach is to turn around a method used to calculate the average angular momentum of fission fragments from isomeric ratios determined experimentally. The method is based on a statistical theory developed by Huizenga and Vandenbosch [59] and applied to fission fragments by several authors, e.g., [60-63].

The statistical model predicts the angular momentum density distribution P(J) to be of the form

$$P(J) = P_0\ (2J+1)\ \exp\left[-(J+1/2)^2/\overline{J^2}\right] \qquad (14)$$

which describes the probability to find a fission fragment in a state with particular spin J as a function of the average $J_{rms} = \sqrt{\overline{J^2}}$ induced in the fission process.

J_{rms} is assumed constant for all fragment masses in the neutron induced fission of all actinide systems but varying with incident neutron energy.

The branching mechanism assumed to either one of the two isomeric states is that excited fragments with J values near that of the isomeric

state (Jm) γ-decay to the isomeric state, fragments with J values near the ground state (Jg) γ-decay to the ground state and fragments with J values exactly between Jg and Jm divide equally among ground and isomeric states. This relation may be written

$$\frac{IN^h}{IN^h + IN^l} = \frac{\int_{Jc}^{\infty} P(J)\, dJ}{\int_{0}^{\infty} P(J)\, dJ} \qquad (15)$$

IN^h independent yield of high spin isomer

IN^l independent yield of low spin isomer

When Jc is chosen according to the recipe given above four different cases are resulting which differ according to whether the mass number A and/or the value of [Jm-Jg] are even or odd.

The value of $J_{rms} = \sqrt{\overline{J^2}}$ required to solve equation (14) and correspondingly (15) has been obtained, by fitting experimental isomeric yield ratios, to be J_{rms} = 7.5 ± 0.5 for thermal neutron induced fission

≈ 8 for fast neutron induced fission

≈ 9 for 10 MeV proton (neutron) induced fission and

≈ 10 for 14 MeV neutron induced fission.

The predictions are compared to a set of six experimental values not used in the determination of J_{rms} and general agreement as found.

Values that have more recently been determined or values given in [29] subject to discussion are compiled in TableIV together with the values predicted according to the model.

The agreement found is varying.

Especially, the yields of ^{97}Nb and ^{99}Nb are found to be off the predicted values by more than an order of magnitude.

It ought to be stated that Huizenga and Vandenbosch [59] mention the possibility that isomeric ratios may be found that do not allow to draw conclusions on J_{rms} due to different reasons like competing levels of intermediate spin between the levels of the two isomeric states or a level of intermediate spin just above the metastable

Table IV

Experimental ratios of formation cross-sections of high spin isomer (σ_h) to total ($\sigma_h+\sigma_l$) and predictions according to the model /29/

Fission-reaction	Isotope	I^π		$\sigma_h/(\sigma_h+\sigma_l)$		Ref.
		low-spin state	high-spin state	predicted	experimental	
$^{235}U(n_{th},f)$	^{97}Nb	$1/2^-$	$9/2^+$	0.81	≥ 0.99	64, 65
	^{99}Nb	$1/2^-$	$9/2^+$	0.81	0.077 ± 0.009	64, 65
	^{128}Sb	5^+	8^-	0.37	≥ 0.413 [1]	66
	^{130}Sb	5^+	8^-	0.37	0.41 ± 0.11 [2]	66
	^{132}Sb	4^+	8^-	0.42	0.31 ± 0.03	67
	^{132}Sb	4^+	8^-	0.42	0.28 ± 0.03	68
	^{132}Sb	4^+	8^-	0.42	$0.29^{+0.08}_{-0.12}$	69, 70 [3]
$^{239}Pu(n_{th},f)$	^{132}Sb	4^+	8^-	0.42	0.25 ± 0.03	67
$^{249}Cf(n_{th},f)$	^{132}Sb	4^+	8^-	0.42	0.32 ± 0.03	67

[1] This value was by mistake not given as a lower limit in /29/

[2] This value, as given in /29/ should be cited with caution. The authors of /66/ (p.1208) write: If the 1.6 min isomeric state of 130-Sn recently reported by Kerek (/71/) has an appreciable fission yield ... the ratio of the 130-Sb independent yields would be affected in an unknown way since the fission yield of 1.6 min 130-Sn and the fraction of it decaying to each 130-Sb isomer are unknown.

[3] The ratio of $Sb(4^+)$ to $Sb(8^-)$ as given in /70/ is actually the reciprocal of the value given in /69/. We assume that the two isomeric states have been confused in /70/.

state decaying by a cross-over transition to the ground state. Other non-statistical phenomena are also not excluded. Therefore, predictions of isomeric yields based on the model and the experimental values may differ considerably in some cases.

Outliers have to be expected even when an uncertainty of 50 % is attributed to the predicted ratios (σ_h/σ_l).

The model is applied by Meek and Rider [22] to any sum yield of two isomeric states, without introducing an error for the subdivision.

The difficulty of differentiating the experimental error of a sum yield (which ought to be given) and the uncertainty in subdividing this sum is recognized.

The author feels that a subdivision of sum yields according to a model should not be applied in a compilation of experimental yields (e.g., it should not be used in the Table 'Original Reference Data' [21]) but should be restricted to the systematics developed from the original data (e.g., Table 'Averaged and Evaluated Data' [21]).

Ternary Fission Products

Ternary fission, i.e., binary fission accompanied by the emission of light ($A \leq 10$) (charged) particles is a rare process ($\sim$0.2% of all fission events) in low energy nuclear fission. It has some importance for the normalization and charge conservation in fission yield sytematics and shall therefore be mentioned briefly here. A recent summary [72] gives a compilation of the experimental results on the total number of light particles (N) emitted per 1000 fissions in various fission processes (^{232}Th, ^{233}, ^{235}, ^{238}U, ^{239}, ^{241}Pu by neutrons; ^{232}Th, ^{238}U by α-particles and ^{238}U by protons at various energies).

A fit of the experimental results as a function of A_F and Z_F the atomic mass and nuclear charge of the compound nucleus and of ε_b, the excitation energy of the compound nucleus at the outer fission barrier (as defined for equation (10) of this paper) has been attempted and has led to the two following equations (16 a+b) which are valid for two different and non overlapping regions of excitation energy.

$$\text{(a)}\quad N = -33.395 + 8.295\ \varepsilon_b + (0.263 - 0.0613\ \varepsilon_b)(4\ Z_F - A_F) \qquad (16)$$

χ^2 = 11.9 per degree of freedom (20 data points, 4 degrees of freedom)

for $0.5 \leq \varepsilon_b \leq 3.5$ MeV

and

(b) $N = -6.935 - 1.410\varepsilon_b + (0.0604 + 0.0111\ \varepsilon_b)(4\ Z_F - A_F)$

$\chi^2 = 4.9$ per degree of freedom (17 data points, 4 degrees of freedom)

for $12.5 \leqslant \varepsilon_b \leqslant 32.5$ MeV

No function could be defined for the intermediate energy range of $3.5 \leqslant \varepsilon_b \leqslant 12.5$ MeV due to lack of data. Information on the particle spectrum is given for the three reactions $^{233}U(n_{th},f)$, $^{235}U(n_{th},f)$ and ^{252}Cf(sp.f.). The particle spectrum is found very similar in the three cases with the following nuclides in decreasing order of intensity: ^{4}He, ^{3}H, ^{6}He, ^{1}H, ^{2}H.

Single Fission Yield Systematics and Estimation Methods

The principles discussed above with a more or less direct feed-back to experimental data have been used by several authors to produce tables of predicted yields or to recommend recipes to calculate unmeasured fission yields.

The most important studies produced after 1969 and generally accompanied by compilations of experimental yields will be enumerated in the following and their particular characteristics will be presented.

A.C. Wahl [17] is presenting an evaluated fission yield compilation of $^{235}U(n_{th},f)$ and a recipe to calculate 'normal fission yields' discussed above (see eq. (7)). Deviation from the 'normal yields' are recognized and discussed to be a consequence of odd-even and shell effects.

S. Amiel and H. Feldstein give a yield compilation for the most abundant mass chains (A=83-97 and 130-145) for $^{235}U(n_{th},f)$[23] and for $^{233}U(n_{th},f)$ (A=82,84-94 and 131-143) as well as for $^{235}U(n_f,f)$(7 mass chains)[24]. An (incomplete) set of recommended ('corrected') yields is included. Recommended yields have been obtained by the evaluation of experimental data or, in their absence, may be obtained using a recipe developed in the papers and which consists in multiplying the predicted 'normal yields' |17| (see above) with a factor $(1 \pm X)$ for proton pairing as determined in |23,24|. ($X=0.25$ for $^{235}U(n_{th},f)$ [23] and $X=0.22\pm0.07$ for both $^{235}U(n_{th},f)$ and $^{233}U(n_{th},f)$ and $X=0.08\pm0.05$ for $^{235}U(n_f,f)$ [24]).

K. Wolfsberg |25| is presenting estimated values of fractional yields and a compilation of experimental data for the following reactions: thermal neutron induced fission of ^{233}U, ^{235}U and ^{239}Pu ; fission spectrum neutron induced fission of ^{235}U, ^{238}U, and ^{239}Pu and 14 MeV neutron induced fission of ^{235}U,^{238}U, and^{239}Pu. The calculations are based on a value of σ=0.56 with error margins between ±0.06 (high yield regions) and 0.12 (low yield regions). ΔZ for all fission reactions except Pu-239 is assumed ±0.45±0.1 (high yield asymmetric region) ±0.45±0.2 (low yield asymmetric region) and 0.0±0.2 (region of symmetry). For ^{239}Pu fission a 'Zp function similar to that given by Reisdorf et al. ([73]) for low-energy fission of plutonium nuclides' was used. The numbers of prompt neutrons evaporated were obtained as described above. Independent yields calculated from the Gaussian according to eq. (5), (6) and (6a) were multiplied or divided by the following odd-even factors: $\overline{EOZ}$=1.25±0.10, for thermal neutron and fission spectrum induced fission and $\overline{EOZ}$=1.15±0.15 for 14 MeV neutron induced fission. In the case of plutonium fission the three factors 1.00±0.20, 1.00±0.15 and 1.00±0.15 were used for the three cases. The Gaussians are renormalized to 1 after applying the odd-even factors. The maximum errors are propagated resulting in estimated fractional yields with carefully evaluated limits of uncertainty.

Yamamoto and Sugiyama [38]estimate the fractional independent yields in the thermal neutron induced fission of ^{232}U and ^{238}Pu and in the 2 MeV neutron induced fission of ^{234}U, ^{236}U, ^{240}Pu, and ^{242}Pu based on the ΔZ-values obtained from K-X-ray measurements [73] for the similar nuclides ^{233}U, ^{235}U and ^{239}Pu. The width parameter of the Gaussian charge dispersion curve is selected σ=0.56±0.06. A proton pairing factor (1±X) and a subsequent renormalization are applied.

The values of X used are

X = 0.15 (^{232}U), X = 0.20 ($^{234,236}U$) and X = 0.10 ($^{238,240,242}Pu$).

Correction for prompt neutron emission is made according to the measurements of Apalin |41|, subject to doubt as discussed before.

Meek and Rider [20-22] provide the most complete source of information on fission yield data in the form of a compilation of fission product yields. Chain yield data as well as independent yield data of the following

fission processes are covered: thermal neutron induced fission of ^{233}U, ^{235}U, ^{239}Pu, ^{241}Pu, fast neutron induced fission of ^{232}Th, ^{233}U, ^{235}U, ^{236}U, ^{238}U, ^{237}Np, ^{239}Pu, ^{240}Pu, ^{241}Pu, ^{242}Pu, 14 MeV neutron induced fission of ^{232}Th, ^{233}U, ^{235}U, ^{238}U, ^{239}Pu and the spontaneous fission of ^{252}Cf. The latest issue [22] contains approximately 18 000 entries from 1030 references. The data are available in report form and on magnetic tape in different formats.

The report is composed of two parts mainly: (a) Original Reference Data and (b) Averaged and Evaluated Data. The values given in part (b) are also based on experimental results whereever such data are available. The systematics are used only when experimental values are missing. However, in more rare fission reactions and in the low yield regions of all fission reactions the lack of experimental data is still prevailing.

Concerning the experimental data compiled, it is obvious that a bulk of 18 000 values is difficult to handle and the weading out of errors as discussed above under data requirements is an immense task in which the scientific community should be urged to help the compilers.

The systematical approach used to predict yields ('calculated yields') is based on the principles discussed above. In the earlier compilation [21] Zp-values were obtained according to the principle of a constant ΔZ (0.45 in the region of asymmetry and 0.0 in the region of symmetry) for all fission reactions [74]. The values of $\nu(A)$ used for the different fission reactions are not stated.

In the later compilation [22] the method of Nethaway [48] was adopted to find the Zp-values necessary for the calculation of fractional yields according to equation (5). The width parameter of this equation was always kept constant at $\sigma=0.56\pm0.06$ for all fission reactions.

Odd-even corrections are carried out in [22] according to [51] as described and discussed above. The corrected yield values are renormalized so that the sum of the fractional independent yields along a decay chain equals 1. A complete set of recommended absolute independent yields is produced for each fission reaction using experimental data where available and calculated yields where necessary. Small conservation corrections are applied to all data forcing the sum of all chain yields in the light and heavy mass peaks to equal 100% each and enforcing mass and charge balance of compound nucleus and fission products including neutrons.

An attribution of yields to single isomeric states with known sum yields (experimental or calculated) is done according to the procedure discussed in chapter Isomeric Yield Ratios when the spins of the single isomeric states are known. For isomers with unknown spins a 50 to 50 ratio is assigned.

E.A.C. Crouch A compilation and evaluation of fission yields similar to the one of Meek and Riders is in preparation by E.A.C. Crouch [76] as announced in [75]. This compilation was not available to the author.

Prediction Methods Based on Theory

Introductory Remarks

The plain fact that low energy nuclear fission proceeds in an asymmetric way was a long standing puzzle to theoreticians.

It is therefore not surprising that predictions of fission yields from theory have been formulated only lately.

The author believes, however, that recently theories, due mainly to the possibility to describe shell effects as a function of deformation [77] in the compound nucleus and in fission fragments have attained a state of accuracy for practical use.

Therefore, the main theoretical approaches leading to predictions of yields will be enumerated in the following. The basic physical principles underlying them will be briefly discussed, the predictions derived concerning yields will be presented and attempts will be made to test the accuracy of the predicted values.

Such a test is, however, not always easy. It is possible only in cases where experimental data already exist. The optimum test of prediction methods is probably a comparison with experimental data that have been measured after the theory has been formulated. This situation is not frequently encountered.

A particular problem exists in the case of charge distribution even of well studied reactions like $^{235}U(n_{th},f)$ as the bulk of data is very complex as pointed out in section Data Requirements. In addition to the high number of values which have to be compared many yields have been measured with contradictory results. Error assignments have been based on different criteria etc. Therefore an evaluation of the experimental data is required.

In the present case the agreement of predictions from theories with experiment shall be discussed in terms of their agreement with the two systematics believed most reliable

(a) the systematics based on the 'normal yield' concept in particular equation (7) and

(b) the most recent results from the global fitting procedure, in particular the EOZ-model (straight line NOT sine function in Fig. 1 of [31] and the results given in Table III of [31]) with its most important deviation from the 'normal yield' systematics: The fine structure at the 50 proton shell.

The existence of odd-even effects is introducing a certain inaccuracy into the comparison, since the theoretical prediction methods referred do not consider odd-even factors.

The models to be discussed are using quite different approaches. They are also quite different in the theoretical involvement and in the number of parameters to be fitted.

In the following, four groups of theories will be discussed

(a) a single particle approach at the scission point (Greiner et al., Nörenberg);

(b) a more phenomenological model describing a random distribution of the neutrons exceeding the β-stability of both fragments;

(c) a statistical approach describing the probability of formation of a fission product as a function of the number of quantum states available to this fragment;

(d) an approach combining aspects of (a) and (c).

The discussion of the models will essentially be limited to the resulting predictions on fission yields and their comparison with the experiment.

The Single Particle Approach

Two theories will be discussed (1) the ATCS model of Greiner and coworkers and (2) the molecular model of fission by Nörenberg. Both models are con-

sidering fission to be a nearly adiabatic process as illustrated in Fig. 1a.

The ATCS-model (Asymmetric Two-Center Shell model) [78] is considering the protons and neutrons in two separate single particle potentials representing two deformed fragments not necessarily of the same size and connected by a neck.

The model has been used [79] to calculate mass distributions for the fission of ^{226}Ra, ^{236}U and ^{258}Fm as a function of nuclear temperatures and elongation parameter without any free parameter. Since the calculations involving a three dimensional minimization are very time consuming only 5 mass pairs could be calculated for each mass curve (temperature and elongation). 'Semiquantitative agreement' with experiment is found in all three cases. In particular, the double humped (^{236}U), triple humped (^{226}Ra), and single peaked (^{258}Fm) shape found experimentally is reproduced (Fig. 12).

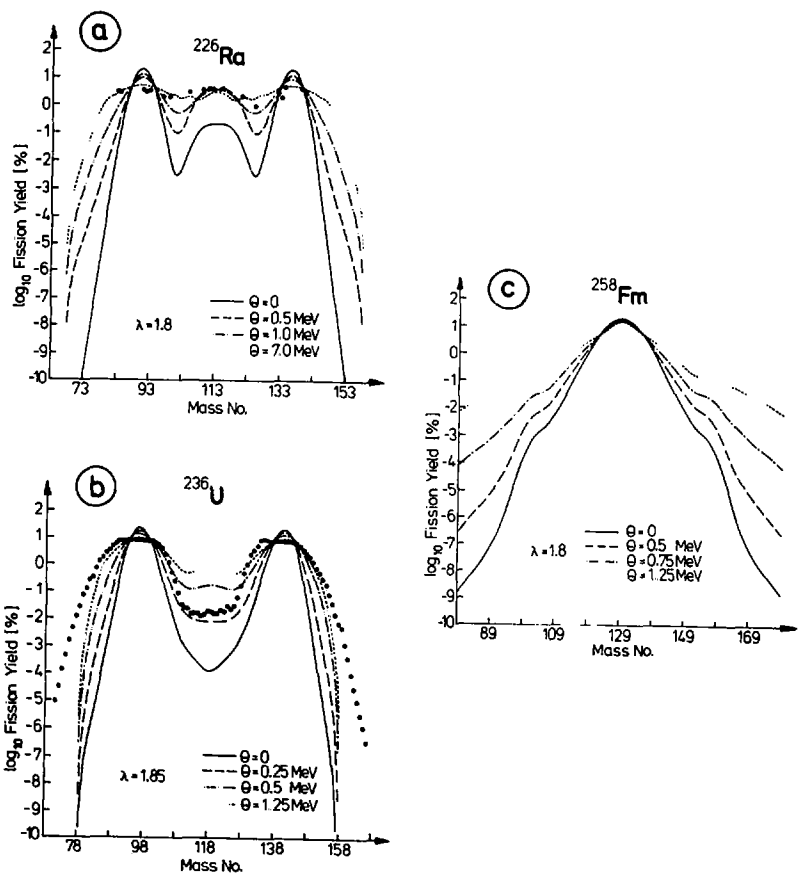

Fig. 12. Mass yield curves calculated according to the ATCS-Model for varying nuclear temperatures indicated below in the order of full, dashed, dash-dotted, and dotted lines and compared (in cases a and b) with experimental results (larger points). a) ^{226}Ra (0, 0.5, 1, 7 MeV); b) ^{236}U (0, 0.25, 0.5, 1.25 MeV); c) ^{258}Fm (0, 0.5, 0.75, 1.25 MeV).

The ratio of the asymmetric to symmetric fission is reproduced fairly well at a nuclear temperature of 0.5 MeV (^{236}U) and 1 MeV (^{226}Ra). The model appears suitable for predictions of mass yields in fission reactions difficult to study experimentally.

The same model has been applied for the calculation of charge distribution [80] in the spontaneous fission of ^{236}U, without refitting a single parameter. Only two mass pairs, probably due to lack of computer time, could be calculated (A_H/A_L = 141/95 and 142/94). The calculated charge dispersion curves show a Gaussian form with σ=0.60±0.05 and a charge displacement* ΔZ=0 (141/95) and $\Delta Z=\mp 0.16$ (142/94). This is somewhat less accurate than could be expected for a prediction derived from the systematics discussed above.

Nörenberg in his molecular model of fission [81,82] is emphasizing the treatment of charge distribution rather than mass distribution.

A single particle description in the configuration of two deformed fragments is used taking into account a nuclear interaction between the two partly deformed fragments.

The distance (d) between the centers of mass of both fragments at scission is an important parameter controling the size of the interaction between the two fragments.

The prediction of a charge displacement curve for various values of d is shown in Fig. 13. The strong fine structure around fragment mass 132 seen for the larger values of d is due to the neighbourhood of the double shell closure in $^{132}_{50}$ Sn. This structure disappears for d=12.5 fm due to the interaction of the complementary fragment. The choice of the mean charge distribution (broken line in Fig. 13) and the corresponding value of d (∿15 fm) is based on measurements of the kinetic energies of fission fragments but may have been influenced by an exceptionally high

---

* The comparison with experimental data in [80] is not quite correct since predictions for (preneutron emission) fragments are compared to experimental measurements of (post neutron emission) products. Also the two fission processes compared are different ^{236}U(sp.f) and ^{236}U(n_{th},f).

experimental value of ΔZ(=-1.6) for chain 132 [83, 84] which was subsequently shown to be incorrect [11,12,85].

In a more recent paper [82] on charge distribution in the fission of ^{240}Pu and ^{242}Pu the maximum of a 'scission barrier' obtained from a minimization of the total energy with respect to the deformations has been used to define d. A value of d=13.8 fm has been obtained and the fine structure has almost disappeared from the charge displacement (ΔZ) curve for this reaction, as can be seen from Fig. 14. The agreement of the predic-

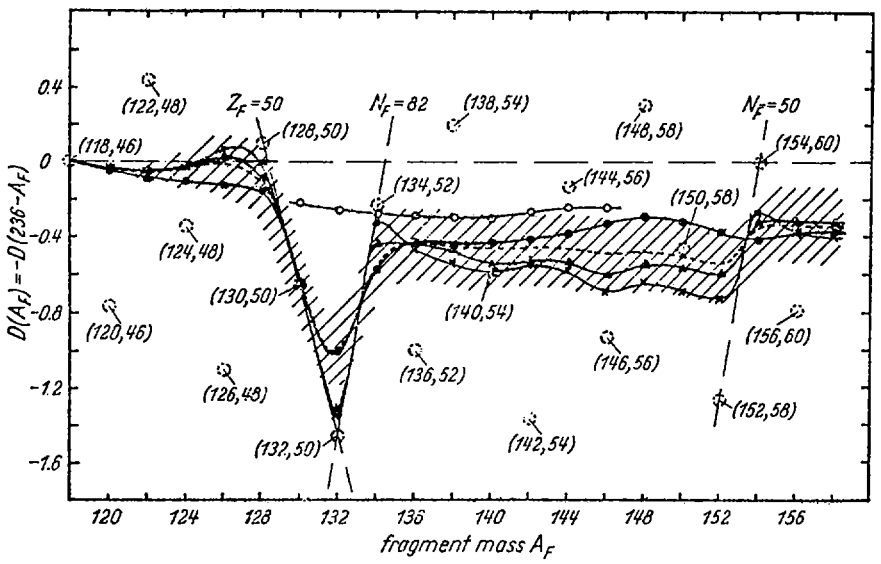

Fig. 13. Calculated charge displacement (ΔZ) curve for $^{235}U(n_{th},f)$ assuming various fragment distances (d=12.5 fm (o); 14.0 fm (•); 15.5 fm (Δ) and 17.0 fm (x)). (From /81/).

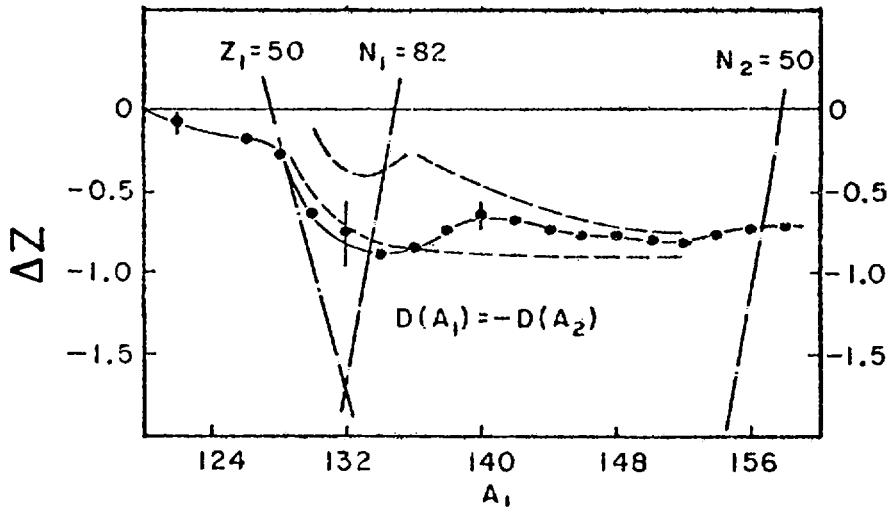

Fig. 14. Calculated charge displacement (ΔZ) curve for $^{239}Pu(n_{th},f)$ assuming a fragment distance d=13.8 fm. The range of experimental data has been indicated by the broken lines. (From /82/).

tion with the experimental data as indicated in the Figure is satisfactory. The prediction $\Delta Z \approx \pm 0.75$ as read from the Figure is, however, consistently higher than the best evaluated value $\Delta Z = \pm 0.57 \pm 0.03$ for $^{239}Pu(n_{th},f)$ as obtained from Table III in [31].

Random Distribution of Excess Neutrons

Iyer and Ganguly[87] propose a model - resembling a bit the ECD-rule - in which for each possible fragment combination in Z the β stable fragment mass is calculated, using a mass formula [86].

Since the compound nucleus possesses more neutrons than both β-stable fragments together, the remaining neutrons are distributed in a random way between the two fragments. This calculation results in a mass distribution of isotopic yield curves which can be converted into a charge distribution of isobaric chains and be compared to radiochemical results.

Fig. 15 shows a plot of $\Delta Z (= Zp - Z_{UCD})$ obtained from the model compared

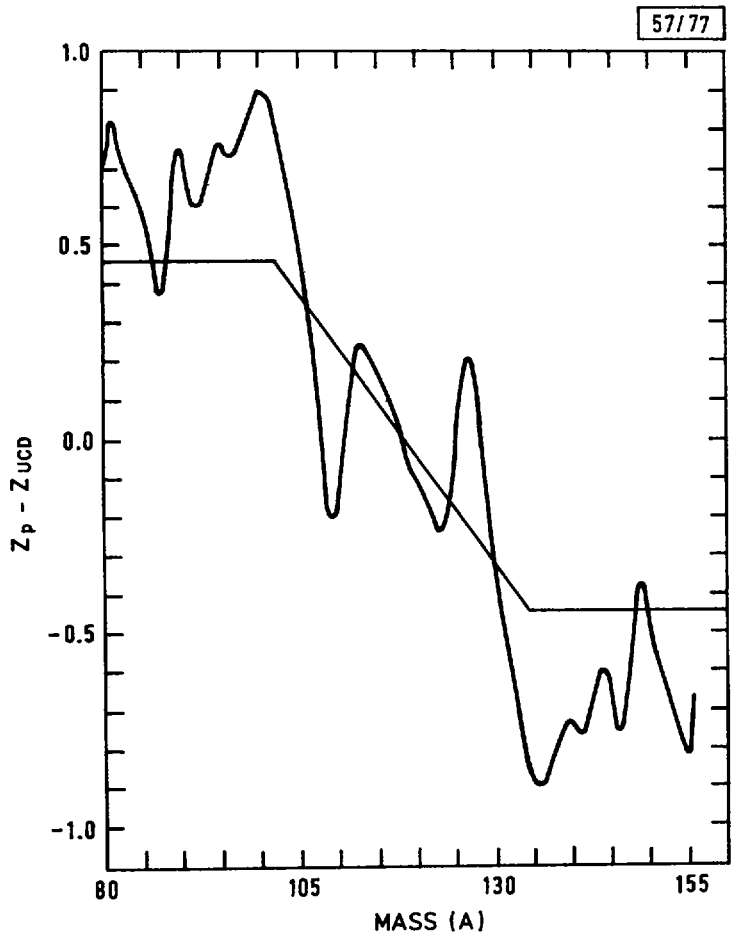

Fig. 15. Charge displacement (ΔZ) curve for $^{235}U(n_{th},f)$ as calculated in /87/ (curved line) compared to the "normal yield" concept (straight lines). (After /87/).

to the radiochemically developed prescription (Eq. (7)). The strong fluctuations in the curve are due to the systematics of β-stability and may be correlated to an odd-even effect. The average value of $|\Delta Z|$ seems definitely too large in the region of asymmetry compared with the radiochemical result of $\Delta Z=0.45$ (or 0.51) fairly well established in that region. In the region of symmetry the prediction derived from radiochemical results is much less reliable and the most recent analysis (see Fig. 1 of [31]) is indeed indicating a fine-structure of the size shown in Fig. 15 at the masses A=109 and 127.

A very narrow width of the Gaussian charge distribution of c=0.45 ($\sigma \approx \sqrt{\frac{c}{2} + \frac{1}{12}} = 0.38$) agrees also with findings discussed in [31].

The model has recently been applied to the reactions $^{235}U(n_{2MeV},f)$ and $^{235}U(n_{14MeV},f)$ [100].

The Statistical Model

The statistical model as initially developed by Fong [88] describes the probability of formation of a fission product (its 'yield') as a function of the number of quantum states available to the fragment pair at the moment of scission. The scission configuration is approximated by two deformed fragments in contact. The number of quantum states available is related directly to the density of excitation levels of a nucleus and this is increasing exponentially with its excitation energy.

The (maximum) total excitation energy (G) of the fragments is given by the total energy release (F) of the fission reaction (resulting from the mass balance of the compound nucleus and the primary fission fragments in their ground states) minus the coulombic potential (C) and the deformation energy (D) of the fragments in the scission configuration.

$$G = F - C - D \quad * \qquad (17)$$

The terms in the equation (17) are functions of the mass numbers, charge numbers and the coulombic energy. Their knowledge should enable us to derive the mass distribution, charge distribution, and the kinetic

* G is actually the sum of the energy available for internal excitation (E) and center of gravity motion (k) of the fragments at the scission moment. k is neglected in Fong's approach but has a final value in studies to be discussed later.

energy distribution in nuclear fission.

At the early time of the work there was no sufficiently accurate mass formula extending to the short-lived primary fission fragments, nor an appropriate level density formula. Coulombic and deformation energies could be calculated only in the liquid drop model neglecting shell effects. Corrections were applied to the mass formula, especially, based on experimental β-decay energies and mass spectroscopically determined masses of neighbouring stable isotopes. Two parameters of the level density formula have been fitted to experimental data of fast neutron capture cross sections.

The result of the calculation is the mass yield curve shown in Fig. 16 which is in good agreement with the experimental values shown, and in somewhat less good agreement with later experimental data showing more fine-structure [26]. However, this fine-structure is at least partly due to the structures in prompt neutron emission, see Fig. 7 in this paper, that Fong could not correct adequately for as they were not known.

However, application of the model to $^{239}Pu(n_{th},f)$ gave a four humped mass distribution [89].

A number of older modifications of the statistical model are discussed in [90]. A detailed study of Ignatyuk |91| should also be mentioned.

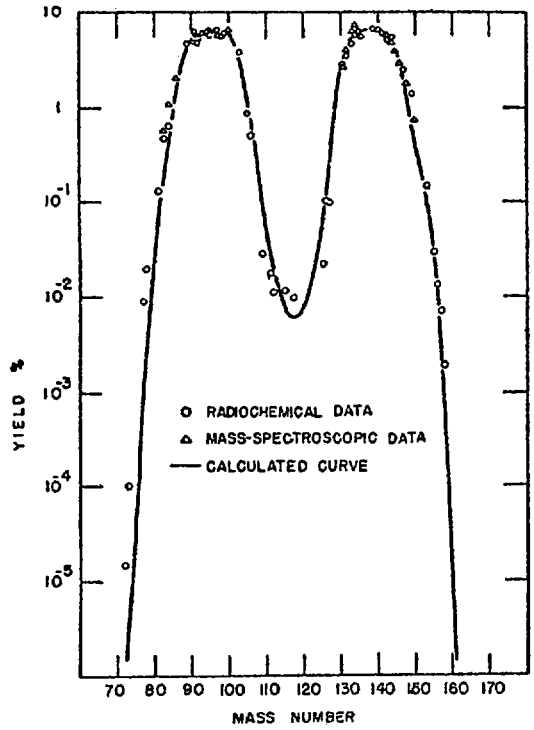

Fig. 16. Mass distribution curve of $^{235}U(n_{th},f)$ calculated by Fong compared with experimental data (from /88/).

More recently Okamoto, Nakahara and Nishi [92] have shown for the fission of ^{241}Am with thermal neutrons that poor agreement with experimental values is found for charge distribution, mass yield and total energy release in spite of the use of shell corrections expressed as a function of deformation and applied to mass and level density formulae.

Yamamoto and Sugiyama |93| use a distance (d) between the two fragments in the scission configuration as a free parameter to be fitted as a function of A to a known mass yield curve. The results for a fixed d=3 fm (dotted curve) are shown in Fig. 17 and may be compared with the experimental data by Schmitt et al. [94] and the fitted curve (solid line through the points) calculated with the values of d shown in the inset. It is obvious that a small change in d is affecting the yields very much.

However, the values of d of one fissioning nuclide show a similar behavior at different masses, as shown in Fig. 18. Interpolation or extrapolation of the values of d (A) to neighboring nuclides have been used to calculate the fragment mass yield values predicted for the fission of ^{232}U and ^{238}Pu by thermal neutrons and the fission of ^{234}U, ^{236}U, ^{240}Pu and ^{242}Pu by 2 MeV neutrons [38]. The fragment yields were subsequently converted to product yields using the values of prompt neutron emission from [41] subject to doubt (see above). For the case of ^{240}Pu(n_f,f)

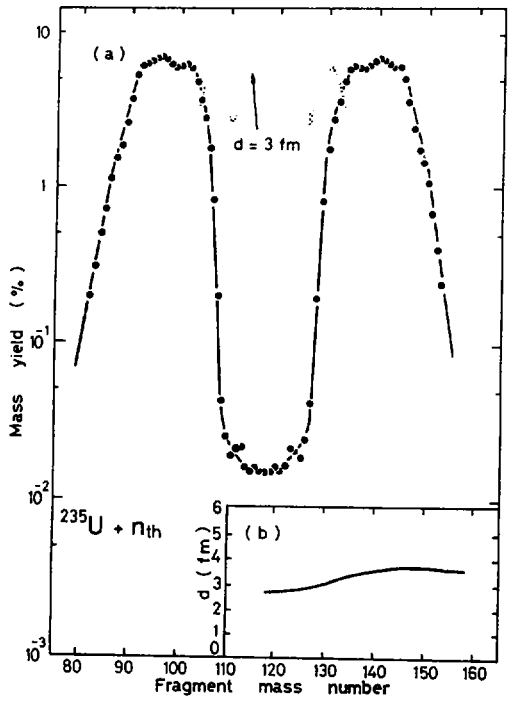

Fig. 17. Mass yield curves for ^{235}U(n_{th},f). Dotted curve: calculated with a fixed d=3fm. Solid curve: calculated using the values of d as shown in the inset (b). Full points: Experimental results /94/.(From /93/).

very recently experimental values have become available [36,37]. They are compared with this and another prediction in Fig. 6.

The agreement found is surprisingly good. It may still be improved if the $\nu(A')$ values from [41] used in the conversion of fragment yields to product yields are replaced by better values. Possibly, however, ^{240}Pu is a particularly well suited case since the values of d (Fig. 18) of ^{239}Pu and ^{241}Pu used for the interpolation are particularly similar.

A modified statistical model has been proposed by Facchini and coworkers [95-97]. The assumption of a statistical distribution of energy between kinetic (collective) and intrinsic states - leading to a negligible kinetic energy in Fong's model - has been dropped on the basis of new experimental results on ternary fission indicating the the fragments move at the scission point with a kinetic energy of the order of 10-20 MeV [98]. The binding energies as a function of deformation have been calculated according to the results of [99]. It has, however, turned out that spherical scission fragment shapes with a scission distance of 8 fm gave the best results.

Typical fractional independent yield values (blank circles) are given in Fig. 19 and may compared with experimental recommended yields (black triangles) from [23]. Since predicted yields are referring to fragments prior to prompt neutron emission they have been converted to product yields by a simple interpolation method for the purpose of comparison.

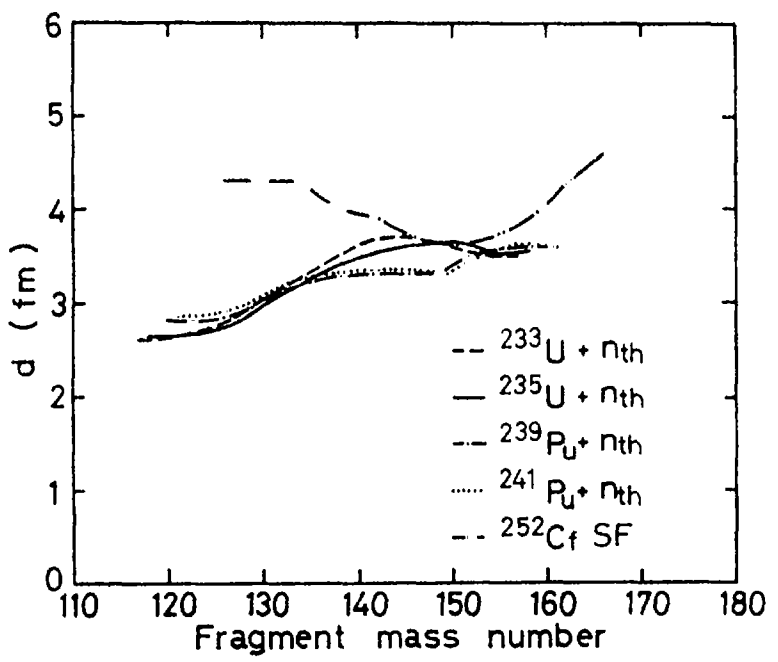

Fig. 18.
Values of the scission point distance d as a function of heavy fragment mass for various fissioning systems (from /93/).

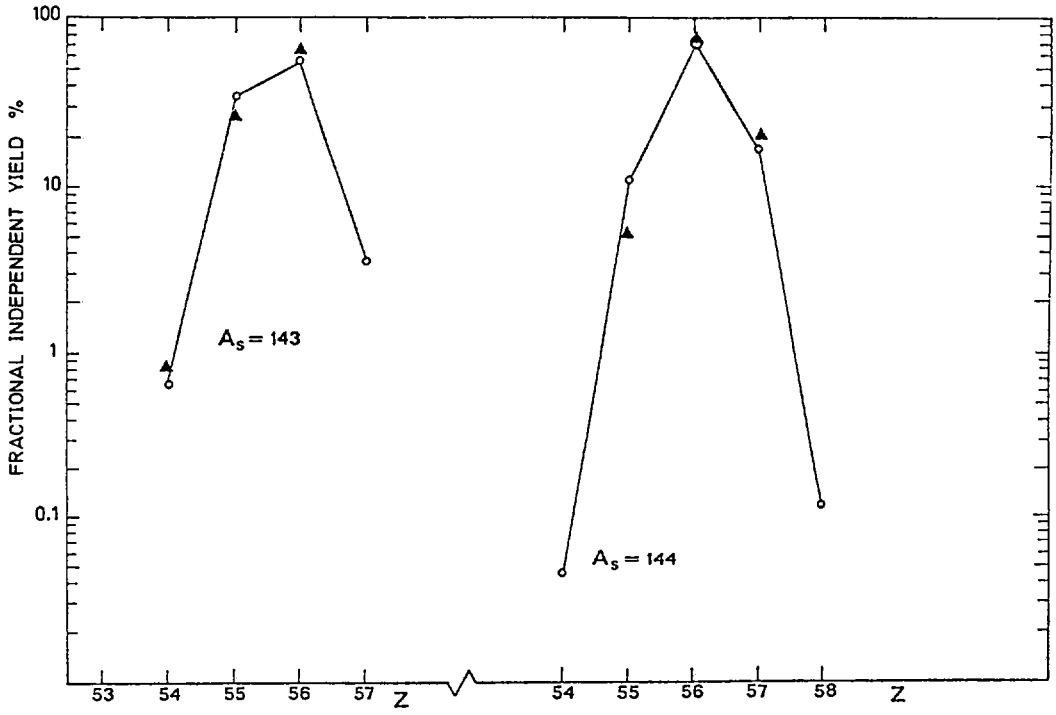

Fig. 19. Fractional independent yields in mass chains 143 and 144. Open circles: calculated. Closed triangles: experimental values /23/. (From /96/).

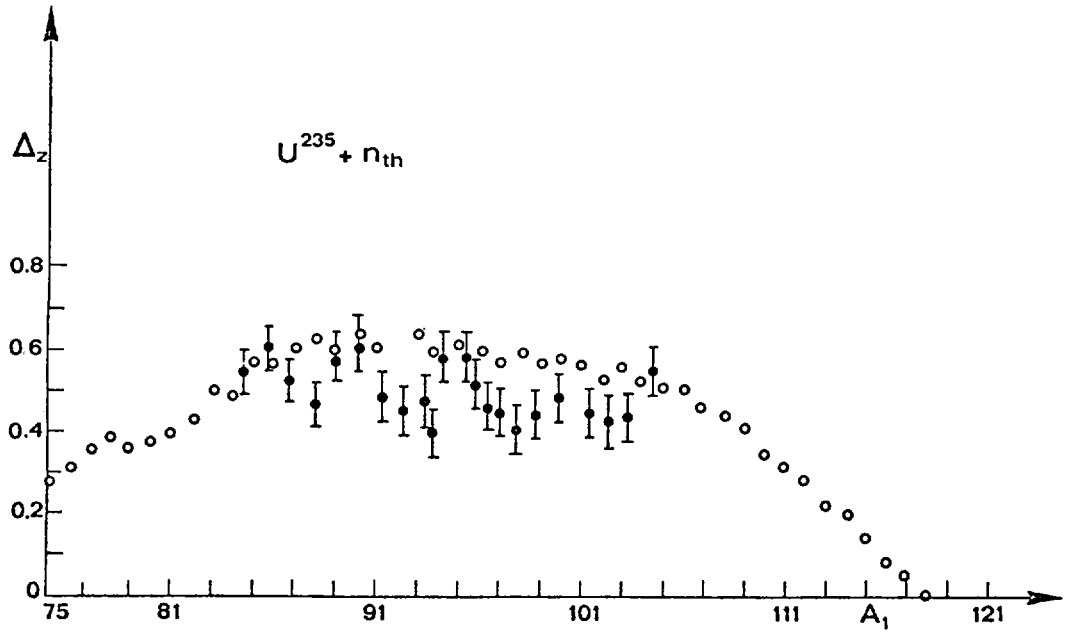

Fig. 20. Charge displacement (ΔZ) curve. Open circles: prediction. Closed circles: experimental results /19,23/. (From /96/).

The predicted ΔZ-values are given in Fig. 20 (blank circles) and may be compared to experimental values [23] (full circles) or to the rules (a) and (b) developed from systematics and discussed above.

The agreement is quite good except (possibly) around A'=107/129 where the fine-structure discussed in rule (b) is not found. Because of the generally good agreement between predictions and experiment it would be desirable that these calculations be extended to other fission reactions.

Scission Point Model based on Deformed Shell Effects

A recent model of Wilkins, Steinberg and Chasman [56] is in a way bridging the statistical (nonadiabetic) and single particle (adiabetic) approaches. Like in the model of Facchini no complete equilibrium between collective and single particle states is assumed as opposed to the pure statistical model. However, as opposed to adiabetic models, some coupling of collective and single particle states is assumed and is described by two different nuclear temperatures (τ_{int}=0.75 MeV and T_{coll}=1.0 MeV).

The probability of formation of any fission fragment pair is calculated from the potential energy surface according to:

$$P(N,Z,\tau,d) = \int_{\beta_1=0}^{\beta_{max}} \int_{\beta_2=0}^{\beta_{max}} \exp[-V(N,Z,\beta,\tau,d)/T_{coll}]\, d\beta_1\, d\beta_2 \qquad (18)$$

- N Neutron number
- Z Proton number
- τ intrinsic single particle excitation
- d distance between the tips of the spheroids in the scission configuration $\equiv$1.4 fm
- β_1,β_2 deformation parameters for fragments 1 and 2
- V total potential energy

Equation (18) allows to calculate mass- (P(N+Z)) and charge- (P(N,Z)) distribution as well as the distributions in kinetic energy and internal excitation energy resulting in predictions on the number of prompt neutrons emitted from single fragments.

The potential energy $V(N,Z,\beta,\tau,d)$ is calculated as a function of the neutron and proton numbers of the complementary fragments (N_1, N_2, Z_1, Z_2) and their deformation parameters (β_1,β_2). Liquid drop terms are corrected for shell- and pairing-effects. Coulombic and some nuclear potential terms describe the interaction between two coaxial spheroids whose tips are separated by the distance (d=1.4 fm).

The results of interest for the present topic are mass- and charge yield predictions as well as predicted values of prompt neutron emission. They are shown in Figs. 21 to 24 .

Fig. 21 shows that the trends in mass yield distribution are generally well reproduced: 'From a narrow, symmetric mass distribution in the region of Po the mass distribution becomes triple peaked at Ra. It rapidly changes to an asymmetric distribution for nuclides from Th - Cf before once more favoring symmetry at ^{258}Fm. The nearly constant position of the heavy mass group .... (is) reproduced'. In this respect the results are about equivalent to those of the ATCS-model, see above.

The quantitative agreement with experimental results is, however, by far not sufficient to allow reasonable predictions on mass yields as appears from a comparison in Fig. 22 for the fission of ^{235}U by thermal neutrons.

It must be stated that in the present work the parameters (d=1.4 fm, τ_{int}=0.75 MeV and T_{coll}=1.0 MeV) were kept constant throughout the treatment of very different fissioning systems and that fits may be improved by varying these parameters. A number of other possible improvements are discussed by the authors and, hopefully, will be tested.

The correlation between the calculated average deformation of the fragments in ^{252}Cf(sp,f) and the experimental number of prompt neutrons emitted attributed to be a consequence of this deformation, shown in Fig. 23, is very good and may turn out useful in estimating $\nu(A)$ if $\bar{\nu}$ is known.

A plot of $(Z-Z_{UCD})$ values as predicted (blank circles) and as obtained experimentally by Clerc et al. [11] (full points) is shown in Fig. 24 It may be stressed that $\bar{Z}$, the average nuclear charge in an isobaric chain, has been plotted (rather than Zp). A comparison with the complete set of data including radiochemical values should therefore be made using the data points and the sine function in Fig. 1 of [31]. This curve coincides almost with Clerc's data and stresses the accuracy of these data.

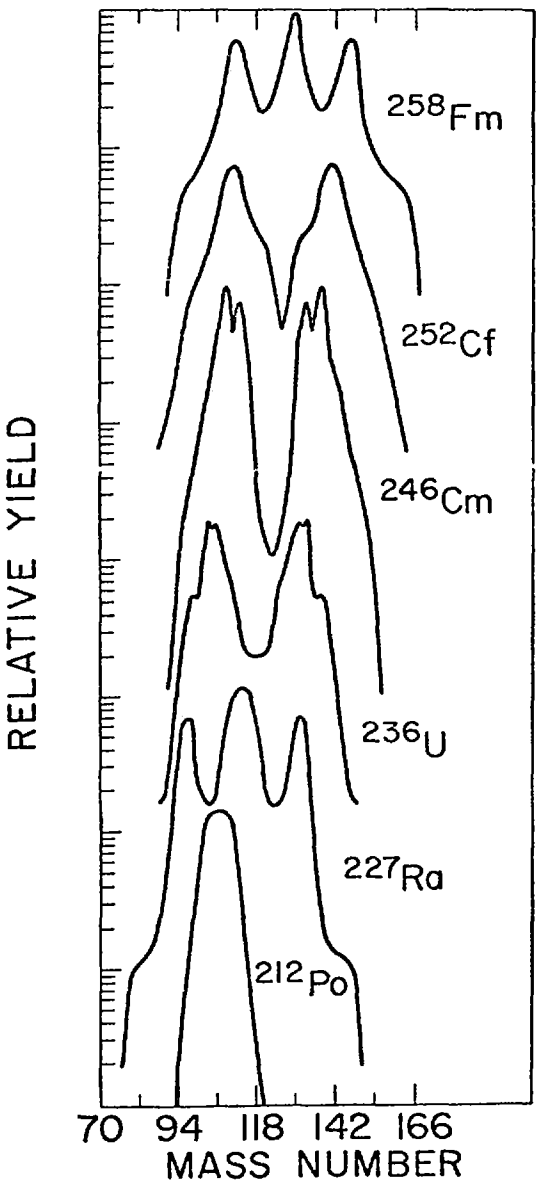

Fig. 21.
Calculated mass yield distributions for various fissioning systems (from /56/).

The fine structure in both curves due mainly to the odd-even proton effect coincide mainly in the region of asymmetric fission products.

The (absolute) predicted values are, however, systematically lower by about 0.2 Z units in the mass range $102 \geq A \geq 134$. An important deviation is found around A'=128/108 where Clerc's data confirm the fine structure seen in the radiochemical data [19,31].

It is interesting to note that this fine structure which is interpreted as an effect of the closed 50 proton shell is predicted only in Iyer and

Ganguly's model which is considering fission fragments in their ground states. If it could be confirmed further experimentally it could probably be interpreted as indicating that the effect of the 50 proton shell is underestimated possibly because the deformation of fragments around A=130 is overestimated.

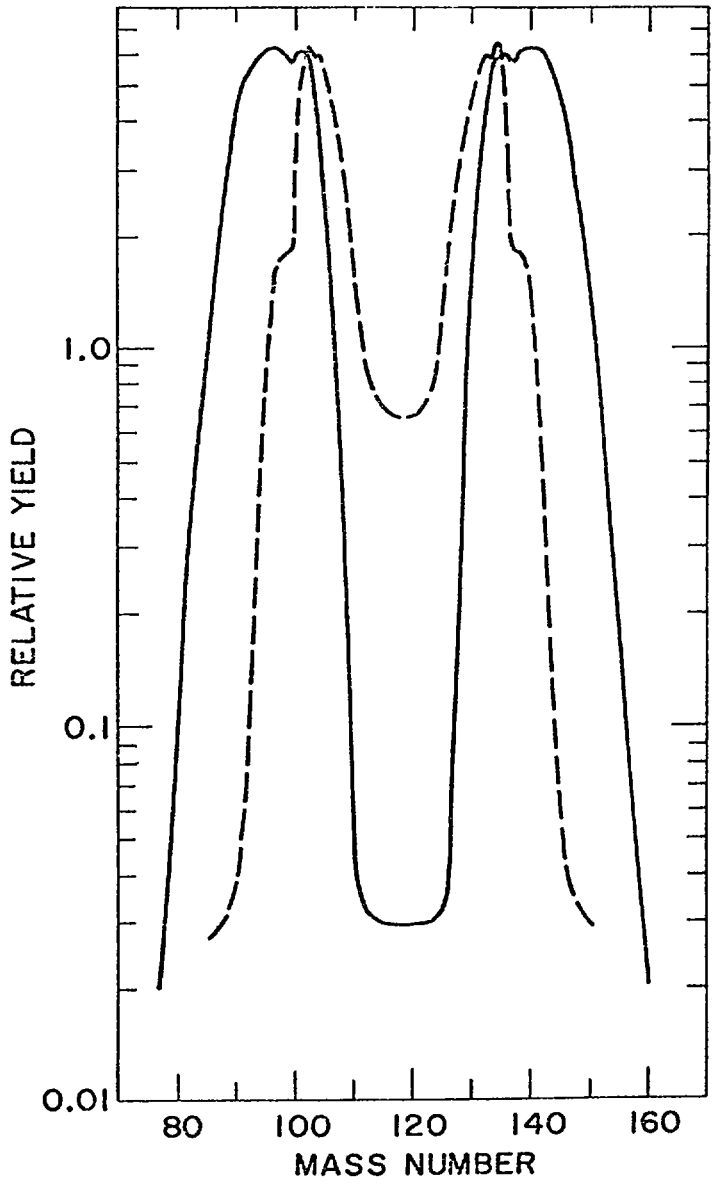

Fig. 22. Comparison of the calculated mass distribution for $^{235}U(n_{th},f)$ (dashed line) with the experimental data /73/ (solid line). (From /56/).

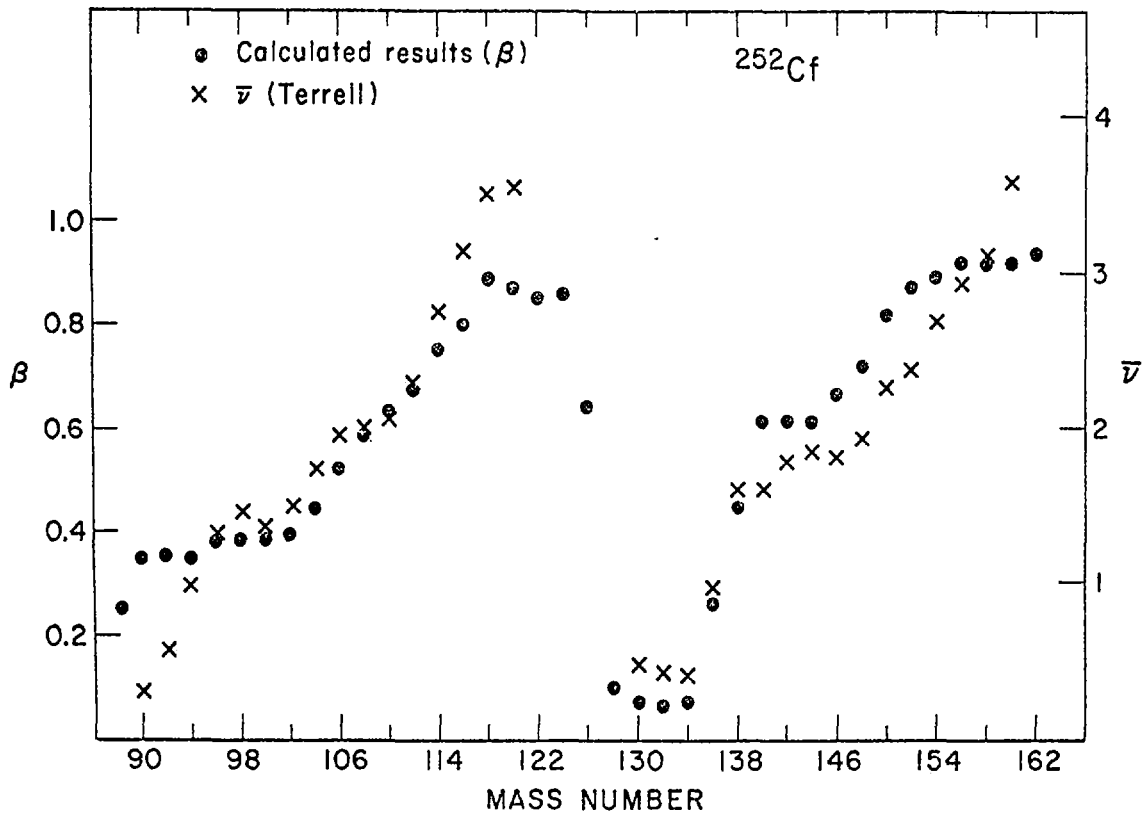

Fig. 23. Average deformation β of the fragments (full points) calculated for ^{252}Cf(sp,f) compared to the number of prompt neutrons emitted (ν(A)) in the spontaneous fission of ^{252}Cf /45/. (From /56/).

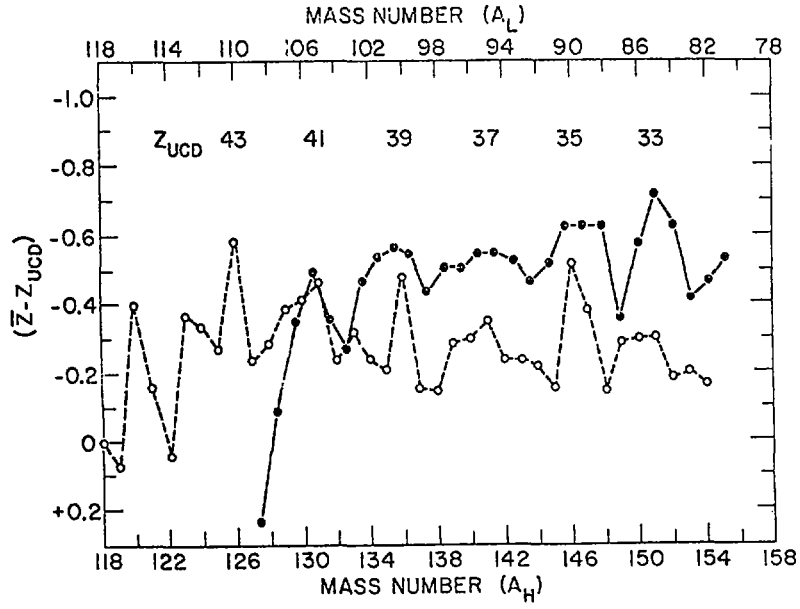

Fig. 24. The quantity $\bar{Z}-Z_{UCD}$ as a function of A for $^{235}U(n_{th},f)$ as calculated by Wilkins, Steinberg and Chasman (dashed line, open circles) compared to the experimental results of Clerc et al. /10/. (Solid line, full points) (From /56/).

Concluding Remarks

Concluding, a few notes will be made on predictions developed from systematics and theories.

Prediction of mass yields from both, systematics and theories for fissioning nuclides far away from the well studied processes are only semiquantitative.

Various methods are, however, available allowing to interpolate between different excitation energies or mass- and charge-numbers of fissioning nuclei. Voids in an otherwise well measured mass yield curve may also be closed by interpolation.

An interesting proposal is to obtain product mass yield curves by converting fragment mass distributions, which can be measured more easily, using simple assumptions on prompt neutron emission.

Concerning charge distributions, two main concepts are being pursued at present. They have been called 'Normal Yield' concept and 'Global Fitting Procedure' in the foregoing. Both are suffering from a lack of experimental data for the more exotic fission reactions and in the low yield regions of the better known fission processes. The systematics of odd-even factors which may have to be treated as a function of four parameters (mass- and charge-number and excitation energy of the fissioning nucleus as well as fragment proton (or neutron) number) is suffering from lack of data, especially in fission reactions with very high or very low pairing effects.

Some prediction methods of charge distribution from theories have attained a degree of precision comparable with that of predictions from systematics. Different approaches (adiabatic and nonadiabatic) seem to develop toward a common (semiadiabatic) approach.

The comparison of theoretical predictions and experiment in the present paper is somewhat indirect due to the lack of a generally accepted evaluated data set. The development of such data sets seems an important task for the future.

Acknowledgments

It is a pleasure to thank Professor A.C. Wahl (St. Louis) for his continuous interest in the present work and for many helpful discussions he had with the author during his stay at Mainz.

Dr. Rider provided the author with a draft of his most recent compilation and with detailed information on the mathematical treatment of data and predictions.

Helpful correspondence with him, Dr. J.L. Cook and Dr. U. Facchini is gratefully acknowledged.

The author also thanks to the following authors for sending reprints, preprints and other documents: Prof.Dr. A.H.W. Aten, Dr. J.L. Cook, Dr.England, Dr. D. Madland, Dr. A.R. del Musgrove, Dr. D.N. Sharma and Prof.Dr. K. Sugiyama.

The organizational support by Dr. G. Lammer (IAEA) is acknowledged.

This work was supported by the German Bundesministerium für Forschung und Technologie (BMFT).

References

1. A.R. deL. Musgrove, J.L. Cook, G.D. Trimble Proceedings of a Panel on Fission Product Nuclear Data (Bologna, 1973), IAEA, Vienna (1974) Vol. II, p. 163
2. R. Vandenbosch, J.R. Huizenga, Nuclear Fission, Academic Press N.Y., London (1973)
3. N. Bohr, J.A. Wheeler, Phys. Rev. 56, 426 (1939)
4. V.M. Strutinsky, Nucl. Phys. A122, 1 (1968)
5. A. Bohr, Proc. Intern. Conf. on Peaceful Uses Atomic Energy, Geneva 2, 151 (1955)
6. W.J. Swiatecki, S. Bjornholm, Physics Reports 4, 325 (1972)
7. J.P. Unik, J.E. Gindler, L.E. Glendenin, K.F. Flynn, A. Gorski, R.K. Sjoblom, Proceedings of the Third IAEA Symposium on the Physics and Chemistry of Fission, Rochester (1973) IAEA, Vienna (1974), Vol. II, p. 19
8. G. Siegert, J. Greiff, H. Wollnik, G. Fiedler, M. Asghar, G. Bailleul, J.P. Bocquet, J.P. Gautheron, H. Schrader, H. Ewald, P. Armbruster, Phys. Rev. Letters 34, 1034 (1975)
9. G. Siegert, J. Greif, H. Wollnik, R. Decker, G. Fiedler, W. Kaiser, B. Pfeiffer, Contribution DPG, OePG Tagung Kernphysik, Baden, Austria, AED-Conf-76-072-007
10. H.-G. Clerc, W. Lang, H. Wohlfahrt, K.-H. Schmidt, H. Schrader, K.E. Pferdekämper, R. Jungmann, Z. Phys. A274, 203 (1975)
11. H.-G. Clerc, K.H. Schmidt, H. Wohlfarth, W. Lang, H. Schrader, K.E. Pferdekämper, R. Jungmann, M. Asghar, J.P. Bocquet, G. Siegert, Nucl. Phys. A247, 74 (1975)

12. H.O. Denschlag, W. Faubel, G. Paffrath, T. Tamai, K. Wolfsberg, J. Blachot, G. Siegert, ILL-Annex to the Annual Report (1975), p. 18
13. H. Braun, Z. Alfassi, H.O. Denschlag, W. Faubel, G. Fischbach, T. Izak-Biran, G. Paffrath, T. Tamai, H. Schrader, G. Siegert, ILL-Annex to the Annual Report (1976), p. 24 and H. Braun, H.O. Denschlag, W. Faubel, G. Fischbach, T. Izak-Biran, G. Paffrath, H. Schrader, G. Siegert, T. Tamai. Jahresbericht 1976, Institut für Kernchemie, Universität Mainz, p. 92
14. W. Faubel, H. Braun, H.O. Denschlag, T. Izak-Biran, J. Leuthner, H. Meixler, G. Paffrath, T. Tamai, H. Schrader, G. Siegert, ILL-Annex to the Annual Report (1976), p. 23 and Jahresbericht 1976, Institut für Kernchemie Universität Mainz, p. 96
15. G. Paffrath, H.O. Denschlag, W. Faubel, K. Wolfsberg, T. Tamai, J. Blachot, H. Schrader, G. Siegert, 173rd ACS National Meeting New Orleans, Louisiana (1977)
16. A.C. Wahl, R.L. Ferguson, D.R. Nethaway, D.E. Troutner, K. Wolfsberg, Phys. Rev. 126, 1112 (1962)
17. A.C. Wahl, A.E. Norris, R.A. Rouse, J.C. Williams in Proceedings of the 2nd Symposium on the Physics and Chemistry of Fission, IAEA Vienna (1969), p. 813
18. H.R. von Gunten, Actinides Review 1, 275 (1969)
19. H.O. Denschlag, Habilitationsschrift, Mainz (1971)
20. M.E. Meek, B.F. Rider, Report NEDO-12154, January 1972
21. M.E. Meek, B.F. Rider, Report NEDO-12154-1, January 1974
22. M.E. Meek, B.F. Rider, Report NEDO-12154-2, March 1977 (Draft)
23. S. Amiel, H. Feldstein in Proceedings of the Third IAEA Symposium on the Physics and Chemistry of Fission, Rochester (1973), IAEA, Vienna (1974), Vol. II, p. 65

24. S. Amiel, H. Feldstein, Phys. Rev. C11, 845 (1975)

25. K. Wolfsberg, Report LA-5553 MS

26. W.H. Walker in Proceedings of a Panel on Fission Product Nuclear Data Bologna (1973), IAEA, Vienna (1974) Vol. I, p. 285

27. J.G. Cuninghame, Proceedings of a Panel on Fission Product Nuclear Data Bologna (1973), IAEA, Vienna (1974), Vol. I, p. 353

28. J.G. Cuninghame, these proceedings, paper 10

29. D.G. Madland, T.R. England, Report LA-6595

30. E. Moll, H. Schrader, G. Siegert, M. Asghar, J.P. Bocquet, G. Bailleul, J.P. Gautheron, J. Greif, G.I. Crawford, C. Chauvin, H. Ewald, H. Wollnik, P. Armbruster, G. Fiebig, H. Lawin, K. Sistemich, Nucl. Instr. Methods 123, 615 (1975)

31. A.C. Wahl, Contribution to R.P. 11, these proceedings (INDC(NDS)-87)

32. L.A. Busing, H.A. Levy, Report ORNL-TM-271 (1962)

33. H.-G. Clerc, W. Lang, H. Wohlfarth, K.H. Schmidt, H. Schrader, Report IKDA 76/5, Technische Hochschule Darmstadt, Germany

34. J.L. Cook, E.K. Rose, G.D. Trimble, Austral. J.Phys. 29, 125 (1976)

35. J.L. Cook, E.K. Rose, Report AAEC/E 386, March 1976

36. L. Koch, Inst. für Transurane, Karlsruhe, Prog. Rep. 21, 98 (1976) referred in R.P. 10 of these proceedings

37. W.A. Myers, M.V. Kantelo, A.L. Prindle, D.R. Nethaway unpublished results (1977) referred in R.P. 10 of these proceedings

38. T. Yamamoto, K. Sugiyama, Report NETU-20, April 1977, Tokohu University, Sendai, Japan

39. J. Terrell, Proceedings of the IAEA Symposium on the Physics and Chemistry of Fission (Salzburg, 1965) IAEA, Vienna, 1965, Vo. II, p. 3

40. E.A.C. Crouch, Report AERE-R 7209 (1973) and Report AERE-R 7394 (1973)

41. V.F. Apalin, Yu.N. Gritsyuk, I.E. Kutikov, V.I. Lebedev, L.A. Mikaelyan, Nucl. Phys. 55, 249 (1964)

42. E.E. Maslin, A.L. Rodgers, W.G.F. Core, Phys. Rev. 164, 1520 (1967)

43. J.W. Boldeman, A.R. deL Musgrove, R.L. Walsh, Aust. J. Phys. 24, 821 (1971)

44. J.C.D. Milton, J.S. Fraser, Proceedings of the IAEA Symposium on the Physics and Chemistry of Fission (Salzburg 1965), IAEA, Vienna, 1965, Vol. II, p. 39

45. J. Terrell, Phys. Rev. 127, 880 (1962)

46. E. Cheifetz, Z. Fraenkel, Phys. Rev. Letters 21, 36 (1968)

47. K. Wolfsberg, Phys. Rev. 137, B 929 (1965)

48. D.R. Nethaway, Report UCRL-51640 and UCRL-51538

49. T. Izak-Biran, S. Amiel pers. communication 1976, T. Izak-Biran, Doctoral Thesis, Jerusalem (1976) (in Hebrew).

50. S. Amiel, H. Feldstein, T. Izak-Biran, Phys. Rev. C15, 2119 (1977)

51. D.G. Madland, T.R. England, Report LA-6430-MS

52. J.R. Nix in Ann. Rev. of Nucl. Science Vol. 22 [E. Segrè, Editor, Annual Reviews Inc., Palo Alto, California] (1972)

53. H.C. Britt, M. Bolsterli, J.R. Nix, J.L. Norton, Phys. Rev. C7, 801 (1973)

54. B.B. Back, Ole Hansen, H.L. Britt, J.D. Garrett, Phys. Rev. C9, 1924 (1974)

55. B.B. Back, H.C. Britt, Ole Hansen, B.Leroux, J.D. Garrett, Phys. Rev. C10, 1948 (1974)

56. B.D. Wilkins, E.P. Steinberg, R.R. Chasman, Phys. Rev. C14, 1832 (1976)

57. L. Yaffe, Symposium on the Physics and Chemistry of Fission IAEA, Vienna (1969) p. 701

58. J.K.P. Lee, G. Pilar, B.L. Tracy, L. Yaffe, J. Inorg. Nucl. Chem. 37, 2035 (1975)

59. J.R. Huizenga, R. Vandenbosch, Phys. Rev. 120, 1305 (1960)

60. H. Warhanek, R. Vandenbosch, J. Inorg. Nucl. Chem. 26, 669 (1964)

61. D.G.Sarantites, G.E. Gordon, C.D. Coryell, Phys. Rev. 138, B353 (1965)

62. C. Rudy, R. Vandenbosch, C.T. Ratcliffe, J. Inorg. Nucl. Chem. 30, 365 (1968)

63. W.D. Loveland, Y.S. Shum, Phys. Rev. C4, 2282 (1971)

64. M. Weis, H.O. Denschlag, Jahresbericht 1975, Institut für Kernchemie, Universität Mainz, p. 84

65. M. Weis, H.O. Denschlag, Jahresbericht 1976, Institut für Kernchemie, Universität Mainz

66. M.M. Fowler, A.C. Wahl, J. Inorg. Nucl. Chem. 36, 1201 (1974)

67. G. Paffrath, H.O. Denschlag, Jahresbericht 1975, Institut für Kernchemie, Universität Mainz, p. 90-94 and G. Paffrath, Dissertation, Mainz (1976)

68. W. Rudolph, Dissertation, Mainz (1976)

69. G. Bailleul, J.P. Bocquet, H. Schrader, M. Asghar, C. Chauvin, J.P. Gautheron, J.Greif, G. Siegert, Fission Information Meeting and Workshop ILL, Grenoble (1974) p. 106

70. G. Bailleul, J.P. Bocquet, H. Schrader, A. Stippler B. Pfeiffer, M. Asghar, C. Chauvin, J.P. Gautheron, J. Greif, G. Siegert, P. Armbruster, H. Ewald, Z. Phys. A273, 283 (1975)

71. A. Kerek, et.al Annual Report of the Research Institute for Physics, Stockholm, Sweden (1972), p. 72

72. D.G. Madland, L. Stewart, Report: LA-6783-MS, (ENDF-247) (1977)

73. W. Reisdorf, J.P. Unik, H.C. Griffin, L.E. Glendenin, Nucl. Phys. A177, 337 (1971)

74. K. Wolfsberg, G.P. Ford, B.R. Erdal, private communication to B.F. Rider, October 1973, The Z_p-values quoted are similar to but not identical with those quoted in Ref. 25

75. G. Lammer, Report INDC (NDS)-86/G+P Progress in Fission Product Nuclear Data No. 3 (1977)

76. E.A.C. Crouch, Atomic Data and Nuclear Data Tables 19, No. 5 (1977)

77. V.M. Strutinsky, Nucl. Phys. A95, 420 (1967) and ibid. A122, 1 (1968)

78. J. Maruhn, W. Greiner, Z. Phys. 251, 431 (1972)

79. J. Maruhn, W. Greiner, Phys. Rev. Letters 32, 548 (1974)

80. R.K. Gupta, W. Scheid, W. Greiner, Phys. Rev. Letters 35, 353 (1975)

81. W. Nörenberg, Z. f. Physik 197, 246 (1966)

82. W. Nörenberg, Phys. Rev. C5, 2020 (1972)

83. E. Konecny H. Opower, H. Gunther, H. Göbel, Proceedings of the IAEA Symposium on the Physics and Chemistry of Fission, Salzburg (1965), p. 461

84. E. Konecny, H. Gunther, H. Rösler, G. Siegert, H. Ewald, Z. Physik 231, 59 (1970)

85. R. Naeumann, H. Folger, H.O. Denschlag, J. Inorg. Nucl. Chem. 34, 1785 (1972)

86. H.B. Levy, Phys. Rev. 106, 1265 (1957)

87. M.R. Iyer, A.K. Ganguly , Phys. Rev. C3, 785 (1971)

88. P. Fong, Phys. Rev. 102, 434 (1956)

89. J.K. Perring, J.S. Story , Phys. Rev. 98, 1525 (1955)

90. J.E. Gindler, J.R. Huizenga, Nuclear Fission in L. Yaffe, Ed. Nuclear Chemistry, Academic Press, New York (1968) Vol. II

91. A.V. Ignatyuk, Sov. J. Nucl. Phys. 9, 208 translated into english from: Yad. Fiz 9, 357 (1969)

92. H. Okamoto , H. Nakahara, T. Nishi, J. Phys. Soc. Japan 34, 588 (1973)

93. T. Yamamoto , K. Sugiyama, J. Nucl. Science and Technology 11, 461 (1974)

94. H.W. Schmitt, J.H. Neiler, F.J. Walter, Phys. Rev. 141, 1146 (1966)

95. U. Facchini, E. Saetta-Menichella, J. Physics A, 7, 975 (1974)

96. U. Facchini, G. Sassi, Contribution to IAEA Consultants Meeting on the Use of Nuclear Theory in Neutron Nuclear Data Evaluation, Trieste, December 1975

97. U. Facchini, G. Sassi, J. Physics G, 3, 269 (1977)

98. F. Fossati, T. Pinelli, Nucl. Phys. A249, 185 (1975)

99. P.A. Seeger, W.M. Howard, Nucl. Phys. A238, 491 (1975) and private communication to the authors of Ref. 97

100. D.N. Sharma, M.R. Iyer, A.K. Ganguly, Phys. Rev. C14, 181 (1976)

101. A.H. Wapstra. N.B. Gove, Nuclear Data Tables A9,265(1971)

Review paper 12

STATUS OF DECAY DATA OF FISSION PRODUCTS

Jean BLACHOT

CENTRE d'ETUDES NUCLEAIRES de GRENOBLE
Département de Recherche Fondamentale
Laboratoire de Chimie Physique Nucléaire
85 X - 38041 GRENOBLE CEDEX - France -

Abstract

Fission products (F.P.) are neutron rich isotopes ranging from Zn to Tm. If we take into account the 700 F.P. nuclides of the French file*, we have

121	stable nuclides		
82	nuclides with	T-1/2 < 1 s	
195	"	"	1 s ≤ T-1/2 < 1 m
141	"	"	1 m ≤ T-1/2 < 1 h
62	"	"	1 h ≤ T-1/2 < 1 d
54	"	"	1 d ≤ T-1/2 < 100 d
42	"	"	100 d ≤ T-1/2

The status of decay data of F.P. was described at the Bologna Panel 1973 by Rudstam /1/. Since then, FPND have improved in general, but still much is valid of what Rudstam said about the accuracies of FPND. The lack of decay data for the short lived F.P. has been considerably reduced, and some of the short lived F.P. have now well studied decay data.

The present status of decay data is given in this review, which is composed of six sections. In the first one, the principal new facilities used in decay data measurements are reviewed. The second part is devoted to the total decay energy (Q). In the third Section, the half lives are treated. In the fourth and fifth Sections, beta and gamma energies and intensities, and also average values are discussed. Finally, the last Section considers the different files and compilations devoted to the decay of F.P.

* The French file is described in Sect. VI D and also in Annex 2 to this review /75/.

I. - FACILITIES -

Successful study of short lived FP can be achieved only by the development and the progress of new facilities and new methods

I.A/-Modern separators-

The different methods used for the separation of the short-lived isotopes have been reviewed by Ambruster [2]. In his paper he gives a figure of the schemes of the different methods (Figure I). The Kinematic Separator is not convenient for the study of decays. It allows one to deal with the products of reaction before decay.

I.A.1/- ISOL system -

Most of the systems were already working in 1973.

a)-OSIRIS -

A review of the OSIRIS isotope-separator on-line facility is described by Rudstam [3]. Eighteen elements, Zn, Ga, Ge, As, Br, Kr, Rb, Sr, Ag, Cd, In, Sn, Sb, Te, I, Xe, Cs, Ba are processed. With Se, Y, La, Ce produced as daughters, the total number of fission products available for measurements is about 210. Future plans to raise the temperature of the source will allow that some other elements, in particular rare earth, will be released.

b)- ISOL with a target in the form of uranyl stearate. The TRISTAN I system at Ames Laboratory USA, the ARIEL system at Grenoble, France, the IALE in Bueno Aires, Argentine, and SOLIS at Soreq Israël are the main systems which have been the most fruitful in the nuclear spectroscopic studies of short lived F.P. in the last years. Because of source limitation, only rare gases, Kr, Xe and their daughters and very few halogens have been studied.

c)- TRISTAN II (Ames) [4] -

A new in-beam source of the Studsvik type was also set up at the Tristan II facility. As at Osiris, this source produces good yields of the elements Br-Sr, Ag, Ba. The figure II_a shows the results of $4\pi\beta$ run done to determine the yield as a function of mass. The figure II_b gives the activity collected at OSIRIS for comparison.

d)- OTHER SYSTEMS -

The progress in on-line isotope separators has been described by Ravn [5], in particular the development of new ion sources and new targets. The formation of very pure beams of the Rb, Cs elements, by a combination of surface ionization with their fast diffusion in graphite was pioneered by the ORSAY group [6]. This group has mainly devoted their system to mass determination [7].

OSTIS [8] -

A system with the same kind of target was set up at ILL Grenoble by a German Group [8]. OSTIS has mass resolution $M/\Delta M^2 \simeq 500$ and gives very low contamination ($< 10^{-5}$ Rb, 10^{-4} Cs), with good transmission (> 3%).

e)- NEW DEVELOPMENTS -

A promising approach to developing an ISOL facility which is applicable to non-gaseons F.P. is the coupling of the fission source to the ion source of an isotope separator by means of a gas-jet transport system. Many groups [4,9] have tried to develop this technique, but up to now the efficiency seems too low, and no new decay data have been obtained with this approach.

I.A.2/-LOHENGRIN -

The performances of the recoil separator LOHENGRIN installed at the Grenoble High Flux Reactor are given by Armbruster [10]. It focuses on a parabola resulting from a magnetic sector field and a cylindrical condenser. The fission products are separated into spectra of A/q lines (A = mass number, q = ionic charge) with a mass dispersion perpendicular to the parabola (3.24 cm for a 1% mass difference). The exit slit of the instrument of 72 cm length lies along the parabola where it is approximatively a straight line.

The figure III shows an example of FP spectra recorded for the light group by varying the magnetic field for a constant electric field (350 KV). The mass resolution achieved for this spectrum is of $A/\Delta A \simeq 900$.
(f w 1/10 m)

The exit slit length of LOHENGRIN has some inconvenience for decay measurements. Therefore two special techniques have been developed to achieve a concentration of the radioactivity : figure IIIb

1/- a moving tape system with a zig-zag pattern device to concentrate the activity in front of the detector.

2/- a gas-jet transport system using 17 capillaries to evacuate the thermalization chamber and a final single tube giving a spot of 5 mm diameter of radioactivity.

The intensity of F.P. on 72 cm length can vary from 1.7×10^5 to 9×10^3 (F.P./S) (target 400 $\mu g/cm^2$ UO_2, and mass chain yield of 6.4%).

The time of flight of F.P. into the system (about 2μs) is much shorter than any β half-life.

I.A.3/-JOSEF - [11]

JOSEF (the Jülich on-line separator for fission products).

The separator consists of a focusing magnetic system containing a convenient gas at a pressure of a few torr. It separates F.P. according to their mass and nuclear charge. The separator is described by Sistemich et al. [11]. Ions with mass number A, ionic charge number q and velocity v are deflected in a magnetic field of flux density B on trajectories with radius ρ, the magnetic rigidity being

$$B\rho = 226.8 \frac{Av/vo}{q} \quad (G.m)$$

$$\text{with } vo = e^2/h = 2.19 \times 10^8 \text{ cm/s.}$$

A drawback of this separator is the relatively low mass resolution $A/\Delta A = 79$. But it has a charge resolution of $Z/\Delta Z = 38$ for the light F.P.

JOSEF allows to study half lives down to 10^{-6} S. A moving tape arrangement is also set up, and all the detector systems useful for the decay study are also present. A rate of about 2.3×10^4 cm^{-2} S^{-1}, for a single mass number (chain yield 6.4%) is observed. The figure IV shows :

a) Schematic presentation.

b) Intensity distributions of selected isotopes as a function of Bρ, demonstrating the mass and atomic number resolution.

c) Bρ values of primary fission products as a function of mass for He of 4 Torr as a filling.

The Table Ia gives the characteristics of existing facilities described above and also those of a few others.

I.B/ - Radiochemical Separations -

A survey on the progress of fast chemical separations procedures is given by Trautman [19]. Examples of fast, discontinuous separation procedures from aqueous solutions are shown in Table 1b of Trautman [19].

A great deal of attention has been devoted to explore the possibility of performing chemistry at the end of the gas-jet system. The advantage of such a system is that the rapid chemical separations can be done completely on-line. An example of this system is the on-line system SISAK [12]. Other examples of the rapid chemical separations can be found in [12]. The description of SISAK, and its application to the study of short lived F.P. is given in the recent thesis of Skarnemak [13].

The figure V (taken from his thesis), gives the flow sheet of the chemical system used for the isolation of Ce isotopes.

II. - Q_β .

Many new measurements of total β-decay energies were made since Bologna. P.F are neutron-rich isotopes. So we'll treat only $Q_{\bar{\beta}}$

$$Q_\beta(Z,A) = M(Z,A) - M(Z+1,A) \qquad (1)$$

Z proton number,

N neutron number,

A mass number,

M mass excess.

It is possible to measure either the mass excess, or the $Q_{\bar{\beta}}$.

II.A - ON LINE MASS-SPECTROMETRIC MEASUREMENTS -

II.A.1/ Mass determinations

a)- The method described by Thibault [7] has been used for the Rb and Cs masses. The principle of the method is based on the theorem that the product of the mass M by the applied potential V is constant if the ions follow the same trajectories in a constant magnetic field.

$$M_A V_A = M_B V_B = M_C V_C$$

The originality of this method is that A,B,C are isotopes of the same element (Rb or Cs). M_A and M_B are two known masses used to detect and calibrate any possible systematic error and M_C is the unknown mass. The results are not yet published.

b)- Precise direct mass measurement. With the LOHENGRIN separator, they [10] were able to resolve masses of ^{94}Rb and ^{94}Sr. But to obtain a mass resolving power of $M/\Delta M \simeq 15000$ which corresponds to a difference in binding energy of about 6.5 MeV, several technological problem have yet to be surmounted.

II.A.2/- Beta end point measurement. (Total β^- decay energy). The most important facilities have groups doing this kind of measurement. In general the beta spectra of the sources were recorded by a beta detector in coincidence with a gamma detector so the total β-decay energy is evaluated from the sum of the energy of a β branch, that leads to an excited state of the daughter nuclide and the energy of the subsequent γ cascade which depopulates this state. This Q_β method requires a comprehensive knowledge of the decay scheme. With this method, it is possible also to investigate isomeric states and to give Q_β values for both isomers. But sometimes the

energy of the isomeric state is known with much higher precision from another kind of measurement (electron or gamma transition).

Two recent theses [14][15] describe the method used OSIRIS, and present a lot of measurements. [56]

The comparison of different Q_β spectrometer is made in Table II.

There is not too much overlapping between the measurements, as it is possible to see from the table III. In this table, we have put the values of the French file, the data of Wapstra and Bos (1977) [19], and the results of the OSIRIS group [14,15], LOHENGRIN collaboration [18],AMES Laboratory [68,69],OSTIS [8] group, and ORSAY group [7].

II.B/- MASS PREDICTIONS -

No experimental values exist for roughly a third of F.P., far off the stability line. Different methods of calculation have been developed to predict masses and binding energies.

Very recently Atomic Data and Nuclear Data Tables [20] have included in the same table nine different and recent predictions of mass excesses and "The 1975 Midstream Atomic Mass Evaluation" by Wapstra and Bos [21].

A brief comparison of Mass formulas is given in the table taken from ADNDT [20]. Table n° IV.

The methods of calculation are explained by the authors in the introductions, and it is outside the scope of this review to describe in detail all the mass formulae . Below ,we give only their principal features and their classification.

II.B. 1/- Droplet model mass equations -

Myers [22], Groote et al. [23], Seeger et al. [24] belong to this class. The macroscopic part is similar for all three, but for the microscopic part their approaches are different.

II.B. 2/- Shell model mass equations -

The semi empirical shell model formula is developped by Liran et al.[25] Their equation contains 178 independent coefficients adjusted to experimental data. As boundaries of the shell regions they adopt the magic numbers N,Z = 2, 8, 20, 28, 50, 82 ...

II.B.3/- Mass relations -

The transversal and longitudinal mass relationships described by Garvey and Kelson [30] have been used by Jänecke [27] who updated the results,using as input the new experimental mass values of Wapstra and Bos [21]. Comay and Kelson [28] have generated mass tables with the transverse Garvey Kelson equation and by averaging over the ensemble to predict unknown masses. Jänecke and Eynon [29] obtain mass predictions from the solutions of inhomogeneous partial difference equations with the help of liquid-drop model expressions.

II.B.4/- Energy-density concept -

Beiner et al. [26] use expressions for energy density with the parameters related to infinite nuclear-matter properties.

Atomic mass evaluation of Wapstra and Bos. An "interim" evaluation of experimental atomic masses excess has been presented in the same table that the mass predictions. This set of some 1300 values is a revision of 1971 Atomic Mass evaluation [19].

It contains more experimentally determined masses (1330 instead of 1160). All the masses were adjusted in one run (requiring inversion of a 687 x 687 matrix). A complete atomic mass evaluation will be published in an other volume of A.D.N.DT [19] and was sent to all users by Wapstra as microfilm.

From the Mass predictions, written on a magnetic tape, we have calculated the Q_β values for 700 isotopes including the most of known and unknown F.P.

The results are given in Annex $n^o 5$ and shown in the figures VI - X. The figures VI, VII, VIII show the difference between Q_β calculated by the different models, and the adjusted Q_β of Wapstra 1975, if they exist. The Q_β calculated with the mass of Janëcke [27] are in the best agreement with the Q_β of Wapstra 1975. The values derived from Liran [25] also agree well with those of Wapstra.

The figures IX, X, represent the upper value and the lower value for the masses without experimental data. The difference between these two values is about 1.5 MeV for Q_β of 8 to 10 MeV. It seems also that often the upper value is from Liran [25].

III - HALF LIVES -

III.1/- Experimental problems and errors -

It is not easy to assign correctly errors to measured half lives, especially the systematic error. Certainly the utilisation of isotopic separation, and also gamma counting have reduced the errors coming from contamination. For short lived isotopes the development of good electronic systems allows a

better correction for dead time. Half-life determination of very long lived nuclides (> 1 year) is also difficult and the data are spread. The statistical analysis of all the errors given in the French library shows, that the average error for nuclides less than 1 min. is 8%, for those around 1 day ≃ 1% and about 4% for those greater than 3 years [65]. The U.K. contribution [46] asks for some expression of the "confidence factor" for ^{154}Eu $t_{1/2}$ = 8.5 years which is in disagreement with the often used 16 years.

Some recent works in LOHENGRIN, JOSEF, OSTIS have shown the interest of doing the measurement on nuclides coming from different reactions. For instance the relative intensity of some γ rays of ^{146}La was not the same, when ^{146}La was produced in LOHENGRIN or in OSTIS. With OSTIS the ^{146}La isotope is coming only as a daughter of ^{146}Ba, while in LOHENGRIN the ^{146}La is also produced directly by fission. After a careful analysis of the decay of many γ rays, 2 half lives were assigned to ^{146}La [47]. A lot of other isomers have been found recently in ^{96}Y [48] ^{97}Y [49] ^{98}Y [50] ^{148}Pr [45] etc .. Also a "good confidence factor" for the half lives of short-lived isotopes is the agreement in results coming from many facilities, mainly if the groups have used different ways to produce and to measure the half lives.

Due to the continuous production of activity in the on line system, some new approaches to measurement have been developed. In LOHENGRIN a fast transport of the F.P. from the exit slit to the detector area has been achieved with a continuous moving tape collector. The β or γ activity of a single isobar with a radioactive

decay constant λ is then a function of the speed v of the tape as follows

$$H(v) = K \frac{v}{\lambda} [1 - \exp(-\lambda \frac{x_1}{v})] x \exp(-\lambda \frac{x_2}{v}) [1 - \exp(-\lambda \frac{x_3}{v})]$$

where x_1 , x_2 , x_3 represent respectively : the collecting length, the shielded length and the measuring length of the tape. This function has a fixed and known shape for a given set of parameters x_1, x_2, x_3 whose maximum corresponds to v/λ constant.

The fig.VII shows the relative activity of some γ rays of mass 132.

The SISAK group has also developed the TDD (two detector delay) method [13]. A TDD measurement requires two Ge(Li) detectors equiped with coil, i.e. teflon tubing wound around each detector head. The ratio between the areas of the corresponding γ ray peaks in detectors 2 and 1, respectively are plotted against the delay time.

III.2/- Determination of unknown half lives -

The number of unknown half lives of F.P. has been reduced since Bologna. 57 F.P. have estimated half lives in the French file. The half-life calculation has been done by different methods.

a)- ENDF/B-IV -

Dr. Schenter [52] uses the following equation suggested from "β-strength function" theories

$$\lambda = \alpha X^4 (X^2 + 6 \gamma X + 15 \delta) ANZ$$

with

$N = A-Z$

$EC = \beta Q$

$X = (Q-Ec)/0.511 = Q(1-\beta)/0.511$

$ANZ = 1.0 + A\epsilon + (N-Z+\eta)$

$= \alpha X^4(X^2+6\gamma X+15\delta)ANZ$

$t1/2 = \ell n\ 2/\lambda$ sec

$\alpha = 40.25 \times 10^{-8}$
$\beta = 0.2552$
$\gamma = -20.92$
$\delta = 172.3$
$\epsilon = -0.01072$
$\zeta = 0.04339$
$\eta = -19.0$

The constants α, β, γ, δ, ϵ, ζ, η, were found by a least squares adjustment to the "known" (experimental) values of T 1/2 originating from ENDF/B-IV.

b)- YOSHIDA [53] -

Using the gross theory of beta decay developed by Takahashi and Yamada [66], Yoshida has derived three formulas which are functions of the Q value and mass number of the nuclides,

For odd-A nuclides

$$\log t1/2 = -(5.345 + 0.00294A)\log Q + 5.444-0.00102A,$$

For odd-odd nuclides

$$\log t1/2 = (0.0172-0.000194A)Q - (5.954-0.00059A)\log Q + 6.193 - 0.00215A,$$

For even-even nuclides

$$\log t1/2 = -(5.211 + 0.00003A)\log Q + 4.957 - 0.00419A.$$

c)- Extrapolation -

If we plot the Log of $T_{1/2}$ versus the mass number for a given element, we obtain two straight lines, one for odd A and one for even A. We have used this method to estimate the unknown half-lives of 57 F.P.

The fig.VI shows some examples. The Table V gives the values obtained with this method, and for comparison the data of ENDF/B-IV and also those of Yoshida [53] with the Q_β used for calculation.

The agreement exists only for less than half of the nuclides. For the others ENDF/B-IV has in general higher values and Yoshida yet higher. Dr. Yoshida thinks that the formulas given in his paper [53] are mainly aimed at an estimation for high Q value (Q_β larger than 3.4 MeV). He suggests also in a recent paper [54] to take a proper consideration of nuclear shell effect in the gross theory. This will probably decrease the calculated $T_{1/2}$. The fact that the $T_{1/2}$ which need to be calculated have decreased allows to use the extrapolation method more confidently. This method seems also more reliable.

III.3/- Recent Results -

The recent results of measurements of short lived F.P., those of LMRI Saclay [70], Debertin [62], those of Martin [34] are given in the Table VI . The recent results of Lohengrin and Josef are not written in a separate column, but can be found in the data of the French file.

IV- BETA SPECTRA -

In β^- decay, an antineutrino ($\bar{\nu}$) and a negative electron β^- are emitted from the nucleus as a result of the process $n \rightarrow p + \beta^- + \nu^-$.

For decay to a particular level in the daughter nucleus, the maximum energy available (also called end-point) is $Emax = Q_\beta^- - E$ (level). The intensity of each transition is derived from γ-ray intensity balance for each level in the daughter. The energy released in a β-transition is divided between the β-particle and the antineutrino.

a)- The average energy of Beta spectra -

The average energy E_{av} of a β particle is given by

$$E_{av} = \int_o^{E_{max}} E \; N(E) \; d\,E \Big/ \int_o^{E_{max}} N(E) \; d\,E \qquad \text{with}$$

N(E) number of particles of energy E

It is customary to use $W = E/m_oC^2 + 1$ = total electron energy (in units of m_oC^2), then

$$N(W) \; d\,W = p\,W\,(W_o - W)^2\,F(\pm Z,W)\,\{1 + \delta_R(W,Z)\}\,C(W)\,dW$$

with $p = \sqrt{W^2 - 1}$

F(Z,W) is called Fermi function

C(W) denotes the so called shape factor of which the form is different for decays of different degrees of forbiddenness. A compilation of the existing experimental data on the shapes of beta spectra is given by Behrens and Szybisz [73]. It contains the shape factor, the experimental method used, and the reference. The FP isotopes having data in this compilation are listed in the TABLE VII a . The expression $\delta(W,Z)$ is the model independant electro-magnetic radiative correction. In general it is small $\simeq$ 0,04.

b)- Calculations of the average β^- energy -

1)- Gove and Martin [41] have developed a LOGFT program. Its documentation is given in Nuclear Data Tables. The program performs a

direct integration over the theoretical β-distribution to the measured end-point. Corrections to the spectrum shape are made for first or second forbidden unique transitions.

2)- Barré and de Tourreil [42] have written a code for calculating the average energy of an allowed β^- transition. They use the FERMI function tabulated by Rose et al. [67].

3)- Tobias [43] has developed a FORTRAN and a BASIC program. The program is able to take account of the nature of the transitions (allowed, first forbidden, etc ..), and evaluates the FERMI and forbidden beta functions. This can be run on a small computer. This program is derived from the equations given by Dillman [44].

4)- ENDF/B IV [31]
The average beta energies tabulated are calculated from the following equations.

$$\bar{E}_\beta = \frac{F_\beta}{100} \sum_i E_{\beta i}\, I_{\beta i}\, fi\,(E_{\beta i})$$

$$f_i(E_{\beta i}) = \frac{1}{4} \frac{2\,W_o^2 + 8\,Wo + 10}{W_o^2 + 5\,Wo + 10}$$

where $W_o = \frac{E_{\beta i}}{0.511 \times 10^6}$ is the beta end-point energy in $m_o c^2$ units and $fi(E_{\beta i})$ is the approximate ratio of the average beta energy to the beta end-point energy. $F_\beta/100$ is a normalization factor. This equation has been proposed by England [45].

5)- Stamatelatos and England [71] have published recently a new approximation for calculating average beta energy. They propose equation with some coefficients given in a table as a function of the atomic number Z. Their calculated values differ from those calculated by "exact" method by < 1%.

c)- Comparison -

The Table VII b gives the values computed by Martin [35], Tobias [43] and the Barré Code [42], ENDF/B-IV for some beta transitions of four F.P. (first forbidden and second forbidden transitions). Always Tobias gives the highest values ($\leq$ 1%). Without taking in account the degree of forbidenness, the values of the Barré Code, and of ENDF/B-IV show differences up to 10%.

d)- Evaluation of unknown average beta and gamma energy ($\bar{E}_\beta$, $\bar{E}_\gamma$)

1)- The gross theory of beta decay has been applied by Yoshida [53] to estimate the average energies of the emitted β and γ rays. By fitting parameters to the experimental values of $\bar{E}_\beta$ and $\bar{E}_\gamma$, Yoshida has derived equations giving $\bar{E}_\beta/Q$ and $(\bar{E}_\beta + \bar{E}_\gamma)/Q$. As for the half lives, they are functions of the Q value and mass number of the nuclides. The theory gives deviations for some well known nuclides (Rb 88), but the author expects improvement in consistency by applying a new treatment.

2)- C.W. Reich and R.L. Bunting [74] suggest that data from recent experiments designed to measure β-strength functions for a large number of short-lived fission products may also be used to provide average β- and γ-decay energies for these nuclides. They give the methods employed to do this and present the results for the average β-decay energies, $\langle E_\beta \rangle$, per decay. For ~10 cases, $\langle E_\beta \rangle$ values from decay-scheme studies are available. A comparison of their deduced values with the latter ones is presented and generally good agreement is found.

3)- ENDF/B-IV uses the following equations:

$$\bar{E}_\beta = Q\,(0.47 + 0.02P + 0.0041\,(N-Z) - 0.0025A)$$
$$\bar{E}_\gamma = Q\,(0.04 - 0.01P + 0.01\,(N-Z) + 0.0002A)$$

P is a pairing factor, and is $\simeq 1$

As for T1/2 the constants were derived from a least squares adjustment to the "known" experimental values of $\bar{E}_\beta$ and $\bar{E}_\gamma$.

V - GAMMA -

V. 1/- Gamma ray energies -

The excellent energy resolution characteristics of the Ge(Li)γ-ray detector has provided great improvements in the quality of γ-ray spectral data. At present it is common that the energies of two different measurements by two groups differ by less than 0.1 keV for the most intense γ-rays up to 3000 keV.

Helmer et al. [55] have reevaluated some precise γ-ray energies for calibration of Ge(Li) spectrometers up to 1300 keV. These energies are based, either on the energy scale referenced to $WK\alpha_1$ X ray energy, or that referenced to the electron mass, $m_o c^2$. The energies and uncertainties for 4 F.P., from their paper [55] are given in Table VIII.

For high energy, there are not enough standards. However the uncertainties are in general about 0.2 - 0.4 keV. For instance the 4078.5 ± 0.5 keV γ-ray of ^{91}Rb reported by Achteberg [56] is found at 4078.25 ± 0.19 by Wohn [57] and 4078.5 ± 0.5 keV by Mason [58].

V. 2/- Relative γ-ray intensity -

Measurements with a precision of ∿ 1-2% have been reported for some cases in the range of 150 - 2000 keV. Below 150 keV the errors are greater due to many corrections (absorption, etc ...).

V. 3/- Internal conversion coefficients -

The experimental results on internal conversion coefficients are not very numerous, especially for short lived F.P. Several tabulations of calculated internal conversion coefficients exist. The

tables of Hager and Seltzer [59] have been written on magnetic tape [63]. The ICC of any transition with a known multipolarity can be obtained by computer interpolation. Raman et al. [64] have compared experimental values with the theoretical values. They found that for 15 E_3 and M_4 transitions the theoretical values are systematically 2 - 3% higher.

V. 4/- Absolute gamma ray intensity -

To deduce absolute decay rates, we consider first the relationships between β and γ intensities normalized to 100 β decays of the parent.

Let βi be the number of β decays to the excited state i, γij be the number of γ transitions from state i to state j, and $N_{\gamma g.s}$ be the total number of transitions from excited states to the ground state with α_{ij} denoting the total internal conversion coefficient for the transition γij, then

$$N_{\gamma g.s.} = \sum_i \gamma i_o \ (1 + \alpha i_o)$$

and $100 - \beta_{g.s} = \Sigma \ \beta i = N_{\gamma g.s.}$

If $\beta_{g.s.}$ is equal to zero and if the g.s. γ's have high energy ($\alpha \simeq 0$), then absolute normalisation is easy. When the α's are not negligible the main error arises from a possibly wrong assignment of the multipolarity. Unfortunately the determination of $\beta_{g.s.}$ is difficult and very few measurements exist.

In a recent work the Ames group [57] have measured the $\beta_{g.s.}$ for the decays of several Kr and Rb nuclides ^{88}Kr, ^{88}Rb, ^{89}Kr, ^{89}Rb, ^{90}Kr, ^{90}Rb, ^{91}Kr, ^{91}Rb. They have done absolute β counting with a 4π-geometry plastic scintillation detector and have taken γ spectra simultaneously with a Ge(Li) detector.

The determinations of $\beta_{g.s.}$ have also been done by other methods. Taking into account fission yield data with Ge(Li) gamma spectrometry, one can obtain absolute intensities of γ lines. This method was used by Cavallini et al. [60] for ^{94}Y and De Freune et al. [61] for ^{118}In.

If a nuclide has only one daughter isotope with a longer half life and a well-known absolute γ intensity, it is also relatively easy to derive the absolute γ intensity from measurements of γ intensities during decay of parent and daughter nucleus. In this case for the determination of the $\beta_{g.s.}$, the level scheme has to be established. An example is found in the paper of Cavallini et al. [60].

Debertin et al. have determined the absolute γ-ray intensities for 5 important F.P. ^{103}Ru, ^{132}Te, ^{134}Cs, ^{140}Ba, ^{140}La with an accuracy around 1%. Their method was already described as a contribution to the Bologna Panel. They [62] give their results compared with the American and the French file.

Nuclides of the French file having absolute γ intensity were entered in the Table IX. For each nuclide, the intensity of βg.s, and error, and the total conversion coefficient are given. For gamma we have written M, if many gammas, and 1, if only 1 gamma, are used for the normalisation. "?" means the gamma has ICC not negligible, but not reported in the file. This table allows to see the relative part of the different terms (Iβg.s, γ, αt).

VI - FILES -

A/- The ENDF/B-IV is described in La 6116 [31] by England and Schenter. One hundred eighty nuclides have experimental data on β^- end-point energies and γ line data (energies and intensities). All radioactive nuclides (711) have evaluated data for the average β^- energy ($\bar{E}_\beta$), total γ energy ($\bar{E}_\gamma$), half-lives, branching, and other data. Rose and Burrows have prepared a publication "ENDF/B fission product Decay Data" [32].

The purpose of this publication is to provide comprehensive radioactive decay data for the F.P. nuclides in a convenient book format. Sample pages for A chain 79 are given in Annex n° 1 [75].

B/- ENSDF

The ENSDF (Evaluated Nuclear Structure Data File) system has been developed by the staff of the Nuclear Data Project. This system was chosen for the international file of Evaluated Data. The description of all the format, the structure, etc .. of this file is given by Ewbank et al. [36] [37]. Table X shows an example of data set in card image form for ^{88}Y decay. The following status of the ENSDF is derived from a paper of Ewbank [38]: As of January 1, 1977, the data file contained 1443 decay schemes. The inventory of the ENSDF data bank is given in the Figure X. Approximatively 200 F.P. are already in the bank. The extent and depth of ENSDF continues to improve as new and revised evaluations are added to the file. In order to maintain a four-year cycle, evaluations will be performed at several centers around the world. A complete magnetic tape copy of all data included in ENSDF is prepared regularly from the master file at Oak Ridge, and can be obtained from the Neutron Data Centers (NNCSC Brookhaven, IAEA/NDS Vienna, CCDN Saclay).

The half lives of FP, as extracted by Dr. Ewbank from the ENSDF file, July 1977, are given in Annex No. 4 [75]. These tables give a good picture of the completeness of the ENSDF file.

C/- The MEDLIST output -

Atomic and Nuclear Radiations from ENSDF Decay Data sets are obtained as output of the MEDLIST program [34]. The format for detailed spectrum information has been simplified to make the information more accessible and to shorten the file, but it is a very close approximation of ENDF/B-V. The description of all the formats can be obtained from the Nuclear Data Group of Oak Ridge. Table XII represents card images of the ENDF-style format, and Table XI gives the output as it appears in the Martin Table [34].

D/- The French file exists at two levels :

1)- an expanded working file,

2)- an evaluated file used with the Pepin code for summation calculations [35].

The description of the file is given in Annex $n^{o}2$ [75]. A comparison between the ENDF/B-IV and the French file was made by Fiche. The results are shown in Annex n^{o} 3. Table XI shows the output of the French file for ^{88}Y. The data for this nuclide have been obtained directly by computer program [72] from the ENSDF file.

E/- ENDF/B-V -

The Radioactive Decay Data are given in section 457. The main purpose of MT = 457 is to describe absolutely the energy spectra resulting from radioactive decay and to give average parameters useful for different applications. A lot of new parameters have been added to the ENDF/B-IV mainly for the processes of Int. Conv. X-ray...

These will lengthen the file. The first version of this file will be ready in about two years. The description of the file can be found in ENDF-102 (Data Formats and Procedures for the Evaluated Nuclear Data File, BNL-NCS 50496).

F/- Decay Data Master File at INEL [39]

The PDMF is a computer file of evaluated decay schemes. The purpose of this file is to provide the data base necessary to generate,

a) updates of their GAUSS-VI nuclide identification library,

b) revisions of the "Tables of the Isotopes",

c) an expanded working file for ENDF/B,

d) other specialized decay data and dosimetry files,

The total number of entries exceed or will exceed soon 200.

G/- TABLE of ISOTOPES [40]

The 7th edition of Table of Isotopes will be published late in 1977. It will include selected experimental data on decay properties (as did the 6th), this time with experimental uncertainties. Adopted values for half-lives, E_γ,I_β, I_α, and level properties will appear on the schemes (rounded, without uncertainties). Adopted normalization factors for I_γ (absolute), with uncertainty where possible, will be given with the tabular entries on γ-rays.

ACKNOWLEDGEMENTS

I want to thank my colleage of the French file, C. FICHE for fruitful discussions, suggestions, and also Prof. A. MOUSSA, C. DEVILLERS, E. MONNAND, J. BOCQUET, F. SCHUSSLER.

I would like to thank particularly Drs. EWBANK and BAMBYNEK for careful reading of the first version of this review.

It is also a pleasure to acknowledge all my colleagues who sent to me a contribution.

Prof. A.H. ATEN
Dr. K. DEBERTIN*
Dr. T.R. ENGLAND
Dr. W.B. EWBANK
Dr. J.C. HILL
Dr. C.M. LEDERER
Dr. A.L. NICHOLS
Dr. Y. NIR-EL
Dr. T. NISHI
Dr. J. PEROLAT
Dr. C.W. REICH *
Dr. R.E. SCHENTER
Dr. K. SISTEMICH
Dr. C. THIBAULT
Dr. A. WAPSTRA
Dr. K. WUNSCH
Dr. T. YOSHIDA

* These contributions are published in INDC(NDS)-87.

REFERENCES

1. G. RUDSTAM "Status of Decay Data of Fission Products", Bologna Panel of F.P. (1973).

2. P. ARMBRUSTER, in Proc. 3 rd Int. Conf. on Nuclei far from Stability, Cargèse 1976, CERN-Report 76-13.

3. G. RUDSTAM, Nucl. Instr. and Meth. 139 (1976) 239.

4. W.L. TALBERT, JR., F.K. WOHN, A.R. LANDIN, J.C. PACER, R.L. GILL, M.A. CULLISON, G.A. SHEPPARD, K.A. BURKE, K.L. MALABY and A.F. VOIGT, Nucl. Instr. and Meth. 139 (1976) 257.

5. H.L. RAVN, 3 rd International Conference on Nuclei far from Stability, Cargèse (1976), CERN 76-13 p. 22.

6. R. KLAPISCH, Annu. Rev. Nuclear Sci. 19, (1969) 33.

7. C. THIBAULT, see reference n° 5 p. 93.

8. K. WÜNSCH, Private communication April 1977.

9. R.A. ANDERL et al. Annual Report of EG.6 Idaho ANCR-1255 and private communication C.W. REICH.

10. P. ARMBRUSTER, M. ASGHAR, J.P. BOCQUET, R. DECKER, H. EWALD, J. GREIF, E. MOLL, B. PFEIFFER, H. SCHRADER, F. SCHUSSLER, G. SIEGERT and H. WOLLNIK, Nucl. Instr. and Meth. 139 (1976) 213.

11. K. SISTEMICH, Nucl. Instr. and Meth. 139 (1976) 203.

12. N. TRAUTMANN, see reference n° 5 p. 30.

13. G. SKARNEMARK, Thesis Chalmers University of Technology Göteborg, Sweden May 1977.

14. K. ALEKLETT, Thesis Chalmers University of Technology, Göteborg, Sweden (1977).

15. E. LUND, Thesis Chalmers University of Technology, Göteborg Sweden 1977.

16. E. LUND, G. RUDSTAM, Nucl. Instr. and Meth. 134 (1976) 173.

17. F.K. WOHN, J.R. CLIFFORD, G.H. CARLSON, W.L. TALBERT, Nucl. Instr. and Meth. 101 (1972) 343.

18. The LOHENGRIN Collaboration see reference n° 5 p. 109.

19. A.H. WAPSTRA, K. BOS, private communication and to be published in ADNDT.

20. S. MARIPUU, AT. DAT. NUC. DAT. TAB. 17 (1976) 411.

21. A.H. WAPSTRA, K. BOS, see reference n° 20 p.474.

22. W.D. MYERS, see reference n° 20 p. 411.

23. H.V. GROOTE, E.R. HILF, K. TAKAHASHI, see reference n° 20 p. 418.

24. P.A. SEEGER, W.M. HOWARD, see reference n° 20 p. 428.

25. S. LIRAN, N. ZELDES, see reference n° 20 p. 431.

26. M. BEINER, R.J. LOMBARD, D. MAS, see reference n° 20 p.450.

27. J. JANËCKE, see reference n° 20 p. 455.

28. E. COMAY, I. KELSON, see reference n° 20 p. 463.

29. J. JANËCKE, B.P. EYNON, see reference n° 20 p. 467.

30 G.T. GARVEY et al., Rev. Mod. Phys. 41, S1 (1969).

31 T.R. ENGLAND, R.E. SCHENTER, La-6116-MS and ENDF-223

32 P.F. ROSE, T.W. BURROWS "ENDF/B Fission Product Decay Data"(in press)

33 J. BLACHOT, C. FICHE, Atomic Data & Nucl. Data Tables 20, n°4 (1977)

34 Nuclear Decay Data for Selected Radionuclides, édited by M.J.MARTIN ORNL-5114 (March 1976).

35 C. DEVILLERS, note CEA

36 W.B. EWBANK, 5th International CODATA Conference Boulder Colorado June 28 (1976).

37 NUCLEAR DATA PROJECT, ENSDF styles and conventions ORNL 5054.

38 W.B. EWBANK, Private communication, April 1977.

39 R.L. BUNTING, R.G. HELMER, C.W. REICH, ANCR-1255, p.27.

40 C.M. LEDERER, Private communication, April 1977.

41 N.B. GOVE, M.J. MARTIN, Nucl. Dat. TAB. 10 (1971) 206.

42 B. BARRE, R. De TOURREIL, Note CEA N.1285 (1970).

43 A. TOBIAS, RD/B/N 3740 (1976).

44 L.T. DILLMAN, J. Nuc. Medicine, Suppl. 2, Pamphlet n°4 (1969).

45 T.R. ENGLAND, "An investigation of Fission Product Behavior in Nuclear Reactors", PHD Thesis, Univ. Wiscousin (1969).

46 U.K. Contribution to this panel CNDC (77) p.3.

47 E. MONNAND et al. , to be published.

48 G. SADLER et al. , Nucl. Phys. A 253 (1975) 365.

49 E. MONNAND et al. , see reference n°5 p. 477.

50 K. SISTEMICH et al. , Z. Physik A 281 (1977) 169.

51 Y. NIR-EL et al. , see reference n° 5 p.501 and private communication.

52 R.L. SCHENTER, private communication, Feb. 1977.

53 T. YOSHIDA, private communication and to be published.

54 T. KONDOH et al. , supplement of Progr. Theor. Phys., 60 (1976) 136 Kyoto.

55 R.G. HELMER et al. , see reference n° 9 p. 35.

56 E. ACHTEBERG et al. , Phys. Rev. C 9 (1974) 299.

57 F.K. WOHN et al. , Phys. Rev. C 13 (1976) 2492.

58 J.F. MASON, an J. Phys. 48 (1970) 2895.

59 R.S. HAGER, E.C. SELTZER, Nucl. Dat. A9, 119.

60 P. CAVALLINI et al., R. Rad. Lett. 21 (1975) 151 et 157.

61 D. DE FRENNE et al. , Phys. Rev. C 15 (1977) 1440.

62 K. DEBERTIN et al. , contribution to this paper. Published in [75].

63 D.G. VALLIS, private communication (1977).

64 S. RAMAN et al. , Phys. Rev. C 7 (1973) 2531.

65 C. DEVILLERS et al. , Bul. Am. Phys. Soc. 20 (1975) 135.

66 K. TAKAHASHI et al. Atomic Dat. Nucl. DAT. TAB. 12 (1973) 101.

67 K. SIEGBAHN, α, β, γ - ray spectroscopy, North-Holland Publishing company, Amsterdam (1965).

68 J.P. ADAMS et al., Phys. Rev. C8 (1973) 767.

69 J.R. CLIFFORD et al., Phys. Rev. C7 (1973) 2535.

70 J.P. PEROLAT, communication privée, Janvier 1977.

71 M.G. STAMATELATOS, T.R. ENGLAND, N.S.E. (1977) 204.

72 A. FORTRAN PROGRAM written by C. FICHE (1976).

73 M. BEHRENS, L. SCYBISZ, Z.A.E.D. 6-1 (1976).

74 C.W. REICH, R.L. BUNTING, Private communication and contribution to this review. The contribution is published in [75].

75 "Annexes and selected contributions to the review papers of this meeting", INDC(NDS)-87 (1978).

FIGURE CAPTIONS

1. Schemes of different methods to separate short lived isotopes.

2. a)- Activity measured with a 4π beta-detector at the Tristan II facility
   b)- Activity measured with a 4π beta-detector at OSIRIS.

3. a)- A/q spectrum recorded with constant electric field HT = 460 KV for the light group.
   b)- The moving tape system arrangement at the exit slit of LOHENGRIN.

4. a)- Schematic view of the gas filled separator JOSEF.
   b)- Calibration of JOSEF for light fission products. Gas-filling He at 4 torr.
   c)- Intensity distribution vs the magnetic rigidity of ^{96}Sr and ^{96}Y, ^{97}Y.

5. Flow sheet showing the chemical system rised for the isolation of Ce isotopes with SISAK.

6. Interpolation of known and unknown half lives.

7. The mass chain 132 γ-activity as a function of tape speed.

8. Difference between calculated masses and experimental masses of Wapstra, Bos (1975) [21]
   a [24] b [23] c [24] a1 [29] b1 [28] c1 [27] a2 [26] b2 [25]

9. a, b Upper and lower mass for nuclides without experimental data.

10. ENSDF data bank inventory 03-23-77.

Table I a

CHARACTERISTICS OF EXISTING ISOL FACILITIES AT REACTORS

Name, location (initial operation)	Target and target conditions	Neutron flux at target (cm^{-2} sec^{-1})	Delay time from production to ionization	Type of ion source (temperature)	Elements extracted, with decay products excluded	Approximate overall efficiency
TRISTAN, Ames (Nov. 1966)	^{235}U as UO_2 (0.2g at 600°C	2×10^{13} th.	12 sec trans.	oscil. elect. (1700°C)	Kr, Xe	10^{-2}–10^{-1}
	^{235}U as stearate (2-4g at 20°C)	3×10^{9} th.	1.2 sec trans.	"	Br,Kr,I,Xe	10^{-3}–10^{-1}
	^{235}U as UO_2+ UC (1g at 1500°C)	"	diffusion limit	oscil. elect. (1500°C)	(As),(Se),Br,Kr,Rb,Sr, Ag,Cd,In,Sn,Sb,Te,I,Xe,Cs,Ba	10^{-4}–10^{-2}
ARIEL, Grenoble (June 1968)	$^{233,35,38}U$, ^{232}Th (4g UO_2 or stearate)	10^{8} 14-MeV	4-6 sec diff.	oscil. elect. (1700°C)	Kr,Xe	10^{-2}–10^{-1}
	^{235}U as UO_2 (10g at 20°C)	3×10^{8} th.	"	"	"	"
SOLIS, Soreq (July 1968)	^{235}U as stearate (2-4g at 20°C)	2×10^{9} th.	0.3 sec trans.	oscil. elect. (1700°C)	Kr,Xe	10^{-2}–10^{-1}
	^{235}U as UO_2 (1g at 1800°C)	"	diffusion limit	surface ion. (1800°C)	Rb,Cs;Br,I	10^{-3}
OSIRIS, Studsvik (July 1968)	^{235}U as UO_2+ UC (0.2g at 1500°C)	4×10^{11} th.	diffusion limit	oscil. elect. (1500°C)	Zn,Ga,Ge,As,Br,Kr,Rb,Sr, Ag,Cd,In,Sn,Sb,Te,I,Xe,Cs,Ba	10^{-4}–10^{-2}
	^{235}U as UO_2+ UC (2g at 1500°C)	"	"	"	"	"
IALE, Buenos Aires (March 1969)	^{235}U as stearate (14g at 20°C)	5×10^{8} th.	1 sec trans.	oscil. elect. (1700°C)	Br,Kr,I,Xe	10^{-3}–10^{-1}
JOSEF, Jülich (Nov. 1972)	^{235}U as UO_2 (40mg at 500°C)	1×10^{14} th.	μsec recoil	none - recoil in Torr gas	all fission products (there is no chemical selectivity)	10^{-5}–10^{-4}
SIRIUS, Strasbourg (June 1973)	^{235}U as UO_2 (10mg at 20°C)	5×10^{10} th.	8 sec trans.	hollow cath. (2200°C)	Sn,Sb,Te,I,Xe,Cs,Ba,Ce,Pr + others (survey incomplete)	10^{-4}
	"	"	sec trans.	"		
	^{235}U as UO_2 (0.6g at 50°C)	5×10^{11} th.	sec trans.	"		
SOLAR, Pullman (Jan. 1974)	^{235}U as UO_2 (1g at 1600°C)	5×10^{9} th.	0.1 sec diff. Sr,Ba = 7 min.	surface ion. (1600°C)	Rb,Cs;Br,I;Sr,Ba	10^{-5}–10^{-3}
LOHENGRIN, Grenoble (March 1974)	^{235}U as UO_2 (3mg at 500°C)	5×10^{14} th.	μsec recoil	none - recoil in vacuum	all fission products (there is no chemical selectivity)	10^{-6}–10^{-5}
OSTIS, Grenoble (Oct. 1975)	^{235}U as UO_2 (2g at 1800°C)	3×10^{9} th.	0.1 sec diff.	surface ion. (1800°C)	Rb,Cs	10^{-3}
"ISOL", Mainz (Dec. 1975)	^{235}U as UO_2 (1g at 1800°C)	5×10^{9} th.	0.1 sec diff.	surface ion. (1800°C)	Rb,Cs	10^{-3}

Table I b

Technique	Element[production]	Procedure	Nuclide/Half-life
Solvent extraction	Zr [U+n]	TBP/7.5 N HNO_3	^{101}Zr 2.0 sec
	Mo [U,Pu+n]	Amylalcohol/NH_4SCN	^{107}Mo 3.5 sec
	Tc [Pu,Cf+n]	$AsPh_4Cl$/0.1 N HNO_3	^{110}Tc 1.0 sec
	Ru [Pu,Cf+n]	Petrolether/5 N $HClO_4$	^{112}Ru 3.6 sec
Ion exchange resins	Y [U+n]	Cation resin/1 M α-HIB	^{97}Y 1.5 sec
	Ce [U+n]	Anion resin/PbO_2/9 N HNO_3	^{150}Ce 3.4 sec
Sorption	Nb [Pu,Cf+n]	Glass/10 N HNO_3	^{104}Nb 0.8 sec
Exchange with solids	Ag [Cf+n]	$AgCl/Ag^+$	^{118}Ag 4.0 sec
	I [U+n]	AgI/I^-	^{140}I 0.8 sec
Volatilization	As [U+n]	AsH_3 from HCl+Zn	^{86}As 0.9 sec
	Se [U+n]	SeH_2 from HCl+Zn	^{88}Se 1.4 sec
	Sb [U,Pu+n]	SbH_3 from HCl+Zn	^{136}Sb 0.8 sec
	Te [U,Pu+n]	TeH_2 from HCl+Zn	^{137}Te 3.5 sec
	Sn [U,Pu+n]	SnH_4 from HCl+$NaBH_4$	^{132}Sn 39 sec

Rapid discontinuous separation procedures from aqueous solutions

Table II

Comparison of different Q_β spectrometers

SYSTEM	OSIRIS [16]	AMES [17]	LOHENGRIN [18]	OSTIS [8]
β detection	Si(Li) 25 mm Ø 5 mm thick	Well type cylindrical. Scintillator (Pilot B plastic). Well : truncated cone Ø &,9 cm depth 2,3 cm.	β detector telescope 75 mm x 75 mm Ø plastic scintillator (NE 102 A) 0,5 mm thick plastic ΔE PM EMI 9531	Hyperpure intrinsic germanium detector.
γ detection	Ge/Li or Na(I) for highly excited levels	Ge/Li	Ge/Li	Ge/Li
Energy calibration	^{207}Bi, ^{228}Th, ^{206}Rh	^{85}Kr, ^{207}Bi, ^{141}La, ^{144}Ce, ^{137}Xe, ^{38}Cl, ^{88}Kr.	^{90}Y, ^{94}Si, ^{106}Rh, ^{38}Cl ^{94}Y, ^{90}Rb, ^{92}Rb.	with well known γ rays
Response function	Measured using conversion electrons from ^{207}Bi (up to 1.7 MeV) used other work up to 5 MeV.	Magnetic spectrometer with a source of ^{144}Ce up to 2,5 MeV and of ^{88}Kr up to 5 MeV.	Linearity tested with the beta spectrometer BILL	tested with the beta spectrometer BILL
Data Analysis	Computer program a/- using the response and efficiency fonctions for a conversion of the pulse spectrum in a true electron energy distribution. b/- determining the end point energy corresponding to the electron distribution by a Kurie plot.	Computer program FERMI is a two parameter fitting routine which can fit a spectrum consisting of up to 5 individual β group provided the relative intensity and end point energy of each group being held fixed relative to the most energetic group.	Computer program a/- low counting rates. The counting rate Nn in channel number n is transformed by the Lindahle method b/- Kurie plot calculation with a detector response function of gaussian shape.	Computer program square root plot and fit the high energy part of the spectrum.
Accuracy	$\sigma = (\bar{\sigma}^{-2} + \bar{\sigma}^{-2}(\mathrm{Ecal})\|^{1/2}$ $\bar{\sigma} = (\Sigma\, \bar{\sigma}_1^{-2})^{-1/2}$ σ(Ecal) = the largest calibration uncertainty	Not given	Not given	Not given

Table III

Recent data of Qβ

NUCLIDE	CLEF	ENERGY	ERROR	REF	77WAP		OSIRIS		76LOH	AMES
29CU 71	QBF-	4530.0	0.0	69GA						
30ZN 71M	QBF-	2979.0	11.0	74WA						
30ZN 71F	QBF-	2822.0	11.0	74WA	2818.0	100.0				
29CU 72	QBF-	8260.0	0.0	69GA						
30ZN 72	QBF-	458.0	6.0	74WA	457.0	6.0				
31GA 72	QBF-	3990.2	3.2	74WA	3991.6	3.1				
30ZN 73	QBF-	4700.0	200.0	74WA	4700.0	200.0				
29CU 73	QBF-	6150.0	0.0	69GA						
31GA 73	QBF-	1560.0	40.0	77WA	1560.0	40.0				
30ZN 74	QBF-	2350.0	100.0	76KO	2350.0	100.0				
31GA 74	QBF-	5500.0	50.0	71WA	5400.0	100.0				
30ZN 75	QBF-	5620.0	200.0	76AL			5620.0	200.0		
31GA 75	QBF-	3300.0	200.0	74CH	3300.0	200.0				
32GE 75F	QBF-	1174.0	3.7	74WA	1177.8	2.6				
30ZN 76	QBF-	3890.0	80.0	77WA	3890.0	80.0	3980.0	120.0		
31GA 76	QBF-	6770.0	150.0	77WA	6770.0	150.0	6770.0	150.0		
33AS 76	QBF-	2968.8	1.9	74WA	2968.6	1.8				
30ZN 77	QBF-	6910.0	220.0	76AL			6910.0	220.0		
31GA 77	QBF-	5340.0	60.0	76AL			5340.0	60.0		
32GE 77M	QBF-	2861.2	10.0	77WA						
32GE 77F	QBF-	2701.5	3.0	77WA	2701.5	3.0				
33AS 77	QBF-	690.4	3.9	77WA	690.4	3.9				
30ZN 78	QBF-	5600.0	250.0	77WA			6010.0	180.0		
33AS 78	QBF-	4310.0	70.0	76EN	4290.0	70.0				
30ZN 79	QBF-	8660.0	0.0	76JA						
31GA 79	QBF-	6760.0	80.0	77WA	6760.0	80.0	6770.0	80.0		
32GE 79	QBF-	4300.0	200.0	70KA	4150.0	140.0	4090.0	180.0		
33AS 79	QBF-	2200.0	50.0	77WA	2200.0	50.0				
34SE 79F	QBF-	142.0	7.0	74WA	149.0	5.0				
31GA 80	QBF-	8600.0	600.0	76AL			8600.0	600.0		
32GE 80	QBF-	2630.0	70.0	77WA	2630.0	70.0	2640.0	70.0		
33AS 80	QBF-	5700.0	300.0	77WA	5700.0	300.0	5370.0	120.0		
35BR 80F	QBF-	2010.0	12.0	74WA	2006.0	11.0				
31GA 81	QBF-	7230.0	190.0	76AL			7230.0	190.0		
32GE 81	QBF-	5570.0	0.0	69GA						
33AS 81	QBF-	3800.0	200.0	74WA	3750.0	100.0				
34SE 81M	QBF-	1686.1	10.0	69ZO						
34SE 81F	QBF-	1583.0	10.0	74WA	1585.0	7.0				
36KR 81M	QBF-	480.0	100.0	74WA						
36KR 81F	QBF+	269.0	19.0	74WA	269.0	19.0				
31GA 82	QBF-	12350.0	0.0	69GA						
32GE 82	QBF-	3580.0	0.0	69GA						
33AS 82M	QBF-	7200.0	0.0	76EN						
33AS 82F	QBF-	7200.0	0.0	76EN						
35BR 82M	QBF-	3138.6	5.0	77WA						
35BR 82F	QBF-	3092.6	1.5	77WA	3092.6	1.5				
31GA 83	QBF-	11410.0	0.0	69GA						
32GE 83	QBF-	8680.	0.0	69GA						
33AS 83	QBF-	5460.0	220.0	77WA	5460.0	220.0	5460.0	220.0		
34SE 83M	QBF-	3835.0	31.0	77WA						

Table III (continued)

NUCLIDE	CLEF	ENERGY	ERROR	REF	77WAP		OSIRIS		76LOH + 76OSTIS		AMES	
34SE 83F	QBF-	3615.0	31.0	77WA	3615.0	31.0						
35BR 83	QBF-	969.0	6.0	74WA	960.0	15.0						
31GA 84	QBF-	13710.0	0.0	76JA								
32GE 84	QBF-	6760.0	0.0	69GA								
33AS 84	QBF-	9900.0	0.0	69GA								
34SE 84	QBF-	1818.0	29.0	77WA	1818.0	29.0						
35BR 84M	QBF-	4700.0	0.0	67LE								
35BR 84F	QBF-	4673.0	26.0	77WA	4673.0	26.0						
32GE 85	QBF-	10080.0	0.0	76JA								
33AS 85	QBF-	9050.0	0.0	72KR								
34SE 85	QBF-	5920.0	0.0	69GA								
35BR 85	QBF-	2800.0	100.0	74WA	2800.0	100.0	2870.0	19.0				
36KR 85M	QBF-	992.2	2.0	73MA								
36KR 85F	QBF-	687.2	2.0	74WA	687.0	2.0						
32GE 86	QBF-	9060.0	0.0	76JA								
33AS 86	QBF-	10183.0	0.0	69GA								
34SE 86	QBF-	4970.0	0.0	69GA								
35BR 86	QBF-	7300.0	400.0	74WA	7300.0	400.0	7610.0	60.0				
37RB 86F	QBF-	1771.8	2.8	74WA	1774.4	1.9						
33AS 87	QBF-	10410.0	0.0	69GA								
34SE 87	QBF-	7270.0	0.0	71ND								
35BR 87	QBF-	7060.0	100.0	77WA			6840.0	120.0				
36KR 87	QBF-	3889.0	5.0	77WA	3889.0	5.0						
37RB 87	QBF-	273.7	1.9	74WA	273.3	1.9						
38SR 87M	QBF+	2249.8	1.4	74WA								
33AS 88	QBF-	13010.0	0.0	76JA								
34SE 88	QBF-	6330.0	0.0	71TO								
35BR 88	QBF-	8200.0	0.0	76BU			8200.0	500.0	8550.0	150.0		
36KR 88	QBF-	2913.0	17.0	77WA	2913.0	17.0					2930.0	0.3
37RB 88	QBF-	5312.0	12.0	74WA	5309.0	11.0	5500.0	200.0	5303.+	6.+	5300.0	60.0
34SE 89	QBF-	8630.0	0.0	69GA								
35BR 89	QBF-	8040.0	0.0	69GA								
36KR 89	QBF-	4930.0	60.0	77WA	4930.0	60.0					4930.0	60.0
37RB 89	QBF-	4486.0	12.0	71WA	4486.0	12.0			4490.+	10.+		
38SR 89	QBF-	1489.3	3.4	74WA	1492.2	3.3						
34SE 90	QBF-	7470.0	0.0	69GA								
35BR 90	QBF-	10330.0	0.0	69GA								
36KR 90	QBF-	4390.0	30.0	74WA	4390.0	30.0			4390.0	100.0	4350.0	50.0
37RB 90M	QBF-	6426.0	70.0	74WA					6540.+	30.+(D)		
37RB 90F	QBF-	6320.0	70.0	74WA			6910.0	120.0	6415.0	100.0	6320.0	70.0
38SR 90	QBF-	546.0	2.0	71WA	546.0	2.0						
39 Y 90M	QBF-	2961.5	3.2	74WA								
39 Y 90F	QBF-	2279.2	3.2	74WA	2283.9	2.5						
34SE 91	QBF-	10310.0	1000.0	69GA								
35BR 91	QBF-	9180.0	0.0	69GA								
36KR 91	QBF-	6200.0	100.0	74WA	6200.0	100.0					6120.0	70.0
37RB 91	QBF-	5700.0	40.0	74WA	5700.0	40.0			5810.+	50.+	5680.0	40.0
38SR 91	QBF-	2684.0	4.0	77WA	2684.0	4.0						
39 Y 91F	QBF-	1545.0	5.0	74WA	1543.0	2.0						
34SE 92	QBF-	8730.0	0.0	69GA								
35BR 92	QBF-	12010.0	0.0	69GA								
36KR 92	QBF-	5970.0	80.0	74WA	5970.0	80.0			5915.0	120.0	5970.0	80
37RB 92	QBF-	7700.0	250.0	74WA	7770.0	200.0			7980.0	100.0	7580.0	150
									8045.0+	50.0+		
38SR 92	QBF-	1930.0	30.0	73CL	1930.0	30.0					1930.0	30.(
39 Y 92	QBF-	3623.0	20.0	74WA	3634.0	16.0						
36KR 93	QBF-	7700.0	1000.0	74WA							8300.0	500.(
37RB 93	QBF-	7360.0	70.0	77WA	7360.0	70.0			7410.0	100.0	7230.0	100.(
									7433.0+	35.0+		

Table III continued

NUCLIDE	CLEF	ENERGY	ERROR	REF	77WAP		OSIRIS		76LOH + 76OSTIS		AMES
38SR 93	QBF-	4190.0	50.0	74WA	3950.0	150.0	4150.0	200.0	4130.0	100.0	
39 Y 93F	QBF-	2890.0	2.0	74WA	2890.0	20.0					
40ZR 93	QBF-	90.0	3.0	72KO	92.3	1.9					
36KR 94	QBF-	6560.0	0.0	69GA							
37RB 94	QBF-	9700.0	1000.0	74WA					10260.+	30.+	
38SR 94	QBF-	3420.0	70.0	74WA	3420.0	70.0					
39 Y 94	QBF-	4860.0	15.0	74WA	4882.0	12.0					
41NB 94M	QBF-	2088.0	2.6	74WA							
41NB 94F	QBF-	2046.0	2.6	74WA	2045.2	2.6					
36KR 95	QBF-	9650.0	0.0	76JA	8590.0	300.0					
37RB 95	QBF-	8590.0	300.0	74WA							
38SR 95	QBF-	6090.0	90.0	77WA	6090.0	90.0			6060.0	100.0	
39 Y 95	QBF-	4430.0	20.0	71WA	4430.0	20.0					
40ZR 95	QBF-	1123.0	3.6	74WA	1123.1	2.7					
41NB 95F	QBF-	925.5	0.5	72ME	925.6	0.5					
37RB 96	QBF-	11630.0	500.0	74WA							
38SR 96	QBF-	5360.0	100.0	77WA	5360.0	100.0			5350.0	100.0	
39 Y 96M	QBF-	7020.0	100.0	77WA	7020.0	100.0					
39 Y 96F	QBF-	7020.0	100.0	77WA							
41NB 96	QBF-	3187.0	4.0	71WA	3187.0	4.0					
37RB 97	QBF-	9060.0	0.0	69GA							
38SR 97	QBF-	7400.0	300.0	74WA					7450.0	120.0	
39 Y 97M	QBF-	7337.0	130.0	77WA							
40ZR 97	QBF-	2657.4	20.0	77WA	2657.4	2.0					
41NB 97M	QBF-	1189.0	0.0	77WA							
41NB 97F	QBF-	1932.9	2.0	77WA	1932.9	2.0					
37RB 98	QBF-	12110.0	0.0	69GA							
38SR 98	QBF-	5810.0	120.0	76SI	5810.0	120.0			5880.0	120.0	
39 Y 98M	QBF-	7300.0	9.0	77SI							
39 Y 98F	QBF-	7400.0	100.0	75LO					8750.0	120.0	
40ZR 98	QBF-	2239.0	21.0	77WA	2239.0	21.0					
41NB 98M	QBF-	4585.0	6.0	77WA					4580.0	100.0	
41NB 98F	QBF-	4585.0	6.0	77WA	4585.0	6.0					
43TC 98	QBF-	1795.0	22.0	76EN	1792.0	8.0					
37RB 99	QBF-	10070.0	0.0	69GA							
38SR 99	QBF-	8450.0	1000.0	69GA							
39 Y 99	QBF-	6390.0	200.0	76MO	6390.0	200.0					
40ZR 99	QBF-	4445.0	120.0	75LO	4460.0	100.0			4545.0	120.0	
41NB 99M	QBF-	3632.0	20.0	74WA	3624.0	16.0					
41NB 99F	QBF-	3632.0	20.0	74WA							
42MO 99	QBF-	1356.6	1.0	74WA	1356.7	1.0					
43TC 99F	QBF-	292.1	2.7	74WA	293.6	1.8					
39 Y100	QBF-	9590.0	1000.0	69GA							
40ZR100	QBF-	3360.0	150.0	77WA	3360.0	150.0			3340.0	130.0	
41NB100M	QBF-	6230.0	130.0	77WA							
41NB100F	QBF-	6230.0	130.0	77WA	6230.0	130.0			6240.0	100.0	
43TC100	QBF-	3202.8	2.2	77WA	3202.8	2.2					
39 Y101	QBF-	7700.0	0.0	76JA							
40ZR101	QBF-	6100.0	1000.0	74WA							
41NB101	QBF-	4570.0	100.0	77WA	4570.0	100.0			4570.0	100.0	
42MO101	QBF-	2821.0	25.0	74WA	2811.0	24.0					
43TC101	QBF-	1633.0	24.0	76EN	1625.0	24.0					
39 Y102	QBF-	10830.0	0.0	76JA							
40ZR102	QBF-	2920.0	0.0	69GA							
41NB102	QBF-	7000.0	1000.0	74WA					7250.0	130.0	
42MO102	QBF-	1040.0	1000.0	74WA							
43TC102M	QBF-	4367.0	0.0	69BL							
43TC102F	QBF-	4150.0	100.0	69BL							
40ZR103	QBF-	7000.0	0.0	76JA							
41NB103	QBF-	5600.0	1000.0	74WA							

Table III (continued)

NUCLIDE	CLEF	ENERGY	ERROR	REF	77WAP		OSIRIS	76LOH	AMES
42MO103	QBF-	4100.0	1000.0	74WA					
43TC103	QBF-	2350.0	100.0	74WA	2350.0	100.0			
44RU103	QBF-	762.9	3.9	77WA	762.9	3.9			
40ZR104	QBF-	5150.0	0.0	76JA					
41NB104M	QBF-	8800.0	0.0	69GA					
41NB104F	QBF-	8800.	0.0	76AH					
42MO104	QBF-	2400.0	1000.0	74WA					
43TC104	QBF-	5400.0	1000.0	74WA					
45RH104M	QBF-	2573.0	12.0	71WA					
45RH104F	QBF-	2444.0	7.0	74WA	2448.0	7.0			
41NB105	QBF-	6940.	0.0	76AH					
42MO105	QBF-	5400.0	1000.0	74WA					
43TC105	QBF-	3200.0	200.0	75SU	3400.0	200.0			
44RU105	QBF-	1916.8	3.7	74WA	1917.0	3.7			
45RH105F	QBF-	565.0	2.9	74WA	566.9	2.9			
41NB106	QBF-	9900.0	0.0	76AH					
42MO106	QBF-	3340.0	0.0	69GA					
43TC106	QBF-	6300.0	1000.0	74WA					
44RU106	QBF-	39.4	0.3	71WA	39.4	0.3			
45RH106M	QBF-	3678.0	9.0	74WA					
45RH106F	QBF-	3540.0	9.0	74WA	3541.0	9.0			
42MO107	QBF-	6190.0	0.0	69GA					
43TC107	QBF-	4200.0	1000.0	74WA					
44RU107	QBF-	3150.0	300.0	74WA	3150.0	300.0			
45RH107	QBF-	1510.0	40.0	74WA	1510.0	40.0			
46PD107F	QBF-	33.1	3.0	74WA	33.1	3.0			
42MO108	QBF-	4900.0	0.0	72ND					
43TC108	QBF-	7990.0	0.0	69GA					
44RU108	QBF-	1320.0	100.0	75FE	1200.0	850.0			
45RH108M	QBF-	4500.0	600.0	74WA					
45RH108F	QBF-	4500.0	600.0	74WA	4500.0	600.0			
47AG108M	QBF+	2028.0	11.0	74WA					
47AG108F	QBF-	1643.0	8.0	74WA	1649.0	8.0			
43TC109	QBF-	6280.0	0.0	69GA					
44RU109M	QBF-	4300.0	1000.0	74WA					
44RU109F	QBF-	4300.0	1000.0	74WA					
45RH109	QBF-	2500.0	1000.0	74WA					
46PD109F	QBF-	1116.0	2.0	76EN	1115.9	2.0			
48CD109	QBF+	202.0	0.0						
42MO110	QBF-	5620.0	0.0	76JA					
43TC110	QBF-	8000.0	0.0	76JA					
44RU110	QBF-	1810.0	0.0	69GA					
45RH110M	QBF-	5400.0	100.0	74WA					
45RH110F	QBF-	5400.0	100.0	74WA	5400.0	100.0			
47AG110M	QBF-	3009.1	2.0	74WA					
47AG110F	QBF-	2892.0	2.0	75PE	2892.8	1.9			
44RU111	QBF-	5560.0	0.0	76JA					
45RH111	QBF-	3500.0	1000.0	74WA					
46PD111M	QBF-	2372.0	50.0	74WA					
46PD111F	QBF-	2200.0	50.0	74WA	2200.0	50.0			
47AG111M	QBF-	1088.0	3.0	71ND					
47AG111F	QBF-	1028.0	3.0	71ND	1028.0	3.0			
43TC112	QBF-	10420.0	0.0	76JA					
44RU112	QBF-	3630.0	0.0	76JA					
45RH112	QBF-	7170.0	0.0	76JA					
46PD112	QBF-	293.0	19.0	74WA	293.0	19.0			
47AG112	QBF-	3958.0	29.0	74WA	3958.0	29.0			
44RU113	QBF-	6660.0	0.0	76JA					
45RH113	QBF-	5240.0	0.0	76JA					
46PD113	QBF-	3500.0	1000.0	74WA					
47AG113M	QBF-	2060.0	0.0	74WA					
47AG113F	QBF-	2010.0	20.0	77WA	2010.0	20.0			

Table III continued

NUCLIDE	CLEF	ENERGY	ERROR	REF	77WAP		OSIRIS		76LOH	AMES
48CD113M	QBF-	583.7	7.0	74WA						
45RH114	QBF-	8270.0	0.0	76JA						
46PD114	QBF-	1450.0	0.0	75BR						
47AG114M	QBF-	4860.0	140.0	74WA						
47AG114F	QBF-	4860.0	140.0	77WA	4860.0	140.0				
49IN114M	QBF+	1638.0	7.0	74WA						
49IN114F	QBF-	1983.8	2.8	74WA	1984.6	2.7				
46PD115	QBF-	4620.0	0.0	69GA						
47AG115M	QBF-	3180.0	100.0	71WA						
47AG115F	QBF-	3180.0	100.0	74WA	3180.0	100.0				
48CD115M	QBF-	1608.6	9.0	77WA						
48CD115F	QBF-	1447.6	2.0	77WA	1447.6	2.0				
49IN115M	QBF-	829.0	8.0	74WA						
49IN115F	QBF-	493.0	8.0	74WA	495.0	8.0				
46PD116	QBF-	2610.0	200.0	75BR						
47AG116M	QBF-	6200.0	0.0	69GA						
47AG116F	QBF-	6100.0	1000.0	74WA			5300.0	200.0		
49IN116N	QBF-	3380.0	0.0	67LE						
49IN116F	QBF-	3271.0	8.0	74WA	3273.0	8.0				
46PD117	QBF-	5720.0	0.0	69GA						
47AG117M	QBF-	4180.0	100.0	77WA						
47AG117F	QBF-	4180.0	100.0	77WA	4180.0	100.0	4180.0	100.0		
48CD117M	QBF-	2526.0	14.0	74WA						
48CD117F	QBF-	2526.0	14.0	74WA	2528.0	14.0				
49IN117M	QBF-	1769.3	8.0	74WA						
49IN117F	QBF-	1454.0	8.0	74WA	1455.0	8.0				
46PD118	QBF-	3850.0	0.0	69GA						
47AG118M	QBF-	7230.0	0.0	69GA						
47AG118F	QBF-	7230.0	0.0	69GA						
48CD118	QBF-	740.0	300.0	71WA	750.0	300.0				
49IN118M	QBF-	4200.0	300.0	71WA						
49IN118N	QBF-	4200.0	200.0	71WA						
49IN118F	QBF-	4200.0	300.0	71WA	4200.0	300.0				
46PD119	QBF-	6610.0	0.0	76JA						
47AG119	QBF-	5360.0	0.0	69GA						
48CD119F	QBF-	3500.0	300.0	77WA	3500.0	300.0	3940.0	130.0		
49IN119M	QBF-	2639.0	18.0	74WA						
49IN119F	QBF-	2339.0	18.0	74WA	2337.0	18.0				
46PD120	QBF-	4620.0	0.0	76JA						
47AG120M	QBF-	6000.0	0.0	76KO						
47AG120F	QBF-	6000.0	0.0	76KO						
48CD120	QBF-	1720.0	100.0	76KO	1720.0	100.0				
49IN120M	QBF-	5400.0	100.0	77WA						
49IN120F	QBF-	5400.0	100.0	77WA	5400.0	100.0	5430.0	290.0		
47AG121	QBF-	5420.0	0.0	69GA						
48CD121F	QBF-	4500.0	0.0	71WA						
49IN121M	QBF-	3672.0	33.0	74WA						
49IN121F	QBF-	3359.0	27.0	77WA	3359.0	27.0	3410.0	50.0		
50SN121M	QBF-	387.3	2.5	71WA						
50SN121F	QBF-	386.0	2.6	74WA	386.6	2.5				
47AG122	QBF-	8400.0	0.0	69GA						
48CD122	QBF-	2620.0	0.0	69GA						
49IN122M	QBF-	6500.0	200.0	74WA			6300.0	500.0		
49IN122F	QBF-	6500.0	200.0	74WA	6350.0	150.0	6250.0	190.0		
51SB122F	QBF-	1978.2	3.1	74WA	1980.9	3.8				
47AG123	QBF-	7280.0	0.4	69GA						
48CD123	QBF-	5590.0	0.0	69GA						
49IN123M	QBF-	4380.0	40.0	74WA			4690.0	210.0		
49IN123F	QBF-	4380.0	40.0	74WA	4381.0	40.0	4440.0	60.0		
50SN123M	QBF-	1424.0	5.0	74RA						
50SN123F	QBF-	1400.0	5.0	74WA	1397.0	4.0				
52TE123F	QBF+	51.9	2.6	74WA	52.0	2.3				

Table III (continued)

NUCLIDE	CLEF	ENERGY	ERROR	REF	77WAP		OSIRIS		76LOH	AMES
48CD124	QBF-	4700.0	0.0	74FO						
49IN124	QBF-	7140.0	90.0	77WA	7140.0	90.0	7180.0	50.0		
51SB124N	QBF-	2914.0	18.0	74WA						
51SB124F	QBF-	2904.1	1.9	74WA	2905.0	1.9				
47AG125	QBF-	8090.0	0.0	76JA						
48CD125	QBF-	6240.0	0.0	76JA						
49IN125M	QBF-	5400.0	100.0	77WA			5660.0	120.0		
49IN125F	QBF-	5400.0	100.0	77WA	5400.0	300.0	5480.0	80.0		
50SN125M	QBF-	2376.0	8.0	77WA						
50SN125F	QBF-	2350.0	6.0	77WA	2350.0	6.0				
51SB125	QBF-	766.0	2.0	74WA	766.8	2.0				
48CD126	QBF-	4600.0	1000.0	69GA						
49IN126	QBF-	8120.0	120.0	77WA	8120.0	120.0	8060.0	170.0		
50SN126	QBF-	378.0	30.0	77WA	378.0	30.0				
51SB126M	QBF-	3682.0	18.0	77WA						
51SB126F	QBF-	3665.0	32.0	77WA	3665.0	32.0				
49IN127M	QBF-	6430.0	80.0	77WA			6650.0	180.0		
49IN127F	QBF-	6430.0	80.0	77WA	6430.0	80.0				
50SN127M	QBF-	3100.0	100.0	77WA			3206.0	240.0		
50SN127F	QBF-	3100.0	100.0	77WA	3100.0	100.0	3201.0	240.0		
51SB127	QBF-	1581.0	5.0	74WA	1581.0	5.0				
52TE127M	QBF-	781.0	5.0	74WA						
52TE127F	QBF-	693.0	5.0	74WA	694.0	5.0				
48CD128	QBF-	5280.0	0.0	76JA						
49IN128	QBF-	9100.0	200.0	77WA	9100.0	200.0	9310.0	160.0		
50SN128	QBF-	1290.0	10.0	77WA	1290.0	10.0	1290.0	40.0		
51SB128M	QBF-	4250.0	150.0	74WA						
51SB128F	QBF-	4250.0	150.0	74WA	4260.0	150.0	4390.0	40.0		
53 I128	QBF-	2127.0	5.0	74WA	2127.0	5.0				
49IN129M	QBF-	7520.0	120.0	77WA						
49IN129	QBF-	7520.0	120.0	77WA	7520.0	120.0	7600.0	120.0		
50SN129M	QBF-	3900.0	0.0							
50SN129F	QBF-	4000.0	120.0	74WA			4000.0	120.0		
51SB129	QBF-	2376.0	21.0	74WA	2377.0	21.0				
52TE129M	QBF-	1608.5	18.0	74WA						
52TE129F	QBF-	1503.7	3.5	74WA	1498.0	4.0				
53 I129	QBF-	190.8	1.0	77PE	192.0	4.0				
49IN130	QBF-	9300.0	500.0	73KE						
50SN130M	QBF-	5000.0	0.0	73KE			4000.0	310.0		
50SN130F	QBF-	2040.0	100.0	74WA	2000.0	100.0	2190.0	30.0		
51SB130M	QBF-	4970.0	80.0	77WA						
51SB130F	QBF-	4970.0	80.0	77WA	4970.0	80.0	5020.0	80.0		
53 I130F	QBF-	2984.0	10.0	74WA	2984.0	100.0				
49IN131M	QBF-	12780.0	0.0	69GA						
49IN131	QBF-	12780.0	0.0	69GA						
50SN131M	QBF-	4790.0	440.0	77WA						
50SN131F	QBF-	4620.0	300.0	77WA	4620.0	300.0	4590.0	200.0		
51SB131	QBF-	3100.0	1000.0	74WA			3180.0	90.0		
52TE131M	QBF-	2250.0	6.0	76EN						
52TE131F	QBF-	2250.0	6.0	74WA	2249.0	6.0				
53 I131	QBF-	970.8	0.6	71WA	970.8	0.6				
49IN132	QBF-	9800.0	0.0	69GA						
50SN132	QBF-	3220.0	100.0	74WA	3220.0	100.0	3080.0	40.0		
51SB132M	QBF-	5600.0	200.0	77WA						
51SB132F	QBF-	5600.0	200.0	77WA	5600.0	200.0	5530.0	70.0		
52TE132	QBF-	493.0	4.0	77WA	493.0	4.0				
53 I132M	QBF-	3700.0	0.0	73DI						
53 I132F	QBF-	3580.0	20.0	76EN	3580.0	20.0				

Table III (continued)

NUCLIDE	CLEF	ENERGY	ERROR	REF	77WAP		OSIRIS		76LOH + 76OSTIS		AMES	
50SN133	QBF-	7240.0	0.0	69GA								
51SB133	QBF-	3950.0	200.0	74WA	3950.0	200.0						
52TE133M	QBF-	3304.0	100.0	77WA								
52TE133F	QBF-	2970.0	60.0	77WA	2970.0	60.0						
53 I133F	QBF-	1760.0	30.0	76EN	1760.0	30.0						
54XE133F	QBF-	427.3	3.0	74WA	427.3	3.0						
50SN134	QBF-	6070.0	0.0	69GA								
51SB134M	QBF-	8400.0	300.0	72KE								
51SB134F	QBF-	8400.0	300.0	72KE			8240.0	210.0				
52TE134	QBF-	1700.0	300.0	76EN			1560.0	90.0				
53 I134M	QBF-	4466.3	60.0	74WA								
53 I134F	QBF-	4150.0	60.0	76EN	4150.0	60.0						
55CS134F	QBF-	2058.5	0.4	74WA	2058.0	0.4						
50SN135	QBF-	8080.0	0.0	69GA								
51SB135	QBF-	7520.0	0.0	69GA								
52TE135	QBF-	6200.0	250.0	77WA	6200.0	250.0	5950.0	240.0				
53 I135	QBF-	2711.0	30.0	77WA	2711.0	30.0						
54XE135F	QBF-	1159.0	9.0	74WA	1159.0	9.0						
55CS135	QBF-	210.0	5.0	74WA	205.0	5.0						
50SN136	QBF-	6950.0	0.0	69GA								
51SB136	QBF-	9540.0	0.0	69GA								
52TE136	QBF-	5000.0	200.0	75LO								
53 I136M	QBF-	7000.0	100.0	74WA								
53 I136F	QBF-	7000.0	100.0	74WA	7000.0	100.0	6600.0	200.0				
55CS136	QBF-	2547.5	2.0	76EN	2548.1	2.0						
51SB137	QBF-	8150.0	0.0	76JA								
52TE137	QBF-	6480.0	0.0	69GA								
53 I137	QBF-	5500.0	200.0	77WA	5500.0	200.0	5500.0	200.0				
54XE137	QBF-	4344.0	23.0	77WA	4344.0	23.0						
55CS137	QBF-	1173.2	0.9	75BU	1173.2	0.9						
52TE138	QBF-	5340.0	1000.0	69GA								
53 I138	QBF-	8300.0	1000.0	77WA			7300.0	500.0				
54XE138	QBF-	2740.0	50.0	74WA	2740.0	50.0					2830.0	80.0
55CS138M	QBF-	5369.9	70.0	76PA								
55CS138F	QBF-	5290.0	70.0	76MA					5300.+		5290.0	70.0
52TE139	QBF-	7610.0	0.0	69GA								
53 I139	QBF-	6700.0	0.0	69GA			6000.0	400.0				
54XE139	QBF-	4880.0	60.0	73AD	4880.0	60.0	4570.0	200.0			4880.0	60.0
55CS139	QBF-	4290.0	70.0	74WA	4290.0	70.0	4440.0	60.0	4196.+	10+	4290.0	70.0
56BA139	QBF-	2307.0	5.0	76EN	2306.0	5.0						
52TE140	QBF-	6100.0	0.0	69GA								
53 I140	QBF-	8930.0	0.0	69GA								
54XE140	QBF-	4060.0	60.0	74WA							4060.0	60.0
55CS140	QBF-	6050.0	250.0	74WA					6150.+	50.+	5800.0	100.0
56BA140	QBF-	1035.0	10.0	74WA	1035.0	10.0						
57LA140	QBF-	3760.8	2.0	74WA	3760.5	2.0						
52TE141	QBF-	8400.0	0.0	76JA								
53 I141	QBF-	7420.0	0.0	69GA								
54XE141	QBF-	6000.0	100.0	73AD	6000.0	100.0					6000.0	100.0
55CS141	QBF-	4990.0	80.0	73AD	4980.0	80.0			5177.+	25.+	4980.0	80.0
56BA141	QBF-	3030.0	50.0	74WA	3030.0	50.0					3010.0	60.0
57LA141	QBF-	2430.0	30.0	73AD	2430.0	30.0						
58CE141	QBF-	580.9	1.5	74WA	580.0	1.5						
54XE142	QBF-	4900.0	100.0	73AD	4900.0	100.0					4900.0	100.0
55CS142	QBF-	6900.0	100.0	73AD	6870.0	90.0			7266.+	40.+	6890.0	60.0
56BA142	QBF-	2200.0	100.0	71WA	2200.0	100.0						
57LA142	QBF-	4517.0	6.0	71WA	4517.0	6.0						
59PR142F	QBF-	2164.0	1.9	74WA	2158.8	2.6						
54XE143	QBF-	6650.0	0.0	69GA								
55CS143	QBF-	5650.0	200.0	77WA	5650.0	200.0			6000.+	30.+		
56BA143	QBF-	4200.0	1000.0	74WA								
57LA143	QBF-	3380.0	40.0	74WA	3300.0	80.0						

Table III (continued)

NUCLIDE	CLEF	ENERGY	ERROR	REF	77WAP		OSIRIS	76LOH + 76OSTIS		AMES
58CE143	QBF-	1444.0	5.0	74WA	1455.0	3.6				
59PR143	QBF-	932.1	2.0	74WA	935.3	1.9				
54XE144	QBF-	4670.0	0.0	69GA						
55CS144	QBF-	8050.0	0.0	69GA	8100.0	300.0		8140.+	100.+	
56BA144	QBF-	2900.0	1000.0	74WA						
57LA144	QBF-	5300.0	300.0	75MO						
58CE144	QBF-	315.5	1.5	74WA						
59PR144M	QBF-	3055.6	18.0	74WA						
59PR144F	QBF-	2996.6	2.9	74WA						
54XE145	QBF-	6300.0	1000.0	69GA						
55CS145	QBF-	6100.0	500.0	74WU						
56BA145	QBF-	4150.0	300.0	76PF						
57LA145	QBF-	3700.0	200.0	76PF						
58CE145	QBF-	2500.0	100.0	76PF	2500.0	90.0				
59PR145	QBF-	1805.0	10.0	71WA	1805.0	10.0				
55CS146	QBF-	8540.0	0.0	69GA						
56BA146	QBF-	2970.0	0.0	69GA						
57LA146M	QBF-	5950.0	150.0	76MO						
57LA146F	QBF-	5950.0	150.0	76MO						
58CE146	QBF-	1080.0	60.0	76EN	1080.0	60.0				
59PR146	QBF-	4080.0	100.0	71WA	4080.0	100.0				
54XE147	QBF-	7870.0	0.0	76JA						
55CS147	QBF-	7000.0	0.0	76JA						
56BA147	QBF-	5520.0	0.0	69GA						
57LA147	QBF-	4700.0	1000.0	74WA						
58CE147	QBF-	3200.0	1000.0	74WA						
59PR147	QBF-	2700.0	200.0	71WA	2700.0	200.0				
60ND147	QBF-	894.5	1.0	74WA	895.8	0.9				
61PM147	QBF-	224.5	0.4	67ND	224.7	0.4				
56BA148	QBF-	3920.0	0.0	69GA						
57LA148	QBF-	6930.0	0.0	69GA						
58CE148	QBF-	1800.0	1000.0	74WA						
59PR148M	QBF-	3960.0	150.0	76MO						
59PR148F	QBF-	3960.0	150.0	76MO						
61PM148M	QBF-	2464.0	9.0	76EN						
61PM148F	QBF-	2464.0	9.0	76EN	2464.0	9.0				
57LA149	QBF-	5400.0	0.0	76JA						
58CE149	QBF-	3900.0	1000.0	74WA						
59PR149	QBF-	3000.0	0.0	76PI	3000.0	200.0				
60ND149	QBF-	1680.0	7.0	76EN	1689.0	4.0				
61PM149	QBF-	1072.0	2.0	71WA	1071.3	3.7				
57LA150	QBF-	7740.0	0.0	76JA						
58CE150	QBF-	2360.0	0.0	69GA						
59PR150	QBF-	5000.0	1000.0	74WA						
61PM150	QBF-	3500.0	80.0	71WA	3500.0	80.0				
58CE151	QBF-	4610.0	0.0	76JA						
59PR151	QBF-	3500.0	1000.0	74WA						
60ND151	QBF-	2441.0	10.0	77WA	2441.0	10.0				
61PM151	QBF-	1188.0	10.0	71WA	1188.0	10.0				
62SM151	QBF-	76.1	0.6	74WA	76.1	0.6				
59PR152	QBF-	6130.0	0.0	76JA						
60ND152	QBF-	1120.0	150.0	74WA	1150.0	130.0				
61PM152M	QBF-	3600.0	200.0	71DA						
61PM152F	QBF-	3500.0	150.0	74WA	3470.0	130.0				
63EU152N	QBF-	1877.0	0.0	71BA						
63EU152F	QBF-	1821.0	4.0	74WA	1819.2	3.3				
59PR153	QBF-	4900.0	0.0	76JA						
60ND153	QBF-	3400.0	1000.0	74WA						
61PM153	QBF-	1800.0	100.0	71WA	1800.0	100.0				
62SM153	QBF-	808.6	3.5	74WA	805.2	2.9				
60ND154	QBF-	1700.0	0.0	69GA						
61PM154M	QBF-	3900.0	140.0	74WA	4000.0	100.0				

Table III (continued)

NUCLIDE	CLEF	ENERGY	ERROR	REF	77WAP		OSIRIS	76LOH	AMES
61PM154F	QBF-	3900.0	200.0	71DA					
63EU154	QBF-	1975.9	3.7	74WA	1978.0	5.0			
60ND155	QBF-	3990.0	0.0	76JA					
61PM155	QBF-	3100.0	1000.0	74WA					
62SM155	QBF-	1624.0	5.0	74WA	1629.4				
63EU155	QBF-	246.6	2.9	71WA	246.0	2.9			
61PM156	QBF-	5340.0	0.0	69GA					
62SM156	QBF-	735.0	13.0	76BU	714.0	11.0			
63EU156	QBF-	2453.0	9.0	74WA	2433.0	9.0			
61PM157	QBF-	4040.0	0.0	76JA					
62SM157	QBF-	2600.0	200.0	73KA	2600.0	200.0			
63EU157	QBF-	1360.0	15.0	74WA	1360.0	15.0			
62SM158	QBF-	1090.0	0.0	69GA					
63EU158	QBF-	3430.0	120.0	74WA	3450.0	80.0			
62SM159	QBF-	3270.0	0.0	76JA					
63EU159	QBF-	2630.0	50.0	71WA	2630.0	30.0			
64GD159	QBF-	971.4	2.3	74WA	974.7	1.8			
63EU160	QBF-	4400.0	1000.0	74WA					
65TB160	QBF-	1838.8	2.1	74WA	1833.4	1.7			
63EU161	QBF-	3470.0	0.0	76JA					
64GD161	QBF-	1959.0	1.7	77WA	1959.1	1.7			
65TB161	QBF-	590.5	1.7	77WA	590.5	1.7			
63EU162	QBF-	5420.0	0.0	76JA					
64GD162	QBF-	1400.0	100.0	70CH	1400.0	100.0			
65TB162M	QBF-	2460.0	70.0	74WA					
65TB162F	QBF-	2420.0	70.0	74WA	2420.0	70.0			
64GD163	QBF-	2450.0	0.0	69GA					
65TB163	QBF-	1700.0	50.0	74WA	1700.0	50.0			
64GD164	QBF-	1580.0	0.0	69GA					
65TB164	QBF-	3860.0	150.0	74WA	3860.0	150.0			
65TB165	QBF-	2950.0	0.0	76JA					
66DY165M	QBF-	1399.0	0.0	74BU					
66DY165F	QBF-	1291.0	4.0	74BU	1285.1	3.9			
65TB166	QBF-	4920.0	0.0	69GA					
66DY166	QBF-	481.0	5.0	74WA	484.0	5.0			
67HO166M	QBF-	1865.0	1.5	74WA					
67HO166F	QBF-	1856.1	1.5	74WA	1854.3	1.7			
66DY167	QBF-	2350.0	60.0	77TU					
67HO167	QBF-	970.0	20.0	76EN	970.0	20.0			
66DY168	QBF-	920.0	0.0	69GA					
67HO168	QBF-	2750.0	8.0	74WA	2720.0	100.0			
66DY169	QBF-	2850.0	0.0	69GA					
67HO169	QBF-	2124.0	24.0	77WA	2124.0	20.0			
68ER169	QBF-	352.2	1.5	71WA	352.0	1.5			
66DY170	QBF-	2090.0	0.0	69GA					
67HO170M	QBF-	4000.0	200.0	74KA					
67HO170F	QBF-	4000.0	200.0	74KA	4000.0	200.0			
69TM170	QBF-	967.0	0.0	67LE					

Table IV

Brief Comparison of Mass Formulas

Authors	Features	No. of Coefficients	Fitted to	Goodness of Fit†	σ + for F.P.
Myers	Improvement of droplet model via higher-order terms	16	1971 W-G*	Fig. 3, p. 415	0.020
Groote, Hilf, Takahashi	Shell correction from bunching of average single-particle spectra	50	1975 W-B*	$\sigma = 0.67$	0.0205
Seeger Howard	Shell and deformation energies from Nilsson model and BCS pairing	9	1971 W-G	$\sigma = 0.704$§	0.019
Liran Zeldes	Strong pairing, lowest seniority, some single-nucleon excitation	178	1975 W-B	$\sigma = 0.276$	0.0127
Bauer	Liquid-drop parameters which depend on shell structure	11	1971 W-G	Fig. 3, p. 448	
Beiner, Lombard, Mas	Self-consistent energy-density method	12	1971 W-G	Fig. 2, p. 453	
Jänecke	Garvey-Kelson method $M(N,Z) = g_1(N) + g_2(Z) + g_3(A)$	500	1975 W-B	$\sigma = 0.118$	0.010
Comay Kelson	Average values and uncertainties from ensembles of G-K mass tables	Subsets of known masses	1975 W-B	$<\|M - M_{exp}\|> = 0.102$	0.016
Jänecke Eynon	Inhomogeneous partial difference equation solved	220	1975 W-B	$\sigma = 0.289$	0.014

*1971 W-G 1971 Atomic Mass Evaluation, A. H. Wapstra and N. B. Gove, NUCLEAR DATA TABLES **9**, 267 (1971). 1160 values
1975 W-B 1975 Midstream Atomic Mass Evaluation, A. H. Wapstra and K. Bos, this issue. 1300 values

†Of course, a good fit to presently known masses is not necessarily an indication of good fit to masses of nuclei far from stability which will be measured in the future

§For binding energies. Values of other authors are for masses or mass excesses

σ Root-mean-square error, $[(x_i - \bar{x})^2/n]^{1/2}$, in MeV

σ_+ calculated with the 700 isotopes of TABLE V

Table V

Calculated half lives

Nuclide	T1/2 (present work) S	T1/2 (ENDF B/4) S	T1/2 (YOSHIDA) S	QB. (KeV)	Ref.
29CU 71	1.0			4530.	69GAR
29CU 72	0.5	6.	4.4	8260.	69GAR
29CU 73	0.5	3.9	9.6	6150.	69GAR
30ZN 78	1.6	2.42	7.2	5600.	77WAR
30ZN 79	0.35	0.38	1.3	8660.	76JAN
31GA 84	0.2	0.098	0.2	13710.	76JAN
32GE 85	0.4	0.23	0.5	10080.	76JAN
32GE 86	0.26	0.25	0.4	9060.	76JAN
33AS 88	0.19	0.12	0.25	13010.	76JAN
34SE 90	0.2	0.55	1.0	7470.	69GAR
34SE 92	0.1	0.24	0.34	8730.	69GAR
36KR 95	0.1	0.50	0.64	9650.	76JAN
39 Y101	0.8	0.97	2.1	7700.	"
39 Y102	0.5	0.27	0.7	10830.	"
40ZR103	1.	1.77	3.6	7000.	"
40ZR104	0.1	3.7	6.4	5150.	
42MO110	0.2	1.89	3.8	5620.	76JAN
43TC112	0.12	0.35	0.8	10420.	"
45RH113	0.9	0.90	17.	5240.	"
45RH114	0.4	1.7	3.2	8270.	"
46PD119	1.1	1.71	4.4	6610.	"
46PD120	0.35	4.27	9.7	4620.	"
47AG125	0.15	0.38	1.3	8090.	"
48CD125	0.5	1.66	5.9	6240.	"
48CD128	0.15	1.29	4.4	5280.	"
50SN135	0.2	0.29	1.32	8080.	69GAR
50SN136	0.2	0.41	0.9	6950.	"
51SB137	0.1	0.28	1.1	8150.	76JAN
51SB138	0.1	0.13	0.59	10670.	
52TE139	0.7	0.42	1.7	7610.	69GAR
52TE140	0.5	0.75	1.8	6100.	"
52TE141	0.55	0.23	0.9	8400.	76JAN
54XE144	0.3	1.	7.2	4670.	69GAR
54XE147	0.1	0.26	2.5	7870.	76JAN
57LA149	0.25	2.86	11.	5400.	"
57LA150	0.4	0.64	3.6	7740.	"
58CE151	0.34	1.0	28.	4610.	"
59PR152	0.4	8.31	14.	6130.	"
59PR153	0.3	7.74	19.	4900.	"
60ND153	14.	67.	161.	3400.	74WAP
60ND154	33.	6.E05	2.E04	1790.	69GAR
60ND155	1.2	26.01	63.	3990.	76JAN
61PM155	4.	36.	272.	3100.	74WAP
61PM156	1.7	13.1	33.	5340.	69GAR
61PM157	1.	68.0	58.	4040.	76JAN
62SM158	2.2M	2638.5	1.E04	1090.	69GAR
62SM159	160.	162.2	195.	3270.	76JAN
63EU161	25.	42.05	136.	3470.	76JAN
63EU162	5.	269.8	29.	5420.	"
64GD163	0.5	92.7	1000.	2450.	69GAR
64GD164	1.0	1301.4	1712.	1580.	"
65TB165	30.	32.75	344.	2950.	76JAN
65TB166	52.		51.	4920.	69GAR
66DY168	1.6H		2.7E04	920.	"
66DY169	7.1		411.	2850.	"

Table VI - Half lives of the French file and some other works
(for references see end of Table)

NUCLIDE,	T1/2	DT1/2		REFE	Other works
29CU 71	1.00	.0	S	68DET	
30?N 71M	3.92	.500E-01	H	73ALV	
30?N 71F	2.40	.200	M	73ALV	
29CU 72	.500	.0	S	68DET	
30?N 72	46.5	.100	H	74ALV	
31GA 72	14.1	.200	H	74ALV	14.1 ± .2 H /d/
29CU 73	.500	.0	S	76BLA	
30ZN 73	23.5	1.00	S	72ERD	
31GA 73	4.91	.500E-01	H	74ALV	
32GE 73M	.530	.300E-01	S	66NDS	
30?N 74	98.0	2.00	S	76KOC	
31GA 74	8.25	.500E-01	M	71CAM	
30?N 75	10.2	.300	S	73RUD	
31GA 75	126.	2.00	S	73RUD	
32GE 75M	48.3	.600	S	75HOR	
32GE 75F	82.8	.400E-01	M	75HOR	
30?N 76	5.70	.500	S	73RUD	
31GA 76	27.6	1.10	S	73RUD	
33AS 76	26.3	.700E-01	H	72EME	26.32 ± .07 H /d/
30?N 77	1.40	.300	S	70GRA	
31GA 77	12.7	2.00	S	70GRA	
32GE 77M	54.0	1.00	S	70GRA	
32GE 77F	11.3	.100	H	73RAM	11.30 ± .01 H /d/
33AS 77	38.8	.300	H	68ARD	38.8 ± .3 H /d/
34SE 77M	17.5	.100	S	66NDS	
30?N 78	1.60	.0	S	76BLA	
31GA 78	5.09	.500E-01	S	73RUD	
32GE 78	87.0	1.00	M	75URO	
33AS 78	90.7	.200	M	76END	
30ZN 79	.350	.0	S	76BLA	
31GA 79	3.00	.800E-01	S	73RUD	2.63 ± .09 S /e/
32GE 79	42.0	2.00	S	70KAR	
33AS 79	8.20	.0	M	70GRA	
34SE 79M	3.91	.500E-01	M	75URO	
34SE 79F	.650E+05	.0	A	66NDS	
35BR 79M	4.88	.500E-01	S	75URO	
31GA 80	1.70	.200	S	70GRA	1.66 ± .02 S /e/
32GE 80	24.5	1.00	S	72DEL	
33AS 80	16.5	.300	S	71MCM	
35BR 80M	4.42	.100E-01	H	75GRE	
35BR 80F	17.6	.0	M	66NDS	
31GA 81	1.23	.100E-01	S	75RUD	
32GE 81	10.1	.800	S	72DEL	
33AS 81	35.8	1.60	S	74CHA	
34SE 81M	57.3	.100	M	69ZOL	
34SE 81F	18.5	.100	M	75LEM	
36KR 81M	13.0	.0	S	66NDS	
36KR 81F	.210E+06	.0	A	66NDS	2.165 ± .2 A /d/
31GA 82	.600	.100E-01	S	75RUD	0.60 ± .01 S /e/
32GE 82	4.60	.350	S	72DEL	
33AS 82M	13.0	.600	S	70KAR	
33AS 82F	21.0	2.00	S	76END	
35BR 82M	6.13	.800E-01	M	75LEM	
35BR 82F	35.4	.100	H	69LIU	35.30 ± .03 H /d/
31GA 83	.310	.100E-01	S	75RUD	
32GE 83	1.90	.300	S	72DEL	
33AS 83	13.3	.500	S	75KRA	
34SE 83M	70.4	.300	S	67SCH	
34SE 83F	22.6	.0	M	67MAR	
35BR 83	2.39	.200E-01	H	75KOC	
36KR 83M	1.86	.100E-01	H	73MAR	
31GA 84	.200	.0	S	76BLA	
32GE 84	1.20	.300	S	72DEL	
33AS 84	5.40	.0	S	72KRA	
34SE 84	3.10	.200	M	68REN	
35BR 84M	6.00	.0	M	70HAT	
35BR 84F	31.8	.800	M	70HAT	
32GE 85	.400	.0	S	76BLA	
33AS 85	2.05	.0	S	72KRA	2.08 ± .05 S /e/
34SE 85	31.4	1.00	S	75HUR	
35BR 85	175.	4.00	S	73RUD	
36KR 85M	4.48	.100E-01	H	73MAR	4.48 ± .01 H /d/
36KR 85F	10.7	.600E-01	A	73MAR	
32GE 86	.260	.0	S	76BLA	
33AS 86	.800	.0	S	72KRA	
34SE 86	16.0	.0	S	60NDS	
35BR 86	54.0	.0	S	72ACH	
37RB 86M	61.0	.0	S	67YUL	
37RB 86F	18.8	.0	J	67LED	18.66 ± .02 J /d/
33AS 87	.300	.0	S	72KRA	
34SE 87	5.80	.0	S	71NDS	
35BR 87	55.7	.0	S	67DEL	55.5 ± .3 S /e/
36KR 87	76.3	.500	M	73MAR	76.3 ± .5 M /d/

Table VI (continued)

NUCLIDE.	T1/2	DT1/2	REFE	Other works	
37RB 87	.472E+11	.400E-01A	66MCM		
38SR 87M	2.83	.200E-01H	67LED		
33AS 88	.190	.0 S	76BLA		
34SE 88	1.52	.600E-01S	77PFE		
35BR 88	16.3	.300 S	76BUN	16.5 ± 0.5 S /e/	
36KR 88	2.80	.200E-01H	72EHR	2.84 ± 0.02 H /a/	
37RB 88	17.8	.110 M	69RAG	17.8 ± 0.1 M /d/	
34SE 89	.410	.400E-01S	71TOM		
35BR 89	4.55	.100 S	70GRA		
36KR 89	3.18	.200E-01M	69CAR	3.17 ± 0.02 M /d/	
37RB 89	15.1	.110 M	66KIT	15.2 ± 0.1 M /d/	
38SR 89	50.8	.250 J	72LAG	50.5 ± 0.1 J /d/	
39 Y 89M	16.1	.400E-01S	67YUL		
34SE 90	.200	.0 S	76BLA		
35BR 90	1.96	.500E-01S	75RUD	1.96 ± 0.05 S /e/	
36KR 90	32.3	.900E-01S	70MAS		
37RB 90M	4.18	.100 M	69CAR		
37RB 90F	2.55	.500E-01M	69CAR		
38SR 90	28.1	.800 A	75KOC	28.15 ± 0.1 A /b/	28.5 ± 0.8 A /d/
39 Y 90M	3.19	.0 H	73HAN		
39 Y 90F	64.2	.0 H	68LAG	64.0 ± 0.1 J /d/	
40ZR 90M	.830	.300E-02S	70MAS		
34SE 91	.270	.500E-01S	75GAU		
35BR 91	.541	.500E-02S	75RUD	0.541 ± 0.005 S /e/	
36KR 91	8.57	.400E-01S	69CAR		
37RB 91	58.2	.200 S	69CAR	59.6 ± 0.2 S /g/	
38SR 91	9.48	1.00 H	69KNI		
39 Y 91M	49.7	.400E-01M	69KNI		
39 Y 91F	58.5	.0 J	71BAB		
34SE 92	.100	.0 S	68DET		
35BR 92	.365	.700E-02S	75RUD	0.365 ± 0.007 S /e/	
36KR 92	1.92	.700 S	72OLS		
37RB 92	4.48	.300E-01S	72OLS	4.34 ± 0.06 S /e/	4.57 ± 0.07 S /g/
38SR 92	2.71	.100E-01H	71PAR		
39 Y 92	3.53	.200E-01H	66NOR		
36KR 93	1.20	.100 S	72AMI	1.33 ± 0.05 S /e/	
37RB 93	5.89	.400E-01S	67GAU	5.85 ± 0.03 S /e/	5.92 ± 0.09 S /g/
38SR 93	7.30	.100 M	71CAV		
39 Y 93M	1.70	.500 S	74SCH		
39 Y 93F	10.1	.200 H	69GUN		

Table VI (continued)

NUCLIDE,	T1/2	DT1/2	REFE	Other works		
40ZR 93	.153E+07	.100E+07A	72KOC			
41NB 93M	16.4	.400 A	77LLO			
36KR 94	.200	.100E-01S	67AMI			
37RB 94	2.67	.400E-01S	67GAU	2.69 ± 0.02 S /e/	2.81 ± 0.04 S /g/	
38SR 94	76.1	.300 S	73GRI	76.6 ± 1.0 S		
39 Y 94	18.7	.100 M	71CAV			
41NB 94M	6.26	.100E-01M	73KOC	6.26 ± 0.01 M /d/		
41NB 94F	.203E+05	.0 A	73KOC	2.03 E 4 + 0.16 A /d/		
36KR 95	.100	.0 S	76BLA			
37RB 95	.360	.200E-01S	67GAU	0.400 ± 0.004 S /e/	0.402 ± 0.008 S /g/	
38SR 95	28.0	3.00 S	73RUD	25.1 + 0.2 S /g/		
39 Y 95	10.6	.300 M	71CAV			
40ZR 95	64.0	.600E-01J	71DEB			
41NB 95M	86.6	.800 H	69FOI			
41NB 95F	35.1	.300E-01J	72MFD			
37RB 96	.280	.500E-01S	67GAU	0.203 ± 0.003 S /e/	0.225 ± 0.012 S /g/	
38SR 96	.900	.0 S	74LOH	1.103 ± 0.022 S /g/		
39 Y 96M	6.00	.300 S	75SAD	6.32 ± 0.18 S /g/		
39 Y 96F	10.0	.300 S	75SAD	9.6 ± 0.3 S /a/		
41NB 96	23.4	.0 H	67LED			
37RB 97	.172	.500E-02S	74ROE	0.150 ± 0.030 S /f/	0.181 ± 0.010 S /g/	
38SR 97	.430	.500E-01S	75LOH	0.400 ± 0.100 S /f/		
39 Y 97M	1.21	.300E-01S	76MON	1.5 ± 0.3 S /a/	1.1 ± 0.16 S /f/	1.5 ± 01 S /g/
39 Y 97F	3.70	.200 S	76MON	3.6 ± 0.3 S /a/	3.3 ± 0.2 S /g/	
40ZR 97	17.0	.200 H	73MED	16.90 ± 0.05 H /d/		
41NB 97M	60.0	8.00 S	73MED	60 ± 1. S /d/		
41NB 97F	72.0	.700 M	73MED	72.1 ± 0.7 M /d/		
37RB 98	.131	.0 S	70KLA	0.108 ± 0.013 S /f/	0.098 ± 0.018 S /g/	
38SR 98	.650	.500E-01S	76SIS	0.670 ± 0.090 S /f/	0.6 ± 0.1 S /g/	
39 Y 98M	2.00	.200 S	77SIS	2.1 ± 0.3 S /g/		
39 Y 98F	.650	.500E-01S	77SIS			
40ZR 98	30.7	.400 S	76HER			
41NB 98M	51.3	.400 M	76HER			
41NB 98F	2.86	.600E-01S	76HER			
43TC 98	.420E+07	.300E+06Y	76END			
37RB 99	.760E-01	.0 S	70KLA			
38SR 99	.600	.200 S	75GAU			
39 Y 99	1.50	.500 S	75LOH			
40ZR 99	2.40	.200 S	72TRA	2.0 ± 0.2 S /a/		
41NB 99M	2.60	.200 M	71CAV			
41NB 99F	15.0	.200 S	72TRA			
41NB 99	15.0	.200 S	72TRA			
42MO 99	66.0	.100E-01H	72EME	66.0 ± 0.2 H /d/		
43TC 99M	6.02	.300E-01H	70NDT	6.02 ± 0.03 H /d/		

Table VI (continued)

NUCLIDE,	T1/2	DT1/2		REFE	Other works	
43TC 99F	.213E+06	.0	A	70MOT		
39 Y100	.800	.300	S	75LOH		
40ZR100	7.10	.400	S	74KOC	7.1 ± 0.4 S /a/	
41NB100M	3.10	.300	S	74KOC	3.1 ± 0.3 S /a/	
41NB100F	1.50	.300	S	74KOC	1.5 ± 0.2 S /a/	
43TC100	15.8	.0	S	69BER		
39 Y101	.800	.0	S	76BLA		
40ZR101	2.00	.300	S	72TRA	2.0 ± 0.3 S /a/	
41NB101	7.10	.300	S	72TRA	7.1 ± 0.3 S /a/	
42MO101	14.6	.500E-01	M	73TOD		
43TC101	14.2	.100	M	76END		
39 Y102	.500	.0	S	76BLA		
40ZR102	.800	.300	S	72TRA	9.9 + 0.2 S /a/	
41NB102	4.50	.500	S	72TRA	4.3 + 0.4 S /a/	
42MO102	11.5	.0	M	67LED		
43TC102M	4.50	.0	M	69BLA		
43TC102F	5.00	.0	S	69BLA		
40ZR103	1.00	.0	S	76BLA		
41NB103	1.50	.200	S	76KAF	1.5 ± 0.2 S /a/	
42MO103	68.0	1.00	S	76KAF	68.0 ± 1.0 S /a/	
43TC103	54.2	.800	S	76KAF	54.2 ± 0.8 S /a/	
44RU103	39.3	.500E-01	J	75PER	39.276 ± 0.009 J /c/	39.35 ± 0.05 J /d/
45RH103M	56.1	.300E-01	M	75PER	56.112 ± 0.028 M /b/	56.12 ± 0.01 M /d/
40ZR104	.100	.0	S	76BLA		
41NB104M	4.80	.400	S	76AHR	4.8 ± 0.4 S /a/	
41NB104F	.800	.200	S	76AHR	0.8 ± 0.2 S /a/	
42MO104	60.0	2.00	S	76KAF	60.0 + 2.0 S /a/	
43TC104	18.2	.400	M	75TIV	18.5 + 0.5 M /a/	
45RH104M	4.34	.500E-01	M	76SAM		
45RH104F	42.3	.400	S	76SAM		
41NB105	2.80	.300	S	76AHR		
42MO105	36.0	2.00	S	76KAF	36.0 ± 2.0 S /a/	
43TC105	7.70	.400	M	67KAU	7.6 ± 0.1 M /a/	
44RU105	4.40	.200E-01	H	74BER		
45RH105M	45.0	.0	S	74BER		
45RH105F	35.4	.600E-01	H	74BER		
41NB106	1.00	.0	S	76AHR	1. S /a/	
42MO106	8.20	1.00	S	76AHR	8.2 ± 1.0 S /a/	
43TC106	36.0	.0	S	70HER	36.0 ± 0.1 S /a/	
44RU106	369.	2.00	J	70NDT	371.63 ± 0.17 J /c/	
45RH106M	2.18	.0	H	71TAK		
45RH106F	29.9	.100	S	76END		
42MO107	3.50	.500	S	76KAF	3.5 ± 0.5 S /a/	
43TC107	21.2	.200	S	70WIL	21.0 ± 1.0 S /a/	

Table VI (continued)

NUCLIDE,	T1/2	DT1/2		REFE	Other works
44RU107	4.55	.0	M	72FRA	
45RH107	21.7	.400	M	72NDS	
46PD107M	22.0	1.00	S	67LED	
46PD107F	.650E+07	.300	A	72NDS	
47AG107M	44.3	.200	S	67LED	
42MO108	1.50	.400	S	72TRA	
43TC108	5.00	.200	S	72TRA	5.0 ± 0.2 S /a/
44RU108	4.50	.200	M	72NDS	4.6 ± 0.1 M /a/
45RH108M	6.90	.200	M	69PIN	
45RH108F	16.8	.500	S	72NDS	17. ± 1. S /a/
47AG108M	127.	21.0	A	72NDS	127. ± 21 A /d/
47AG108F	2.41	.100E-01	M	72NDS	2.37 ± 0.01 M /d/
43TC109	1.40	.400	S	76KAF	1.4 ± 0.4 S /a/
44RU109M	12.9	1.00	S	75FRA	12.9 ± 1.0 S /a/
44RU109F	34.5	2.90	S	70WIL	34.5 ± 1.0 S /a/
45RH109	80.0	.0	S	75FRA	79.8 ± 0.1 S /a/
46PD109M	4.69	.100E-01	M	71BER	
46PD109F	13.5	.200E-01	H	76END	13.46 ± 0.02 H /d/
47AG109M	39.6	.200	S	71BER	
48CD109	453.	6.00	J	75PER	453. ± 2. J /d/
42MO110	.200	.0	S	76BLA	
43TC110	.820	.400E-01	S	72WIL	1.0 ± 0.2 S /a/
44RU110	12.6	.500	S	76KAF	12.6 ± 0.5 S /a/
45RH110M	28.5	1.50	S	70PIN	
45RH110F	3.30	.300	S	75FRA	3.3 ± 0.3 S /a/
47AG110M	250.	1.00	J	75PER	250.8 ± 0.3 J /d/
47AG110F	24.7	.300	S	75PER	24.6 + 0.2 S /d/
44RU111	3.00	1.00	S	75FRA	3. ± 1. S /a/
45RH111	11.0	1.00	S	76KAF	11. ± 1. S /a/
46PD111M	5.50	.200	H	71NDS	
46PD111F	22.0	1.00	M	71NDS	
47AG111M	74.0	3.00	S	71NDS	
47AG111F	7.48	.100E-01	J	71NDS	7.45 ± 0.01 J /d/
48CD111M	49.6	.700	M	72NDS	
43TC112	.120	.0	S	76BLA	
44RU112	3.60	.500	S	75FRA	3.6 ± 0.5 S /a/
45RH112	1.50	.0	S	75FRA	1.5 S /a/
46PD112	20.1	.600	H	71BAB	
47AG120M	.320	.400E-01	S	76KOC	
47AG120F	1.17	.500E-01	S	71BAC	
48CD120	50.8	.210	S	76KOC	
49IN120M	44.4	1.00	S	70GRA	
49IN120F	3.08	.800E-01	S	73SCH	
47AG121	.800	.100	S	73RUD	

NUCLIDE,	T1/2	DT1/2		REFE	Other works
48CD121M	4.50	.400	S	74SCH	
48CD121F	12.0	.500	S	70GRA	
49IN121M	3.76	.600E-01	M	70GRA	
49IN121F	23.1	.600	S	73RUD	
50SN121M	50.0	.0	A	71NDS	
50SN121F	27.1	.400E-01	H	68ERD	
47AG122	1.50	.500	S	71FOG	
48CD122	5.78	.900E-01	S	73SCH	
49IN122M	10.0	.500	S	71TAK	
49IN122F	1.50	.300	S	71TAK	
51SB122M	4.20	.200	M	72NDS	
51SB122F	2.71	.600E-01	J	72EME	2.70 ± 0.01 J /d/
47AG123	.390	.300E-01	S	75RUD	
48CD123	3.80	.100	S	74GRA	
49IN123M	47.8	.500	S	70GRA	
49IN123F	5.97	.500E-01	S	70GRA	
50SN123M	40.1	.700E-01	M	68ERD	
50SN123F	129.	.400	J	72NDS	
52TE123M	120.	.100	J	72NDS	
52TE123F	.120E+14	.0	A	67LED	
48CD124	1.00	.200	S	74GRA	
49IN124	3.17	.500E-01	S	73RUD	
51SB124M	20.2	.200	M	73BER	
51SB124N	93.0	5.00	S	73BER	
51SB124F	60.2	.300E-01	J	73BER	60.20 ± 0.03 J /d/
47AG125	.150	.0	S	76BLA	
48CD125	.500	.0	S	76BLA	
49IN125M	17.9	.0	S	66ERD	
49IN125F	2.33	.0	S	76FOG	
50SN125M	9.52	.500E-01	M	68ERD	
50SN125F	9.64	.300E-01	J	68ERD	
51SB125	2.77	.400E-01	A	72NDS	
52TE125M	57.4	.150	J	77PER	57.4 ± 0.15 J /b/
48CD126	.530	.100	S	74GRA	
49IN126	1.53	.100E-01	S	73RUD	
50SN126	.100E+06	.0	A	73AUB	
51SB126M	19.0	.300	M	71ORT	
51SB126F	12.4	.100	J	71ORT	
49IN127M	3.10	.310	S	70RUD	3.76 ± 0.0d S /e/
49IN127F	1.09	.300E-01	S	73RUD	
50SN127M	4.40	.100	M	72NDS	
50SN127F	2.10	.400E-01	H	72NDS	
51SB127	3.85	.500E-01	J	72NDS	
52TE127M	109.	2.00	J	72NDS	

Table VI (continued)

NUCLIDE.	T1/2	DT1/2		REFE	Other works		
52TE127F	9.35	.700E-01	H	72NDS			
48CD128	.150	.0	S	76BLA			
49IN128	3.70	.500	S	74GRA	0.94 ± 0.05 S /e/		
50SN128	59.1	.500	M	76LEW			
51SB128M	9.10	.300E-01	H	70FOW			
51SB128F	10.0	.500E-01	M	70FOW			
53 I128	25.0	.200E-01	M	73AUB			
49IN129M	1.20	.0	S	74GEE	2.5 ± 0.2 S /e/		
49IN129	.800	.300	S	70GRA	0.99 ± 0.02 S /e/		
50SN129M	7.50	.100	M	66CHU			
50SN129F	2.52	.120	M	72IZA			
51SB129	4.32	.300	H	72NDS			
52TE129M	34.1	.200	J	72EME	33.6 ± 0.1 J /d/		
52TE129F	69.6	.400	M	72NDS	69.6 ± 0.2 M /d/		
53 I129	.157E+08	.400E-01	A	72NDS	1.57 E 7 + 0.04 A /d/		
54XE129M	8.87	.300E-01	J	75HOF	8.0 ± 0.2 J /d/		
49IN130	.530	.500E-01	S	73KER			
50SN130M	1.70	.100	M	73KER			
50SN130F	3.70	.200	M	74FOW			
51SB130M	40.0	1.00	M	74FOW			
51SB130F	6.30	.200	M	74FOW			
53 I130M	9.20	.0	M	70QUA			
53 I130F	12.4	.100E-01	H	74HID	12.36 ± 0.01 H /d/		
49IN131M	.270	.200E-01	S	74GEE			
49IN131	.300	.100	S	70GRA	0.29 ± 0.01 S /a/		
50SN131M	39.0	2.00	S	76SCH			
50SN131F	50.0	2.00	S	76SCH			
51SB131	23.0	.0	M	70ERT			
52TE131M	30.0	2.00	H	76END			
52TE131F	25.0	1.00	M	76AUB			
53 I131	8.04	.100E-02	J	72EME	8.020 ± 0.003 J /b/	8.02 ± 0.01 J /c/	8.04 ± 0.01 J /d/
54XE131M	11.9	.100	J	72EME	11.9 ± 0.1 J /d/		
49IN132	.120	.200E-02	S	73KER	0.3 ± 0.1 S /e/		
50SN132	39.0	.190	S	72NAE			
51SB132M	4.10	.100	M	70ERT			
51SB132F	2.80	.100	M	76HID			
52TE132	3.24	.0	J	67BEM	76.9 ± 0.3 H /c/	78.2 ± 0.8 H /d/	
53 I132M	83.6	.700	M	73DIK			
53 I132F	2.30	.300E-01	H	76END	2.30 ± 0.03 H /d/		
50SN133	1.70	.300	S	70GRA	1.47 ± 0.07 S /e/		
51SB133	2.43	.0	M	70RUD			
52TE133M	55.4	.400	M	74HEN			

Table VI (continued)

NUCLIDE,	T1/2	DT1/2		REFE	Other works
52TE133F	12.4	.280	M	74HEN	
53 I133M	9.00	.0	S	74HEN	
53 I133F	20.8	.100	H	76END	20.8 ± 0.1 H /d/
54XE133M	2.19	.500E-01	J	75HOF	2.188 ± 0.008 J /d/
54XE133F	5.25	.200E-01	J	75HOF	5.245 ± 0.006 J /d/
50SN134	1.04	.200E-01	S	75RUD	1.04 ± 0.02 S /e/
51SB134M	.850	.100	S	72KER	
51SB134F	10.3	.500	S	72KER	10.3 ± 0.4 S /e/
52TE134	41.8	.800	M	76END	41.8 ± 0.8 M /d/
53 I134M	3.80	.200	M	72COR	
53 I134F	52.6	.500	M	76END	52.6 ± 0.5 M /d/
55CS134M	2.91	.200E-01	H	75PER	
55CS134F	2.06	.500E-02	A	75PER	2.062 ± 0.005 A /d/
50SN135	.200	.0	S	68DET	
51SB135	1.70	.200E-01	S	73TOM	1.82 ± 0.04 S /a/
52TE135	18.0	2.00	S	69DEN	
53 I135	6.70	.0	H	70MAC	6.61 ± 0.01 H /d/
54XE135M	15.6	.100	M	73MAR	15.29 ± 0.03 M /d/
54XE135F	9.15	.200E-01	H	73MAR	9.09 ± 0.01 H /d/
55CS135	.300E+07	.0	A	67LED	
56BA135M	28.7	.200	H	67LED	
50SN136	.200	.0	S	68DET	
51SB136	.820	.200E-01	S	75RUD	0.82 ± 0.02 S /e/
52TE136	20.9	.0	S	70FOL	17.5 ± 0.4 S /e/
53 I136M	48.0	.0	S	74CAR	
53 I136F	83.0	.0	S	74CAR	
55CS136	13.1	.100	D	76END	13.1 ± 0.1 J /d/
56BA136M	.320	.0	S	67LED	
51SB137	.100	.0	S	76BLA	
52TE137	3.50	.500	S	69HER	
53 I137	24.6	.100	S	73RUD	24.25 ± 0.12 S /e/
54XE137	3.83	.100E-01	M	73MAR	
55CS137	30.2	.340E-01	A	75RUN	30.0 ± 0.2 A /d/
56BA137M	2.55	.200E-02	M	76MAR	2.552 ± 0.02 M /d/
52TE138	1.60	.100	S	75GAU	
53 I138	6.46	.150	S	75RUD	6.46 ± 0.15 S /a/
54XE138	14.2	.700E-01	M	73MAR	14.17 ± 0.07 M /d/
55CS138M	2.90	.100	M	71CAR	32.2 ± 0.1 M /d/
55CS138F	32.2	.100	M	76MAR	
52TE139	.700	.0	S	68DET	
53 I139	2.61	.110	S	73TOM	2.30 ± 0.05 S /e/
54XE139	39.7	.700	S	69CAR	
55CS139	8.98	.300	M	70RUD	
56BA139	82.7	.200	M	76END	82.7 ± 0.2 M /d/

NUCLIDE,	T1/2	DT1/2		REFE	Other works
52TE140	.500	.0	S	68DET	
53 I140	.590	.100E-01	S	75RUD	0.59 ± 0.01 S /e/
54XE140	13.6	.100	S	69CAR	
55CS140	63.7	.300	S	69CAR	
56BA140	12.8	.660E-02	J	74PEK	12.746 ± 0.01 J /c/
57LA140	40.2	.200	H	74PEK	40.272 ± 0.007 H /c/
52TE141	.550	.0	S	76BLA	
53 I141	.480	.120	S	71KRA	0.48 ± 0.03 S /e/
54XE141	1.72	.130E-01	S	69CAR	
55CS141	24.9	.400	S	71TAL	29.3 ± 0.1 S /g/
56BA141	18.0	.700E-01	M	69CAR	
57LA141	3.93	.600E-01	H	69CAR	
58CE141	32.4	.130	J	72EME	32.50 ± 0.07 J /d/
54XE142	1.22	.200E-01	S	73LEM	

Table VI (continued)

NUCLIDE,	T1/2	DT1/2		REFF	Other works		
55CS142	1.70	.100	S	73LEM	1.69 ± 0.09 /e/	1.78 ± 0.02 /g/	
56BA142	10.7	.100	M	73LEM			
57LA142	92.7	.700	M	73LEM			
58CE142	.500E+17	.0	A	67NDS			
59PR142M	14.6	.500	M	67KER			
59PR142F	19.1	.400E-01	H	73LEM	19.13 ± 0.04 H /d/		
54XE143	.960	.0	S	67NDS			
55CS143	1.78	.100E-01	S	75RUD	1.78 ± 0.01 /e/	1.78 ± 0.01 /g/	
56BA143	12.0	.0	S	70GRA	15.17 ± 0.38 /g/		
57LA143	15.0	1.00	M	76BLA	14.23 ± 0.14 M /h/		
58CE143	32.7	.0	H	70FAS	33.0 ± .2 H /d/		
59PR143	13.6	.0	J	67NDS	13.56 ± 0.02 J /d/		
54XE144	.350	.0	S	68DET			
55CS144	1.06	.100	S	67GAU	1.00 ± 0.02 /e/	1.011 ± 0.021 /f/	1.02 ± 0.03 /g/
56BA144	10.7	.200	S	74GRA	11.22 ± 0.78 /f/	12.0 ± 0.4 /g/	
57LA144	42.4	.600	S	72OHY	40. ± 3.5 /g/	42.1 ± 0.7 /h/	
58CE144	285.	.800	J	75PER			
59PR144M	7.20	.200	M	70FAS			
59PR144F	17.3	.800E-01	M	75PER	17.28 ± 0.03 M /d/		
60ND144	.210E+16	.0	A	67NDS			
54XE145	.900	.300	S	71WOL	0.589 ± 0.028 /f/		
55CS145	.563	.270E-01	S	71TRA	0.65 ± 0.04 /g/		
56BA145	4.33	.150	S	76PFE	4.24 ± 0.34 /f/	3.79 ± 0.19 /g/	
57LA145	24.0	5.00	S	70FAS	21. ± 5. /g/	25. ± 5. /h/	
58CE145	2.98	.600E-01	M	70FAS	3.0 ± 0.1 M /h/		
59PR145	5.98	.0	H	67NDS			
55CS146	.189	.110E-01	S	71TRA	0343 ± 0.007 /e/	0.315 ± 0.012 /f/	
56BA146	2.00	.400	S	75LOH	2.18 ± 0.11 /f/	2.14 ± 0.37 /g/	
57LA146M	6.20	.500	S	76MON	8.5 ± 1 /h/		
57LA146F	10.0	.500	S	76MON	9.0 ± 0.6 /g/		
58CE146	14.2	.500	M	76END	14.2 ± 0.3 M /h/		
59PR146	24.2	.0	M	67NDS			
54XE147	.100	.0	S	76BLA			
55CS147	.218	.900E-02	S	77WUN			
56BA147	.720	.700E-01	S	76AMI	0.72 ± 0.07 /g/		
57LA147	4.00	1.00	S	75LOH	4.43 ± 0.54 /g/	2.2 ± 0.4 /h/	
58CE147	55.0	3.00	S	75LOH	56.7 ± 2.3 /h/		
59PR147	12.5	.400	M	70FAS	12.0 ± 0.2 M /h/		
60ND147	11.1	.160	J	67NDS	11.06 ± 0.03 J /d/		
61PM147	2.62	.100E-01	A	67NDS	2.6234 ± .0002 A /d/		
62SM147	.107E+08	12.0	A	67NDS			
56BA148	.470	.200	S	76AMI	0.47 ± 0.20 /g/		

Table VI (continued)

NUCLIDE,	T1/2	DT1/2		REFF	Other works	
57LA148	1.70	.300	S	75LOH	2.62 ± 0.61 /g/	1.0 /h/
58CE148	48.0	4.00	S	70FAS	50.5 ± 1.6 /h/	
59PR148M	134.	7.00	S	76MON	2.2 ± 0.1 M /h/	
59PR148F	149.	3.00	S	76MON		
61PM148M	41.3	.100	D	76END	41.3 ± 0.1 J /d/	
61PM148F	5.37	.900E-02	D	76END	5.370 ± .009 J /d/	
57LA149	.250	.0	S	76BLA	1.2 ± 0.4 /g/	
58CE149	3.00	.500	S	75LOH	4.7 ± 0.8 /g/	5.7 ± 0.5 /h/
59PR149	2.25	.800E-01	M	76PIN	2.9 ± 0.3 M /h/	
60ND149	1.73	.100E-01	H	76END	1.73 ± 0.01 H /d/	
61PM149	2.21	.0	J	66MCI		
62SM149	.400E+15	.0	A	67LED		
57LA150	.400	.0	S	76BLA		
58CE150	5.90	.300	S	75LOH	4.8 ± 0.5 S /h/	
59PR150	6.10	.0	S	70WAR	6.2 ± 0.2 S /h/	
61PM150	2.70	.0	H	67LED		
58CE151	.340	.0	S	76BLA		
59PR151	4.00	.700	S	70WIL		
60ND151	12.4	.200	M	75REI		
61PM151	28.0	.0	H	69GUN		
62SM151	87.0	.0	A	67LED		
59PR152	.400	.0	S	76BLA		
60ND152	11.4	.0	M	71DAN		
61PM152M	7.50	1.00	M	71DAN		
61PM152F	4.10	.0	M	71DAN		
63EU152M	1.60	.200E-01	M	75PRU		
63EU152N	9.30	.0	H	67LED	9.32 ± 0.02 H /d/	
63EU152F	12.4	.180	A	67NDS	13.3 ± 0.1 A /d/	
64GD152	.110E+15	.0	A	67LED		
59PR153	.300	.0	S	76BLA		
60ND153	14.0	.0	S	68DET		
61PM153	5.30	.300	M	69SMI		
62SM153	46.7	.100	H	75RFI	46.7 ± 0.1 H /d/	
64GD153	242.	1.00	D	76END	242. ± 1. J /d/	
60ND154	33.0	.0	S	68DET		
61PM154M	1.80	.200	S	71DAU		
61PM154F	2.80	.200	M	71DAU		
61PM154	2.80	.200	M	71DAU		
63EU154	7.84	.0	A	69GUN	8.6 ± 0.1 A /d/	
60ND155	1.20	.0	S	76BLA		
61PM155	4.00	.0	S	68DET		
62SM155	22.4	.300	M	69UNG		
63EU155	4.65	.200	A	70MOW	4.96 ± 0.01 A /d/	
61PM156	1.70	.0	S	68DET		

Table VI (continued)

NUCLIDE,	T1/2	DT1/2		REFE
62SM156	9.40	.200	H	70GRI
63EU156	15.2	.100	J	69GUN
61PM157	1.00	.0	S	76BLA
62SM157	8.00	.500	M	73KAF
63EU157	15.1	.400E-01	H	66DAN
62SM158	2.20	.0	M	68DET
63EU158	45.9	.200	M	74TUL
62SM159	160.	.0	S	76BLA
63EU159	18.7	.400	M	73TUL
64GD159	18.6	.800E-01	H	73TUL
63EU160	52.8	10.0	S	73MOR
65TB160	72.3	.200	J	74TUL
63EU161	25.0	.0	S	76BLA
64GD161	3.70	.100	M	74TUL
65TB161	6.91	.200E-01	J	74TUL
63EU162	5.00	.0	S	76BLA
64GD162	8.20	.300	M	70CHA
65TB162M	2.20	.0	H	67LED
65TB162F	7.75	.310	M	66SCH
64GD163	.550	.0	S	68DET
65TB163	19.5	.300	M	72BUY
64GD164	1.00	.0	S	68DET
65TB164	3.00	1.00	M	74BUY
65TB165	30.0	.0	S	76BLA
66DY165M	1.26	.600E-02	M	74BUY
66DY165F	2.32	.600E-02	H	74BUY
65TB166	52.0	.0	S	68DET
66DY166	81.6	.100	H	75BUY
67HO166M	1200.	.400	A	67LED
67HO166F	26.8	.300E-01	H	68NET
66DY167	6.20	.800E-01	M	77TUU
67HO167	3.10	.100	H	76END
68ER167M	2.28	.300E-01	S	72JOH
66DY168	1.60	.0	H	68DET
67HO168	2.99	.700E-01	M	74GRE
66DY169	7.10	.0	S	68DET
67HO169	4.40	.200	M	66FUN
68ER169	9.30	.200	J	73HAR
66DY170	1.60	.0	M	68DET
67HO170M	2.80	.200	M	74KAW
67HO170F	43.0	2.00	S	74KAW
69TM170	130.	.0	J	67LED

Other works

(a) K. KAFFRELL et al, 3rd International Conference on nuclei from stability, CARGESE, 1976, CERN 76-13, p. 483

(b) J.P. PEROLAT , Private Communication, 1977

(c) K. DEBERTIN, Private Communication, 1977

(d) M.J. MARTIN, ORNL 5114

(e) E. LUND, G RUDSTAM, Phys. Rev. C13, 1976, p. 321, p. 1544

(f) K. WUNSCH, Private Communication, 1977

(g) I. NIR EL, (see reference (a)), p. 501, Private Communication

(h) G. SKARNEMARK, Thesis Chalmers University, GOTEBERG, SWEDEN, 1977

128.6 ± 0.3 J /d/

69MOR1 MORET R. JOUR. DE PHYS. 30(1969)497
69PIN PINSTON J.A. ET AL. NUCL. PHYS. A133(1969)124
69RAG RAGAINI R.C. KNIGHT J.D. NUCL.PHYS. A125(1969)97
69SCH SCHICK W. C. ET AL. NUCL. PHYS. A128(1969)353
69SMI SMITHER R.K. ET AL. PHYS. REV. 187(1969)1632
69UNG UNGRIN J. NUCL. PHYS. A127 (1969) 353
69WEI WEISS H. V. PHYS. REV. 188(1969)1893
69ZOL ZOLLER W.H. ET ALL NUCL. PHYS. A130(1969) 293
70APT APT K.E. ET AL. NUCL.PHYS. A 152(1970)344
70ARA ARAD R. ET AL CAN. J. OF PHYS. 48 (1970) 1378
70ARO ARONSSON P.O. AT AL. PHYS. REV. LETTERS 25(1970)590
70BAE BAEDECKER P.A. NUCL. PHYS. A 158 (1970)
70BAR BARRETTE J. ET AL CAN. J. OF PHYS. 48 (1970) 11
70CAL CALWAY P.G. ET AL. NUCL. PHYS. A156(1970)338
70CHA CHANG J.C. ET AL. NUCL.PHYS. A142(1970)634
70ERT ERTEN H.N. ET ALL A.P.S. (1970) MEETING HOUSTON
70FAS FASCHING THESE MIT 1970
70FAS1 FASCHING J.L. ET AL. PHYS. REV. C1(1970)1126
70FOL FOLGER H. RAP. BMBW-FBK 70-04 P25
70FOW FOWLER ET AL. A.C.S. MEETING CHICAGO SEPT 70
70GRA GRAPPENGISSER ET AL CERN 70 30 P 1093
70GRI GRITCHENKO Z.G. ET AL.SOV. J. NUC. PHYS. 10(1970)536
70HAT HATTULA J. THESE Z. PHYSICAL 231 (1970) 203
70HEL HELPPI H. HATTULA J. PHYS. SCR. 2 (1970) 155
70HER HERMANN G. CERN 70 30 P 985
70HNA HNATOWICH D.J. ET AL. NUCL. PHYS. A143(1970)289
70KAR KARRAS M. ET AL NUCL. PHYS. A 147 (1970) 120
70KLA KLARISCH CERN 70 30 P 40
70KRA KRACIKOVA J.I. CSFCH J. PHYS. B20 10(1970) 1138
70MAC MACIAS E.S. NUCL. PHYS. A160(1970) 274
70MAS MASON J. F. CAN. J. OF PHYS. 48 (1970) 2895
70MAS1 MASON J.F. ET AL. CAN. J. OF PHYS. 48(1970)2056
70MCD MCDONALD J.A. ET AL. NUCL. PHYS. A156(1970)321
70MCI MCISAAC L.D. ET AL. NUCL. PHYS. A156(1970)212
70MER MEREDITH ET AL. NUCL. PHYS. A 142 (1970) 513
70MOW MOWATT R.S. CANAD. J. PHYS. 48(1970) 1933
70NDT NUCLEAR DATA VOL. 8A N 1
70PIN PINSTON J. A. ET AL. NUCL. PHYS. A157(1970)323
70QUA QUAIM S.M. NUCL. PHYS. A154(1970)145
70REI REICH C.W. CLINE J.E. NUCL. PHYS. A159 (1970) 181
70RUD RUDSTAM G. ET AL.CERN 70 3 P 341
70TAL TALBERT W.L. ET AL. NUCL. PHYS. A146(1970)149
70VAN VAN HISE J.R. PHYS. REV. C 15 (1970) 1861
70WAR WARD T. E. ET AL NUCL. PHYS. A 154(1970) 665
70WIL WILHELMY J.B. UCRL 19530(1970) 178
70ZOL ZOLLER W.H. ET AL. NUCL. PHYS. A142(1970)177
71APT APT F. E. THESE MIT (1971)
71BAR BARA S. J. INORG. NUCL.. CHEM. 33(1971) 592
71BAC BACKLIN A. ET ALL CERN 70 3 (1971) P1069
71BER BERDRAND NUCL. DATA TAB. B 6 1 (1971)
71BLA BLACHOT J. ET AL PHYS. REV. C4(1971) 214
71CAM CAMP D.C. ET AL NUCL. PHYS. A 163 (1971) 145
71CAR CARRAZ ET AL NUCL. PHYS. A171 (1971) 209
71CAV CAVALLINI P. ET AL NUCL. PHYS. A175 (1971) 363
71DAN DANIELS W.R. HOFFMAN D.C. PHYS. REV. C4 (1971) 919
71DAU DAURIA ET AL NUCL. PHYS. A 178 (1971) 172
71DER DERTIN K. Z. NATURFORF. 26 A (1971)596
71FOG FOGELBERG B. PHYS. LETTERS B36 N4(1971) 334
71GUJ GUJRATHI S.C. ET AL NUCL. PHYS. A 172 (1971) 353
71HNA HNATOWICH D.H.J. THESE MIT 1968
71KAF KAFFREL ET AL. Z. PHYSIK 245 (1971) 451
71KRA KRATZ K.L. RAPPORT BMBW FB-K 71.12 MAINZ (1971)71
71LAR LARSEN ET AL. PHYS. REV. C3(1971)1372
71LIU LIUKKONEN Z. PHYS. 241 (1971) 150
71LUD LUDINGTON M.A. PHYS. REV. 4 (1971) 647
71MAC MACIAS M.I. THESIS PARIS UNIV. ORSAY (1971) FRNC TH 136
71MAC1 MACIAS ET AL NUCL. PHYS. A 169 (1971) 305
71MCD MCDONALD J. NUCL. PHYS. A 176 (1971) 526
71MCM MC MILLAN D.K. NUCL. PHYS. A174 (1971) 593
71NDS HOREN D.J. NDS B6 (1971) 75
71NDS2 RAMAN S. KIM H.J. NDS B VOL 6 (1971) 1-104
71NDS5 HOREN D.J. NDS B6 (1971) 75
71NDT WAKAT M. A. NUCL. DATA TAB. A 8 (1971
71OKA OKANO K. ET AL NUCL. PHYS. A 164 (1971) 545
71ORT ORTH C J. PHYS. REV. C3(1971)2402
71PAR PARSA B. ET AL NUCL. PHYS. A 175 (1972) 629
71RES RESTER A.C. ET AL. NUCL. PHYS. A162(1971)461
71SCH SCHICK W.C. TALBERT W. MCDONNEL PHYS. REV. C4(1971) 507
71TAK1 TAKAHASHI K. ET AL NUC. PHYS. A 167 (1971) 183
71TAK2 TAKAHASHI ET AL PHYS. REV. C4 (1971) 214
71TAL TALBERT W.L. COMMUNICATION PRIVEE (1971)
71TOM TOMLINSON L. ET AL INORG. AND NUCL. CHEM.33(1971) 3609
71TRA TRACY B.L. PHYS. LET. VOL. B34 N4 (1971) 277
71WOL WOLSFBERG K. J. INORG. NUCL. CHEM. 33 (1971) 589
72ACH ACHTERBERG E. ET AL PHYS. REV. C 5 (1972) 1759
72AMI AMIEL S. ET AL PHYS. REV.C5(1972) 270
72ARD ARDISSON G. ET AL NUCL. PHYS. A 179 (1972) 545
72BAK BAKER K.R. ET AL Z. PHYSIK 256 (1972) 387
72BUY BUYRN A. NDT VOL. 8 (1972) 295
72CAR CARTER BAPS (1972) 514
72CAV CAVALLINI P. J. DE PHYSIC (1972) 676
72COO COOK W. B. CAN. J. PHYS. 50 (1972) 1957
72COR CORYELL ET AL NUC. PHYS. A 179 (1972) 689
72DEL DEL MARMOL P. FETTWEIS P. NUC. PHYS. A 194 (1972) 140
72EHR EHRENBERG B. AMIEL S. PHYS. REV. C6 (1972) 618
72EME EMERY J. F. REYNOLDS NUCL. SCIE. ENG. 48 (1972) 319
72ERD ERDAL L. ET AL NUCL. PHYS. A 194 (1972) 449
72FRA FRANZ H. KRATZ J.V. ET AL BMBWFBK 15 (1972)
72GRE GREGORY P. R. CAN. J. PHYS. 50 (1972) 012
72HER HERZOG W. GRIMM W. ET AL Z. PHYSICS 257 (1972) 424
72HOP HOPKINS F.F. PHYS. REV. C5 (1972) 1015
72IZA IZAK T J. INORG. NUCL. CHEM. 34 (1972) 1469
72JOH JOHNSON W.T.K. NUCL. INST. METH. 99 (1972) 221
72KER KERFK A. CARLF P. ET AL NUCL. PHYS. A 198 (1972) 466
72KOC KOCHER D.C. NUCL. DATA B 8 (1972) 527
72KRA KRATZ J.V. BMBW FBK 15 (1972) 32
72LAG LAGOUTINE M. INST. J. OF APPLIED RAD. AND ISOT. 23(72)21
72MAU MAURON G. KERN J. ET AL NUCL. PHYS. A 181 (1972) 489
72MCI MCISAAC L.D. ET AL ANCR 1088 (1972) 387
72MED MEDSKER L.R. NUCL. DATA B 8 (1972) 599
72NAF NAFUMANN ET AL J. INORG. NUCL. CHEM. 34 (1972) 1785
72NDS BERTRAND F.E. NDS B7(1972) 33
72NDS2 KOCHER D.C. NDS B VOL 7 (1972) 299 - 418
72NDS4 BERTRAND F.E. NUCL. DAT. SHEET B7 (1972) 1
72NDS5 AUBLE R.L. NDS B7(1972) 465
72NDS6 AUBLE R L. NDS B7(1972)363
72NDS7 BERTRAND F.E. NDS B7 (1972) 1
72NDS8 BERTRAND F.E. NDS B7(1972) 33
72OHY3 OHYOSHI A. ET AL J. OF NUCL. SCIE. AND TEC. 9 (1972) 658
72OLS OLSON R. J. FT AL PHYS. REV. 5(1972) 2095
72TRA TRAUTMANN N. ZAFFRELL RAD. CHEM. ACTA 18 (1972) 86
72WAH WAHL A.C. J. INORG. NUCL. CHEM. 34 (1972) 1767
72WIL WILHELMY J.B. ET AL PHYS. REV. C5 (1972) 2041
73ALV ALVAR K.R. NUCL. DAT. SHEETS 10(1973) 205
73AUB AUBLE R. L. NUCL. DATA SHEET 9 157 (1973)
73AUB1 AUBLE R.L. NUCL. DATA SHEETS 10(1973) 151
73BER BERTRAND F.E. ET AL NUCL. DATA 10 91(1973)
73BLA BLACHOT J. CARRAZ L.C. RCEA (1973) 4437

73BOR BORG S. HOLM G.B. ET AL NUCL. PHYS. A212(1973)197
73COO COOK W.B. ET AL CAN. J. PHYS. 51 (1973) 1978
73DAU DAURIA J.M. ET AL CAN. J. OF PHYS. 51 (1973) 686
73DIK DIKSIC M. INORG. NUCL. CHEM. LETTERS 9 (1973) 1057
73FET FETTWEIS P. SADASIVAN Z. PHYSIK 263 (1973)99
73FRE DE FRENNE D. Z. PHYSIK 258 (1973) 38
73GRI GRIMM W. HERZOG W. Z. PHYS. 259 (1973) 67
73GRI1 GRIMM W. HERZOG W. Z. PHYSIK 266(1974)397
73HAN HANSER A. NUCL. INST. METH. 107 1973) 187
73HAR HARMATZ B. NUCL. DAT. SHEET 10 (1973) 359
73HEN HENRY PHYS. REV. C 7 222 (1973)
73KAF KAFFRELL N. PHYS. REV. VOL 8 1 (1973) 320
73KER KEREK A. ET AL NUCL. PHYS. A209 (1973) 520
73KOC KOCHER D.C. NUCL. DATA SHEET 10(1973) 241
73LEM LEMMING J.F. RAMAN S. NUCL. DAT. SHEET 10 (1973) 309
73MAR MARTIN M.J. NUCL DAT. ORNL 4923
73MED MEDSKER L.R. NUCL. DATA SHEETS 10 (1973) 1
73MON MONNAND E. BLACHOT J. RAPPORT CEA
73MOR ORCOS N.A. ET AL. J. INOR. NUC. CHEM. 35 (1973) 3659
73RAM1 RAMAN S. NUCL. DATA SHEETS 9 (1973) 229
73RAM3 RAMAN S. ET AL NUCL. PHYS. A206 (1973) 343
73RUD RUDSTAM G. I.A.E.A. BOLOGNE (1973)
73SCH SCHEIDELMANN J. INORG. NUCL. CHEM. 35 (1973) 3055
73SCH1 SCHUSSLER F. BRISSOT R. NUCL. PHYS. A 209 (1973) 589
73SER SERGEEV V. BECKER J. NUCL. PHYS. A 202 (1973) 385
73TAL TALBERT W.L. ET AL PHYS. REV.8(1973) 1945
73TIR TIRSELL K.G. PHYS. REV. C7(1973)2108
73TOD TODD R.R. KELLY W.H. NUCL. DAT. SHEET 10 (1973) 47
73TOM TOMLINSON L. NDT 12(1973) 179
73TUL TULI J.K. ET AL NDS 9 15 (1973) 435
74ACH ACHTERBERG E. ET AL PHYS. REV. C9 1(1974)299
74ALV ALVAR K.R. NUCL DAT SHEETS 11(1974)121
74ALV1 ALVAR K.R. N.D.S. 13(1974)305
74BER BERTRAND F.E. NUCL. DAT. SH. 11 (1974) 449
74BJO BJORNSTAD T. ALSTAD J. J. INORG. NUCL. CHEM. 36(1974)215
74BRI BRISSOT R ET AL NUC. PHYS. A (1974)
74BUY BUYRN A. NUCL. DAT. SHEETS 11(1974) 279
74BUY1 BUYR A. NUCL. DAT. SH. 11(1974)157
74CAR1 CARRAZ L. NUCL. PHYS. A158(1970)403 ET THESE GRENOBLE197
74CHA CHACKO M.C. HEYDE K. ET AL Z. PHYSIK 266(1974)337
74CHA1 CHACKO M. C. ET AL Z. PHYSYK 267(1974)359
74FOG FOGELBERG B. ET AL NUCL. PHYS. A230 (1974)214
74FOW FOWLER M.M. ET AL J. INORG. NUCL. CHEM. 36(1974)1191
74GEF DE GEER L.E. ET AL ANNUAL REPORT 1974 R.I.P. STOCKHOLM
74GRA GRAPENGIESSER B. LUND E. JINORG NUCL CHEM 36(1974)2409
74GRE GREENWOOD L.R. NUCL. DAT. SH. 11 (1974)385
74GRI GRIGORIAN N. COMMUNICATION PRIVEE 1674 MOSCOU
74HEN HENRY E.A. NUCL. DAT. SH. 11 (1974) 495
74HID HIDDLESTON H.R. NDS 13(1974) 133
74KAW KAWADE K. ET AL JOUR. OF PHYS. SOC. JAP. 36(1974E1221
74KER KEREK A. ET AL NUCL. PHYS. A224 (1974)367
74KLU KLUGE A. KROTH K. ET AL NUCL. PHYS. A224(1974)1
74KOC KOCHER D.C. NUCL. DAT. SH. 11 (1974)279
74KOC1 KOCHER D.C. N.D.S. 13(1974)337
74LOH LOHENGRIN COLLABORATION ILL GRENOBLE 1974
74MCD MCDONALD J. FOGELBERG ET AL NUCL. PHYS. A224(1974)13
74PEK PEKER L.K. ETAL. NUC.DAT.SH. 12(1974)343
74RAM RAMAN S. ET AL. PHYS.REV. C9 (1974)426
74ROE ROECKL E. ET AL NUCL. PHYS. A222(1974)621
74SCH SCHICK W.C. JR. TALBERT W.L. PHYS. REV. C9(1974)2328
74TUL TULI J.K. NUC.DAT.SH. 12(1974)477
74TUL1 TULI J.K. NUCL. DAT. SH. 12 (1974) 245
74TUL2 TULI J.K. N.D.S. 13(1974)493
74WAP WAPSTRA COMMUNICATION PRIVEE

75RAT RAILLEUL G. BOCQUET J.P.Z. PHYSIK A273(1975)273
75BRU1 BRUCHLE W. REPORT MAINZ (1975)95
75BRU2 BRUCHLE W. REPORT MAINZ (1975)90
75RUN RUNTING R.L. NUCL. DAT. SH. 15(1975)335
75RUY BUYRN A. NUCL. DAT. SH. 14 (1975) 471
75FET FETTWEIS P. DEL MARMOL P. Z.PHYSIK A275(1975)359
75FRA FRANZ G. HERRMANN G. INORG. NUCL. CHEM. LETT.11(1975)857
75FRA1 FRANZ G. REPORT MAINZ (1975)81
75GAS GASSER M. KERN J. ET AL NUCL. PHYS. A250 (1975)106
75GAU GAUTHERON J.P. ET AL THESE 1975
75GRE GREENWOOD L.R. NUCL. DAT. SH. 15(1975)289
75HEN HENRY E.A. NUCL. DATA SH. 14(1975)191
75HIL HILLIS D.L. BINGHAM C.R. PHYS. REV. C 12(1975)260
75HOF HOFFMAN D.C. ET AL J. INORG. NUCL. CHEM. 37(1975)2336
75HOR HOREN D.J. LEWIS M.R. NUCL. DAT. SH. 16(1975)25
75HUR HURDUS M.H. TOMLINSON L. J. INORG. NUCL. CHEM. 37(1975)1
75KAW KAWASE Y. FOGELBERG NUCL. PHYS. A241(1975)237
75KIM KIM H.J. NUCL. DAT. SH. 16(1975)107
75KOC KOCHER D.C. NUCL. DAT. SH. 15(1975)169
75KOC1 KOCHER D.C. NUCL. DAT. SH. 16 (1975)445
75KRA KRATZ J.V. FRANZ H. ET AL NUCL. PHYS. A 250(1975)13
75KRA1 KRATZ K.L. ET AL INORG. NUCL. CHEM. LETTERS 11(1975)331
75LEM LEMMING J.F. NUCL. DAT. SHA. 15(1975)137
75LOH LOHENGRIN COLLABORATION ILL GRENOBLE 1975
75MON MONNAND E. ET AL J. DE PHYS. 36(1975)1
75MON1 MONNAND E. COMMUNICATION PRIVEE 1975
75NAM NAMIK K. ARAS ET AL PHYS. REV. 11(1975)927
75NUH NUH M.F. SLAUGHTER D.R. NUCL. PHYS. A 250(1975)P1
75PER PEROLAT J.P. LMRI COMMUNICATION PRIVEE (1975)
75PIN PINSTON J.A. ET AL NUCL. PHYS. A246(1975)395
75PRU PRUYS H.S. HERMES E.A. J. INORG. NUCL. CHEM37(1975)1587
75REI REICH C. COMMUNICATION PRIVEE 1975
75RUD RUDSTAM G. LUND E. LA-60 RESARCH REPORT 1975
75SAD SADLER G. KHAN T.A. ET AL NUCL. PHYS. 252(1975) 365
75SUM SUMMERER K. KAFFREL N. ET AL SUBMITTED TO Z. PHYSIK (197
75TIV TIVIN P. ET AL Z. PHYSIK A 273(1975)339
75TOV TOVEDAL H. FOGELBERG B. NUCL. PHYS. 252 (1975)253
75URO URONE P.P. NUCL. DAT. SH. 15(1975)107
75URO1 URONE P.P. KOCHER D.C. NUCL. DAT. SH. 15(1975)257
76AHR AHRENS H. PATZELT P. ET AL J. INORG. NUCL. CHEM.38(76)19
76AMI AMIEL S. ENGLER G. CARGESE (1976)
76AUB AUBLE R.L. TODD ET AL NUCL. DAT. SH. 19(1976)1
76AUB1 AUBLE R.L. HIDDLESTON H.R. NUCL. DAT. SH. 17(1976)573
76BLA BLACHOT J. DOUSSON S. ET AL J. DE PHYS. 37(1976)275
76BUN BUNTING R.L. TALBERT W.L. PHYS REV C VOL13N4(1976)1577
76BUR BURROWS T.W. NUCL. DAT. SH. 18(1976)553
76BUY BUYRN A. NUCL. DAT. SH. 17(1976)97
76CAR CARLSON G.H. TALBERT W.L. ET AL NUCL. DAT. SH. 17(1976)
76END ENSDF COMMUNICATION DU DR. EWBANK OCTOBRE 1976
76FOG FOGELBERG B. ET AL Z.PHYSIK A276(1976)381
76HAR HARMATZ NUCL. DAT. SH. 17(1976)143
76HER HERZOG W. TRAUTMANN N. ET AL Z. PHYSIK A276(1976)393
76HID HIDDLESTON H.R. BROWNE C.P. NUCL. DAT. SH. 17(1976)225
76KAF KAFFRELL N. FRANZ GARGESE 1976 CERN-76-13
76KOC KOCHER D.C. NUCL. DAT. 17 (1976)519
76LEW LEWIS L. NUMNELIFY ET AL PHYS. REV. 13 N5(1976)2017
76MAR MARTIN M.J. NUCLEAR DECAY DATA ORNL 5114(1976)
76MON MONNAND E. J. BLACHOT CARGESE CERN-76-13
76PFE PFEIFFER B. COMMUNICATION PRIVEE 1976
76PIN PINSTON J.A. ROUSSILLE P. ET AL COMMUNICATION PRIVEE 197
76SAM SAMUELSON L.E. KELLY W.H. ET AL NUCL. DAT SH. 18(1976)12
76SCH SCHUSSLER COMMUNICATION PRIVEE 1976
76SCH1 SCHUSSLER F. BLACHOT J. & AL.-Z. PHY.-A PARAITRE 1977
76SIS SISTEMICH K. SADLER G. ET AL CARGESE (1976)

76SMI SMITH H.A. BUNKER ET AL PHYS REV VOL 13N1(1976)387
76TAL TALBERT J. COMMUNICATION PRIVEE (1976)
76VAI VAISALA S. GRAEFFE PHYS. REV. VOL13N1(1976)372
76WES WESTERN W.R. HILL ET AL PHYS. REV. CVOL13N1 (1976)275
77PER PEROLAT J.P. TABLE DES RADIONUCLEIDES SACLAY (1977)
77PFE PFEIFFER R. BOCQUET J.P. ET AL JOUR DE PHYS 38(1977)600
77SIS SISTEMICH K. SADLER G. ET AL 1977 A PARAITRE
77TUU TUURNALA T. ET AL. Z. PHYSIK A 280(1977)309
77WOL WOLLNIK H. ET AL. A PARAITRE
77WUN WUNSCH K.D. ET AL. COMMUNICATION PRIVEE (1977)

NOMBRE TOTAL DE SIGLES REFERENCES = 321 DONT 0 ERRONE(S)

REFERENCES TO TABLE VI

60NDS NDS 1960
63NDS NDS 1963
66CHU CHU P. ET AL. J. OF INORG. AND NUCL. CHEM. 28(1966)1339
66DAN DANIELS W. R. ET AL. PHYS. REV. 147(1966)845
66ERD ERDAL R.P. THESE 1966 ST LOUIS MISSOURI
66FUN FUNKE L. ET AL. NUCL. PHYS. A86(1966)345
66KIT KITCHING J.E. ET ALL. CAN. I. OF NUCL. PHYS. 44(1966)266
66MCI MCISAAC L.D. ET AL. PHYS. REV. 150(1966)1033
66MCM1 MCMULLEN C.C. ET AL CAN. J. OF PHYS. 44(1966) 3033
66NDS FWBANK W.B. ET AL NUC. DAT. B1-6 (1966) 1
66NOR NORRIS A.E. PHYS. REV. 146(1966)926
66SCH SCHIMA F. ET AL. PHYS. REV. 151(1966)950
67AMI AMIEL S. VIENNE AVRIL 1967
67REM REMIS C.E. ET AL. ARKIV FUR PHYS. 37(1967)203
67DEL DEL MARMOL P. ET COL. VIENNE AVRIL 1967
67GAU GAUVIN H. PHYS. LET. 24B(1967)402
67KAU KAURANEN P. ET AL. RADIOCHIMICA ACTA 7(1967)203
67KER KERN J. ET AL. PHYS. LET. 24B(1967)400
67LED LEDERER AT AL. 1967 VOL 2 N 6
67MAR MARLOW K.W. ET AL. PHYS. REV. 163(1967)1098
67MUR MURRI F.L. ET AL. PHYS. REV. 155(1967)1263
67NDS RAMAN S. ET AL NUC. DAT. B2-1 (1967) 1
67RAG RAGAINI R.C. ET AL. NUCL. PHYS. A99(1967)547
67SCH SCHRIBER S.O. NUCL. PHYS. A 96(1967) 337
67WIL WILD J.F. NUCL. PHYS. A103(1967)601
67YUL YULE H. P. NUC. PHYS. A94(1967) 442
68ANN ANNE R.G. ET AL. PHYS. REV. 176(1968)1329
68ARD ARDISSON G. ET AL. C. R. ACAD. SCIENCES 267(1968)344
68DET DE TOURREIL CALCUL SYSTEMATIQUE
68ERD ERDAL B.R ET ALL J. OF INORG. AND NUCL. CHEM. 30(1968)19
68LAG LAGOUTINE INT J. OF AP. RAD. AND ISOT. 19 (1968) 475
68MON MONARO S. ET AL. CAN. J. OF PHYS. 46(1968)2375
68NET NETHAWAY D.R. J. INORG. NUC. CHEM. VOL30(1968) 15
68PAR PARSA B. GORDON NUCL. PHYS. A 110 (1968) 674
68REN RENGAN K. ET AL. J. OF INORG. AND NUCL. CHEM.30(1968)2
68WEI WEISS H.V. ET ALL PHYS. REV. 172(1968) 1269
69BER BERG V. ET AL NUCL. PHYS. A 135 (1969) 401
69BLA BLACHOT J. ET AL. NUCL. PHYS. A139(1969)434
69BRA BRAHMAVAR S.M. ET AL NUCL. INST. METH. 69 (1969) 353
69BRO BROWN R.A. CAN. J. OF PHYS. 47(1969)
69CAR CARLSON G.C. ET AL. NUCL. PHYS. A125(1969)267
69DEN DENSCHLAG J. INORG. NUCL. CHEM. 31 (1969) 1873
69DIC DICKINSON W.C. ET AL. NUCL. PHYS. A123(1969)481
69FOI FOIN OMS J. NUCL. PHYS. A123(1969)513
69GAR GARVEY G.T. ET AL. REV. OF MOD. PHYS. VOL. 41 N 4,PART 2
69GRI GRIFFIN H.C. ET AL. PHYS. REV. 183(1969)991
69GUN GUNNINK R. ET AL. UCID 15439 (1969)
69HER HERMANN G. AT AL. ANNUAL REVIEW NUCL. SCIE. 19 (1968)
69HNA HNATOWICH D.J. ET AL. NUCL. PHYS. A130(1969)497
69IMA IMANISHI N. ET AL. J. OF INORG. NUCL. CHEM. 31(1969)228
69KEM KEMNITZ P. ET AL. NUCL. PHYS. A137(1969)679
69KNI KNIGHT J.D. ET AL. NUCL. PHYS. A130(1969)433
69KUG KUGER H. NUCL. PHYS. A137(1969)281
69LIU LIUKKONEN E. ET AL. NUCL. PHYS. A138(1969)163
69MEY MEYER R.A. NUCL. PHYS. A 127 (169) 595

Table VII (a) - Isotopes with experimental data on the shapes of beta spectra (66)

Allowed beta transitions

110 Ag	114 In	115 Cd
130 I	131 I	134 Cs

1st forbidden Non unique β^- transitions

72 Ga	76 As	86 Rb
91 Y	99 Mo	111 Ag
115mCd	100 Sb	124 Sb
137 Xe	139 Ba	140 La
141 Ce	143 Pr	144 Ce
144 Pr	147 Nd	148 Pm
152 Eu	154 Eu	166 Ho
170 Tm		

1st forbidden unique β^- transitions

76 As	86 Rb	89 Sr
90 Sr	90 Y	91 Y
115mCd	142 Pr	144 Pr
158mEu	160 Ho	

Second forbidden Non unique β^- transitions

94 Nb	99 Tc	129 I
135 Cs	137 Cs	

Third forbidden Non unique β^- Transition

87 Rb

Table VII (b)

Comparison of average beta values computed by Martin; Tobias; the Barré Code; ENDF/B-IV.

	MARTIN	TOBIAS	BARRE	ENDF/B4
^{90}SR				
1st Forbidden	546.	546.	546.	546.
Unique	195.8	196.1	174.2	172.5
^{90}Y				
1st Forbidden	2284.	2273.	2273.	2273.
Unique	934.8	931.5(936.)	926.2	930.1
^{137}CS				
1st forbidden	514.	514.	514.	514.
Unique	174.3	174.9	157.8	160.8
2nd Forbidden	1176.	1176.	1176.	1176.
	416.4	426.9	417.2	427.8
^{99}MO				
1st Forbidden	1214.	1234.	1234.(1214.)	1214.
Unique	442.	452.(445.)	452.(443.4)	444.3

Table VIII

Energies of the gamma rays of 4 F.P.

^{94}Nb	702.625(13) 871.094(15)	^{137}Cs	661.646(19)
^{95}Zr-Nb	724.178(14) 756.710(18) 765.781(18)	^{141}Ce	145.4405(28)

Table IX - Intensity of $\beta_{g.s.}$ (IBG.S.), and internal conversion coefficients of nuclides with absolute γ-intensities

NUCLIDE	REFE	FN	IBG.S.		GAMMA *	INT.CON.COEF.	
30ZN 71M	70ZOL	0.9144			M		
30ZN 71F	70ZOL	0.3045	57.		M		
30ZN 72	69KUG	0.8300			1	12.38	
31GA 72	71RES	0.9600			M		
31GA 73	74ALV1	1.0000			M	1103.	
30ZN 74	72ERD	0.7430			1	0.346	
31GA 74	71CAM	0.9170			M		
31GA 75	74CHA1	0.0249	96.		M		
32GE 75M	66NDS	0.4098			1	1.44	0.13
32GE 75F	68ANN	0.1180	87.		M		
31GA 76	71CAM	0.6580			M		
33AS 76	72ARD	0.3820	58.		M		
32GE 77M	69IMA	1.0000	58.		M	0.858	
32GE 77F	73RAM1	0.5320			M		
33AS 77	68ARD	0.0150	97.56		M		
34SE 77M	66NDS	0.5316			1.	0.881	
32GE 78	66NDS	0.9600			M		
33AS 78	76END	0.5400	34.	3.	M		
32GE 79	70VAN	0.2000	80.		1.		
33AS 79	75URO1	1.0000			M	9.56	
34SE 79M	66NDS	0.0947			1.	9.56	
35BR 79M	66NDS	0.7810			1.	0.28	0.05
33AS 80	71MCM	0.4180	56.		M		
35BR 80M	66NDS	0.3860			1.	298.	
35BR 80F	71NDT	1.0000	84.43		M		
33AS 81	74CHA	0.1320	80.				
34SE 81M	69ZOL	0.1050			M	8.40	
34SE 81F	69ZOL	0.0051	99.1				
36KR 81M	66NDS	0.6494			1.	0.54	0.07
36KR 81F	76END	1.0000	96.3		1.		
33AS 82M	76END	0.7400			M		
33AS 82F	76END	0.1500	80.		M		
35BR 82M	75LEM	1.0000			M		
35BR 82F	70MER	1.0000			M		
34SE 83M	73FET	0.1730	31.		M		
34SE 83F	73FET	0.6860			M		
35BR 83	76VAI	0.0140			M		
36KR 83M	73MAR	1.0000			1.	19.83	
34SE 84	68REN	1.0000			1.		
35BR 84M	70HAT	1.0000			1.		
35BR 84F	70HAT	0.4400	31.		M		
34SE 85	77PFE	0.2680			M		
35BR 85	75NUH	1.0000			M	0.5	
36KR 85M	73MAR	1.0000			M	0.456	
36KR 85F	73MAR	1.0000	99.57		M		
35BR 86	72ACH	0.0536	30.		M		
37RB 86F	76MAR	1.0000	91.2		1.		
36KR 87	73MAR	1.0000	30.5	2.2	M		
38SR 87M	67LED	1.0000			1.		
35BR 88	76BUN	0.0770	5.5		M		

* GAMMA - M ... Many γ-rays are used for normalisation
1 ... One γ-ray is " " "

Table IX (continued)

NUCLIDE	REFE	FN	IBG.S.	GAMMA		INT.CON.COEF.	
36KR 88	73MAR	1.0000	14.	4.	M	6.21	
37RB 88	73MAR	1.0000	76.	4.	M		
36KR 89	73HEN	1.0000	14.		M		
37RB 89	73HEN	0.0635	18.		M		
39 Y 89M	76KOC	1.0000			1.	0.0085	
36KR 90	75KOC1	0.0389	27.		M		
37RB 90M	76TAL	0.0952			M		
37RB 90F	76TAL	0.0325	37.		M		
39 Y 90M	73HAN	1.0000			M		
39 Y 90F	70MAC	0.0020	99.8		1.		
40ZR 90M	75KOC	1.0000			1.		
36KR 91	74ACH	0.4320	10.	4.	M	0.115	
37RB 91	74ACH	0.3210	60.	5.	M	1.1	
38SR 91	73BLA	1.0000	30.5		M		
39 Y 91M	69KNI	1.0000			1.	0.786	
39 Y 91F	69GUN	1.0000	99.7				
36KR 92	72OLS	1.0000	50.		M	0.049	
37RB 92	72OLS	1.0000	94.		M		
38SR 92	72OLS	1.0000	3.3		M		
39 Y 92	70TAL	0.1390	85.8		M		
36KR 93	74BRI	1.0000	5.		M		
37RB 93	74BRI	1.0000	42.		M		
38SR 93	72HER	1.0000			M		
39 Y 93F	73TAL	0.0069	90.3		M		
37RB 94	72CAR	0.0999	81.		M		
38SR 94	73GRI	0.8110	15.		M		
39 Y 94	71CAV	0.5600	41.		M		
41NB 94M	73KOC	1.0000			1.	1238.	
41NB 94F	73KOC	1.0000			1.		
38SR 95	73GRI1	1.0000	52.9		M		
39 Y 95	72CAV	0.1878	58.		M		
40ZR 95	72MED	1.0000	0.4		M		
41NB 95M	69FOI	1.0000			1.	3.07	
41NB 95F	69BRA	1.0000	0.1		1.		
39 Y 96F	75SAD	0.8890			M		
41NB 96	68MON	0.9710			M		
38SR 97	76MON	0.2780	20.		M		
39 Y 97M	76MON	0.9940			M		
39 Y 97F	76MON	0.1740	40.	10.	M		
40ZR 97	70ARA	0.9460			M		
41NB 97M	73MED	1.0000			1.	0.021	
41NB 97F	70ARA	1.0000			M		
39 Y 98M	77SIS	2.8600			M		
39 Y 98F	77SIS	0.1290	51.		M		
41NB 98M	76HER	1.0000			M		
41NB 98F	76HER	1.0000	90.		M		
42MO 99	77PER	1.0000			M	0.121	
43TC 99M	76MAR	1.0000			1.	0.095	0.02
40ZR100	75LOH	0.5740			M		
41NB100F	72HER	1.0000	50.		M		

Table IX (continued)

NUCLIDE	REFE	FN	IBG.S.	GAMMA	INT.CON.COEF.	
43TC100	69BER	0.0668	93.3	M		
42MO101	72COO	1.0000		M	969.	
43TC101	76END	0.8800		M	0.24	0.02
43TC102M	76AUB	0.8200		M		
43TC102F	69BLA	0.5315	41.	M		
43TC103	74KOC1	0.3091		M	?	
44RU103	75PER	1.0000		M	1530.	
45RH103M	75PER	1.0000		1.	1530.	
43TC104	75TIV	0.9033		M		
45RH104M	76SAM	1.0000		M	0.98	
45RH104F	76SAM	0.0190	98.	M		
43TC105	75SUM	1.0000	26.4	M	?	
44RU105	75NAM	0.4728		M	3.99	
45RH105M	74BER	0.2028		1.	3.93	
45RH105F	76END	0.1923	75.	M	0.019	
45RH106M	76END	0.8643		M		
45RH106F	76END	0.2060	79.3	M		
44RU107	72FRA	0.2600	74.	1.	?	
45RH107	69GRI	1.0000		M	0.885	
46PD107M	69GRI	0.7140		1.	0.4	
47AG107M	67LED	0.0002		1.	4280.	
44RU108	75FET	1.0000	68.	1.	?	
45RH108M	69PIN	0.8288	9.	M		
45RH108F	75FET	0.4300	53.5	M		
47AG108M	72NDS	1.0000		M	0.25	
47AG108F	71OKA	0.0175	96.	M		
45RH109	75FRA1	1.0000		M	?	
46PD109M	71BER	0.4700		1.	1.1	
47AG109M	71BER	1.0000		1.	25.9	
45RH110M	70PIN	0.9346		M		
47AG110M	75PER	1.0000		M		
47AG110F	75PER	1.0000	94.	0.1 M		
46PD111M	69SCH	0.3240		M	188.	
46PD111F	69SCH	0.5790		M	188.	
47AG111M	69SCH	1.0000		M	188.	
47AG111F	71HNA	0.0730	91.2	M		
48CD111M	72NDS2	0.9430		1.	0.06	
46PD112	67LED	0.0400		1.	24.	
47AG112	70MCD	0.4330	54.	M		
46PD113	75BRU2	0.0440	91.	M	?	
47AG113F	69HNA	0.0830	88.	M		
48CD113M	71NDS	1.0000	99.9	1.	3.0	
49IN113M	76MAR	1.0000		1.	0.54	
46PD114	75BRU1	0.0407	94.2	M	?	
47AG114F	75BRU1	0.1156	88.	M		
49IN114M	75KIM	1.0000		1.	4.32	
49IN114F	75KIM	1.0000	99.8	1.		
47AG115F	70HNA	0.3623	35.9	M		
48CD115M	73SER	0.0205	97.	M		
48CD115F	74GRI	1.0000		1.	0.998	

Table IX (continued)

NUCLIDE	REFE	FN	IBG.S.	GAMMA	INT.CON.COEF.	
49IN115M	69GUN	1.0000		1.	0.998	
46PD116	75BRU1	0.1855		M	?	
47AG116M	71BAC	0.9407		M		
47AG116F	74BJO	0.4248		M		
49IN116N	76END	0.8442		M	1.6	
49IN116F	76END	1.0000	98.8	1.		
48CD117M	72GRE	1.1260		M		
49IN117F	70BAE	1.0000		1.	0.157	
50SN117M	76END	1.0000		1.	0.157	
47AG118F	76CAR	0.8500	15.	1.		
49IN118M	70HAT	0.9600		M		
49IN118N	76CAR	1.0000		1.	2.	
49IN118F	78FRE	0.05	94.9	M		
48CD119M	74MCD	1.0000	30.	M		
48CD119F	74MCD	1.0000		M	1.55	
49IN119M	73RAM3	0.0270	92.	M	1.55	
50SN119M	76MAR	1.0000		1.	5.19	0.15
47AG120F	76KOC	0.8000	20.	1.		
49IN120M	71LIU	0.9709		M		
49IN120F	73SCH	1.0000	81.	M		
49IN121F	76FOG	1.0000		M	?	
50SN121M	67LED	0.0826		1.	11.1	
49IN122M	71TAK2	1.0000		1.		
49IN122F	71TAK2	1.0000		1.		
51SB122M	72NDS	1.0000		1.	?	
51SB122F	72NDS	0.7120	27.4	1.		
50SN123M	74RAM	0.9997		M	?	
50SN123F	74RAM	0.0050	99.37	1.		
52TE123M	72NDS6	0.8370		1.	0.194	
48CD124	74FOG	1.0000	0.1	1.	9.54	
51SB124N	69MEY	1.0000		M		
51SB124F	69MEY	1.0000		M		
50SN125M	72NDS5	0.9957		M		
50SN125F	67WIL	1.0000	82.5	M		
51SB125	75PER	1.0000		M	13.9	
52TE125M	75PER	1.0000		1.	13.9	
50SN126	76SMI	0.3680		M	2.15	
51SB126M	73AUB	0.8600		M		
51SB126F	73AUB	1.0000		1.		
50SN127F	71APT	0.2978	40.	M		
51SB127	67RAG	0.3570		M	0.62	
52TE127M	70APT	0.0040		M	4.8	
52TE127F	70APT	0.0074	98.	M	?	
50SN128	76LEW	1.0000		1.	6.010	
51SB128M	72KER	1.0000		1.		
51SB128F	71MCD	1.0000		1.		
53 I128	73AUB	1.0000	77.7	M		
49IN129M	74GEE	0.3968		M		
51SB129	70CAL	0.4350		M		

Table IX (continued)

NUCLIDE	REFE	FN	IBG.S.		GAMMA	INT.	CON.COEF.
52TE129M	72NDS4	0.0500	32.52		M	4.8	0.4
52TE129F	69DIC	1.0000			M	4.8	0.4
53 I129	76MAR	1.0000			1.	12.3	
54XE129M	72NDS	1.0000			1.	12.3	
49IN130	73KER	1.0000			1.		
50SN130F	76END	0.7125			M	1.7	
51SB130M	76END	0.9980			M		
51SB130F	74KER	1.0000			1.		
53 I130F	70QUA	0.9974			M		
49IN131M	74GEE	0.9259			M		
51SB131	71BLA	0.4400			M		
52TE131M	76END	0.0386	3.8	0.4	M	0.241	
52TE131F	71MAC	0.6691			M	0.257	
53 I131	70NDT	1.0000			M	1.45	
54XE131M	73MAR	1.0000			1.	49.	
50SN132	72KER	1.0000			M	?	
51SB132M	74KER	1.0000			1.		
51SB132F	74KER	1.0000			1.		
52TE132	76HID	1.0000			M	5.31	
53 I132M	73DIK	0.1320			M	21.8	
53 I132F	76END	0.9870			M		
52TE133M	68PAR	0.8700			M		
52TE133F	68PAR	0.7262			M		
53 I133F	76END	0.8730			M	8.7	
54XE133M	75PER	1.0000			1.	8.7	0.4
54XE133F	76END	1.0010			M	1.69	
51SB134F	72KER	0.9992			M		
52TE134	76END	0.3070			M	1.53	
53 I134M	72COR	0.7900			M	6.46	
53 I134F	76END	0.9540			M		
55CS134M	75PER	1.0000			1.	136.	
55CS134F	75PER	1.0000			M		
53 I135	71MAC1	0.3028			M		
54XE135M	73MAR	1.0000			1.	0.232	
54XE135F	73MAR	1.0000			M	0.073	
56BA135M	75HEN	1.0000			1.	5.42	
53 I136F	74CAR1	0.6930			M		
55CS136	76END	0.9990			M		
54XE137	75MON	0.0318	66.	23.	M		
56BA137M	76MAR	1.0000			1.	0.112	
53 I138	76WES	0.0980			M		
54XE138	73MAR	1.0000	18.	3.	M	?	
55CS138M	71CAR	0.2500			M	218.	
55CS138F	76MAR	0.0763			M		
54XE139	71TAL	0.5683	22.		M		
55CS139	73MON	0.0802	84.		M		
56BA139	76END	1.0000	75.	3.	M	0.251	
55CS140	73SCH1	0.0083	14.		M		

Table IX (continued)

NUCLIDE	REFE	FN	IBG.S.	GAMMA		INT.CON.COEF.	
56BA140	70NDT	1.0000			M	4.65	
57LA140	72MCI	1.0000			M		
54XE141	71TAL	0.0260	49.		M	?	
55CS141	71TAL	0.0510	5.9		M	8.5	
56BA141	70MCI	0.0460	10.		M	0.18	
57LA141	70MCI	0.0026	97.		M		
58CE141	73AUB1	1.0000	30.		1.	0.456	
56BA142	71LAR	0.2996			M	?	
57LA142	71LAR	0.4901	13.		M		
59PR142F	67NDS	1.0000	96.28		1.		
57LA143	76BLA	1.0000			M	?	
58CE143	71LUD	1.0000			M	6.546	
55CS144	76MON	0.7130			M	?	
57LA144	75MON1	0.9033			M		
58CE144	75PER	1.0000	75.8	0.9	M	1245.	60.
59PR144M	75PER	1.0000			M	1245.	60.
59PR144F	75PER	1.0000	97.96	0.07	M		
56BA145	76PFE	0.1370	39.		M	4.56	
57LA145	76PFE	0.0350	17.		M	4.56	
58CE145	76PFE	0.6330			M	4.65	
59PR145	75HIL	0.0069	98.18		M		
58CE146	76END	0.5500			M	3.2	
59PR146	70FAS	0.8758			M		
57LA147	75LOH	0.4550			M	?	
58CE147	75LOH	0.3598			M	?	
59PR147	75PIN	1.0000	5.0		M	12.26	
60ND147	69GUN	1.0000	0.5		M	2.1	
61PM147	67NDS	1.0000	99.92				
61PM148M	76END	0.0878			M	3.51	
61PM148F	76END	0.0233	54.3	1.4	M		
59PR149	76PIN	1.0000	17.5		M	1.11	
60ND149	76END	0.2730			M	348.	
61PM149	66MCI	1.0000	96.		M		
61PM150	70BAR	0.7415			M		
60ND151	75REI	0.1653			M	3.96	
61PM151	73COO	0.2400	11.		M	?	
62SM151	67LED	1.0000	98.4		1.	3.55	
60ND152	71DAN	1.0000			M	?	
61PM152M	71DAN	1.0000	70.		M		
61PM152F	71DAN	1.0000	61.		M		
63EU152N	75PRU	0.0173	73.		M		
63EU152F	72BAK	0.2640			M		

Table IX (continued)

NUCLIDE	REFE	FN	IBG.S.	GAMMA	INT.CON.COEF.
61PM153	69SMI	1.0000		M	319.
62SM153	75REI	1.0000	21.	M	1.721
64GD153	76END	0.2950		M	3.83
61PM154F	71DAU	0.6849		M	?
63EU154	69GUN	1.0000		M	1.2
62SM155	76END	0.0375		M	4.38
63EU155	76END	0.3267	13.	M	9.59
62SM156	76BUR	0.1390		M	6.
63EU156	74KLU	0.1030	27.	M	0.977
62SM157	63NDS	1.0000		M	
63EU157	66DAN	1.0000		M	?
63EU159	69KEM	1.0000		M	?
64GD159	69BRO	0.1040	63.7	M	11.
63EU160	73DAU	1.0000		M	?
65TB160	69GUN	1.0000		M	4.67
64GD161	75GAS	1.0000		M	13.6
65TB161	74TUL2	0.2810	10.	M	2.52
65TB162F	76BUY	0.7890	0.4	M	7.14
65TB163	71KAF	1.0000		M	7.9
65TB164	71GUJ	0.2010		M	9.
66DY165M	72MAU	0.0013		M	31.5
66DY165F	74BUY1	0.0008	83.	M	3.13
66DY166	75BUY	0.0597	5.	M	35.9
67HO166M	70REI	1.0000		1.	7.
67HO166F	70REI.	1.0000	51.	1.	6.92
66DY167	77TUU	0.0470		M	0.97
67HO167	76END	1.0000	15.	M	5.7
67HO168	73TIR	0.6276		M	1.
67HO169	73HAR	0.6514		M	?
68ER169	75PER	1.0000	58. 3.	1.	215. 110.
67HO170M	74KAW	0.1956	23.	1.	7.52
67HO170F	74KAW	0.0238	64.	M	7.52
69TM170	67LED	1.0000		M	7.55

Table X

Standart output and input format from ENSDF. Data set for 88Y decay

```
88SR     88Y EC DECAY                    NBS-MJM                              750912
88SR  N 0.9935      3
88SR CN NR          FROM RI(1836+2734+3220G)=100
88Y   P 0.0           4-                107 D      1              3619       4
88SR  L 0.0           0+                STABLE
88SR  L 1836.06     2 2+
88SR  E 1783          4 0.20     1 5.8      6 9.76     5              6.0        7 1U
88SR2 E K=0.840  $ L=0.101  $ M+=0.022  $ EAV=358 2$
88SR CE IB          FROM 63RH01 (0.20% 1), 04BA26 (0.203% 16)
88SR  G 1836.04     2 100
88SR  L 2734.08     3 3-
88SR  E 885           4            94.6     7 6.849    7
88SR2 E K=0.873  $ L=0.105  $ M+=0.023  $
88SR  G 898.02      2 94.0     7
88SR  G 2734.03     7 0.64     3
88SR  L 3218.47     5 2+
88SR  E 401           4            0.032    5 9.37     7                          1U
88SR2 E K=0.852  $
88SR  G 1382.39     5 0.024    5
88SR  G 3218.48     8 0.0078   17
88SR  L 3584.7      8
88SR  E 34            4            0.066    13 6.8     2
88SR2 E K=0.69  5$
88SR  G 850.6       8 0.066    13
```

Table XI

γ ray energies and intensities. Character editing and page lay out by the Medlist programm

88Y EC DECAY (107 D 1) I(min)=0.10%

Radiation Type	Energy (keV)	Intensity (%)	Δ(g-rad/μCi-h)
Auger-L	1.79	105 6	0.0040
Auger-K	12	27.1 23	0.0070
β+ 1 max	761 4		
avg	358.0 20	0.200 10	0.0015
X-ray L	1.8	1.7 6	=0
X-ray $K\alpha_2$	14.09790 2	17.6 8	0.0053
X-ray $K\alpha_1$	14.16500 2	33.9 14	0.0102
X-ray Kβ	15.8	9.1 4	0.0031
γ 2	898.020 20	93.4 7	1.79
γ 4	1836.040 20	99.35 3	3.89
γ 5	2734.03 7	0.64 3	0.0370

3 weak γ's omitted (ΣIγ = 0.10%)
Maximum γ±-intensity = 0.40%

Table XII

ENDF/B-V style format of ENSDF data, useful for computer processing

```
3.9088) 04 0.0                    0          0          0          2  83 8451     1
0.0          0.0                  0          0          2          0  83 8451     2
88Y EC DECAY (107 D 1)                                NBS-MJM/ENSDF/750912      83 8451     3
88Y EC DECAY (107 D 1)              1(MIN)= 0.10%                               83 8451     4
0.0          0.0                  1        451          6          0  83 8451     5
0.0          0.0                  1        457         27          0  83 8451     6
                                                                     83 3   0     7
3.9088) 04 0.0                    0          0          0          3  83 8457     8
9.2448) 06 8.5400) 06             0          0          6          0  83 8457     9
5.8797) 03 2.9560) 02 2.5921D 06  0 1.0578D 02 2.2020D 04 0.0           83 8457    10
0.0          0.0                  0          0          6          1  83 8457    11
2.0000) 00 0.0          3.5190D 06 4.0000D 03 1.0000D 00 0.0           83 8457    12
2.0000) 00 1.0000) 00             0          0          5          1  83 8457    13
1.0000) 00 0.0          7.1600D 02 3.6023D 01 1.0000D-03 0.0           83 8457    14
2.0000) 00 8.0000) 00             0          0          5          3  83 8457    15
1.0000D 00 0.0          5.1637D 03 2.9340D 02 1.0000D-03 0.0           83 8457    16
2.0000) 00 0.0                    0          0          5          9  83 8457    17
1.0000) 00 0.0          2.5921D 06 1.0578D 02 1.0000D-03 0.0           83 8457    18
1.0000) 00 2.0000) 00             0          0          6          1  83 8457    19
3.5800) 05 2.0000) 03 2.0000D-03  1.0000D-04 7.6094D 05 4.0000D 03     83 8457    20
8.0000) 00 2.0000) 00             0          0         18          3  83 8457    21
1.7900) 03 0.0          1.0530D 00 5.2866D-02-2.0000D 00 0.0           83 8457    22
1.2100) 04 0.0          2.7099D-01 2.2952D-02-1.0000D 00 0.0           83 8457    23
0.0         -1.0000) 00 0.0         0.0          3.0000D 01 0.0        83 8457    24
0.0          2.0000) 00           0          0         54          9  83 8457    25
1.8100) 03 0.0          1.7121D-02 5.4183D-03-4.0000D 00 0.0           83 8457    26
1.4099) 04 2.0000)-01 1.7559D-01 7.2791D-03-2.0000D 00 0.0             83 8457    27
1.4165) 04 2.0000D-01 3.3917D-01 1.3453D-02-1.0000D 00 0.0             83 8457    28
1.5800) 04 0.0          9.1131D-02 3.9492D-03-3.0000D 00 0.0           83 8457    29
8.9802) 05 2.0000) 01 9.3389D-01 6.9602D-03 2.0000D 00 0.0             83 8457    30
1.8360) 06 2.0000) 01 9.9350D-01 3.0000D-04 4.0000D 00 0.0             83 8457    31
2.7340) 06 7.0000D 01 5.3584D-03 2.9806D-04 5.0000D 00 0.0             83 8457    32
1.1699) 06-1.0000) 00 9.7164D-04 0.0        3.0000D 00 0.0             83 8457    33
5.1100) 05 0.0          4.0000D-03 2.0000D-04-1.0000D 01 0.0           83 8457    34
                                                                     83 9   0     35
                                                                     83 0   0     36
                                                                      0 0   0     37
```

Table XIII

French file format obtained directly from the ENSDF format by program

```
                    39 Y  88
                    ******
   PERIODE T1/2= 107.000 +/-  1.000 D

          ENERGIE +/- ERREUR  KEV        BRANCHEMENT +/- ERREUR  % A
QBM+    3619.000     4.000                    0.0        0.0

** BETAS+     NB+=  4                    ABSOLU

   ENERGIE +/- KEV     INTENSITE +/-
    34.000    4.000      0.0       0.0
   401.000    4.000      0.0       0.0
   885.000    4.000      0.0       0.0
  1783.000    4.000      0.20      0.01

** GAMMAS      NG =  6                  RELATIF          A/R=.9935

  ENERGIE +/- KEV     INTENSITE +/-          ALFA T    +/-     POLAR   % M
   850.600    0.800      0.066     0.013      0.0       0.0             0.0
   898.020    0.020     94.000     0.700      0.0       0.0             0.0
  1382.390    0.050      0.024     0.005      0.0       0.0             0.0
  1836.040    0.020    100.000     0.0    *   0.0       0.0             0.0
  2734.029    0.070      0.640     0.030  *   0.0       0.0             0.0
  3218.479    0.080      0.008     0.002  *   0.0       0.0             0.0

COMMENTAIRES:EDITION DU 12/ 9/75
ENSDF=      NRS-MJM
```

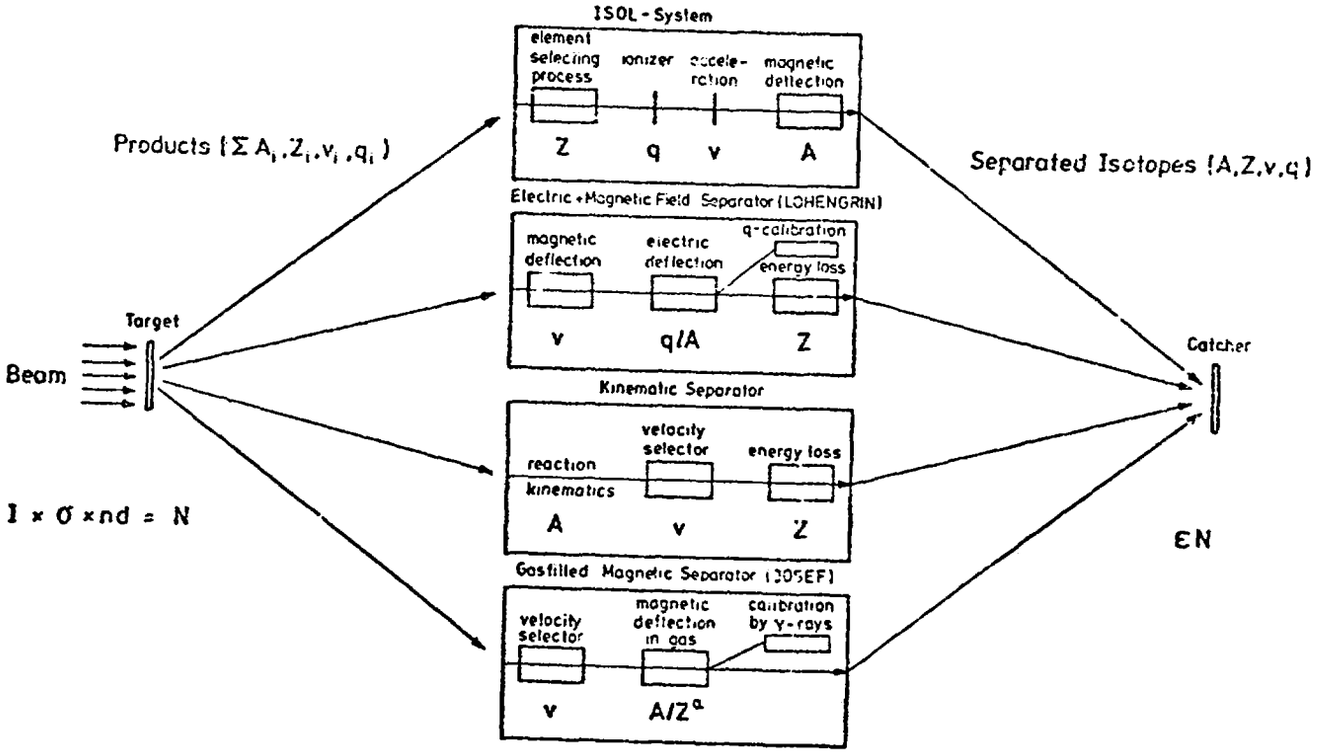

Figure I : Schemes of different methods to separate short lived isotopes

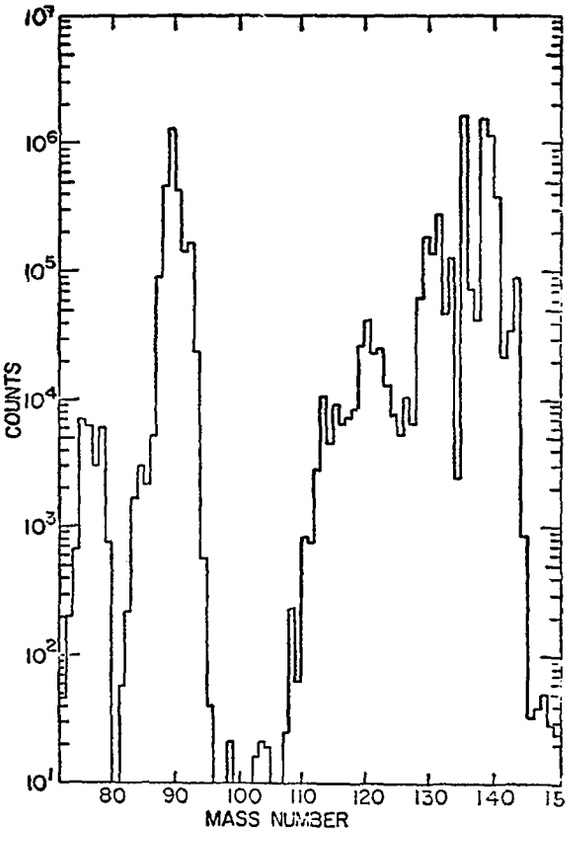

a) Activity measured with a 4π beta detector at the Tristan II facility

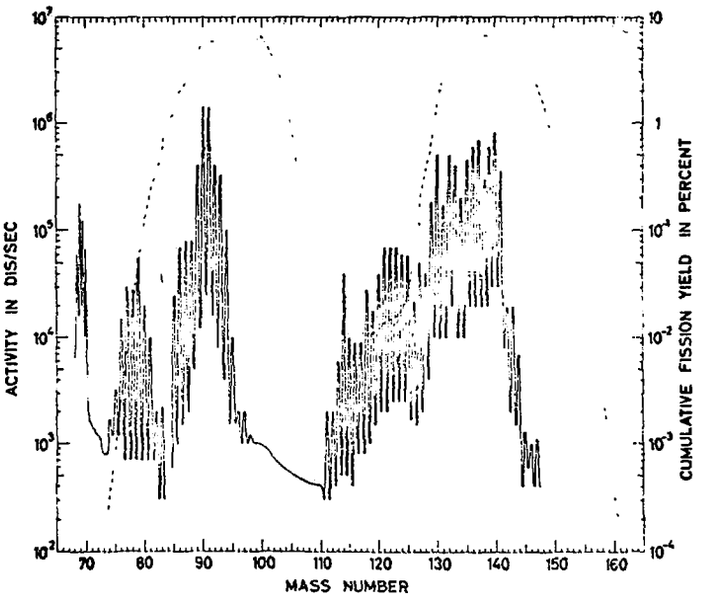

b) Activity measured with a 4π beta detector at OSIRIS

Figure II

Figure III

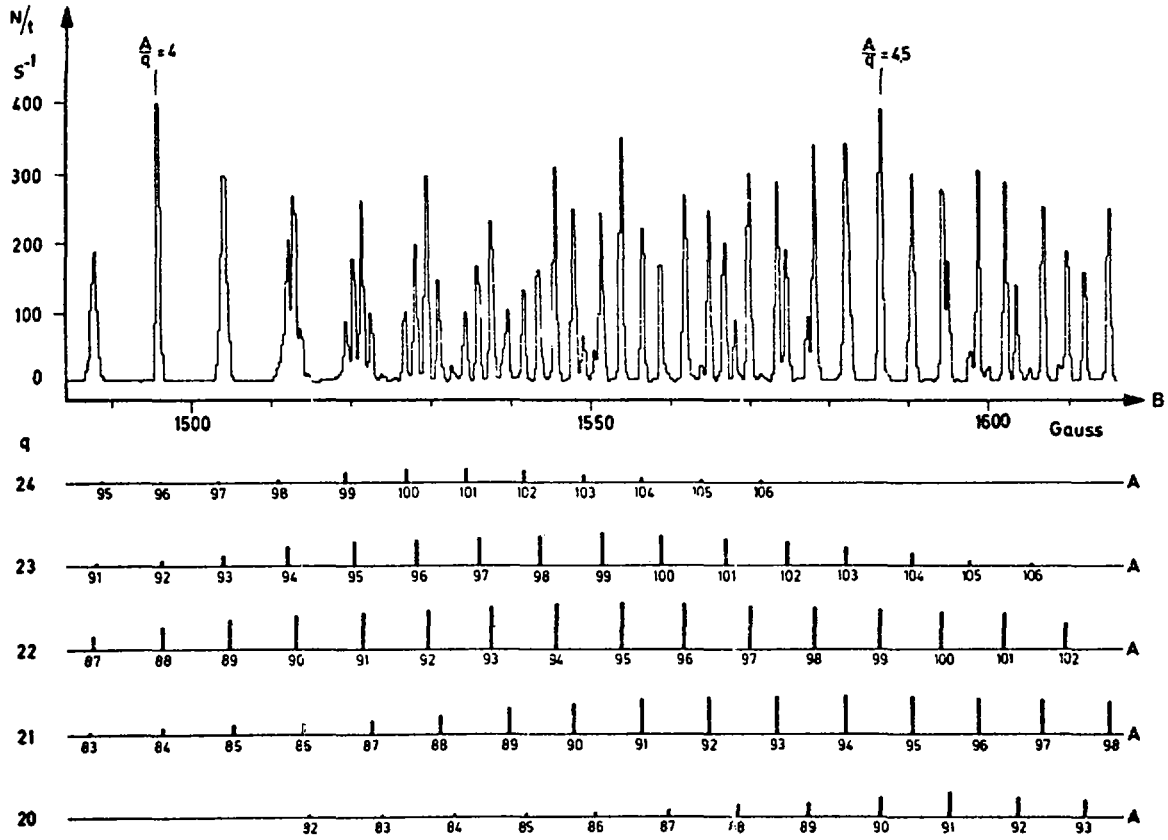

a) A/q spectrum recorded with constant electric field HT = 460 KV for the light group F.P.

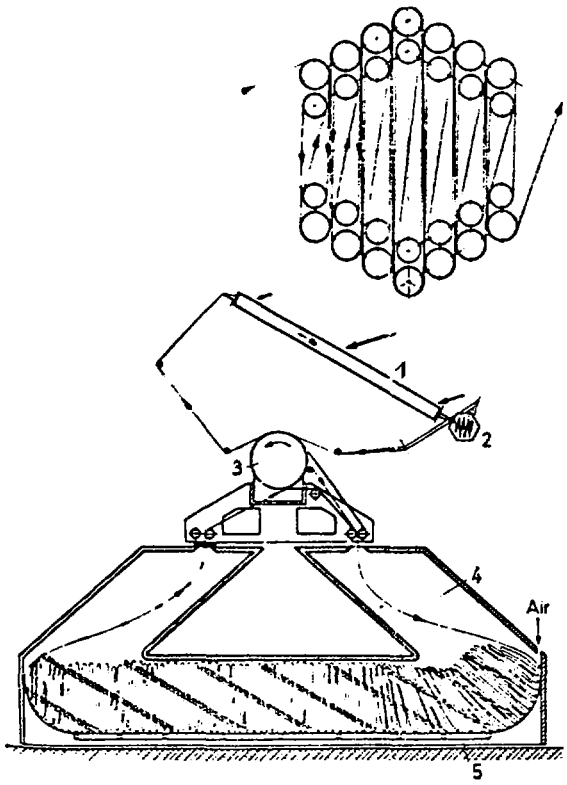

b) The moving tape system arrangement at the exit slit of LOHENGRIN:
(1) Exit slit of the separator.
(2) Zig-zag pattern device to concentrate the activity.
(3) Driving wheel,
(4) Tape reservoir,
(50 Loop transport system.

Figure IV

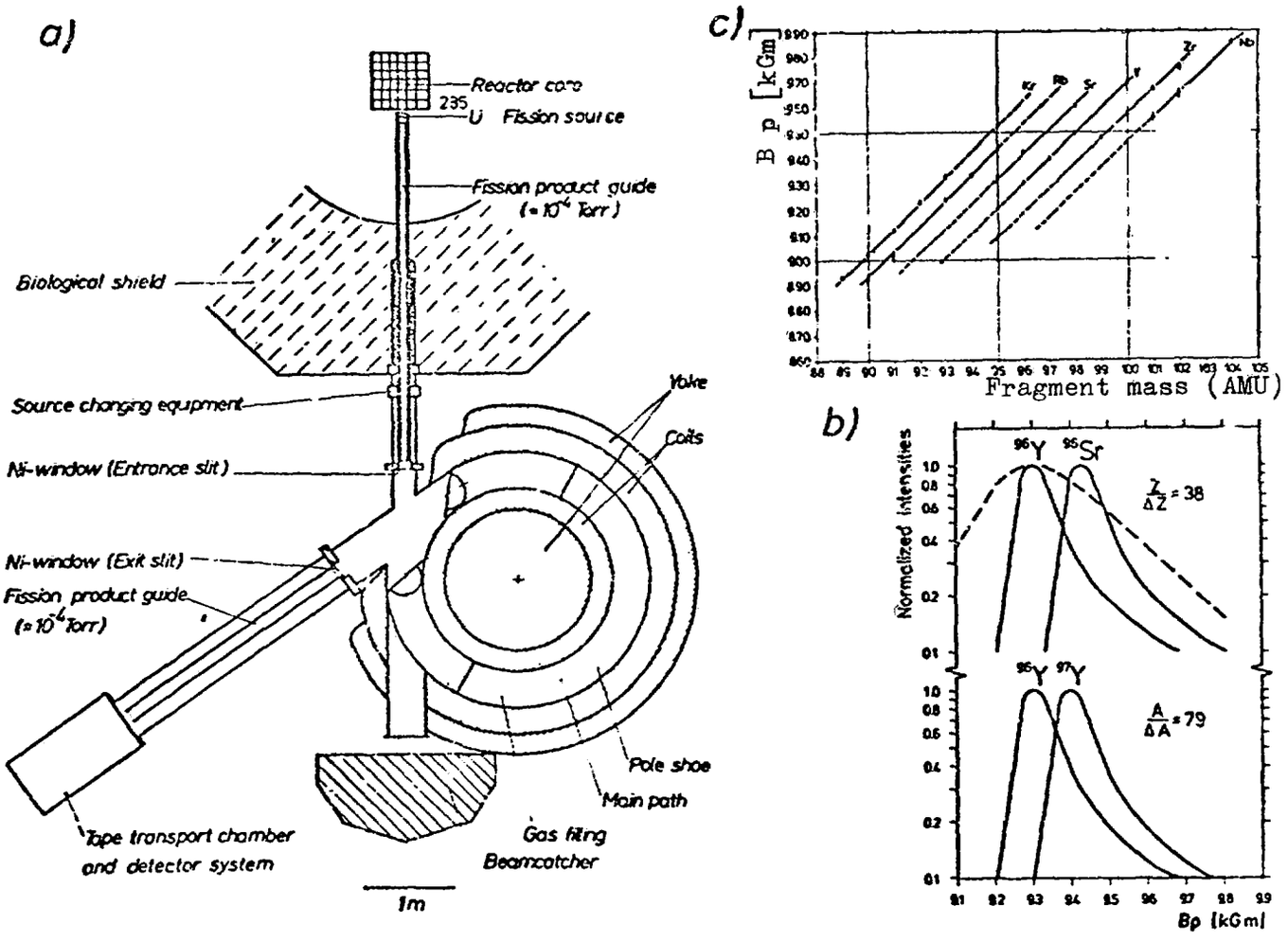

a) Schematic view of the gas filled separator JOSEF.

b) Intensity distribution vs the magnetic rigidty of ^{96}Sr and ^{96}Y, ^{97}Y.

c) Calibration of JOSEF for light fission products, gas-filling He at 4 torr.

Figure V

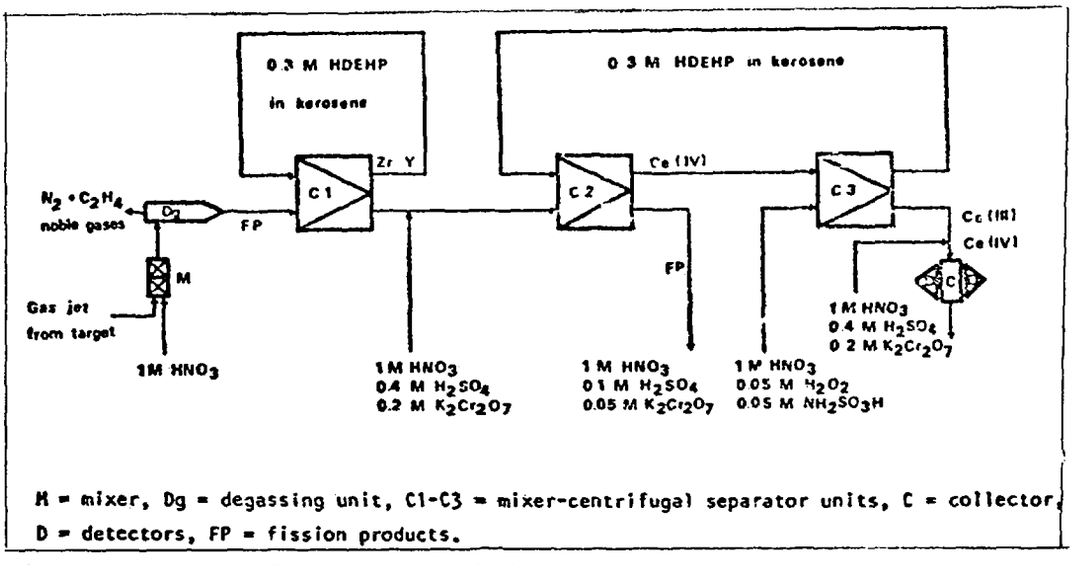

Flow sheet showing the chemical system used for the isolation of Ce isotopes with SISAK.

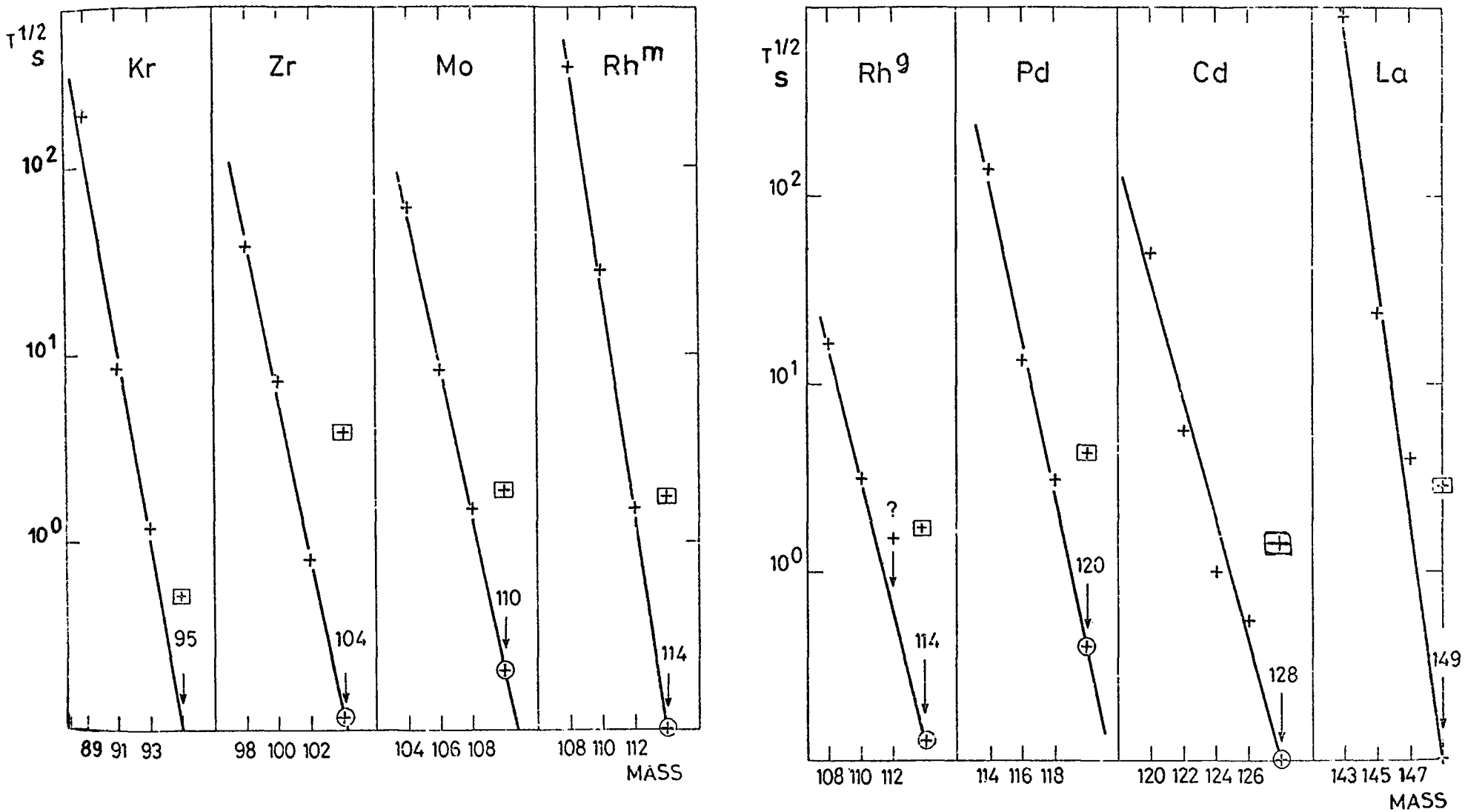

Figure VI: Interpolation of known and unknown half lives

Figure VII

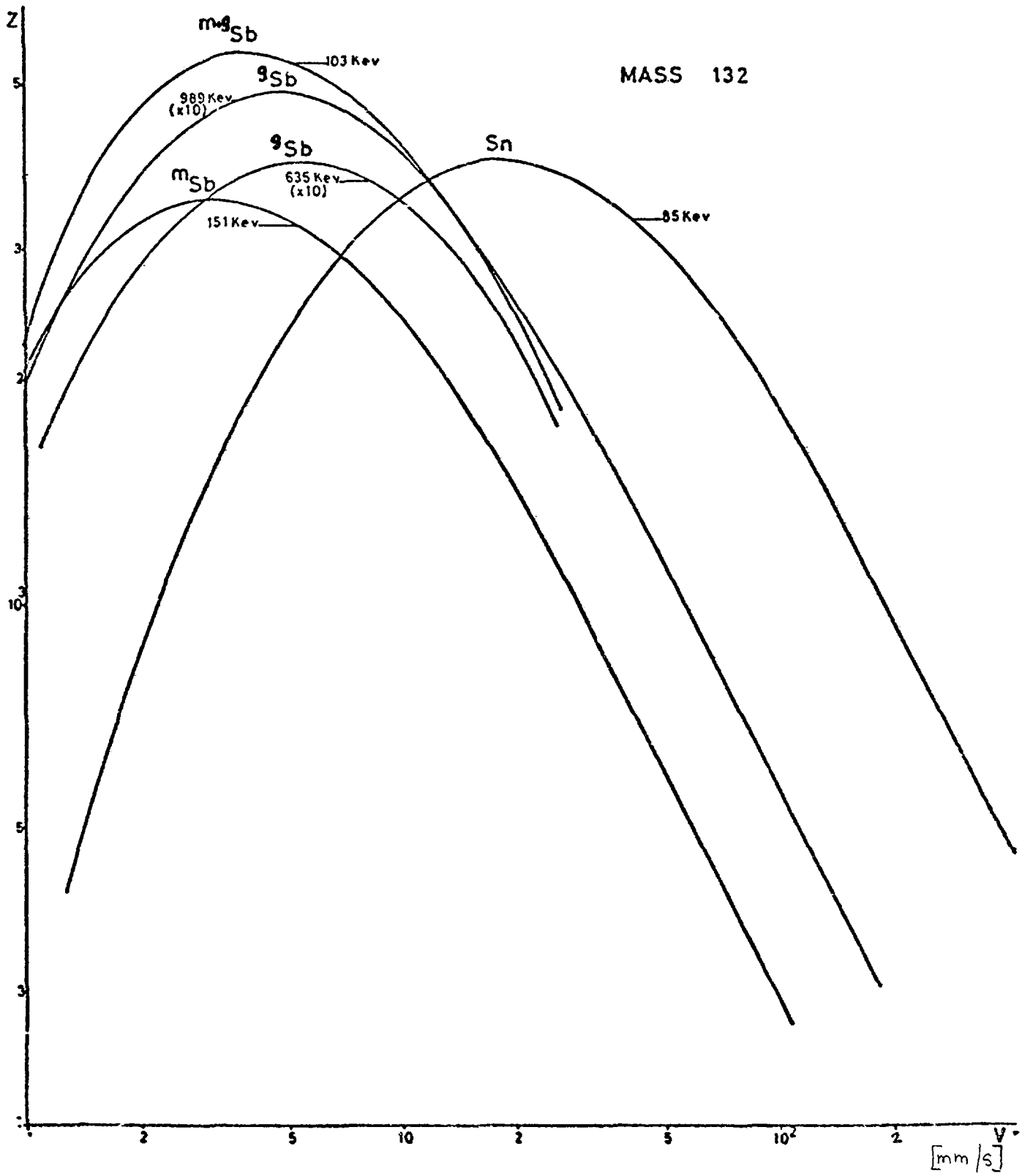

The mass chain 132 γ-activity as a function of tape speed

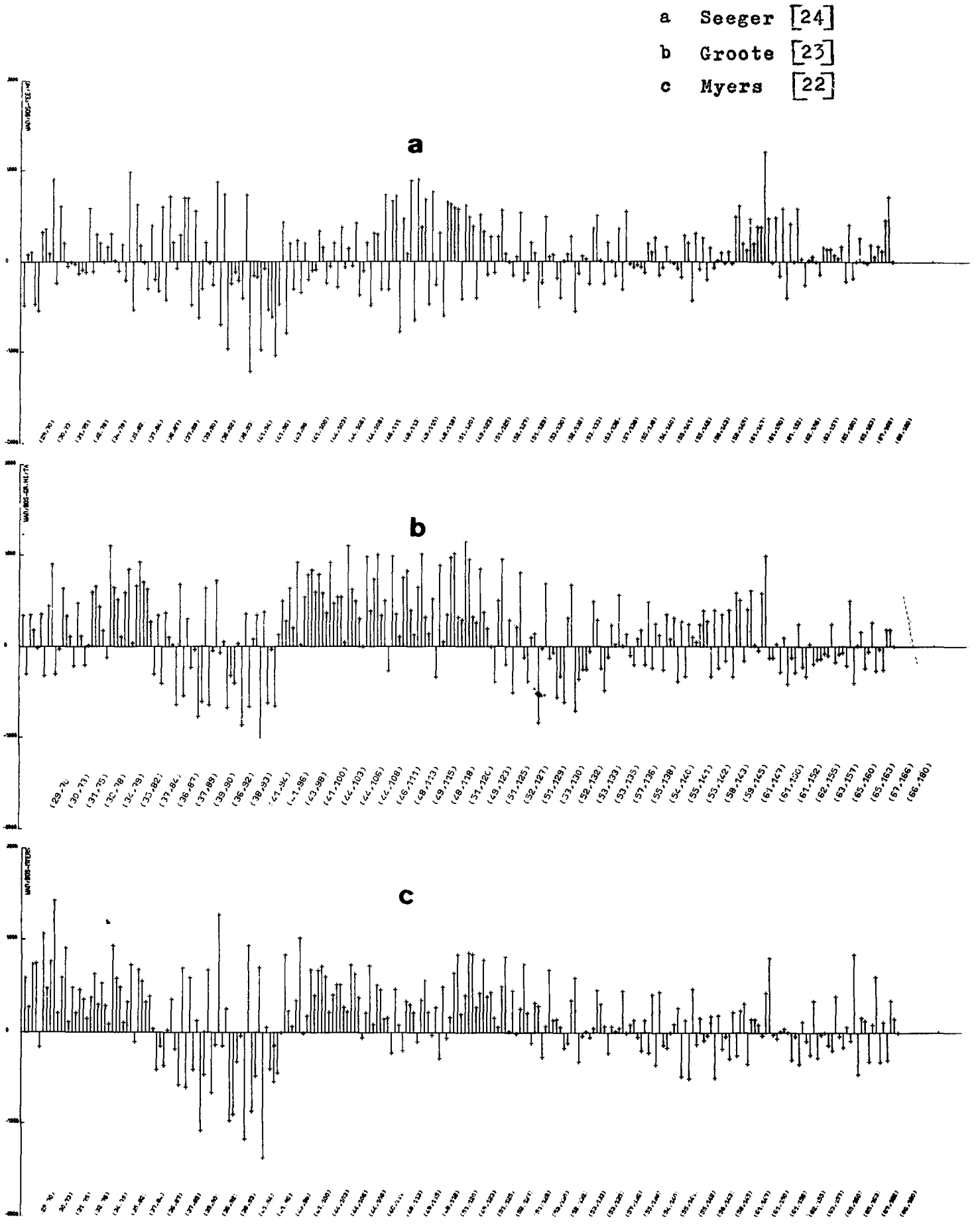

Figure VIII

Difference between masses calculated and experimental masses of Wapstra, Bos (1975), [21]

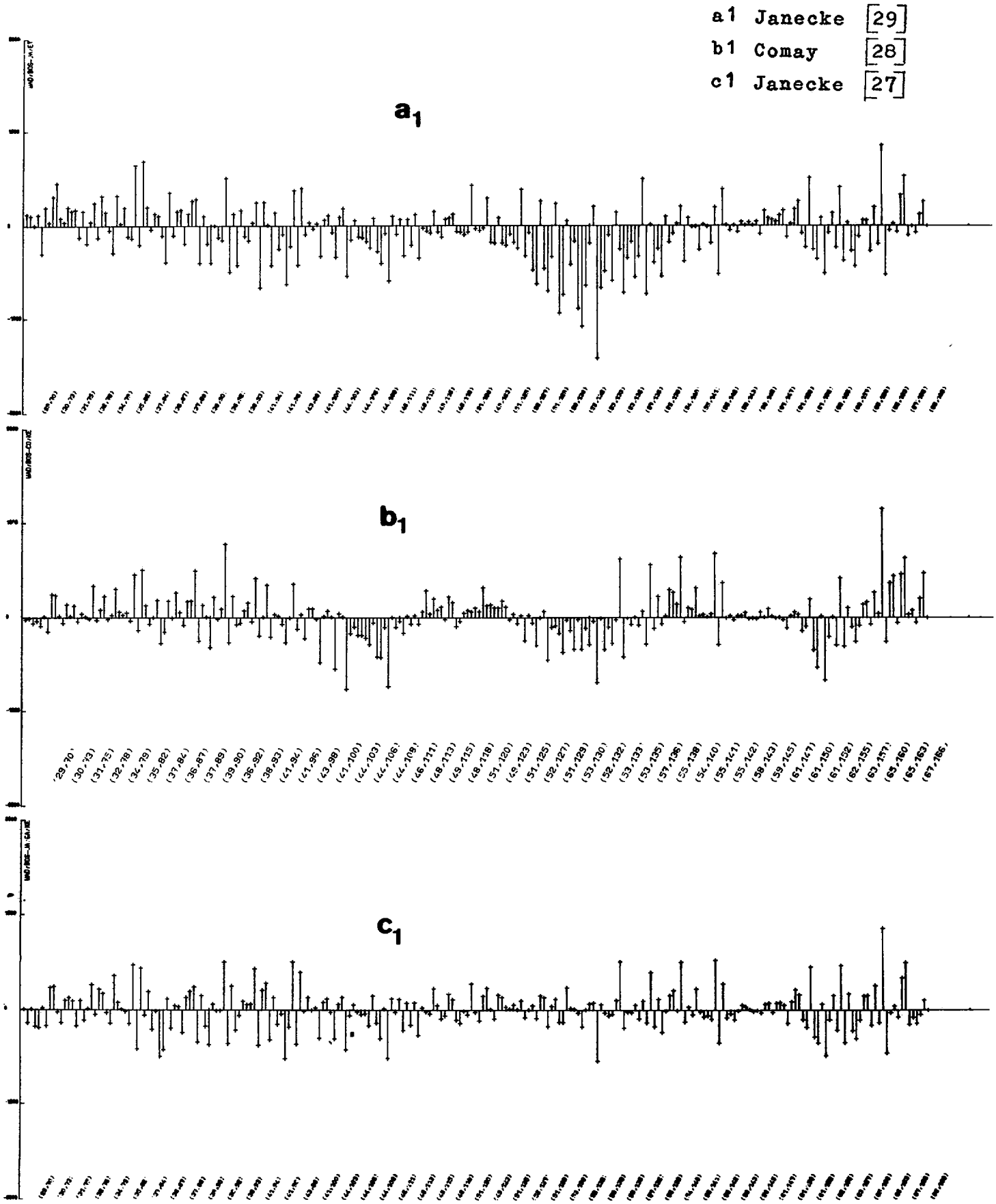

Figure VIII

Difference between masses calculated and experimental masses of Wapstra, Bos (1975), [21]

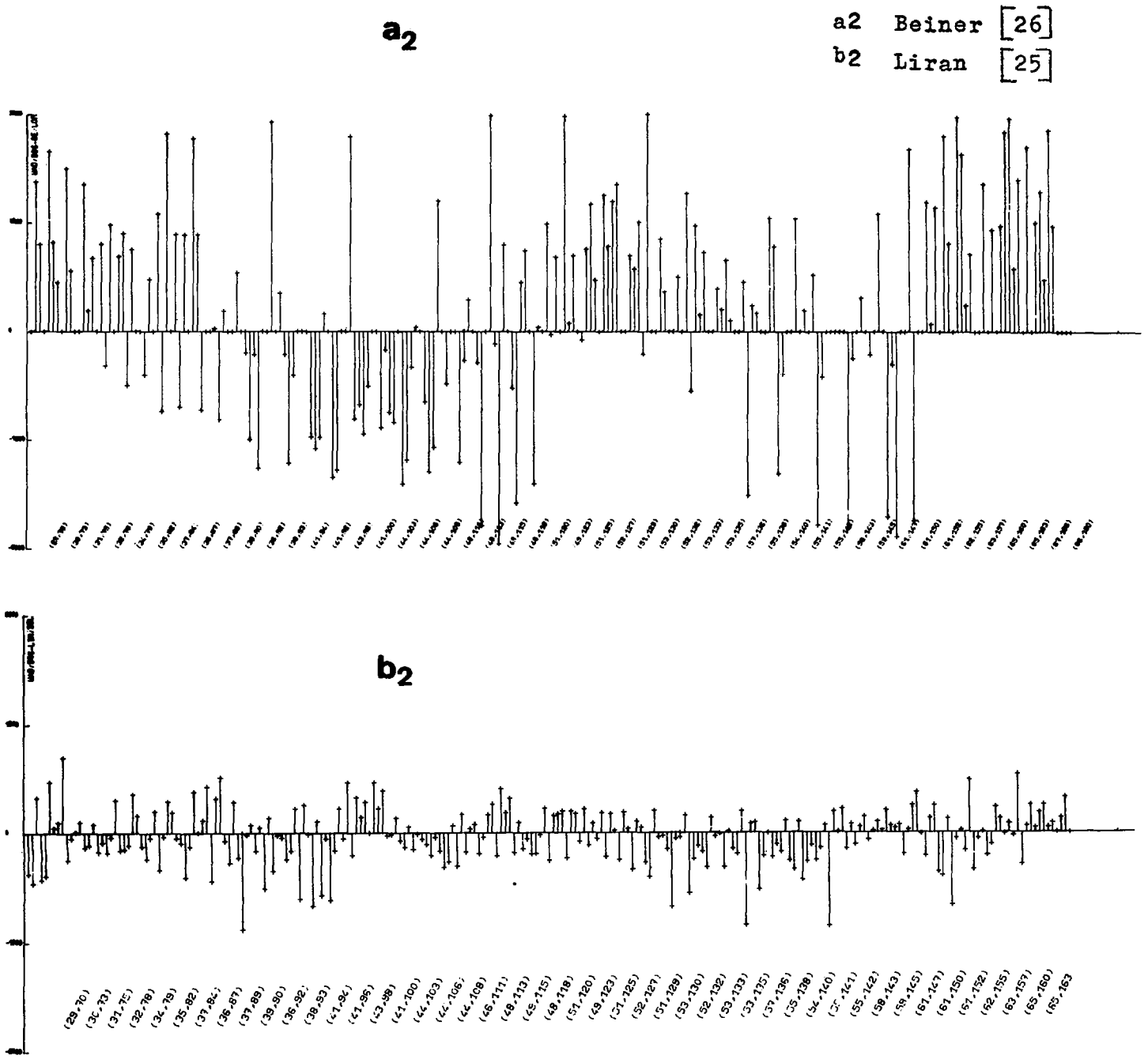

Figure VIII

Difference between masses calculated and experimental masses of Wapstra, Bos (1975),[21]

a)

Figure IX

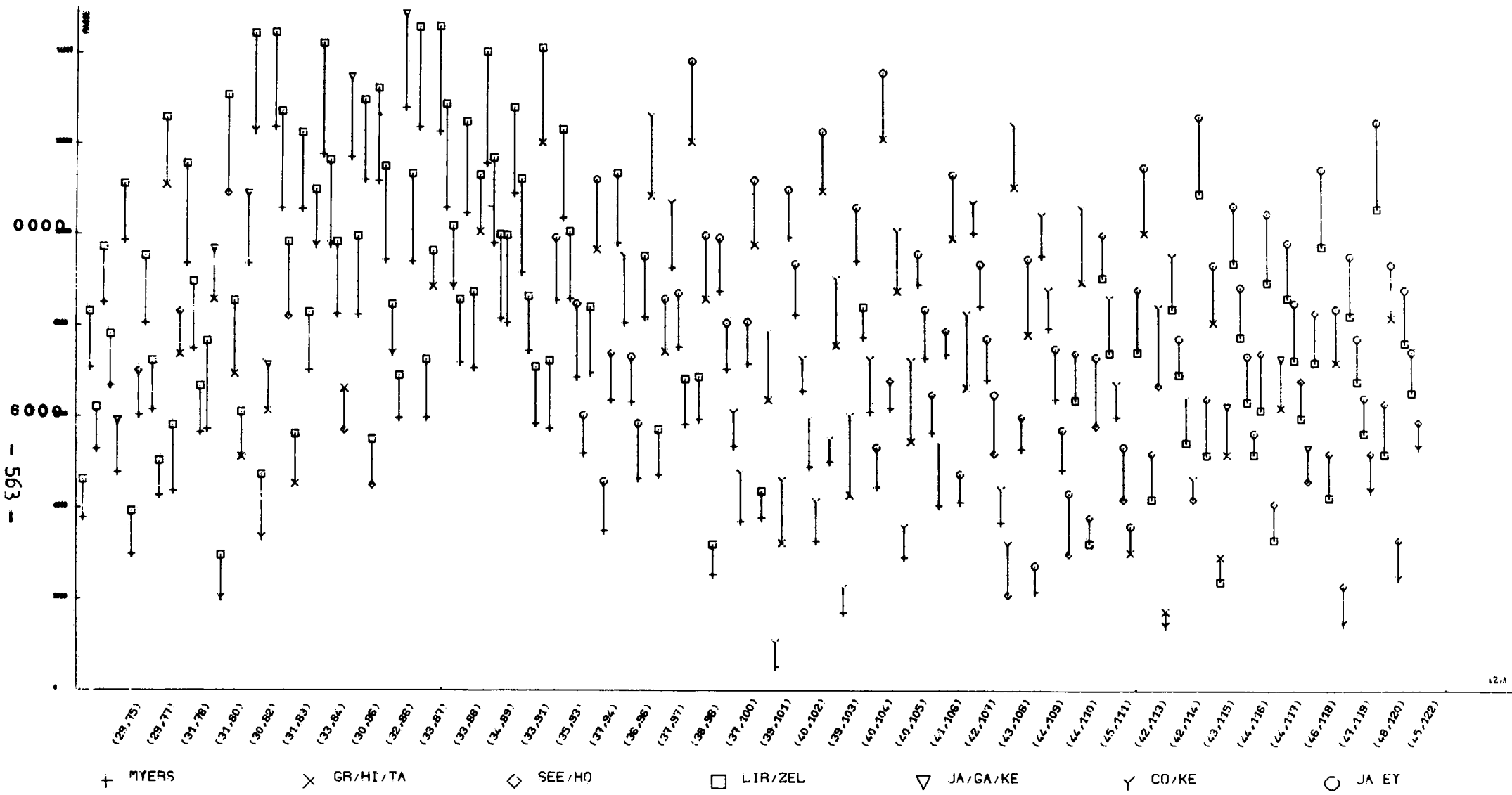

Upper and lower mass for nucleides without experimental data

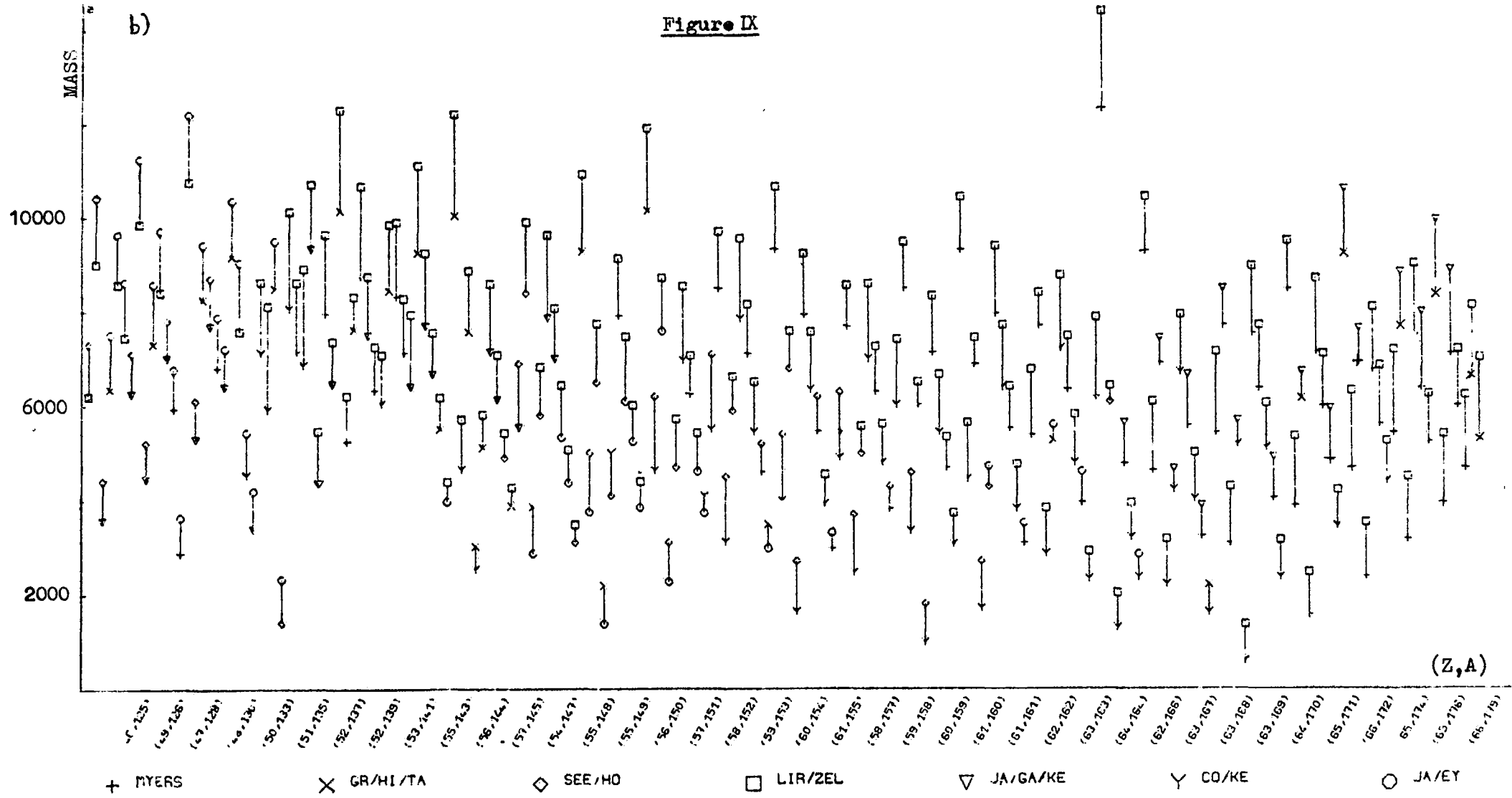

Figure IX

Upper and lower mass for nuclides without experimental data

Figure X : ENSDF Decay Data

03-24-77

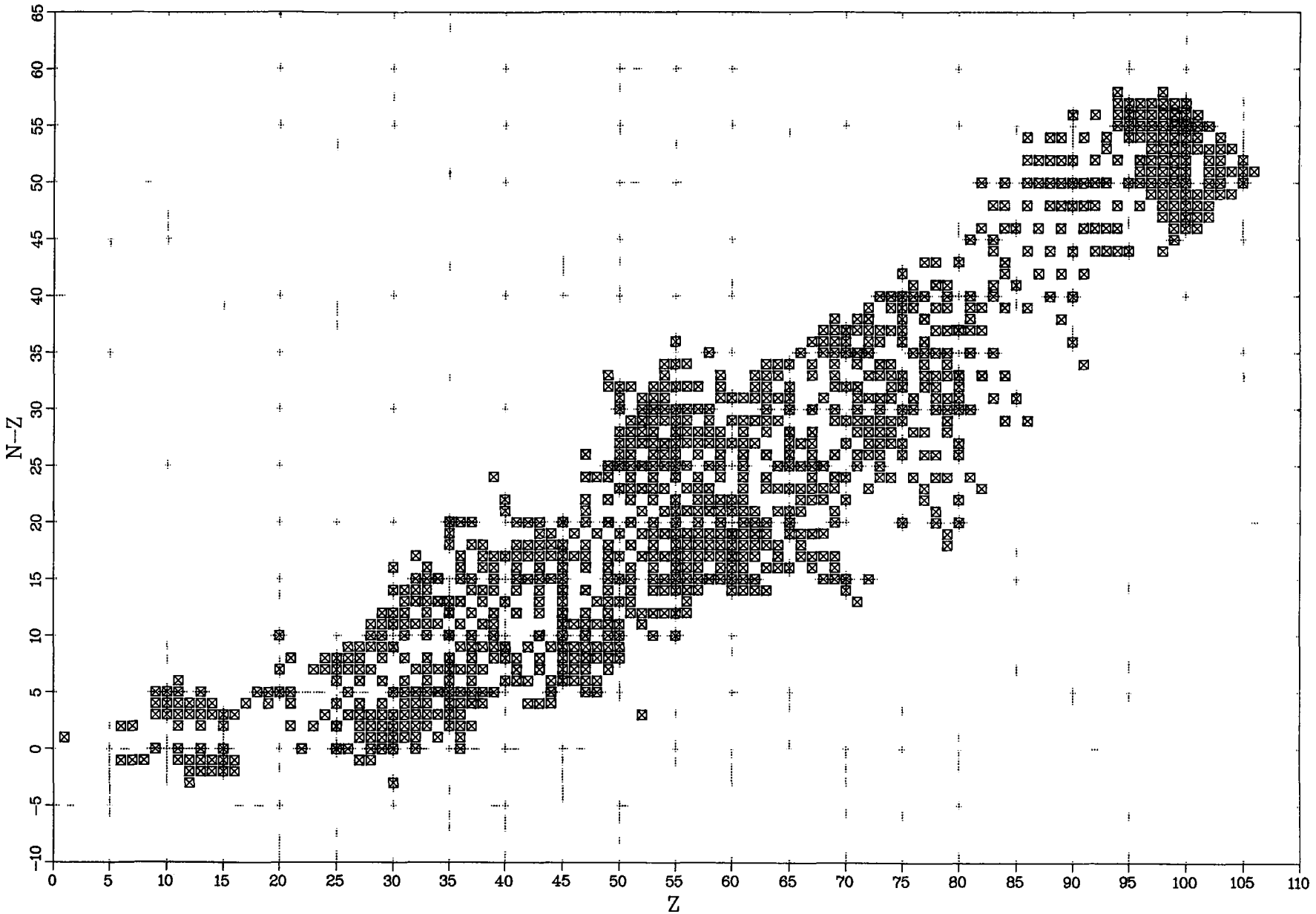

Review paper 13

STATUS OF DELAYED NEUTRON DATA

by

G Rudstam

The Swedish Research Councils'
Laboratory, Studsvik, Fack,
S-611 01 Nyköping, Sweden

Abstract

Our knowledge about the emission of delayed neutrons from fission products has improved considerably since the last FPND-panel at Bologna in 1973. The development is summarized in the present review with special regard to the following items

- the identification of delayed-neutron precursors including their labelling by half-life determinations,
- the neutron branching ratios,
- the neutron energy spectra of individual precursors,
- the yields and decay properties of delayed neutrons in nuclear fuel,
- the composite delayed-neutron spectrum in nuclear fuels.

The field of delayed neutrons is quite well covered by now, at least as far as reactor applications are concerned. Some points needing further attention are discussed at the end of the review.

1. INTRODUCTION

The field of delayed-neutrons has been intensively studied during the time since the last FPND-panel at Bologna in 1973. The reason is mainly the extensive use of the isotope-separator-on-line technique which has enabled us to investigate even very short-lived nuclides in a very convenient way. As a result of all these efforts the field of

delayed-neutron emission is now quite well known although a number of points remain to be elucidated.

In this review the development of our knowledge about delayed-neutron emission since the Bologna panel will be discussed. In the present situation with a large amount of data available it seems logical to start with a survey of the properties of the individual precursors and then to use these data to build up the combined effects of the precursors in nuclear fuel for comparisons with the results of integral measurements.

2. PROPERTIES OF INDIVIDUAL DELAYED-NEUTRON PRECURSORS

2.1. Identification of delayed-neutron precursors

In his Bologna review Amiel[1] lists 42 delayed-neutron precursors among the fission products. To-day the number of known cases is 67, i.e. a considerable increase in only three years. They are tabulated in Table 1, and their positions are indicated in the isotopic chart shown in Fig. 1.

Table 1 also contains average half-life values evaluated from published results. In general, different determinations agree very well. The reason is obvious - many of them have been obtained by neutron counting which is clean and little disturbed by other activities, especially for mass-separated samples. In a few cases listed below discrepancies occur which need be clarified:

^{79}(Zn,Ga). As discussed in ref.[48] mass-separated samples of mass 79 probably contain two delayed-neutron precursors - ^{79}Zn and ^{79}Ga. The difference between half-life determinations using delayed-neutron counting[2] and beta counting[3] might well be real reflecting differences in the P_n-values.

^{140}I. Experiments using chemical separation[20,45] have yielded half-life results in the range 0.86 - 0.89 s whereas experiments using mass separation give a smaller value, or 0.60 s. There are reasons to believe that the results with mass-separated samples are the more reliable ones because there is only one neutron activity in the sample.

After chemical separation of iodine there will be many neutron activities present. This must lead to great difficulties in the half-life determinations.

^{143}Xe. For this nuclide there are two experimental determinations yielding very different results. The determination obtained by neutron counting of mass-separated samples has been preferred.

^{146}Cs. The nuclide ^{146}Cs has been studied with mass-separated samples. The low value from ref.[32] disagrees with the others, among which there is also a determination by the same research group[30]. No explanation of the discrepancy has been offered. Since the higher result is backed up by two other independent experiments, it should be chosen.

At least one delayed-neutron precursor is now known for each mass in the ranges 79 - 99 and 127 - 146. Furthermore, one precursor of mass 123 is known. Clearly, there is still a large number of delayed-neutron precursors to be detected over the whole isotopic chart because all nuclides sufficiently far away from stability are expected to be delayed-neutron precursors. Most of these precursors will be of comparatively little interest for nuclear technology, however, (but certainly not for basic science) because of too low fission yields (cf. Section 3.1).

2.2 Branching ratios

The fraction of decays of a precursor leading to the emission of a neutron, i.e. the P_n-value, has been listed in Table 2. This list comprises 46 precursors which means that the branching ratio has only been measured for two thirds of the number of known cases.

The straight-forward way to determine the branching ratio is to measure, for the same sample or for different samples monitored in a suitable way, both the neutron activity and the sample strength, the latter by measuring the beta activity or counting the number of atoms (or ions). Then, after a proper calibration of the counters, the branching ratio is ob-

tained directly. It has been common practice, however, to use indirect methods for evaluating the sample strengths. These methods may make use of yields which have not been measured but are obtained from fission yield systematics. Experiments have shown that the pattern of independent fission yields is far from smooth. Rather, it exhibits a pronounced fine structure[53,54]. This makes earlier P_n-value determinations using indirect methods and assuming the yield pattern to be smooth questionable. Thus, erroneous indirect determinations might explain certain of the large differences in the P_n-determinations revealed in Table 2. Still, deviations between direct determinations far outside of what to be expected from the limits of errors given are frequent (cf., for instance, ^{88}Se, ^{135}Sb, ^{142}Cs, ^{144}Cs). Factors of two or more, corresponding to tens of standard deviations, may be found. There must be systematic errors involved which give rise to such large deviations.

Izak-Biran and Amiel have tried to reevaluate P_n-determinations involving fission yield values[55]. Still, the results must be regarded with some caution unless all fission yields appearing in the treatment are based on measurements.

The P_n-values obtained by direct and indirect methods are kept apart in Table 2. In some cases with large discrepancies direct determinations have been preferred (^{88}Se, ^{86}As). For ^{142}Cs direct determinations are so different that it seems meaningless to give an average value.

Evidently, a great effort is required before our knowledge about P_n-values can be considered to be in a satisfactory state. In addition to the cases with large discrepancies quoted above there are others with only indirect determinations or where the limits of error are too large. This list comprises ^{86}As, ^{89}Se, ^{94}Kr, ^{99}Sr, ^{97}Y, ^{99}Y, ^{134}Sn, ^{136}Sb, ^{136}Te, ^{137}Te, ^{140}I, and ^{141}I. This means that about half of the measured cases should be remeasured. Furthermore, for about the same number of precursors no P_n-value measurement has yet been carried out.

2.3 Estimates of P_n-values

There have been many attempts to predict P_n-values theoretically but the results have been modest. For theoretical estimates one needs information on total decay energies (Q_β) and neutron separation energies (B_n), on the competition between neutron and gamma emission, and on the shape of the beta strength function. There are considerable uncertainties in all these items. The decay energies and separation energies have to be extracted from mass formulas whose applicability far from stability may be questionable. The relative neutron and gamma widths are little known, and also the energy dependence of the beta strength function is under debate. In a recent report Rudolph and Kratz[56] have studied the possibility to estimate the P_n-values of the known precursors using simple assumptions concerning the quantities involved in the calculation. The authors interprete the failure to make accurate predictions using statistical models by the persistance of nuclear structure effects which manifest themselves in strong resonances in the beta strength functions and in the gamma-to-neutron competition. Still, there are correlations between the P_n-values and the "neutron window" $Q_\beta - B_n$ which can be used for crude estimates of P_n-values of unknown precursors. Thus, Kratz and Herrmann[57] find a linear relationship when plotting $\log P_n$ *versus* $\log\left\{(Q_\beta - B_n)/(Q_\beta - C)\right\}$, where C is a constant depending on the nuclear type of the precursor. In a similar treatment by Amiel and Feldstein[58] further elaborated by Nir-El and Amiel[59] the form

$$P_n = a\,(Q_\beta - B_n)^m \qquad (1)$$

is chosen to represent the branching ratios. The precursors are grouped according to nuclear type, and the constants a and m are determined for each type (and also for heavy and light precursors).

As an illustration a comparison between different methods to estimate P_n-values is given in Table 3.

2.4 Energy spectra

A field with considerable development since Bologna is the study of the energy spectra of delayed neutrons from individual precursors. In such studies isotope or chemical separation is mandatory. The techniques used are time-of-flight measurements, proton-recoil deter-

minations or ^{3}He-spectrometry. The ^{3}He-spectrometer seems to be the best tool for high energies whereas time-of-flight and proton recoil spectrometry are superior at low energies.

The energy resolution of the ^{3}He-spectrometer varies with energy. Franz et al.[60] have reached a resolution of 12 keV (FWHM) for thermal neutrons and about 20 keV for 1 MeV neutrons. The time-of-flight method is capable of an excellent resolution at low energies, but the resolution is rapidly lost at energies above a few hundred keV. The proton-recoil spectrometer resembles the time-of-flight method: the resolution is good at low energies deteriorating at high energies.

The precursors for which the spectra have been measured are indicated in Table 4. A surprising result is the fine-structure appearing in many cases. It is especially pronounced for precursors where the emitter contains a single neutron in excess of the 50- and 82-closed shells (^{85}As, ^{87}Br, ^{134}Sn, ^{135}Sb, ^{136}Te, ^{137}I). This is shown in Fig. 2. The fine structure gradually diminishes in importance as one moves away from the closed shells as shown in the series ^{87}Br, ^{88}Br, ^{89}Br, and ^{90}Br (cf. Fig. 3). Several suggestions have been put forward to explain this structure. One is that the density of those levels which can be fed by allowed beta decay is sufficiently low so that the neutron spectrum simply gives a picture of the levels fed[67] Another explanation connects the structure to statistical fluctuations in the beta decay step and in the subsequent neutron-gamma competition[72,104]. A third explanation takes into account the presence of antianalogue states, core-polarized states and spin-flip states with preferential beta-feeding leading to fine-structure in the beta strength.[73]

It should be noted that the antianalogue state lies within the neutron window in all the cases shown in Fig. 2 except for ^{137}I. This supports the hypothesis of favoured beta decay to certain levels. It is somewhat embarrassing, though, that all the cases in Fig. 3 also have their antianalogue state within the window. It is true that they also exhibit fine structure, but it is much less prominent than for the other cases.

The question about the origin of the fine structure in the neutron spectra is still open, and more work is needed in order to solve it. Among the interesting investigations to be carried out is an experimental determination of the level density of the neutron emitters. This can be done for ^{87}Kr and ^{137}Xe by measuring the (n,γ)-cross sections of ^{86}Kr and ^{136}Xe as a function of the neutron energy[74]. Such an experiment could decide whether the level density is low enough to be resolved by the neutron spectrometers, or whether it more corresponds to the density required in order to give rise to fine structure in a statistical treatment based on Porter-Thomas fluctuations.

One might expect fine structure in the beta strength to show up in the studies of the beta strength functions described in ref.[75]. The latter experiments were of a low-resolution type, however, tending to smearing out any fine structure. The strong increase in the beta strength with increasing excitation energy encountered for many nuclides is not in disagreement with preferential feeding of high-lying states.

For a few precursors neutron spectra have been measured at different laboratories. The ^{3}He-measurements of the spectrum of ^{137}I carried out at Mainz[66] and at Studsvik[67] have been closely compared. Both energies and intensities agree well. The spectrum given in ref.[66] is slightly harder, but this may be due to statistical uncertainties in the upper end of the neutron spectrum. For ^{135}Sb, however, the energies agree but there is disagreement concerning the intensities. The spectrum measured at Mainz[66] is considerably harder than that measured at Studsvik[67]. The source of the discrepancy is probably to be found in the conversion of the pulse spectrum to neutron energy spectrum (insufficiently known response functions at neutron energies $\gtrsim$ 1 MeV).

In the case of ^{87}Br the neutron spectrum has been measured using ^{3}He-spectrometers by the groups at Mainz[68] and Studsvik[67], and also using a proton-recoil spectrometer by Ray and Kenney[76]. There is a general agreement about the energy of the neutron peaks. The latter authors claim, however, that the spectrum should be considerably softer than found by the other groups. This is an important point which has to be looked into. In order to make possible a detailed comparison the spectra obtained in the three different experiments have been divided into 100-keV intervals starting from 100 keV (the lower limit for the proton-recoil experiment).

The relative distribution of the neutrons in the different intervals is given in Table 5. Obviously, the two ^{3}He-measurements agree well with one another whereas the proton-recoil measurement gives a spectrum which falls off much more rapidly with increasing energy.

It is difficult to see how large errors can appear in the ^{3}He-spectrometry where the calibration and the determination of the response function are straight-forward. Thus, at least until more evidence to the contrary has been gathered, it seems prudent to rely on the intensities obtained by this technique. The results from the proton-recoil spectrometry have to be analyzed in a rather complicated manner which is possibly subject to errors.

2.5 Average neutron energy

From the measured neutron spectra the average neutron energy can easily be evaluated. This has been done for a number of cases, and the results are included in Table 4. Results obtained from an analytical description of the spectra[61] are also given in the table. Differences between these two sets of values are due to the fact that the analytical description covers the whole energy range from zero energy up to the full neutron window whereas the experimental spectra usually are cut at both ends. For most precursors the differences are small.

The average neutron energy has also been measured directly. Reeder, Wright, and Alquist[62] have used a detector arrangement consisting of three rings of ^{3}He-counters with different amounts of moderator. This means different energy dependence of the response of the three rings and, suitably calibrated, the ratio between the count rates of the rings can be used for measuring the average neutron energy. The results determined for halogen and alkali isotopes using two methods - either each ring scaled individually (A) or the outer rings scaled together (B) - are given in Table 4 where they can be compared to those obtained from the spectra.

If we judge an agreement within some 20 % to be satisfactory (note that the errors of the direct determinations are statistical only and do not include possible systematic errors), there is disagreement in three cases, i.e. ^{89}Br, ^{93}Rb, and ^{94}Rb. The directly determined average energy is much higher than that obtained from the spectra. This discrepancy is

hard to explain as none of these precursors have an appreciable fraction of their neutrons above 1 MeV where the discrepancy between ^{3}He-results make the average energy deduced from the spectra questionable (cf. preceding section). The fact that the direct determinations lead to high average energies cannot be used as an argument against the proton-recoil determinations giving softer spectra because Reeder et al. used spectra obtained with ^{3}He-spectrometry in calibrating their equipment.

2.6 Other properties of delayed-neutron precursors

In the preceding sections those properties of individual delayed-neutron precursors which are the most important ones for nuclear technology, i.e. the half-life, the P_n-value, and the neutron spectrum, have been discussed. There are other properties of less importance for technology but certainly of high scientific interest. One such property is the competition between neutron and gamma emission from the same excited level in a nucleus. Studies of this kind require complementary investigations of the gamma-rays emitted from levels at excitation energies above the neutron separation energy. The existence of such gamma-rays has been proven[68,77,78]. For an evaluation of the neutron/gamma-ray competition it is not sufficient to measure only the high-energy gamma-rays which are ground state transitions or transitions to some low-lying level in the beta-decay daughter. It is necessary to measure also the gamma-chains cascading down from the levels of interest, and this requires the determination of the whole disintegration scheme, or at least the important features of it. This is a large experiment, and it has not yet been completed for any particular case. Experiments are under way, however[79].

In order to determine whether a gamma-ray is really emitted in competition with neutron emission it is necessary to measure the neutron separation energy with precision. Until recently, only the separation energy of ^{87}Kr was accurately known. However, that of ^{137}Xe has recently been measured[80] and this measurement, yielding B_n = 4025.2±0.6 keV, revealed that two gamma-rays of energy 3907 and 3994 keV claimed to be emitted from regions above the neutron separation energy after the beta decay of ^{137}I did, in fact, correspond to energies below the separation energy. The authors used an old value of this quantity which is in error by 165 keV.

Also the neutron separation energy of ^{87}Kr has recently been remeasured with the result B_n = 5515.5±0.9 keV[82], in agreement with earlier determinations.

Another property of the delayed-neutron emission of great scientific interest is the extent of feeding of those excited levels in the final nucleus which are energetically within reach. For ^{85}As, ^{94}Rb, and ^{135}Sb gamma-rays following neutron emission have been reported[83], and neutron emission to excited states has also been proposed for ^{95}Rb, ^{96}Rb, and ^{97}Rb[84]. Similar studies are in progress at Studsvik[85].

3. MACROSCOPIC PROPERTIES

3.1 Completeness of the set of known precursors

When the properties of the individual precursors are known any macroscopic quantity pertinent to nuclear technology can be easily calculated for any conditions as regards fuel composition and irradiation history. The further quantities needed for such a calculation are the fission yields. As these are treated in another review at this panel, they will not be discussed here.

Obviously, the kind of treatment proposed will only succeed if the set of known precursors is reasonably complete. Otherwise, the macroscopic quantities obtained will only be partial.

Thus, the first problem to tackle is to test the completeness of the set of precursors known today. For this purpose the quantity $P_n \times Y_c$, where Y_c is the cumulative fission yield, has been calculated for the various precursors, with the P_n-values from Table 2 and Y_c-values from the recent evaluation of Rider and Meek (ref.[110]). The results for thermal-neutron induced fission of ^{235}U and ^{239}Pu and for fast-neutron induced fission of ^{238}U are tabulated in Table 6. Under saturation conditions the contribution of a given precursor to the effective delayed-neutron activity in nuclear fuel will be $P_n \times Y_c$.

By summing those contributions one gets for the number of delayed neutrons per 10^4 fissions 170 ± 7 for thermal neutron induced fission of ^{235}U, 70 ± 4 for thermal neutron induced fission of ^{239}Pu, and 298 ± 23 for fast neutron induced fission of ^{238}U.

A comparison of these numbers with results of direct measurements (Table 8) indicates that there is no significant difference between calculated and experimental delayed neutron yields for ^{235}U and ^{239}Pu. The contributions from precursors not included in the summation because of unmeasured branching ratios or because they are still unknown, can at most correspond to a few percent of the total effect.

Concerning ^{235}U, still unknown precursors of some importance may be found at masses 100 and 147 and a few units above these mass numbers. Further away the fission yields drop so fast as to make possible delayed-neutron precursors umimportant. Among the known precursors whose P_n-values have not yet been measured, only ^{97}Sr, ^{98}Sr, and ^{98}Y have fission yields that are large enough to give non-negligible contributions to the neutron activity. The magnitude of their effect can be estimated using predicted P_n-values of Table 3. It comes out to be about 1 neutron per 10^4 fissions.

The situation is different, however, for ^{238}U. Whereas an older evaluation of fission yields (ref.[87]), combined with a more preliminary set of P_n-values (see footnote to Table 2) leads to 383 $\pm$ 33 delayed neutrons per 10^4 fissions, which corresponds to 87 $\pm$ 8% of the measured value (Table 8), the new number of 298 $\pm$ 23 amounts to only 66 $\pm$ 5% of the measured total delayed neutron yield. This decrease is essentially caused by lower fission yields of a number of important precursors (^{87}Br, ^{89}Br, ^{90}Br, ^{96}Rb, ^{135}Sb, ^{136}Sb, ^{138}I, ^{139}I, ^{140}I, ^{141}I). In the case of ^{135}Sb and ^{136}Sb the effect is enlarged by lower P_n-values. As it seems improbable that as much as one third of the delayed-neutron yield should be attributable to precursors not included in the summation, for the moment one is led to question the reliability of the new set of yields for fast-neutron induced fission of ^{238}U.

Calculations of neutron yields have been carried out many times. A recent analysis of the energy dependence of the yield in neutron-induced fission of ^{235}U has been published by Alexander and Krick[103]. Their result for thermal neutrons is 154±8 neutrons per 10^4 fissions assuming a smooth fission yield pattern, and this number increases to 169±17 when odd-even effects in the fission yields are included. Their results are systematically higher than the experimental values which is somewhat surprising. Again they indicate, however, that all the important precursors are known by now. In order to draw further-reaching conclusions from this kind of comparison it is necessary to reduce the errors of the calculated yields by improving the P_n-values (cf. Section 2.2) and, above all, by producing solid experimental data on the fission yields of the precursors.

Extrapolated values with crude estimates of the odd-even effect are not sufficiently accurate.

3.2 Delayed-neutron groups

In evaluating macroscopic features it has been customary to classify the precursors in a series of "half-life groups". It was early found that six groups, of half-lives approximately 55.7 s, 22.7 s, 6.22 s 2.30 s, 0.61 s, and 0.23 s (for ^{235}U), served the purpose well[86,105]. It is interesting to check the basis for this classification. The nuclide ^{235}U is again chosen as an example, and the quantity P_nY_c has been plotted versus the half-life in Fig. 4. The figure shows clearly that ^{87}Br falls in the most long-lived group whose half-life agrees with that of ^{87}Br.

The next group consists mainly of ^{137}I and ^{88}Br with some contribution from ^{136}Te and ^{141}Cs. The half-life should be closer to that of ^{137}I than to that of ^{88}Br which is also the case.

For the third group, however, the situation is more complicated. One would have expected the half-life to be lower than 6.2 s because of the important contribution from 4.38 s ^{89}Br. Apparently, influence from 16 s ^{88}Br keeps it up. This shows that the physical basis for this group is weak.

Looking at Fig. 4 there does not seem to be any physical basis at all for the three short-lived groups. The P_nY_c-values are more or less randomly scattered in the region of short half-lives, and all the groups will be composed of many precursors, most precursors in addition giving contributions to two groups. Only by disregarding ^{97}Y one does find some tendency for grouping around 2.3 s, 0.6 s, and 0.2 s (the P_n-value of ^{97}Y is deduced indirectly, and it must therefore be regarded with caution). Nevertheless, the basis for the three short-lived groups is very weak indeed.

In summary, the methods of dividing the precursors into six half-life groups is artificial. It might also be dangerous. A grouping based on the decay of the neutron activity might not be applicable for features such as the effective delayed-neutron spectrum. There other properties of the individual precursors come into play, and a different grouping

might be called for.

The approach of grouping the precursors was very useful at the time when the knowledge about the individual precursors was incomplete, or even hardly existant. This is no longer the case. The old classification cannot be made accurate in view of the large number of precursors contributing to the total effect, and it should be abandoned wherever possible in favour of a more accurate treatment involving the summing of the properties of the individual precursors. Such a treatment is easily adjusted to any experimental conditions which happen to be of interest.

For situations where the old group classification is still of interest reference is made to the review given by Amiel at the Bologna panel[1] and to a more recent analysis by Tuttle[90]. These reviews cover a wide band of fissile nuclides: ^{232}Th, ^{233}U, ^{238}U, ^{239}Pu, ^{240}Pu, ^{241}Pu, and ^{242}Pu. Fractional group yields and decay constants are given for the six half-life groups. There is also a new experimental report dealing with fast fission of ^{235}U, ^{238}U, and ^{239}U by Besant et al[91] made available to this panel. On the whole, the latter work confirms the group constants found earlier.

In this connection it may be mentioned that Aten[92] has tried to simplify the situation further by expressing the delayed-neutron activity by one term only, of the type

$$I = N\left(\frac{n}{F}\right) e^{-k\sqrt{t}}, \qquad (2)$$

where N = number of fissions per unit time up to t =0,

$\left(\frac{n}{F}\right)$ = delayed neutron yield per fission,

I = delayed-neutron production per unit time,

t = time, and

k = a constant depending on the fissile nuclide.

The degree of agreement with experimental results for ^{235}U can be seen in Table 7. The neutron activity is underestimated at short decay times and overestimated at long decay times. The formula works best in a medium range of decay times.

3.3 Delayed-neutron yields

The delayed-neutron yields have been touched upon earlier in connection with the discussion of the completeness of the set of known precursors (Section 3.1). Generally, the yields are independent of the incident neutron energy up to a point at which second-chance fission becomes energetically possible[1]. Thus, thermal-neutron induced fission and fast fission can be compared. In his extensive review Tuttle[90] has analyzed all experimental evidence available to him and reevaluated the results wherever appropriate. His list of yields is reproduced in Table 8. The new experimental values obtained by Besant et al[91] have also been introduced in the table. They are systematically lower than Tuttle's recommended values and, in fact, in better agreement with Keepin's old set of data[86]. The authors offer no explanation to this discrepancy which, by the way, does not seem too serious in view of the limits of error given.

Another recent publication[101] reports relative delayed-neutron yields in the fission of ^{237}Np induced by 0.4 - 1.2 MeV neutrons.

It was early noted that there exists a linear relationship between the logarithm of the neutron yield and the parameter A - 3Z where A and Z are the mass number and the atomic number of the fissioning nuclide[86,93]. Tuttle[90] uses a slightly different parameter, or (A - 3Z)(A/Z). This kind of relationship might be useful for estimating yields of unmeasured nuclides. The reason for the shift in yields when changing the fissile material is obviously connected to a change in the cumulative yields of the precursors since the P_n-values are independent of the nuclide fissioning. This shift in the fission yield pattern is smooth, and therefore one should certainly expect a smooth change of the neutron yields as a function of the fissioning nuclide. Aten has analyzed the situation and finds that a relationship such as the one mentioned above is compatible with reasonable assumptions concerning the development of the yields[92].

In a contribution to this panel Pai also follows this line and makes theoretical predictions of delayed-neutron yields of all actinides and transuranics of interest to nuclear industry[94].

3.4 Time dependence of the delayed-neutron emission as obtained by the summing procedure

In this section the delayed-neutron effect in nuclear fuel will be calculated as a sum of contributions from the individual precursors. Denoting the abundance of the precursor j at time t by $N_j(t)$ the total production rate $D(t)$ is equal to

$$D(t) = \sum_j \lambda_j N_j(t) P_{nj}, \tag{3}$$

where λ_j and P_{nj} are the decay constant and the P_n-value of the precursor j.

In order to calculate the abundances one needs to know the original composition of the fuel, the irradiation history, the half-lives, the delayed-neutron branching ratios, and the neutron capture cross sections of all the fission products and actinides. The general evaluation gets quite complicated but, fortunately, the calculation can be simplified because of the position of most of the precursors way out on the neutron-richer side of the peaks of the charge distributions. This means that the parent effect is usually small - the parents have smaller yields than the precursors. In addition, the parents are usually more short-lived than the precursors and rapidly saturated. It is then sufficient to take them into account by using the cumulative yields of the precursors in the following - approximate but quite accurate - formula for the delayed-neutron activity as a function of time t after stopping the fission process of length T:

$$D(t) = n \sum_j P_{nj} Y_j \, (1 - e^{-\lambda_j T}) \, e^{-\lambda_j t} \tag{4}$$

where n is the fission rate during the irradiation, and Y_j is the yield (cumulative and properly weighted if the fuel contains several fissile components) of the precursor j. A calculation of the time variation of the number of delayed neutrons based on Eq. (4) with nuclear data taken from Tables 1 and 2 (half-lives and P_n-values, respectively) and with fission yields from Table 6 has been carried out for ^{235}U-containing fuel. The result can be compared to a more elaborate calculation using the code INVENT[95], and with experimental results from refs.[86] and [91] in Table 7. The summation results agree well with each other proving that the simple expression (4) is sufficiently accurate. They also agree

well with the integral measurements with a maximum deviation of a few per cent in the intermediate cooling time range. This is another proof that the set of known precursors is reasonably complete.

3.5 Effective energy spectrum of delayed neutrons in nuclear fuel

A number of recent integral determinations of delayed-neutron spectra have been carried out using either ^{3}He-spectrometry[97,102] or proton-recoil spectrometry[98,99,100]. Spectra corresponding to the different half-life groups have been recorded. Near-equilibrium spectra are available for thermal-neutron induced fission of ^{235}U[98,99] and for fast-neutron induced fission of ^{232}Th[100], ^{233}U[100], ^{235}U[100,102], ^{238}U[100,102], and ^{239}Pu[100,102].

When comparing the equilibrium spectra obtained by different methods it turns out that those reported by Evans and Krick using ^{3}He-spectrometry[102] are systematically harder than those obtained by Eccleston and Woodruff using proton-recoil spectrometry[100]. Evans and Krick attribute this difference to the fact that their spectra contain a larger fraction of the most short-lived precursors with presumably higher energies than the spectra given in ref.[100]. The discrepancy might also be connected to the difference between the ^{3}He-spectrometer technique and the proton-recoil technique as discussed in Section 2.4. It seems necessary to straighten out this point.

The effective energy spectrum of the delayed neutrons in nuclear fuel can also be evaluated along the same line as the decay curve. Using the same approximation as in the preceding section one can write

$$P(E_n)dE = n\sum_j Y_j(1 - e^{-\lambda_j T})e^{-\lambda_j t} P_j(E_n)dE_n, \qquad (5)$$

where $P(E_n)dE_n$ is the energy distribution resulting from adding all the spectra of the precursors, properly weighted by the abundances. The delayed-neutron energy spectrum, normalized to the P_n-value and corresponding to the precursor j, is denoted by $P_j(E_n)dE_n$.

From here on one can choose two different paths. One approach is to introduce the various precursor spectra in tabular form. This has

been done by Saphier et al.[96] who compose the effective delayed-neutron spectrum from the spectra of 21 precursors. They also construct spectra corresponding to the six half-life groups in thermal-neutron induced fission of ^{233}U, ^{235}U, ^{239}Pu, and ^{241}Pu, in fast-neutron induced fission of ^{232}Th, ^{235}U, ^{238}U, ^{239}Pu, and in 14.7 MeV neutron induced fission of ^{235}U and ^{238}U, and they present the results in a 54-energy group representation.

3.5 Effective energy spectrum of delayed neutrons in nuclear fuel

A number of recent integral determinations of delayed-neutron spectra have been carried out using either ^{3}He-spectrometry[97,102] or proton-recoil spectrometry[98,99,100]. Spectra corresponding to the different half-life groups have been recorded. Near-equilibrium spectra are available for thermal-neutron induced fission of ^{235}U[98,99] and for fast-neutron induced fission of ^{232}Th[100], ^{233}U[100], ^{235}U[100,102], ^{238}U[100,102], and ^{239}Pu[100,102].

When comparing the equilibrium spectra obtained by different methods it turns out that those reported by Evans and Krick using ^{3}He-spectrometry[102] are systematically harder than those obtained by Eccleston and Woodruff using proton-recoil spectrometry[100]. Evans and Krick attribute this difference to the fact that their spectra contain a larger fraction of the most short-lived precursors with presumably higher energies than the spectra given in ref.[100]. The discrepancy might also be connected to the difference between the ^{3}He-spectrometer technique and the proton-recoil technique as discussed in Section 2.4. It seems necessary to straighten out this point.

The effective energy spectrum of the delayed neutrons in nuclear fuel can also be evaluated along the same line as the decay curve. Using the same approximation as in the preceding section one can write

$$P(E_n)dE = n\sum_j Y_j(1 - e^{-\lambda_j T})e^{-\lambda_j t} P_j(E_n)dE_n, \qquad (5)$$

where $P(E_n)dE_n$ is the energy distribution resulting from adding all the spectra of the precursors, properly weighted by the abundances. The delayed-neutron energy spectrum, normalized to the P_n-value and corresponding to the precursor j, is denoted by $P_j(E_n)dE_n$.

From here on one can choose two different paths. One approach is to introduce the various precursor spectra in tabular form. This has been done by Saphier et al.[96] who compose the effective delayed-neutron spectrum from the spectra of 21 precursors. They also construct spectra corresponding to the six half-life groups in thermal-neutron induced fission of ^{233}U, ^{235}U, ^{239}Pu, and ^{241}Pu, in fast-neutron induced fission of ^{232}Th, ^{235}U, ^{238}U, ^{239}Pu, and in 14.7 MeV neutron induced fission of ^{235}U and ^{238}U, and they present the results in a 54-energy group representation.

If ^{239}Pu is chosen instead of ^{235}U as the fissionable material, the 25 cases treated correspond to 80 % of the total neutron activity of identified precursors, and this percentage increases to 95 % when the estimated spectra are included.

The use of Eq.(5)now permits the calculation of the effective delayed-neutron energy distribution in nuclear fuel for any irradiation and cooling conditions. An example is given in Fig. 6 containing delayed-neutron spectra for a long irradiation of ^{235}U with thermal neutrons and varying the cooling times. The origin of the main fine structure peaks is indicated. The evolution of the spectra with cooling time is clearly seen.

It should be noted that the experimental data for individual precursors used as basis for describing the spectra do not extend below about 70 keV. Consequently, any possible fine structure below this energy is not reproduced.

So far, the neutron spectra have been calculated for thermal neutron induced fission of ^{235}U. In a similar way the spectra can be calculated for any fissile material or mixture of fissile components.

A comparison between the effective spectra calculated by the technique used in ref.[61] and various integral measurements may also be done. Excellent agreement is obtained with Shalev and Cuttler's data[97] and with Fieg's data[98] (the "short cycle" results of Fieg are compared to the calculated curve in Fig. 7). On the other hand, the spectra measured by Sloan and Woodruff[99] do not agree well with the calculated ones as is evident

from Fig. 8 showing the "4-second cycle" results of ref.[99] and a calculated spectrum corresponding to the same conditions. As mentioned above the peaks at energies below about 70 keV cannot be reproduced in the calculated curves. The other peaks found by Sloan and Woodruff have their counterparts in the calculated curve except the one at 215 keV. As for the general shape of the distributions the agreement is rather poor. The neutron spectrum reported in ref.[99] is considerably softer than the calculated one. Similar results are obtained for the "12-second cycle" and the "25-second cycle" of ref.[99]. Again, it might be possible to attribute the discrepancy to differences in the proton-recoil spectrometry and the ^{3}He-spectrometry, but it should then be noted that Fieg[98] also used the proton-recoil method and his result agree well with the calculated spectrum.

Evans and Krick[102] find a much stronger peaking in the energy range 370 - 380 keV than other experimentalists[97-100]. The spectra of known precursors can hardly account for an effect of this size[61,96]. If it is real it might be connected to the fact that Evans and Krick have measured their spectra closer to equilibrium than other investigators thereby including contributions from precursors which escape detection in other experiments because of too short half-lives.

4. NEUTRONS RESULTING FROM (γ,n)-PROCESSES IN NUCLEAR MATERIALS

Many of the fission products emit high-energy gamma-rays. This means that there is a possibility of neutron production by (γ,n)-reactions in various nuclear materials. Especially deuterium is of interest in this context. Its threshold for this reaction is 2.23 MeV, and the cross section then rises rapidly to a maximum of about 2.5 mb at about 4 MeV gamma-energy. Many fission products possess gamma-rays of energies in this range, especially the short-lived ones with high disintegration energies. One should therefore expect a neutron component very much like the delayed-neutrons. There will be contributions from many fission products, and the decay of this neutron component will be composite. For an evaluation of the effect three pieces of information are needed: 1° the distribution of high-energy gamma-rays from the fission products, 2° the cross sections versus gamma energy for the reactor materials, and 3° the composition and geometrical arrangement of these materials. For the gamma-ray emission integral measurements exist[25]. The excitation functions are either known or can

be measured. The third component will vary from reactor to reactor, however, which makes it difficult to draw general conclusions.

The problem of photoneutrons is somewhat outside of the scope of the present review, and it will therefore not be treated in any detail.

5. SUMMARY AND RECOMMENDATIONS

At least one delayed-neutron precursor is known for each mass in the range 79 - 99 and 127 - 146 (in addition, one at mass 123). The search for precursors of mass a few units above 99 and 146 may still be of some interest for nuclear technology, but further away the fission yields drop so fast as to make delayed-neutron precursors unimportant.

The precursor half-lives are generally known with great precision. No further work seems to be necessary in this field.

The branching ratios have been measured only for about two thirds of the known precursors. The remaining gap should be filled. In addition, existing measurements often disagree severely. For about half the number of measured cases remeasuring is called for. Thus, a considerably effort is required to improve our knowledge about branching ratios.

The neutron energy spectra have been measured for 27 precursors, including those of primary interest for nuclear technology. For most spectra the low energy part up to about 100 keV is lacking and should be measured. Among the cases of some importance which have not yet been studies might be mentioned ^{93}Kr, ^{97}Y, ^{99}Y, ^{137}Te, ^{138}Te. and ^{145}Cs. There is no strong motivation from the technological point of view to measure these precursors, however.

The spectrum measurements agree well as far as energy values are concerned. There is a discrepancy between the proton-recoil spectrometry and the ^{3}He-spectrometry in the determination of the intensities, however. This discrepancy must be clarified.

The set of known precursors is now sufficiently complete to permit a satisfactory evaluation of the macroscopic effects of delayed neutrons in nuclear fuel.

ACKNOWLEDGEMENTS

It is a pleasure to acknowledge the valuable assistance offered to me by many colleagues in the form of unpublished manuscripts, communications and suggestions. Especially, I would like to express my gratitude to Prof A H W Aten, Dr A E Evans, Dr H V Klapdor, Dr K L Kratz, Dr M H McTaggart, Dr Y Nir-El, Dr Hsiang Lin Pai, Prof S G Prussin, Dr P L Reeder, Dr D Saphier, Dr J M Stevenson, and Prof G L Woodruff.

REFERENCES

1) S Amiel, Proceedings of a Panel on Fission Product Nuclear Data, IAEA, Bologna, 26-30 November 1973, Volume 2, p. 33.

2) G Rudstam and E Lund, Phys Rev C 13 (1976) 321.

3) B Grapengiesser, E Lund, and G Rudstam, J Inorg Nucl Chem 36 (1974) 2409.

4) T Matsushigues and L Matsushigues (private communication).

5) P del Marmol and P Fettweis, Nucl Phys A194 (1972) 140.

6) P del Marmol, J Inorg Nucl Chem 30 (1968) 2873.

7) J V Kratz, H Franz, and G Herrmann, J Inorg Nucl Chem 35 (1973) 1407.

8) P del Marmol and M Nêve de Mévergnies, J Inorg Nucl Chem 29 (1967) 273.

9) L Tomlinson and M H Hurdus, J Inorg Nucl Chem 30 (1968) 1649.

10) J V Kratz and G Herrmann, J Inorg Nucl Chem 32 (1970) 3713.

11) P del Marmol and D C Perricos, J Inorg Nucl Chem 32 (1970) 705.

12) L Tomlinson and M H Hurdus, J Inorg Nucl Chem 33 (1971) 3609.

13) M Asghar, J P Gautheron, G Bailleul, J P Boquet, J Greif, H Schrader, and G Siegert, Nucl Phys A247 (1975) 359.

14) E T Williams and C D Coryell, Nucl Appl 2 (1966) 256.

15) M D Silbert, and R H Tomlinson, Radiochim Acta 5 (1966) 223.

16) P del Marmol, P Fettweis, and D C Perricos, Radiochim Acta 16 (1971) 4.

17) N Sugarman, J Chem Phys 17 (1949) 11.

18) G J Perlow and A F Stehney, Phys Chem 107 (1957) 776.

19) G J Perlow and A F Stehney, Phys Rev 113 (1959) 1269.

20) K L Kratz and G Herrmann, Nucl Phys A229 (1974) 179.

21) W L Talbert, A B Tucker, and G M Day, Phys Rev 177 (1969) 1805 and W L Talbert, Phys Rev C1 (1970) 1135 (addendum).

22) G C Carlson, W C Schick, W L Talbert, and F K Wohn, Nucl Phys A125 (1969) 267.

23) P L Reeder and J F Wright, Phys Rev C 12 (1975) 718.

24) P Patzelt and G Herrmann, Proc Symp "Physics & Chemistry of Fission" Vol 2 p. 243, IAEA Vienna (1965).

25) S Amiel, J Gilat, A Notea, and E Yellin, "Delayed Fission Neutrons" (Panel Proceedings) p. 115, IAEA, Vienna (1968).

26) S Amiel, H Feldstein, M Oron, and E Yellin, Phys Rev C5 (1972) 270.

27) H K Carter, F K Wohn, W L Talbert, and J R McConnell, Bull Am Phys Soc II, 17 (1972) 514.

28) I Amarel, R Bernas, R Foucher, J Jastrzebski, A Johnson, J Teillac, and H Gauvin, Phys Letters 24B (1967) 402.

29) P L Reeder, J F Wright, and L J Alquist, Communication to this panel.

30) E Roeckl, P F Dittner, R Klapisch, C Thibault, C Rigaud, and R Prieels, Nucl Phys A222 (1974) 621.

31) S Amiel, G Engler, Y Nir-El, and M Schmid, Proceedings from the Cargèse 3rd International Conference far from Stability, Cargèse, 19 - 26 May 1976, CERN Report 76-13 (1976) p 501.

32) B L Tracy, J Chaumont, R Klapisch, J M Nitschke, A M Poskanzer, E Roeckl, and C Thibault, Phys Letters 34B (1971) 277.

33) I Amarel, H Gauvin, and A Johnson, J Inorg Nucl Chem 31 (1969) 577.

34) J Eidens, E Roeckl, and P Armbruster, Nucl Phys A141 (1970) 289.

35) E Lund and G Rudstam, Phys Rev C13 (1976) 1544.

36) A Kerek, G B Holm, S Borg, and P Carlé, Nucl Phys A209 (1973) 520.

37) L-E De Geer, S Borg, and G B Holm, Nucl Phys (to be published).

38) A Kerek, G B Holm, L-E De Geer, and S Borg, Phys Letters 44B (1973) 252.

39) S Borg, G B Holm, and B Rydberg, Nucl Phys A212 (1973) 197.

40) L Tomlinson and M H Hurdus, Phys Letters 25 B (1967) 545.

41) A A Delucchi, A E Greendale, and P O Strom, Phys Rev 173 (1968) 1159.

42) A Kerek, G B Holm, S Borg, and L E de Geer, Nucl Phys A195 (1972) 177.

43) W Rudolph, K-L Kratz, and G Herrmann, J Inorg Nucl Chem 39 (1977) 753.

44) H D Schüssler, H Ahrens, H Folger, H Franz, W Grimm, G Herrmann, J V Kratz, and K L Kratz, Proc 2nd Symp "Physics and Chemistry of Fission", p. 591, IAEA, Vienna (1969).

45) G Herrmann, N Kaffrell, N Trautmann, R Denig, W Herzog, D Hübscher, and K L Kratz, CERN Report 70-30 (1970) p 985.

46) New determination at OSIRIS (1975) in order to check the discrepancy between published values.

47) O L Cordes, J E Cline, and C W Reich, Nucl Instr Meth 48 (1967) 125.

48) G Rudstam and E Lund, Nucl Sci Eng (to be published).

49) P M Aron, O I Kostochkin, K A Petrzhak, and V I Shpakov, Atomnaya Energiya 16 (1964) 368; Eng trans Soviet J Atom Energy 16, 447.

50) R L Reeder, J F Wright, and L J Alquist, Proceedings from the Cargèse International Conference on Nuclei far from Stability, Cargèse, 19-26 May 1976, CERN Report 76-13 (1976) p 327.

51) H D Schüssler, and G Herrmann, Radiochim Acta 18 (1972) 123.

52) M Asghar, J Crançon, J P Gautherin, and C Ristori, J Inorg Nucl Chem 37 (1975) 1563.

53) S Amiel and H Feldstein, Phys Rev C11 (1975) 845.

54) G Siegert, J Greif, H Wollnik, G Fiedler, R Decker, M Asghar, G Bailleul, J P Bocquet, J P Gautheron, H Schrader, P Armbruster, and H Ewald, Phys Rev Letters 34 (1975) 1034.

55) T Izak-Biran and S Amiel, Nucl Sci Eng 57 (1975) 117.

56) W Rudolph and K L Kratz, Z für Physik A 281 (1977) 269.

57) K-L Kratz and G Herrmann, Z Physik 263 (1973) 435.

58) S Amiel and H Feldstein, Phys Lett 31B (1970) 59.

59) Y Nir-El and S Amiel, Proceedings from the Cargèse 3rd International Conference on Nuclei far from Stability, Cargèse 19-26 May 1976, CERN Report 76-13 (1976) p 322.

60) H Franz, W Rudolph, H Ohm, K-L Kratz, G Herrmann, F M Nuh, D R Slaughter, and S G Prussin, submitted to Nucl Instr Methods (1977).

61) G Rudstam, J Radioanal Chem 36 (1977) 591 and The Swedish Research Councils' Laboratory Report LF-70 (1976) revised (INDC (SWD)9/G+P).

62) P L Reeder, J F Wright, and L J Alquist, Battelle Pacific Northwest Laboratories Report BNWl-SA-5890 Rev (1976).

63) R Brissot, J Crançon, Ch Ristori, J P Bocquet, and A Moussa, submitted to Nucl Phys.

64) H Franz, J-V Kratz, and G Herrmann, private communication (1972).

65) H Franz, J-V Kratz, K-L Kratz, W Rudolph, G Herrmann, F M Nuh, S G Prussin, A A Shibab-Eldin, Phys Rev Lett 33 (1974) 859.

66) K-L Kratz, W Rudolph, H Ohm, H Franz, C Ristori, M Zendel, G Herrmann, F M Nuch, D R Slaughter, A A Shibab-Eldin, and S G Prussin, Proceedings from the 3rd International Conference on Nuclei far from Stability, Cargèse, 19-26 May 1976, CERN Report 76-13 (1976) p 304.

67) S Shalev and G Rudstam, Nucl Phys A230 (1974) 153.

68) F M Nuh, D R Slaughter, S G Prussin, H Ohm, W Rudolph, and K-L Kratz, submitted to Nucl Phys (1977).

69) S Shalev and G Rudstam, Nucl Phys A275 (1977) 76.

70) G Rudstam and S Shalev, Nucl Phys A235 (1974) 397.

71) K-L Kratz, H Ohm, W Rudolph, K Sümmerer, M Zendel, K D Wünsch, G Jung, H Wollnik, C Ristori, and J Crançon, Int Workshop on Gross Properties of Nuclei and Nuclear Excitation, Hirschegg, 17-22 January 1977.

72) P G Hansen, in Advances in Nuclear Physics, Vol 7, Edited by M Baranger and E Vogt, Plenum Press, N Y (1973).

73) H V Klapdor, Proceedings from the 3rd International Conference on Nuclei far from Stability, Cargèse, 19-26 May, CERN Report 76-13 (1976) p 311.

74) B Fogelberg, work in progress.

75) K Aleklett, G Nyman, and G Rudstam, Nucl Phys A246 (1975) 425.

76) P K Ray and E S Kenney, Nucl Instr Methods 134 (1976) 559.

77) D R Slaughter, F M Nuh, A A Shibab-Eldin, and S G Prussin, Phys Lett 38B (1972) 22.

78) H Tovedal and B Fogelberg, Nucl Phys A252 (1975) 253.

79) H Tovedal and B Fogelberg, work in progress (1977).

80) B Fogelberg and W Mampe, Z Physik A281 (1977) 89.

81) F M Nuh, D R Slaughter, S G Prussin, K-L Kratz, H Franz, and G Herrmann, Phys Lett 53B (1975) 435.

82) C M Jensen, K G Lanier, L G Mann, ans S G Prussin, Phys Rev C (to be published).

83) K-L Kratz, W Rudolph, H Ohm, H Franz, G Herrmann, C Ristori, J Crançon, M Asghar, G I Crawford, F M Nuh, and S G Prussin, Phys Lett 65B (1976) 231.

84) H Gunther, G Siegert, K Wünsch and H Wollnik, Nucl Phys A242 (1975) 56.

85) P Hoff and B Fogelberg, work in progress (1977).

86) G R Keepin, Physics of Nuclear Kinetics, Addison Wesley, Reading (1965).

87) M E Meek and B F Rider, USA Report NEDO-12154-1 (1974).

88) S J Balestrini and L Forman, Phys Rev C10 (1974) 1872.

89) L Tomlinson, Atomic Data and Nuclear Data Tables 12 (1973) 179.

90) R J Tuttle, Nucl Sci Eng 56 (1975) 37.

91) C B Besant, P J Challen, M H McTaggart, P Tavoularidis, and J G Williams, communication to this panel.

92) A H W Aten, communication to this panel.

93) G Moscati and J Goldenberg, Phys Rev 126 (1962) 1098.

94) H L Pai, communication to this panel.

95) G Rudstam, INVENT - a computer programme for evaluating the inventory of fission products in nuclear fuel, internal report of the Swedish Research Councils' Laboratory (1977).

96) D Saphier, D Ilberg, S Shalev, and S Yiftah, Nucl Sci Eng 62 (1977) 660.

97) S Shalev and J M Cuttler Nucl Sci Eng 51 (1972) 52.

98) G Fieg, J Nucl Energy 26 (1972) 585.

99) W R Sloan and G L Woodruff, Nucl Sci Eng 55 (1974) 28.

100) G W Eccleston and G L Woodruff, Nucl Sci Eng 62 (1977) 636.

101) B P Maksyutenko, Yu F Balaskshev, and G I Volkova, Sov J Nucl Phys 19 (1974) 380.

102) A E Evans and M S Krick, Nucl Sci Eng 62 (1977) 652.

103) D R Alexander and M S Krick, Nucl Sci Eng 62 (1977) 627.

104) P Hoff, thesis, University of Oslo, 1976.

105) D J Hughes, J Dabbs, A Cahn, and D Hall, Phys Rev 73 (1948) 111.

106) J Crançon et al, unpublished data from LOHENGRIN collaboration, Grenoble (1977).

107) C Ristori et al, unpublished data from OSTIS collaboration, Grenoble (1977).

108) S Amiel et al, contribution to RP 10.

109) K L Kratz, Annual Report, Inst f Kernchemie, Univ Mainz (1977) p 34.

110) B F Rider and M E Meek, US Report NEDO - 12154-2 (D) (1977).

Table 1

Half-lives of delayed-neutron precursors (errors correspond to one standard deviation).

Precursor	Half-life, s	Average value, s	Comments
^{79}(Zn,Ga)	2.63 ± 0.09[a] 3.00 ± 0.09[b]	-	Probably mixture of two precursors contributing differently to neutron activity[a] and beta activity[b], cf. ref.[48]
^{80}Ga	1.66 ± 0.02[a] 1.7 ± 0.2[b]	1.66 ± 0.02	
^{81}Ga	1.23 ± 0.01[a] 1.2 ± 0.2[c]	1.23 ± 0.01	
^{82}Ga	0.60 ± 0.01[a]	0.60 ± 0.01	
^{83}Ga	0.31 ± 0.01[a]	0.31 ± 0.01	
^{83}Ge	1.9 ± 0.4[d]	1.9 ± 0.4	
^{84}Ge	1.2 ± 0.3[d]	1.2 ± 0.3	
^{84}As	5.8 ± 0.5[e] 5.4 ± 0.4[f]	5.6 ± 0.3	
^{85}As	2.15 ± 0.15[g] 2.028± 0.012[h] 2.05 ± 0.05[f] 2.08 ± 0.05[a]	2.03 ± 0.01	
^{86}As	0.9 ± 0.2[f]	0.9 ± 0.2	
^{87}As	0.6 ± 0.3[i] 0.73 ± 0.06[au]	0.73 ± 0.06	

Table 1 (cont'd)

Precursor	Half-life, s	Average value, s	Comments
^{87}Se	5.9 ± 0.2[j]	5.60 ± 0.16	
	5.85 ± 0.15[i]		
	5.41 ± 0.10[k]		
^{88}Se	1.3 ± 0.3[j]	1.52 ± 0.06	
	1.4 ± 0.3[i]		
	1.53 ± 0.06[k]		
^{89}Se	0.41 ± 0.04[k]	0.41 ± 0.04	
^{91}Se	0.27 ± 0.08[ℓ]	0.27 ± 0.08	
^{87}Br	55.4 ± 0.35[m]	55.6 ± 0.1	
	55.8 ± 0.25[n]		
	55.6 ± 0.15[o]		
	55.5 ± 0.3[a]		
	56.3 ± 0.5[b]		
^{88}Br	15.5 ± 0.3[p]	16.0 ± 0.2	
	15.5 ± 0.4[q]		
	16.3 ± 0.8[r]		
	15.9 ± 0.1[n]		
	16.7 ± 0.2[a]		
	16.5 ± 0.5[b]		
^{89}Br	4.4 ± 0.5[r]	4.38 ± 0.03	
	4.5 ± 0.4[n]		
	4.37 ± 0.03[a]		
	4.55 ± 0.10[b]		
^{90}Br	1.96 ± 0.05[a]	1.92 ± 0.06	
	1.80 ± 0.15[ℓ]		
	1.71 ± 0.14[s]		

Table 1 (cont'd)

Precursor	Half-life, s	Average value, s	Comments
^{91}Br	0.541± 0.005[a]	0.542± 0.008	
	0.60 ± 0.05[ℓ]		
	0.63 ± 0.07[s]		
^{92}Br	0.365± 0.007[a]	0.362± 0.012	
	0.26 ± 0.04[s]		
	0.35 ± 0.04[au]		
^{92}Kr	1.86 ± 0.01[t]	1.85 ± 0.01	
	1.840± 0.008[u]		
^{93}Kr	1.17 ± 0.04[w]	1.29 ± 0.01	
	1.19 ± 0.05[x]		
	1.30 ± 0.01[t]		
	1.289± 0.012[u]		
	1.33 ± 0.05[a]		
	1.27 ± 0.02[ℓ]		
^{94}Kr	0.20 ± 0.01[y]	0.208± 0.009	
	0.23 ± 0.02[z]		
	0.22 ± 0.02[ℓ]		
^{92}Rb	4.43 ± 0.05[aa]	4.50 ± 0.02	
	4.48 ± 0.02[t]		
	4.50 ± 0.03[u]		
	4.34 ± 0.06[a]		
	4.54 ± 0.02[v]		
	4.50 ± 0.04[b]		
	4.57 ± 0.07[aw]		
^{93}Rb	5.89 ± 0.04[aa]	5.85 ± 0.04	
	5.60 ± 0.05[x]		
	6.18 ± 0.06[t]		
	5.86 ± 0.13[u]		
	5.8 ± 0.1[y]		
	5.85 ± 0.03[a]		
	5.80 ± 0.05[b]		
	5.86 ± 0.05[ℓ]		
	5.82 ± 0.03[ab]		
	6.12 ± 0.08[v]		
	5.92 ± 0.09[aw]		

Table 1 (cont'd)

Precursor	Half-life, s	Average value, s	Comments
^{94}Rb	2.67 ± 0.04[aa]	2.76 ± 0.02	
	2.8 ± 0.1[y]		
	2.79 ± 0.08[z]		
	2.69 ± 0.02[a]		
	2.78 ± 0.05[b]		
	2.76 ± 0.08[ac]		
	2.67 ± 0.06[l]		
	2.73 ± 0.01[ab]		
	2.83 ± 0.03[v]		
	2.80 ± 0.04[aw]		
	2.73 ± 0.02[av]		
^{95}Rb	0.36 ± 0.02[aa]	0.384 ± 0.005	
	0.400± 0.004[a]		
	0.383± 0.006[ac]		
	0.402± 0.008[ad]		
	0.369± 0.005[ab]		
	0.377± 0.004[v]		
	0.377± 0.006[av]		
^{96}Rb	0.207± 0.003[ae]	0.201 ± 0.002	
	0.203± 0.003[a]		
	0.199± 0.004[ac]		
	0.197 ± 0.002[ab]		
	0.205 ± 0.004[v]		
	0.197 ± 0.005[av]		
	0.220 ± 0.010[aw]		
^{97}Rb	0.135± 0.010[af]	0.170 ± 0.002	
	0.176± 0.005[ae]		
	0.172± 0.003[a]		
	0.172± 0.003[ac]		
	0.181± 0.010[ad]		
	0.167± 0.002[ab]		
	0.182± 0.007[v]		
	0.171± 0.004[av]		
^{98}Rb	0.136± 0.008[ae]	0.119 ± 0.007	
	0.14 ± 0.01[a]		
	0.106± 0.006[ac]		
	0.098± 0.018[ad]		
	0.114± 0.013[av]		

Table 1 (cont'd)

Precursor	Half-life, s	Average value, s	Comments
^{99}Rb	0.076 ±0.005[ae]	0.076 ±0.005	
^{97}Sr	0.4 ± 0.3[ag] 0.43 ± 0.03[aw]	0.43 ± 0.03	
^{98}Sr	0.85 ± 0.05[ae] 0.6 ± 0.1[aw]	0.80 ± 0.10	
^{99}Sr	0.6 ± 0.2[ℓ]	0.6 ± 0.2	
^{97m}Y	1.11 ± 0.03[ag] 1.11 ± 0.14[ae] 1.3 ± 0.1[aw]	1.13 ± 0.04	
^{99}Y	0.8 ± 0.7[ag] 1.45 ± 0.22[ℓ]	1.4 ± 0.2	
^{123}Ag	0.39 ± 0.03[ah]	0.39 ± 0.03	
^{127}In	3.76 ± 0.03[ah] 3.7 ± 0.1[b]	3.76 ± 0.03	
^{128}In	0.94 ± 0.05[ah] 0.80 ± 0.03[b]	0.84 ± 0.06	A long-lived component found at this mass (cf. ref.[35]) might be due to contamination.
^{129}In	0.99 ± 0.02[ah] 0.8 ± 0.3[b]	0.99 ± 0.02	
^{129}In	2.5 ± 0.2[ah]	2.5 ± 0.2	
^{130}In	0.58 ± 0.01[ah] 0.53 ± 0.04[ai]	0.58 ± 0.01	
^{131}In	0.29 ± 0.01[ah] 0.27 ± 0.012[aj]	0.28 ± 0.01	
^{132}In	0.3 ± 0.1[ah] 0.12 ± 0.02[ak]	0.13 ± 0.04	

Table 1 (cont'd)

Precursor	Half-life, s	Average value, s	Comments
^{133}Sn	1.47 ± 0.07[ah]	1.47 ± 0.03	
	1.47 ± 0.04[aℓ]		
^{134}Sn	1.04 ± 0.02[ah]	1.04 ± 0.02	
	0.7 ± 0.2[ℓ]		
^{134}Sb	11.3 ± 0.3[am]	10.4 ± 0.1	
	11.1 ± 0.8[an]		
	10.3 ± 0.15[ao]		
	10.3 ± 0.4[ah]		
	10.2 ± 0.3[b]		
	10.5 ± 0.6[ap]		
	10.43± 0.14[ap]		
^{135}Sb	1.696 ± 0.021[h]	1.71 ± 0.02	
	1.82 ± 0.04[ah]		
	1.706 ± 0.014[ap]		
	1.60 ± 0.05[au]		
^{136}Sb	0.82 ± 0.02[ah]	0.82 ± 0.02	
	0.75 ± 0.20[ap]		
	0.9 ± 0.1[au]		
^{136}Te	17.5 ± 0.4[ah]	17.5 ± 0.2	
	17.5 ± 0.2[au]		
^{137}Te	3.5 ± 0.5[aq]	2.8 ± 0.7	
	2.1 ± 0.5[ℓ]		
^{138}Te	1.4 ± 0.4[ℓ]	1.4 ± 0.4	
^{137}I	24.4 ± 0.4[r]	24.5 ± 0.1	
	24.7 ± 0.1[o]		
	24.25± 0.12[ah]		
	24.5 ± 0.2[b]		
	24.8 ± 0.2[ℓ]		

Table 1 (cont'd)

Precursor	Half-life, s	Average value, s	Comments
^{138}I	6.46 ± 0.15^{ah} 6.62 ± 0.09^{b} $6.5 \pm 0.2^{\ell}$ 6.21 ± 0.20^{s}	6.53 ± 0.08	
^{139}I	2.7 ± 0.1^{p} 2.30 ± 0.05^{ah} 2.47 ± 0.15^{b} $2.4 \pm 0.2^{\ell}$ 2.27 ± 0.27^{s}	2.38 ± 0.07	
^{140}I	0.86 ± 0.04^{ar} 0.89 ± 0.12^{s} 0.59 ± 0.01^{ah} 0.61 ± 0.01^{as}	0.60 ± 0.01	Large discrepancy between two sets of experiments. Those of refs.[ah] and [as] are preferred because they were obtained with mass-separated samples (cf.text).
^{141}I	0.48 ± 0.03^{ah} 0.43 ± 0.08^{ar} 0.41 ± 0.08^{s}	0.47 ± 0.03	
^{141}Xe	1.73 ± 0.01^{t} 1.720 ± 0.013^{u}	1.73 ± 0.01	
^{142}Xe	1.15 ± 0.04^{w} 1.18 ± 0.04^{at} 1.32 ± 0.03^{t} 1.24 ± 0.02^{u}	1.24 ± 0.03	
^{143}Xe	0.96 ± 0.02^{w} 0.30 ± 0.03^{y}	0.30 ± 0.03	The experimental results disagree. The one from ref.[y] is chosen because it was obtained by neutron counting of mass-separated samples.

Table 1 (cont'd)

Precursor	Half-life, s	Average value, s	Comments
^{141}Cs	24.7 ± 0.2[u] 24.9 ± 0.2[t] 22.2 ± 0.4[ah] 25.6 ± 0.3[b] 29.3 ± 0.1[aw]	24.9 ± 0.2	The values from refs.[ah] and [aw] disagree with the others for unknown reasons. They are disregarded in calculating the average value.
^{142}Cs	1.68 ± 0.02[t] 1.68 ± 0.02[u] 1.69 ± 0.09[ah] 1.70 ± 0.02[v] 1.70 ± 0.09[ab] 1.78 ± 0.02[aw]	1.71 ± 0.01	
^{143}Cs	1.78 ± 0.01[ah] 1.78 ± 0.01[ad] 1.79 ± 0.02[v] 1.79 ± 0.04[ab] 1.77 ± 0.03[av]	1.78 ± 0.01	
^{144}Cs	1.06 ± 0.10[aa] 1.05 ± 0.14[af] 1.00 ± 0.02[ah] 1.00 ± 0.01[av] 0.99 ± 0.02[ab] 1.00 ± 0.04[v] 1.04 ± 0.03[aw]	1.002 ± 0.005	
^{145}Cs	0.563± 0.027[ae] 0.58 ± 0.01[ah] 0.61 ± 0.02[ac] 0.577± 0.006[ab] 0.65 ± 0.03[v] 0.616± 0.020[av] 0.65 ± 0.03[aw]	0.585± 0.008	
^{146}Cs	0.189± 0.011[ae] 0.343± 0.007[ah] 0.28 ± 0.03[ab] 0.352± 0.042[ac] 0.325± 0.010[av] 0.31 ± 0.06[aw]	0.335 ± 0.007	The value from ref.[ae] disagrees with the others for unknown reasons. It is disregarded in calculating the average value (cf. text).
^{147}Cs	0.214± 0.030[av]	0.21 ± 0.03	

a = ref.[2]
b = ref.[3]
c = ref.[4]
d = ref.[5]
e = ref.[6]
f = ref.[7]
g = ref.[8]
h = ref.[9]
i = ref.[10]
j = ref.[11]
k = ref.[12]

l = ref.[13]
m = ref.[14]
n = ref.[15]
o = ref.[16]
p = ref.[17]
q = ref.[18]
r = ref.[19]
s = ref.[20]
t = ref.[21]
u = ref.[22]
v = ref.[23]

w = ref.[24]
x = ref.[25]
y = ref.[26]
z = ref.[27]
aa = ref.[28]
ab = ref.[29]
ac = ref.[30]
ad = ref.[31]
ae = ref.[32]
af = ref.[33]
ag = ref.[34]
ah = ref.[35]
au = ref.[106]
av = ref.[107]

ai = ref.[36]
aj = ref.[37]
ak = ref.[38]
al = ref.[39]
am = ref.[40]
an = ref.[41]
ao = ref.[42]
ap = ref.[43]
aq = ref.[44]
ar = ref.[45]
as = ref.[46]
at = ref.[47]
aw = ref.[108]

Table 2

Branching ratios for delayed-neutron precursors (errors correspond to one standard deviation).

Precursor	P_n-value,% direct determination	P_n-value, % indirect determination	Average value,%	Comments
^{84}As		0.13 ± 0.06[a]	0.13 ± 0.06	
^{85}As	22 ± 8[w]	23 ± 3[a] 22 ± 5[c]	23 ± 3	
^{86}As	10.5 ± 2.2[w]	$3.8\ ^{+1.7}_{-1.0}$[a]	10.5 ± 2.2	Large discrepancy between experiments. Direct determination preferred
^{87}As	44 ± 14[x]		44 ± 14	
^{87}Se	0.25 ± 0.06[d]	0.23 ± 0.07[e] 0.16 ± 0.03[f]	0.21 ± 0.03	The value[f] is given the same weight as[d].
^{88}Se	0.15 ± 0.09[d]	0.75 ± 0.06[f]	0.15 ± 0.09	Large discrepancy between experiments. Direct determination preferred.
^{89}Se		5.0 ± 1.5[f]	5.0 ± 1.5	
^{91}Se	21 ± 8[g]		21 ± 8	
^{87}Br	3.1 ± 0.6[h] 2.1 ± 0.3[i] 2.5 ± 0.3[j] 2.16± 0.33[k] 2.56± 0.38[x]		2.37 ± 0.14	
^{88}Br	6.0 ± 1.6[h] 7.4 ± 0.5[j] 6.3 ± 0.9[k] 6.47 ± 0.70[x]		6.9 ± 0.3	

* This table is a revision of the table 2 included in the preliminary version of this review which was distributed before the meeting.

Some old values mainly based on indirect determinations have been omitted, and a number of new direct determinations have been added. This has led to a better consistency between different measurements and to smaller errors of the average values. Except for a couple of precursors, notably ^{86}As, ^{88}Br, and ^{135}Sb, the difference between the new and old average values is within limits of error, however.

These changes have also been implemented in the calculation of neutron yields (see Table 6).

The author is grateful to Dr K L Kratz for reporting new experimental results from Grenoble and Mainz .

Table 2 (cont'd)

Precursor	P_n-value, % direct determination	P_n-value, % indirect determination	Average value, %	Comments
^{89}Br	7 ± 2[h]		13.5±2.3	
	16.9 ± 1.7[j]			
	16.5 ± 2.5[k]			
	12.5 ± 2.0[x]			
^{90}Br	22.6 ± 3.1[g]		21.2 ± 2.4	
	18.9 ± 3.9[x]			
^{91}Br	9.9 ± 2.0[g]		10.8 ± 1.7	
	14.1 ± 3.9[w]			
^{92}Br	21 ± 8[w]		22 ± 6	
	24.5 ± 10[x]			
^{92}Kr	0.0323 ± 0.0026[i]	0.040 ± 0.007[p]	0.033± 0.003	
^{93}Kr	1.9 ± 0.2[g]	3.9 ± 0.6[o]	2.1 ± 0.3	
	1.92± 0.14[n]	2.60± 0.50[p]		
^{94}Kr	5.7 ± 2.2[g]		2.2 ± 1.4	
	1.6 ± 0.9[g]			
^{92}Rb	0.012 ± 0.002[j]	0.012 ± 0.004[p]	0.012 ± 0.001	
	0.0125± 0.0015[n]			
^{93}Rb	1.43 ± 0.18[q]	2.6 ± 0.4[o]	1.38 ± 0.11	
	1.24 ± 0.14[r]	1.65 ± 0.30[p]		
	1.86 ± 0.13[j]	2.1 ± 0.6[ℓ]		
	1.75 ± 0.15[k]			
	1.2 ± 0.1[g]			
	1.16 ± 0.08[n]			
^{94}Rb	11.1 ± 1.1[q]	11± 2[ℓ]	10.6 ± 0.7	
	8.5 ± 0.9[r]			
	13.7 ± 1.0[j]			
	12.8 ± 0.7[k]			
	9.6 ± 0.8[g]			
	9.7 ± 0.5[z]			

Table 2 (cont'd)

Precursor	P_n-value, % direct determination	P_n-value, % indirect determination	Average value, %	Comments
^{95}Rb	7.1 ± 0.9[s]		8.9 ± 0.5	
	8.5 ± 0.9[r]			
	11.0 ± 0.8[j]			
	10.9 ± 0.8[k]			
	8.4 ± 0.5[g]			
	8.55 ± 0.5[z]			
^{96}Rb	12.7 ± 1.5[q]		14.2 ± 1.0	
	13.0 ± 1.4[r]			
	17.0 ± 1.2[j]			
	16.2 ± 1.2[k]			
	12.5 ± 0.9[z]			
^{97}Rb	27.2 ± 3.0[r]		30 ± 3	
	35.9 ± 2.6[j]			
	39.0 ± 3.4[k]			
	25.2 ± 1.8[z]			
^{98}Rb	13.3 ± 2.1[r]		15.0±2.4	
	18.4 ± 2.9[z]			
^{99}Sr		3.4 ± 2.4[g]	3.4 ± 2.4	
^{97}Y		1.6 ± 0.3[v]	1.6 ± 0.3	
^{99}Y		1.2 ± 0.8[g]	1.2 ± 0.8	
^{134}Sn	15 ± 8[g]	24 ± 15[g]	17 ± 7	
^{134}Sb	0.090 ± 0.015[t]	0.08 ± 0.02[c]	0.086 ± 0.012	
^{135}Sb	19.9 ± 2.1[t]	8 ± 2[c]	13.9 ± 2.4	
	14 ± 1[w]			
^{136}Sb	32 ± 14[t]	19 ± 9[w]	23 ± 8	
^{136}Te	0.7 ± 0.4[t]	2.0 ± 1.0[w]	0.9 ± 0.4	
^{137}Te	2.5 ± 0.5[g]		2.2 ± 0.5	
	1.3 ± 0.8[g]			

Table 2 (cont'd)

Precursor	P_n-value, % direct determination	P_n-value, % indirect determination	Average value, %	Comments
^{138}Te	6.3 ± 2.1^{g}	4.6 ± 2.5^{g}	5.6 ± 1.6	
^{137}I	6.1 ± 0.5^{x} 8.6 ± 1.2^{i} 8.5 ± 0.9^{j} 7.8 ± 1.2^{k} 6.1 ± 0.8^{g}		6.7 ± 0.5	
^{138}I	2.0 ± 0.5^{h} 6.0 ± 3.5^{j} 5.7 ± 3.3^{k} 2.58 ± 0.22^{g} 4.5 ± 0.9^{x}		2.6 ± 0.3	
^{139}I	10.2 ± 0.9^{g} 10.1 ± 3.6^{x}		10.2 ± 0.9	
^{140}I	21.7 ± 5.6^{x}		22 ± 6	
^{141}I	39 ± 13^{x}		39 ± 13	
^{141}Xe	0.0426 ± 0.0023^{n}	0.054 ± 0.009^{p}	0.043 ± 0.003	
^{142}Xe	0.406 ± 0.034^{n}	0.45 ± 0.08^{p}	0.41 ± 0.03	
^{141}Cs	0.043 ± 0.007^{j} 0.0529 ± 0.0029^{n}	0.073 ± 0.011^{p}	0.053 ± 0.004	
^{142}Cs	0.096 ± 0.008^{j} 0.086 ± 0.010^{k} 0.285 ± 0.026^{n}	0.27 ± 0.07^{p}	($\sim$0.18)	Large differences between experimental values.

Table 2 (cont'd)

Precursor	P_n-value, % direct determination	P_n-value, % indirect determination	Average value, %	Comments
^{143}Cs	1.13 ± 0.25[q]		1.82 ± 0.12	
	1.95 ± 0.14[j]			
	1.93 ± 0.10[k]			
	1.74 ± 0.12[z]			
^{144}Cs	1.10 ± 0.25[q]		3.0 ± 0.7	Large differences between experimental values. Unweighted average.
	4.3 ± 0.3[j]			
	3.67 ± 0.59[k]			
	2.95 ± 0.25[z]			
^{145}Cs	12.1 ± 1.4[r]		14.3 ± 1.9	
	21.8 ± 1.5[j]			
	18.0 ± 2.7[k]			
	12.5 ± 3.0[w]			
	12.2 ± 0.9[z]			
^{146}Cs	14.2 ± 1.7[z]		13.4 ± 0.7	
	13.2 ± 0.8[z]			
^{147}Cs	25.4 ± 3.2[z]		25 ± 3	

a = ref.[7]
b = ref.[8]
c = ref.[9]
d = ref.[10]
e = ref.[11]
f = ref.[12]
g = ref.[13]
h = ref.[49]
i = ref.[16]
j = ref.[29]
k = ref.[50]
l = ref.[51]
m = ref.[20]
n = ref.[52]
o = ref.[25]
p = ref.[21]
q = ref.[33]
r = ref.[30]
s = ref.[28]
t = ref.[43]
u = ref.[44]
v = ref.[89]
w = ref.[106]
x = ref.[109]
z = ref.[107]

Table 3

Predicted P_n-values for unmeasured precursors

Precursor	P_n-value, % ref.[56]	P_n-value, % ref.[57]	P_n-value, % ref.[59]
^{80}Ga	1.2		0.197
^{83}Ge	0.2		1.9
^{84}Ge	4.3	4.5	1.2
^{99}Rb	41		68.5
^{97}Sr	0.3	0.05	0.2
^{98}Sr	0.5	0.34	0.596
^{98}Y		0.30	0.079
^{133}Sn	$3x10^{-5}$		0.072
^{143}Xe	4.0		1.24

Table 4

Average energy of delayed neutrons

Precursor	Reference for spectrum	Average neutron energy, keV			
		From experimental spectrum[a]	From analytical representation[b]	Reference [c] Method A	Method B
^{79}(Zn,Ga)	d	250[d]	360		
^{80}Ga	d	240[d]	250		
^{81}Ga	d	370[d]	360		
^{85}As	e, f, g	610[e]	570		
^{87}Br	h, i, m	170[h]	220		150 ± 10
^{88}Br	j	260[j]	240		330 ± 30
^{89}Br	k	470[k]	440		>710
^{90}Br	j	460[j]	420		
^{91}Br	k	510[k]	500		
^{92}Rb				180 ± 40	120 ± 30
^{93}Rb	k, ℓ	340[k]	330	560 ± 10	630 ± 10
^{94}Rb	d,ℓ	350[d]	310	570 ± 10	610 ± 10
^{95}Rb	d,ℓ	520[d]	540	530 ± 10	570 ± 10
^{96}Rb	ℓ			560 ± 10	540 ± 10
^{97}Rb	ℓ			> 720	>620
^{129}In	d	550[d]	440		
^{130}In	d	420[d]	420		
^{134}Sn	h	540[h]	520		
^{135}Sb	f, h	610[h]	600		

Table 4 (cont'd)

Precursor	Reference for spectrum	Average neutron energy, keV			
		From experimental spectrum[a]	From analytical representation[b]	Reference [c] Method A	Method B
^{136}Te	h	220[h]	210		
^{137}I	g, h	510[h]	490		530 ± 50
^{138}I	j	390[j]	370		
^{139}I	k	370[k]	390		
^{140}I	j	450[j]	430		
$^{141}(I,Cs)$	k	270[k]	320		240 ± 50(Cs)
$^{142}(Xe,Cs)$	j	200[j]	200	240 ± 60(Cs)	130 ± 10(Cs)
^{143}Cs	k	240[k]	220	350 ± 10	320 ± 20
^{144}Cs	j	280[j]	310	290 ± 20	330 ± 20
^{145}Cs	-			460 ± 30	540 ± 20
^{146}Cs	-				530 ± 70

a = References given in this column indicate the source of the spectrum. The calculation of the average value has been done for the present review.

b = ref.[61]
c = ref.[62]
d = ref.[48]
e = ref.[64]
f = ref.[65]
g = ref.[66]
h = ref.[67]
i = ref.[68]
j = ref.[69]
k = ref.[70]
l = ref.[71]
m = ref.[76]

Table 5

Comparison between different determinations of the delayed-neutron spectrum of ^{87}Br

Energy interval keV	Relative distribution of neutrons, % Ref.[67]	Ref.[68]	Ref.[76]
100-200	46	38	86
200-300	29	32	12
300-400	9	11	1.6
400-500	9	10	0.5
500-600	3	4	0.1
600-700	3	3	
> 700	0.7	1.5	

Table 6

Contribution of individual precursors to the total delayed-neutron effect in thermal-neutron induced fission of ^{235}U and ^{239}Pu and in fast-neutron induced fission of ^{238}U at saturation conditions

Precursor	P_n-value %	Cumulative fission yield Y_c, %			$P_n \times Y_c \times 10^4$		
		^{235}U(a)	^{239}Pu(a)	^{238}U(a)	^{235}U	^{239}Pu	^{238}U
^{80}Ga	-	0.012 ±0.002	(9 ± 6) x 10^{-3}	0.023 ±0.014	-	-	-
^{81}Ga	-	(8 ± 5) x 10^{-3}	(3.3±2.1) x 10^{-3}	0.024 ±0.015	-	-	-
^{82}Ga	-	(2.7±1.7) x 10^{-3}	(5.5±3.5) x 10^{-4}	0.011 ±0.007	-	-	-
^{83}Ga	-	(3.9±2.4) x 10^{-4}	(7 ± 4) x 10^{-5}	(4.3±2.8) x 10^{-3}	-	-	-
^{83}Ge	-	0.051 ±0.004	0.016 ±0.010	0.17 ±0.11	-	-	-
^{84}Ge	-	0.032 ±0.010	(3.0±1.9) x 10^{-3}	0.16 ±0.10	-	-	-
^{84}As	0.13 ±0.06	0.25 ±0.02	0.067 ±0.021	0.47 ±0.30	0.033 ±0.015	(9 ± 5) x 10^{-3}	0.061 ±0.048
^{85}As	23 ±3	0.16 ±0.01	0.023 ±0.007	0.28 ±0.18	3.7 ±0.5	0.53 ±0.18	6.4 ±4.2
^{86}As	10.5 ±2.2	0.086 ±0.014	0.011 ±0.007	0.15 ±0.09	0.90 ±0.24	0.12 ±0.08	1.6 ±1.0
^{87}As	44 ±14	0.071 ±0.023	(1.9±1.2) x 10^{-3}	0.053 ±0.034	3.1 ±1.4	0.084 ±0.059	2.3 ±1.6
^{87}Se	0.21 ±0.03	0.76 ±0.03	0.14 ±0.09	0.93 ±0.21	0.16 ±0.02	0.029 ±0.019	0.20 ±0.05
^{88}Se	0.15 ±0.09	0.38 ±0.06	0.052 ±0.033	0.88 ±0.28	0.057 ±0.035	(8 ± 7) x 10^{-3}	0.13 ±0.09
^{89}Se	5.0 ±1.5	0.118 ±0.019	(6 ± 4) x 10^{-3}	0.38 ±0.24	0.59 ±0.20	0.030 ±0.21	1.9 ±1.3

Table 6 (cont'd)

Precursor	P_n-value %	Cumulative fission yield Y_c, % ^{235}U(a)	^{239}Pu(a)	^{238}U(a)	$P_n \times Y_c \times 10^4$ ^{235}U	^{239}Pu	^{238}U
^{91}Se	21 ±8	(1.6±1.0) x 10^{-3}	(5 ± 3) x 10^{-5}	0.016 ±0.010	0.034 ±0.025	0.11 ±0.08	0.34 ±0.25
^{87}Br	2.37 ±0.14	2.02 ±0.04	0.70 ±0.03	1.48 ±0.06	4.79 ±0.28	1.66 ±0.11	3.51 ±0.24
^{88}Br	6.9 ±0.3	1.96 ±0.12	0.53 ±0.03	1.70 ±0.39	13.5 ±0.6	3.66 ±0.27	11.7 ±2.7
^{89}Br	13.3 ±2.3	1.32 ±0.04	0.35 ±0.02	1.67 ±0.38	17.6 ±3.1	4.66 ±0.85	22.2 ±6.3
^{90}Br	21.2 ±2.4	0.65 ±0.05	0.23 ±0.02	0.85 ±0.40	13.8 ±1.9	4.88 ±0.70	18.0 ±8.7
^{91}Br	10.8 1.7	0.25 ±0.02	0.017 ±0.006	0.49 ±0.24	2.70 ±0.48	0.18 ±0.07	5.3 ±2.7
^{92}Br	22 ±6	0.036 ±0.012	0.018 ±0.012	0.11 ±0.07	0.79 ±0.34	0.40 ±0.29	2.4 ±1.7
^{92}Kr	0.033 ±0.003	1.75 ±0.05	0.316 ±0.013	2.62 ±0.16	0.058 ±0.006	0.010 ±0.001	0.086 ±0.009
^{93}Kr	2.1 ±0.3	0.53 ±0.03	0.071 ±0.004	1.42 ±0.12	1.11 ±0.17	0.15 ±0.02	3.0 ±1.0
^{94}Kr	2.2 ±1.4	0.234 ±0.026	0.020 ±0.006	0.78 ±0.50	0.51 ±0.33	0.044 ±0.030	1.7 ±1.6
^{92}Rb	0.012 ±0.001	4.90 ±0.07	1.96 ±0.20	3.73 ±0.30	0.059 ±0.005	0.024 ±0.003	0.045 ±0.005
^{93}Rb	1.38 ±0.11	3.62 ±0.05	1.82 ±0.30	3.97 ±0.44	5.00 ±0.41	2.51 ±0.46	5.48 ±0.76
^{94}Rb	10.6 ±0.7	1.81 ±0.05	0.81 ±0.13	2.85 ±0.92	19.2 ±1.4	8.6 ±1.6	30 ±10
^{95}Rb	8.9 ±0.5	0.84 ±0.03	0.37 ±0.09	1.67 ±0.38	7.48 ±0.50	3.29 ±0.82	14.9 ± 3.5
^{96}Rb	14.2 ±1.0	0.214 ±0.035	0.049 ±0.016	0.57 ±0.24	3.04 ±0.54	0.70 ±0.23	8.1 ±3.5

Table 6 (cont'd)

Precursor	P_n-value %	Cumulative fission yield Y_c, % ^{235}U(a)	^{239}Pu (a)	^{238}U(a)	$P_n \times Y_c \times 10^4$ ^{235}U	^{239}Pu	^{238}U
^{97}Rb	30 ±13	0.077 ±0.012	(7 ± 2) x 10^{-3}	0.085 ±0.020	2.31 ±0.43	0.31 ±0.06	2.55 ±0.65
^{98}Rb	15.0 ±2.4	(3.1±2.0) x 10^{-3}	(7 ± 2) x 10^{-4}	0.035 ±0.022	0.047 ±0.037	0.011 ±0.004	0.53 ±0.34
^{97}Sr	-	2.05 ±0.06	0.76 ±0.37	3.42 ±0.79	-	-	-
^{98}Sr	-	0.85 ±0.07	0.22 ±0.14	2.45 ±0.56	-	-	-
^{99}Sr	3.4 ±2.4	0.35 ±0.06	0.038 ±0.024	0.86 ±0.39	1.19 ±0.86	0.13 ±0.12	2.9 ±2.4
^{97}Y	1.6 ±0.3	6.87 ±0.13	5.27 ±0.79	6.16 ±0.75	11.0 ±2.1	8.4 ±2.0	9.9 ±2.2
^{99}Y	1.2 ±0.8	2.36 ±0.09	1.20 ±0.28	3.78 ±0.86	2.8 ±1.9	1.4 ±1.0	4.5 ±3.2
^{123}Ag	-	(7 ± 4) x 10^{-4}	(9 ± 6) x 10^{-4}	(9 ± 6) x 10^{-3}	-	-	-
^{127}In	-	0.060 ±0.027	0.16 ±0.10	0.101 ±0.064	-	-	-
^{128}In	-	0.090 ±0.058	0.073 ±0.023	0.30 ±0.19	-	-	-
^{129}In	-	0.013 ±0.008	0.12 ±0.08	0.61 ±0.30	-	-	-
^{130}In	-	0.097 ±0.031	0.026 ±0.017	0.31 ±0.20	-	-	-
^{131}In	-	0.029 ±0.009	(6 ± 4) x 10^{-3}	0.22 ±0.14	-	-	-
^{132}In	-	(7 ± 2) x 10^{-3}	(1.3±0.8) x 10^{-3}	0.069 ±0.044	-	-	-
^{133}Sn	-	0.15 ±0.09	0.032 ±0.021	1.33 ±0.30	-	-	-

Table 6 (cont'd)

Precursor	P_n-value %	Cumulative fission yield Y_c, % ^{235}U (a)	^{239}Pu (a)	^{238}U (a)	$P_n \times Y_c \times 10^4$ ^{235}U	^{239}Pu	^{238}U
^{134}Sn	17 ±7	0.11 ±0.07	(1.9±1.2) x 10^{-3}	0.33 ±0.21	1.9 ±1.4	0.032 ±0.02	5.6 ±4.2
^{134}Sb	0.086 ±0.012	0.41 ±0.05	0.12 ±0.08	1.30 ±0.30	0.038 ±0.007	0.010 ±0.007	0.11 ±0.03
^{135}Sb	13.9 ±2.4	0.148 ±0.009	0.051 ±0.016	0.92 ±0.41	2.06 ±0.38	0.71 ±0.25	12.8 ±6.1
^{136}Sb	23 ±8	0.016 ±0.010	(2.8±1.8) x 10^{-3}	0.21 ±0.15	0.37 ±0.26	0.064 ±0.047	4.8 ±3.8
^{136}Te	0.9 ±0.4	1.53 ±0.25	0.55 ±0.24	4.81 ±0.77	1.38 ±0.65	0.50 ±0.31	4.3 ±2.0
^{137}Te	2.2 ±0.5	0.44 ±0.14	0.13 ±0.08	2.33 ±0.54	0.97 ±0.38	0.29 ±0.19	5.1 ±1.7
^{138}Te	5.6 ±1.6	0.091 ±0.029	0.0106 ±0.0034	0.86 ±0.39	0.51 ±0.22	0.059 ±0.025	4.8 ±2.6
^{137}I	6.7 ±0.5	3.24 ±0.20	2.43 ±0.10	5.30 ±0.85	21.7 ±2.1	16.3 ±1.4	36 ±6
^{138}I	2.6 ±0.3	1.61 ±0.10	1.17 ±0.09	3.08 ±0.71	4.19 ±0.55	3.04 ±0.42	8.0 ±2.1
^{139}I	10.2 ±0.9	0.99 ±0.03	0.31 ±0.15	1.83 ±0.42	10.1 ±0.9	3.2 ±1.6	18.7 ±4.6
^{140}I	22 ±6	0.22 ±0.14	0.060 ±0.019	0.59 ±0.27	4.8 ±3.3	1.32 ±0.55	13.0 ±6.9
^{141}I	39 ±13	0.020 ±0.006	(7 ± 2) x 10^{-3}	0.18 ±0.11	0.78 ±0.35	0.27 ±0.12	7.0 ±4.9
^{141}Xe	0.043 ±0.003	1.33 ±0.04	0.47 ±0.02	3.20 ±0.19	0.057 ±0.004	0.020 ±0.002	0.14 ±0.01
^{142}Xe	0.41 ±0.03	0.45 ±0.03	0.137 ±0.011	1.97 ±0.45	0.18 ±0.02	0.056 ±0.006	0.81 ±0.19
^{143}Xe	-	0.053 ±0.006	(9 ± 1) x 10^{-3}	0.40 ±0.05	-	-	-

Table 6 (cont'd)

Precursor	P_n-value %	Cumulative fission yield Y_c, % ^{235}U (a)	^{239}Pu (a)	^{238}U (a)	$P_n \times Y_c \times 10^4$ ^{235}U	^{239}Pu	^{238}U
^{141}Cs	0.053 ±0.004	4.47 ±0.09	3.31 ±0.36	5.06 ±0.30	0.24 ±0.02	0.18 ±0.02	0.27 ±0.03
^{142}Cs	0.2 ±0.1	2.67 ±0.11	1.49 ±0.24	3.92 ±0.43	0.53 ±0.27	0.30 ±0.15	0.78 ±0.39
^{143}Cs	1.82 ±0.12	1.48 ±0.06	0.54 ±0.12	2.33 ±0.37	2.69 ±0.21	0.98 ±0.23	4.24 ±0.73
^{144}Cs	3.0 ±0.7	0.36 ±0.03	0.13 ±0.06	1.14 ±0.26	1.08 ±0.27	0.39 ±0.20	3.4 ±1.1
^{145}Cs	14.3 ±1.9	0.058 ±0.009	0.022 ±0.014	0.49 ±0.11	0.83 ±0.17	0.31 ±0.20	7.0 ±1.8
^{146}Cs	13.4 ±0.7	0.017 ±0.004	(1.4±0.9) x 10^{-3}	0.11 ±0.03	0.23 ±0.06	0.019 ±0.012	1.47 ±0.41
^{147}Cs	25 ±3	-	-	-	-	-	-
				SUM	170 ±7	70 ±4	298 ±23

(a) = ref.[110]

Table 7

Comparison between integral measurements of the decay of the delayed-neutron activity in ^{235}U[86,91] and summation of contributions of individual precursors using Eq. (4) and also using the computer-code INVENT[95]. The results for the approximate decay formula (2) are also shown. The activity is normalized to unity at zero cooling time.

Decay time	Neutron activity				
s	Integral measurements		Eq. (4)	INVENT	Eq. (2)
	Keepin[86]	Besant[91]			
0	1.000	1.000	1.000	1.000	1.000
0.1	0.962	0.960	0.959	0.960	0.883
0.2	0.929	0.925	0.924		0.839
0.4	0.872	0.868	0.862	0.866	0.780
0.8	0.786	0.783	0.766		0.703
1.6	0.668	0.664	0.641	0.649	0.608
3.2	0.522	0.517	0.488		0.494
6.4	0.365	0.364	0.334	0.339	0.369
12.8	0.232	0.231	0.210	0.214	0.245
25.6	0.136	0.134	0.123	0.127	0.136
51.2	6.41×10^{-2}	6.23×10^{-2}	5.86×10^{-2}		5.98×10^{-2}
102.4	1.89×10^{-2}	1.76×10^{-2}	1.77×10^{-2}	1.83×10^{-2}	1.86×10^{-2}
204.8	3.03×10^{-3}	2.74×10^{-3}	3.01×10^{-3}		3.57×10^{-3}
409.6	2.06×10^{-4}	1.71×10^{-4}	2.03×10^{-4}	2.14×10^{-4}	3.46×10^{-4}
819.2	1.28×10^{-6}	8.30×10^{-7}	1.23×10^{-6}		1.28×10^{-5}

Table 8

Absolute delayed-neutron yields from neutron-induced fission in terms of number of delayed neutrons per 10^4 fissions

Nuclide	Ref.[a]		Ref.[b]	Summing known precursors[c]	
	Combined[d]	Fast	Thermal	Fast	Thermal
^{232}Th	545 ±11	547 ±12			
^{233}U	69.8 ±1.3	72.9 ±1.9	66.4 ±1.8		
^{234}U	106 ±12	106 ±12			
^{235}U	169.7 ±2.0	171.4 ±2.2	165.4 ±4.2	164 ±6	170 ±7
^{236}U	231 ±26	231 ±26			
^{238}U	450.8 ± 6.0	451.0 ± 6.1		439 ±17	298 ±23 [383[e] ±33]
^{238}Pu	45.6 ±5.1	45.6 ±5.1			
^{239}Pu	65.5 ±1.2	66.4 ±1.3	62.4 ±2.4	59.8 ±2.2	70 ±4
^{240}Pu	96 ±11	96 ±11			
^{241}Pu	160 ±16	163 ±16	156 ±16		
^{242}Pu	228 ±25	228 ±25			

a) = ref.[90] b) = ref.[91] c)= this review Section 3.1

d)=recommended by Tuttle[90] e)= calculated with Y_c from ref.[87] (see Sect. 3.1.)

Figure captions

Fig. 1. Isotopic chart showing the position of known delayed-neutron precursors (hatched areas).

Fig. 2. Pulse spectra of delayed neutrons from the precursors ^{134}Sn, ^{135}Sb, ^{136}Te, and ^{137}I. The pulse spectra obtained from the ^{3}He-spectrometer are shown rather than the neutron spectra in order to indicate the statistical errors ($\pm$ one standard deviation) of the measured points.

Fig. 3. Pulse spectra of delayed neutrons from the precursors ^{87}Br, ^{88}Br, ^{89}Br, and ^{90}Br. The pulse spectra obtained from the ^{3}He-spectrometer are shown rather than the neutron spectra in order to indicate the statistical errors ($\pm$ one standard deviation) of the measured points.

Fig. 4. Product of branching ratio and cumulative fission yield plotted versus the half-life of the precursor. The broken vertical lines correspond to a set of group half-lives.

Fig. 5. Experimental and calculated delayed-neutron spectra for the precursor ^{137}I. Histogram: Experimental spectrum[67)]
Dashed curve: Calculated spectrum
Dash-dot curve: s-wave component
Dash-dot-dot curve: d-wave component
Dash-dot-dot-dot curve: g-wave component.

Fig. 6. Delayed-neutron spectra for a long irradiation of ^{235}U and cooling times 0, 2.3 s, 23 s, and 220 s.[61)]
The origin of the fine structure peaks is indicated.

Fig. 7. Experimental and calculated effective delayed-neutron spectra in the fission of ^{235}U.
Dashed curve: Experimental "short-cycle" spectrum from ref.[98)]
Solid curve: Calculated spectrum.

Fig. 8. Experimental and calculated effective delayed-neutron spectra in the fission of ^{235}U.
Dashed curve: Experimental "4-second cycle" spectrum from ref.[99)]
Solid curve: Calculated spectrum.

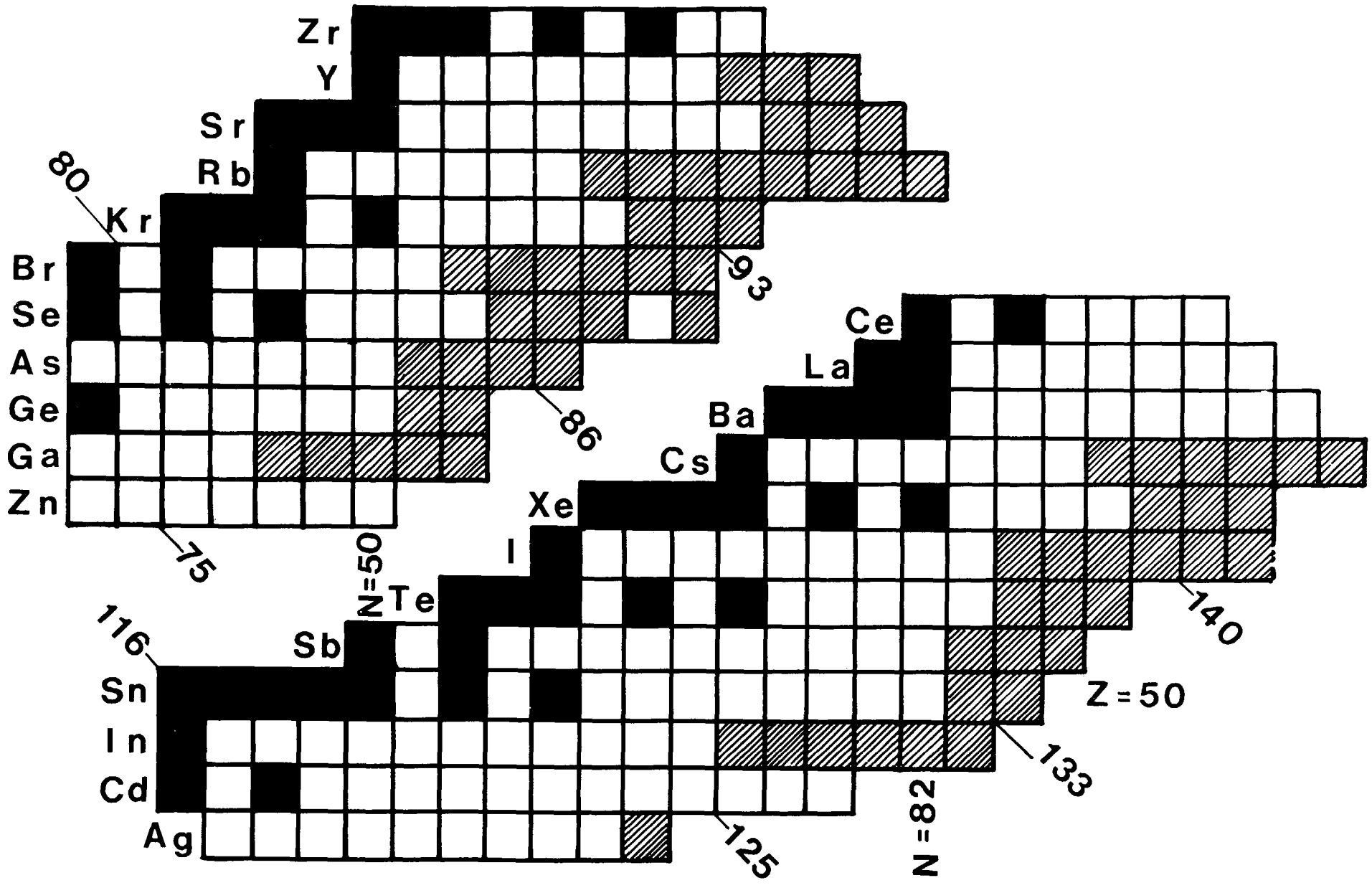

Fig. 1. Isotopic chart showing the position of known delayed-neutron precursors (hatched areas).

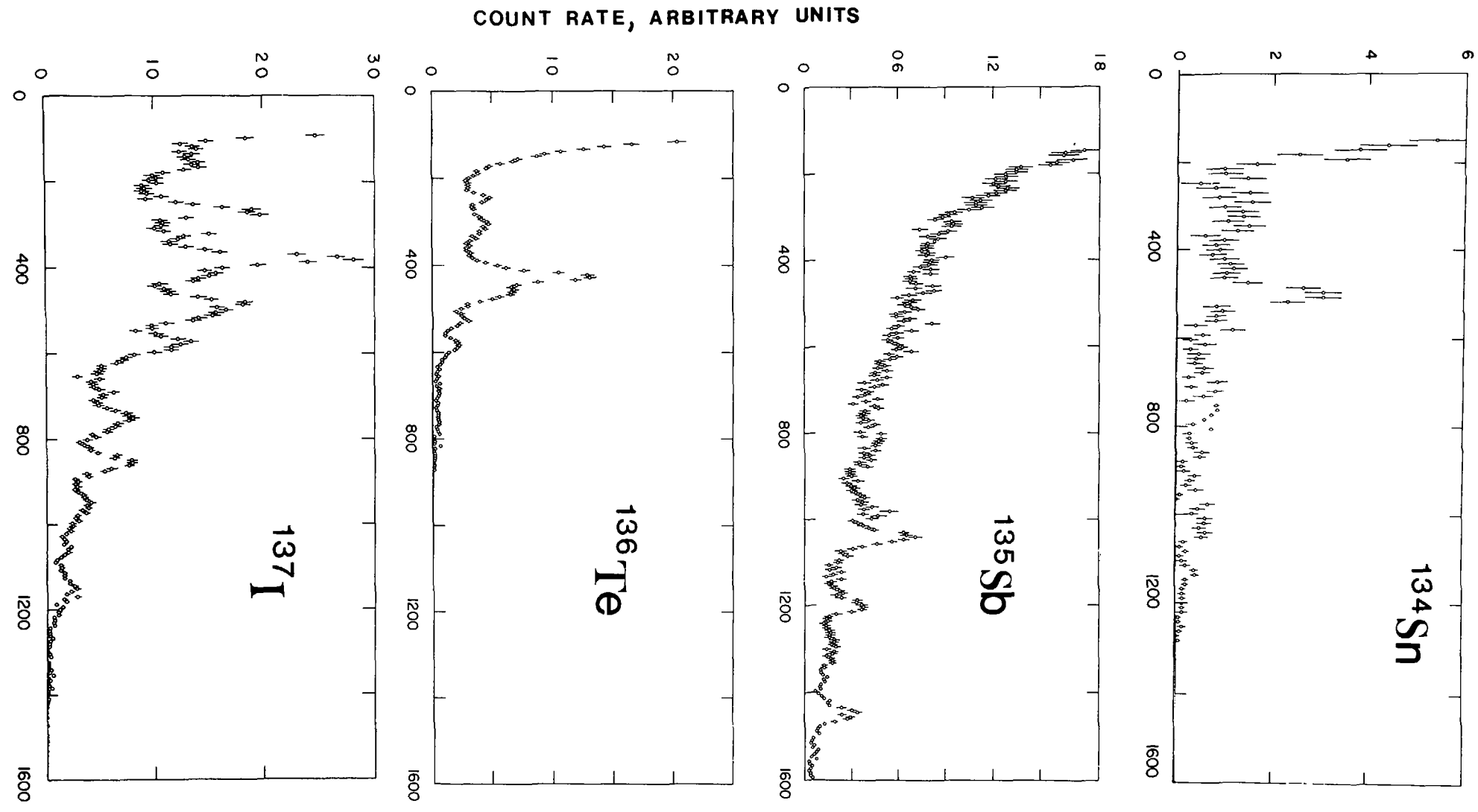

Fig. 2. Pulse spectra of delayed neutrons from the precursors ^{134}Sn, ^{135}Sb, ^{136}Te, and ^{137}I. The pulse spectra obtained from the ^{3}He-spectrometer are shown rather than the neutron spectra in order to indicate the statistical errors ($\pm$ one standard deviation) of the measured points.

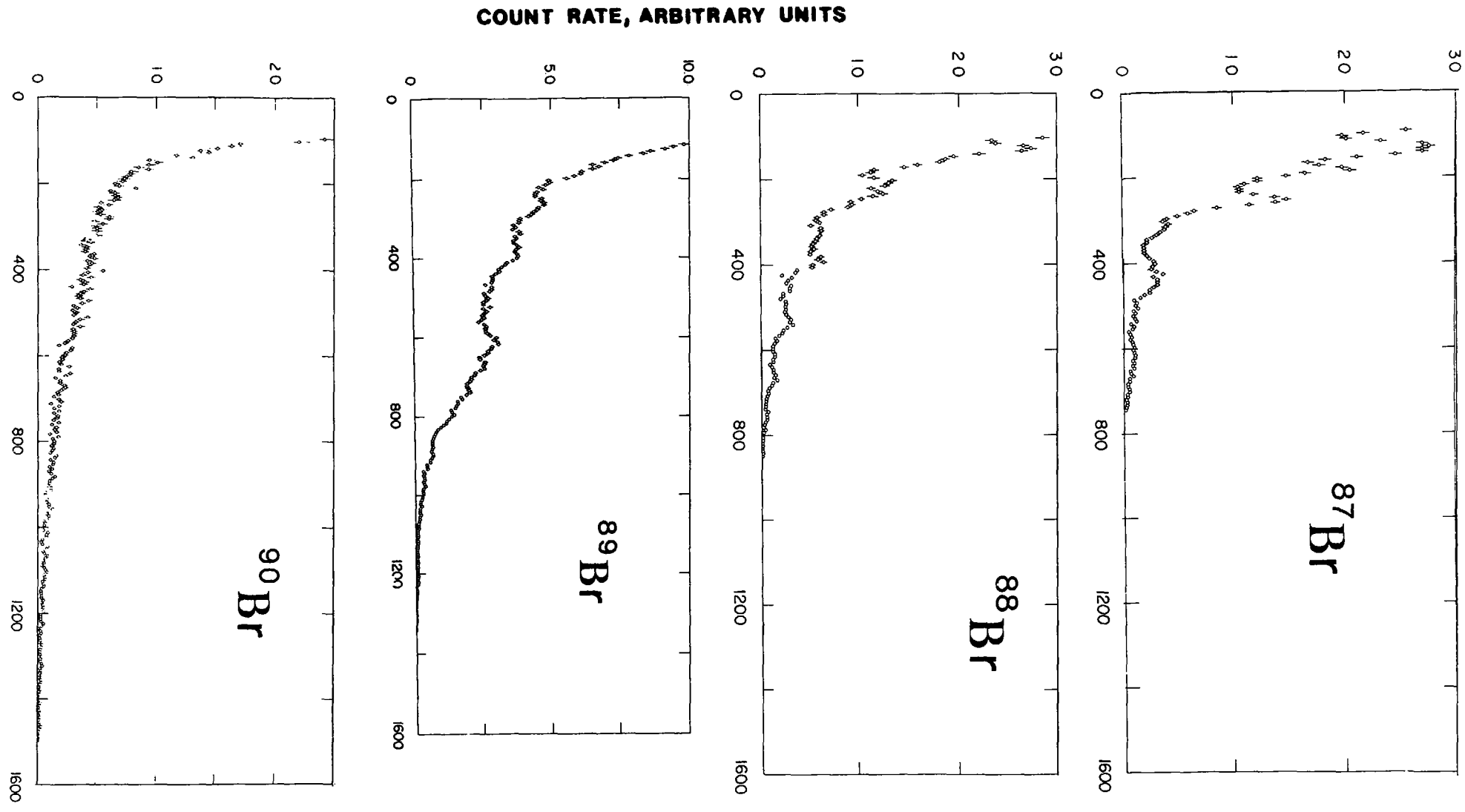

Fig. 3. Pulse spectra of delayed neutrons from the precursors ^{87}Br, ^{88}Br, ^{89}Br, and ^{90}Br. The pulse spectra obtained from the ^{3}He-spectrometer are shown rather than the neutron spectra in order to indicate the statistical errors ($\pm$ one standard deviation) of the measured points.

Fig. 4. Product of branching ratio and cumulative fission yield plotted versus the half-life of the precursor. The broken vertical lines correspond to a set of group half-lives.

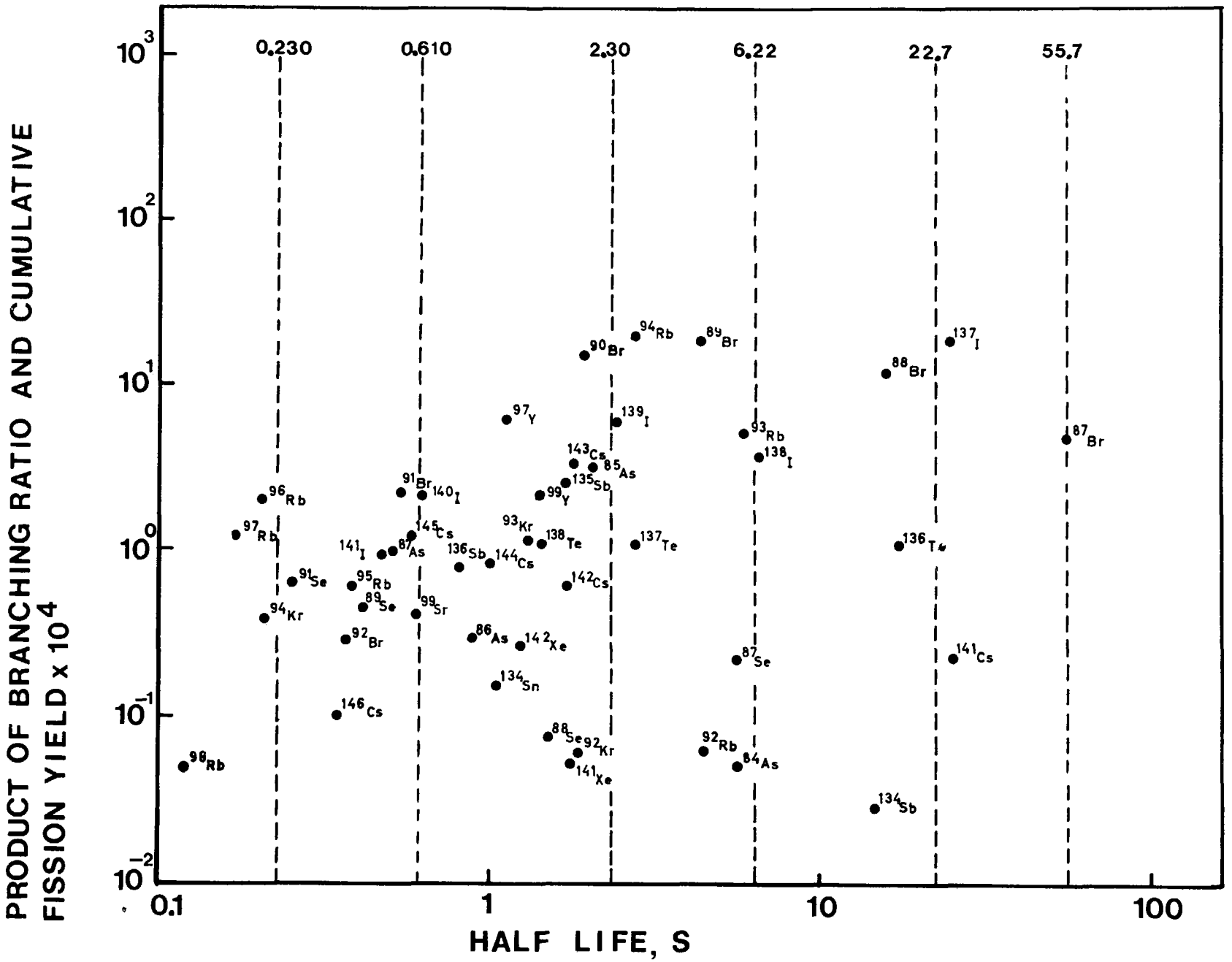

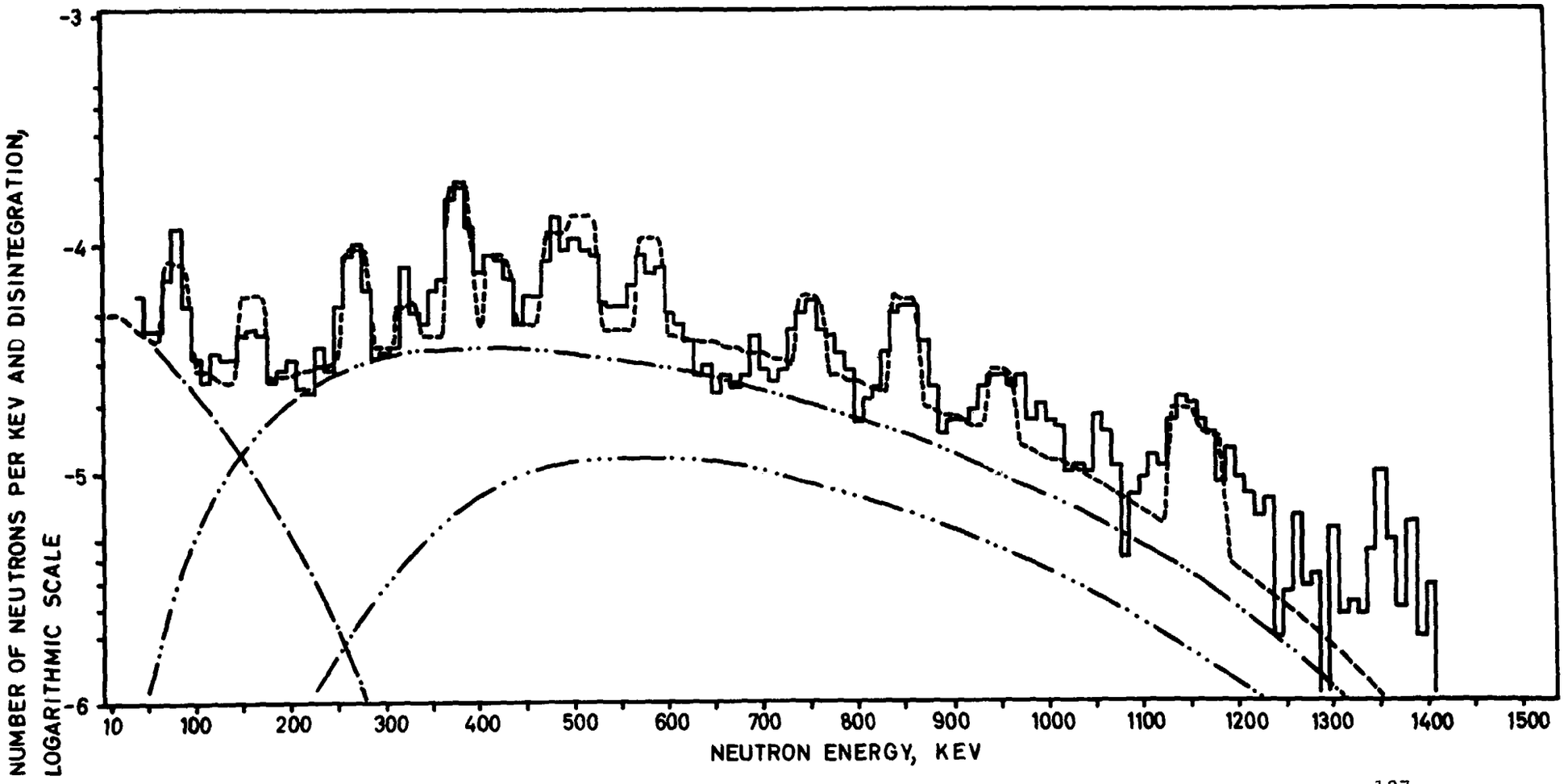

Fig. 5 . Experimental and calculated delayed-neutron spectra for the precursor ^{137}I.
Histogram: Experimental spectrum[67)]
Dashed curve: Calculated spectrum
Dash-dot curve: s-wave component
Dash-dot-dot curve: d-wave component
Dash-dot-dot-dot curve: g-wave component

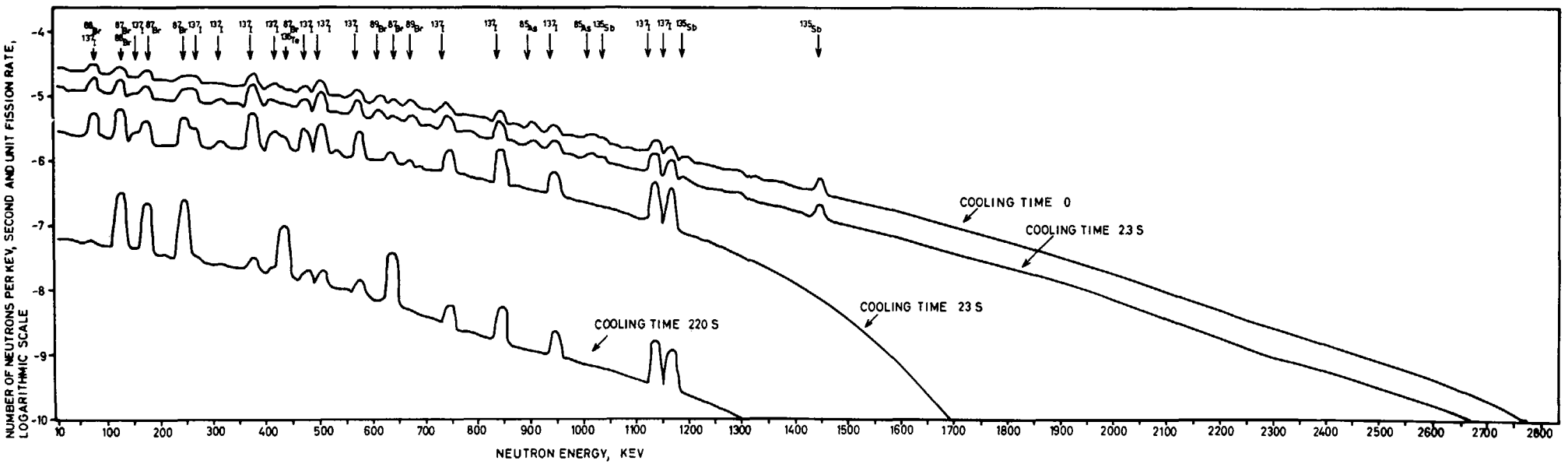

Fig. 6. Delayed-neutron spectra for a long irradiation of ^{235}U and cooling times 0, 2.3 s, 23 s, and 220 s.[61] The origin of the fine structure peaks is indicated.

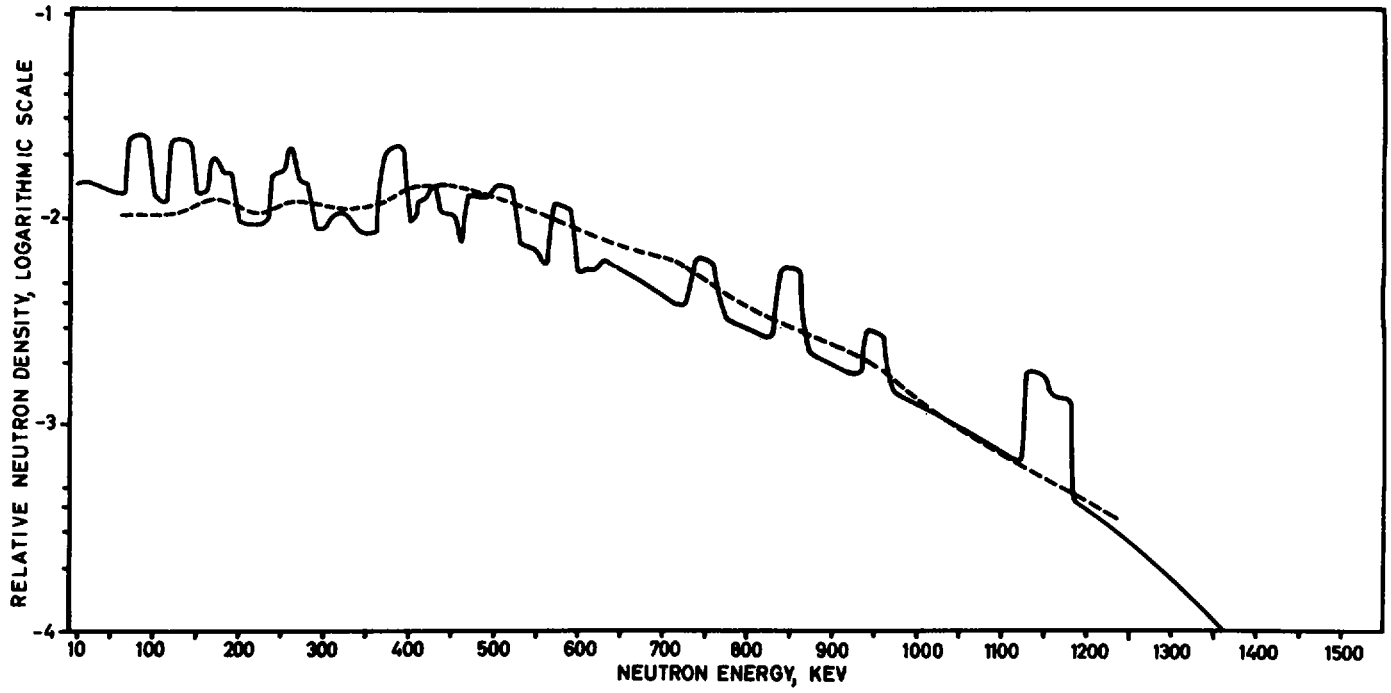

Fig. 7. Experimental and calculated effective delayed-neutron spectra in the fission of ^{235}U.
Dashed curve: Experimental "short-cycle" spec-rum from ref.[98]
Solid curve: Calculated spectrum.

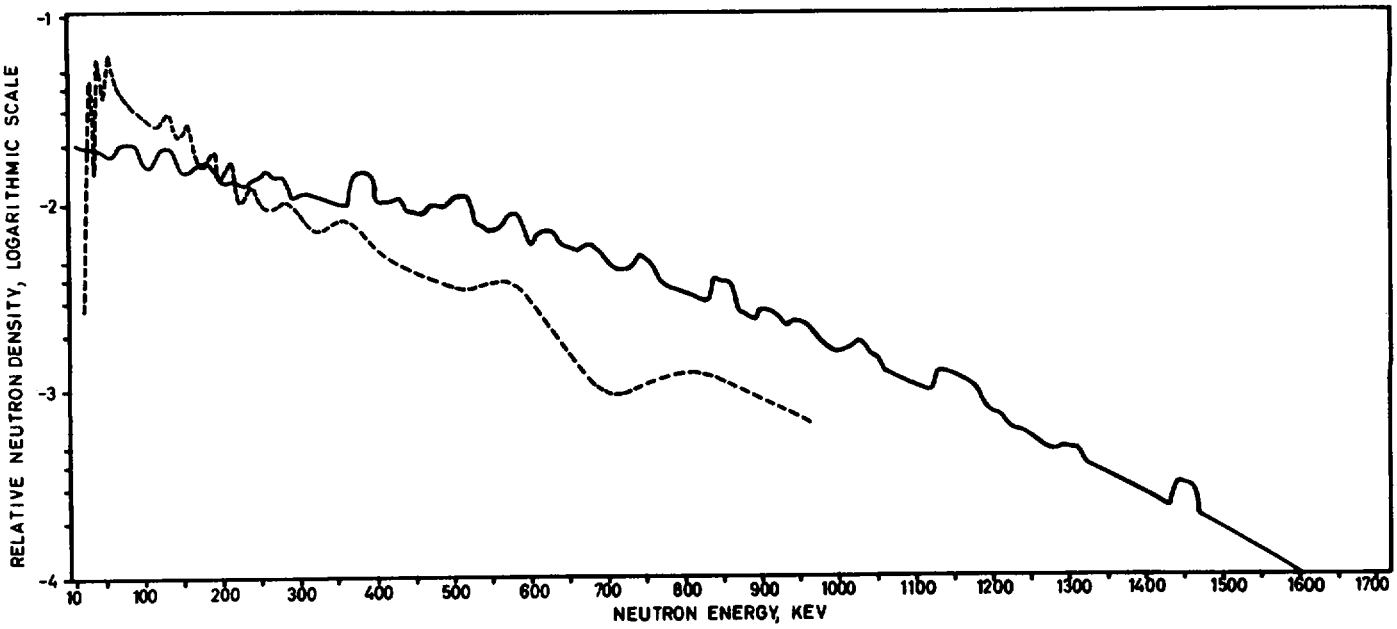

Fig. 8. Experimental and calculated effective delayed-neutron spectra in the fission of ^{235}U.
Dashed curve: Experimental "4-second cycle" spectrum from ref.[99]
Solid curve: Calculated spectrum.

Review paper 14

INTEGRAL DETERMINATION OF FISSION PRODUCT NEUTRON CAPTURE CROSS SECTIONS

M. Bustraan
J.W.M. Dekker
R.J. Heijboer
A.J. Janssem

Netherlands Energy Research Foundation ECN, Petten (N.H.), The Netherlands.

ABSTRACT

Integral measurements of fission product capture cross sections in fast reactors performed and analysed up to now are reviewed. A comparison is made with calculated integral data using various fission product cross section evaluations. This is done for individual nuclides as well as for gross mixtures of fission products.

1. REVIEW OF EXPERIMENTS

1.1. Introduction

At the 1973 Fission Product Nuclear Data Panel (Bologna) a review paper was presented on "Integral determination of neutron absorption by fission products" |1|. The present report is intended to review the progress that has been made since 1973 on the same subject. For general information on measuring techniques etc. the reader is referred to the 1973 review paper. The present report is restricted to integral measurements in fast spectra. Since 1973 only one (but quite extensive) experimental program on integral determination of fission product absorption in thermal systems has been reported |40|.

At the 1973 Bologna panel only some preliminary results of the STEK measurements were available. The analysis of the STEK measurements has

been performed now in great detail for 32 isotopes. For 30 other isotopes the analysis is still going on. Since 1973 also more accurate data became available from CFRMF |17, 21|.
Furthermore, fission product sampels have been irradiated in EBR-II. However, the results of these transmutation experiments were not yet available when this report was written.
Since no new developments took place at FRO |3|, the results of FRO quoted in this report are the same as those used in ref. |1|.
Up to now no data or results were received from the extensive French fission product program. This program comprises reactivity worth measurements in ERMINE and MASURCA with separated fission product isotopes and with samples of irradiated fuel. Also irradiations are performed in RAPSODIE and PHENIX.

1.2. Measurements in STEK

1.2.1. The STEK facility

STEK |4| was specially built for the integral determination of fission product capture cross sections in fast reactor spectra. It was a fast-thermal coupled critical facility. In the central fast zone effective cross sections were determined from central reactivity worth measurements using the oscillator technique. The measurements were performed with gram quantities of bulk fission products in irradiated fuel samples, of fission product elements, and of separated isotopes. The fuel of STEK in the fast zone consisted of highly enriched uranium and graphite in various ratios. Five STEK cores have been used with $C/^{235}U$ atomic ratios of about 72, 48, 35, 23, and 11, which cores were called, in order of increasing hardness of the spectrum: STEK-4000, -3000, -2000, -1000, and -500, respectively.
A description of the facility, the measuring techniques, and detailed results are given in |5| and |6|.
Only the most important information needed for a judging of the results will be given here.

1.2.2. STEK neutron spectra

The spectra used for the interpretation of the reactivity worth measurements in the five STEK cores were derived from:

a. Calculations,

b. Differential measurements,

c. Integral measurements.

Ad a.

Group fluxes (and adjoint group fluxes) have been calculated in the well-known ABBN 26 group structure. All group constants were taken from the KFK-INR set |7|, except for the $\Sigma^{sc}_{g,g+1}$ of C and Al. For g = 1-14 their elastic downscattering cross sections were derived from a 208 fine group calculation |8|. Below this region the elastic downscattering cross sections were calculated by an iterative procedure taking into account the flux energy spectrum in that region. Full core calculations were made with a two-dimensional RZ diffusion code. In some cases S_8 transport calculations with the code TWOTRAN |9| were made. Homogenized group constants were obtained from a volume and flux weighting of the outcome of cell calculations. In a later stage the $\Sigma^{sc}_{g,g+1}$ of C were derived from a bilinear (flux times adjoint) weighting scheme.

Ad b.

Four types of differential spectrum measurements have been performed in the five STEK cores by:

i) ^{6}LiF semiconductor sandwiches in the range of 0.4 MeV to 10 MeV (no measurements in STEK-500);

ii) ^{3}He proportional counter from 0.1 MeV - 2.5 MeV;

iii) Proton recoil counters from about 50 keV to 1.4 MeV;

iv) Time-of-flight from about 5 eV to 0.1 MeV.

In comparing the results of these measurements with the calculated spectra important discrepancies were detected. For the time being these discrepancies could not yet be resolved. Therefore these measurements were not taken into account in deriving the final STEK spectra.

Ad c.

Two types of integral measurements were performed.

i) Fission rate ratios relative to ^{235}U;

ii) Central reactivity worths of ^{10}B and ^{235}U.

Fission rate ratios relative to ^{235}U have been measured in all five STEK cores for $^{233,238}U$, ^{237}Np, and $^{239,240,242}Pu$. Only the fission

rates of the threshold fission detectors relative to ^{235}U were used in the subsequent analysis and adjustment procedure of the neutron spectrum. Since the cross sections of ^{10}B and ^{235}U can be assumed to be fairly well known, their central reactivity worths may be looked upon as an integral check on the neutron spectrum and the adjoint spectrum.

In first instance also the calculated integral spectral data were discrepant with the measured ones.

In order to resolve the discrepancies in the spectral data it has been tried to adjust the calculated STEK spectra (within their error bounds, determined by errors in core material nuclear data and taking into account the correlations between different errors), such that a better fit with the measured integral spectral data (again within their error bounds) was obtained. This adjustment was done with a modified version of the ECN adjustment program for adjusting fission product cross sections.

The nuclear data for this spectrum adjustment were again taken from the KFK-INR set. For ^{10}B the ENDF/B-III cross sections were used except for the region 4.65 - 1000 keV, where recent experimental data of Friesenhahn |10| were used.

The STEK spectrum adjustments have been effectuated by means of adjustment of the most important nuclear parameters, i.e. σ_f and α of ^{235}U. In ABBN groups 7 - 14 (400 keV - 2.15 keV) a downward adjustment of σ_f of 5% to 6% resulted, which is not in contradiction with recent measurements |11|. Also the adjustments of the α-values in groups 11 and 12 are confirmed by recent measurements |12|.

The STEK spectra are given in fig. 1. Further information, especially on the adopted adjustment procedure, is to be found in |13|.

1.2.3. Normalization of reactivity worths in STEK

The central reactivity worth of a sample is given by

$$\rho = -\delta\left(\frac{1}{k}\right) = \frac{\int_{\text{sample}} \phi^{+}\left(\frac{1}{k}\,\delta\nu F - \delta L - \delta S\right)\phi \; \mathrm{d}r\mathrm{d}E}{\int_{\text{reactor}} \phi^{+}\,\nu\Sigma_f\,\phi \; \mathrm{d}r\mathrm{d}E}, \qquad (1)$$

in which δF, δL, and δS represent the fission, the absorption and the scattering of the samples. For finite samples selfshielding and flux depression should be taken into account.

The denominator of eq. (1), the so-called normalization integral (NI), is difficult to calculate accurately for a fast-thermal

coupled facility because of the large variations in spectrum and importance over such a system. The method used in STEK for the elimination of the normalization integral has been the use of the apparent reactivity worth of a ^{252}Cf neutron source of well known strength |14|. This worth is

$$\rho_S = \frac{S \int \chi_S(E)\ \phi^+(E)\ dE}{NI}, \qquad (2)$$

in which S is the source strength and χ_S the neutron spectrum of the source. If ρ_S is multiplied by the absolute fission rate per gram of ^{235}U at the same position and at the same power level at which ρ_S has been determined, and divided by S one obtains:

$$\rho_o = \frac{\int \Sigma_f\ \phi\ dE \int \chi_S\ \phi^+\ dE}{NI}, \qquad (3)$$

which can be considered as a standard for reactivity worths (Σ_f is the fission cross section per gram ^{235}U). The quantity

$$\frac{\rho}{\rho_o} = \frac{\int_{sample} \phi^+ \left(\frac{1}{k}\delta\nu F - \delta L - \delta S\right) \phi\ dr dE}{\int \Sigma_f\ \phi\ dE \int \chi^S\ \phi^+\ dE} \qquad (4)$$

can be compared more easily with the corresponding experimental value $\left(\frac{\rho}{\rho_o}\right)_{exp}$ because now only the ϕ and ϕ^+ at the sample position have to be known.

All experimental reactivity worth data in STEK are normalized to this quantity ρ_o.

1.2.4. STEK data reduction and analysis

The main objective of the STEK reactivity worth measurements is to use the results for adjustment of evaluated fission-product capture group cross sections |19|.

In reactivity worth measurements also a signal is obtained due to elastic and inelastic scattering. This contribution is proportional to

$$\iint \Sigma_{sc}(E \to E')\ (\phi^+(E') - \phi^+(E))\ dE\ dE'$$

In STEK, $\phi^+(E)$ decreases monotonically with increasing E. This is different from systems with a high content of ^{238}U where the adjoint rises

for energies above the fission threshold of ^{238}U. The result is that in STEK the scattering contribution is positive. In other systems this may be negative. In STEK the scattering contributions were calculated for all measurements and were then subtracted from the measured total reactivity effects. The corrections for admixtures like O and Cl were deduced from separate measurements of the effect of known amounts of these materials.

The majority of the STEK samples exhibit a selfshielding effect, especially in the softer STEK cores. A simple extrapolation to zero mass of measurements with samples with different masses turned out in most cases to be impossible (by lack of measurements with sufficiently small samples) or inaccurate (due to the limited accuracy obtainable per measurement, especially for the small samples).
If one assumes that the resonance parameters which govern the selfshielding are sufficiently well known, one can try to correct for selfshielding by applying a correction calculated from the resonance parameters. As long as the corrections are small this might be an acceptable procedure. Since in STEK, however, this correction was in many cases and in most cores not small (a factor 2 to 3 in some cases!), a more sophisticated procedure has been applied. In this procedure the selfshielded capture group cross sections associated with each nuclide in a sample with a certain thickness form the adjustable quantities. Essential for this method is the introduction of a strong correlation of the errors in the group cross sections, for each nuclide, differing only in the degree of selfshielding. Thus adjustment is performed for a number of samples in one adjustment calculation at the same time. Since for a number of isotopes different sample materials with different isotopic compositions had to be used in order to correct for minor isotopes, also the samples with these other materials had to be treated in the same adjustment run. In an extreme case for Mo a total of 100 different integral data had to be handled in one adjustment calculation. The advantage of this method is that all experimental information is used at its full weight. The only disadvantage inherent in the method is that no "measured" infinite dilution data are obtained, since the measurements as such are not extrapolated to zero thickness. In fact, adjusted integral data for pure nuclides are obtained which in some way depend on a-priori calculated group cross sections and on assumed resonance parameters used in calculating the selfshielding. The measure of this dependency

is closely connected to the quality, or accuracy of the measurements. For measurements with uncertainties small compared to those originating from the uncertainties in the a-priori capture data this dependency is weak. This holds for the majority of the STEK measurements.
In ref. |15| the measured reactivity worths are given together with the a-priori calculated values and the adjusted values for each sample in each STEK core.*) From the adjusted group cross sections an infinite dilution reactivity effect has been calculated in each STEK core for each nuclide. These data, also given in ref. |15|, can be considered as the results from STEK extrapolated to infinite dilution. In table I these "experimental" results are compared with calculated results using the ENDF/B-IV file (see sect. 3).
An alternative method would have been to calculate from the tables in ref. |15| the selfshielding after the adjustment and to apply these calculated adjusted selfshielding correction factors to the measured shielded values to obtain infinite dilution values. Then these results would have to be averaged for the different sample sizes, taking into account the correlations of the errors and the corrections for contaminants, etc., to obtain one infinite dilution value per isotope per STEK core.
The measurements on irradiated fuel samples and on a mock-up fission product sample are treated in chapter 4 dealing with mixtures of fission products.

1.3. Measurements in CFRMF

1.3.1. Facility

The Coupled Fast Reactivity Measurement Facility has been used for two types of measurements on fission product cross sections, i.e.
a) Activation measurements;
b) Reactivity worth measurements.

CFRMF is extensively described in |2,16|. It is a critical assembly with a zoned core. It consists of a 14.5 cm square, 61 cm high ^{238}U (99.7%) block in a MTR type core, in a water pool about 5 m deep. The ^{238}U block has an axial central hole of 5.3 cm diameter. The block and hole are covered with boral. Inside the hole there is a 0.9 mm sleeve of

*) An example is given in fig. 2, to be discussed in sect. 3.4.

^{235}U. Inside this dry hole the reactivity worth and activation measurements are performed. For the activation measurements the power level can be raised to 100 kW giving a peak flux of 1.2×10^{12} n/cm^2.s. When at top and bottom ^{10}B plugs are present the axial flux distribution is a pure cosine.

1.3.2. CFRMF spectra

The CFRMF spectrum (see fig. 1) has been deduced from

a) differential spectrum measurements,

b) calculations,

c) reaction rate measurements as check on the calculations.

Ad a.

Differential spectra were measured by:

i) Proton recoil in three series comprising cylindrical and spherical counters, some filled with hydrogen, some with methane at different pressures. The overlapping energy regions run from 48 keV up to 2 MeV. The results of both types of counters agree within statistical errors.

ii) ^6Li semiconductor sandwich. Two types were used, one with a 4π geometry for the α- and tritium particles and one with an energy-independent collimation geometry. There is some disagreement between the results of the two systems which is thought to be due to neutron spectrum anisotropy for which the collimated detector is more sensitive. There is a rather significant disagreement between the H(n,p) and the $^6Li(n,\alpha)T$ measurements between 0.2 and 0.5 MeV which could not yet be resolved.

Ad b.

The spectrum and adjoint spectrum is calculated by a transport code SCAMP (1D, P_1, S_6). Occasional checks have been made with Monte Carlo calculations. The calculations are done in 71 energy groups, 0.25 lethargy spacings from 21 MeV down. Cell and full core calculations have been made. Cross sections from ENDF/B-III and -IV have been used.
The presently recommended spectrum is the full core cylindrical one-dimensional model calculation using ENDF/B-IV cross sections. The spectrum agrees very well for energies above about 50 keV with the H(n,p) and the $^6Li(n,\alpha)T$ measured ones, except for the above mentioned disagreement between 0.2 and 0.5 MeV. The CFRMF spectrum is drawn in fig. 1 together with STEK and FRO spectra.

Ad c.

For a number of fissionable and non-fissionable dosimetry materials integral reaction rates relative to ^{235}U fission rates have been measured and compared with calculations. In most cases there is a good agreement, which might be interpreted as a confirmation of the calculated flux spectrum.

1.3.3. CFRMF activation measurements

The measurements are performed by exposing a well characterized sample together with flux monitors to the neutron flux in the centre of CFRMF. Reaction rates are thus derived by measuring the activity of the reaction products via γ-ray spectroscopy. Run to run normalization is done by gold foils, while the fission rate of ^{235}U is used as a final standard.

In the original results [17,21] no corrections for selfshielding were applied yet. In some cases these corrections have been estimated by us. The results of these measurements, relative to calculated values using ENDF/B-IV cross sections, are given in table 1. The errors quoted for these measurements mainly stem from the uncertainties associated with the decay data of each reaction component. At this time the errors are conservative estimates based on a preliminary evaluation of the decay data. It is expected that a future evaluation of these data will decrease the uncertainties. The present agreement between measurements and calculations is in the range of 10 - 25%. For other materials for dosimetry applications the overall agreement is of the order of 5%, which substantiates that the activation method is capable of accuracies of at least this magnitude.

1.3.4. CFRMF reactivity worth measurements

CFRMF has been used also for central reactivity worth measurements. The reactivity effects were measured by a control rod calibrated against periods. The reactivity worth measurements in CFRMF exhibit some special difficulties, which renders this facility less suitable for studies of absorption responses. These difficulties are:

a. The rather low sensitivity resulting in a need for rather large samples (tens to hundreds of grams), causing a non-negligible flux perturbation which complicates the analysis by a need for specially

calculated perturbed fluxes.

b. The large reactivity effect of scattering caused by the increase of the adjoint flux with increasing energy. The result of this high scattering sensitivity is that the corrections to be applied for the oxygen and the water present in the samples tend to be large (sometimes the tenfold of the absorption effect). Although the effects of oxygen and water have been measured separately, the accuracy of the final absorption results is badly affected. Even if completely dry and oxygen-free material had been used, the correction for the inelastic and elastic scattering in the sample material would, in a number of cases, remain a considerable source of uncertainty.

For these reasons it has been decided for the purpose of this review paper not to take into account these reactivity worth measurements of CFRMF. However, these measurements may be of interest to test total reactivity worths calculated from a fission product nuclear data file.

1.4. Measurements in FRO

Since 1973 no further work on FRO [3] took place. For the sake of completeness a few important aspects of FRO are repeated here.
FRO was a fast critical reactor using ^{235}U (20%) as fuel, and graphite, stainless steel, aluminium and polythene as diluents. Three different cores with different neutron spectra were used for reactivity worth measurements of 10 fission product nuclides. The spectra were derived only from calculations. The reactivity worths were normalized to the reactivity worths of a sample of ^{235}U (93%). For the effects of self-shielding calculated corrections were applied. The FRO spectra are also given in fig. 1.

2. SOURCES OF ERRORS WHICH PLAY A ROLE IN THE INTERPRETATION OF INTEGRAL MEASUREMENTS

Of the three types of integral measurements (reactivity-, activation- and transmutation measurements) only the first two are dealt with in this report. Some sources of errors are typical for a specific type of measurement, whereas others are important for all measuring methods. One can make a distinction between errors in the integral measurements and uncertainties in the interpretation of the measurements and comparison with calculated integral data. One can further divide the errors in

statistical and systematic errors. When experimental and calculated integral data are compared all errors and their correlations must be taken into account.

2.1. Errors in measured integral data

Statistical errors in experimental reactivity worths are determined by measuring time, reactor noise and drift effects. Numerical values for the STEK and FRO measurements are given in ref.|6| and ref. |3|, respectively. The statistical errors for the important fission product samples (with relatively high capture cross sections) are generally rather small, so that they play only a minor role in the total error which appears in the comparison with calculated reactivity worths.

For STEK several sources of systematic errors have been investigated |6|:

- The point-reactor model used in the inverse kinetics calculations to obtain the experimental reactivity worths might be inadequate for the two-zone reactor. The associated error appeared to be less than the statistical error in the reactivity measurements;
- The effect of uncertainties in the parameters used in the inverse kinetics calculations (reduced neutron generation time, delayed neutron parameters) on absolute reactivity worths (in $) is less than 0.8%. The effect on normalized worths will be even smaller.

Fission product activation data from CFRMF have uncertainties which are mainly due to the uncertainty associated with the decay data of the reaction products. Improvement of the CFRMF data seems possible if more accurate decay data would become available |17|.

2.2. Uncertainties in the experimental conditions

Proper interpretation of the measurements calls for accurate knowledge of the compositions of the samples. Moisture contamination of the samples can be a serious problem in reactivity measurements in all facilities considered in this paper. For the STEK samples moisture contamination had to be far below 1 weight %, sometimes even below 0.1% (for weakly absorbing fission products), in order to keep the disturbing effect due to moisture below an acceptable level. For the CFRMF reactivity measurements the situation is still worse due to the strong energy dependence of the adjoint flux. For the STEK samples a very careful and elaborate

drying and packing procedure has been adopted. The amount of moisture in the samples used for reactivity measurements in CFRMF has been determined afterwards, so that (sometimes quite large) corrections had to be applied to the experimental reactivity worths.

The isotopic composition of the samples used for reactivity worth measurements introduces additional uncertainties only for the mixed fission product samples in irradiated fuel (see sect. 4 and ref. |1|).

Neutron selfshielding plays an important role in the reactivity worth measurements of most isotopic and elemental samples, in particular in the softer STEK and FRO spectra. In order to take into account this selfshielding, the dimensions of the samples should be known accurately. For the powdery STEK samples additional information concerning the distribution of the sample material within the capsules has been obtained from X-ray photographs of the samples.

2.3. Normalization of integral data

Integral data are usually normalized to a standard in order to avoid complications in the comparison of measured and calculated data. The only exception regarding the integral data considered in this paper concerns the reactivity worths measured in CFRMF. The comparison of measured and calculated absolute reactivity worths is complicated since the normalization integral (see sect. 1) is difficult to calculate accurately, in particular for zoned reactor facilities such as CFRMF and STEK. Assessment of the uncertainty in the calculated normalization integral is also quite difficult.

The standard sample material used for normalization should satisfy three requirements:

1. Its reactivity worth or reaction rate can be measured accurately,
2. Its cross sections should be well known,
3. The energy dependence of its cross sections should be similar to the energy dependence of the fission product cross sections, so that any errors or inaccuracies in the neutron spectra are more or less cancelled in the ratio of calculated integral quantities of the fission product and the standard.

2.3.1. Reactivity effect normalization

In ref. |6| three possible standards for reactivity effect normalization

have been considered: (a) the reactivity effect of ^{235}U; (b) the reactivity effect of natural boron, and (c) the (apparent) reactivity effect of a ^{252}Cf source in combination with the absolute ^{235}U fission rate.

a. ^{235}U

^{235}U is often used as a standard material in reactivity worth measurements (e.g. in FRO). Its fission cross section is accurately known, but its capture cross section is less well known. Moreover, the reactivity effect of ^{235}U (ρ_U) consists of a fission part which is partly compensated by an absorption part, whereas the main effect of fission products stems from absorption. Therefore, the variation of ρ_U with neutron spectrum hardness is completely different from the same variation for fission product reactivity effects, which is contrary to requirement (3) given above.

b. Boron

The (n,α) cross section of ^{10}B is well known (except above 50 keV where there are some uncertainties). Moreover, its $1/\sqrt{E}$ energy dependence resembles the energy dependence of the capture cross section of an "average" fission product, although the low energy side might get a somewhat too large weight. Owing to its very large cross section the measurement of the boron reactivity effect might give some problems in the interpretation because of possible flux distortion effects, especially in soft spectra.

c. ^{252}Cf source

STEK reactivity worths have been normalized to ρ_o, the product of the apparent reactivity worth of a ^{252}Cf source and the absolute fission rate of ^{235}U (see sect. 1). The ^{235}U fission rate can be measured accurately with absolute fission chambers. The fission spectrum of a ^{252}Cf source and σ_f of ^{235}U are accurately known, and the characteristics of σ_f of ^{235}U are fairly similar to those of the capture cross section of an "average" fission product. A disadvantage of normalization on ρ_o is the effect of possible inaccuracies in the adjoint spectrum: only the high-energy tail of $\phi^+(E)$ affects ρ_o, whereas in the absorption effect of fission products the adjoint at intermediate energies play a dominant role.

The uncertainty in ρ_o measured in STEK is made up of the following

contributions |6|:

a) Absolute fission rate

1. Amount of ^{235}U in fission chamber: ±1.1%,
2. Systematic error in counting rate: ±0.3%,
3. Statistical error in counting rate: ≤0.2%.

b) Source strength

1. Calibration of ^{252}Cf source: ±1.0%.
2. Effect of uncertainty in half-life of the source: <0.7%.

c) Apparent reactivity effect

1. Statistical error: ≤2.0%.
2. Normalization to the same reactor power of apparent reactivity effect and absolute fission rate: <1.3%.

2.3.2. Activation rate normalization

Three ways of normalization of activation rates measured in CFRMF have been used in subsequent phases of the experimental program:

1. Normalization on the activation rate of gold;
2. Normalization of the integrated flux determined with multi-foil dosimetry methods;
3. Normalization of the fission rate of ^{235}U determined with an NBS fission chamber. On an absolute basis this measured fission rate is much more accurate than the gold capture rate or the measured integrated flux |17|. Further advantages of this method of normalization have been mentioned already in section 2.3.1. The total error in the normalization of fission product activation rates relative to $^{235}U(n,f)$ has been reported to be only 1.7% |17|.

2.4. Errors in calculated integral data

Errors in calculated integral data are due to errors in the fission product cross sections, in the neutron spectra and in the calculated normalization of the integral data.

2.4.1. Sample dependent data

Mostly fission product capture cross sections are the quantities to be

improved with the aid of the integral measurements. Errors in these cross sections are discussed in refs.|18,19|.

Errors in calculated selfshielding factors and flux depression effects are partly due to uncertainties in the fission product cross sections and partly due to approximations in the calculation models. For the STEK samples the first error source is completely taken into account in the cross section error calculation (see sect. 1 and |19|). The magnitude of the second source is estimated from a comparison of the results of different calculation models (analytical resonance integral calculation, collision probability calculation, see |19|): the resulting uncertainty in calculated reactivity worths is of the order of a few per cent and much less than the error due to evaluated cross section uncertainties.

Many samples used for reactivity worth measurements in CFRMF are so large that they seriously perturb the neutron flux. Some perturbed flux calculations using a one-dimensional (cylindrical geometry) S_n-code have been performed |17|.

The samples used for activation measurements in CFRMF are so small that (calculated) selfshielding effects are of the order of only a few per cent.

The measured reactivity effects must be corrected for the effects due to neutron scattering in order to obtain the capture effects. These calculated corrections are sometimes quite large, in particular for nuclides with small capture cross sections and in hard spectra, such as CFRMF, STEK-500 and STEK-1000. For CFRMF the scattering effects often cannot be considered as corrections and it has been suggested |17| to use the CFRMF reactivity worths as integral checks on evaluated inelastic scattering cross sections. For STEK some numerical values for scattering corrections are given in section 3.5; uncertainties in these corrections have been estimated by the evaluator of the RCN-2 set to be about 25% to 50%.

2.4.2. Sample independent data

For STEK a rather complete analysis of all sources of errors in adopted neutron spectra has been made |13|. Some results of this investigation will be mentioned here.

In the early stages of the STEK project it was found that the calculated

reactivity effects of isotopes with fairly well known cross section (e.g. ^{235}U, ^{10}B, ^{103}Rh) differed substantially from the measured values (up to 15%). Since none of the error sources mentioned in the foregoing sections could explain the discrepancies, the origin of the discrepancies had to be sought in the flux and adjoint spectra and/or the calculated normalization quantity ρ_o.

Possible sources of errors in the calculated (normalized) spectra have been investigated:

- Calculation models. Comparison of calculations made at Petten with results obtained with French codes of CEA (which have been extensively tested against experiments in various fast assemblies) did not give any doubt about the calculation models used at Petten.
- Uncertainties in the cross sections of the reactor materials have been estimated and used in spectrum error calculations. It was found that at least a substantial part of the observed reactivity worth discrepancies could be ascribed to the uncertainties (up to 10% in σ_f and α of ^{235}U) in the cross sections of the reactor materials.
- The iterative determination of the elastic slowing down cross section Σ_{de} (in 26 group ABBN scheme) turned out to be highly uncertain. Uncertainties up to 40% had to be attributed to Σ_{de} and were applied in the spectrum error calculations mentioned above.
- Selfshielding factors of reactor materials were found to be rather uncertain. But estimated errors in these factors were less important than the uncertainties in the (infinite dilution) cross sections.
- Bilinear weighting of cross sections should be applied instead of flux weighting to calculate ϕ_g^+ and reactivity effects. The effect of bilinear weighting on calculated reactivity effects was found to be at most 1% to 2%. A complication in bilinear weighting, viz. the coincidence of resonance fine structure in $\phi(E)$ and $\phi^+(E)$, has been investigated. The effect of this coincidence could be calculated only approximatively, but effects of more than 2% on calculated reactivity worths were never found.

The calculated spectrum errors were used in the spectrum adjustment calculations described in sect. 1 and ref.|13|. With the adjusted spectra (and adjusted ^{235}U fission cross sections used in ρ_o) discrepancies between measured and calculated integral quantities of nuclides with fairly well known cross sections (reactivity worths of ^{235}U, ^{10}B, several fis-

sion products, fission rates of ^{238}U, ^{237}Np) are at most of the order of 1 standard deviation of the measured values. Uncertainties in calculated capture reactivity worths due to uncertainties in normalized spectra are of the order of 5%, but depend on the shape of the capture cross section relative to the ^{235}U fission cross section.

Many of the above mentioned sources of errors in (normalized) STEK spectra will also be important for the other facilities CFRMF and FRO, although the magnitude of their influence is difficult to estimate by us. Direct information on errors in the neutron flux spectrum in CFRMF is not available, but the generally good agreement between calculated and measured central neutron spectra gives much confidence in the use of the activation measurements*). For the interpretation of the reactivity worth measurements in CFRMF the normalization integral is needed which is difficult to calculate accurately in this heterogeneous system. Furthermore, the central hole in CFRMF may introduce leakage effects which are difficult to estimate with a one-dimensional cylindrical geometry reactor model.

2.5. Errors in adjusted integral data

All errors mentioned in the previous sections have to be taken into account when calculated and measured integral data are compared and used for adjustment of evaluated cross sections. Correlations between errors are equally important. For the STEK data and CFRMF activation data the uncertainties in the adjusted quantities include all above mentioned error sources. Adjusted infinite dilution integral data and their uncertainties for separated isotopes are given in table 1. Further comments to this table are given in section 3. A discussion on adjustment methods and the impact of adjustment on (errors in) integral data can be found in ref. |18|.

---

*) These measurements have been used by us to adjust evaluated capture cross sections (see section 3). For these adjustment calculations we made a rough estimate of the errors in the neutron spectrum by comparing various sources of information on this spectrum |2|. Five coarse energy groups were defined; within each coarse group fully correlated identical relative errors in the group fluxes were assumed; no correlations of errors were assumed for fluxes in different coarse groups. Further details are given in |20|.

3. COMPARISON OF INTEGRAL DETERMINATIONS OF NEUTRON CAPTURE CROSS SECTIONS OF FISSION PRODUCT NUCLIDES

3.1. Available data

Integral experimental data on neutron capture can be derived from measurements in STEK [6], CFRMF [17],[21] and FRO [3]. In STEK and in FRO central reactivity worth measurements have been made; in CFRMF capture rates as well as reactivity worths have been measured. For reasons already discussed in section 1, the reactivity measurements in CFRMF are not considered in the comparison of data to be discussed in this section. The reactivity measurements in FRO were already available at the Bologna Meeting [1]. At present it is possible to compare these data with data from STEK and CFRMF. Results from French facilities have not been published.

3.2. Neutron spectra

The integral measurements to be compared in this section have been made in nine different spectra (see fig. 1). In order of decreasing average capture cross section, $\bar{\sigma}_c = \int \sigma_c^{fp} \phi dE / \int \phi dE$, of a ^{239}Pu pseudo fission product (burn-up 42 MWd/kg, see sect. 4) they can be ranked as follows: ($\bar{\sigma}_c$ is given in barn/fission for each core in parenthesis):
STEK-4000 (2.20), STEK-3000 (1.22), STEK-2000 (0.88), FRO5 (.79), STEK-1000 (0.56), FRO8 (.35), STEK-500 (.34), CFRMF (.29) and FRO3 (.22). The corresponding quantity for the SNR-300 reactor is: 0.45, thus intermediate between STEK-1000 and STEK-500.

3.3. Results of integral capture cross section determinations compared with ENDF/B-IV calculations

In table 1 the following quantities, relative to the ones calculated with ENDF/B-IV [22] cross sections, are given: 1) Adjusted renormalized reactivity worths derived from STEK; 2) Experimental activation rates from CFRMF, normalized to the fission rate of ^{235}U; 3) Experimental reactivity worths from FRO, normalized to the reactivity worth of ^{235}U. See also footnotes to table 1.

In order to relate the integral quantities given in table 1 with those from other evaluated cross section sets, table 2 has been constructed.

In this table $\bar{\sigma}_c$ values for various fission product nuclides are given for the SNR-300 flux spectrum |23|, using the RCN-2 set |24|, RCN-2A (adjusted set |15|), JENDL-1 |25| and the CNEN/CEA set |26|, all relative to ENDF/B-IV quantities. Furthermore errors, if available, are given in both tables (see also footnotes at the tables).

An extensive comparison between integral quantities from measurements and from various cross section sets has been given recently by the Japanese Nuclear Data Committee |27|. Recent cross section sets have been intercompared (for capture only) also in ref. |28|. Part of the conclusions to be drawn from the tables 1 and 2 can be found in these references and has also been reviewed in |18|.

The STEK results in table 1 are the RCN-2A adjusted renormalized reactivity worths in infinite dilution. Arguments for this way of presentation of the STEK results were given in section 1. Some nuclides, measured in STEK, are not yet fully analysed. Blank spaces are given at the appropriate places in tables 1 and 2. The errors associated with the STEK results as given in tables 1 and 2 are taken from ref. |15|. They are the results of uncertainties in the cross sections used in the calculation of the renormalized STEK reactivity worths. The errors given do *not* contain the influence of uncertainties in the spectra used to calculate the renormalized integral quantities (i.e. $\phi_g \phi_g^+$ for the five STEK cores and ϕ_g for SNR-300). However, the uncertainties in the adjusted capture group cross sections (and thus the adjusted integral quantities) contain a component originating from uncertainties in the spectra, see ref. |15|.

The capture rates measured in CFRMF have been taken from |17|. The selfshielding correction for these measurements is small, but not always negligible (see section 2). For the larger part of the CFRMF capture rate measurements this effect is estimated in |20|. For these nuclides the corrected experimental data have been used in table 1. Beside the measured data relative to ENDF/B-IV quantities, adjusted values for $\bar{\sigma}_c$ in the CFRMF spectrum (again relative to ENDF/B-IV quantities) are given in table 1. These adjusted data have been obtained |20| by performing an adjustment calculation completely equivalent to the one made for STEK. The errors associated with the CFRMF measurements are mainly due to uncertainties in the decay parameters, used in the data reduction of the measurements.

The reactivity measurements in FRO have been taken from |3|, i.e. normalized to the measured worth for ^{235}U. Corrections for selfshielding and for scattering have been applied as given in |3|. The errors in the quantities given in table 1 are only due to statistical uncertainties in the experimental data.

3.4. Global comparison of integral data

In general the agreement between STEK and CFRMF data is good, taking into account the quoted uncertainties, i.e. standard deviations. The comparison between STEK and FRO is somewhat less satisfactory.
The errors in the adjusted RCN-2A data are mostly much smaller than the errors in the corresponding unadjusted RCN-2 data (see columns 5 and 4 of table 2). The same applies for errors in adjusted CFRMF data. For CFRMF adjusted errors can also be compared with errors in the measurements (columns 8 and 7 of table 1). The error reduction relative to errors in the measurements is mostly small and the adjusted quantities are not much different from the measured data. For STEK this comparison between adjusted and experimental data is not given in table 1, but from graphs in ref. |15| it follows that the adjusted data are very close to the "weighted average" of the experimental data, see for example fig. 2. In this figure measured and adjusted reactivity worths for ^{105}Pd samples with a certain degree of self-shielding are compared with calculated values.
As a conclusion it may be stated, that the adjusted data are not very much dependent on a-priori cross sections used, especially when accurate measurements have been made for nuclides with fairly large a-priori uncertainties in the cross sections.
From table 2 it can be concluded that relatively large differences exist between $\overline{\sigma}_c$ values of fission product nuclides, calculated with different evaluated cross section sets. In general, the evaluated errors in $\overline{\sigma}_c$ of the RCN-2 set are consistent with these differences. The differences between RCN-2 and RCN-2A quantities are generally smaller than the differences between the evaluated sets (viz.: ENDF/B-IV, RCN-2, JENDL-1 and CNEN/CEA).
As stated above there is a considerable reduction of errors going from RCN-2 to RCN-2A. For some nuclides the error reduction is such, that one of the values calculated with the other sets can be ex-

cluded, i.e. the differences with the RCN-2A set are larger than three times the standard deviation, given with the adjusted (RCN-2A) quantities. Following this rule, the integral quantities for ^{99}Tc, ^{107}Pd, ^{109}Ag, ^{129}I, ^{141}Pr, ^{147}Sm and ^{149}Sm calculated with ENDF/B-IV can be excluded, as well as the JENDL-1 value for ^{129}I.
Furthermore it can be seen from table 2 that the differences between RCN-2, JENDL-1 and CNEN/CEA among each other are smaller than the differences with ENDF/B-IV for quite a number of nuclides.
Very large differences between the values obtained with RCN-2, JENDL-1 or CNEN/CEA and those obtained with ENDF/B-IV are observed for ^{107}Pd, ^{109}Ag, ^{135}Cs, ^{147}Sm and ^{149}Sm. A discussion about the origins of these differences has been given in refs. |28| and |18|.
The net effects of these differences on an average pseudo fission product mixture will be discussed in section 4 of this report.

3.5. Comparison of measurements for individual nuclides

^{93}Nb

For this nuclide the CFRMF measurement comes out much higher than the trend indicated by the STEK measurements. However, there is a very large uncertainty assumed for the CFRMF reaction rate. In fact this latter measurement has practically no weight, as can be judged from the adjusted value for CFRMF, which is almost equal to the a-priori value calculated with RCN-2 cross sections. Furthermore, there is very good agreement for the adjusted STEK and ENDF/B-IV data, as follows from the ratios (in table 1) almost identically equal to 1.00 for the five STEK cores.

^{95}Mo

For this nuclide a comparison between STEK and FRO can be made.
A good agreement between the measurements in the two facilities can be observed.

^{97}Mo

A difference of about 10% can be estimated between the STEK and FRO measurements. At least for the FRO5 measurement and corresponding STEK measurements (STEK-2000) a discrepancy can be observed. It has to be noted, however, that for the FRO5 measurements only a small statistical error has been taken into account.

^{98}Mo, ^{100}Mo

For these two nuclides a comparison between STEK and CFRMF can be made. The measured value in CFRMF for ^{98}Mo is somewhat higher than indicated by the STEK measurements. Taking into account the error limits, the agreement is fairly good. For ^{100}Mo the CFRMF measurement points to a somewhat lower value than the STEK measurements. It has to be noted that for these two nuclides extremely large scattering corrections, even larger than the remaining capture effects have been applied to the STEK measurements, so that especially for these nuclides the CFRMF data form a valuable supplement to the integral data measured in STEK.

^{99}Tc

For this nuclide data from three different facilities can be compared. The general trend indicated by the measurements in STEK is about 30% higher than indicated by CFRMF and FRO. Scattering corrections in STEK-500 were about 12%. For FRO3 a correction of about 4% has been applied, so that the opposite tendency between STEK and FRO (and CFRMF) cannot be attributed to large scattering corrections.

^{101}Ru, ^{102}Ru, ^{104}Ru

For these nuclides the agreement between STEK, CFRMF and FRO is good. Some of the FRO measurements are outside the general trend, but in view of the error limits these discrepancies are not significant.

^{103}Rh

In this case the agreement between STEK and CFRMF data is very good. The ratio measurement over calculation (see table 1) for the FRO5 core seems much too large. About 40% of the calculated reactivity worth in FRO5 originates from the large resonance in ABBN group 23 (2.15 - 1.0 eV). In this low energy region large uncertainties have to be attached to the neutron flux spectrum, used to calculate the reactivity worth. Probably this fact explains the observed discrepancy. No significant adjustment occurs because of an excellent agreement between measurement and calculation using RCN-2 cross sections.

^{108}Pd, ^{110}Pd

For ^{108}Pd the agreement between STEK and CFRMF is excellent taking into account the fairly wide error limits associated with CFRMF and STEK-500

data. This last error limit (20%) is clearly caused by a rather large and uncertain scattering correction of about 50%, with an estimated uncertainty of 50%.

For ^{110}Pd the CFRMF measurement points to an extremely low value of about 5% of the value calculated with ENDF/B-IV. This tendency is only partly confirmed by the STEK measurements. A re-evaluation of the decay data used for the CFRMF activation measurements may perhaps solve this discrepancy. The adjusted value based on the CFRMF measurement is intermediate between the measured and the a-priori calculated value, although a very large error (90%) has been attributed to this last quantity. This exceptional adjustment originates from the fact that a "logarithmic" adjustment procedure has been applied (see ref. |19|) mainly to avoid negative adjusted group cross sections.

^{109}Ag

The CFRMF measurement is much larger than the value calculated with ENDF/B-IV cross sections. The greater part of this tendency is confirmed by the STEK data.

^{127}I, ^{129}I

The CFRMF measurement for ^{127}I points to a value somewhat lower (about 15%) than indicated by the STEK data. In view of the fairly wide error limits it is doubtful whether this difference is significant. For ^{129}I the agreement between STEK and CFRMF data is excellent.

^{133}Cs

The CFRMF measurement comes out somewhat lower (about 10%) than expected from the STEK data. The measurements in the cores FRO8 and FRO3 are much lower than expected from STEK and CFRMF. Moisture contamination of the FRO samples could be a reason for this discrepancy.

^{139}La

The CFRMF measurement indicates a somewhat lower value than the tendency shown by STEK data. It has to be noted that very large scattering corrections had to be applied to the STEK data. Therefore the measurements in STEK-2000, -1000 and -500 have not been taken into account in the adjustment procedure for the STEK data.

^{141}Pr

The agreement between STEK and CFRMF data is good, although large scattering corrections have been applied to the STEK data in the cores 1000 and 500.

^{147}Pm

For this nuclide the CFRMF measurements can be compared with the FRO results. A discrepancy between the measurements in CFRMF and FRO seems to exist. Future analysis of the STEK measurements might help to resolve this discrepancy.

^{149}Sm

For this nuclide there is a good agreement between STEK and FRO results.

^{152}Sm, ^{154}Sm

For ^{152}Sm a fairly good agreement between the results of STEK and CFRMF can be observed. For the rather unimportant nuclide ^{154}Sm the situation is somewhat less satisfactory.

4. MIXTURES OF FISSION PRODUCTS

4.1. Comparison of different cross section sets when used for calculating absorption in fission product mixtures

4.1.1. The different cross section evaluations considered (status 1977)

For the calculation of absorption in fission product mixtures the following evaluated cross section sets were defined and used:

(1) The RCN-2A (recommended) set, containing 31 nuclides from the RCN-2A (adjusted) library |15|, two nuclides from the unadjusted RCN-2 library |24|, one nuclide (^{135}Cs) from the recent evaluation of CNEN/CEA |26|, seven nuclides from the Australian library |29|, and all other nuclides from ENDF/B-IV |22|.

(2) The RCN-2 (unadjusted) set: in this set the adjusted RCN-2 cross sections were replaced by their corresponding unadjusted values |24|.

(3) The ENDF/B-IV set: ENDF/B-IV cross sections |22| supplemented with cross sections of the Australian library |29| for 7 nuclides.

(4) The JNDC set: JENDL-1 cross sections for 28 nuclides |25,30|, supplemented with (3).

(5) The CNEN/CEA set: Cross sections from the joint CNEN/CEA evaluation for 50 nuclides |26|, supplemented with (3).

These sets of 26-group cross sections were calculated, using the cross section data files indicated, and the SNR-300 spectrum as a weighting function. In this way a direct comparison of the different evaluations is possible. In addition, in the comparison made below, also some other group cross section sets will be mentioned, namely the same as above, but as for status April 1976 |23,27| and some older evaluations available in 1973.

The RCN-2A set was derived from the RCN-2 set by adjusting the group cross sections of the individual nuclides such that an optimal fit to the integral experimental data from STEK |15| was obtained.

4.1.2. Calculation of pseudo fission product cross sections

With each of the five cross section sets mentioned in the previous section macroscopic cross sections were calculated for five mixtures of fission products generated by fissions of ^{235}U, ^{238}U, ^{239}Pu, ^{240}Pu and ^{241}Pu respectively.

The concentrations of the f.p. nuclides in the mixtures were obtained in burn-up calculations for SNR-300 (fundamental mode model), the fuel having obtained an irradiation of about 42 MWd/kg metal |23|; the sum of the concentrations of the nuclides in each mixture was normalized at a value of 2.0. The group cross sections thus obtained are so-called pseudo fission product cross sections, expressed in barn/fission.
As an example we have given in table 3 for the pseudo fission product of ^{239}Pu the 26-group capture cross sections as calculated with the five cross section sets. An intercomparison of the cross section evaluations commenting on differences in the group cross sections can be found in |28|.
The 26 group cross sections were collapsed into one group using an SNR-300 neutron spectrum (from |23|) and a second series using a 1000 MWe FBR spectrum (from |27|). See respectively tables 4-7.
The differences between tables 4 and 5 are mainly caused by the number of newly evaluated cross sections in the CNEN/CEA and RCN-2 sets.
In the CNEN/CEA set this increase from 22 to 50 led to a reduction of

about 1% in $\bar{\sigma}_c$, whereas in the RCN-2 set, which increased from 20 to 33 nuclides while some were revised, this led to an increase of 1½-2% in $\bar{\sigma}_c$. These two evaluations now seem to be quite near to each other. It is rather striking that the result of the ENDF/B-IV set is some 10% lower than those of the other evaluations. On closer examination it was found that of the 34 nuclides for which different evaluations are used in the recommended set and in ENDF/B-IV, there are only five which contribute significantly (more than 1%) to the difference between $\bar{\sigma}_c$ of the pseudo fission products:

Nuclide	Contribution to difference between recommended set and ENDF/B-IV	Comments
^{101}Ru	+ 1.8%	RCN-2A supported by STEK and FRO results
^{99}Tc	+ 1.5%	RCN-2A not in agreement with CFRMF and FRO
^{149}Sm	+ 2.0%	RCN-2A supported by STEK and FRO
^{107}Pd	+ 2.3%	Only STEK measurements available, these are not very accurate
^{135}Cs	+ 2.1%	No analysed measurements available. The CNEN/CEA evaluation is used in the recommended set
Total	+ 9.7%	

Each of the other 29 nuclides contributes less than 0.8% (positive or negative) to the total difference of 10%.

The Japanese set seems to be somewhat high for the ^{235}U pseudo fission product (about 3%).

In 1976 adjustment of capture cross sections of contributing nuclides, using experimental results from STEK, caused a reduction of 1.4 - 2.2% in $\bar{\sigma}_c$. In 1977, with a larger number of adjusted nuclides, this has been reduced to 0.3 - 0.8%. This change is partly due to small changes in the adopted adjustment procedure, i.e. slightly different flux and adjoint spectra, and no "implicit spectrum adjustment" (see ref.|15|). Not only for the nuclides most recently evaluated this revised adjustment procedure has been used, but also the nuclides that already had been analysed were processed again.

In general it has to be remarked that, although the adjustment may in-

fluence cross sections of individual nuclides appreciably (see e.g.|15|), their combined effect in a fission product mixture may be small because of a cancellation of corrections. However the accuracy of $\bar{\sigma}_c$ may still have been improved. Here, comparing the situations in 1976 and 1977, this is probably the case. One sees for example that most evaluations (ENDF/B-IV excepted) are now in better agreement with the values of $\bar{\sigma}_c$ given by RCN-2A of which the values contain more (integral) information.

Let us now consider table 6, the first part of which gives the situation in 1973, and has been taken from refs.|1,31|. The adjustment of the RCN-1 set at that time was done for the fission product mixture as a whole (not for individual nuclides). Use was made of reactivity effects measured in STEK of some samples containing gross mixtures of fission products (samples HFR-101, HFR-102, KFK, see ref.|31|). The resulting adjustments ranged from 1% to 8%. However, because of the fact that these experimental results were not very accurate, the adjustments were not considered as statistically significant. It is satisfying, however, that nevertheless these adjustments already reduced the average cross sections ($\bar{\sigma}_c$) in the direction of the values that are now considered as the most likely values (compare with table 4). In 1973 it was recognized that the UKNDL set |34| most probably gave too high values for $\bar{\sigma}_c$. The Australian set |29| still seems to be not bad for a fission product mixture: however, it is known that for individual nuclides the cross sections may be much different from most other evaluations. Compared with RCN-2A the Australian set gives a 8.2% too high value for the ^{235}U pseudo product, 6.4% too high for ^{238}U, 0.4% too high for ^{239}Pu, and 4.6% too low for the ^{241}Pu pseudo product. This "bandwidth" of about 13% (from +8.2% to -4.6%) is much wider than for the other - more recent - evaluations given in table 4, which also points to important discrepancies for individual fission product nuclides. It is known for example that the cross section of ^{101}Ru is probably about 100% too high, of ^{105}Pd about 40% too low, etc.

The set of Benzi et al. |35| gave reasonably good values, whereas the old Russian set for the ^{239}Pu fission product |36| was remarkably good. However, several of these old evaluations had their shortcomings, and when one compares with the situation in 1977 (table 4), one sees that much progress has been made.

The second part of table 6 was taken from ref. |27|, table 8 (the capture rate has been translated into $\overline{\sigma}_c$). It is based on the situation in July 1976, but the fission product concentrations used were the same as those in the first half of the table (these concentrations were published in 1974 |31|). However the resulting difference in $\overline{\sigma}_c$ will not be large when comparing with the 1976 concentrations |23|. For these cases the 26-group cross section sets were derived from the data files using a "1/E + fission" spectrum as weighting function. That is probably the reason why the values for "Cook" are about 1.5% higher than the values quoted some lines higher in the same table for "Cook", which are based on a 26-group set derived with an SNR-300 weighting function.
Comparing the ENDF/B-IV values of table 6 with those in table 4, a difference of 2 - 5% can be observed. It is not clear whether this is only caused by the differences in weighting function and the difference in burn-up (concentration). Comparing the JNDC values with those in table 4, a difference of 3 - 5% can be seen for the uranium pseudo products, but for the plutonium products it is only 0.6%. In both cases these differences of more than 2% are not easy to explain. One difference between these JNDC sets is that in the case of table 4 the 28 JENDL-1 nuclides have been supplemented with ENDF/B-IV, while in the case of table 6 these were supplemented with the Australian evaluation. However this probably will not explain the differences observed.
The preliminary Japanese evaluation JNDC-P |37| appears to give rather high values, which is caused by some shortcomings in the nuclear theory used (no width fluctuation correction factor was taken into account for example).

In table 7 the one-group cross sections for the case of a 1000 MWe FBR neutron spectrum are given (this spectrum was taken from |27|, table 2). Comparing with table 4 one sees that the values of $\overline{\sigma}_c$ are about 10% higher, but the relative differences between the evaluations remain the same.

4.2. Results of experiments and comparison with calculations

Central reactivity worths of a number of samples containing mixtures of fission product nuclides have been measured in the past in FRO |3,38| and in STEK |1,31|. Also comparisons with calculations (based on different cross section sets) were published. Since part of the analysis of the experimental results as presented in 1973 is obsolete now, and

also the neutron cross section sets have been renewed, it seemed worthwhile to review the results now again.

4.2.1. Measurement of a fission product mock-up sample in FRO

The sample was obtained from KFK, Karlsruhe |39| and simulates a fission product mixture at a burn-up of 23 MWd/kg metal in a steam-cooled fast reactor. The results of the reactivity measurements and a comparison with calculations were first reported in 1970 |38|. The cross sections used were those of a pair of fission products of ^{239}Pu as given in the Russian ABBN set |36|. The calculations turned out to give a much higher effect than the measurements in the different neutron spectra. In 1973 at the Bologna conference on fission products, in ref. |1|, table IX, a comparison was made with calculations using other cross section sets. The agreement was still rather bad. It was stated that a certain amount of moisture might be present in the sample, which would partly explain the discrepancies found in the five spectra.
In the meantime it has been found at STEK, where a similar sample has been measured, that this type of sample may contain an appreciable amount of moisture. However, even if one assumes an amount of 3 wt.% water in the sample, no satisfactory agreement can be found for all cores (for this investigation we made use of calculated values for the reactivity effect of water, as in the Swedish report |3| no experimental values are given): using RCN-2A cross sections the ratios of calculated over experimental values of the total reactivity effects of the sample (normalized on the reactivity effect of ^{235}U) for the cores 3 and 8 are then respectively 1.12 and 0.97, while for the two samples measured in core 5 one finds 0.74 and 0.86. It is also strange that these last two values are so much different.
In conclusion, it seems that these experimental data are not of very much use because not enough is known about the experimental conditions.

4.2.2. Measurement of gross mixtures of fission products in STEK

Three samples were measured in STEK and analysed |1|: the first two (HFR-101 and HFR-102) are samples produced mainly by thermal fission of ^{235}U. They were cut from MTR type fuel plates of the HFR (at Petten) at two locations having a burn-up of about 60% and 30% FIMA*). The

* Fissions per initial metal atom.

third sample (KFK) is an integral mock-up fission product sample prepared by R. Schröder |39|.

Results of the measurements and of comparison with calculations were reported in 1973 |1,31|.

Since 1973, however, a number of corrections had to be made in the measured reactivity worths, while also in the meantime the STEK spectra had been modified. Therefore in November 1976 a short summary of the re-evaluated results was given |23|.

At present the final STEK spectra have become available, while also the CNEN/CEA and RCN-2 cross section sets have been extended. So we will now again review the results. In table 8 the ratios of calculated over experimental values are given for different cross section sets.

Since 1973 the following two corrections have been made in the measured reactivity worths:

- A destructive analysis of the samples showed some contamination by moisture. A correction for the reactivity effect of this moisture had to be made. For the HFR-101 sample this correction was very small, for HFR-102 the experimental fission product capture effects had to be increased by several per cent, and for the KFK sample, which contained 1% of water, the correction was rather large, especially in the hard neutron spectra.
- The measured normalization factor ρ_o has been re-examined. It had to be increased by 0.6%.

Other factors affecting the comparison in table 8 between the results of 1973 and 1976 and the recent calculations are:

- For a number of nuclides (no fission products) in the KFK sample no cross sections were available in 1973. They could now be extracted from the RCN-2 and ENDF/B-IV libraries.
- In 1977 the STEK neutron spectra have been re-evaluated.
- Also the calculated normalization factor ρ_o has been re-evaluated.

These last two points, and the extension of some of the libraries since 1976, are the cause of the difference between table 8 and table 14 of ref.|23| of 1976.

Table 8 reveals that:

- The recent evaluations, except ENDF/B-IV, give a good prediction of the reactivity effects of HFR-101 and KFK samples.

- The agreement for HFR-102 is still rather bad, the discrepancy remains of the order of one or two standard deviations of the measurements.

It must be emphasized that the results presented in table 8 have to be considered as the present state of the art and cannot be considered as finally settled, for two reasons:

- Experiments are planned to obtain more accurate values for the uranium contents of the HFR samples.
- Flux distortion calculations have not been made for all samples in all STEK cores; in several cases corrections to the measured reactivity worths had to be made by extrapolation. More extensive calculations have to be performed.

Whatever the results of all these studies may be, it seems that the experimental information obtained with these integral samples is not (and will not be) accurate enough to bring about much further improvement of the recently evaluated fission product cross section sets. Only experimental results obtained with enriched isotopic fission product samples may lead to an improvement of the existing cross section sets.

5. SOME CONCLUSIONS

Since 1973 several improvements in the knowledge of fast integral capture data can be observed mainly due to an extensive analysis of the STEK reactivity worth measurements and of the inclusion of the CFRMF activation data.

The main sources of uncertainties remaining in the analysis of reactivity worth measurements of isotopic samples are:

- Limited knowledge of the fast scattering cross sections together with the limited knowledge of the fast neutron adjoint spectrum.
- Corrections to be made for impurities and admixtures, especially for water, unless special care is taken to remove the water.
- Non-negligible selfshielding effects and local flux disturbances even in hard spectra, especially for the larger samples.
- Limited knowledge of the neutron spectrum in the actual position where and when the measurements are made.

For measurements on irradiated fuel samples the corrections for the residual fuel (and other materials) constitute a main source of errors.

The interpretation of the CFRMF reactivity worth measurements is difficult because of the low sensitivity of this facility and the relatively large scattering contribution to the measured worths.
For activation measurements the flux levels in STEK and other zero power facilities are too low. CFRMF when operated in the 10 - 100 kW range can, and did already, provide very useful activation data. The main source of error in this case is the limited knowledge of the relevant decay data of the daughter product.
Transmutation requires power reactor flux levels as obtainable in EBR-II, RAPSODIE and PHENIX. No results of transmutation experiments in these reactors were available yet when this report was written.
The accuracy of the results of these experiments will depend on the purity of the samples and on the knowledge of the flux spectrum and the irradiation history.

From a comparison of the analysed integral data one can see that there is in general quite good agreement between the STEK data and the CFRMF activation data. However, for ^{99}Tc new integral measurements might be advisable. The curious discrepancy between STEK and CFRMF measurements for (the unimportant nuclide) ^{110}Pd may be due to unreliable decay data.

From comparison of adjusted integral data and integral quantities calculated from several fission product libraries it follows that for a number of nuclides the calculated values differ more than three standard deviations from the adjusted data. A more detailed discussion of these results is given in ref. |18|.

There are still quite a lot of STEK measurements to be analysed (for isotopes of Zr, Cd, Te, Xe, ^{135}Cs, Ce, Nd, Pm, Eu, Gd and Tb), so that a still larger part of the total fission product poisoning of a fast breeder will be covered by integral measurements. But in view of the limited accuracy of the experimental data |6| it is now already clear that further measurements would be advisable for the nuclides ^{93}Zr and ^{135}Cs. For the rather important nuclide ^{103}Ru no experimental data are available at all.
The uncertainty in the calculated fission product poisoning of a fast breeder could still further be reduced if more accurate neutron capture data would become available for several important nuclides, such as ^{105}Pd, ^{107}Pd, ^{149}Sm and ^{151}Sm.

One can observe that there is some lack of information on radioactive nuclides. Transmutation measurements may help to fill this gap.

In order to answer the question whether new *integral* measurements are needed for all the above mentioned nuclides, one should take into account the *differential* measurements being made or planned for these nuclides.

Systematic errors in series of measurements ultimately limit the accuracy with which the poisoning effect of mixtures of fission products can be predicted. The systematic error in the (comparison of calculated and) measured STEK data is about 5 to 7% |23|. There is still a need for comparison of measured and calculated data for standard materials in different facilities. ^{103}Rh may be a useful standard, although there is still some uncertainty in the capture cross section for the energy range 1 keV to about 10 keV. The combined use of STEK and CFRMF data in cross section adjustment calculations has been proved to be very useful. This combination of integral data from different sources should be extended (STEK, CFRMF, EBR-II, ERMINE, PHENIX, etc.).

Much effort has been devoted in the past to integral measurements with mixtures of fission products. Two of the three samples measured in STEK (the HFR-101 and KFK samples) now show good agreement between experimental values and theoretical values calculated with the recent evaluations RCN-2, RCN-2A, JENDL-1 and CNEN/CEA. The systematic difference between the measured values for HFR-101 and HFR-102 (which samples were obtained from the same fuel irradiated in the same reactor) must be due to inaccurate knowledge of the compositions of the samples (in particular HFR-102) and may be reduced in future after a more detailed destructive analysis of the samples.

As stated earlier, the usefulness of measurements with fission product mixtures heavily depends on the accuracy with which the compositions of the samples can be determined. Excluding the consideration that one wants to reduce the *combined* effect of cross section uncertainties and yield uncertainties in order to obtain a more accurate figure for the fission product poisoning in a particular reactor, there seems to be no need for further measurements with fission product mixtures.

ACKNOWLEDGEMENTS

The authors wish to thank Drs. Y.D. Harker, D.A. Millsap and J.W. Rogers for their contribution of unpublished CFRMF data.
Prof.Dr. V. Benzi and Dr. J.Y. Barré are acknowledged for their permission to use the CNEN/CEA fission product cross section library for the intercomparison of cross section data.
The information obtained during the past years from Dr. Y. Kikuchi and other members of the JNDC has been very fruitful in the writing of this paper.
In the discussions on the contents of this paper Dr. H. Gruppelaar made important contributions.
Many special computer calculations have been performed by B.P.J. van den Bos and H.Ch. Rieffe. Their skilful contribution is gratefully acknowledged.

REFERENCES

|1| Bustraan, M., "Integral determination of neutron absorption by fission products", Proceedings of a panel on fission product nuclear data organized by the IAEA, Bologna, November 26-30, 1973, vol. 2, p. 115.

|2| Rogers, J.W., Y.D. Harker, and D.A. Millsap, "The Coupled Fast Reactivity Measurement Facility (CFRMF)", IAEA Consultants Meeting on Integral Cross Section Measurement in Standard Neutron Fields for Reactor Dosimetry, Vienna, November 15-19, 1976.

|3| Anderson, T.L., Integral measurement of fission product reactivity worths in some fast reactor spectra, Aktiebolaget Atomenergi, AE-428 (1971).

|4| Bustraan, M. (comp.), Determination of effective cross sections of fission products for fast breeders in the fast-thermal coupled critical reactor STEK, RCN-150 (1971).

|5| Klippel, H.Th., and J. Smit, The Coupled Fast-Thermal Critical Facility STEK, RCN-209 (1974).

|6| Veenema, J.J., and A.J. Janssen, Small-sample reactivity worths of fission product isotopes and some other materials measured in STEK, ECN-10 (1976).

|7| Kiefhaber, E., The KFK-INR set of group constants, KFK-1572 (1972).

|8| Kiefhaber, E., Fine group calculations for reactivity coefficients of structural materials in fast reactors, KFK-1759 (1973).

|9| Lathrop, K.D., User's guide for the TWOTRAN program, LA-4058 (1969).

|10| Friesenhahn, S.J., The (n,α) cross sections of ^{6}Li and ^{10}B between 1 and 1500 keV, INTEL-RT-7011-001 (1974).

|11| Poenitz, W.P., and A.B. Smith, Proceedings of the NEANDC/NEACRP specialist meeting on fast neutron fission cross sections of ^{233}U, ^{235}U, ^{238}U and ^{239}Pu, Argonne National Laboratory, Argonne (Ill.), USA, June 1976.

|12| Gwin, R., E.G. Silver, R.W. Ingle, and H. Weaver, Measurement of the neutron capture and fission cross sections of ^{239}Pu and ^{235}U, 0.02 eV to 200 keV, the neutron capture cross sections of ^{197}Au, 10 to 50 keV, and the neutron fission cross sections of ^{233}U, 5 to 200 keV, Nucl. Sci. Eng. 59 (1976) 79.

|13| Dekker, J.W.M., J.B. Dragt, A.J. Janssen, R.J. Heijboer and H.Th. Klippel, Neutron spectra of STEK cores for reactivity calculations, ECN-report to be published.

|14| Karam, R.A., et al., Proceedings of the International Conference on Fast Critical Experiments and their Analysis, p. 403-420, ANL-7320 (1966).

|15| Dekker, J.W.M., Tables and figures of adjusted and unadjusted capture group cross sections based on the RCN-2 evaluation and integral measurements in STEK, vol. I, ECN-14 (1977); and recent data to be published.

|16| Rogers, J.W., D.A. Millsap, and Y.D. Harker, CFRMF Neutron Field Flux Spectral Characterization, Nuclear Technology 25 (1975) 330.

|17| Harker, Y.D., D.A. Millsap, and J.W. Rogers, private communication (1977).

|18| Gruppelaar, H., and J.W.M. Dekker, Impact of integral measurements on the capture cross section evaluations of individual fission product isotopes, ECN- (1977).

|19| Dragt, J.B., et al., Methods of adjustment and error evaluation of neutron capture cross sections; Application to fission product nuclides, Nucl. Sci. Eng. 62 (1977) 117.

|20| Dekker, J.W.M., and H.Ch. Rieffe, Adjusted capture cross sections of fission product nuclides from STEK reactivity worths and CFRMF activation data, ECN-report to be published.

|21| Harker, Y.D., and E.H. Turk, The use of CFRMF data in cross section evaluations, Proc. National topical meeting on new developments in reactor physics and shielding, Kiamesha Lake, Conf-720901 (Book 2), (1972) p. 614.

|22| National Neutron Cross Section Centre (Brookhaven), Evaluated Nuclear Data File B, version 4 (1974).

|23| Heijboer, R.J., and A.J. Janssen, Pseudo fission-product cross sections for a fast breeder reactor, ECN-11 (1976).

|24| Gruppelaar, H., Tables of RCN-2 fission-product cross section evaluation, Vol. 1 (24 nuclides), ECN-13 (1977); and recent data to be published.

|25| Iijima, S., et al., Evaluation of neutron cross section of 27 fission product nuclides important for fast reactor, J. of Nucl. Sci. and Techn. 14 (3), (1977) 161-176.

|26| Centro di Calcolo del CNEN (Bologna) and Commissariat à l'Energie Atomique CEA (Saclay and Cadarache), Fission product library for 50 isotopes, unpublished (1977).

|27| Kikuchi, Y., et al., Fission product fast reactor constants system of JNDC, JAERI-1248 (1976).

|28| Gruppelaar, H., A.J. Janssen, and J.W.M. Dekker, Intercomparison of recent evaluations for the capture cross sections of some fission-product nuclides, ECN-12 (1976).

|29| Rose, E.K., The AAEC fission product cross section libraries FISPROD.POINTXSL and FISPROD.GROUPXSL, AAEC/TM-587 (1971).

|30| Igarasi, S., et al., Proc. of a Conf. on Nuclear cross sections and Technology, Washington DC, 1975, NBS-SP425, vol. 1, p. 320 (1975). (Data of the JNDC evaluation available at NEA data centre, Saclay).

|31| Gruppelaar, H. (comp.), RCN-1 pseudo fission product capture group cross sections, RCN-205 (1974).

|32| Dragt, J.B., and H. Gruppelaar, Error analysis of neutron capture group cross sections for fast reactors, applied to fission products, RCN-192 (1973).

|33| Lautenbach, G., Calculated neutron absorption cross sections of 75 fission products, RCN-191 (1973).

|34| Norton, D.S., The UKAEA nuclear data library, February 1968, AAEW-M824 (1968).

|35| Benzi, V., R. d'Orazi, G. Reffo, and M. Vaccari, Fast neutron radiative capture cross sections of stable nuclei with $29 \leq A \leq 79$, CNEN-report RT/FI(72) 6 (1972).

|36| Abagyan, L.P., et al., Group constants for nuclear reactor calculations, New York, Consultants Bureau (1964).

|37| Kikuchi, Y., et al., JNDC fission product group constants - preliminary version -, JAERI-M6001 (1975).

|38| Anderson, T.L., Integral measurements of fission product reactivity worths in some fast reactor spectra, Proc. IAEA Conf. on Nuclear Data for Reactors, Helsinki, 1970, paper CN-26/51.

|39| Schröder, R., Zur Simulation von Spaltprodukten in schnellen kritischen Anordnungen, Nukleonik 10 (1967) 1, 18-27.

|40| Gunst, S.B., J.C. Connor and D.E. Conway, Measured and calculated fission-product poisoning in neutron-irradiated uranium-233, Nucl. Sci. and Eng. 58 (1975) 387.

|41| Hellstrand, E., private communication (1973).

Table 1. Integral determination of neutron capture cross sections relative to calculated values derived from ENDF/B-IV |22| for a number of fission-product nuclides.

nuclide	STEK [a] 4000	3000	2000	1000	500	CFRMF [b] meas.	adjusted	FRO [c] core 5	core 8	core 3
Zr 40090										
40091										
40092										
40093										
40094										
40096										
Nb 41093	1.00 (03)	1.00 (04)	1.00 (04)	1.00 (05)	1.01 (06)	*1.53 (77)	1.02 (08)			
Mo 42094	1.44 (18)	1.45 (20)	1.46 (21)	1.48 (24)	1.50 (30)					
42095	1.07 (06)	1.05 (05)	1.02 (05)	.98 (06)	.95 (08)			.95 (05)	1.02 (05)	.91 (06)
42096	1.23 (15)	1.22 (15)	1.21 (14)	1.17 (15)	1.07 (27)					
42097	1.16 (04)	1.15 (05)	1.15 (06)	1.13 (07)	1.10 (10)			.99 (01)	1.04 (07)	.99 (06)
42098	.91 (03)	.91 (03)	.90 (04)	.87 (05)	.82 (08)	*.95 (10)	.92 (09)			
42100	1.06 (07)	1.06 (08)	1.06 (10)	1.05 (13)	1.02 (21)	*.75 (07)	.89 (08)			
Tc 43099	1.12 (04)	1.19 (04)	1.23 (05)	1.25 (07)	1.31 (09)	*1.03 (11)	1.10 (10)	1.00 (05)	1.01 (13)	.98 (17)
Ru 44101	1.30 (05)	1.41 (06)	1.44 (07)	1.40 (08)	1.27 (10)			1.43 (06)	1.37 (11)	1.07 (12)
44102	.89 (10)	.88 (10)	.87 (11)	.86 (11)	.82 (14)	*.71 (06)	.75 (06)	1.22 (18)	.84 (18)	.80 (18)
44104	1.00 (09)	1.00 (10)	1.00 (10)	1.00 (12)	1.00 (17)	*.95 (06)	.99 (07)	1.19 (21)	.81 (38)	1.33 (44)
Rh 45103	1.06 (05)	.98 (04)	.95 (04)	.92 (05)	.91 (06)	*.94 (23)	.91 (07)	1.78 (05)	1.02 (03)	.97 (05)
Pd 46104	.94 (16)	.90 (15)	.87 (13)	.81 (12)	.74 (16)					
46105	1.18 (05)	1.16 (05)	1.14 (05)	1.09 (06)	1.04 (07)					
46106	1.41 (11)	1.40 (12)	1.40 (13)	1.38 (13)	1.35 (17)					
46107	1.74 (14)	1.67 (08)	1.66 (08)	1.67 (11)	1.63 (17)					
46108	.88 (07)	.90 (08)	.92 (09)	.97 (11)	1.02 (19)	*.92 (23)	.93 (21)			
46110	1.46 (67)	1.05 (47)	.85 (34)	.67 (27)	.68 (41)	*.06 (01)	.60 (20)			
Ag 47107						*1.08 (16)	1.02 (10)			
47109	1.01 (02)	1.11 (03)	1.19 (04)	1.32 (05)	1.49 (10)	*1.78 (12)	1.63 (13)			
Cd 48111										

Table 1 (continued).

nuclide	STEK [a] 4000	3000	2000	1000	500	CFRMF [b] meas.	adjusted	FRO [c] core 5	core 8	core 3
In 49115						.94 (07)				
Sb 51121						.90 (06)				
51123						.92 (08)				
Te 52128										
52130										
I 53127	.97 (03)	.97 (03)	.98 (04)	1.02 (06)	1.06 (08)	*.86 (16)	.94 (10)			
53129	.85 (07)	.85 (07)	.84 (07)	.82 (08)	.79 (09)	*.78 (07)	.80 (07)			
Xe 54131										
54132						.85 (06)				
54134						.61 (04)				
Cs 55133	1.14 (05)	1.16 (05)	1.15 (05)	1.12 (06)	1.06 (08)	*.93 (06)	.96 (06)	1.07 (06)	.74 (06)	.56 (06)
55135										
55137										
La 57139	1.02 (06)	1.02 (06)	1.01 (06)	.99 (09)	.95 (11)	*.80 (05)	.81 (05)			
Ce 58140						.06 (01)				
58142						.74 (08)				
Pr 59141	.87 (06)	.86 (06)	.84 (06)	.81 (06)	.75 (06)	*.80 (08)	.81 (07)			
Nd 60142										
60143										
60144										
60145										
60146						.72 (10)				
60148						.66 (06)				
60150						.66 (14)				
Pm 61147						1.01 (12)		.71 (03)	.78 (11)	.56 (16)

Table 1 (continued).

nuclide	STEK [a] 4000	3000	2000	1000	500	CFRMF [b] meas.	adjusted	FRO [c] core 5	core 8	core 3
Sm 62147	1.13 (06)	1.22 (08)	1.30 (09)	1.43 (11)	1.50 (13)					
62148	1.34 (18)	1.17 (13)	1.05 (11)	.88 (10)	.76 (11)					
62149	1.34 (05)	1.58 (08)	1.64 (10)	1.63 (11)	1.61 (14)			1.85 (05)	1.52 (16)	1.42 (22)
62150	1.01 (12)	1.05 (10)	1.09 (08)	1.16 (09)	1.24 (11)					
62151	.91 (06)	.85 (09)	.82 (11)	.80 (12)	.79 (11)					
62152	1.14 (07)	1.16 (08)	1.18 (08)	1.19 (08)	1.18 (10)	.97 (05)				
62154	1.05 (13)	1.05 (12)	1.05 (11)	1.05 (10)	1.05 (15)	.75 (03)				
Eu 63151						1.15 (07)				
63153						1.07 (08)				
Gd 64156										
64157										
64158						.98 (12)				
64160						.64 (05)				
Tb 65159										

The numerators of the ratios given in this table are:

a) STEK : *Adjusted renormalized infinite dilution reactivity worths* $\int \sigma_c$ (RCN-2A) $\phi\phi^+ dE / \int \phi\phi^+ dE$ from |15|. Data are given only for those nuclides which were fully analysed at the time of writing this report.

b) CFRMF: *Experimental reaction rate ratios* $\int \sigma_c \phi dE / \int \sigma_f$ (^{235}U) ϕdE; revised data have been used |17| instead of older values |21|. Entries marked by an asterisk are corrected for selfshielding (see |20|). *Adjusted reaction rates* were obtained from measured reaction rates and the RCN-2 cross section set.

c) FRO : *Experimental reactivity worths* ρ_c corrected for selfshielding and scattering as given in |3| and normalized to ρ_{tot} (^{235}U).

The denominators of the ratios are the calculated quantities corresponding with the numerators. Capture cross sections for f.p. nuclides were taken from ENDF/B-IV. In case of FRO shielded σ_f(^{235}U) of |41| have been used. In case of CFRMF σ_f (^{235}U) have been taken from ENDF/B-IV.
Absolute errors in the last two digits are given in parenthesis.
Errors are only due to uncertainties in the numerators of the ratios given in the table.

Table 2. Average capture cross sections in SNR-300 [23] from various nuclear data libraries compared with ENDF/B-IV.

nuclide	$y*\bar{\sigma}_c$	$\bar{\sigma}_c$ ENDF/B-IV ref.[22]	$\bar{\sigma}_c$ divided by $\bar{\sigma}_c$ (ENDF/B-IV) RCN-2 [24]	RCN-2A [15]	JENDL-1 [25]	CNEN/CEA [26]
40090	.0000	.0231	0.00	0.00	.62	0.00
40091	.0014	.0838	0.00	0.00	.92	.84
40092	.0012	.0404	0.00	0.00	.95	.87
40093	.0033	.0861	0.00	0.00	1.91	1.30
40094	.0010	.0228	0.00	0.00	1.05	1.07
40096	.0019	.0381	0.00	0.00	1.36	.94
41093	0.0000	.2130	1.00 (08)	1.02 (07)	1.10	0.00
42094	0.0000	.0479	1.66 (60)	1.54 (33)	0.00	0.00
42095	.0062	.2933	1.02 (18)	.95 (08)	1.01	.93
42096	.0000	.0591	1.43 (62)	1.07 (29)	0.00	0.00
42097	.0143	.2751	1.10 (19)	1.10 (10)	1.13	1.01
42098	.0057	.1013	.84 (07)	.83 (07)	0.00	1.03
42100	.0050	.0781	1.29 (35)	1.03 (21)	0.00	1.05
43099	.0267	.4850	1.11 (18)	1.32 (09)	1.12	1.12
44101	.0340	.5324	1.29 (21)	1.27 (10)	1.33	1.42
44102	.0128	.1874	1.07 (39)	.82 (15)	1.19	1.18
44104	.0090	.1381	1.26 (37)	1.01 (17)	1.15	1.32
45103	.0336	.6977	.91 (08)	.92 (06)	.93	.90
46104	.0003	.2662	.70 (43)	.75 (16)	.94	1.10
46105	.0401	.8296	.98 (15)	1.06 (07)	.91	1.02
46106	.0017	.1570	1.20 (73)	1.38 (17)	0.00	1.23
46107	.0174	.5658	1.69 (92)	1.65 (17)	1.32	1.40
46108	.0038	.1587	1.15 (96)	1.05 (20)	0.00	1.25
46110	.0013	.1453	1.18 (103)	.63 (38)	.70	.69
47107	0.0000	.6968	.87 (08)	0.00	.88	0.00
47109	.0078	.4789	1.42 (17)	1.49 (10)	1.70	1.35
48111	.0017	.4072	0.00	0.00	0.00	0.00
49115	.0004	.4415	0.00	0.00	0.00	0.00
51121	.0003	.4750	0.00	0.00	0.00	0.00
51123	.0001	.2640	0.00	0.00	0.00	0.00
52128	.0008	.0953	0.00	0.00	.37	0.00
52130	.0003	.0158	0.00	0.00	.85	0.00
53127	.0024	.5384	.96 (09)	1.05 (07)	1.02	0.00
53129	.0034	.3793	.88 (22)	.80 (06)	1.15	0.00
54131	.0087	.2090	0.00	0.00	1.78	0.00
54132	.0362	.0687	0.00	0.00	0.00	0.00
54134	.0025	.0347	0.00	0.00	0.00	0.00

Table 2 (continued).

nuclide	$y*\bar{\sigma}_c$	$\bar{\sigma}_c$ ENDF/B-IV ref.|22|	$\bar{\sigma}_c$ divided by $\bar{\sigma}_c$ (ENDF/B-IV) RCN-2 |24|	RCN-2A |15|	JENDL-1 |25|	CNEN/CEA |26|
55133	.0308	.4778	1.06(12)	1.08(08)	.95	1.03
55135	.0050	.0670	0.00	0.00	4.04	3.09
55137	.0009	.0145	0.00	0.00	1.49	0.00
57139	.0023	.0381	.82(13)	.92(11)	.95	.74
58140	.0009	.0179	0.00	0.00	1.64	.56
58142	.0017	.0340	0.00	0.00	1.57	1.22
59141	.0071	.1547	.82(10)	.78(06)	.77	.82
60142	.0000	.0402	0.00	0.00	0.00	0.00
60143	.0119	.2997	0.00	0.00	.95	1.12
60144	.0008	.0933	0.00	0.00	.96	.97
60145	.0103	.3308	0.00	0.00	1.03	1.10
60146	.0032	.1263	0.00	0.00	.66	.56
60148	.0031	.1808	0.00	0.00	.98	.86
60150	.0023	.2195	0.00	0.00	.80	.94
61147	.0209	1.2539	0.00	0.00	.86	.86
62147	.0011	.7945	1.66(32)	1.51(14)	1.50	0.00
62148	.0003	.3349	.81(33)	.78(11)	1.01	0.00
62149	.0179	1.4144	1.59(23)	1.56(13)	1.41	1.25
62150	.0004	.3957	1.02(17)	1.26(12)	1.22	0.00
62151	.0168	2.2071	.97(08)	.81(11)	.94	.95
62152	.0030	.3965	1.04(13)	1.18(10)	1.13	0.00
62154	.0007	.2067	1.02(20)	1.09(15)	1.06	0.00
63151	.0001	3.6259	0.00	0.00	.91	0.00
63153	.0106	2.2926	0.00	0.00	1.06	1.08
64156	.0007	.4407	0.00	0.00	1.70	1.22
64157	.0033	3.5413	0.00	0.00	.45	.32
64158	.0002	.2791	0.00	0.00	0.00	0.00
64160	.0001	.1998	0.00	0.00	0.00	0.00
65159	.0006	1.3946	0.00	0.00	0.00	1.10

y = normalized concentrations in a ^{239}Pu pseudo fission product, burn-up 42 MWd/kg, see |23|.

$\bar{\sigma}_c$ = average capture cross section $\int \sigma_c \phi_{SNR} dE / \int \phi_{SNR} dE$ (in barn).

Errors: see footnote table 1.

Table 3. Capture group cross sections of the pseudo fission product of ^{239}Pu at a burn-up of 42 MWd/kg (see section 4.1.2).

group number	Evaluation (status May 1977, see section 4.1.1)				
	RCN-2A	RCN-2	ENDF/B-IV	JENDL-1	CNEN/CEA
1	0.004	0.004	0.006	0.004	0.006
2	0.015	0.017	0.016	0.017	0.020
3	0.039	0.042	0.041	0.047	0.043
4	0.065	0.068	0.068	0.081	0.065
5	0.089	0.092	0.088	0.104	0.082
6	0.119	0.122	0.108	0.130	0.117
7	0.178	0.181	0.156	0.184	0.180
8	0.254	0.256	0.227	0.256	0.257
9	0.383	0.386	0.346	0.384	0.382
10	0.590	0.593	0.541	0.595	0.599
11	0.878	0.887	0.821	0.889	0.899
12	1.307	1.320	1.218	1.314	1.324
13	1.925	1.922	1.752	1.935	1.925
14	3.000	2.966	2.643	2.995	3.002
15	4.582	4.573	4.040	4.635	4.579
16	9.60	9.58	7.65	8.89	9.13
17	12.64	12.80	10.56	12.22	12.82
18	18.81	18.12	17.25	18.72	19.70
19	32.93	32.54	31.70	35.61	36.44
20	53.17	53.57	54.16	53.38	55.56
21	109.07	107.40	111.92	106.54	110.55
22	23.88	24.76	21.30	27.25	30.04
23	59.34	57.77	51.91	54.97	53.60
24	107.22	107.34	95.34	95.34	103.16
25	52.83	54.32	55.71	60.56	61.06
26	1093	1113	1119	1136	1113

Table 4. Pseudo fission product one-group capture cross sections $\bar{\sigma}_c$ (in barn/fission) for 5 fissionable nuclides in the spectrum of SNR-300 (within parentheses the value relative to RCN-2A). Cross section sets status May 1977.

Cross section set (status May 1977) *)	Pseudo fission product of				
	^{235}U	^{238}U	^{239}Pu	^{240}Pu	^{241}Pu
RCN-2A	0.365 (1.0)	0.453 (1.0)	0.498 (1.0)	0.511 (1.0)	0.528 (1.0)
RCN-2	0.366 (1.003)	0.456 (1.007)	0.501 (1.006)	0.514 (1.006)	0.532 (1.008)
ENDF/B-IV	0.335 (0.918)	0.415 (0.916)	0.450 (0.904)	0.459 (0.898)	0.473 (0.896)
JNDC	0.375 (1.027)	0.459 (1.013)	0.503 (1.010)	0.512 (1.002)	0.527 (0.998)
CNEN/CEA	0.367 (1.005)	0.455 (1.004)	0.500 (1.004)	0.510 (0.998)	0.525 (0.994)

*) Cross section sets as described in section 4.1.1.

Table 5. Pseudo fission product one-group capture cross sections $\bar{\sigma}_c$ (in barn/fission) for 5 fissionable nuclides in the spectrum of SNR-300 (within parentheses the value relative to RCN-2A). Cross section sets status April 1976, see ref. |23|.

Cross section set (status April 1976) *)	Pseudo fission product of				
	^{235}U	^{238}U	^{239}Pu	^{240}Pu	^{241}Pu
RCN-2A	0.355 (1.0)	0.439 (1.0)	0.483 (1.0)	0.495 (1.0)	0.512 (1.0)
RCN-2	0.360 (1.014)	0.447 (1.018)	0.493 (1.021)	0.506 (1.022)	0.522 (1.020)
ENDF/B-IV	0.335 (0.944)	0.415 (0.945)	0.450 (0.932)	0.459 (0.927)	0.474 (0.926)
JNDC	0.377 (1.062)	0.460 (1.048)	0.504 (1.043)	0.513 (1.036)	0.529 (1.033)
CNEN/CEA	0.371 (1.045)	0.461 (1.050)	0.506 (1.048)	0.517 (1.044)	0.533 (1.041)

*) In the status 1976 the RCN-2 and CNEN/CEA sets contained a smaller number of nuclides of own evaluation, namely RCN-2 (and RCN-2A): 19 nuclides RCN-2 adjusted, one unadjusted, 3 nuclides from CNEN/CEA, rest ENDF/B-IV and Australian.
CNEN/CEA: 22 nuclides of own evaluation (against 50 in 1977).
In ENDF/B-IV and JNDC some small errors were not yet corrected (giving some difference with the figures of 1977).

Table 6. Pseudo fission product one-group capture cross sections $\bar{\sigma}_c$ (in barn/fission) for 4 fissionable nuclides in the spectrum of SNR-300 (within parentheses the value relative to RCN-1A). First part of table : cross section sets available in 1973 |1,31|. Second part of table: cross section sets available in 1976, from Japanese ref. |27|.

Cross section set (situation 1973)	Pseudo fission product of *)				
	^{235}U	^{238}U	^{239}Pu	^{240}Pu	^{241}Pu
RCN-1A |31,32|	0.393 (1.0)	0.478 (1.0)	0.510 (1.0)	-	0.534 (1.0)
RCN-1 |33|	0.397 (1.010)	0.492 (1.029)	0.532 (1.043)	-	0.575 (1.077)
UKNDL |34|	0.421 (1.071)	0.538 (1.126)	0.585 (1.147)	-	0.619 (1.159)
Austr. (Cook)|29|	0.395 (1.005)	0.482 (1.008)	0.500 (0.980)		0.504 (0.944)
Benzi et al. |35|	0.393 (1.000)	0.490 (1.025)	0.520 (1.020)	-	0.546 (1.022)
Russian(ABBN) **) |36|	0.443 (1.127)	-	0.534 (1.047)	-	-
Cross section set **) (situation July 1976, figures from Japanese report |27|, table 8)					
JNDC	0.387 (0.985)	0.480 (1.004)	0.506 (0.992)	-	0.530 (0.993)
JNDC-P	0.486 (1.237)	0.587 (1.228)	0.625 (1.225)	-	0.654 (1.225)
Cook	0.401 (1.020)	0.490 (1.025)	0.506 (0.992)	-	0.510 (0.955)
ENDF/B-IV	0.348 (0.886)	0.435 (0.910)	0.461 (0.904)	-	0.484 (0.906)

*) In this table the pseudo products correspond to a burn-up of about 50 MWd/kg metal. The difference in $\bar{\sigma}_c$ compared with 42 MWd/kg, however, is of the order of only 0.2% for the RCN-2 set.

**) The 26-group cross sections of these sets were derived using a $\frac{1}{E}$ spectrum below 1 MeV and a fission spectrum above 1 MeV. This is in contrast with the sets in the first half of the table, and the sets in the other tables (4, 5, 7) which were based on a SNR-300 spectrum to obtain the 26 group cross sections.

Table 7. Pseudo fission product one-group capture cross sections $\bar{\sigma}_c$ (in barn/fission) for 5 fissionable nuclides in the spectrum of a 1000 MWe FBR |27| (within parentheses the value relative to RCN-2A).
Cross section sets status May 1977.

Cross section set (status May 1977)	Pseudo fission product of				
	^{235}U	^{238}U	^{239}Pu	^{240}Pu	^{241}Pu
RCN-2A	0.406 (1.0)	0.502 (1.0)	0.550 (1.0)	0.566 (1.0)	0.584 (1.0)
RCN-2	0.407 (1.002)	0.505 (1.006)	0.553 (1.006)	0.569 (1.005)	0.588 (1.007)
ENDF/B-IV	0.370 (0.911)	0.458 (0.912)	0.494 (0.898)	0.505 (0.892)	0.522 (0.894)
JNDC	0.415 (1.022)	0.507 (1.010)	0.554 (1.007)	0.564 (0.996)	0.582 (0.997)
CNEN/CEA	0.408 (1.005)	0.505 (1.006)	0.553 (1.005)	0.563 (0.995)	0.581 (0.995)

Table 8. Calculated to Experimental ratio (C/E) of normalized capture reactivity effects of integral samples in STEK.

STEK core	integral sample	1) RCN-1 1973	calculations with various cross section evaluations (situation in May 1977) 2)					3) experimental error (%)
			ENDF/B-IV	JENDL-1	CNEN/CEA	RCN-2	RCN-2A	
4000	HFR-101	.94	.94	.98	1.00	.99	1.00	3.5
	HFR-102	.88	.87	.91	.92	.92	.93	6.0
	KFK	1.08	.93	.98	.99	1.00	1.01	2.6
3000	HFR-101	.90	.91	.97	.96	.96	.97	5.1
	HFR-102	.83	.82	.87	.86	.87	.88	8.4
	KFK	1.06	.94	1.00	1.00	1.02	1.02	1.0
2000	HFR-101	.88	.92	.99	.97	.97	.99	6.1
	HFR-102	.76	.76	.82	.80	.81	.82	9.3
	KFK	1.04	.94	1.00	.99	1.01	1.02	1.5
1000	HFR-101	.91	.92	.99	.95	.96	.97	8.2
	HFR-102	.81	.75	.81	.78	.79	.80	14.6
	KFK	1.14	.91	.97	.94	.97	.97	1.6
500	HFR-101		1.01	1.08	.99	1.03	1.04	8.7
	HFR-102		.74	.80	.74	.77	.77	16.1
	KFK		.99	1.05	.99	1.03	1.02	6.5

1) Results as reported in 1973 [31]; calculation with RCN-1 cross sections.

2) See section 4.1.1. for a description of these libraries.

3) These comprise the statistical errors in the reactivity measurements as well as the uncertainties in the compositions of the samples.

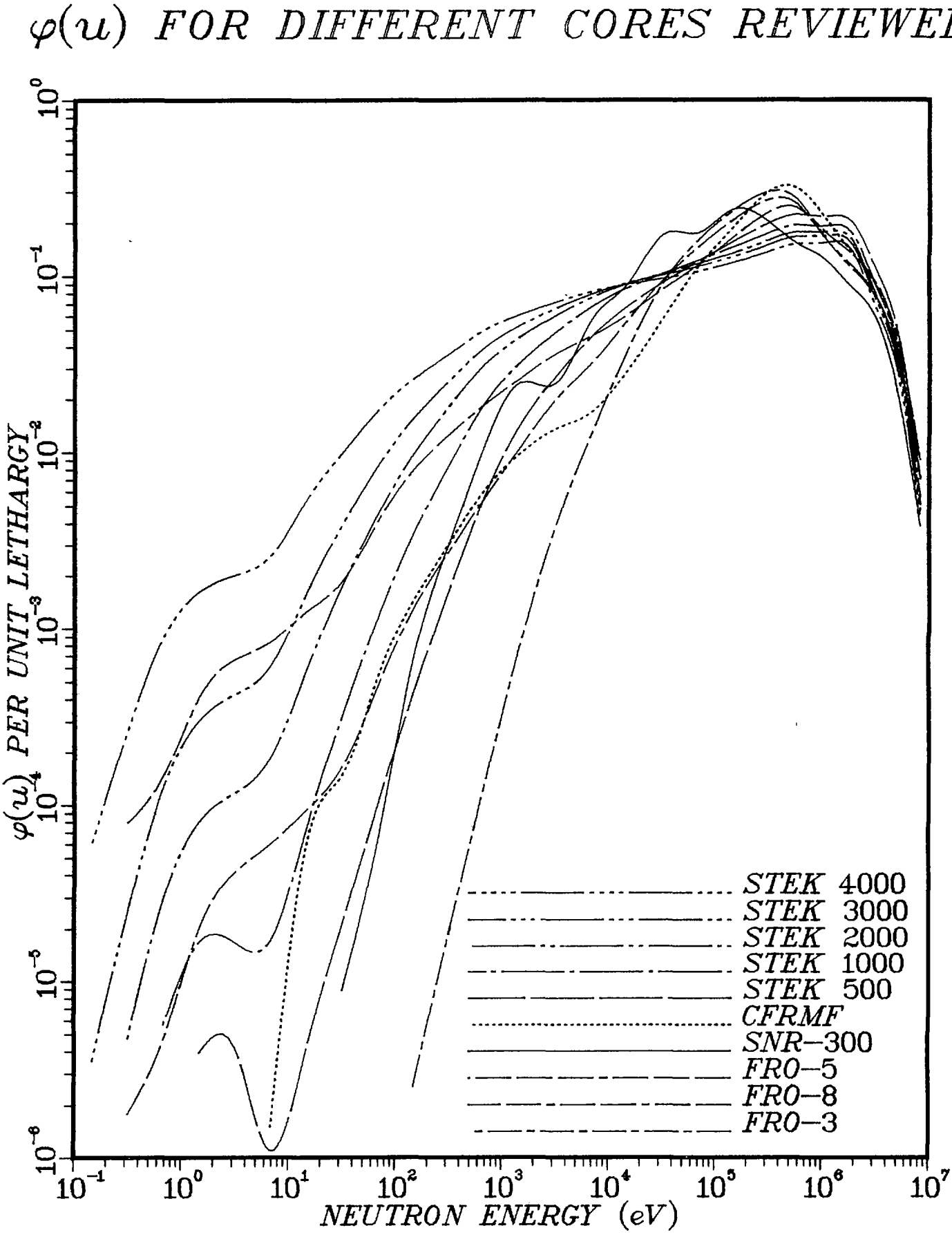

Fig. 1 Comparison of neutron flux spectra in several reactor cores

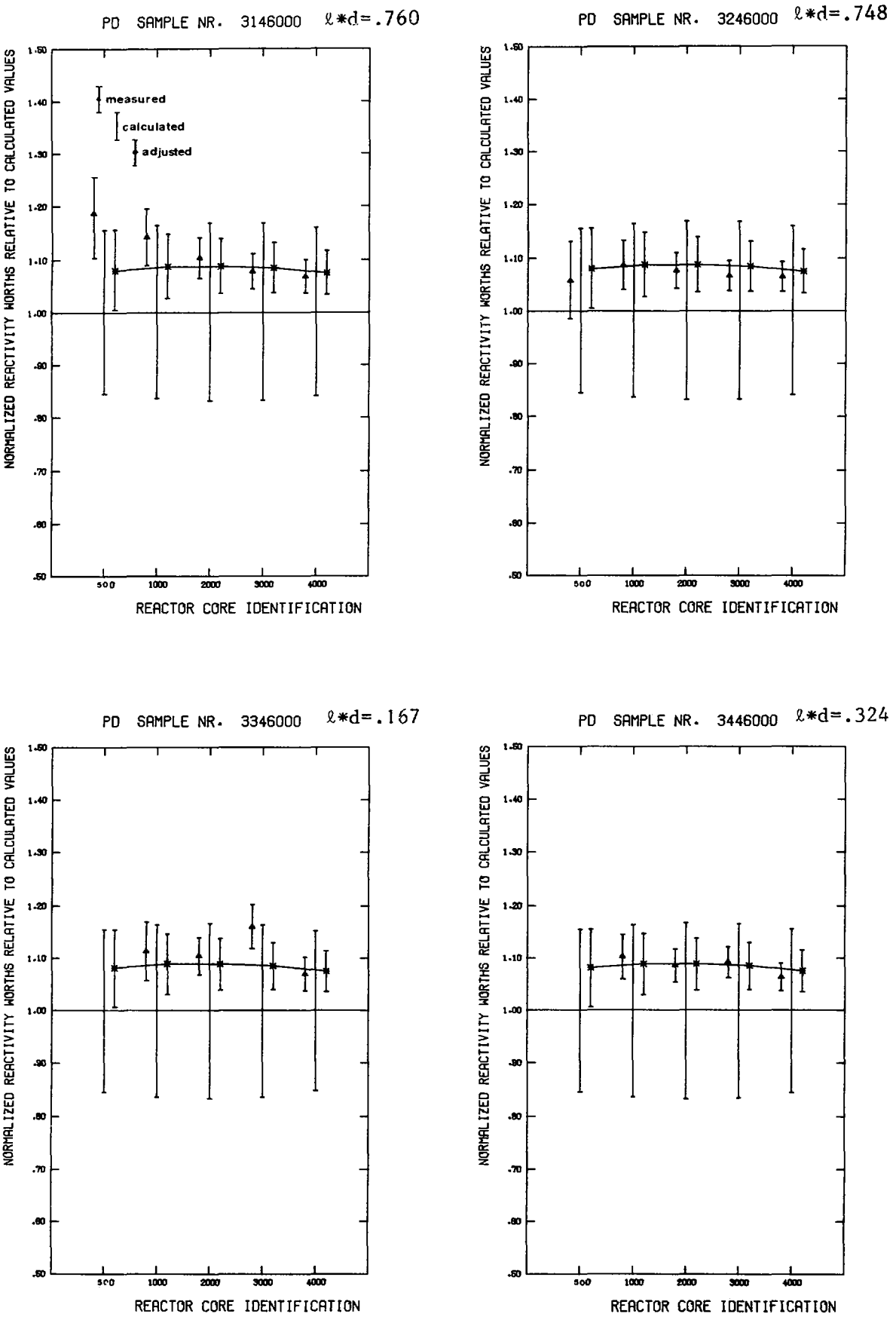

Fig. 2 Reactivity worths of samples with main component ^{105}Pd (93 at $^{0}/_{0}$), measured in STEK, compared with calculations; ℓ *d is the product of mean chord length and density of the samples (in g/cm^2).

Review paper 15

INTEGRAL DETERMINATION OF FISSION PRODUCT INVENTORY AND DECAY POWER

Reviewed by

R. E. Schenter
F. Schmittroth

Hanford Engineering Development Laboratory
Richland, Washington, U.S.A.

T. R. England

Los Alamos Scientific Laboratory
Los Alamos, New Mexico, U.S.A.

Abstract:

Results from nine recent integral decay heat experiments are presented and compared with summation calculations made with several fission product data libraries. Significant improvement has resulted in the agreement between experiments and the comparisons to calculations since last reviewed at the Bologna meeting. Comparisons with experiments are also given for β and γ spectra calculations applying the summation method and using the ENDF-IV decay data library. Generalized least-squares methods are applied to the recent decay-heat experiments and summation calculations to arrive at evaluated values and uncertainties. Results for thermal fission of ^{235}U imply uncertainties less than 2% (1σ) for the "infinite" exposure case for all cooling time greater than 10 seconds. In addition, related topics such as gas content in fission products, absorption effects on decay heating, absorption buildup in reactors, photoneutron spectra, summation calculation uncertainties and analytical representations of decay power are reviewed.

TABLE OF CONTENTS

1. INTRODUCTION - SUMMARY

Extensive progress has been made since the Bologna meeting in both experimental and calculational integral decay power determinations. Since 1973 we have been aware of ten different laboratories completing measurements of fission product decay heat (decay power) following thermal fission of ^{235}U. These experiments were very carefully performed and several of them can be used as "benchmarks" to test the calculational methods to compute decay heat. On the calculational side extensive fission product data libraries have recently been developed in England, France, Japan, Sweden, and the United States which are used to calculate decay heat using the summation method. In addition, several groups have studied and published uncertainty analyses of the summation calculations and least-squares techniques. These methods have been developed and applied to combining experimental and calculational results. As a consequence of this, important advances have been made towards solving the problem of accurately determining the fission-product source terms during operation and following shutdown of power reactors. A particularly important example of this is determining the decay heat following a "loss of coolant" accident situation. Figures 1 and 2 illustrate this point where in Figure 1 decay heat curves corresponding to "infinite irradiation" on ^{235}U are given for the ANS 5.1 Standard, the ANS 5.1 augmented by 20%, ENDF/B-IV summation results and the nominal curve resulting from a least-squares analysis combining four experiments and ENDF/B-IV calculations (Figure 2). The uncertainty associated with the nominal curve has been found to be less than 2% (1σ) for cooling times greater than 10 seconds. Hence the "ANS 5.1 + 20" curve, which is the required curve for U.S. thermal reactor design, is extremely conservative ($\sim 10\sigma$).

Tables I and II summarize the total decay heat determinations for ^{235}U covered in this review for the "Infinite" and "Burst" irradiation cases. There the percent deviation from the least-squares result are given for both calculations and experiments extended and unfolded to infinite and zero cooling times, respectively. Individual β and γ power and spectra experiments and calculations are also considered in this review. Figures 3-5 show typical comparisons of spectra results for experiments at LASL, ORNL, and UI to calculations using ENDF/B-IV. In addition, related topics (see Table of Contents) such as gas content in fission products, absorption effects on decay heating, absorption build-up in reactors, photoneutron spectra and analytical representations of decay power are reviewed.

Table I

% Difference From Nominal Decay Heat For

"Infinite Irradiation" - ^{235}U

	Experiments				Summation Calculations			
t_c(s)	LASL	IRT	ORNL	F-a-R	ENDF/B-IV	FISP	PEPIN	FP-S
20	+0.7	-2.2	-5.4	-	-0.4	+3.8	-	-
10^2	+0.6	-1.7	-4.7	-1.8	-0.2	+4.5	+0.6	+4.4
10^3	+0.1	-1.9	-3.0	+0.0	-0.2	-0.9	-2.1	+0.0
10^4	+0.4	-1.4	+0.3	-0.4	+0.3	+0.6	-0.9	+0.6

Table II

% Difference From Nominal Decay Heat For

"Burst Irradiation" - ^{235}U

	Experiments - Unfolded				Summation Calculations				
t_c(s)	LASL	IRT	ORNL	F-a-R	ENDF/B-IV	FISP	PEPIN	FP-S	NAIG
20	-	-2.7	-7.3	-	-4.9	- 8.1	-	-14.7	-7.6
10^2	+0.3	-1.6	-6.4	-14.5	+1.8	+12.0	+2.9	+ 1.1	+4.4
10^3	+0.2	+0.1	-7.5	+ 0.5	-6.4	- 1.8	-4.8	- 4.4	-4.5
10^4	-1.3	-4.0	+0.2	+ 3.3	+2.4	+ 0.5	-2.1	- 1.5	-

2. DECAY HEAT EXPERIMENTS

A number of benchmark experiments have recently (1973-1977) been completed which measure total, beta and/or gamma decay-energy release from fission products for thermal and fast fission in ^{235}U. Similar experiments for fission in ^{239}Pu and ^{233}U are underway. Table III summarizes these eleven recent experiments and Section 2.1 gives a more detailed description of the individual measurements. Results compared to ENDF/B-IV summation calculations for nine of the experiments are given in Section 2.2. Appendix A1 provides tables of values and additional figures with comparisons to calculations for these experiments.

2.1. Experiment Descriptions

2.1.1. Yarnell and Bendt (1977) [2] used a liquid-helium boil-off calorimeter with a 1-s time constant to measure ^{235}U fission product decay heat at times between 10 and 10^5s following a 2×10^4s thermal neutron irradiation. The uncertainty in the data was ∿2% (1σ) except at the shortest cooling times, where it rose to ∿4%.

Table III

Fission Product Decay-Heat Experiments - ^{235}U

1973-1977*

Experimenter (Date)	Lab	Type	Exposure
1)Yarnell and Bendt (1977)	LASL	Thermal Calorimeter	$2x10^4$s
2)Friesenhahn and Lurie (1977)	IRT	β,γ Nuclear Calorimeter	24h
3)Dickens et al (1977)	ORNL	β,γ Spectroscopy	1,10,100s
4)Lott et al (1973)	F-a-R	Thermal Calorimeter	100,1000,5000s
5)Alam and Scobie (1974)	SURRC	β Spectroscopy	10,100s
6)Jurney (1977)	LASL	γ Spectroscopy	$2x10^4$s
7)Johansson and Nilsson (1977)	STUDSVIK	γ Spectroscopy	4,10,120s
8)Gunst et al (1974)	BAPL	Thermal Calorimeter	---
9)Grossman et al (1977)	UC Berkeley	Calorimeter	1,4,22.4h
10)Murphy and Taylor (1977)	AEE Winfrith	β-Decay Power in Reactor	10^5s
11)Fiche (1976)	CADARACHE	Thermal Calorimeter	---

* Experiments previous to 1973 were reviewed by Lott in the Bologna RP 15. Perry et al. [1] also reviewed and summarized the pre-1973 work.

2.1.2. Friesenhahn and Lurie (1977)[3] made measurements using a "nuclear calorimeter" which is based on a large (4000 liter) liquid scintillator. Initial measurements were made for ^{235}U fission for 24 hour irradiation times and for cooling times between 1 to 10^5s. Later measurements were taken for 1000s and 20000s irradiation times. The irradiations were made in a water-moderated ^{252}Cf source.

2.1.3. Dickens et al. (1977) [4] irradiated with thermal neutrons ^{235}U samples of mass 1 to 10μgm for 1 to 100s using the fast pneumatic-tube facility at Oak Ridge Research Reactor. The resulting β and γ-ray

emissions were counted for times-after-fission between 2 and 14,400s. The data were obtained for β and γ rays separately as spectral distributions. For the γ-ray data, the spectra were obtained using a NaI detector; for the β's, the spectra were obtained using an NE-110 detector. The raw data were unfolded to provide spectral distributions which were integrated to provide energy integrals as a function of time after fission.

2.1.4. Lott et al. (1973) [5] irradiated samples of ^{235}U for periods of 100, 1000, and 5000s which were then transferred to a calorimeter and observed for periods up to 70,000s (19.4h). Error bars of 5% (1σ) were assigned for all irradiation and cooling times.

2.1.5. Alam and Scobie (1974) [6] provided beta-energy release rates for extremely short cooling times (.2-26s). Previous measurements were restricted by experimental limitations to cooling times greater than three seconds. In this experiment the "rabbit" was driven pneumatically instead of manually from the irradiation to the beta detector. Irradiations were for ^{235}U for 10s and 100s periods. An 8% (1σ) experimental uncertainty was assigned.

2.1.6. Jurney (1977) [2] made spectroscopic measurements of γ-rays in support of the LASL calorimetric experiment described in 2.1.1.

2.1.7. Johansson and Nilsson (1977) [7] irradiated ^{235}U for 4, 10, and 120s with thermal neutrons generated in a 6 MeV van de Graaf accelerator (100μA protons). Fast neutrons produced in the $^{9}Be(p,n)^{9}B$-reaction were thermalized using a cube-shaped moderator of paraffin. The neutron flux available was about $10^{8} n/(cm^{2})$. These measurements, performed at the Neutron Physics Laboratory, Studsvik, were aimed at studying the energy distribution and the total energy of γ-radiation emitted in the interval

10-1500s after fission. The total uncertainty in the unfolded γ-burst function was estimated to be less than 7%.

2.1.8. Gunst et al. (1974) [8] irradiated samples of ^{232}Th, ^{233}U, ^{235}U, and ^{239}Pu in high neutron fluxes [$>10^{14}$ n/(cm^{2}s)] and their decay heat was measured for cooling times of 14 to 4500h. To measure the rate of heat emission, an underwater calorimeter was used.

2.1.9. Grossman et al. (1977) [9] used a fast response calorimeter to measure decay heat from thermal fissions in ^{235}U. Irradiation times were 1, 4, and 22.4h with cooling times from 11 to 10^4s. The estimated uncertainty of the measurement was 3.4% (1σ) from 400 to 10^4s and rises to 22.7% at 11s.

2.1.10. Murphy and Taylor (1977) [10] measured gross β-decay power from products of ^{239}Pu and ^{235}U fission in a fast reactor. The irradiation period was 10^5s, and detection continued up to $3x10^7$s after shutdown.

2.1.11. Fiche (1976) [11] measured decay heat using calorimetry for thermal fissions of ^{233}U, ^{235}U, and ^{239}Pu between 10^2 and 10^5s after shutdown.

2.2. Results- Comparisons to ENDF/B-IV Calculations

Figures 6-15 show the direct experimental results compared to ENDF/B-IV calculations for the actual exposure (irradiation) times of the measurements except for the ORNL, STUDSVIK, and UC Berkeley results. For the first two cases (Figures 8, 9, and 12) energy release rates were measured and reported for extended cooling and counting time intervals. The curves shown correspond to unfolded "burst functions" plotted at "mean" time intervals. For the UC Berkeley plot ("UCB", Figure 15) the experimental results were extended to "infinite" irradiation using summation calculations and uncertainty estimates were assigned.

Figures 10 and 11 also include uncertainty bounds for the ENDF/B-IV summation calculation results.

Tables and figures with additional experimental results are given in Appendix A1 [54].

3. DECAY HEAT SUMMATION CALCULATIONS

Essentially all current decay heat calculations use the summation method, where decay power from several hundred individual fission product nuclides are added up to form the complete sum. The basic summation formula as it relates to reactor operation is given as

$$P(t,T) = \sum_{c} \sum_{i} E_{ic} \lambda_{ic} N_{ic}(t,T),$$

where $P(t,T)$ is the decay power, for a reactor that has operated for a time T, at a time, t (cooling time), after shutdown. The quantities E_{ic}, λ_{ic}, and $N_{ic}(t,T)$ denote the decay energy ($E_{ic} = \overline{E}_{\beta} + \overline{E}_{\lambda}$), decay constant ($\lambda_{ic} = \ln 2 / \text{half life}$), and nuclide concentration, respectively, for the i^{th} nuclide in mass chain, c. The quantities plotted in all the figures in this review are directly related to the decay power $P(t,T)$ and naturally arise in the experimental situation. The first (designated in the figures as FI(T) or Decay Heat) is the "integral after heat function" $F(t,T)$ [1] which when multiplied by the fission rate equals $P(t,T)$. Conventional units for $F(t,T)$ are (MeV/s)/ (fissions/s) = MeV/ fission, or alternatively, a fraction of the operation power. The second function (designated in the figures as F(T), f(t) or h(t)) is the "differential after heat function" $f(t)$ [1] which represents the energy release per unit time following an essentially instantaneous burst of fissions. For the "burst" cases which are shown in the figures $tf(t)$ is actually plotted.

Summation calculations have been recently made by scientists at several laboratories usually with their own codes and basic nuclear data libraries. Previous comparison [12] using most of these codes gave essentially identical results when using the same input data even though they use different mathematical procedures. Consequently, calculational results are indicated by the input nuclear data used (e.g. ENDF/B-IV) and not the codes which produced the values.

A table of data sources and codes is given in Section 3.1. Results of the summation calculations and their comparisons to each other, experiments and the ANS standard are given in Section 3.2. and Appendix A2. "Uncertainty Analyses" and "Neutron Absorption Effects" are covered in Sections 3.3. and 3.4.

3.1. Data Sources and Codes

Table IV lists the recent summation codes and nuclear data libraries used for the decay heat calculations presented in this review. Table V indicates the data content, except for fission yields (13,000 entries) of the ENDF/B-IV FP file [13-17] and is representative of the other libraries. Dr. Blachot will be reviewing in detail these libraries in RP 12.

3.2. Comparisons of Calculations and Experiments

Figures 16-21 show comparisons of decay heat calculations (integral and differential afterheat functions) using the codes and nuclear data libraries given in Table IV for ^{235}U thermal fission. Figures 16, 17 and 18 are for β, γ and total power "bursts", respectively. In Figure 19 total "burst" functions unfolded from experiment using the least-squares methods described in Section 4 are shown with the ENDF/B-IV result. Results using the INVENT code are given in Figure 20 for γ

Table IV
Summation Codes and Libraries
1973-1977

Code	Authors	Current Library	Lab	Users
AKTIVIST III [18]	Zappe	AKTIVIST III	T.U. DRESDEN	Zappe
CINDER-10 [19]	England	ENDF/B-IV	LASL	England
FISP [20]	Tobias	(RD/B/M2669)FISP	BERKELEY	Tobias
FISPROD [21]	Walker	ENDF/B-IV	CRNL	Walker
FP-S [21]	Tasaka Sasamoto	JAERI-M5997(75)	JAERI	Tasaka Sasamoto
INVENT [23]	Rudstam	OSIRIS and FISP	STUDSVIK	Rudstam
ORIGEN [24]	Bell	ENDF/B-IV	ORNL	Dickens & Weisbin
ORIGEN [24]	Bell	Yoshida [25] Tasaka [26]	NAIG N.R.L.	Yoshida
PEPIN [27]	de Tourreil	"French File" [40]	SACLAY	Devillers
RIBD-II [28]	Marr	ENDF/B-IV	HEDL	Schenter Schmittroth
ROPEY [29]	Spinrad	ENDF/B-IV	OSU	Bjerke & Spinrad
ZPOWR [30]	Schmittroth	ENDF/B-IV	HEDL	Schmittroth

TABLE V

ENDF/B-IV FP DATA FILE

824 FP NUCLIDES

182 WITH CROSS SECTIONS

182 WITH INDIVIDUAL β & γ "LINES"

712 WITH AVERAGE DECAY DATA ($\bar{E}_\beta$, $\bar{E}_\gamma$, HALFLIVES, BRANCHING RATIOS,...)

300,000 DATA ENTRIES

power and 10^5s irradiation results for β power comparing pre-1973 experiments with calculations are given in Figure 21. Appendix A2 provides additional summation calculation results.

3.3. Uncertainty Analyses

Several studies of the uncertainties in summation calculations have been made [31-35]. In contrast to direct comparisons with experimental values, these studies are basically sensitivity analyses that propagate uncertainties in the basic nuclear data such as fission yields and average decay energies. (Fortunately, there is no significant error associated with the calculational process itself.)

There are a number of incentives for this approach. First of all, it is desirable to ascertain which basic data have the largest impact on the accuracy of the calculations so that future work on the nuclear data libraries can be properly directed. Secondly, in comparisons with experimental measurements, an independent assessment of the summation uncertainties allows one to decide whether or not any observed discrepancies are normal or are indicative of undetected errors. Another point is that except for fission yields, all the decay data is the same for different fissionable nuclides. Thus, an understanding of the sensitivity of summation calculations to the basic data allows one to extrapolate experimental results for one nuclide, such as ^{235}U, to other less studied nuclides.

A particularly important aspect of these uncertainty calculations is to delineate the relationship between the uncertainties for a pulse irradiation and for a finite irradiation more typical of actual reactor operations. Because the summation uncertainties turn out to be much smaller for the longer irradiations, a comparison of the discrepancies between calculated and experimental decay-heat values for a very short irradiation is not indicative of the accuracy of summation calculations for the longer irradiations, even for short cooling times.

Uncertainties in summation calculations arise from several sources. These include errors in fission-product yields, average decay energies, and half-lives. One must also consider metastable states and branching ratios. For short cooling times ($t_c<10^4$s), one can neglect errors due to secondary corrections such as neutron capture. Despite different approaches to the various sources of error by different workers, a number of general conclusions can be drawn. As seen in Figures 22 - 25 taken from Ref. 32, the total uncertainties for cooling times greater than 100s are quite small for both ^{235}U and ^{239}Pu. Also as seen in Figures 22 - 25 and emphasized in Fig. 26, there is a sharp reduction in the calculated uncertainties with increased irradiation times, especially for the shorter cooling times. Work by Spinrad [33] is in quantitative agreement with these conclusions for ^{235}U, although his approach to yield uncertainties is quite different. Spinrad's approach utilizes individual yield uncertainties whereas Schmittroth and Schenter [32] describe yield uncertainties in terms of chain yield uncertainties and the uncertainties in the parameters that describe the Gaussian charge-distribution model. Devillers, et al. [34], also use individual yield uncertainties, but do not include the effect of yield constraints in the uncertainty analysis. As a consequence, they estimate somewhat higher uncertainties due to yields.

For cooling times greater than 100s, decay-heat uncertainties due to decay-energy uncertainties are on the order of 1-3% for a fission burst and ~1% for a long irradiation. For shorter cooling times, Schmittroth and Schenter, in agreement with recent work by Spinrad, show that because of the use of model Q-values possible correlations in average decay energies lead to increased decay-heat uncertainties. This effect is readily apparent in Figures 22 - 25, especially in the decay-energy component. In connection with this problem, Rudstam at Studsvik is presently working to make use of

expected experimental results at the OSIRIS facility to obtain better average decay energies for the short-lived nuclides far from beta-stability.

In general, half-life uncertainties are relatively unimportant in decay-heat calculations, a result obtained by both Devillers, et al. [34], and Schmittroth and Schenter [32]. Nevertheless, one must recognize that gross errors in an individual nuclide can alter this conclusion. As an example, the ENDF/B-IV library contains a value of 2.3m for the half-life of ^{96}Y while recent measurements [35] indicate both a ground and metastable state with respective half-lives of 6.0s and 10.0s. This drastic change, which is far beyond the expected uncertainties, changes the decay-heat calculations for a pulse irradiation by as much as 8%. Fortunately, the effect is much smaller for longer irradiations ($\sim$2.5% for an infinite irradiation).

The problem of gross errors discussed for half-lives in the previous paragraph is also of concern for metastable states and their associated branching ratios. A branching ratio error can shift the decay of a parent nuclide between daughter states of widely different half-lives with an effect equivalent to a large half-life change. In one study [31], the metastable states were excluded from the ENDF/B library in order to test their significance. As long as decay energies were consistently changed to reflect conservation of decay energy in the mass chains, the main consequence of eliminating the metastable states was to alter the time dependence of when the energy was released and the split between beta and gamma energy. For a longer irradiation ($T=10^7$s), which tends to average out time variations, the maximum change in decay heat was $\sim$6%. However, a major portion of this change can arise from a single nuclide as was found to be the case for ^{98}Zr. In the ENDF/B-IV library, this nuclide is mistakenly listed as branching to the metastable state of ^{98}Nb. Experience with these types of errors indicates that errors in a single nuclide can affect decay-heat values by a few percent for a finite-irradiation exposure. Nevertheless, larger errors are very unlikely. Constraints on decay energies, statistical cancellation of errors,

the small contributions of individual nuclides, and the time-averaging that occurs in finite irradiations all combine to keep these problems at a minimum. In order to crudely account for additional errors of this sort, the total uncertainties in Figures 22 - 25 include an extra term (not separately shown) that is as large as 4% for a burst exposure at short cooling times.

A number of conclusions can be drawn. In spite of the need for further testing and library improvements, summation methods are already useful for decay-heat calculations including the short cooling times less than 1000s important for loss-of-coolant accidents. Until recently, summation calculations have been particularly suspect for short cooling times because of their reliance on model data for short-lived nuclides. Also, the sensitivity of summation methods to yield errors is small enough that comparisons of calculated decay-heat values with experimental values for the thermal fission of ^{235}U give additional confidence that these same calculations can be applied to other fissionable nuclide and neutron spectra. Key items for future improvements include obtaining new measurements of nuclear masses for nuclides far from stability and continuing yield studies to improve our confidence in extrapolating to various systems. Work should continue to isolate important individual nuclides whose decay data are uncertain. And finally, there is continuing need to make detailed comparisons with experiment in order to isolate gross errors that tend to degrade confidence in these methods.

3.4. Neutron Absorption Effects

3.4.1. Effect On Decay Heating For short fission intervals characteristic of the recent benchmark experiments, neutron absorption in the fission products is not important (but it has been included in all direct comparisons we have reported). There are two effects: 1) the flux level can reduce the density of directly yielded products even in a fission pulse, but this would be significant only for nuclides having large cross sections

and large yields (e.g., ^{135}Xe), and 2) nuclide coupling in the stable and long-lived nuclides tends to build up the concentration of more unstable nuclides, and this effect is important in altering individual nuclide concentrations during the fission intervals characteristic of reactor lifetimes. The first effect is not important to aggregate decay heating (its effect on decay spectra has not been examined). The second effect has been evaluated for typical reactor lifetimes and a range of flux levels. Figures 27 and 28 show results for two flux levels. The net effect for cooling times less than 10^3s and a thermal flux of 10^{13} n/cm^{2}s is less than 1%. The effect increases with the flux level and irradiation time. For example, the effect on total heating at a thermal flux of 10^{14} n/cm^{2}s reaches 2.4% for ^{235}U at a 10^3s cooling compared to 0.1% at 10^{13} n/cm^{2}s; the increase for ^{239}Pu is approximately three times these values for cooling time less than 10^3s.

At long cooling times, ($\sim 8 \times 10^7$s) the effect is very large, particularly for the gamma energy, as is evident from Figures 27 and 28. This is due primarily to absorption in the stable nuclide ^{133}Cs which produces the shielded nuclide ^{134}Cs. Therefore, it is readily calculated by use of a simple two-nuclide chain. (For example, the peak deviations in Figures 27 and 28 are 81 and 328%, respectively, and the ^{133}Cs ^{134}Cs chain accounts for 78 and 327%, respectively.) The effect is dependent on the flux spectrum and particularly on the ratio of the resonance to the thermal flux (Figures 27 and 28 used an average epithermal flux 2.5 times that of the thermal flux).

The positive effect of neutron capture on total (β plus γ) heating results primarily from the shielded nuclides ^{134}Cs, ^{136}Cs, ^{148m}Pm, ^{148}Pm, and ^{154}Eu. The contribution of ^{135}Xe to ^{136}Cs is an important exception; absorption in ^{135}Xe decreases the heating rate and this persists for greater

than 10^6s. The effect on β heating is much smaller than the γ component; here, the contribution from the nuclides ^{90}Y, ^{132}Te, and ^{140}La is significantly increased by absorption. Other researchers [26, 30, 34] have reached similar conclusions. Dr. Tasaka [26], in particular, has made extensive studies of absorption on total heating.

3.4.2. Absorption Buildup Absorption buildup in reactors has been extensively studied and compared with long-term irradiations experiments. Results are reported in References 36 and 37 based on the 154 multigroup cross section library described in Reference 37. Absorption buildup is accurately described when integrated over the entire neutron spectrum. Resonance and thermal components do not match experiments satisfactorily, but this may be a result of experimental error in separating thermal and resonance components which is based on a rather complex analysis reactivity model.

4. LEAST-SQUARES EVALUATION OF DECAY HEAT

Least-squares methods [38] have been used to evaluate the results of recent decay-heat experiments along with summation calculations based on ENDF/B-IV. There are several reasons to use the least-squares approach. First of all, since the different experiments represent varying irradiation times, one must use some means to extrapolate or unfold to a common irradiation period in order to compare the various results. One technique is to use calculated values to obtain the desired extrapolation. This method provides a useful comparison of the different experimental results but suffers from the deficiency that one cannot easily weight the various results to obtain an average or evaluated decay-heat curve. Furthermore, the uncertainties one assigns to such an average are necessarily somewhat subjective. The least-squares method automatically accounts for different irradiation

histories and objectively propagates quoted experimental uncertainties to obtain uncertainties for the evaluated results. Another advantage of the generalized least-squares approach used here is that important correlations that affect the weight of each experiment can be incorporated. Specifically, decay-heat experiments typically exhibit normalization uncertainties that affect the entire decay-heat curve in a strongly correlated fashion. And finally, simple statistical tests are available to check for experimental biases and inconsistencies.

While the least-squares method is a useful evaluation tool, one must recognize its limitations. No level of sophistication in data analysis can substitute for a physical understanding of the potential for undetected systematic errors. Also, the confidence one has in the final uncertainties as generated by the least-squares approach must in turn depend on the confidence one has in the quoted experimental uncertainties.

The least-squares method was applied to the data from four recent decay-heat experiments, LASL, IRT, ORNL, and the CEAF (Lott et al.) along with values obtained by summation calculations from ENDF/B-IV. The uncertainties assigned to the ENDF/B values were presented earlier in Section 3.3. Experimental uncertainties used initially were those quoted by the experimentalists although some additional judgement was needed to completely specify the required correlations. No attempt was made to reanalyze the experiments to obtain independently assessed uncertainties.

The least-squares method requires a linear model. For this application, the pulse decay-heat function was represented by a linear sum of decaying exponentials, a form that is easily integrated to obtain an analytic representation for the decay heat for any finite exposure. A large number of terms was used (about 5 exponentials per decade of cooling time) to ensure that the least-squares results reflected the input values rather than the underlying exponential model.

The initial evaluation disclosed that the ORNL values were inconsistent in normalization and that the IRT data showed fluctuations that were large compared to their quoted statistical errors. Consequently, a second evaluation was performed with the ORNL normalization uncertainty increased by about a factor of 2 and with the IRT statistical uncertainties increased by a factor of 2.

Values for a pulse irradiation obtained from the least-squares analysis are given in Table VI along with their corresponding one-sigma uncertainties. These uncertainties reflect the expected variations in the evaluated values due to the uncertainties in the input decay-heat values. They do not reflect experimental biases or inconsistencies that are not accounted for in the input uncertainties. A more detailed comparison is shown in Fig. 29 which displays the fractional deviation of the different inputs from the evaluated or nominal values (the pulse values for the ENDF/B results are shown only for comparison; the 20000s ENDF/B values were used as input in the evaluation).

The inconsistency of the ORNL normalization with the evaluated values is readily apparent in the figure. *It is important to reemphasize the nature of this inconsistency which is a direct consequence of the constraining influence of the LASL and ENDF results.* In order to conclude that the ORNL values are actually low as shown in the figure, one must have confidence that the LASL and ENDF uncertainties used in the evaluation fairly reflect the true uncertainties in the corresponding values. If the quoted ORNL uncertainties represent a truer estimate of the actual uncertainties, the picture would obviously change. The power of the least-squares method lies in its ability to compare the various results and obtain an objective evaluation. It cannot guarantee the validity of quoted uncertainties in the input data sets.

Table VI

Decay Heat Values For A Pulse Irradiation
Obtained From A Least-Squares Analysis

Cooling Time,s	f(t),(MeV/s)/fiss.	% Uncertainty
1	7.457×10^{-1}	23.5
2	5.430	6.8
5	2.851	2.5
1×10	1.509	2.0
2	7.315×10^{-2}	1.6
5	2.811	1.4
1×10^{2}	1.290	1.2
2	5.455×10^{-3}	1.3
5	1.884	1.3
1×10^{3}	9.586×10^{-4}	1.3
2	4.644	1.3
5	1.464	1.4
1×10^{4}	5.909×10^{-5}	1.2
2	2.304	1.0
5	6.925×10^{-6}	1.0
1×10^{5}	2.569	1.0

5. SPECTRA-EXPERIMENTS AND SUMMATION CALCULATIONS

Several compilations of fission-product gamma and beta spectral data exist [13, 15, 39, 40] that could be used in comparisons of calculations with recent experimental measurements. Extensive comparisons have been made between computed spectra and beta and gamma spectra measured at the Los Alamos Scientific Laboratory (LASL) [2, 41], Oak Ridge National Laboratory (ORNL) [4] and the University of Illinois (UI) [42]. Results of these comparisons are summarized here in graphic form for delayed beta and gamma spectra. These comparisons are limited to ^{235}U thermal fission; however, the results tend to qualify the specific ENDF/B-IV data base [13, 15] for all fuels because differences arise only due to fission product yields (for the same irradiation history).

The irradiation times (15 ms, 1, 10, 100s, 5.56 and 8h) used in the various calculational and experimental comparisons may be of limited direct interest. The purpose of the comparisons is to examine the ade-

quacy of the data base used in the calculations; the calculational models can then be used for irradiation and cooling times of more specific interest to users.

Spectral comparisons constitute a very stringent test of the data base, particularly for the adequacy of the data at various cooling times. The spectral calculations rely on the spectral data for the 180 fission products (among a total of 824) that are available in the ENDF/B-IV files [15]. The calculated spectra were normalized so that energy integration over the spectrum produces the total calculated energy release (beta or gamma) for all 824 fission products in ENDF/B-IV. In other words, the spectral shapes are determined by 180 fission products while their magnitudes are determined by all 824 fission products. The comparisons with experiment are absolute.

The libraries of Tobias [39] and Devillers, et al., [40] are more extensive in terms of spectral data than ENDF/B-IV. However, all libraries are being extended, and for most cooling times of interest to users of the ENDF/B-IV data, the 180 nuclides account for >90% of the total energy release.

The inclusion of spectral data for more fission products will improve the accuracy of the spectral calculations at the shortest experimental cooling times. However, the present spectral comparisons indicate that even the presently available fission-product spectral data in ENDF/B-IV are adequate for these relatively short cooling times. Figure 30 shows the contribution of the "theoretical nuclides" (those having beta and gamma energies based on Q-values rather than integrated spectra) to the total gamma heating for several irradiation times. Table VII shows the range of contribution of the 180 nuclides having spectral data to the total beta and gamma energy for the specific experiments used in the graphical comparisons.

TABLE VII

SUMMARY OF
CONTRIBUTION OF NUCLIDES HAVING SPECTRAL
DATA IN ENDF/B-IV TO TOTAL β and γ ENERGY

EXPERIMENT	SPECTRAL TYPE	IRRADIATION TIME (s)	MEAN COOLING TIME RANGE (s)	% CONTRIBUTION RANGE	% CONTRIBUTION MID-POINT
LASL[a]	γ	2×10^4	70-151200	88-99.9	99.9
ORNL	γ	1	2.2-99.7	19-66	50
	γ	10	13.7-694.7	32-91	86
	γ	10^2	90-11950	72-99	>98
	β	1	2.2-99.7	34-62	50
	β	10	13.7-694.7	43-89	82
	β	10^2	90-11950	67-98	98
UI	β	2.28×10^4	6-10950	68-99.7	>99
	β	1×10^{-3}	13-3750	NA[b]	NA[b]

[a] LASL experiments recently extended the lower cooling time to ∿29s.

[b] % contribution not calculated for the UI Pulse experiment. The contribution is determined primarily by the cooling time; based on the ORNL comparison, the contribution range should be 42-96%.

5.1. Codes Used

The specific spectral calculations reported here used the CINDER-10 summation code [19] and the auxiliary codes FPDCYS [43] and FPSPEC [43]; however, several other summation codes (RIBD-II [28], ORIGEN [24], etc.) could also have been used. The summation code is used to calculate fission-product activities and total beta and gamma decay energies from all products at the desired irradiation and cooling times. The FPDCYS code generates multigroup spectra of the 180 individual fission products using the gamma energies and intensities and beta end-point energies and intensities contained in an ENDF/B-IV format. The FPSPEC code combines the outputs of the summation and FPDCYS codes in any desired multigroup structure to calculate the aggregate fission-product spectra normalized to the total beta and/or gamma energy from the summation code.

5.2. Processed Libraries

The summation code library contains all decay parameters (half-lives, branching ratios, total β and γ decay energies), yields, and cross sections necessary to compute the coupled buildup of nuclide densities, activities, energies, etc. for all 824 nuclides in ENDF/B-IV. The basic spectral library produced by FPDCYS consists of multigroup spectra for the 180 nuclides having spectral data in ENDF/B-IV. For beta energies, 75 groups are used in a uniform 100 keV binning between 0 and 7.5 MeV. The beta spectra were derived from the end-point energies and intensities using the accurate procedure described in Reference 44.

The gamma spectra are in 150 groups in a uniform 50 keV binning between 0 and 7.5 MeV. When comparing calculated and experimental gamma spectra it is necessary to broaden the lines before grouping (when using a fine group experimental structure) in order to match the finite resolution and energy dependence of the gamma spectrometer used by each experimenter. Two gamma libraries were therefore generated--one for the LASL and one for the ORNL comparisons. Each gamma line at energy E_0 was assumed to be a Gaussian having an area equal to the line intensity, I:

$$G=\frac{I}{\sqrt{2\pi}\,\sigma}\exp\left[\frac{-(E-E_0)^2}{2\sigma^2}\right]$$

The value of σ at E_0 was prescribed by the experimenter. The unbroadened 150 group spectra are listed in Reference 44.

The total energy in each bin (i.e., summed over all nuclides) rather than total yield per bin are compared. This has the advantage of visually displaying the energy release over the energy axis; a division of the energy plots by the abscissa energy would provide the more conventional spectra in terms of yields. The actual plots are for the quantity

$$\text{MeV/Fission/bin} = \frac{\text{MeV/s/bin}}{\text{Fission/s}}$$

The quantity MeV/s/bin is the energy release rate per bin at the specified mean cooling (decay) time (or, as will be noted, an average over the measurement count time). The quantity Fission/s is the fission rate prior to initiation of the cooling interval; this rate was held constant in each experiment. To the extent that neutron absorption can be ignored, the decay energy release rate is simply the plotted value times any user specified fission rate.

The ENDF/B-IV gamma energies used in the summation code results contain the internal conversion energies. However, the spectral shape does not contain the internal conversion energies. More specifically, the internal conversion energies for the 38 nuclides having conversion coefficients in the ENDF/B-IV spectral data are not included in the library produced by FPDCYS code. (Differences in normalization when internal conversion energies are removed have been evaluated; it amounts to only a few percent, depending on cooling time, and is not evident in graphical comparisons).

All measured spectra are necessarily based on a finite counting time. We have examined the difference between using an integration of the calculated values over the counting interval and that obtained using the rate at the mid-point of the interval. For the spectral comparison plots, there is no observable difference. For the energy integrated values, the difference is ∿1% (i.e., the energy release rate at the mid-point or mean time is ∿1% lower than the average over the counting interval).

The units of MeV/fission (per energy bin) used in the present review and in the ORNL draft of Reference 4 are different quantities. In effect, the values in Reference 4 are an integration of MeV/s over the counting interval divided by the number of fissions. Therefore, the values ex-

tracted from that reference were multiplied by the ratio of the fission time to the counting time in order to obtain the same type of quantity provided by other experiments. This results in the more conventional quantity

$$\text{MeV/fission} = \frac{\text{MeV/s}}{\text{Fission/s}}$$

where MeV/s is, in this case, an average over the counting interval. Reference 4 in draft form also tabulates an "average time" which is defined there as the cooling time up to the start of the counting period plus 1/2 of the sum of the fission and counting times. In this review, the mean or decay times always refer the decay time (subsequent to the fission interval) up to the mid-point of the counting interval.

The irradiation times of the experiments are too brief to cause significant effects due to the coupling of nuclides by neutron absorption; however, individual nuclide densities produced directly in fission or by decay coupling will be lowered by a significantly large cross section. Therefore, the cross sections were included for these comparisons using the flux levels (10^{12} - 10^{13} n/cm^2-s) specified for the experiments. The less significant effects of neutron absorption coupling are also included.

5.3. Results

Figures 31-40 provide a selection of the graphical comparisons and an additional 32 comparisons are included in Appendix A3. A total of 102 such comparisons have been published [45]; other comparisons using ENDF/B-IV and the Tobias library are in press, and similar comparisons are expected for other fuels in the near future.

The agreement between calculated and experimental results varies, but overall, it is remarkably good. Beta spectral measurement are notoriously difficult, and the general shift of the measurements at the lower energies may be experimental.

The most stringent test on the ENDF/B-IV data are the comparisons at short irradiation and short cooling times. At these times, the fission products with spectral data in the ENDF/B-IV files are not represented as well as at longer irradiation and cooling times. At longer cooling times, however, the fission products with spectral data in ENDF/B-IV account for most of the energy release. At these times, also, the agreement between experimental and calculated data is seen to be better, particularly for the gamma spectra.

In conclusion, while it is seen that the ENDF/B-IV files could be improved by inclusion of more spectral data for short-lived fission products, it is adequate, in its present form, for predicting fission-product spectra for the irradiation and cooling times or interest in most applications related to reactor safety and safeguards.

6. ADJUSTMENTS OF DIFFERENTIAL DATA

Summation calculations start from basic nuclear data (differential data) such as decay energies and half-lives and calculate various integral properties (decay heat, gas releases, spectra, and biological doses for example) that depend on decaying fission products. Consequently, one can test the basic nuclear data by both integral and differential measurements as discussed elsewhere in this review paper and others.

In this section, the use of integral tests to identify discrepancies in individual nuclear data is briefly considered. The work is preliminary. The well-known fact [32] that only a few nuclides contribute to the total fission-product decay heat at long cooling times implies that decay-heat measurements can provide rather direct information on the validity of the nuclear data for a few long-lived nuclides. However, as shown by Devillers [40], even at short cooling times, the sensitivity of decay heat to individ-

ual nuclides is enough to at least open up the possibility of identifying discrepancies in individual nuclides. For example, a transcription error in ENDF/B for the ^{98}Zr branching ratio increases the calculated decay heat by more than 8% for cooling times near 6000s for a pulse irradiation. A discrepancy of this magnitude is easily seen in comparisons of decay heat with recent experiments. It is also outside the expected accuracy of the summation calculations [32].

To check for additional errors in the ENDF/B library, summation calculations are compared with nominal values determined by least-squares fitting in Fig. 41. The least-squares values (nominal) are an average of recent experiments plus summation calculations. The values plotted in Fig. 41 represent the fractional deviation, $(f_c-f_n)/f_n$, of the calculated values f_c from the nominal values f_n for a pulse irradiation. The solid curve in Fig. 41a represents the total decay heat based on ENDF/B with only ^{98}Zr corrected. The most notable discrepancies are peaks near 200s and 7000s, a pronounced dip near 1000s and a sharp fall off at 10s.

A very different picture appears when one looks separately at the beta and gamma components as seen in Figs. 41b and 41c. Some caution must be taken however. In this preliminary work, only the experiments by ORNL [4] and IRT [3] along with summation calculations were used to determine the least-squares nominal values; however, for the totals shown in Fig. 41a, the nominal values also include the calorimetric experiments by Yarnell and Bendt [2] and by Lott et al. [5] as described in the section on least-squares. Nevertheless, as a consistency check, the sum of the separately determined nominal values for the beta and gamma components are in good agreement with the total nominal values. One sees that the calculated values are in much better agreement for the total decay heat than for the separate beta and gamma components.

One problem, the high calculated gamma values seen in Fig. 41b for cooling times above 10^4s are likely due to an improper treatment of the conversion electrons in ENDF/B-IV. Preliminary calculations show that 3-4% of the gamma energy can go into conversion electrons for this time range, whereas the ENDF/B-IV library lumps the conversion electron energy with the gamma component.

A second problem, the very large beta discrepancy near 100s is substantially reduced by correcting the ^{96}Y half-life. The ENDF/B-IV value of 2.3m was reduced to 6.0s [35] for the corrected curves shown. A 10.0s metastable state for ^{96}Y was still ignored. Unfortunately, the low gamma values below 10^3s are further reduced by this change. It is possible that the nominal values are in error rather than the calculated values. Experimental gamma results by ORNL [4] and IRT [3] are also below the nominal values for this time range. However, these experiments are also below the nominal values for cooling times greater than 10^3s in disagreement with the ENDF/B results.

Because the total decay heat is subject to fewer problems, there are advantages to considering it separately. It is not as sensitive to branching ratio and metastable state errors, and the conversion electron problem disappears. On the experimental side, one can include the relatively simple calorimetric results that give only the total heat. The anomalous bump in the total calculated decay heat near 7000s seen in Fig. 41a was investigated in some detail. Because the anomaly is a bump and not a dip, one can identify the important contributing nuclides at that time and review their corresponding nuclear data. Although the data for most of these nuclides were well known, a couple of problem areas were identified. Previously recognized problems for the ^{130}Sn branching ratio and the average gamma energy for ^{142}La [14] were noted. In addition, contributions from the decay

of ^{133m}Te led to a reevaluation of the 133 mass chain. The branching ratio of ^{133}Sb to the ground state of ^{133}Te was found to be closer to 0.7 than the value of 0.9776 given in ENDF/B. Also, the average gamma decay energy for ^{133m}Te should be closer to 1.0 MeV than the 1.866 given in ENDF/B. The results of these various changes are depicted in Fig. 41.

7. ANALYTICAL REPRESENTATIONS OF DECAY POWER

7.1. Exponential Sums

Non-linear least-square exponential fits to the "burst" function f(t) have been made by England et al. [46] for fission in ^{235}U, ^{238}U, and ^{239}Pu. The fits were made over a time range of 0 to 10^{13}s (see Figure 42 for ^{235}U) and given in terms of a sum of 23 exponentials:

$$f(t) = \sum_{i=1}^{23} \alpha_i e^{-\lambda_i t} .$$

The fits were extremely close to the original curves and agree to within ∿.4% at all times and are considerably better at most decay times. Table VIII gives the α and λ values for the three fissionable nuclides (^{235}U was the least-squares nominal curve and ^{238}U and ^{239}Pu were ENDF/B-IV summation results).

In the absence of neutron capture effects the finite irradiation function F(t,T) is related to f(t) through the following integral [1]

$$F(t,T) = \int_{t}^{t+T} f(t') \, dt' .$$

Consequently, use can be made of Table VIII to obtain finite irradiation results since with the two above equations

$$F(t,T) = \sum_{i=1}^{23} \frac{\alpha_i}{\lambda_i} e^{-\lambda_i t}(1-e^{-\lambda_i T}).$$

TABLE VIII

Parameters
For
Pulse and Finite Irradiation Decay-Heat
Functions f(t) and F(t,T)

^{235}U Thermal		^{238}U Fast		^{239}Pu Thermal	
α	λ	α	λ	α	λ
6.4447E-1	7.8950E+0	1.2311E+0	3.2881E+0	3.1094E-1	2.8480E+0
4.6408E-1	5.5683E-1	1.1486E+0	9.3805E-1	2.1395E-1	9.8330E-1
2.8883E-1	2.2367E-1	7.0701E-1	3.7073E-1	2.0240E-1	3.8966E-1
1.4815E-1	1.0212E-1	2.5209E-1	1.1118E-1	1.2174E-1	1.1978E-1
5.5143E-2	3.3400E-2	7.1870E-2	3.6143E-2	3.9701E-2	4.0829E-2
2.1950E-2	1.1403E-2	2.8291E-2	1.3272E-2	2.2748E-2	1.4287E-2
3.1497E-3	3.2092E-3	6.8382E-3	5.0133E-3	5.2320E-3	5.2952E-3
6.7681E-4	1.3098E-3	1.2322E-3	1.3655E-3	1.2591E-3	1.5235E-3
8.3288E-4	6.4795E-4	6.8409E-4	5.5158E-4	6.8417E-4	5.6352E-4
2.0207E-4	2.0059E-4	1.6975E-4	1.7873E-4	1.5842E-4	1.8578E-4
3.7154E-5	6.0023E-5	2.4182E-5	4.9032E-5	2.1323E-5	4.9377E-5
8.5033E-6	2.1715E-5	6.6356E-6	1.7058E-5	6.3717E-6	1.6710E-5
2.5441E-6	9.9966E-6	1.0075E-6	7.0465E-6	1.0141E-6	6.5786E-6
4.9828E-7	2.5405E-6	4.9894E-7	2.3190E-6	4.8987E-7	2.2253E-6
1.8522E-7	6.6349E-7	1.6352E-7	6.4480E-7	1.6170E-7	6.3618E-7
2.6606E-8	1.2289E-7	2.3355E-8	1.2649E-7	2.0947E-8	1.2722E-7
2.2397E-9	2.7212E-8	2.8094E-9	2.5548E-8	2.9902E-9	2.4609E-8
8.1609E-12	4.3701E-9	3.6236E-11	8.4782E-9	4.8496E-11	9.2396E-9
8.7797E-11	7.5780E-10	6.4577E-11	7.5130E-10	5.7292E-11	7.4498E-10
2.5129E-14	2.4786E-10	4.4963E-14	2.4188E-10	4.1331E-14	2.4251E-10
3.2190E-16	2.2376E-13	3.6654E-16	2.2739E-13	1.0908E-15	2.2044E-13
4.4911E-17	2.4499E-14	5.6293E-17	9.0536E-14	2.1519E-17	2.6819E-14
7.4776E-17	1.5643E-14	7.1602E-17	5.6098E-15	7.5638E-17	1.1834E-14

7.2. Single Power Function

Dr. Aten [47] in the spirit of Way-Wigner [48] has studied the problem of representing β and γ power by a single power function. Using the notation of this review paper Aten's basic formulas are given as

$$f_\gamma(t) = 2.4\ (t+\theta_\gamma)^{-1.25}$$

$$f_\beta(t) = 2.3\ (t+\theta_\beta)^{-1.25} \quad ,$$

where the constants θ_γ and θ_β depend upon the particular fissionable nucleus. Dr. Aten has developed a set of equations to find θ_γ and θ_β in terms of the James [49] parameter z for nuclei in which θ_γ and θ_β have not been obtained experimentally. These equations are given as

$$\log \theta_\gamma = 4.53 - 6.5 \log z$$

$$\log \theta_\beta = 5.61 - 8.3 \log z$$

$$z = 4.28 + .214\ (A-235) - (U-2.43) - .5(Z-92),$$

where $z = 4.28$ for ^{235}U is the base case.

The total γ energy release per fission, "ΣE_γ", can be calculated from the burst function by the following infinite integral

$$\Sigma E_\gamma = \int_0^\infty f_\gamma(t)dt$$

Table IX gives the Aten parameters and comparisons to James [49] evaluated values of ΣE_γ for several fissionable nuclides.

Table IX

Gamma Power Energy Release Parameters

Nuclide	z	θ	E (MeV)-Aten	E (MeV)-James
^{235}U-T	4.28	2.6	7.55	7.2 ± 1.3
^{239}Pu-T	4.0	2.75	6.9	6.3 ± 1.4
^{238}U-F	4.9	1.23	9.15	9.2 ± 2.0
^{235}U-F	4.25	2.6	7.55	7.1 ± 1.3
^{239}Pu-F	4.0	2.75	6.9	6.2 ± 1.4
^{233}U-F	3.81	6.0	6.1	5.7 ± 1.3
^{232}Th-F	4.64	1.5	8.7	8.6 ± 2.0

8. GAS CONTENT IN FISSION PRODUCTS

Extensive calculations of the gas content (noble gases and halogens) in several irradiated fuels have been made using ENDF/B-IV data and partially reported in Ref. 51. The results are of importance to decay-heat experiments because the energy release is considerable by comparison with the fraction of fission products that

are gases. That is, a relatively small gas loss could constitute a significant loss in decay energy. Realization of the importance and potential magnitude of a gas loss in decay-heat experiments has been based on these calculations. The recent LASL, IRT, ORNL, and Berkeley experiments have included a detection method for gas loss through the cladding of irradiated samples during and following irradiation. The ORNL measurements also include a correction for diffusion of gas through the polyethylene window.

Figures 43 and 44 show the time-dependent results following a ^{235}U and ^{239}Pu fission pulse, and Figure 45 shows the values following an extended ^{235}U fission interval (20000 h). Results in these plots are expressed as fractions of the corresponding quantity in the total fission-product ensemble. The fractional density curves include all gases having halflives less than 10^{10}y, but not the stable gases.

The potential seriousness of a gas loss is illustrated by the contrast at $\sim 10^4$ s cooling. For the ^{235}U thermal fission pulse, $\sim$11% of the fission products are noble gases plus halogens and these constitute greater than 45% of the total gamma energy release rate. The contrast is even larger for the extended fission interval (Figure 45) where the fractional density is only 0.5% and this fraction constitutes 34% of the total gamma energy at 10^4s.

9. PHOTONEUTRON SOURCES IN ^{2}H AND ^{9}Be

Total yields, spectra, and average energies of neutrons from photoneutron reactions in deuterium and beryllium induced by delayed gamma spectra from fission products released from thermal and/or fast fissions in ^{232}Th, ^{233}U, ^{235}U, ^{239}Pu and ^{241}Pu were calculated

at a number of cooling times following fission ranging from 1 to 5000 hours [52]. The results of this study have indicated the possibility of sourceless startups in reactors containing significant amounts of deuterium (light water reactors) or beryllium up to times of several hundred hours after reactor shutdown. An experimental study [53] agrees with this conclusion.

10. CONCLUSIONS

Significant improvement has resulted in the agreement between experiments and the comparisons to calculation for both decay heat and spectra production since last reviewed at the Bologna meeting. Many of the recent experiments should qualify as fine "benchmarks" to test the calculational methods to compute fission product inventory and decay power. Consequently, this review gives confidence that the use of the summation method for calculating input quantities for fission reactor application such as "LOCA" analyses is valid and rapidly improving in accuracy.

Nevertheless, there are remaining discrepancies between calculations based on the different libraries and between different experimental results. Also, in spite of the outstanding success in spectral comparisons of summation calculations with experiment, the split between gamma and beta results is not as well determined as for the total. An example of this is indicated in comparing gamma and beta least-square results shown in Figures 46 and 47 with the total values in Figure 29.

The various nuclear data libraries need additional work in at least two areas. Better values are needed (theoretical, measured or both) for the short-lived nuclides far from beta-stability. Also, many of the better studied nuclei have significant gaps or discrepancies

in their individual data. These nuclides must be identified and their data improved as needed. Work on long-lived nuclides important to fuel cycles, waste management, and transportation of nuclear materials should not be neglected. A report on these areas for this review by Zappe et al [18] has been written.

Thermal fission in ^{235}U has been essentially the only process covered in this review. Recent experimental results for thermal and fast fission in ^{239}Pu, ^{233}U, etc. are presently being completed and analyzed (see Appendix A1). These experiments will help to confirm summation results which require only independent yield differences from the ^{235}U libraries.

11. ACKNOWLEDGEMENTS

Written reports for this paper were received from the following authors:

A.H.W. Aten	B.I. Spinrad
J.K. Dickens	M.G. Stamatelatos
P.I. Johansson	A. Tobias
N.A. Lurie	Y.L. Yarnell
G. Rudstam	T. Yoshida
J. Scobie	D. Zappe

We wish to thank these scientists for their contributions.

Thanks also to our colleagues F.M. Mann and M.G. Stamatelatos for many discussions on topics involved in this paper including beta-decay theories, spectra evaluations and decay branching to isomeric and ground states.

Finally, thanks to S. Foreman, D.E. Lessor, L. Rudisill and M. Schenter for help in preparation of the manuscript and the figures.

REFERENCES

1. A. M. Perry et al., Fission-Product Afterheat, ORNL-TM-4197, October 1973.

2. J. L. Yarnell and P. J. Bendt, Decay Heat from Products of ^{235}U Thermal Fission by Fast-Response Boil-Off Calorimetry, LA-NUREG-6713, Los Alamos Scientific Laboratory report (Draft January 15, 1977).

3. S. J. Friesenhahn, N. A. Lurie, V. C. Rogers, and N. Vagelatos, U-235 Fission Product Decay Heat from 1 to 10^5 Seconds, EPRI-NP-180, Electric Power Research Institute report (February 1976), prepared by IRT Corporation. [Values were modified by IRT in letter Lurie to Schenter, April 14, 1977.]

4. J. K. Dickens et al., Fission-Product Energy Release of ^{235}U Between 2 and 14000 Sec, ORNL/NUREG-14, Oak Ridge National Laboratory report (Draft April 22, 1977).

5. M. Lott, G. Lhiaubet, and F. DuFreche, in J. Nucl. Energy, 27, 597 (1973) [See also translation AEC-TR-7472].

6. B. Alam and J. Scobie, Ann of Nucl. Sci. and Eng., 1 (1974) 537.

7. P. I. Johansson and G. Nilsson, Measurement of Decay Energy Released in Thermal Fission of ^{235}U, contribution to this review paper.

8. S. B. Gunst et al, Nucl. Sci. and Eng., 56 (1975) 241.

9. L. M. Grossman et al., A Fast Response Calorimetric Measurement of Decay Heat, Proceedings of ANS Thermal Reactor Safety Meeting, Sun Valley, Idaho, August 1977.

10. M. F. Murphy and W. H. Taylor, INDC(NDS)-86/G+P, 39 (1977).

11. M. Fiche, INDC(NDS)-70/G+P, 6 (1975).

12. C. W. Kee et al., Trans. Am. Nucl. Soc., 19 (1974) 398.

13. Fission Product Decay Library of the Evaluated Nuclear Data File, Version IV (ENDF/B-IV). [Available from, and maintained by, the National Nuclear Data Center (NNDC) at the Brookhaven National Laboratory; these data were compiled by a task force chaired by R. E. Schenter.]

14. T. R. England and R. E. Schenter, ENDF/B-IV Fission-Product Files: Summary of Major Nuclide Data, LA-6116-MS [ENDF-223], Los Alamos Scientific Laboratory report (October 1975).

15. C. W. Reich, R. G. Helmer, and M. H. Putnam, Radioactive-Nuclide Decay Data for ENDF/B, ANCR-1157 (ENDF-120), Aerojet Nuclear Company, (August 1974).

16. M. E. Meek and B. F. Rider, Compilation of Fission Product Yields, NEDO-12154-1 (Jan. 1974).

17. P. F. Rose and T. W. Burrows, ENDF/B Fission-Product Decay Data BNL-NCS-50545 [ENDF-243], Vols. 1 and 2, Brookhaven National Laboratory report (August 1976, issued May 1977).

18. D. Zappe et al., The Use of Fission Product Nuclear Data, contribution to this review paper, available as printed report from authors.

19. T. R. England et al., CINDER-7: An Interim Report for Users, LA-5885-MS, Los Alamos Scientific Laborabory report (April 1975). [CINDER-10 is described in Applied Nuclear Data Research and Development report LA-6472-PR, p. 13 (1976)].

20. A. Tobias, J. Nucl. Energy, 27, 725 (1973).

21. W. H. Walker et al., FISSPROD-2: An Improved Fission Product Accumulation Program, AECL-5105, August 1975.

22. K. Tasaka and N. Sasamoto, FP-S: Program for Calculation of Atomic Density for Each Fission Product Nuclide, JAERI-1198, JAERI (1971).

23. G. Rudstam, INVENT - A Computer Programme for Evaluating the Inventory of Fission Products in Nuclear Fuel, contribution to this review (July 1977).

24. M. J. Bell, ORIGEN - The ORNL Isotope Generation and Depletion Code, ORNL-4628 (1973).

25. T. Yoshida, "Estimation of Decay Heat Nuclear Data for Short-Lived Fission Products", Nucl. Sci. Eng., (to be published).

26. K. Tasaka and N. Sasamoto, Nucl. Sci. Eng., 54, 177 (1974); Nucl. Sci. Eng., 62, 167 (1977).

27. R. de Tourreil, note CEA.N 824 (1967).

28. D. R. Marr, A User's Manual for Computer Code RIBD-II, A Fission Product Inventory Code, HEDL-TME 75-26, Hanford Engineering Development Laboratory report (January 1975).

29. F. Schmittroth, ZPOWR-FP Decay Power Code, (See References 31 and 32 for description).

30. B. I. Spinrad, Evaluation of Fission Product After Heat, OSU Annual Report, NUREG-0018-4, July 1975-August 1976.

31. F. Schmittroth, Nucl. Sci. Eng., 59, 117 (1976).

32. F. Schmittroth and R. E. Schenter, Nucl. Sci. Eng., 63, 276 (1977).

33. B. I. Spinrad, Nucl. Sci. Eng., 62, 35 (1977).

34. C. Devillers et al., Sensitivity of the Afterheat from ^{235}U and ^{239}Pu Thermal Fission to Errors in Fission Product Nuclear Data, Proc. Conf. Nuclear Cross Sections and Technology, NBS Special Publication 425, National Bureau of Standards (1975).

35. G. Sadler et al., Nucl. Phys., A252, 365 (1975).

36. W. B. Wilson et al., Trans. Am. Nucl. Soc., 26, 592 (June 1977).

37. T. R. England et al., Fission Product Data for Thermal Reactors, Part 1, A Data Set for EPRI-CINDER Using ENDF/B-IV, LA-6745-MS, and Fission Product Data for Thermal Reactors, Part 2, User's Manaul for EPRI-CINDER Code and Data, LA-6746-MS (1977).

38. F. Schmittroth and R. E. Schenter, Application of Least-Squares Method to Decay Heat Evaluation, to be published Nucl. Sci. Eng.(12/77).

39. A Tobias, Data for the Calculation of Gamma Radiation Spectra and Beta Heating from Fission Products (Rev. 3), Central Electricity Generating Board, Berkeley Nuclear Laboratory report, RD/B/M2669 [CNDC(73)P4], June 1973.

40. C. Devillers et al., Fission Product Data Library, in Nuclear Data in Science and Technology (Proc. IAEA Symp., Paris, March 1973), Vol. 1, p. 477, IAEA, Vienna, October 1973. (Referred to as the French File.)

41. M. G. Stamatelatos and T. R. England, Nucl. Sci. Eng., 63, 204, (February 1977). [See also, Beta-Energy Averaging and Beta Spectra, LA-6445-MS (ENDF-242), Los Alamos Scientific Laboratory report (August 1976)].

42. N. Tsoulfanidis et al., Nucl. Sci. Eng., 43, 42 (1971).

43. M. G. Stamatelatos and T. R. England, FPDCYS and FPSPEC, Computer Programs for Calculating Fission-Product Beta and Gamma Multigroup Spectra from ENDF/B-IV Data, LA-NUREG-6818-MS, Los Alamos Scientific Laboratory report (May 1977).

44. T. R. England and M. G. Stamatelatos, Multigroup Beta and Gamma Spectra of Individual ENDF/B-IV Fission-Product Nuclides, LA-NUREG-6622-MS, Los Alamos Scientific Laboratory report (December 1976).

45. T. R. England and M. G. Stamatelatos, Comparisons of Calculated and Experimental Delayed Fission-Product Beta and Gamma Spectra from ^{235}U Thermal Fission, LA-NUREG-6896-MS, Los Alamos Scientific Laboratory report (July 1977).

46. T. R. England et al., Fission-Product Source Terms for Reactor Applications, LA-NUREG-6917-MS, Los Alamos Scientific Laboratory report (to be issued).

47. A.H.W. Aten Jr., Decay of Mixed Fission Products, contribution to this review paper.

48. K. Way and E.P. Wigner, Phys. Rev., 70, 115 (1946).

49. M.F. James, J. Nucl. Energy, 23, 517 (1969); 25, 513 (1971).

50. C. Devillers, Fission Product Nuclear Data (FPND), Vol. II, IAEA-169, 326 (1974).

51. T.R. England, et al., "Gamma and Beta Decay Power Following ^{235}U and ^{239}Pu Fission Bursts," LA-6021-MS, Los Alamos Scientific Laboratory report (July 1975).

52. M.G. Stamatelatos and T.R. England, "Fission-Product Gamma-Ray and Photoneutron Spectra, "Neutron Cross Sections and Technology, NBS Special Publication 425, Vol. 1, p. 193, (March 1975), [See also "Fission-Product Gamma-Ray and Photoneutron Spectra and Energy-Integrated Sources," LA-NUREG-6345-MS, Los Alamos Scientific Laboratory report (December 1976, and Addendum I, March 1977)].

53. J.D. Randall, et al., "An Investigation of the Properties of Photoneutrons in the NSCR Core," Technical Report 20, Nuclear Science Center at Texas A & M University, (May 1967) [See also earlier Technical Report 17, January 1966].

54. "Annexes and selected contributions to the review papers of this meeting", INDC(NDS)-87 (1978)

FIGURE CAPTIONS

Fig. 1. Decay-Heat Comparison With ANS 5.1 Standard (Infinite ^{235}U constant Fission Rate, No Depletion and No Absorption)

Fig. 2. ^{235}U Decay-Heat Comparisons Following Extrapolation To An Infinite Fission Interval (Constant Fission Rate, No Depletion and No Absorption)

Fig. 3. Comparison of calculation with LASL 5.56 h irradiation, 1524 s decay

Fig. 4. Comparison of calculation with ORNL 10 s irradiation experiment, 184.7 s decay

Fig. 5. Comparison of calculation with UI 8 h irradiation, 900 s decay

Fig. 6. Comparison of calculated decay heat with experiment results from LASL

Fig. 7. Twenty-four-hour fission product decay heat data from IRT divided by calculated value

Fig. 8. Photon energy emission rate for thermal-neutron fission of ^{235}U from results obtained at ORNL

Fig. 9. Beta energy emission rate for thermal-neutron fission of ^{235}U from results obtained at ORNL

Fig. 10. Total integral afterheat for U235 thermal fission: Lott experiments compared to calculations

Fig. 11. Beta integral afterheat, U235thermal fission, 10 s and 100 s irradiations: results from Alam-Scobie

Fig. 12. Gamma Energy Release - Studsvik results

Fig. 13. Calorimetric Results: U235 thermal fission, high burnups in MTR and ATR

Fig. 14. Gamma integral afterheat: U235thermal, for 20000s irradiation

Fig. 15. Total integral afterheat, U235thermal fission: UCB data

Fig. 16. Beta differential after heat calculations for U235thermal fission

Fig. 17. Gamma differential afterheat calculations for U235thermal fission

Fig. 18. Total differential afterheat calculations for U235thermal fission

Fig. 19. Total differential afterheat functions unfolded from experiment

Fig. 20. The quantity cooling time multiplied by gamma power (in MeV/fission x s) plotted versus cooling time. Experimental results compared to ENDF-, INVENT- calculations

Fig. 21. Beta integral afterheat for U235thermal fission for irradiation of 10^5 s

Fig. 22. - 25. Uncertainties in calculated decay heat vs. cooling time, and contributions from uncertainties in half life-, yield-, decay energy-data to total uncertainty (^{235}U thermal and ^{239}Pu fast fission, T_{irr} = 0 and 10^7 s)

Fig. 26. Decay Heat Uncertainty vs. Exposure Time, T, and Cooling Time, t, for ^{235}U (Thermal)

Fig. 27. Percent Deviation of Decay Heating due to Neutron Absorption (U-235 Irradiation for 20000 hrs., No Depletion) $\Phi = 10^{13}$ n/cm^2 s

Fig. 28. Percent Deviation of Decay Heating due to Neutron Absorption (U-235 Irradiation for 20000 hrs., No Depletion $\Phi = 10^{14}$ n/cm^2 s

Fig. 29. Fractional deviation of decay-heat measurements and calculations from nominal values as determined by least-squares method

Fig. 30. Gamma heat from theoretical decay energies vs. cooling time

Fig. 31. - 36. Total gamma energy release per fission and gamma energy bin: comparison of calculations with experiments

Fig. 37. - 40. Total beta energy release per fission and beta energy bin: comparison of calculations with experiments

Fig. 41. Calculated decay heat compared to least-squares results:
ENDF/B-IV with ^{98}Zr corrected;
Same as above + mass 133 corrections;
Same as above + ^{130}Sn + ^{142}La corrected;
Same as above + ^{96}Y half-life corrected;

Fig. 42. Total Decay Power from U235 Thermal Burst

Fig. 43. Fractional gas content following a U235 fission pulse (fraction of total products)

Fig. 44. Fractional gas content following a PU239 fission pulse (fraction of total products)

Fig. 45. Fractional gas content following a U235 thermal irradiation of 20,000 h, no depletion (fraction of total products)

Fig. 46. Fractional deviation of gammy decay heat measurements and calculations from least-squares results

Fig. 47. Fractional deviation of beta decay heat measurements and calculations from least-squares results

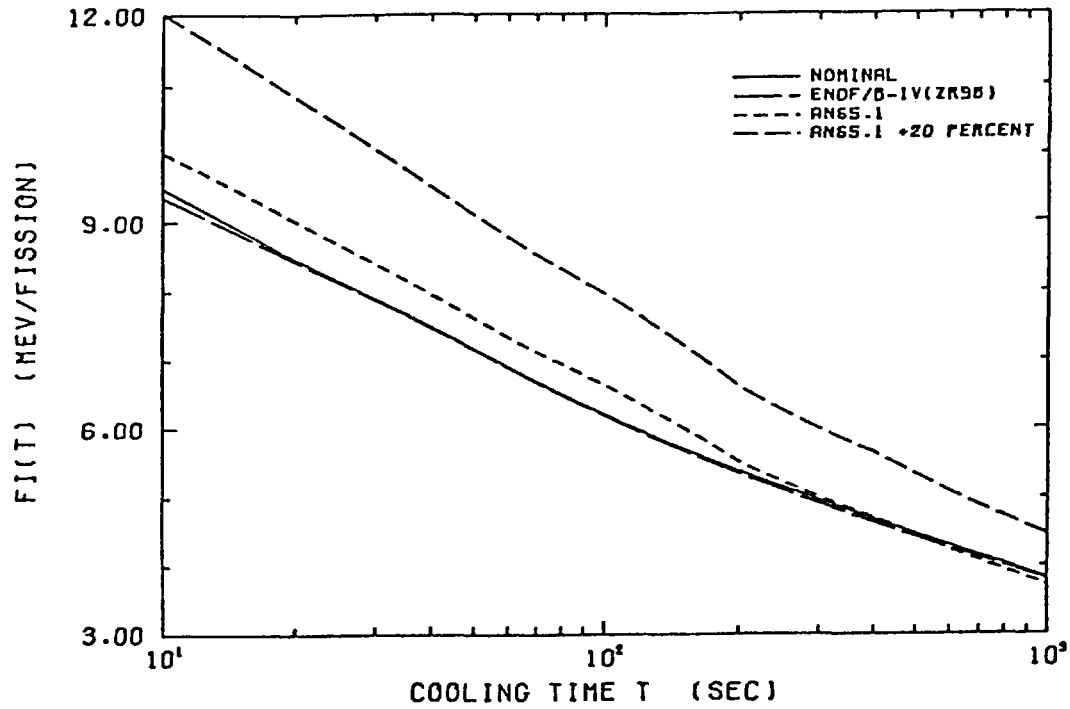

Fig. 1. Decay-Heat Comparisons With ANS 5.1 Standard (Infinite ^{235}U Constant Fission Rate, No Depletion and No Absorption)

Fig. 2. ^{235}U Decay-Heat Comparisons Following Extrapolation To An Infinite Fission Interval (Constant Fission Rate, No Depletion and No Absorption)

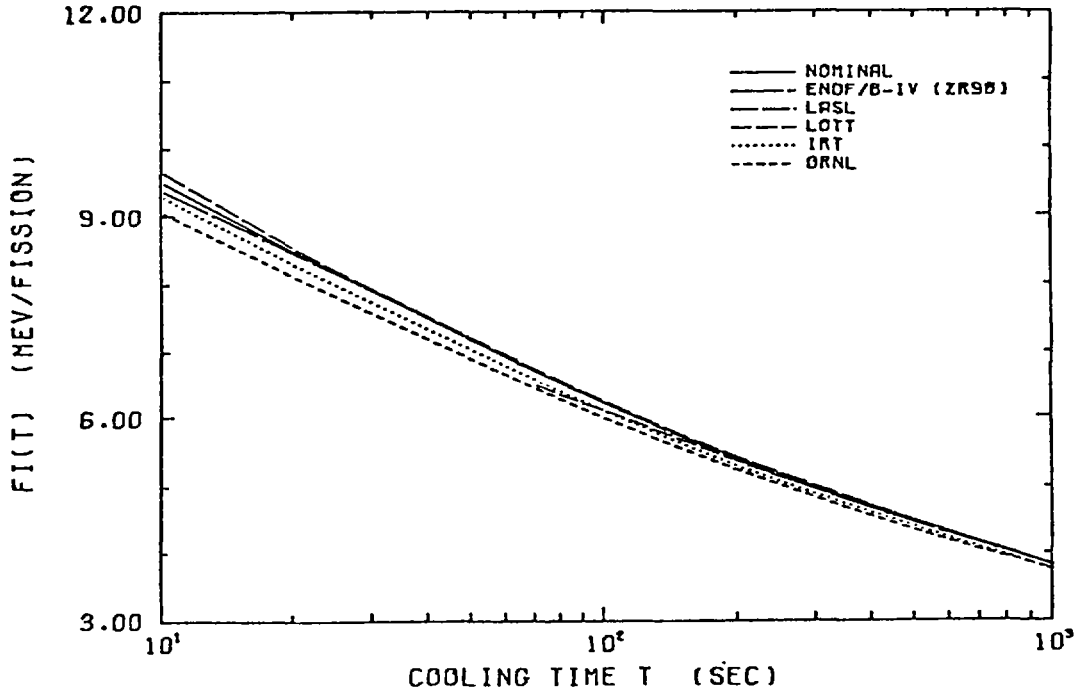

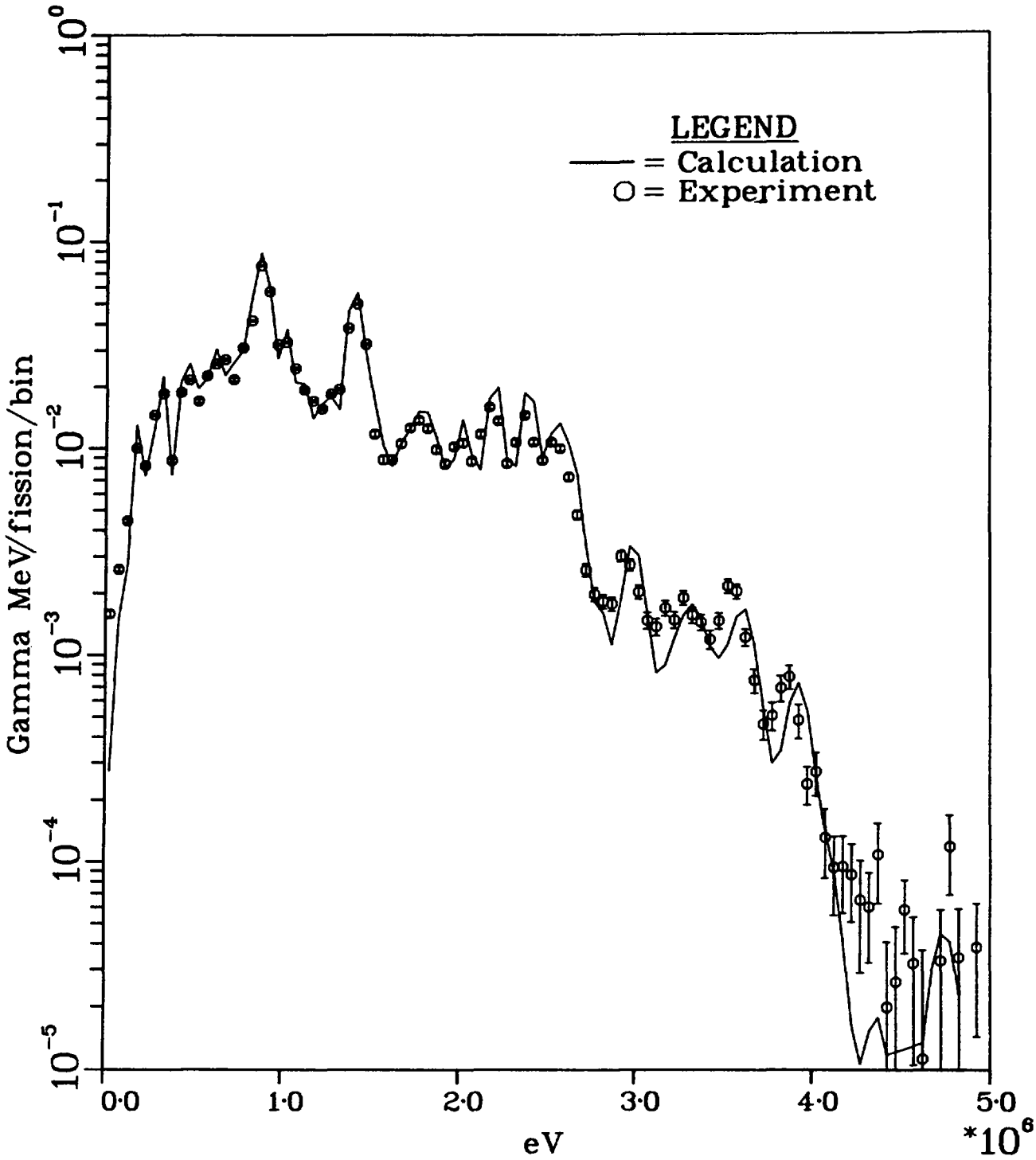

Fig. 3 Comparison of calculation with LASL 5.56 h irradiation, 1524 s decay

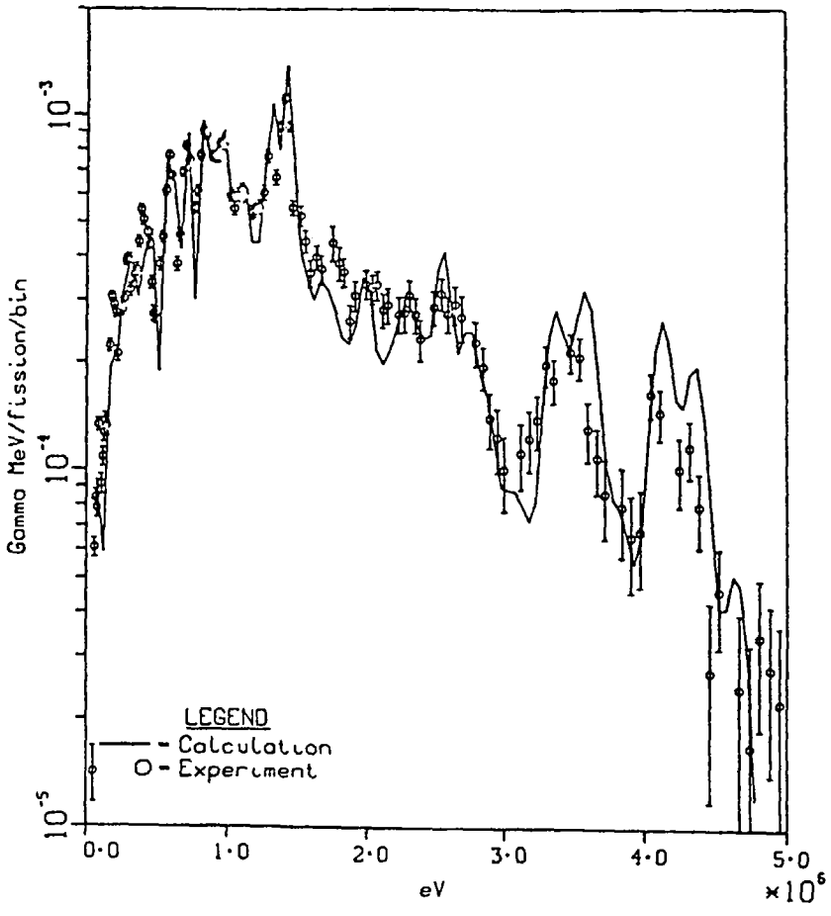

Fig. 4 Comparison of calculation with ORNL 10 s irradiation experiment, 184.7 s decay

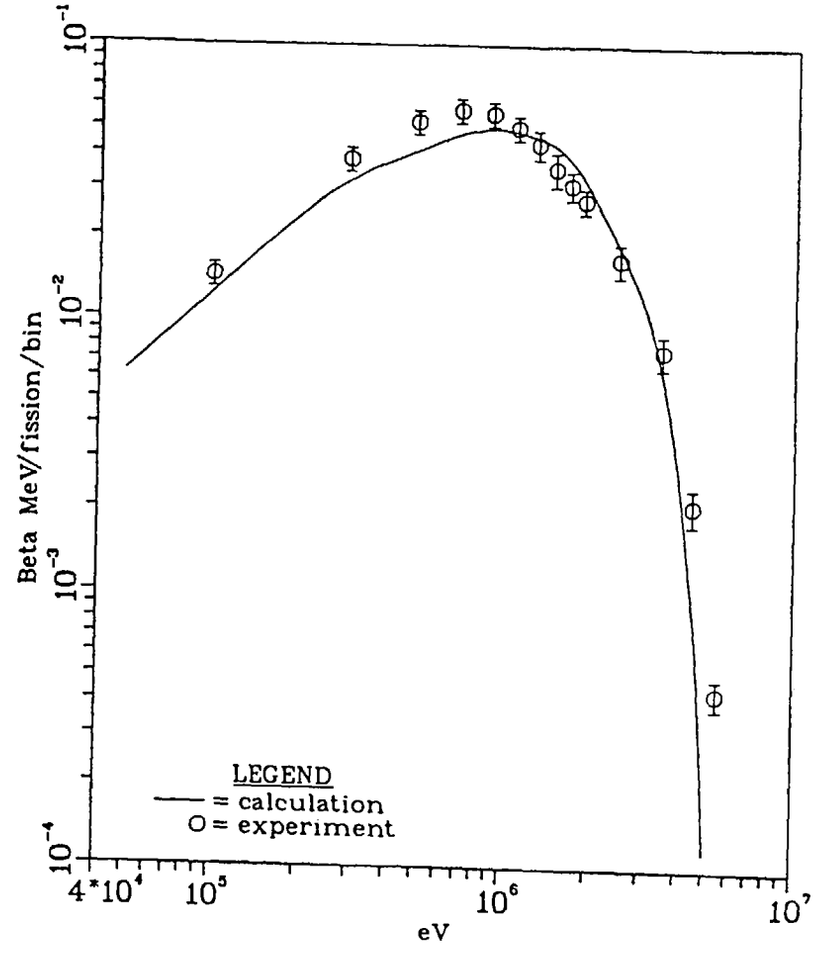

Fig. 5 Comparison of calculation with UI 8 h irradiation, 960 s decay

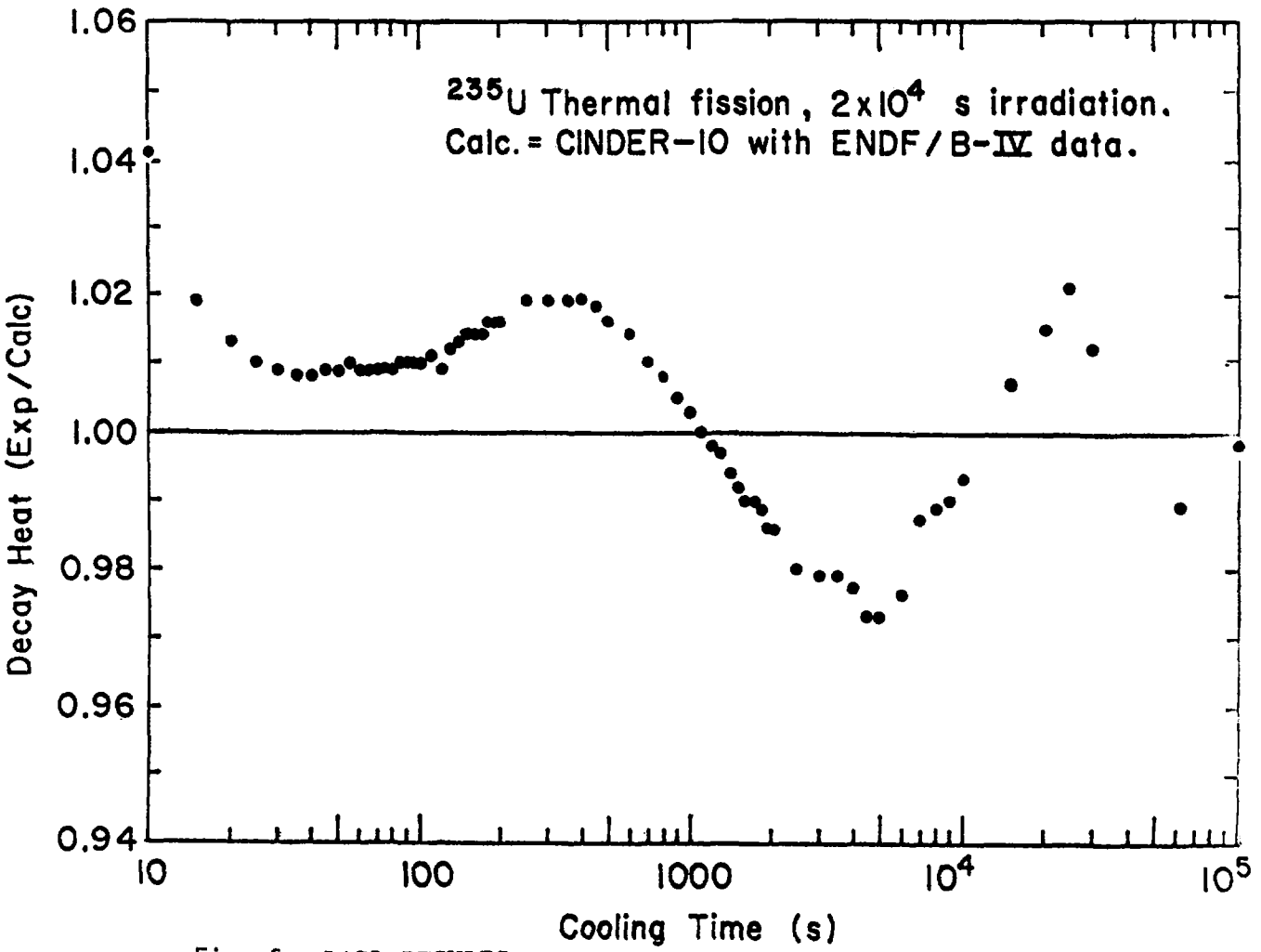

Fig. 6. LASL RESULTS

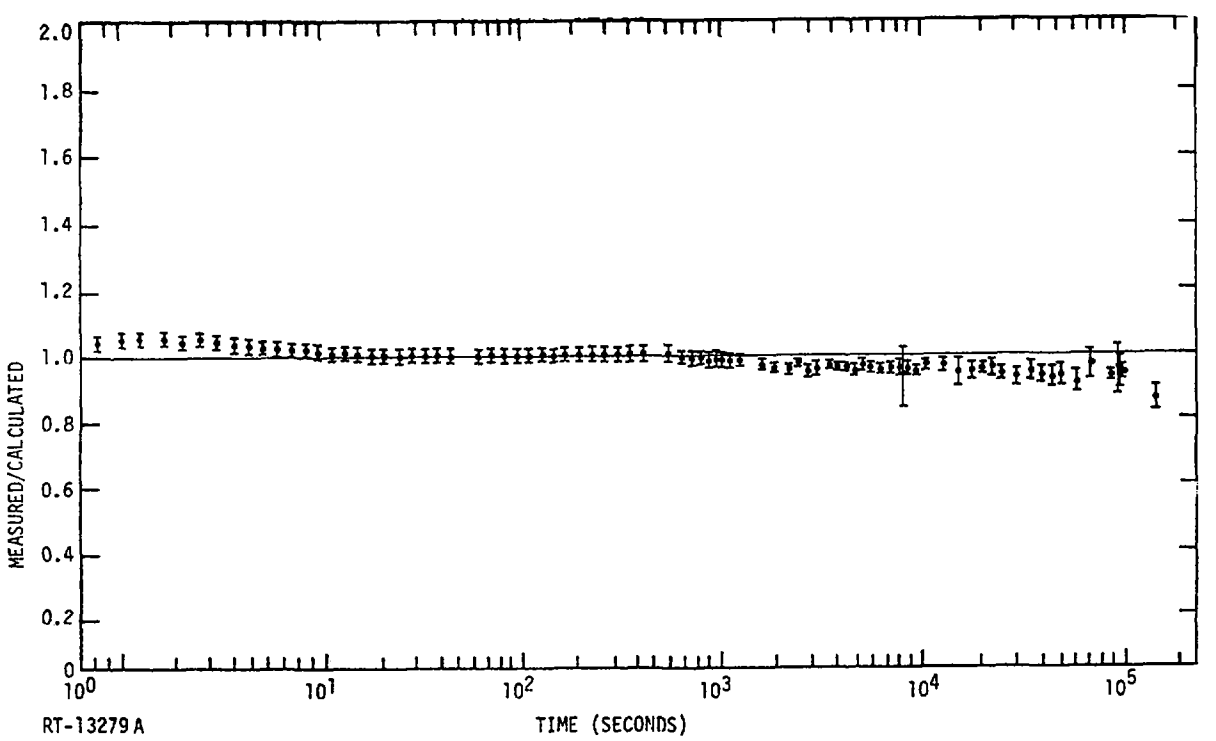

Fig. 7. Twenty-four-hour fission product decay heat data divided by calculated value (IRT RESULTS, U235 THERMAL)

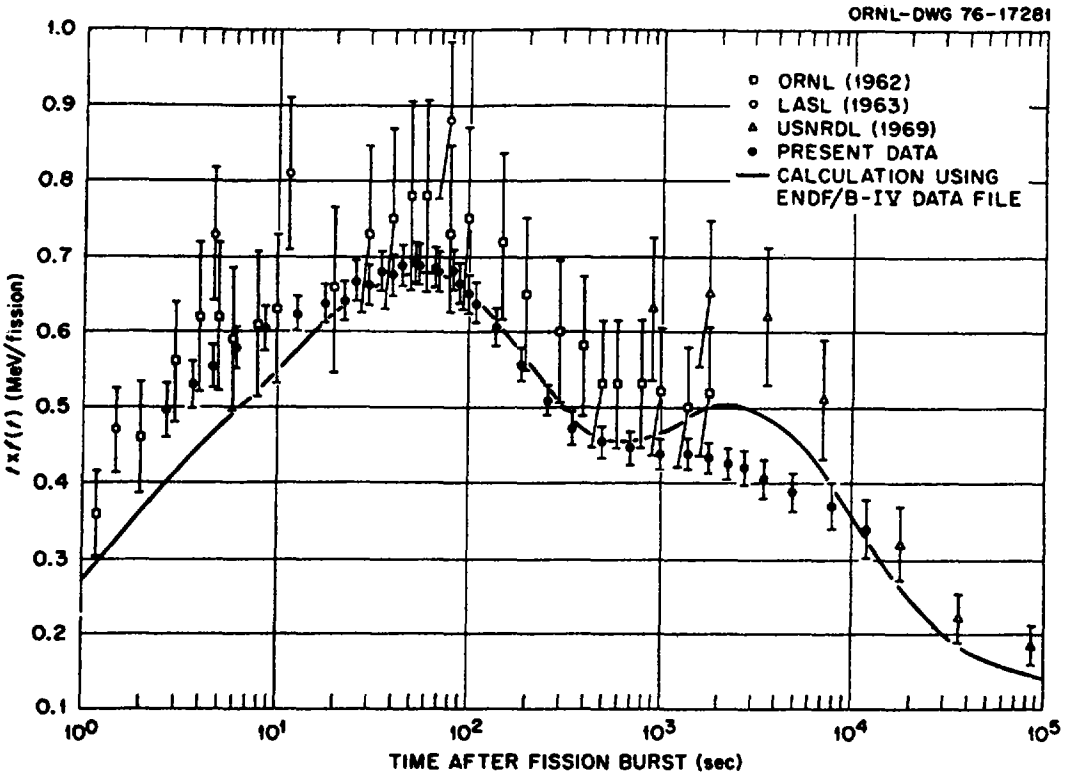

Fig. 8 Photon energy emission rate for thermal-neutron fission of ^{235}U from results of the present work (solid circles).

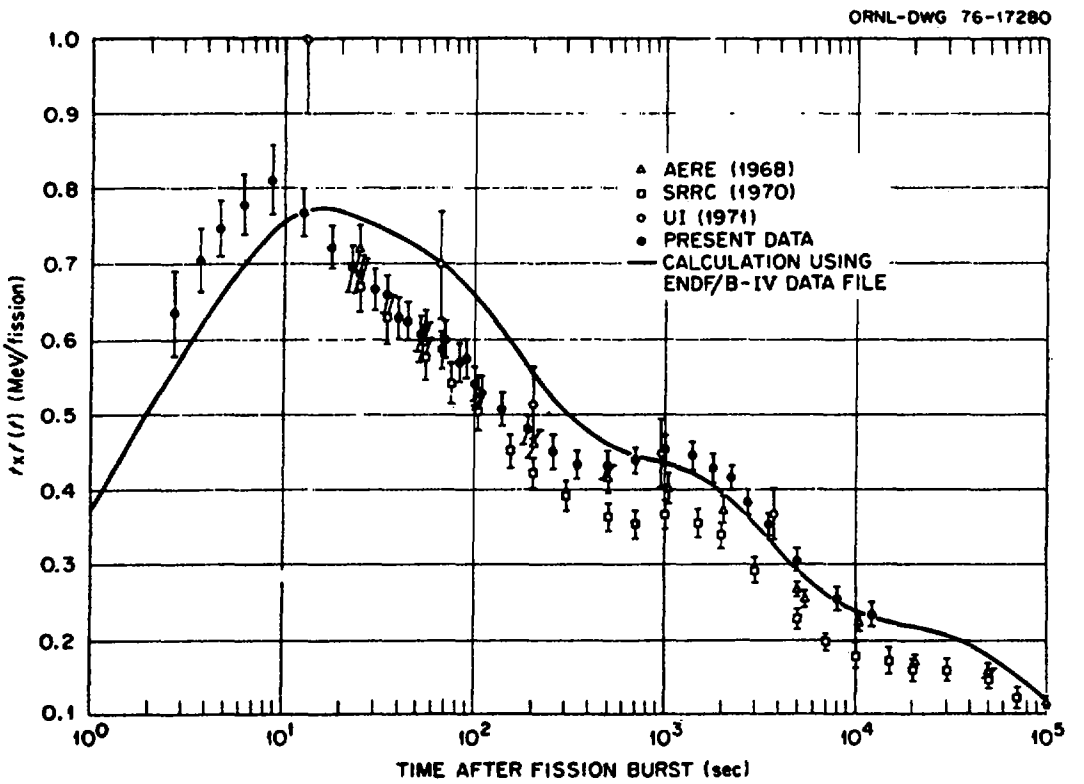

Fig. 9 Beta energy emission rate for thermal-neutron fission of ^{235}U from results of the present work (solid circles).

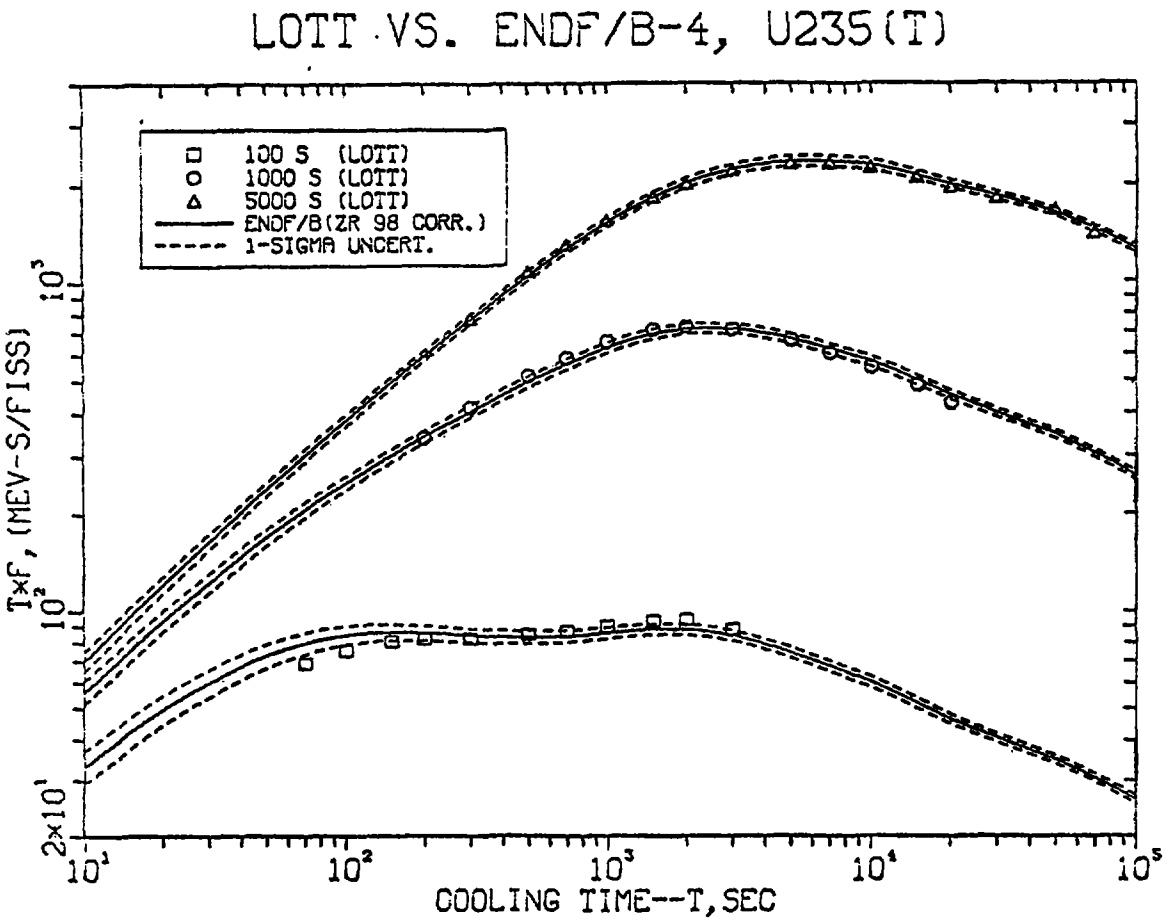

Fig. 10. Total integral afterheat (times time) for U235T

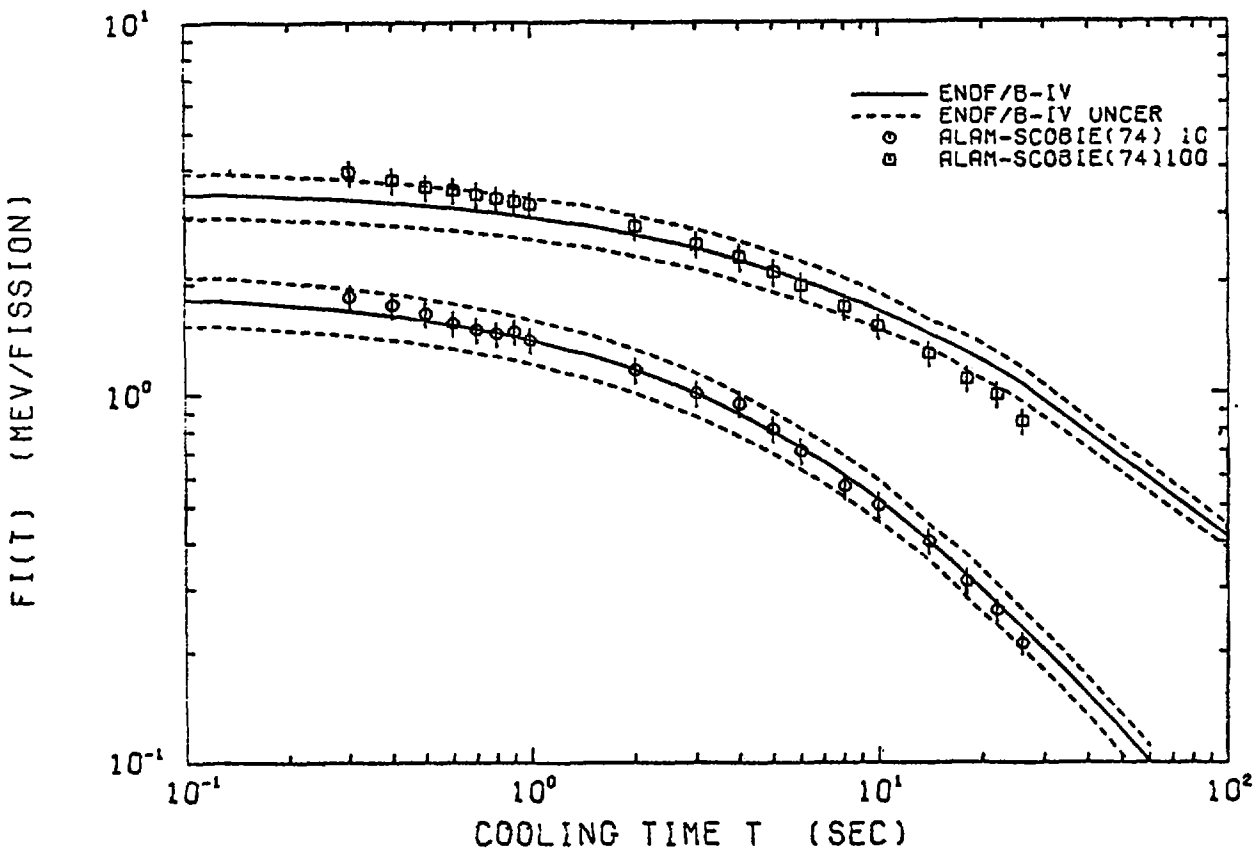

Fig. 11. BETA INTEGRAL AFTERHEAT U235T
10S AND 100S IRRADIATIONS

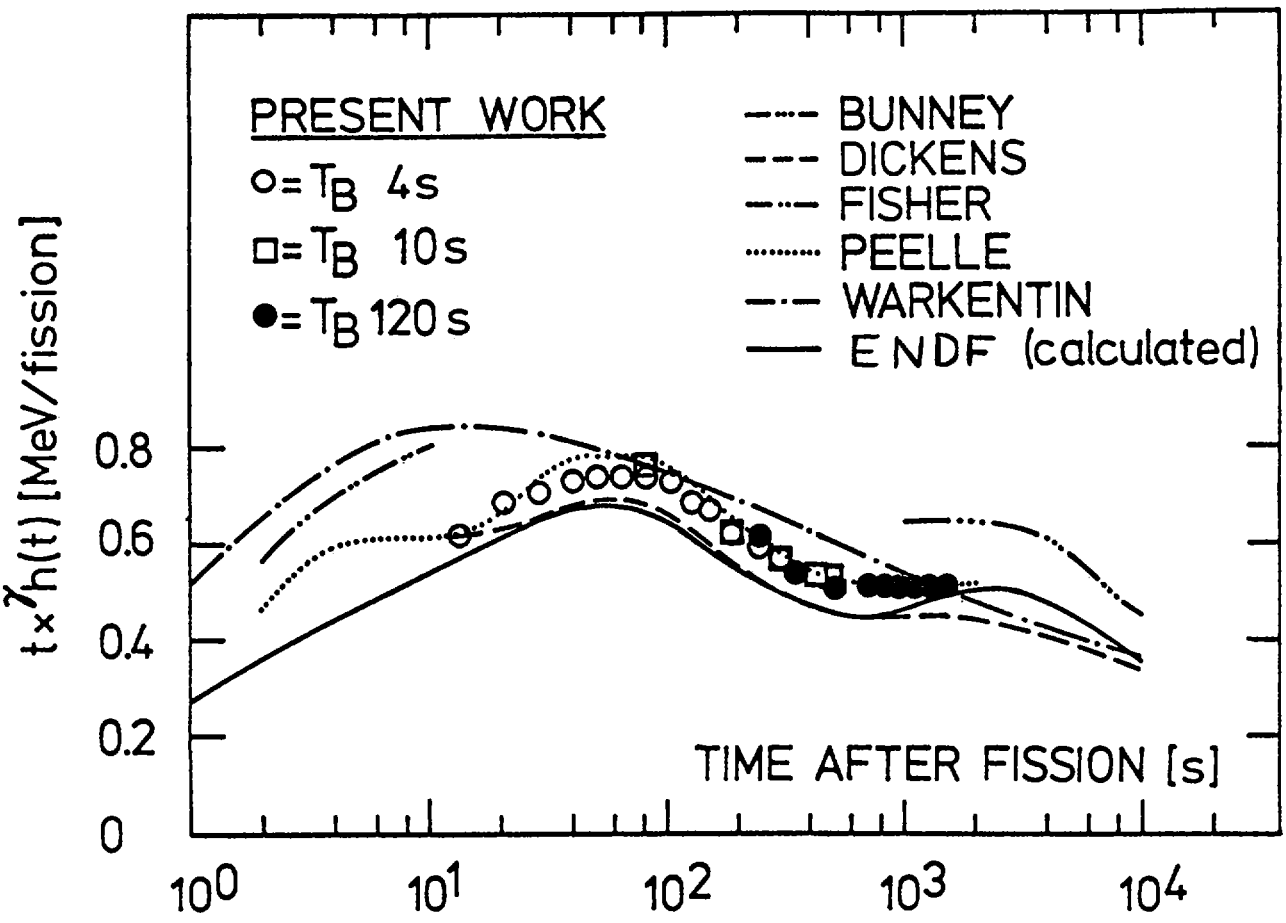

Fig. 12. GAMMA ENERGY RELEASE – STUDSVIK RESULTS (= 'PRESENT WORK' IN FIG.)

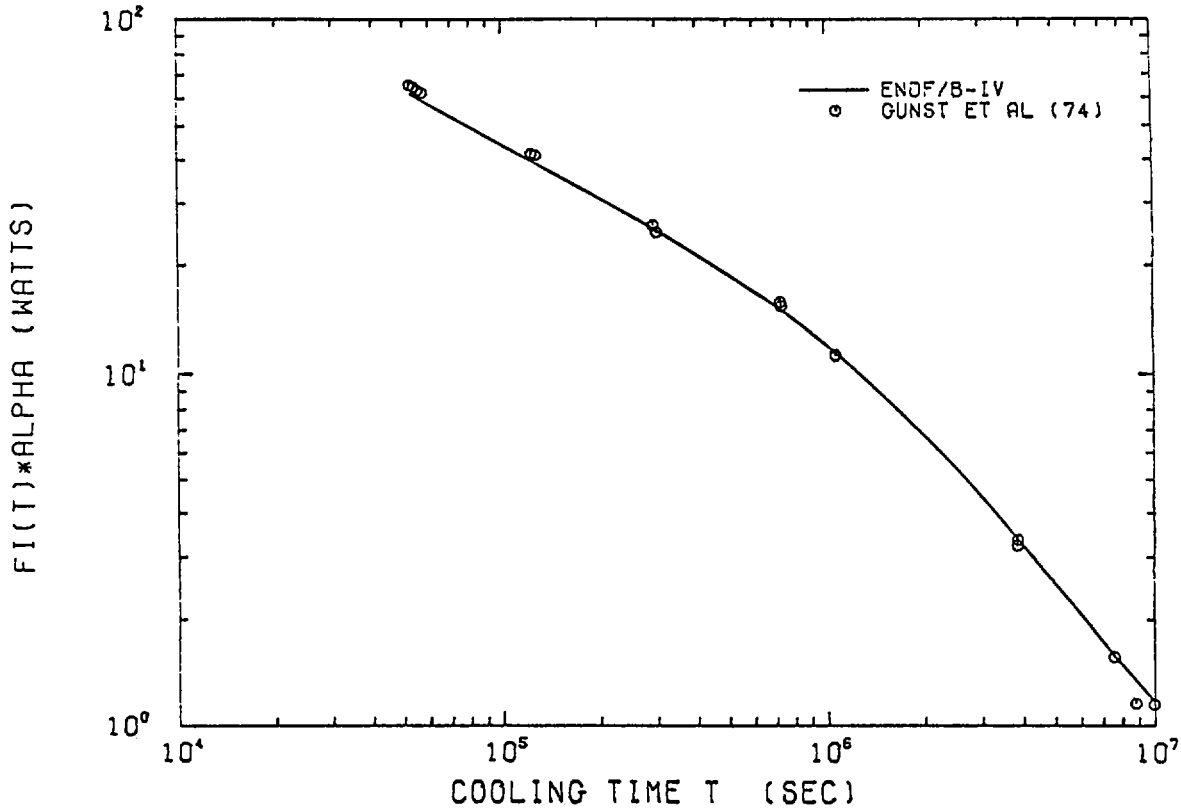

Fig. 13.CALORIMETRIC RESULTS U235T
HIGH BURNUPS IN MTR AND ATR

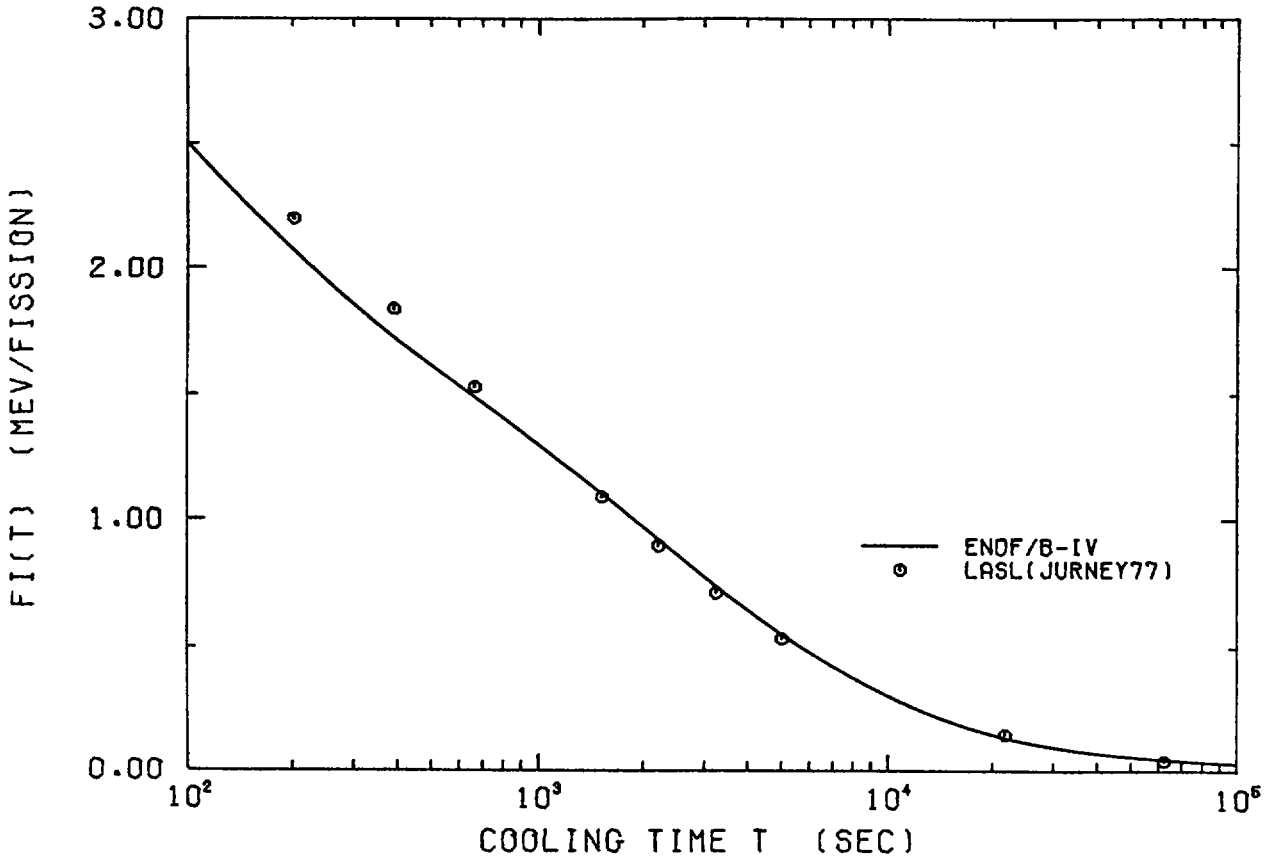

Fig. 14. Gamma integral afterheat U235T for 20000s irradiation

Fig. 15. Total integral afterheat U235T

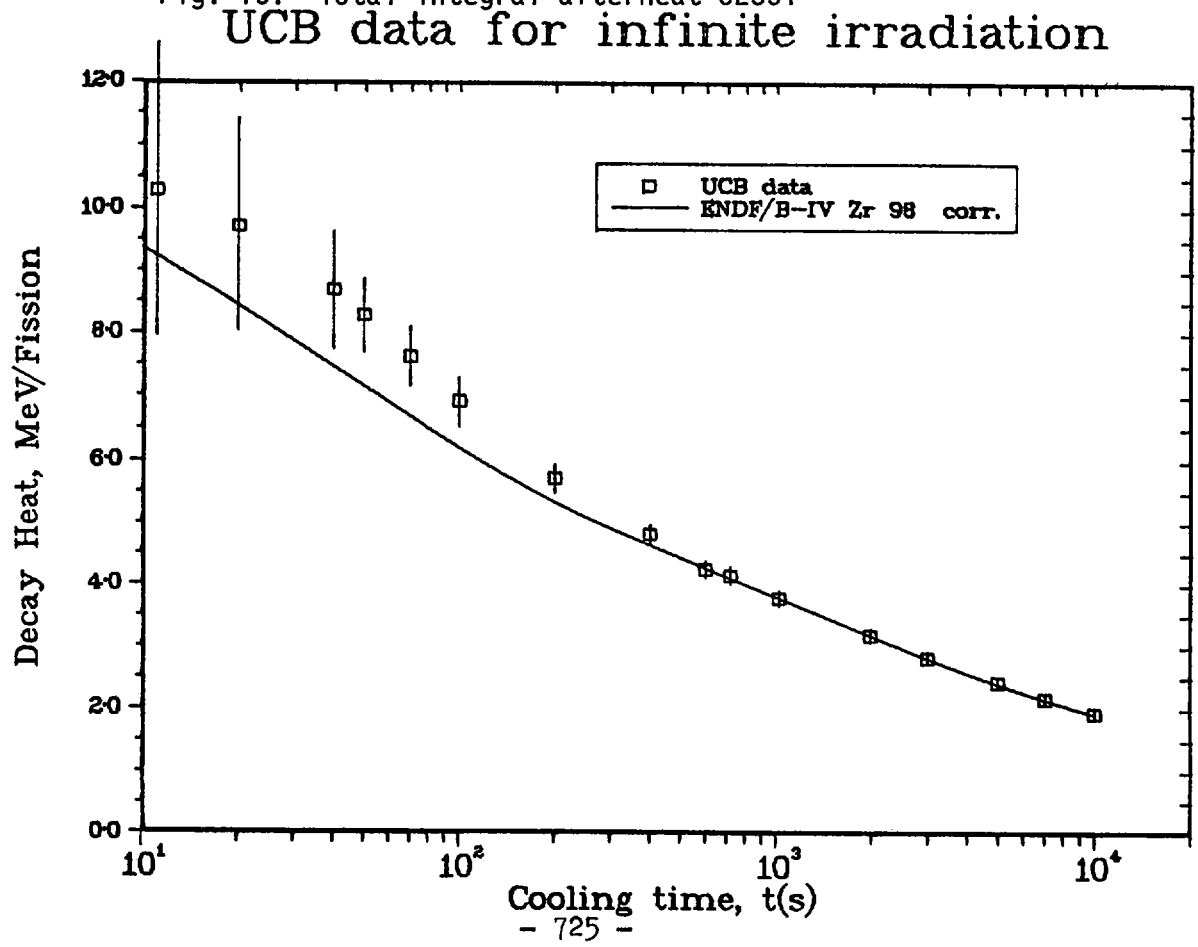

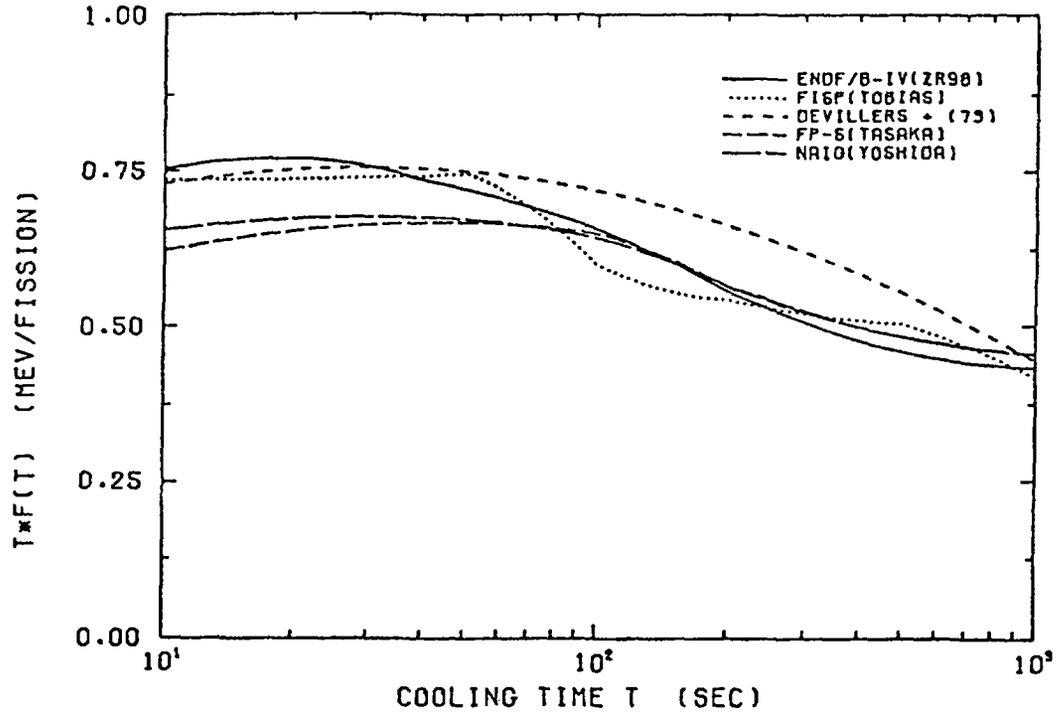

Fig. 16. Beta differential after heat calculations for U235T

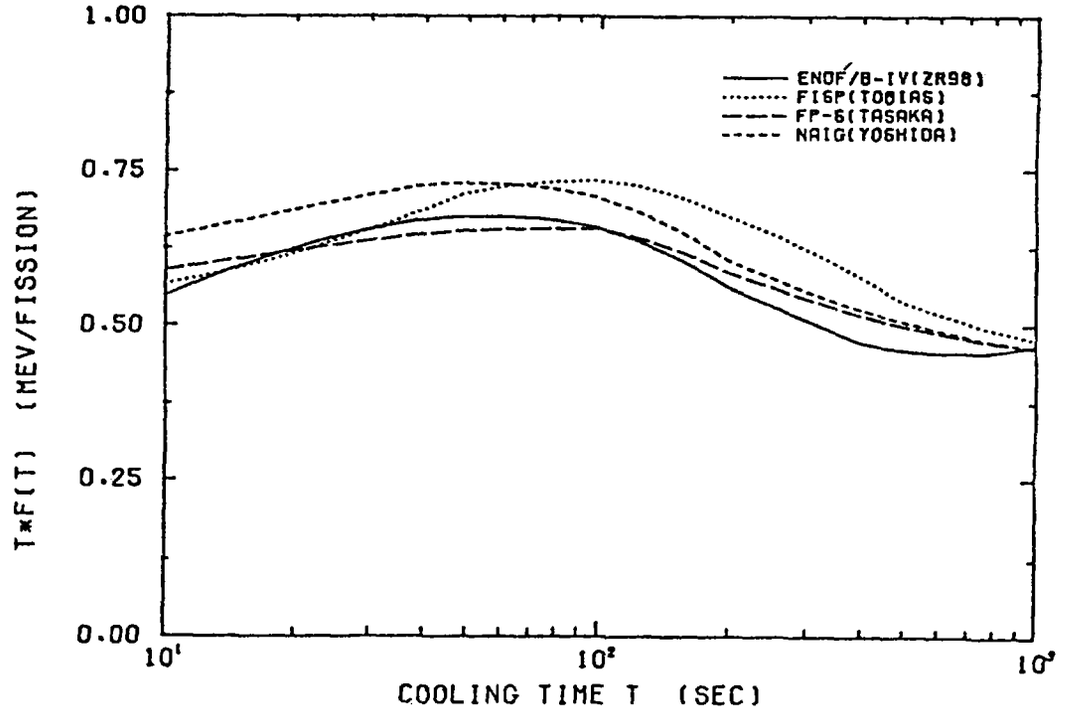

Fig. 17. Gamma differential afterheat calculations for U235T

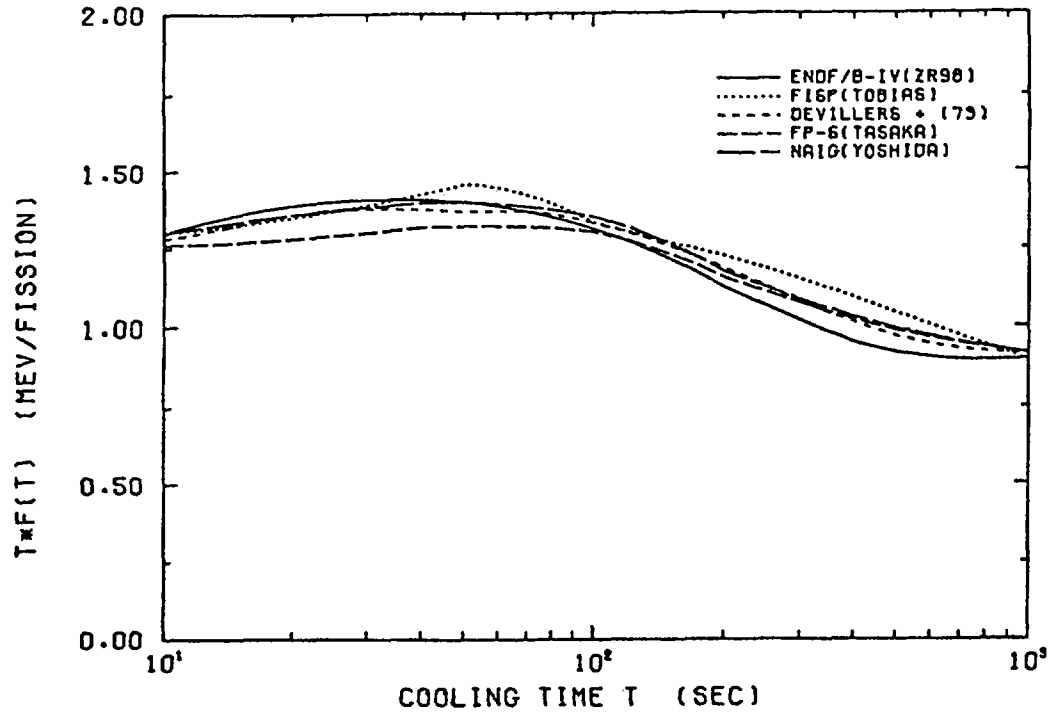

Fig. 18. Total differential afterheat calculations for U235T

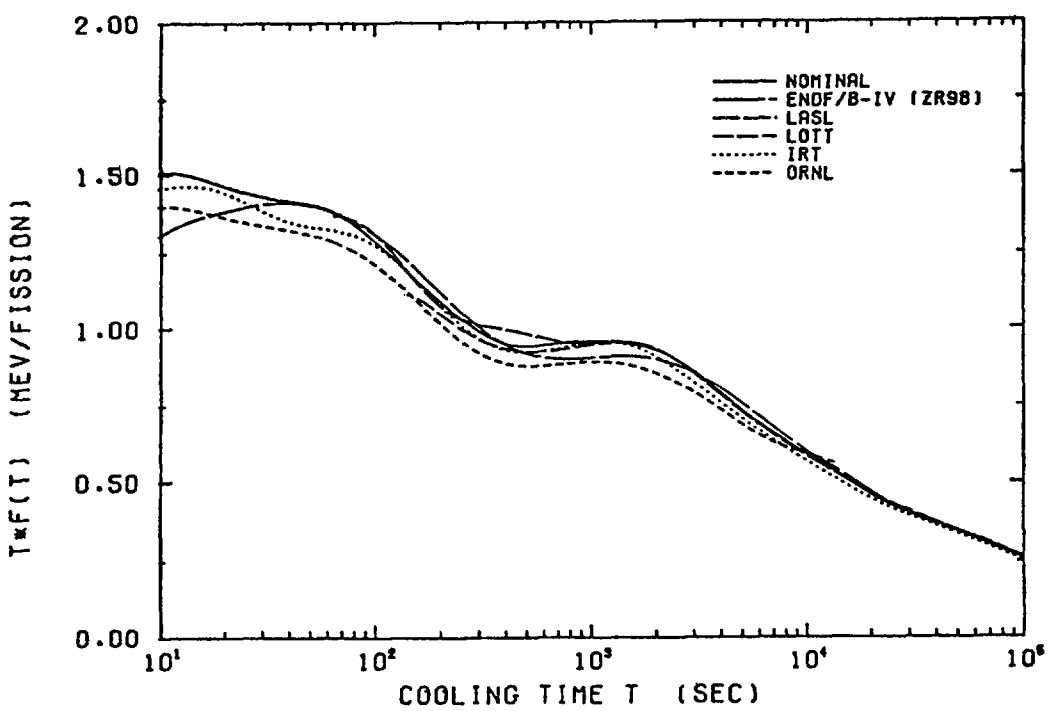

Fig. 19. Total differential afterheat functions unfolded from experiment

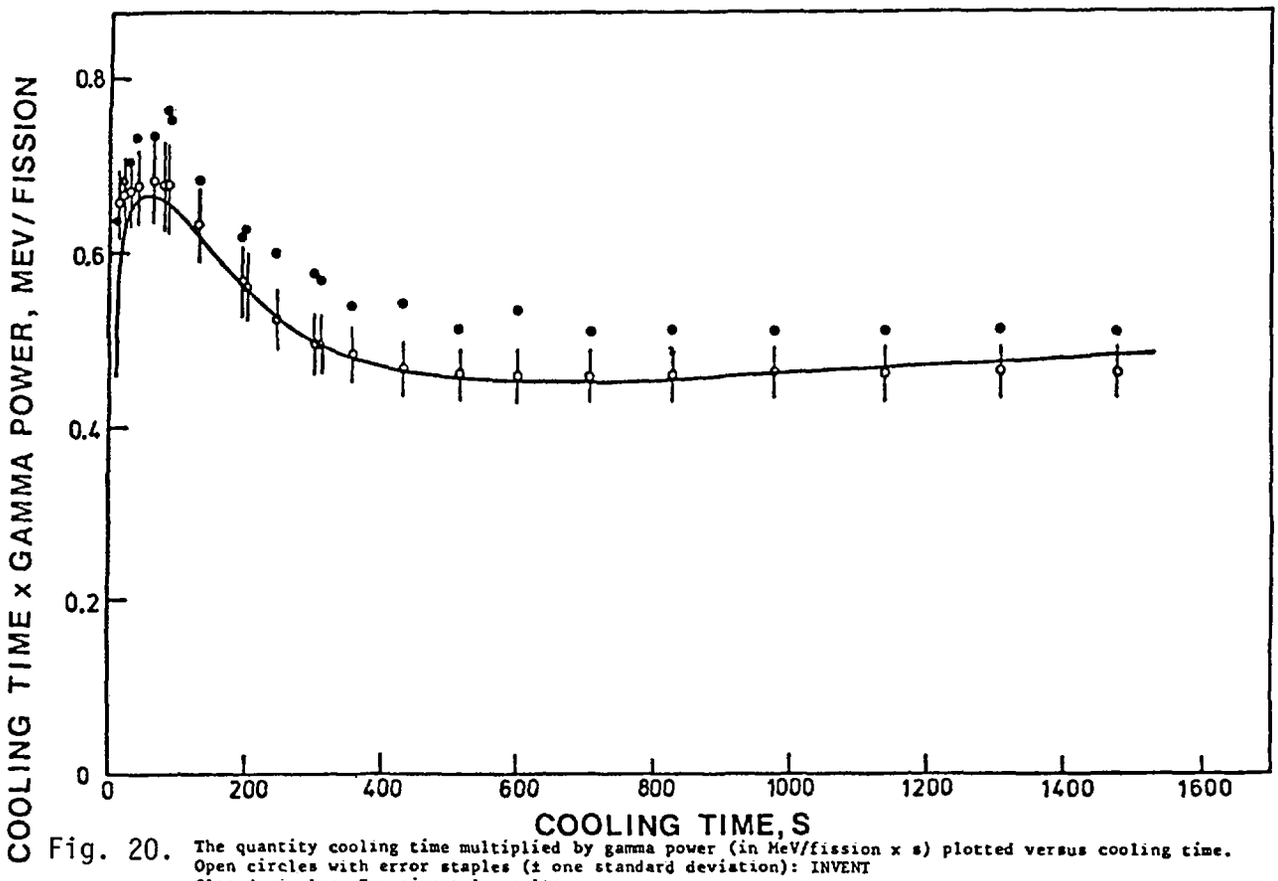

Fig. 20. The quantity cooling time multiplied by gamma power (in MeV/fission x s) plotted versus cooling time.
Open circles with error staples (± one standard deviation): INVENT
Closed circles: Experimental results
Full curve: ENDF calculation

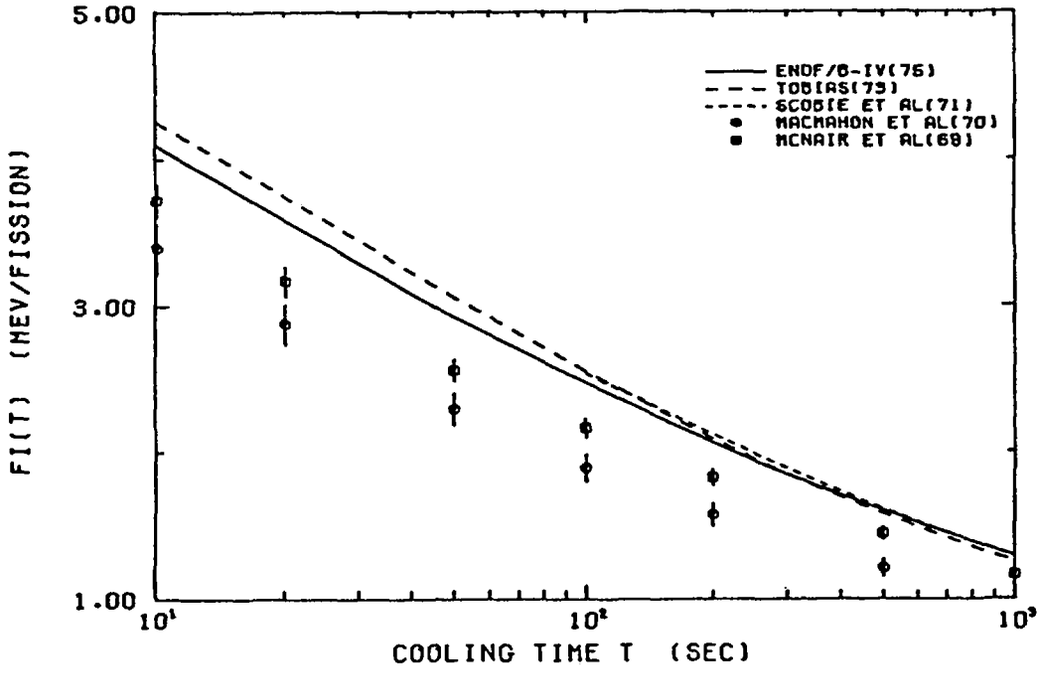

Fig. 21. Beta integral afterheat for U235T for irradiation of 10^5s

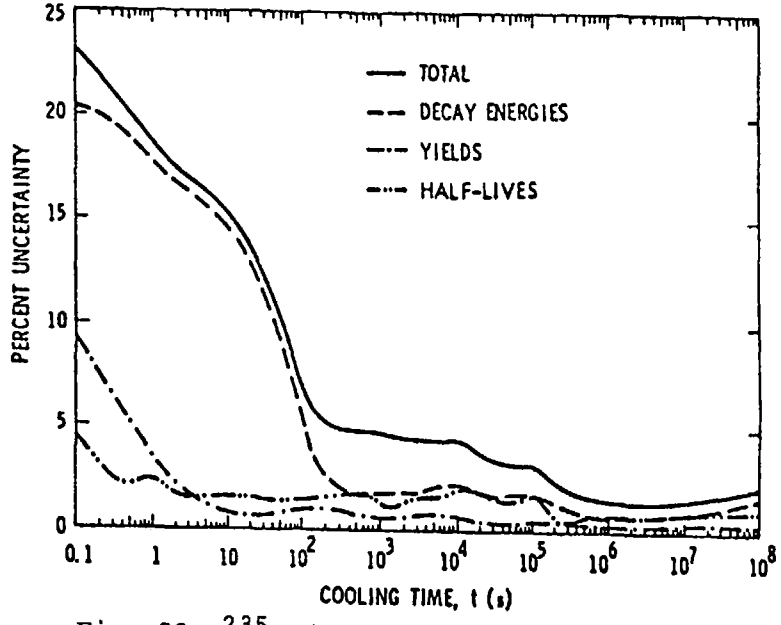

Fig. 22 ^{235}U (Thermal) T = 0 s

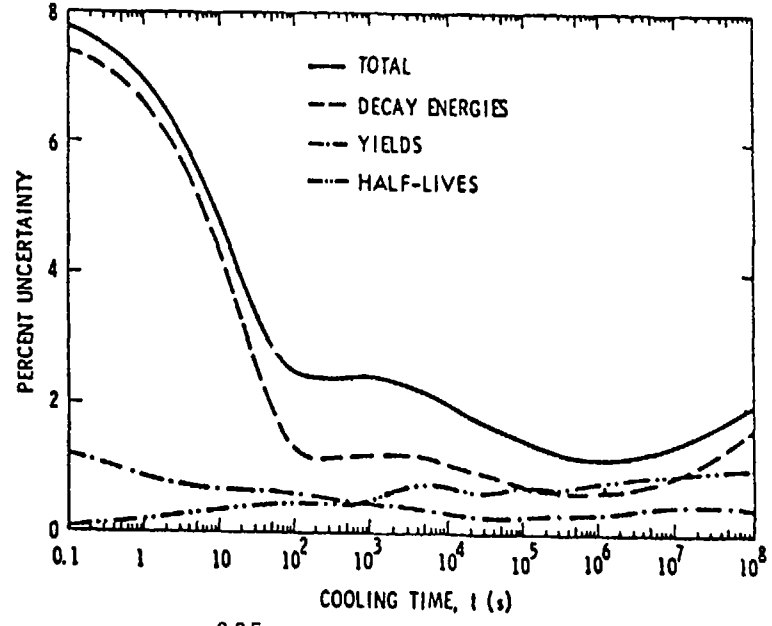

Fig. 23 ^{235}U (Thermal) T = 10^7 s

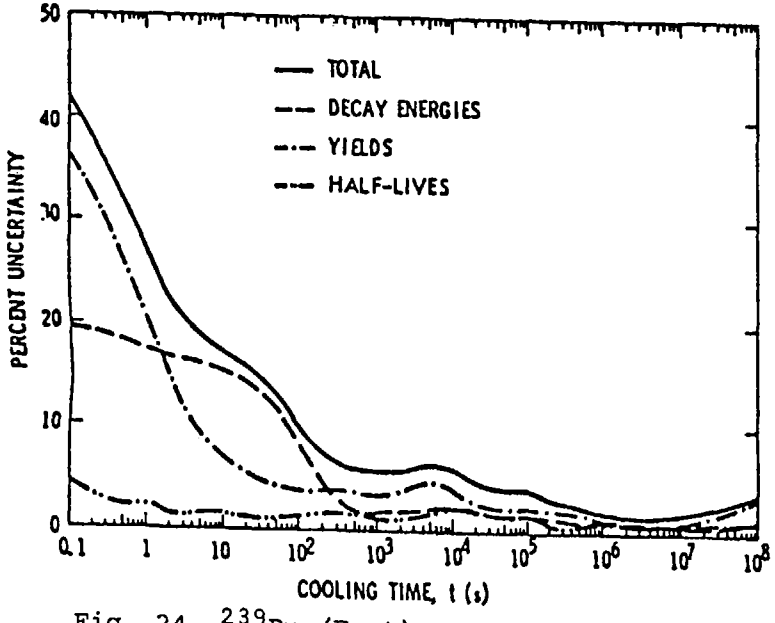

Fig. 24 ^{239}Pu (Fast) T = 0 s

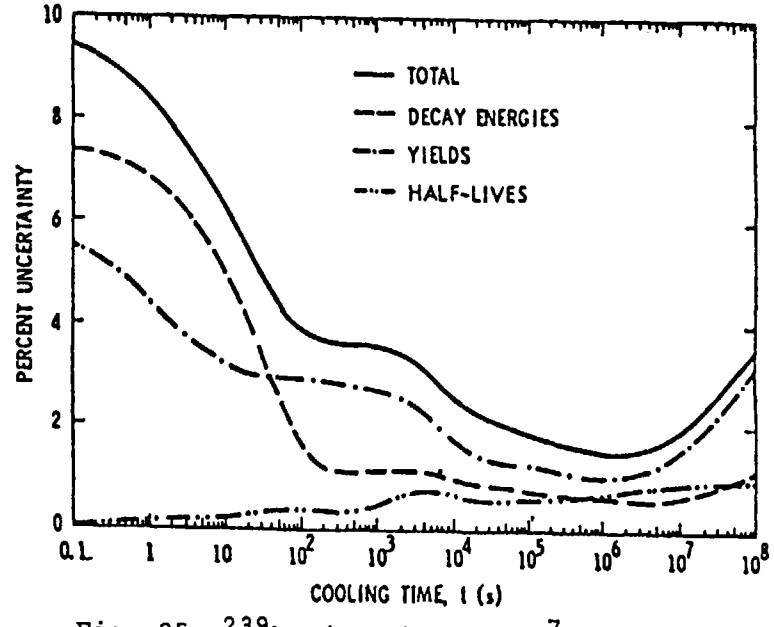

Fig. 25 ^{239}Pu (Fast) T = 10^7 s

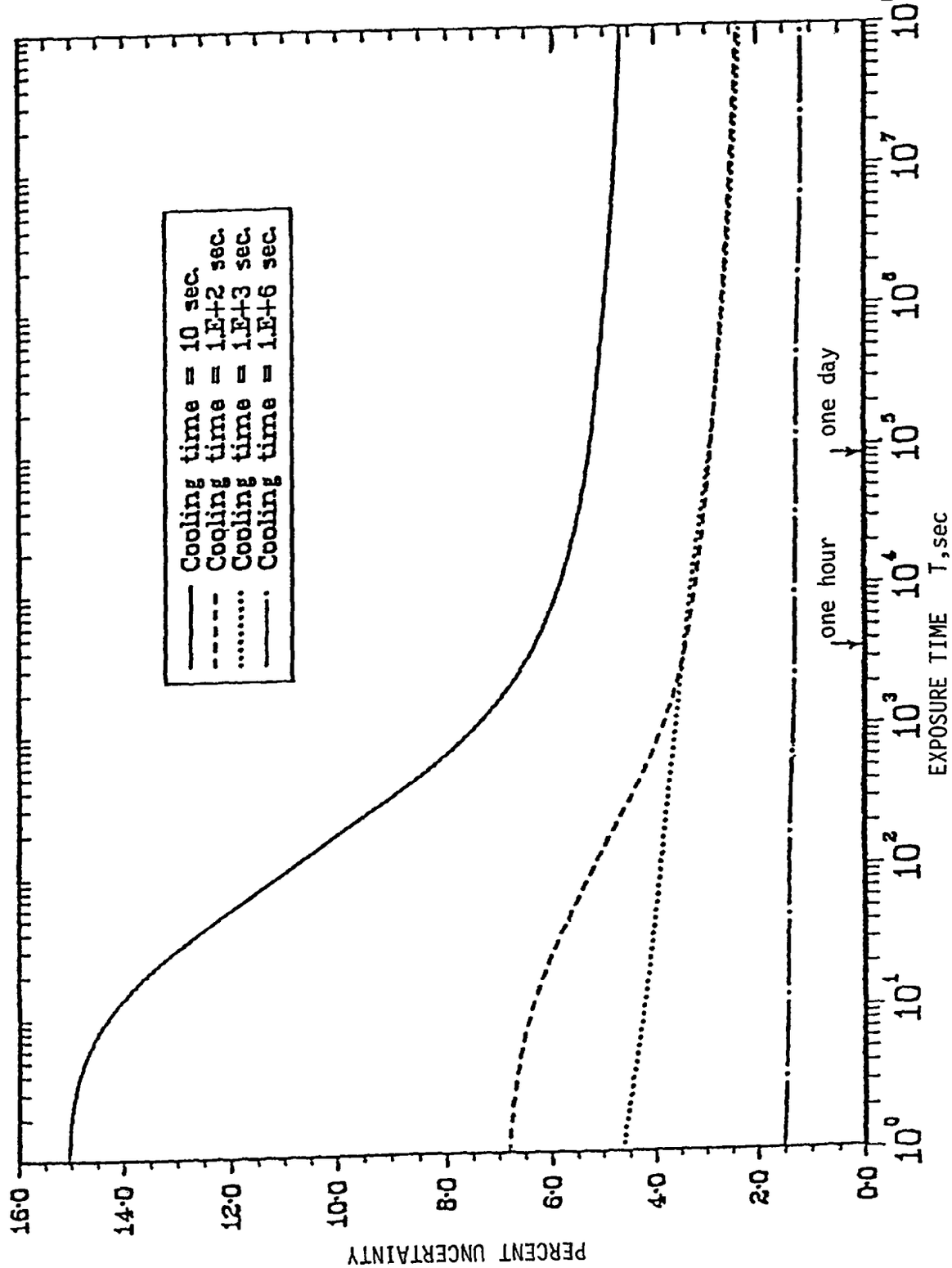

Fig. 26. Decay Heat Uncertainty vs. Exposure Time, T, and Cooling Time, t, for ^{235}U (Thermal)

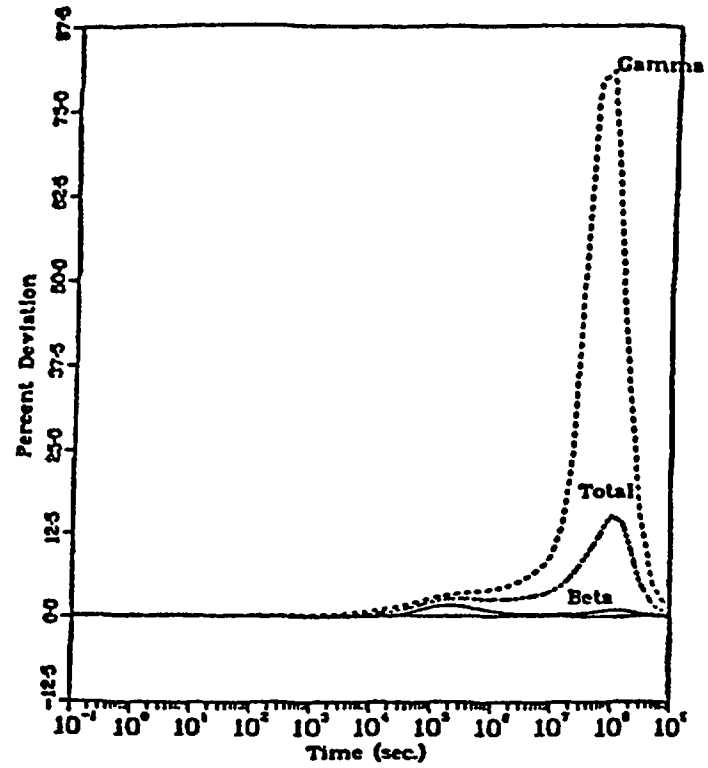

Fig. 27 Percent Deviation of Decay Heating due to Neutron Absorption (U-235 Irradiation for 20000 hrs., No Depletion) $\phi = 10^{13}$

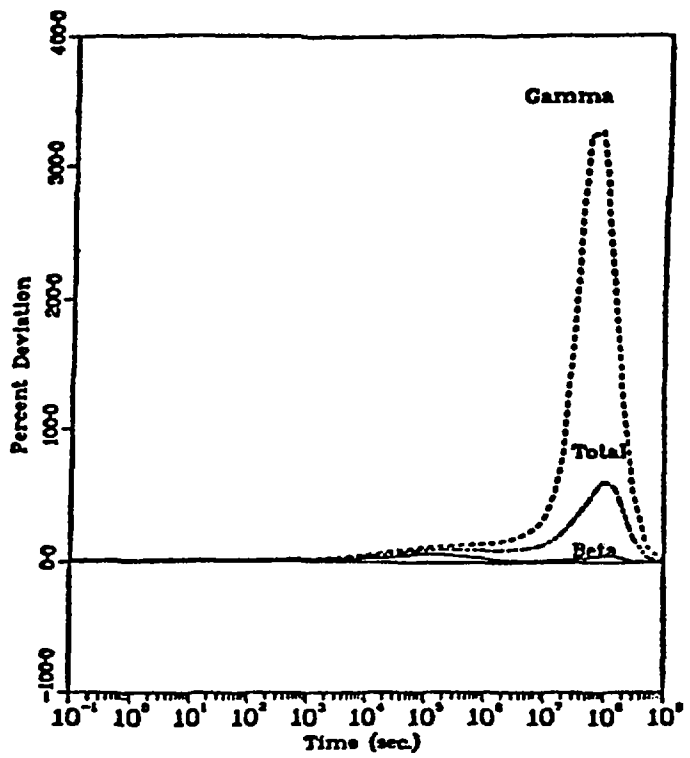

Fig. 28 Percent Deviation of Decay Heating due to Neutron Absorption (U-235 Irradiation for 20000 hrs., No Depletion) $\phi = 10^{14}$

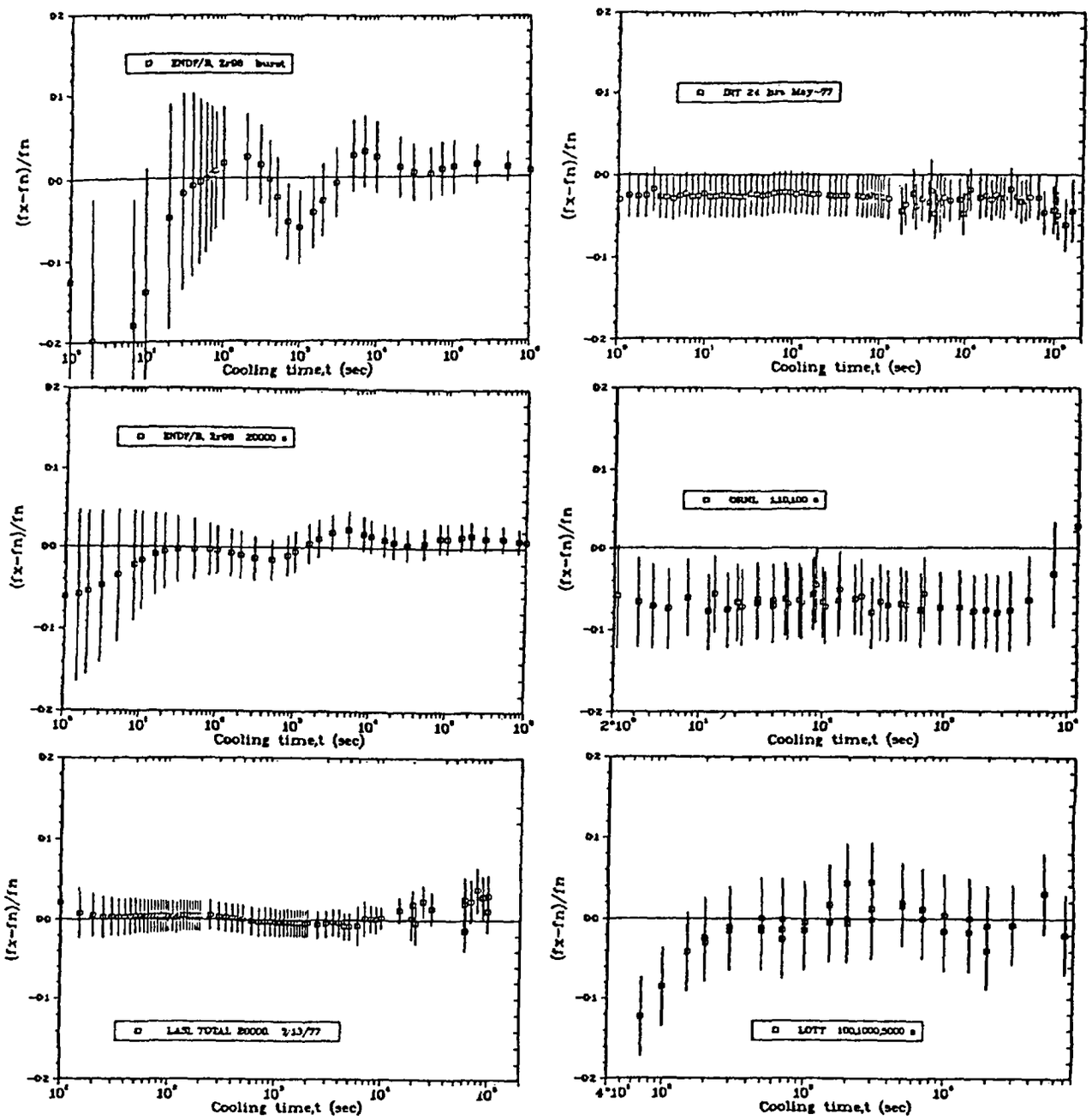

Fig. 29 Fractional deviation of decay-heat measurements and calculations from nominal values as determined by least-squares method.

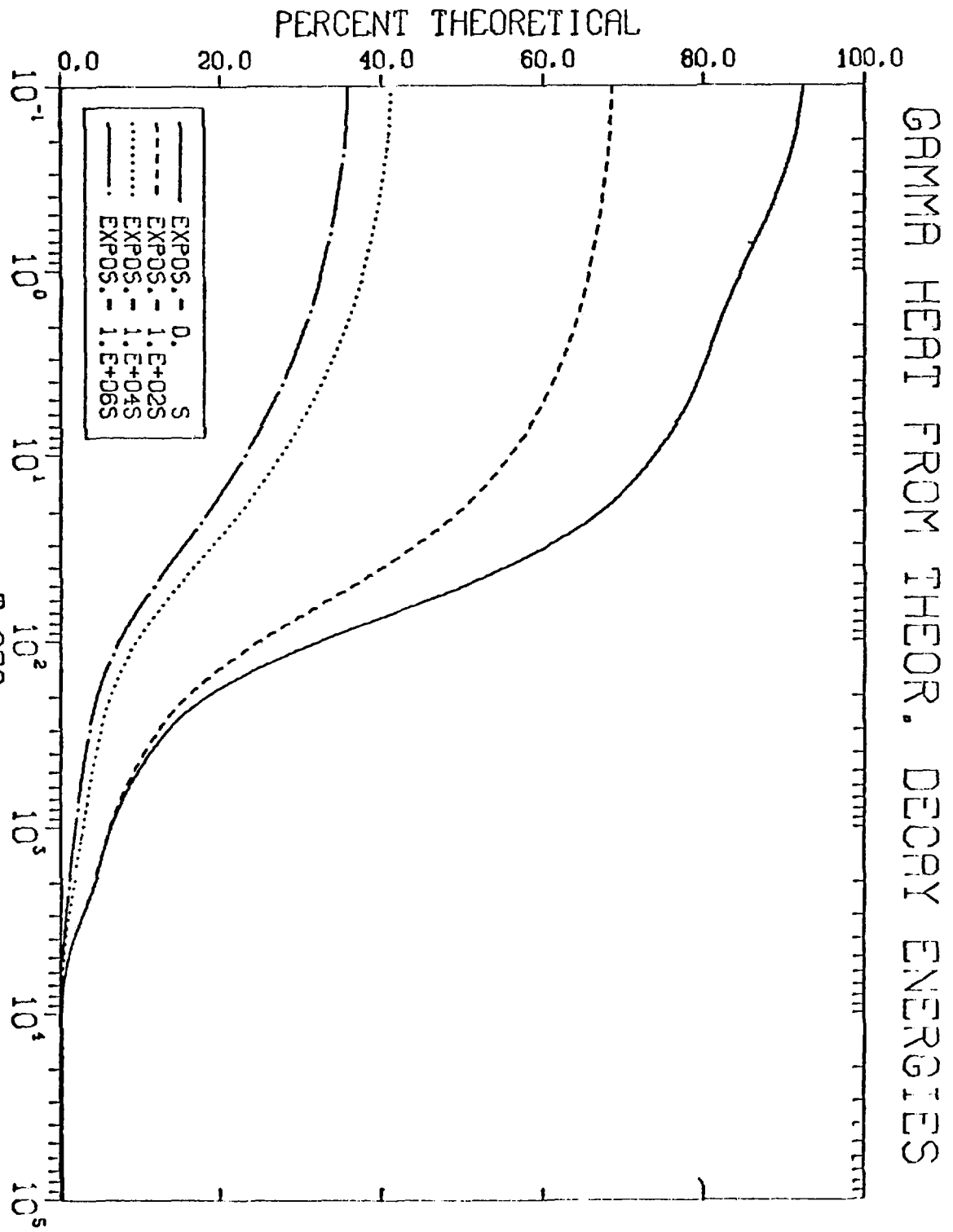

Fig. 30. Gamma heat from theoretical decay energies vs. cooling time

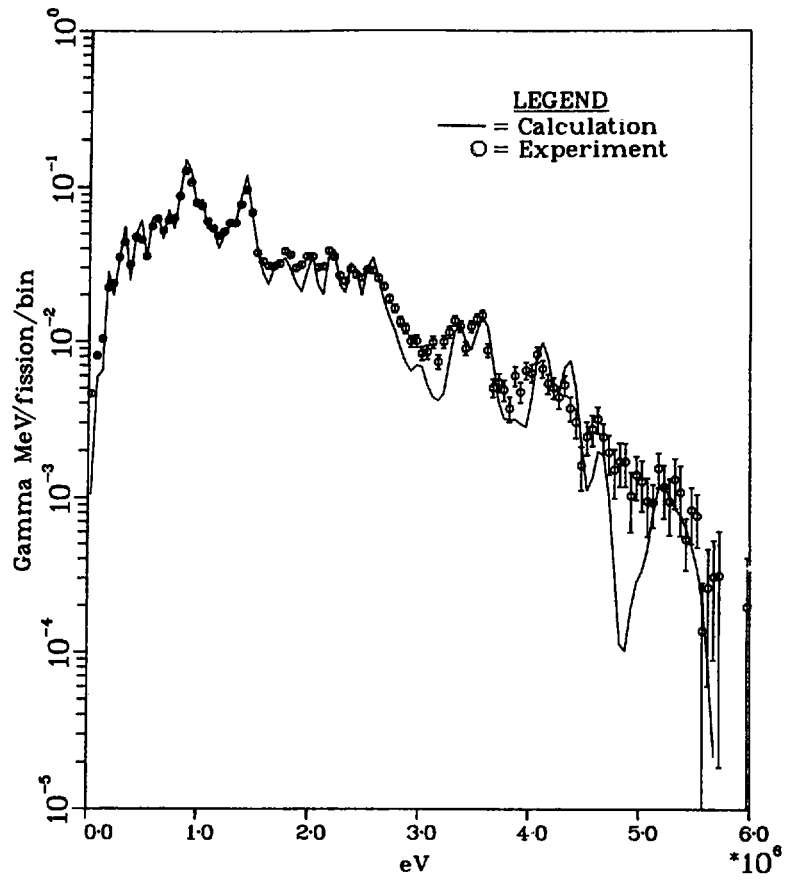

Fig. 31 Comparison of calculation with LASL 5.56 h irradiation, 70 s decay

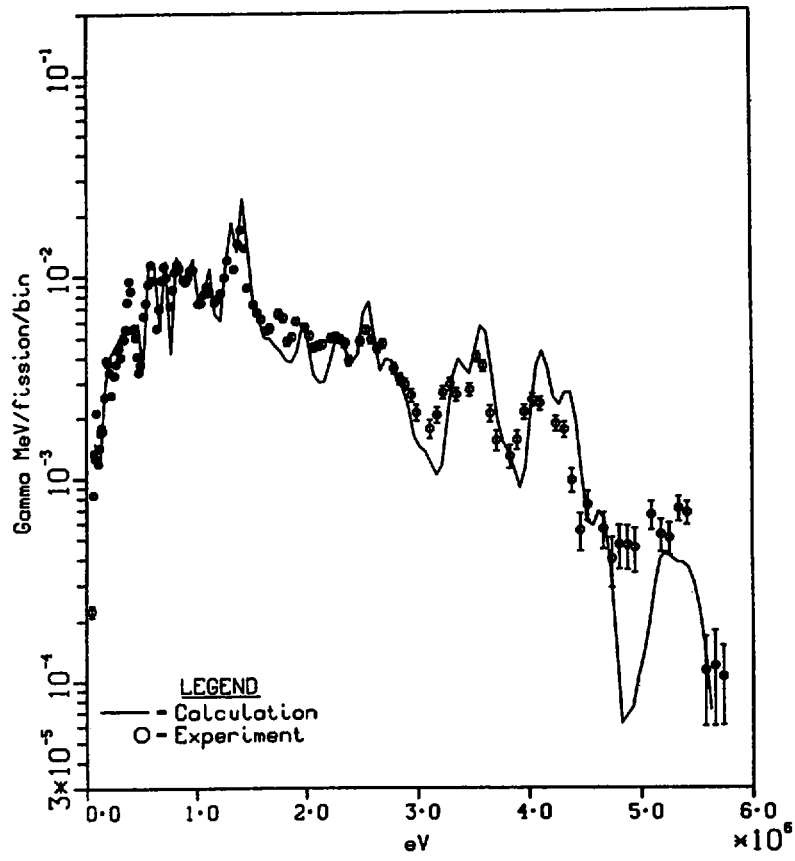

Fig. 32 Comparison of calculation with ORNL 100 s irradiation experiment, 90.0 s decay

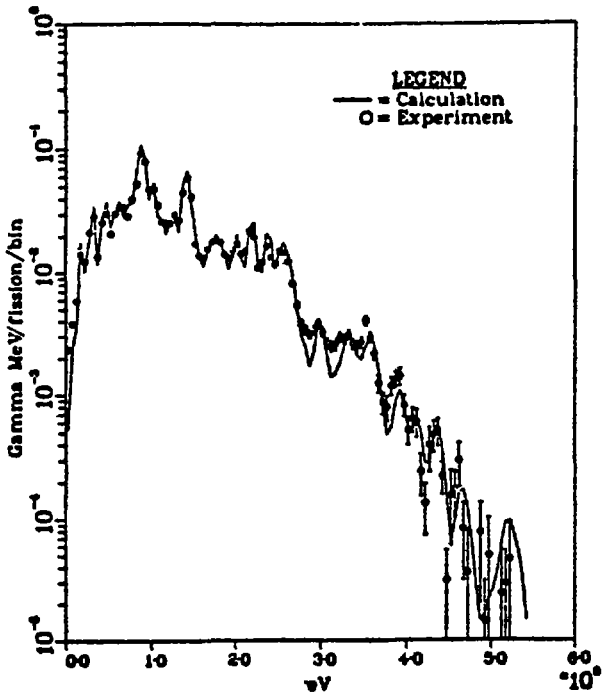

Fig. 33 LASL 5.56 h IRRAD, 660 s Decay

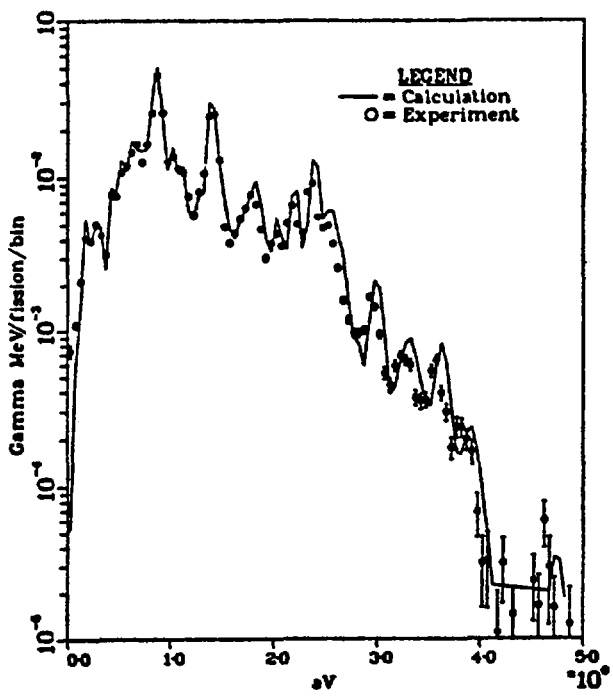

Fig.34 LASL 5.56 h IRRAD, 5000 s Decay

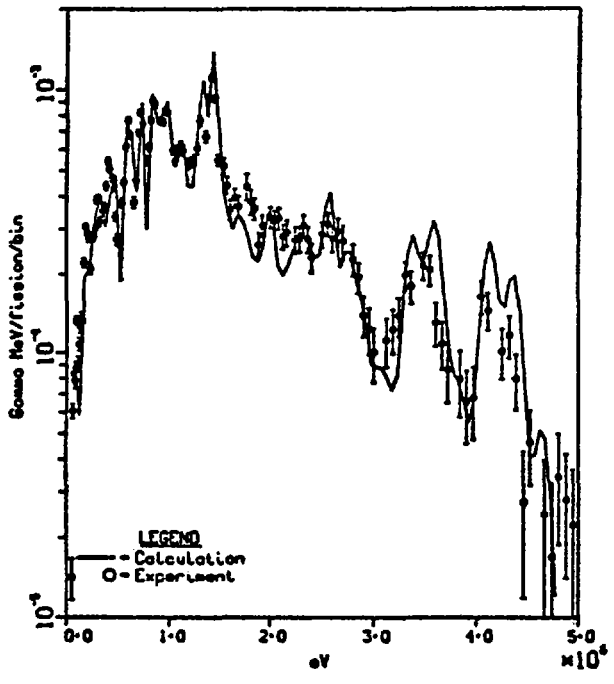

Fig. 35 ORNL 10 s IRRAD, 184.7 s Decay

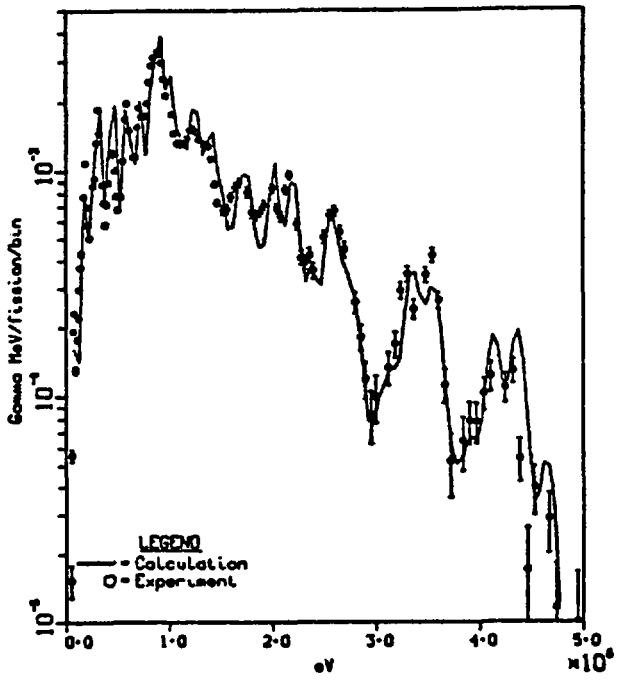

Fig. 36 ORNL 100 s IRRAD, 650.0 s Decay

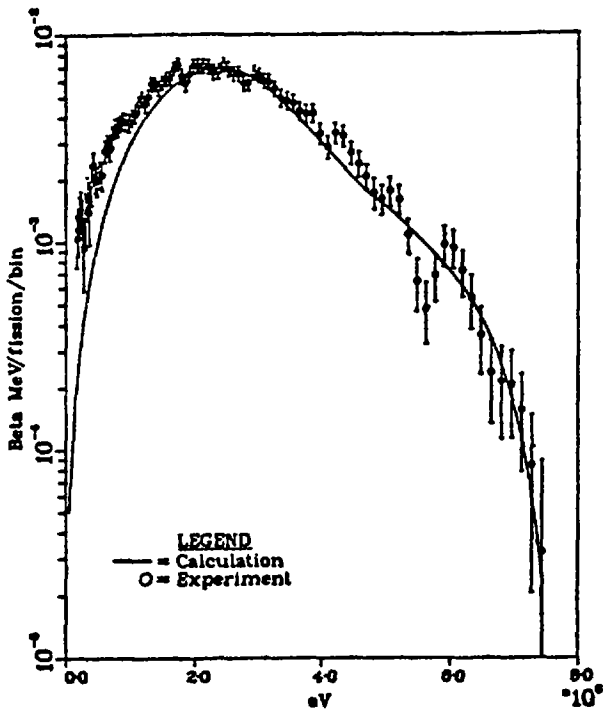

Fig. 37 ORNL 1 s IRRAD, 2.2 s Decay

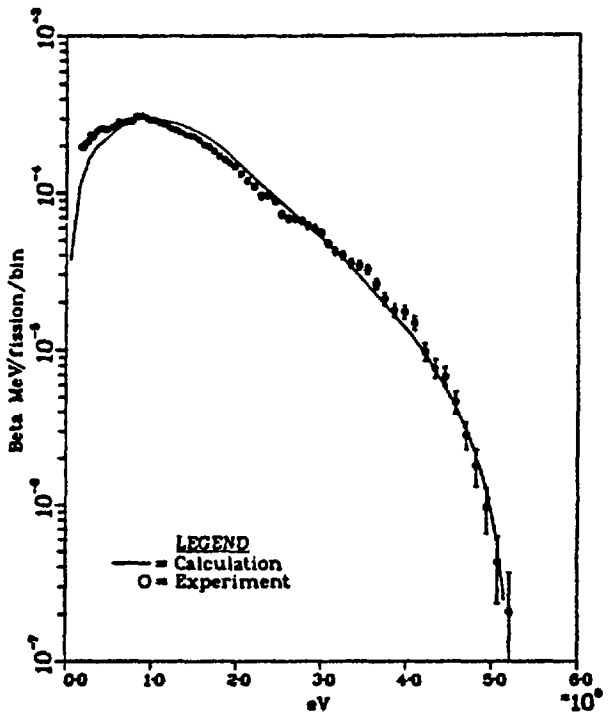

Fig. 38 ORNL 100 s IRRAD, 4950 s Decay

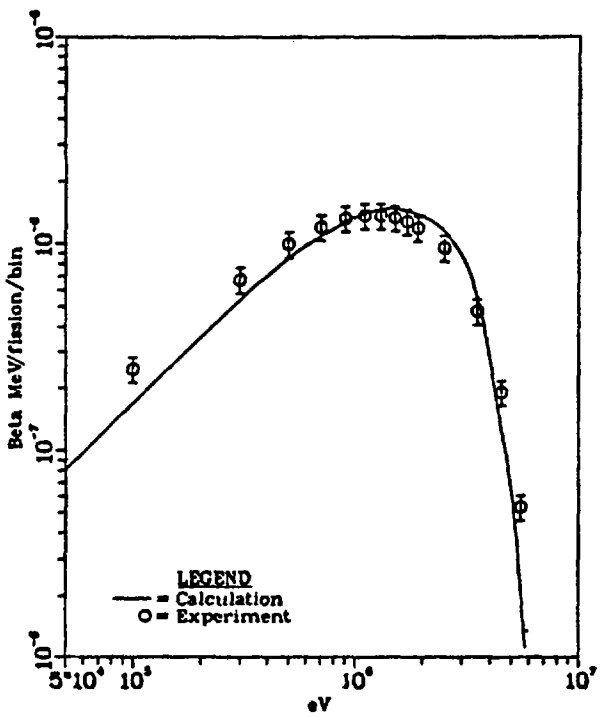

Fig. 39 UI 15 ms IRRAD, 104 s Decay

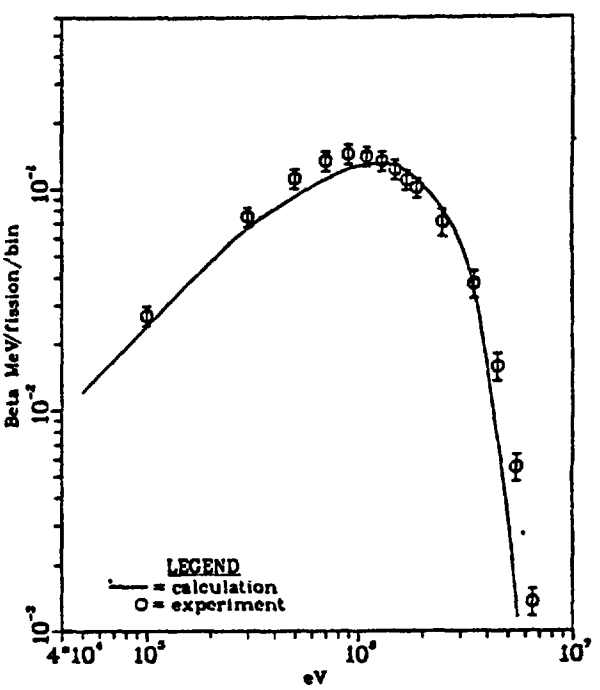

Fig. 40 UI 8 h IRRAD, 21 s Decay

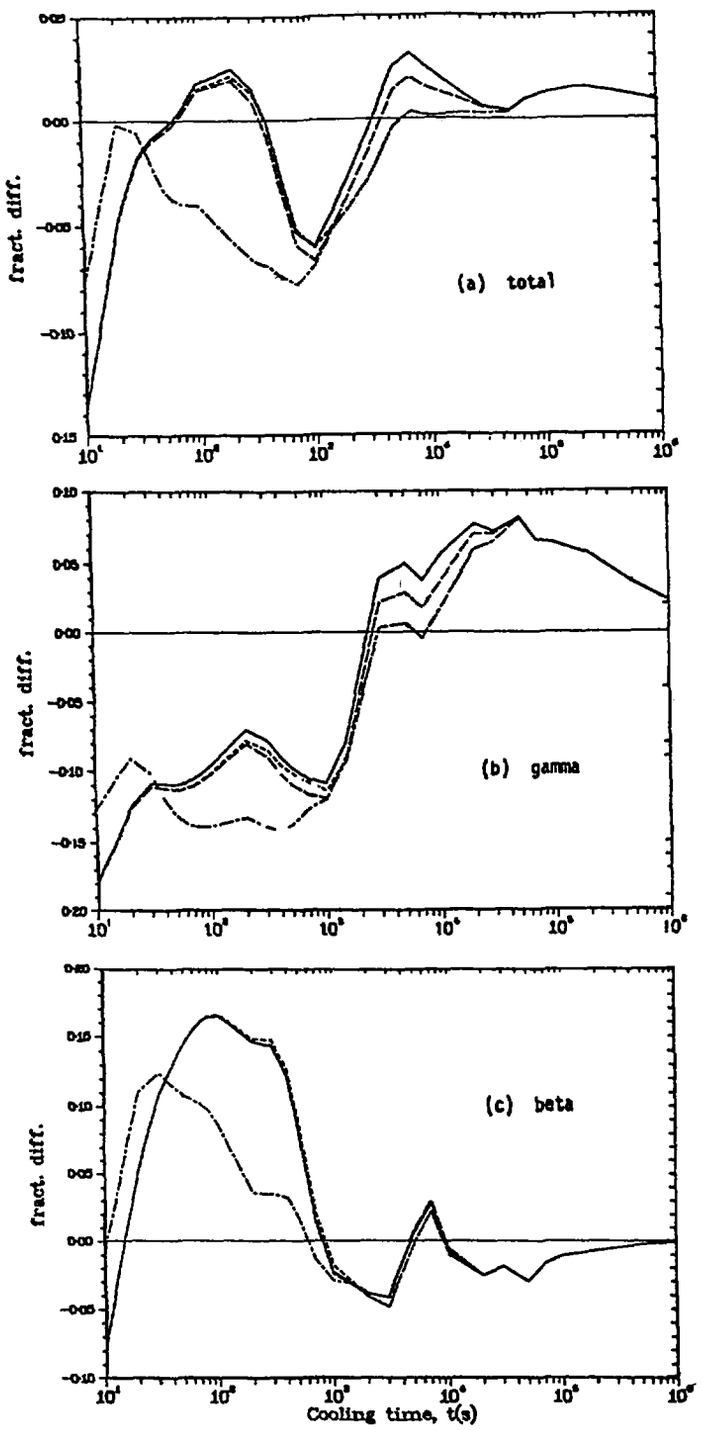

Fig. 41 Calculated decay heat compared to least-squares results:

—— ENDF/B-IV with ^{98}Zr corrected
– – – Same as above + mass 133 corrections
----- Same as above + ^{130}Sn + ^{142}La corrected
– – – – Same as above + ^{96}Y half-life corrected

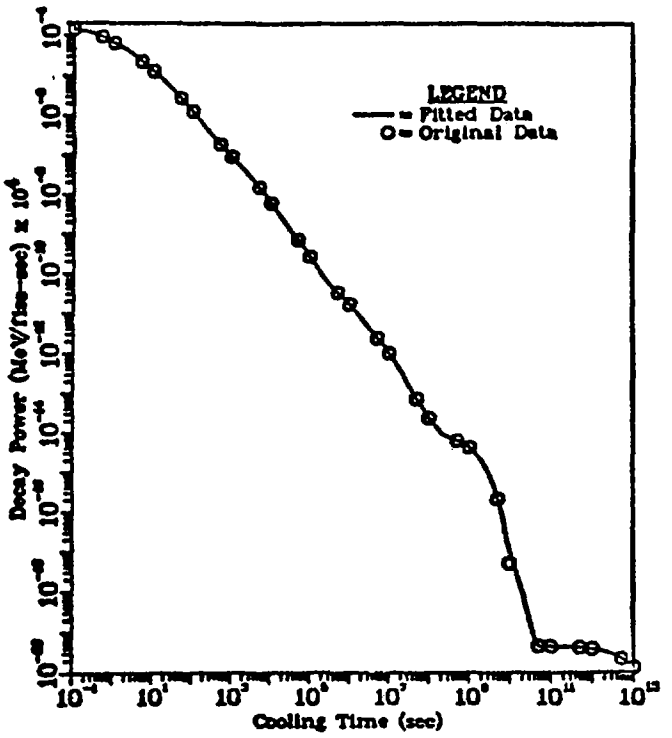

Fig. 42. Total Decay Power From U235 Thermal Burst

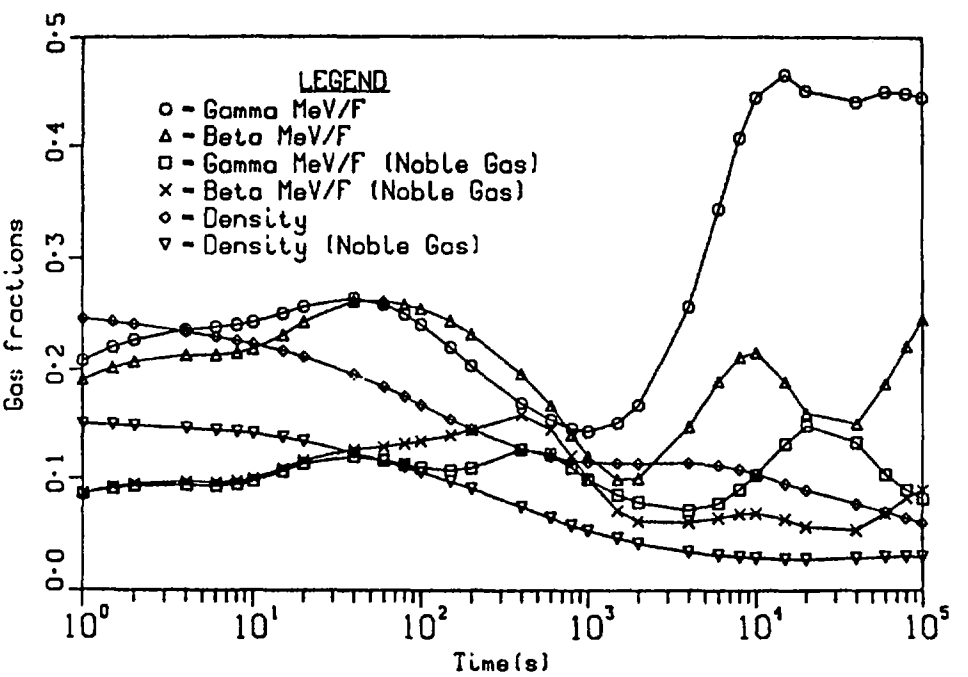

Fig. 43 Fractional gas content following a U235 fission pulse (fraction of total products)

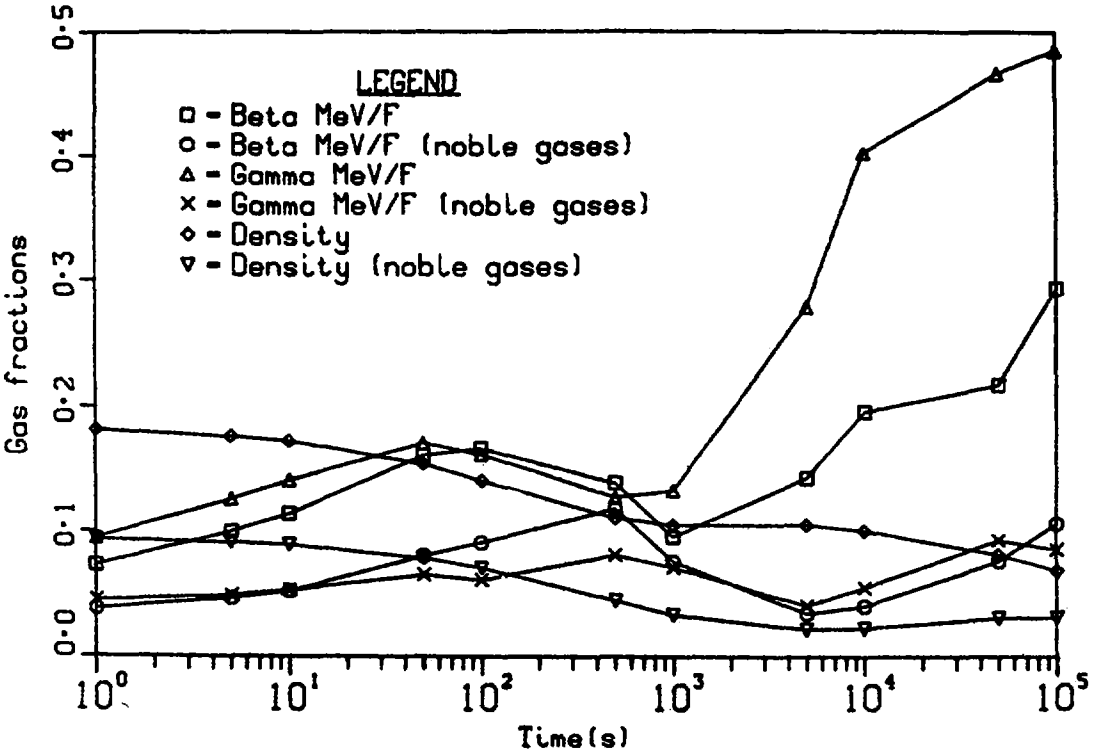

Fig. 44 Fractional gas content following a PU239 fission pulse (fraction of total products)

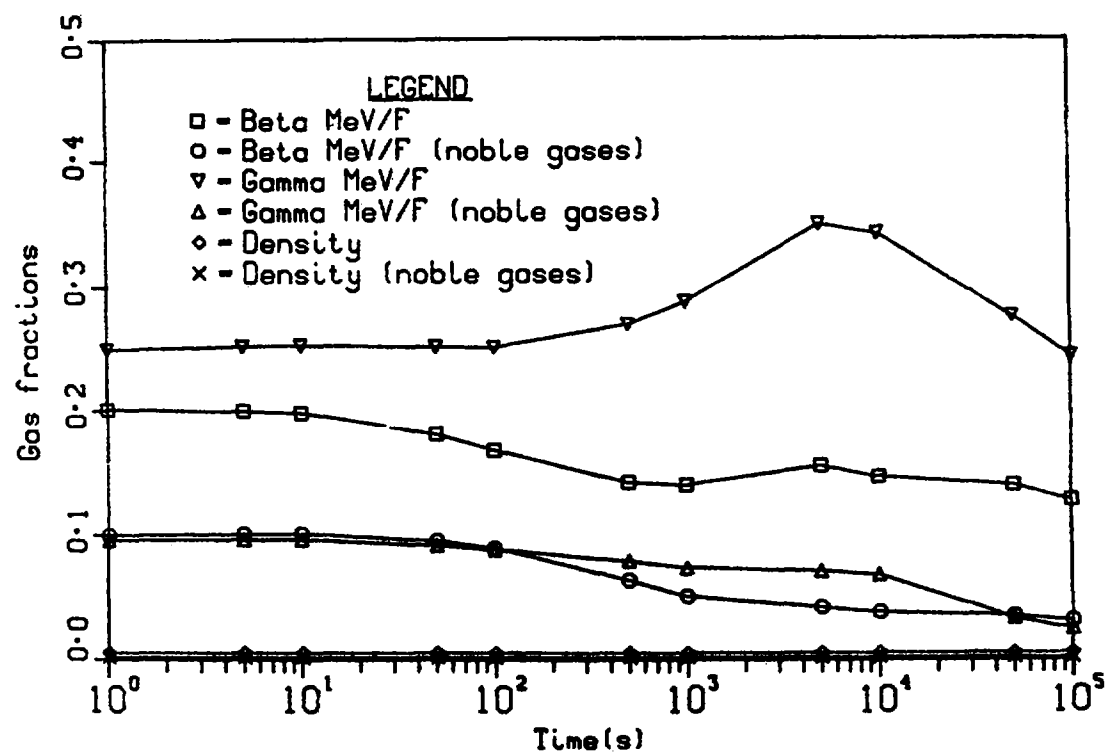

Fig. 45 Fractional gas content following a U235 thermal irradiation of 20,000 h, no depletion (fraction of total products)

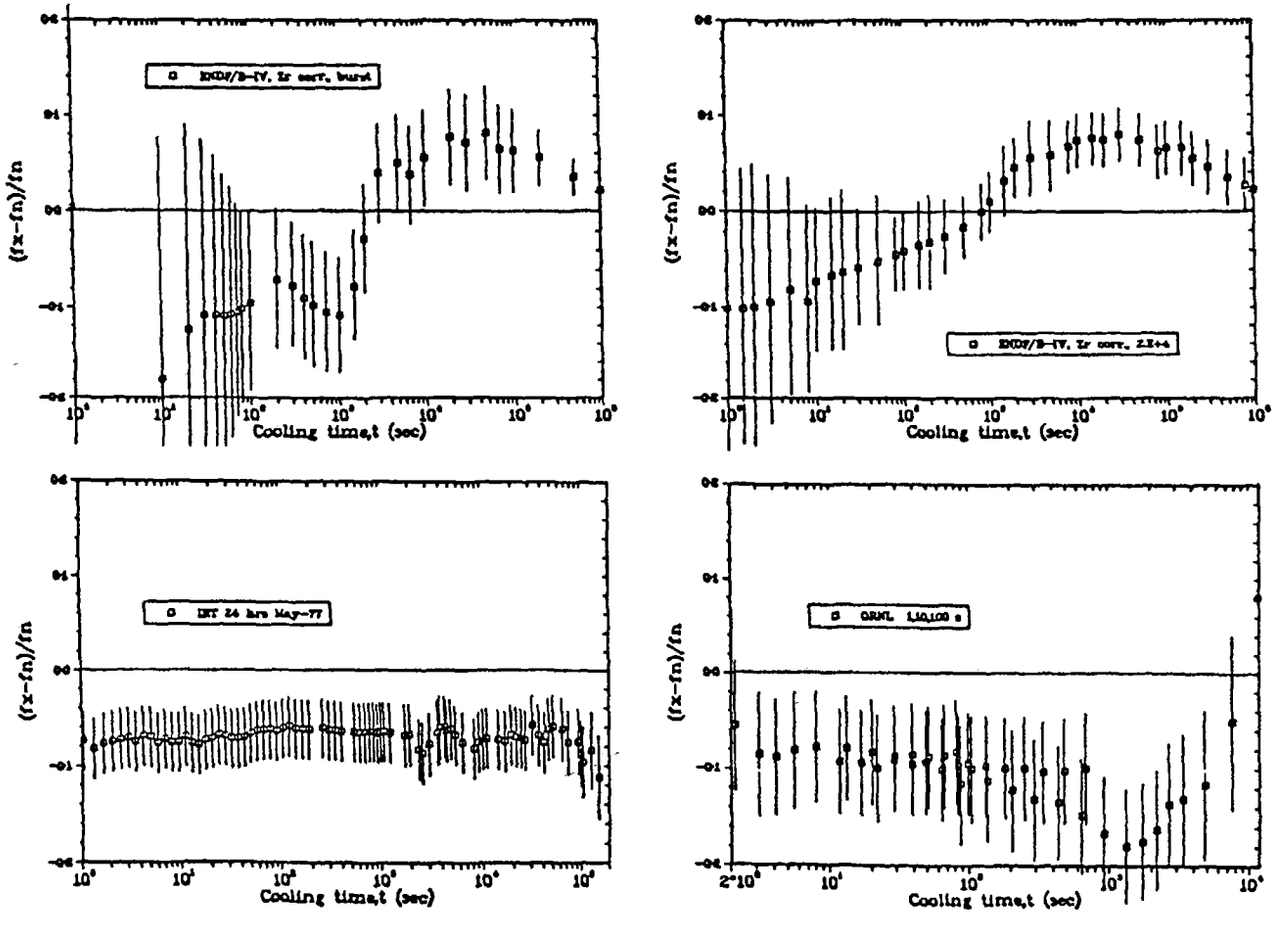

Fig. 46 Fractional deviation of gamma decay heat measurements and calculations from least-squares results.

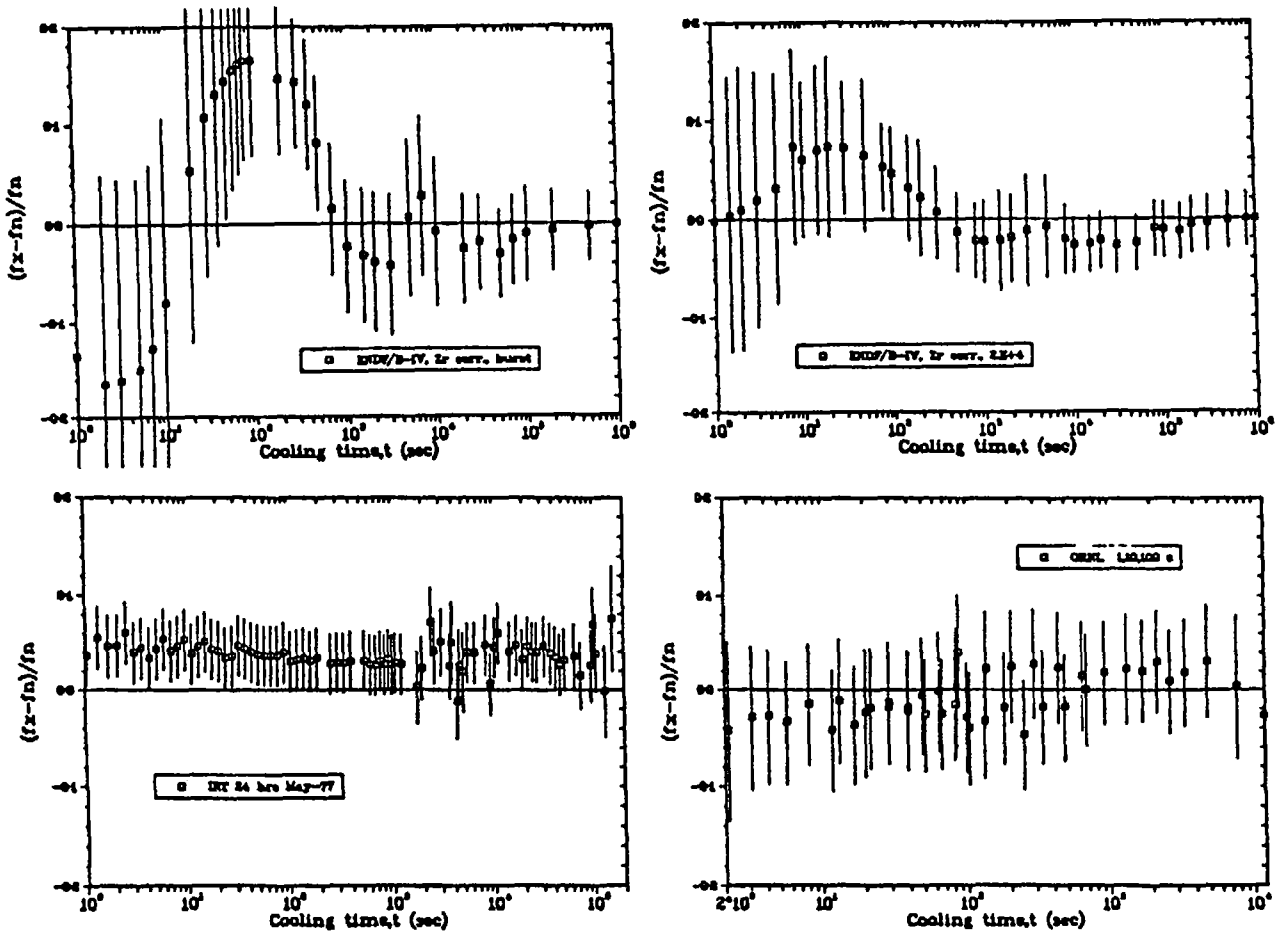

Fig. 47 Fractional deviation of beta decay heat measurements and calculations from least-squares results.

CONCLUSIONS AND RECOMMENDATIONS

Contents

Table of Contents

Page

List of Abbreviations used

BU	Burnup
CFRMF	Coupled Fast Reactivity Measurement Facility, located at Aerojet Nuclear Company, Idaho Falls
CTR	controlled thermonuclear reactors
d	day(s)
D	discrepancy
E	energy
FBR	fast breeder reactor(s)
FP	fission product(s)
FPND	fission product nuclear data
$g\sigma_o$	effective thermal cross section (in a Maxwell spectrum) in Westcott formalism
h	hour(s)
HWR	heavy water reactor
HTGR	high temperature gas cooled reactor
I_{rel}	relative intensity
INDC	International Nuclear Data Committee
LWR	light water reactor
LMFBR	liquid metal fast breeder reactor
NDAT	Non destructive assay techniques (in safeguards)
P_n	delayed neutron emission probability
PWR	pressurized water reactor
RI	resonance integral
RP	review paper (presented at this meeting)
s,sec	second(s)
SPRT-method	a method used to determine optical model parameters ([75Del])

t_{cool}	cooling time
$T_{1/2}$	half life
WRENDA	World Request list for Nuclear Data
y	year(s)
Y_{cum}	cummulative yield
$\overline{\mu}$	average cosine of scattering angle in laboratory system
ν_d	total delayed neutron yield (per fission)
σ_{el}	elastic scattering cross section
σ_γ	capture cross section
σ_{th}	$= g\sigma_o$ (see there)

I. INTRODUCTION

The 15 review papers presented at the meeting covered the applications (review papers 2 to 6) and the status (review papers 1, 7 to 15) of fission product nuclear data of the following categories:

- fission yields;
- decay data;
- delayed neutron data;
- neutron cross section data.

The presentation of the review papers and of several related contributed papers was followed by plenary discussions about questions of general interest such as the justification of requests for improved accuracies, the priorities of the requests, and the comparison of different measurement and evaluation techniques. These discussions led to several general recommendations to the IAEA, which are reproduced in Chapter II.

After the plenary sessions, five working groups were formed (see Appendix C), four of which were each concerned with one of the data types mentioned above, and the fifth dealing with fission product bulk properties required for inventory assessments. On the basis of the review papers and the plenary discussions, the members of the working groups compared the requirements for FPND to the status of the data. The summary reports of the different working groups, which include statements about the present situation in each data field, and recommendations for future work, form the basis of the contents of Chapters III and IV.

On the last day of the meeting, the summaries of the working groups' conclusions and recommendations as well as the general recommendations to the IAEA were presented and discussed in plenary until agreement was reached.

II. GENERAL RECOMMENDATIONS TO THE IAEA

The discussions during the plenary sessions and within the working groups resulted in a number of general conclusions as well as recommendations to the IAEA. Some of them refer to the status of implementation of the general recommendations to the IAEA issued at the First FPND Panel held by the IAEA Nuclear Data Section (NDS) at Bologna in November 1973.

II.1. FPND Progress Report

The meeting participants unanimously agree on the usefulness of the Reports on "Progress in Fission Product Nuclear Data" issued by IAEA/NDS and recommend that they continue to be issued in annual intervals.

In the first issue of the Progress Report, a special circular addressed to FPND measurers had been included in accordance with a recommendation issued by the Bologna Panel. This circular specified the type of experimental and interpretation detail which measurers should include in the reports on their work, and which is needed by FPND evaluators for an adequate judgement and comparison of different experimental results.

It is strongly recommended by this meeting, that a similar circular to FPND measurers be included again in the next issue of the Bulletin. The reason for reiterating this recommendation from the Bologna Panel is that since then no significant improvement in the documentation of experimental work could be noted.

II.2. FPND requests

The participants emphasize the convenience of finding all requests for FPND in WRENDA (World Request List for Nuclear Data), which is published biennially by the IAEA. It is therefore recommended that all requests concerning FPND (e.g. also for β and γ-spectra or delayed neutron spectra from precursors) should be submitted for inclusion in WRENDA. While the conciseness, uniformity and handiness of WRENDA is acknowledged, it is pointed out that the justification of requests as presented in WRENDA is poor. However, if recommendations for new measurements are to be based on user requirements, a more detailed justification than can be given in WRENDA is needed. It is therefore recommended that new FPND requests are to be backed up by detailed studies and explanations which shall be included in the FPND Progress Report, together with a detailed justification.

II.3. List of FPND compilations

The list of FPND compilations and evaluations together with the explanatory text reported in the review paper 1 at this meeting was found to be a very useful, more informative update of the corresponding list prepared for the Bologna Panel. It is recommended that IAEA/NDS update and publish this list in periodic (initially annual) intervals.

II.4. Future coordinating activities

II.4.1. Compilation of decay data

The meeting strongly recommends that IAEA/NDS promote a comprehensive compilation of decay data for all unstable and metastable nuclides over the whole atomic mass range, including fission products and actinides.

II.4.2. Average resonance parameters and level scheme data

Since at higher incident neutron energies (keV-MeV range), only few experimental cross section data are available, evaluated cross-section curves are partially based on nuclear theory. Existing evaluations often show severe discrepancies between each other, which are mainly due to the different models and parameters used.

As the first step towards an improvement of the situation, the IAEA is asked to coordinate an international effort to find the most accurate methods of determining average parameters from resolved resonances. It is suggested that IAEA/NDS initiate an intercomparison of the best available methods. Also, strong support should be given to evaluations of level scheme data, which are needed for statistical theory calculations of inelastic scattering cross-sections.

II.4.3. Fission product yields

It is noted that at present there exist only two extensive evaluations of fission product yields which are continuously updated, namely those of E.A.C. Crouch and of M.E. Meek and B.F. Rider. These two evaluations differ significantly in many of their recommended values, but the most striking discrepancy lies in the assigned uncertainties, those recommended by Crouch being often by a factor 2 to 3 higher than those given by Meek and Rider. In order to resolve these discrepancies, the meeting strongly recommends both national and international support for fission yield evaluations. In a first attempt, the IAEA should try to establish close contacts between measurers and evaluators of fission yields, which should enable the evaluators to better judge the quality of their experimental input data.

II.5. Future meetings

Concerning future FPND meetings, it was agreed that another general meeting devoted to the whole field of FPND would only be needed if and when drastic changes in the requirements for a large variety of data would occur. However, it was recommended that smaller specialists' meetings devoted to only one type of data (like decay data, cross-sections etc) when discrepancies or gaps in the knowledge exists, be organised in the future.

II.5.1. Meetings on cross section-data

In view of the unsatisfactory situation concerning evaluated cross-sections (see section II.4.2.), the participants recommend that IAEA/NDS organise:

(i) a specialist meeting on the systematics of all parameters needed in nuclear model calculations of neutron cross sections; and

(ii) in a few years time, a specialists' meeting on the status of fission product capture cross-sections, where both experimenters and evaluators should re-examine the status of the cross section data.

II.5.2. Meeting 1978 on delayed neutron data

The working group on delayed neutrons endorsed the INDC recommendation to convene a specialists' meeting on delayed neutron data in 1978.

III. SUMMARY OF USER REQUIREMENTS

This chapter is supposed to give a summary of the FPND requirements agreed by the meeting, separated according to user areas. However, a number of requirements expressed in the review papers were not discussed at the meeting; these are assumed to be accepted, and were taken over directly from the review papers.

In order not to duplicate information, some of the data requirements, especially when many nuclides are involved, are not listed in detail in this chapter. A complete survey of all the FPND requirements reviewed by the meeting, and the status of the requested data, is found in Chapter IV.

All accuracies mentioned refer to the 1σ confidence level.

III.1. Environmental aspects

The meeting noted that in the assessment of individual or collective doses from releases of radioactive materials to the environment, the total uncertainty cannot be reduced much below a factor of 2. To this, uncertainties in FPND contribute only a negligible amount, by far the major contribution coming from the uncertainties in the environment transfer factors. It is therefore concluded that, at the present state of knowledge, no further information on FPND is required for environmental assessments.

III.2. Design of power reactors cores

III.2.1. Thermal reactors

The target accuracies required for the prediction of reactivity effects due to fission products, and for the variation of reactivity effects with reactor temperature are the same as at the Bologna meeting: 2% for the prediction of reactivity lifetime and 10% for the variation of the FP reactivity effect with temperature. This requires fission yield and capture cross section data of the most important absorbers:

Tc 99, Rh 103, Xe 131, Xe 135, Cs 133, Nd 143, Pm 147, Sm 149

Sm 151, Sm 152.

Most of the requirements have by now been fulfilled; those still unsatisfied are included in Tables 5 and 11 of Chapter IV.

Tables 5 and 11 include in addition the requests concerning reactivity effects found in WRENDA 76/77, whose number exceeds those expressed in Bologna. Furthermore, a study by Ottewitte, submitted

as contribution to RP 3, pointed to the significance of the half lives of Xe135 and Sm149 precursors for the concentration of these absorbers. From this study, requests for half life data were deduced which are included in Table 6 of Chapter IV.

III.2.2. Fast reactors

(i) Effects of neutron capture on reactivity

The meeting agreed that the present target accuracy for the prediction of reactivity effects of fission products should be 10%. In future, however, for the expected developments of high burnup fast reactors with heterogeneous cores, a target accuracy of 7% would be appropriate. The 10% target implies that the bulk capture effect of FP is required to 10% accuracy.

The resulting accuracies for individual FP capture cross sections are, according to the Bologna Panel, 20 to 30% for the important isotopes. However, the participants from Japan, France and US did not agree with this figure. Whereas S. Iijima felt that reactor designers in Japan would accept capture cross section uncertainties of 20%, the participants from France and US emphasized an accuracy goal of 10% in the main FP capture cross sections. It was finally agreed that, in view of the fact that systematic errors in the capture cross sections of individual FP do not necessarily tend to cancel in the lumped FP, a 10% accuracy for the capture cross sections of main FP should be aimed at.

All capture cross section requirements are included in Table 12 of Chapter IV.

(ii) Effect of neutron scattering on reactivity

The effect of neutron inelastic scattering of the lumped FP is about 10 to 15% of the capture effect on reactivity. This means that an accuracy of 30% would be required for the scattering effect of lumped FP. This requirement is apparently met, as the various recent calculations of the scattering effect do not differ by more than 15%.

If the uncertainty in the scattering effect could be decreased, e.g. to 20%, the requirements for capture cross sections could be relaxed. It is, however, not sure if such an increase in accuracy can be reached with the present evaluation methods.

The transport cross section ($\sigma_{el}(1-\bar{\mu})$) was considered by S. Iijima to be of importance for the determination of the leakage of neutrons from the reactor. According to Iijima the reactivity is affected by the transport cross section to the same degree as by the inelastic scattering, but in the opposite direction.

(iii) Time dependence of reactivity

At short times after reactor start-up the time behaviour of the lumped FP depends partly on the cross sections of some radioactive isotopes ($T1/2 \gtrsim 1d$) such as: Ru103, Rh105, Pm149, Mo99. These cross sections are not well known and it would be valuable to investigate the effect of their uncertainties on the total uncertainty of the time dependence of reactivity.

(iv) Sodium void reactivity

The meeting endorsed the conclusion of J. Rowlands that the effect of FP on sodium void reactivity should be predicted to within 30% accuracy. There was some discussion about the way in which this requirement could be met. J. Rowlands suggested to determine the FP effect on sodium void reactivity as the difference between the FP reactivities in a normal and in a voided core. This difference amounts to about 15% of the total FP reactivity, which leads to the requirement that the total FP reactivities (both in normal and in voided core) should be determined to $\pm$ 3.5%. According to J.Y. Barré, however, it would be sufficient to analyze integral measurements performed in different fast reactor spectra. The meeting concluded that this question needs further investigation.

(v) Doppler reactivity

It was agreed that the contribution of FP to the uncertainty of the Doppler reactivity should be less than 7%. Since according to calculations by Butland [76But], the net contribution of FP to the Doppler reactivity does not exceed 15% (see also RP 3), this leads to the requirement for an accuracy of 50% in the FP effect. For the resulting requirements on the bulk FP cross sections, it has to be taken into account that the effects of capture and inelastic scattering are of opposite sign and that therefore the requirements for these separate components may be more stringent than 50%.

(vi) Determination of reactivity by delayed neutrons

The requirement to be able to measure reactivities from the kinetic response of the reactors leads to a need for delayed neutron data to enable the reactor period-reactivity relationship to be determined to 3 to 5%. This requires:

- total delayed neutron yields per fission from Th232, U233, U235, U238 and Pu239 to $\pm$ 3% (Pu240 and 241 to lower accuracy);
- an accurate knowledge of the time dependence of delayed neutrons in the range of 1 to 100 seconds, in order to be able to determine the relationship between reactor period and reactivity to 3-5%.

- the delayed neutron spectra, so that the reactivity worth of delayed neutrons relative to prompt neutrons can be determined to ± 2%.

Further sensitivity studies are needed to formulate the accuracy requirements for the time dependence and the energy spectra. Calculations made using different sets of data which are available could help to define these requirements.

III.3. Reactor operation

III.3.1. Contamination of reactor components by fission products

The requirements for FPND for the prediction and control of FP release and contamination of reactor components have remained the same as at the Bologna Panel, the tolerable uncertainty in the inventory of important isotopes being 40%. Table 1 lists those dominating FP isotopes for which the 40% accuracy requirement was not met at the time of the Bologna Panel and the present status of the required data. The table shows that the requirements are essentially met, with the exception of Cs 136.

Table 1: Important FP isotopes for the control of contamination of reactor components
(= Table I of RP 4)

FP	data determining precision of inventory	important for reactor type	present accuracy
Ag 110m	σ_γ Ag109	LMFBR	<30%
Sb 125	cum. yield	"	<20%
Te 129m	" "	PWR	<15%
		HTGR	30%
		LMFBR	<30%
Cs 134	σ_γ Cs133	LMFBR	30%
Cs 136	" Cs135	"	30% to factor 2

III.3.2. Failed fuel detection

As already stated at the Bologna Panel, the required precision in the inventory of gaseous FP used for the detection of fuel failure is 40%. The current status of those short lived FP that had not fulfilled the requirements at the time of the Bologna Panel is given in Table 2.

Table 2: Achieved accuracy in the inventory of FP used for failed fuel detection

(= Table II of RP 4)

FP	PWR	HTGR	LMFBR
Kr 90	6	6	20
Kr 91	7	7	30
Xe 138	3	4	9
Xe 139	5	6	13
Xe 140	5	5	12
Xe 141	6	6	29

The table shows that all data of importance to failed fuel detection are known to the required accuracy.

III.3.3. Decay heat

(i) Required bulk accuracies

According to RP 4, the knowledge of the residual heat after reactor shutdown is important in three different respects:

- For the removal of residual heat after normal operation or emergency shutdown, with cooling times ranging from 0 to 10^6 sec.

- For the handling of irradiated fuel and its temporary storage, where cooling times range from a few hours to several months or even years (10^5 to 10^8 sec.)

- For fuel transport, reprocessing and waste packaging.

The highest precision in the prediction of afterheat is demanded for the heat removal after shutdown. The meeting agreed that, for PWR's and BWR's, accuracies as given in Table 3 should be aimed at. As compared to the Bologna Panel, Table 3 includes also requirements for the thorium-cycle, and the target accuracies are higher than those requested at Bologna (which are equal to those listed in RP 4). The needs for higher accuracies w ere particularly emphasized by the US delegates, on the basis of the requirements by the US Nuclear Regulatory Commission as well as by reactor vendors.

(ii) Status of decay heat accuracies

Sensitivity studies performed in France and USA for U235 and Pu239 decay heat from thermal fission are supported by agreement between different summation calculations and the latest experiments. The decay heat accuracies for these 2 cases, as calculated assuming infinite irradiation and neglecting neutron capture, is included in Table 3.

The present status for fast fission in U235 and Pu239 has not yet been evaluated, but is probably represented by the larger uncertainty values of Table 3.

From Table 3 it can be seen that the priority I requests are met for U235, but possibly not for Pu239. The much tighter priority II requirements are not yet met. The status of U233 data is probably similar to that for U235, but experimental support is sparse. Probably the priority I requirements for Pu241 and U238 can be met, but more study is needed.

(iii) Individual FPND requirements

From the above requirements for precisions of decay heat predictions and from the sensitivity studies performed by C. Devillers together with an analysis of the available data (RP 4), a number of requirements for individual FPND has been derived:

- Half life data are required to 5% accuracy for:

  Sr 91; Y 98; Zr 95, 98; Nb 97, 100; I 131, 132, 135;

  Xe 135; Cs 134; and La 140.

  The measurements for these half-lives reveal discrepancies, which may be resolved by evaluation.

- Uncertainties in average decay energies contribute the major part to the overall decay heat uncertainty. A 10% accuracy is required for the decay energies of the following important nuclides whose β-spectra are unknown, namely:

Table 3: Fission product decay heat:

accuracy requirements and their priorities (in brackets) - status [1]

Fissioning system	Cooling time: 1 - 20 s req. %	status %	20 - 10^4 s req. %	status %	10^4 - 10^6 s req. %	status %	10^6 - 10^7 s req. %	status %	10^7 - 10^8 s req. %	status %
thermal										
U 235	10(I) 5(II)	4–8	5(I) 2(II)	2–4	10(I) 5(II)	1.5–3	10(I) 5(II)	3–5	≤5(I)	3–5
Pu 239	10(I) 5(II)	8–15	5(I) 2(II)	2–6	10(I) 5(II)	2–6	10(I) 5(II)	3–5	≤5(I)	3–5
U 233	10(II) 5(III)		5(II) 2(III)		10(II) 5(III)		10(II) 5(III)		≤5(II)	
Pu 241	30(I) 15(II)		15(I) 6(II)		30(I) 15(II)		30(I) 15(II)		≤15(I)	

	10^2 - 10^7 s required %	10^7 - 10^8 s required %	integrated over time 0 - 10^5 s required %
fast			
U 235, Pu 239	10(I) 5(II)	≤ 5(I)	10(I)
U 238 Pu 241	30(I) 15(II)	≤15(I)	30(I)
Th 232	30(II) 15(III)	≤15(II)	30(II)

1) A range of uncertainties is given for each cooling time, reflecting the uncertainty in the estimated standard deviation, and its variation with decay time.

Br 88, 89; Sr 95, 96; Y 96, 96m; Zr 100; Nb 102; Mo 103, 104, 105; Tc 105, 107; Te 135; I 137, 138; Cs 141, 142; Ba 143, 144; La 144, 145, 146.

For some other FP an accuracy of 5% in the decay energy is desirable:

Sr 89; Y 90, 91; Rh 106; Cs 137; Ba 140; La 140; Ce 141; Pr 143,144.

- Independent yields: at short cooling times (10 sec), the influence of yield errors on the decay heat uncertainty is mainly due to the uncertainties in direct yields. In order to achieve an overall accuracy of 5% for this short cooling time, it is required that the uncertainties in direct yields are not larger than those given in the evaluation of Meek and Rider [77Mee], the values of which have mostly been obtained by calculations.

As is pointed out in RP 4 (Table VIII), the effect of neutron capture should increase the decay heat in a power reactor at decay times longer than 10^4 s; in a typical thermal power reactor the increase may amount to more than 8% after 10^7 s (3 months), but the exact figure depends on the fluence.

The prediction of this effect requires the knowledge of the capture resonance integral for Cs 133 and Pm 148m.

III.4. Out of pile fuel cycle

It was indicated at the Bologna Panel that FPND requirements for fuel cycle purposes are not very severe and existing data are mostly adequate. The present meeting found that for most of the problems of the out of pile cycle, this statement is still valid. Some requirements were however expressed, mainly concerning the calculations of decay heat released during interim storage and of the mass balance at the reprocessing stage.

III.4.1. Interim storage and transport

In connection with interim storage and transport of burnt fuel before reprocessing, knowledge of the released fission product decay heat is required to an accuracy of 15% for cooling times $10^5 s \leq t(cool) \leq 10^8 s$. For cooling times > 10^7 sec, after which only a few long lived FP contribute significantly to the decay heat, this requirement is equivalent to the requirement for 5% accuracy in the decay power of each of the dominating FP.

For some of these FP, the 5% accuracy target is not reached different decay power calculations being discrepant by more than 5%; the discrepancies are caused by differences in the

input data. The resulting requirement is:

- 5% accuracy in average ($E_\beta + E_\gamma$) - energy of:
  Sr 89, Cs 137, Ce 141 and Pr 144.

Another problem of concern to irradiated fuel transport, and involving FPND, is the shielding of high energy gamma rays. According to a contribution by Austin et al to RP 5, for a particular flask design uncertainties of 30% in the γ-source strength have been noted, the dominant isotopes being: Ru/Rh106, La140, Cs134, Ce/Pr144.

III.4.2. Reprocessing

It is now generally agreed that cooling times before reprodessing will be $\geq 10^7$ sec, and never as low as 3×10^6 sec as auggested at Bologna for FBR fuel. A range of relatively short-lived FP included at Bologna can therefore be omitted from consideration so far as reprocessing is concerned.

At the reprocessing stage, the decay heat due to FP insolubles, mainly Ru103 and Ru/Rh106, plays an important role, especially for FBR fuels. A 10% accuracy in the total decay heat of the insolubles, for cooling times $\gtrsim 10^7$ sec, is required.

For environmental and reprocessing purposes, a comparison of the material contained in the dissolved spent fuel with the amount of different isotopes in the original fresh fuel is of great interest. In order that such a "mass balance" becomes adequately accurate, extensive calculations, implying fission cross sections, FP yield, decay and capture cross section data, have to be carried out for each fuel type.

The most important FP in this context are the volatile isotopes of impact on the environment, H3 and I129, and the insolubles which remain in the fuel after the first solvent extraction, i.e. Zr/Nb95, Ru103 and Ru/Rh106. For a mass balance, the inventory of H3 should be known to 5%, whereas for the other FP an uncertainty of 10% in the inventory is tolerable.

Assuming that the main quantity affecting the inventory of these isotopes is the fission yield, the following data requirements can be expressed for the purpose of mass balance calculations:

- thermal and fast fission yields from the major and some minor (Pu240, 241) actinides for H3 to ± 5%;

- thermal and fast fission yields from the same actinides for Zr/Nb95, Ru103, Ru106 and I129 to ± 10%.

III.4.3. Shutdown flux

In a contribution to RP 5, Austin mentioned that in some reactors, shutdown flux levels are influenced by photoneutron reactions in light elements. A good example is the Winfrith HWR, for which the dominant neutron source for some hours after shutdown is provided by high energy (γ-n) reactions in deuterium.

A knowledge of this source strength to ~ ± 50% is desirable, both to aid instrumentation design and to assist in interpretation of shurdown reactivity determinations. Br86 would appear to be an important FP contributing energetic γ-rays.

III.4.4. Nuclear incineration of minor actinides

According to the recent Euratom state-of-the-art review (EUR-5801e), FPND requirements for nuclear incineration of minor actinides are already met, as far as establishing technical feasibility is concerned. In the event of a decision to develop the process with a view to its large scale operation, accurate FPND will be needed to evaluate the reactivity effects and to calculate the quantities of FP formed. It was endorsed by the present meeting, that these requirements are unlikely to arise within the next 2 to 3 years.

III.4.5. Alternative fuel cycles

Possible future FPND requirements for alternative fuel cycles as described in RP 5 will have to be assessed as soon as the needs arise. In particular, additional data will probably be required for high burnup and the thorium fuel cycle; these may include further FP cross section data, and further fission yield-data for minor actinides and for fast fission of Th232.

III.5 Investigations on irradiated fuel

Three topics were covered under this title: burnup studies, reactor neutron dosimetry measurements, and non-destructive analysis in safeguards. These studies are related by the method of investigation used, which is to deduce some 'original' quantity (like the number of fissions, the number of fissionable isotopes, the neutron spectrum etc) from the measurement of the amount of a certain FP contained in an irradiated sample.

III.5.1. Burnup

The "burnup" (BU) of an irradiated fuel denotes the relative number of heavy metal isotopes that have been lost through fission:

$$BU = \frac{\text{number of fissions} \times 100}{\text{initial total number of heavy element atoms}} \quad [\text{atom \% fission}]$$

The basic burnup quantity as defined above can be directly related to a number of other quantities like the average or terminal fission rate, the individual sources of fission etc which are required for different applications (a list of such applications if found in RP 6).

According to RP 6, many applications require that the burnup be determined to an accuracy as high as 1.5-2%. This requirement applies particularly to the determination of the number of fissions

(absolute or relative), and to the calculation of the residual fissionable nuclide content and the reactivity worth of fuel.

The most accurate and widely applicable method of measuring the burnup is the FP monitor-residual heavy atom technique. In this method, the fuel specimen is dissolved and the numbers of atoms of a selected FP monitor and of the heavy metal atoms are determined.

This is a destructive method, which is not always desirable and applicable. Non-destructive BU measurements are most often performed by γ-spectrometry of FP. Such measurements provide less accurate BU values ($\gtrsim$ 5%), but have the advantage of giving rapid information on relative BU.

(i) Destructive techniques: choice of FP-monitor

The most accurate technique for destructive BU measurements is isotope dilution mass spectrometry. For this technique, the chemically most suitable elements which may be used as FP monitors are Nd and Ce.

Thermal reactors. For a long time, Nd148 has been considered a nearly ideal BU monitor for thermal LWRs, because its thermal fission yield seemed to be practically identical for U235 and Pu239 (1.68%). Recently however, it was found that Nd147 had a high thermal capture cross section (σ_γ= 440 ± 150 barn [74Hec]), which means that the published and generally accepted yield of Nd148 was probably too high. This assumption is also supported by recent measurements of Nd148 yields by W.J. Maeck [76Mae], which suggest that the thermal U235 fission yield of Nd148 is ~ 1.65%. Therefore, the Nd148 yield for U235 and Pu239 should be carefully remeasured and evaluated, so that Nd148 may be used as monitor for highly accurate BU determinations in mixed U235-Pu239 fuel.

In highly enriched fuel, with only one major source of fission, U235 or Pu239, it is recommended that the sum of Nd145 + Nd146 be used as BU monitor. The sum of these isotopes seems to be nearly independent of the integrated neutron flux [76Mae], and it is therefore probably not affected by capture effects.

For thermal reactor fuels in which U233 and U235 are the principal fission sources, Ce140 should be a better monitor, as its thermal fission yield for these two actinides is nearly the same ($\approx$ 6.35%).

If the purpose of the BU measurement is to determine the individual fission sources, such FP should be chosen as monitors, whose fission yields for the various fissioning nuclides are significantly different. In this case, the most suitable FP monitors for thermal reactors are the Kr-isotopes Kr83,84,86 and the Ru-isotopes Ru101,102,104.

Fast reactors. Nd isotopes may also be used as BU monitors for most of the fast reactor fuels. E.g., Nd143 would be suited for U233-U235 and Pu239-Pu241 fuel, Nd146 (or the sum of all stable Nd-isotopes minus Nd144) for U233-Pu239, Nd148 for U235-Pu239.

The accurate determination of BU in fast reactors requires also a knowledge of the variation of the monitor's fission yield with the neutron spectrum. At present, the neutron energy dependence of Nd-fission yields (and also of some other important FP) is being investigated at different laboratories, by evaluation of existing data as well as in new experiments.

To distinguish fission sources in fast reactor fuels, the stable isotopes of Nd(143,148,150) and Sm(147,149,152,154) are the best monitors.

(ii) Non-destructive technique: γ-ray scanning

Gamma ray activities, or their ratios, of specific FP can be used to derive information on different parameters of the fuel history. In particular, for the applications related to BU studies, the following quantities may be deduced from γ-spectrometric measurements:

- the number of fissions from the activity of Cs137, or after short irradiations, from Ce144;
- the fluence, from which the relative BU can be deduced, from the activity ratios Cs134/Cs137 or Eu154/Cs137;
- the ratio of Pu239 to U235 fissions from Ru106/Ce144 or Ru106/Cs137;
- the fission rate at shutdown ("terminal" fission rate) from Ba/La140 or Zr/Nb95;
- the ratio of the Pu239 to U235 fission rates at shutdown (less important) from Ru103/Ce141 or Ru103/Zr95.

(iii) Required accuracies for individual FPND

The accuracy target of 1.5-2% for burnup determination, means that the fission yields of the stable FP monitors used in destructive techniques are required to 1-1.5%, and the fission yield of the radioactive FP used for γ-scanning to an accuracy of 1.5%. Measurements with γ-spectroscopy require in addition the absolute γ-ray intensities of the major γ-lines to 1%. Furthermore, in order to take the neutron capture into appropriate account, thermal, resonance and fast capture cross sections of those FP whose neutron capture would effect the number of BU monitor isotopes, have to be known; an accuracy of 5-10% is in general sufficient. In summary, the following data are required for BU studies:

- to an accuracy of 1.5%: the thermal and fast fission yields of Nd145,146,148; the thermal yields of Kr83, 84,86, of Ru101,102,104 and of Ce140; the fast yields of Nd143,144,150 and of Sm147,149;

- to an accuracy of 2%: the thermal fission yields of Zr/Nb95, Ru103,106, Cs137, Ba/La140, Ce141,144;

- to an accuracy of 1%: the absolute intensities of the major γ-rays of Zr/Nb95, Ru103,106, Cs137, Ba/La140, Ce141, Ce/Pr144, Nd147, Eu154,155.

- the capture cross sections:
  thermal and resonance to an accuracy of 3-5% for Cs133 and Eu153;

  thermal to 3-5%, resonance to 10% for: Cs134, Pr141, Nd 143,145, Sm153 and Eu154;

  thermal and resonance to an accuracy of 10% for Nd147;

  fast to an accuracy of 10%: for all Nd-isotopes.

III.5.2. Neutron dosimetry

Reactor neutron dosimetry provides information relative to neutron flux densities, fluences and neutron spectra. This information is needed in order to calculate accurately fission rates, burnup, damage rates etc.

At the 1975 ASTM-Euratom Symposium on Reactor Dosimetry, in Petten [75Pet], the accuracy requirements for fission rate determinations were stated to be in the range of 2-5% for FBRs, and somewhat lower for LWRs and CTRs.

At the present time, multiple foil activation is the only practical means for achieving the required accuracies. This technique involves the irradiation of selected materials, which have known neutron activation thresholds, followed by a γ-ray assay of the reaction products. Among others, it is common to use also fission reactions, like U235 (n,f), Pu239 (n,f), Np237 (n,f), Th232 (n,f) and U238 (n,f) and to detect selected FP. The usual detection method is γ-spectrometry, which restricts the suitable FP to those which are fairly longlived and have strong γ-rays, like:

Zr 95, 97; Ru 103; I 131; Te 132; Cs 137; Ba 140; Ce 143,144, or their respective equilibrium daughters.

If an accuracy of 2% in fission rates has to be achieved (FBR programmes), the nuclear data of the above mentioned FP should be known to the following accuracies:

- the fast fission yields and their neutron energy dependence to 2%;

- the absolute γ-ray intensities for the major γ-rays ($I_{rel} \geq 10\%$) to ± 1% (this requirement seems not to be fulfilled for Ru103, Te132, Ce144;

- the half lives to ≤ 1%.

III.5.3. Safeguards

Safeguards uses FPND mainly for its "non-destructive assay techniques" (NDAT). These techniques are at present only used to verify the information released by the reactor operators. NDAT consist in general in γ-ray scanning of burnt fuel and subsequent evaluation of FP γ-ray activity ratios.

The parameters to be checked include those which are determined in BU analysis, plus possibly some others like the irradiation time, cooling time, fuel composition etc. The values of the parameters, given by the reactor operator, may be checked by calculating - with these values - the expected activity ratios and comparing them to the actually measured ratios.

In addition to the quantities required for BU analysis (see section III.5.1.), information on the cooling time and the irradiation time may be of interest to safeguards, which can be deduced from the following activity ratios:

cooling time:	Ba140/Ce141	irradiation time:	Ba140/Cs137
	Ba140/Zr95		Zr95/Cs137
	Ce141/Zr95		Ce144/Cs137
	Zr95/Nb95		

It follows that the FP involved in NDAT are the same as in BU, which are listed in section III.5.1.

Under favourable experimental conditions, the γ-activities of the important FP can be determined to 3%; hence the calculations of activity ratios should reach at least the same accuracy. Sensitivity studies performed by M. Lammer (in a contribution to RP 6) define the accuracies of individual FPND required to meet the global accuracy target of 3%. Table 4 lists those FPND which do not yet fulfill the accuracy requirements.

Table 4: Unsatisfied FPND requirements for NDAT

accuracy requirements (%)

FP	Thermal fission yields U-233	U-235	Pu-239	Pu-241	Cross-section $g\sigma_o$	RI	$T_{1/2}$	γ-emission probability [1]
Ru-103	3	-	3	10	-	-	-	1-1.5 [2]
Ru-106	2	-	2	-	-	-	0,5 [3]	1 [2]
Cs-133	1	1	1	5	2	2 [4]	-	-
Cs-134	-	-	-	-	6		-	1-1.5
Cs-137	-	-	-	-	-	-	≤0,5 [3]	-
Ce-141	3	-	3	-	-	-	-	1-1.5
Ce-144	-	-	-	-	-	-	-	1-1.5 [2]
Sm-149 [5]	5	3-5	5	-	-	-	-	-
Sm-151 [5]	5	3-5	5	-	-	-	-	-
Sm-152 [5]	5	5	5	-	-	-	-	-
Sm-153	2	2	2	-	10^3 b	[4]	-	-
Eu-153	-	-	-	-	2	6	-	-
Eu-154	-	-	-	-	3-5	[4]	1	1-1.5

1) For major γ-rays

2) Accuracy achieved by individual measurements has to be confirmed

3) Accuracy achieved by individual measurements, but discrepancies exceed requirements

4) Significance of RI unknown; data should enable the calculation of the pile-cross-section to the accuracy shown for $g\sigma_o$

5) For Eu-154 activity

IV. CONCLUSIONS AND RECOMMENDATIONS

FOR THE DIFFERENT DATA TYPES

IV.1. Bulk properties of fission products

The contribution of all FP to quantities like absorption, reactivity worth, heat emission etc, is called a FP bulk property in general, and is referred to as (bulk) FP absorption etc in particular.

IV.1.1. Decay heat: technical recommendations

The bulk requirements for decay heat and the present accuracy status are summarized in Table 3 of Sect. III.3.3. The needs deduced for individual FPND accuracies are included in Tables 6 to 9 of Sect. IV.3.1.; the comparison of status and requirements in these Tables implies the recommendation to (re)measure or re-evaluate those data for which the requirements are not yet met. In addition, the following general activities and considerations concerning decay heat are recommended by the meeting:

(i) Decay heat measurements should be treated as benchmarks, and full experimental details made available (e.g. irradiation history, method of measuring the number of fissions; isotopic composition of sample).

(ii) Experiments in progress should be completed.

(iii) More measurements on fast fission decay heat should be made (the accuracy status of fast fission decay heat has not yet been evaluated, but it may be assumed to be approximately represented by the larger uncertainty values given in Table 3 for thermal decay heat).

(iv) A recommended decay heat curve should be produced for each fissile nuclide and be made available to IAEA/NDS for international dissemination.

Note that a curve for U235 thermal fission has already been reported by Schenter et al. (See RP 15, fig. 1 and 2, and Table VIII). This curve shows that the so-called "ANS 5.1," standard decay heat curve [61Shu] augmented by 20 %, which is still considered as guideline for safety requirements in US thermal reactors, is extremenly conservative, corresponding to a 10σ confidence level.

(v) To aid in reviewing and correlating the data needed for contruction of recommended decay heat curves, Schenter and Devillers (see list of participants) should act as collectors for summation calculations, and Yarnell and Dickens (see list of participants) for measurements.

(vi) Measurements at very short and very long decay times should be made if possible; although data for very long decay times (t_{cool} >10^7 s) might better be obtained by measurements n individual fission products (the nuclides important for long decay times may be found from the Table A-5-II in Vol.II of the Bologna meeting proceedings and from the sensitivities in the Appendix of RP 4 of the present meeting; requirements are included in Tables 6 to 9 of Sect.IV. 3.1.).

IV.1.2. Other bulk properties

In this paragraph, all those requirements for FP bulk properties are summarized, for which the needs of individual FPND have not been assessed explicitely. They are all related to the design of fast reactor cores.

(i) Requirements

The target accuracy for the bulk FP capture effect on reactivity of fast reactors is 7 to 10% (see Sect.III.2.2.i). To meet this target, individual FP capture cross sections seem to be required to an accuracy of ± 10%; in addition, experiments on samples of lumped FP are of great value. These requirements are treated in more detail in Section IV.5.1.

Concerning the FP scattering effect on reactivity, S. Iijima recommended that the influence of the transport cross section ($\sigma_{el}(1-\mu)$) on the neutron leakage be investigated. Iijima suggested that this effect may be as important as the inelastic scattering effect, but of opposite sign.

The effect of FP on the sodium void reactivity should be predictable to within 30%. The question how this target should be approached was not solved at the meeting. If, as suggested by J.L. Rowlands, the FP sodium void reactivity is determined as the difference of FP effects in a normal and in a voided core, the total FP effects in each core would have to be known to 3.5% accuracy. According to J.Y. Barré however, it would be possible to fulfill the 30% accuracy goal by an analysis of integral measurements in different fast reactor spectra.

The uncertainty contributed by FP to the total Doppler reactivity should not exceed 7%, which requires that the FP effect on Doppler reactivity should be known within 50% accuracy. The requirements on the bulk scattering and capture cross sections separately may however be more stringent, as the effects of these components are of opposite sign.

The relationship between reactivity and reactor period should be accurate to 3-5%. This requires the knowledge of certain bulk delayed neutron data:

- The total delayed neutron yields per fission from U233, U235, U238 and Pu239 to ± 3% (Pu240 and 241 lower accuracies);

- the time dependence of delayed neutrons in the range of 1 to 100 seconds - sensitivity studies are needed to determine the target accuracy;

- the delayed neutron spectrum, to determine the ratio of delayed neutron to prompt neutron reactivity worths to 2%.

(ii) Conclusions and Recommendations

- In deciding about the requirements on data for individual isotopes to meet the bulk FP requirements, possible systematic errors in the measurements and theoretical methods must be taken into account and can be dominating factors.

- It should be investigated whether the effect of FP on the fast reactor sodium void reactivity has to be measured or whether it can be derived from an analysis of existing integral measurements together with a study of the uncertainty in the differential cross section data.

- For the assessment of the accuracy requirements on the differential cross sections of FP, the influences of inelastic and elastic moderation, as well as capture, on the fast reactor Doppler effect have to be studied in more detail.

- The main parameters determining the time variation of the lumped FP cross sections in a fast reactor and the uncertainties in these parameters should be investigated (see also Sect. III.2.2.iii.).

- Further sensitivity studies are required to define the accuracy requirements for the time dependence of delayed neutron emission and for delayed neutron energy spectra, if possible before the IAEA's delayed neutron specialists' meeting planned for the Fall of 1978.

IV.2. Fission product yields

IV.2.1. Requirements

(i) Chain yields

Table 5 represents a summary of all unsatisfied chain yield requirements expressed at the meeting. Only the most stringent

Table 5: Unsatisfied chain yield requests

Nuclide	fissioning system th..thermal f..fast	Most stringent requirement accuracy 2) (%)	source of request 1)	priority	accuracy given by Meek+Rider 2)	Comment
^{3}H	$^{232}Th_f$ $^{233}U_{th,f}$ $^{235}U_{th,f}$ $^{238}U_f$ $^{239}Pu_{th,f}$ $^{240}Pu_f$ $^{241}Pu_{th,f}$	5-10	MB	I		^{3}H analysis, required to 5-10% in fuel; for yield, 10% essential, 5% desirable
^{95}Zr	$^{232}Th_f$	2	Dos,BU	I	8	Source of request: IAEA consultants meeting on dosimetry [76IAE]
	$^{237}Np_f$				2.8	
	$^{239}Pu_f$				2	
	$^{233}U_{th}$	2	BU	II	4	
^{97}Zr	$^{232}Th_f$	2	Dos,BU	I	6	"
	$^{237}Np_f$				4	
	$^{239}Pu_f$				2	
^{102}Ru	$^{239}Pu_{th}$	1.5	BU	II	2	
^{103}Ru	$^{232}Th_f$	2	Dos	I	6	Source of request: [76IAE]
	$^{237}Np_f$				2.8	
	$^{239}Pu_f$				1.4	
	$^{233}U_{th}$	2	BU	II	4	
^{104}Ru	$^{239}Pu_{th}$	1.5	BU	II	2	
^{105}Rh	$^{233}U_{th}$	5	ρ	II	16	
^{106}Ru	$^{233}U_{th}$	2	Sg	II	4	
	$^{239}Pu_{th}$	2	BU,Sg	II	2.8	
	$^{240}Pu_f$	10	MB	I	8	

Table 5 (continued)

Nuclide	fissioning system th.. thermal f.. fast	Most stringent requirement accuracy 2) (%)	source of request 1)	priority	accuracy given by Meek+Rider 2)	Comment
$^{107}Pd/Ag$	$^{239}Pu_{th}$	5	Dos	II	16	
^{109}Ag	$^{239}Pu_{th}$	5	ρ	II	8	
^{129}I	$^{232}U_{th}$	10	MB	I	16	
	$^{235}U_f$				8	
	$^{238}U_f$				11	
	$^{239}Pu_{th}$				16	
	$^{239}Pu_f$				8	
	$^{240}Pu_f$				16	
	$^{241}Pu_f$				16	
^{131}I	$^{232}Th_f$	2	Dos	I	2.8	
	$^{237}Np_f$				2	
	$^{238}U_f$				2	
^{127}Te	$^{233}U_{th}$	10	ρ	II	16	
^{132}Te	$^{232}Th_f$	2	Dos	I	2.8	
	$^{233}U_f$				8	
	$^{238}U_f$				2.8	
	$^{240}Pu_f$				6	
^{135m}Xe	$^{233}U_{th}$	3	ρ	II	4	
^{135g}Xe	$^{233}U_{th}$	1	ρ	II	2.8	
	$^{239}Pu_{th}$	1			1.4	
^{137}Cs	$^{232}Th_f$	2	BU	I	4	
	$^{233}U_f$				6	
	$^{238}U_f$				1	
	$^{240}Pu_f$				8	
	$^{241}Pu_f$				2	

Table 5 (continued)

Nuclide	fissioning system th.. thermal f.. fast	Most stringent requirement accuracy 2) (%)	source of request 1)	priority	accuracy given by Meek+Rider 2)	Comment
^{140}La	$^{232}Th_f$	2	Dos	I	4	
	$^{233}U_f$				2	
	$^{240}Pu_f$				4	
	$^{241}Pu_f$				1.4	
^{143}Ce	$^{232}Th_f$	2	Dos	I	6	
	$^{233}U_f$				2	
	$^{240}Pu_f$				2.8	
	$^{241}Pu_f$				2	
^{143}Nd	$^{233}U_f$	1.5	BU	I	2	
	$^{237}Np_f$				4	
	$^{242}Pu_f$				4	
^{141}Ce	$^{233}U_{th}$	2	BU	II	2.8	
	$^{239}Pu_{th}$				2.8	
^{144}Ce	$^{232}Th_f$	2	BU	I	4	
	$^{233}U_f$				2.8	
	$^{239}Pu_f$				1	
	$^{240}Pu_f$				6	
^{144}Nd	$^{232}Th_f$	1.5	BU	I	4	
	$^{233}U_f$				2	
	$^{239}Pu_f$				6	
	$^{240}Pu_f$				4	
	$^{242}Pu_f$				4	
^{145}Nd	$^{233}U_f$	1.5	BU	I	2	
	$^{241}Pu_f$				1.4	
	$^{242}Pu_f$				4	
^{146}Nd	$^{233}U_f$	1.5	BU	I	2	
	$^{242}Pu_f$				4	

Table 5 (continued)

Nuclide	fissioning system th..thermal f..fast	Most stringent requirement accuracy 2) (%)	source of request 1)	priority	accuracy given by Meek+Rider 2)	Comment
^{147}Nd	$^{233}U_{th}$	3	ρ	II	4	
^{148}Nd	$^{233}U_f$				2	
	$^{240}Pu_f$	1.5	BU	I	4	
	$^{242}Pu_f$				6	
^{147}Sm	$^{232}Th_f$	1.5	BU	II	4	
^{149}Sm	$^{232}Th_f$	1.5	BU	II	16	
^{150}Nd	$^{232}Th_f$				16	
	$^{233}U_f$	1.5	BU	I	2	
	$^{242}Pu_f$				6	
^{151}Sm	$^{232}Th_f$	15		II	23	
	$^{233}U_{th}$	5	ρ	II	2.8	
^{153}Sm	$^{233}U_{th}$				6	
	$^{235}U_{th}$	2	Sg	II	2.8	
	$^{239}Pu_{th}$				6	
^{155}Eu	$^{239}Pu_{th}$	5	ρ	II	11	

1) Source of request:

MB = fuel cycle mass balance (RP 5); see also Sect. III.4.2.

Dos = neutron dosimetry (RP 6); see also Sect. III.5.2.

BU = burnup (RP 6); see also Sect. III.5.1.

Sg = safeguards (RP 6); see also Sect. III.5.3.

ρ = reactivity changes: the requirements for fission yields which were stated at the Bologna meeting, have by now been met. The origin of the requirements listed here is WRENDA 76/77: some were found directly as requests for yield data, but most of them were taken over from the cross section requests

(for core design) in WRENDA, assuming that the concentrations - and therefore the yields - of the absorbers must be known to an accuracy corresponding to that of the cross section.(RP 3). See also Para. III.2.

2) As the main evaluators are in strong disagreement on uncertainties assigned to chain yields, those of Crough [77Cro] being in general considerably higher than those of Meek and Rider [77Mee], it is in many cases not clear whether requests have been met. The policy followed in producing this table was to be more conservative for the more important cases (priority I) by assuming that Meek and Rider have under-estimated the uncertainties by a factor of two. For the remainder (priority II), it was assumed that the uncertainties given by Meek and Rider are valid.

requirement for each FP is indicated, and the application area from which the request origins.

Additional requests may arise for alternative fuel cycles, as is pointed out in Sect. III.4.5.

(ii) Direct yields

There is only a general request relevant to direct yields: At short cooling times ($\lesssim$10 sec), the decay heat uncertainty due to yield errors comes mainly from inaccuracies in direct yields. The decay heat uncertainty for this interval is to be less than 5%, which leads to the requirement that uncertainties in direct yields (with values exceeding 0.5%) should be comparable to those listed by Meek and Rider [77Mee]. Since these yields are based almost entirely on systematics, their validity cannot be assessed.

(iii) Fission yields versus neutron energy

The requirement for burnup and dosimetry to establish the number of fissions to 1.5-2.0% relative accuracy, requires that fission yields of fission monitors be known to 1.0-1.5% accuracy. This makes a knowledge of the dependence of yields on neutron energy necessary as this dependence is of similar size as the required accuracy. As, at the present time, methods for evaluating the energy dependence are not well established, the development of such methods is required.

IV.2.2. General recommendations and observations

(i) Compilations and evaluations

The tremendous amount of fission yield data available at present calls for both national and international support for evaluators. It is recommended that the support should be given in different forms:

a) The IAEA and other international agencies are asked for appropriate support, e.g. by establishing further contacts between measurers and evaluators.

b) National support should be given by provision of additional staff.

c) Measurers should supply evaluators with information needed. In order to provide revisions of old data, evaluators should send extracts of their files to the measurers concerned, asking for a revision of, or comments to, their entries, e.g. along the following lines:

- The indicated value or its error margins may have to be changed due to better knowledge of the method used or of constants used in the determination (half-lives, decay schemes, branching ratios, newly discovered

isomeric states, neutron capture cross sections, yields of reference nuclides, etc);

- discrepancies to other measurements could be commented;
- duplicates should be removed from the compilation;
- values which have subsequently been shown to be wrong should be withdrawn.

(ii) ENDF/B-V Error Margins

It is understood that a new error evaluation of the yield data entering the ENDF/B-V file in progress and this is welcomed.

IV.2.3. Recommendations for measurements and evaluations

(i) Absolute Fission Yields

It is noted that the results of commonly used evaluation procedures (i.e., normalization of the total sum of mass yields to 200%) are severely influenced by discrepancies in measured element yields, which may comprise significant portions of the mass yield curves. In order to avoid such a bias of evaluated yields and enable the resolution of discrepancies, accurate absolute yield data are required. Experimenters are therefore requested to pay great attention to the absolute calibration of their data and apply two independent methods where possible. Accurate measurements of relative fission yields using gamma-ray spectroscopy can also help to resolve discrepancies, and the use of this technique is recommended for fission yields not having the requested accuracy.

(ii) Chain yields

The requested chain yields as listed in Table 5 should be measured and/or evaluated.

(iii) Direct yields

In order to satisfy the request for decay heat (IV.2.ii.), it is recommended that work on direct yields should continue. Further measurements of fast fission direct yields should be performed, which would also improve the possibilities to predict yields, including a check of the hypothesis of a constant charge dispersion width.

For the purpose of improving systematics, more independent yields of single isomeric states should be measured, with emphasis on the thermal fission of ^{235}U. Measurements of independent

yields, especially for fission reactions showing strong pairing effects (e.g. Th232), would also be needed for the further development of the odd-even systematics.

(iv) Interpretation of fission yields for various neutron energies

It is recommended that the energy dependence of fast fission yields be investigated, especially for those FP which are used in burnup and dosimetry studies (Zr95,97; Ru103; I131; Te132; Cs137; Ba140; Ce143,144; all stable Nd isotopes).

Because the change in many yields with neutron energy is small (<5%), a comparison of absolute literature yields, which often carry uncertainties of 2 to 5%, in general does not allow conclusions to be drawn about the energy dependence. It is therefore recommended, as a first step, that the changes in the relative fission product abundances be evaluated. These are in most cases determined to a much higher accuracy.

(v) Spectral Index

It is strongly recommended that in a measurement of fast-neutron-induced fission, the neutron spectrum should be defined by measurement. As a minimum, the spectral index defined as the ratio of the number of fissions induced in ^{238}U to that in ^{235}U should be indicated.

IV.3. Fission product decay data

IV.3.1. Requirements

Tables 6 to 9 summarize all the accuracy requirements which were expressed at the meeting, the assigned priorities, the sources of the most stringent request, and the accuracy status.

IV.3.2. Observations and recommendations

(i) The detailed requests listed in Tables 6 to 9 which are not yet met should be fulfilled. In addition, comparisons between the data (half-lives, branching ratios, and average energies) in different libraries should continue, and any serious unresolvable discrepancy thus discovered should lead to further request.

(ii) The detailed Request List in the Bologna Panel Proceedings (Vol. II, Table A3-I) should be updated with the help of the information given here and in the Appendix of RP 4. The IAEA should review both the requirements and the status of the

Table 6: Requests for half-life data

Nuclide	required accuracy (%)	priority	source of request 1)	accuracy status (%)	Ref 2)	Comments
Br 87	3-5; met	II		0.2	/1/	for delayed neutron calculation
Sr 91	5	I	DH	11	/2a/	(/3/: accuracy=2%)
Y 98	5	I	DH	8	/2d/	
Zr 95	<1; met	I	Dos	0.1	/2b/	
Zr 97	<1	I	Dos	1	/2c/	(/3/: accuracy=0.3%)
Zr 98	5	I	DH	10	/2e/	
Nb 97	5	I	DH	1	/2c/	discrepancies
Nb 100	5	I	DH	20	/2f/	
Ru 103	<1; met	I	Dos	0.13	/2g/	
Pd 115	5			11	/5/	
Te 132	<1	I	Dos	1	/3/	(new measurement: accuracy=0.4 /4/)
I 131	5	I	DH	0.12	/2h/	
I 133	5	I	DH	0.5	/4/	
I 135	5 met	I	DH, ρ	0.15	/2i/=/3/	
Cs 134	5	I	DH	0.24	/3/	
Cs 137	<1	I	Dos	0.7	/3/	
Xe 135	5; met	I	DH, ρ	0.11	/3/	
Xe 135m	30; met	I	ρ	0.2	/3/	
Ba 140	<1; met	I	Dos	0.1	/2k/;/4/	
La 140	5; met	I	DH	0.5	/2k/	(new measurement: accuracy=0.02/4/)
La 147	5			25	/2L/	
Ce 143	<1; met	I	Dos	0.6	/3/	(new measurement: accuracy=0.1/5/)
Ce 144	<1; met	I	Dos	0.3	/6/	
Nd 149	30; met	I	ρ	0.6	/3/	
Pm 149	5; met	I	ρ	0.1	/3/	
Eu 154	1	II	Sg	D=100 3)		
	5	I				to resolve discrepancy between T1/2=8.5a and T1/2=16a

Table 6 (continued)

1) Sources of requests:

DH ... decay heat calculations (RP 4)
Dos ... neutron dosimetry (RP 6)
ρ ... reactivity changes (RP 3)
Sg ... safeguards (RP 6)

2) References:

The main source for the accuracy status was Table VI of RP 12 /2/. Only in case of default (or serious disagreement with other works), other sources are indicated.

/1/ G. Rudstam, RP 13 of this meeting, Table 1

/2/ J. Blachot, RP 12 of this meeting, Table VI. The following references are quoted in this Table:

/2a/ 69Kni = Knight J.D. et al, Nucl. Phys. A130(1969)753
/2b/ 71Deb = Debertin K., Y. Naturforsch. 26A(1971)596
/2c/ 73Med = Medsker L.R., Nucl. Data Sheets 10 (1973)1
/2d/ 77Sis = Sistemich K. et al, Z. Physik A281(1977)169
/2e/ 76Her = Herzog W. et al, Z. Physik 276(1976)393
/2f/ 74Koc = Kocher D.C., Nucl. Data Sheets 11(1974)279
/2g/ 75Per = Pérolat J.P., LMRI, private communication, 1975
/2h/ 72Eme = Emery J.E., Nucl. Sci. and Engg. 48(1972)319
/2i/ = /3/
/2k/ 74Pek = Peker L.K. et al, Nucl. Data Sheets 12(1974)343
/2L/ 75Loh = LOHENGRIN Collaboration, ILL Grenoble 1975

/3/ D.C. Kocher (editor) "Nuclear Decay Data for Radio-Nuclides Occurring in Routine Releases from Nuclear Fuel Cycle Facilities", ORNL/NUREG/TM-102 (1977)

/4/ K. Debertin, contribution to RP 12. INDC(NDS)-87 (1978)

/5/ G. Skarnemark, Thesis Chalmers University, Goeteborg, Sweden, 1977

/6/ J. Legrand et al, "Table des Radionucléides" (published by CEA, Lab. de Métrologie des Rayonnements Ionisants) (1974)

3) D ... discrepancy

Table 7: Requests for average decay energies ($\bar{E}_\beta + \bar{E}_\gamma$) to calculate decay heat

Nuclide	required accuracy (%)	priority	source of request 1) (RP)	accuracy status 2) (%)	Comments
Br 88,89	10		RP 4	35	
Sr 89	5		RP 4,5	8	discrepancy?
Sr 95	10		RP 4	25	
Sr 96	10			40	
Y 90,91	5		RP 4,5	8	
Y 96,96m				35	
Zr 100				35	
Nb 102				35	
Mo 103,104 105	10		RP 4	35	
Tc 105				25	
Tc 107				35	
Rh 106	5	I		6	
Te 135	10			35	
I 137,138	10			35	
Cs 137	5		RP 5	11	
Cs 141, 142	10			23	
Ba 140	5			7	
Ba 143, 144	10		RP 4	40	
La 140	5; met			2	
La 144	10			25	
La 145,146	10			35	
Ce 141	5		RP 4,5	11	discrepancy ?
Pr 143	5		RP 4	10	
Pr 144	5		RP4,5	7	

1) Source of request:

RP 4 .... removal of decay heat after shutdown

RP 5 .... interim storage and transport

2) The accuracy status was obtained from the Annex to RP4, through the sensitivities and the error in the afterheat due to ($\bar{E}_\beta + \bar{E}_\gamma$)

Table 8: Requests for γ-intensities (γs/disintegr.) of the major γ-rays (i.e. Iγ ≥ 10%)

Nuclide	required accuracy (%)	priority	source of request 1)	accuracy status (%)	Ref 2)	Comments
Br 86	50 ; met	II	RP 5	<25	/9/	high energy γs requested
Zr 95	1	I	BU	1	/2/	
Zr 97	1		Dos	10	/2/	
Nb 94 m	5		σ_{act}	20	/2/	
Nb 95	1 ; met		BU	0.02	/3/	
Mo/Tc 99	5		σ_{act}	< 3	/2/,/4/	
Tc 100	5		σ_{act}	<10	/4/	
Ru 103	1		BU	3 (1)	/2/(/1/)	in brackets: new measurement /1/
Ru/Rh 106	1 3)		BU	< 5 (1)	/2/(/1/)	"
Rh 104	5		σ_{act}	< 5	/4/	
Pd 109				11	/2/	
Ag 108				<20	/10/	
Ag 110				5	/2/	
Ag 110 m				2	/2/	for decay data libraries: γ-transitions see inconsistent and difficult to fit into a coherent scheme
In 116 m (T1/2=54')				< 5	/10/	
Te/I 132	1		Dos	< 4	/2/	
I 128	5		σ_{act}	10	/5/	
I 131	1		Dos	1.5	/2/	
Xe 133	5 ; met		σ_{act}	1	/2/	
Cs 134	1 3)	II	Sg	< 1.5	/1/,/2/	
Cs/Ba 137	1 ; met	I	BU	0.4	/2/,/4/	
Ba 140	1			16(<1.5)	/2/(/1/)	in brackets: new measurement /1/
La 140	1 3); met			<3(<1)	/2/(/1/)	
Ce 141	1			4	/2/,/4/	
Ce 143	5		σ_{act}, Dos	<10	/2/,/4/	
Ce 144	1 3)		BU	4(1.5)	/6/(/1/)	in brackets: new measurement /1/

Table 8 (continued)

Nuclide	required accuracy (%)	priority	source of request 1)	accuracy status (%)	Ref 2)	Comments
Pr 142	5	I	σ_{act}	14	/10/	in brackets: new measurement /1/
Pr 144	1 3)		BU	7 (<1.5)/4/(/1/)		
Nd 147	1		BU	<6	/2/	
Pm 148	5		σ_{act}	<5	/2/,/4/	
Eu154	1		BU, Sg	3	/2/	
Eu 155	1		BU	3	/7/	
Eu 156	1	II	Sg	5	/8/	

1) Sources of request:

RP 5 ... for prediction of high energy (γ,n) reactions in Deuterium (see Sect.III.4.3.)

BU ... burnup, non destructive determination (RP 6, and Sect.III.5.1.)

Dos ... reactor neutron dosimetry (RP 6, and Sect.IV.5.2.)

σ_{act} ... for cross section activation measurements in CFRMF

Sg ... safeguards, non destructive methods (RP 6, and Sect.III.5.3.)

2) References

(The main references for the stuatus of I_γ accuracies were /2/ and /4/; other sources were only consulted when the required information could not be found in /2/ or /4/.)

/1/ K. Debertin, contribution to RP 12

/2/ D.C. Kocher (editor) "Nuclear Decay Data for Radionuclides Occurring in Routine Releases from Nuclear Fuel Cycle Facilities", ORNL/NUREG/TM-102 (1977)

/3/ Nuclear Data Sheets B8 (1972)29

/4/ J. Blachot et al, "Bibliothèque de Données Nucléaires Relatives aux Produits de Fission", CEA-N-1822(1975)

/5/ Nuclear Data Sheets 9 (1973)157

/6/ J. Legrand et al, "Table des Radionucléides" (published by CEA, Lab. de Métrologie des Rayonnements Ionisants) (1974)

/7/ Nuclear Data Sheets 15 (1975)409

Table 8 (continued)

/8/ Nuclear Data Sheets 18 (1976)553

/9/ " " " B5 (1971)151

/10/ M.J. Martin (editor) "Nuclear Decay Data for Selected Radionuclides", ORNL-5114 (1976)

3) Intensity of high energy γ-rays requested to 10% accuracy for shielding during fuel transport. (See Sect. III.4.1.)

Table 9: Request for branching ratio

Nuclide	required accuracy (%) in branching ratio	priority	status	Ref	Comment
I 135	5	I	6	/1/	to g and m; for reactor physics
			3	/2/	

References:

/1/ M.J. Martin, ORNL-5114 (1976)

/2/ H. Feuerstein, J. Oschinski, Inorg + Nucl. Chem. Letters 12 (1976)243

data; assistance in reviewing the status should be sought from the Data Centres and other evaluators. The results should be published in the Newsletter.

(iii) It is highly desirable (for their interchange and comparison) that all evaluated data be stored in a common format. The meeting recommends ENDF/B-IV format at present; and probably ENDF/B-V format when it has been approved and tested. For experimental data the use of the ENSDF format is recommended.

(iv) The meeting notes the incomplete status of uncertainties in beta and gamma transition probabilities in the several data files and recommends as first priority the completion of uncertainty analysis and inclusion of uncertainties in all data files. This is especially important for those nuclides that contribute most to decay heat at longer cooling times.

(v) The meeting recognizes that correlations likely exist among experimental results of decay data (see RP 11 and RP 13) and recommends that consideration be given to encouraging research in quantitative determinations of these correlations among experimental results. Results of these analyses should be included in uncertainties given in the several data files indicating, when possible, the source of the correlation.

(vi) Critical reviews should be made of the different theoretical or semi-empirical methods of predicting decay data when no measurements are available (e.g. half-lives, average energies).

(vii) The greatest source of uncertainty in average β or γ decay energies is frequently the uncertainty in the intensity of the beta-decay to the ground state of the daughter. More experimental effort is needed to measure this as accurately as possible for as many nuclides as possible.

(viii) The meeting recommends remeasuring complete beta-ray spectra of important long-lived fission-product nuclei (see RP 4 Appendix), especially for those nuclides which have not been remeasured since 1960. The measurements should provide beta-ray end point energies, $E_{\beta max}$, to $\pm$10 keV, and the spectra should be measured at least for $E_\beta > 0.05 \times E_{\beta max}$. These measurements are needed to resolve uncertainties and differences in average beta-ray energies among the several data files, as noted in Table VIII (b) of review paper no. 12 (for decay heat calculations).

(ix) It is recognized that decay heat measurements and, even more, γ- and β-spectrum measurements on bulk fission products, can give valuable information on possible errors or discrepancies in the differential data.

(x) There is still a need for more and better data on internal conversion coefficients. Evaluators frequently need to make assumptions about transition types, and interpolate using tables of theoretical data such as that of Hager and Seltzer. Unfortunately there can be large discrepancies and uncertainties in multipolarities in making use of theoretical calculations.

(xi) Frequently it is not known which of two isomers is the ground state. Experiments should be made to remove such uncertainties: but in the meantime compilers of libraries should ensure that all their data (branching ratios, etc) are consistent with whatever choice they make.

IV.4. Delayed neutron data

IV.4.1. Requirements and status of total delayed neutron properties

Apart from the bulk requirements on delayed neutron properties which need further sensitivity studies, requirements on total delayed neutron yield accuracies were expressed for reactor physics purposes (Sect. IV.1.2.):

- to determine ν_d for U233, U235, Pu239 thermal and fast fission and U238 fast fission to $\pm$ 3%.

This requirement has not yet been met, especially for U238.

The meeting noted that, in order to approach the long term goal of assessing individual precursor spectra with sufficient accuracy, also the integral spectra, in equilibrium and time-dependent, require improvement.

At the Bologna Panel, it was recommended that a standard neutron source with an energy spectrum similar to that of total delayed neutrons be prepared for the calibration of the neutron counting facilities in individual laboratories. This has apparently not been done; however americium-lithium sources can be considered adequate and are available with absolute calibration.

IV.4.2. Requirements and status for individual precursor data

From the applications' side, no individual delayed neutron precursor data were requested. Perhaps the bulk requirements relative to reactivity studies (Sect. IV.1.2.) will lead to some needs for precursor data, but sensitivity studies are required first.

Nevertheless, some requirements are expressed below. In general, they refer to the goal of eventually obtaining systematics of delayed neutron precursors which are theoretically well understood and enable reliable predictions of delayed neutron yields, spectra etc.

(i) Half-lives

The status of the half-lives of the 67 precursors identified to date is given in Table 1 of RP 13. The overall accuracy is satisfactory. The only FP whose half-life should be reinvestigated is Cs141: its uncertainties would be required to be $\leq 5\%$, whereas there exists a discrepancy between measurements of $\approx 10\%$.

(ii) Branching ratios (P_n-values)

Table 2 of RP 13 reflects the present status of P_n values. There are 48 precursors having measured P_n-values, with uncertainties between 7 and 50%.

P_n values may be determined directly, by measuring the neutron activity of a separated precursor, or indirectly from the relation $P_n = \frac{\nu_d}{Y_{cum}}$ (Y_{cum} = cumulative yield of precursor under consideration)

The cumulative yields, as sum of independent yields, are very often obtained from systematics - which are not yet well established - and have in general high uncertainties. It is therefore desirable to perform more direct measurements, especially for those FP with unknown or indirect P_n values. An accuracy of 5 to 10% for such measurements is considered to be a realistic goal. This would significantly improve our knowledge of delayed neutron phenomena and would also have a positive impact on yield distribution models.

According to Table 2 of RP 13, direct P_n values have been measured for 43 FPs. The Table includes also the most recent measurements which were performed for As85-87, Br87-92, Rb94-98, Sb135-136, Te136, I132-141 and Cs143-147; but only about 40% of these have errors <10%. They nevertheless suggest immediate reevaluation of the indirectly determined P_n values. The status of P_n values as found in Table 2 of RP 13 is reproduced in Table 10.

For the sake of developing systematics and the yield theory, P_n values of additional even Z isotopes should be measured; this requirement is of less importance to reactor physics.

Y98,99 and In128,129,130 have isomeric states requiring P_n measurements or establishment of the state(s) leading to delayed neutron emission.

Table 10: Status of P_n-values (taken from Table 2 of RP 13)

Precursor	accuracy 1) of P_n (%)	number of 2) direct determinations	number of 2) indirect determinations	Comments
As 84	46		1	
As 85	13	1	2	
As 86	21	1	1	Large discrepancy; direct determination preferred
As 87	32	1		
Se 87	15	1	2	
Se 88	60	1	1	Large discrepancy; direct determination preferred
Se 89	30		1	
Se 91	40	1		
Br 87	6	5		
Br 88	5	4		
Br 89	18	4		
Br 90	11	2		
Br 91	16	2		
Br 92	28	2		
Kr 92	10	1	1	
Kr 93	15	2	2	
Kr 94	64	2		
Rb 92	8	2	1	
Rb 93	8	6	3	
Rb 94	6	6	1	
Rb 95	6	6		
Rb 96	7	6		
Rb 97	10	4		
Rb 98	16	2		
Sr 99	70		1	
Y 97	19		1	
Y 99	67		1	

Table 10 continued

Precursor	accuracy 1) of P_n (%)	number of 2) direct determinations	number of 2) indirect determinations	Comments
Sn 134	42	1	1	
Sb 134	14	1	1	
Sb 135	17	1	1	
Sb 136	35	1	1	
Te 136	45	1	1	
Te 137	23	2		
Te 138	29	1	1	
I 137	8	5		
I 138	12	5		
I 139	9	2		
I 140	28	1		
I 141	34	1		
Xe 141	7	1	1	
Xe 142	8	1	1	
Cs 141	8	2	1	
Cs 142	D=100	3	1	direct exp. values between 0.086 and 0.285
Cs 143	7	4		
Cs 144	24	4		unweighted average, discrepancies between experiments = 100%
Cs 145	14	5		
Cs 146	6	2		
Cs 147	12	1		

1) accuracy given is the error of the weighted average of the P_n values taken into account;

D .... discrepancy

2) in columns 3 and 4 the number of those directly resp. indirectly determined P_n values are given that were taken into account in calculating the weighted average. In general, all values for direct P_n were used, but those for indirect P_n were taken only, when there were less than 2 direct values or when they agreed well with the direct values.

Estimates of unmeasured Pn values based on statistical models are less accurate than was anticipated. Therefore, if estimates are to be made, in the absence of expensive calculations incorporating nuclear structure effects, simple empirical model estimates are still preferred.

(iii) Spectra

Considerable progress on individual spectra has been made since the Bologna meeting. By now, spectra of about 30 precursors have been measured (the nuclides are listed in Table 4 of RP 13.)

Important nuclides still requiring measurement of spectra are

^{93}Kr, ^{97,99}Y, ^{137,138}Te.

The low energy (10 to 100 keV) part of the spectra has been measured for only about half of the precursors, and should be measured for the remaining ones, namely: (Zn,Ga)79; Ga80,81; Br88-91; In129,130; Sn134; I139,140. Of relatively high importance are the spectra of the shortlived halogens.

Further work on assessment of the properties of different spectrometer types, especially concerning response function and detector efficiency is urgently needed: experiments using He^3, time-of-flight, and proton recoil methods show considerable differences.

(iv) Average neutron energies

Average delayed neutron energies for individual precursors have been measured within $\simeq$50 to 100 keV, including systematic errors which can now realistically be kept below 20 to 50 keV. (Note that the errors given by the SOLIS group [76Ree] to date do not include systematic errors.)

IV.4.3. Observations and conclusions

(i) Considerable progress concerning individual precursor data has been made since Bologna, which may be summarized as follows:

- There are 69 known precursors vs. 42 at the time of the Bologna Panel;
- Based entirely on energetics, $\sim$102 potential precursors (including isomeric states) have been identified that have yields of significance in fast or thermal fission.

- There are 48 precursors having measured Pn values (direct or indirect) vs. ~34 reported at Bologna.

- 15 more neutron spectra from individual precursors have been measured since the Bologna Panel. (by the time of the Panel ~12 had been measured)

(ii) The emphasis is shifting from group data towards data for individual precursors. These data constitute the basis for a reliable prediction of macroscopic properties like total number of delayed neutrons, delayed neutron energy spectra etc, and their dependence on all operational conditions (i.e. fuel composition, reactor power, operating history and cooling time).

As a guideline, it may be assumed that for any combination of microscopic quantitites that are worth ~1% of a macroscopic property, a 5-10% accuracy in the microscopic data should be reached.

(iii) The improvement of data for individual precursors presupposes a corresponding improvement in independent fission product yields.

IV.4.4. Recommendations

(i) In accordance with the requirements stated in the previous actions, the following measurements are recommended:

- measurement of fission spectrum averaged total delayed neutron yield (ν_d) of U238;

- improvement of the knowledge of integral equilibrium and time dependent spectra;

- to improve the accuracies of Pn values of the FP listed in Table 10 to become 5 to 10%. At present, this re-requirement seems not to be met for ~70% of the 48 precursors with determined Pn values.

- to determine Pn values of additional even Z isotopes and of the isomeric states of Y98,99 and In128-130;

- to measure the delayed neutron spectra of Kr93; Y97,99; Te137,138. And the low energy part (10 to 100 keV) of (Zn,Ga)79; Ga80,81; Br88-91; In129,130; Sn134; I139,140.

(ii) Delayed neutron spectra from individual precursors measured by different techniques differ considerably. A resolution of these discrepancies is urgently required, in terms

of analyzing response functions and efficiencies of the different detectors.

(iii) The goal of producing macroscopic delayed neutron properties from precursor data will require some additional accurate measurements of equilibrium and group data for comparison purposes.

IV.5. Fission product neutron cross sections

IV.5.1. Requirements and status:

(i) thermal capture cross sections and resonance integral data

A survey of all the requests for thermal neutron capture cross sections and resonance integrals, and the status of these data can be found in Table 11. Below, some comments concerning the requirements and status are given.

At the Bologna meeting, the variation of the Xe135 and Sm149 capture cross sections with neutron energy was required to an accuracy of ± 10% for the calculation of the temperature coefficient of reactivity. Whereas no recent data exist for Xe135, measurements for Sm149 were made at Brookhaven [74Bec], and at the Rensselaer Polytechnic Institute (R.P.I.) [75Hoc]. An evaluation of these data is recommended.

For the resonance integrals of Tc99 and Pd107, a discrepancy between the experimental values and the value obtained from resonance parameters exists.

The accuracy of 2% for the thermal capture cross section of Sm151 originates from recent measurements of Kirouac and Eiland [75Kir].

The requests found in WRENDA 76/77 and included in Table 11 may partly be superseded.

(ii) Fast capture cross sections

Fast capture cross sections are essentially needed for corrections in the burnup determination (Sect. III.5.1.) and for the prediction of the bulk FP reactivity effect (Sect. III. 2.2.).

The element most frequently used as BU-monitor is Nd. Therefore the fast capture cross sections of Nd143-150 are required with high priority: if they are larger than 100mb, they should be known to an accuracy of 10%, preferably as differential data. A more general request for BU monitors, which has much lower priority, is to know the fast capture

Table 11: Requirements and Status for Thermal Capture Cross-Section and Resonance Integral Data

FP	Quantity	required accuracy %	source of request	priority	status g) (%)	E-range of resolved resonances (eV)	Comments
^{83}Kr	σ_{th},RI	10	W	2	15/1/		
^{95}Zr	σ_{th}	20b	W	2	D=5b/4/		radioactive; D between 2 evaluations (/5/,/7/)
	RI	20b			D=3b/4/		
^{95}Nb	σ_{th}	100b	W	2	D=3b/4/		radioactive; "
^{99}Mo	σ_{th}	100b	W	2	D=5b/4/		" "
	RI	1000b			RI=26b/4/		RI= evaluated data (/5/,/7/)
^{99}Tc	σ_{th}	20	DH	1	10[b])/2/	5.6- 280 eV	
	RI	15					
^{101}Ru	σ_{th}	10	W	1	30/1/		
	RI	10			15/1/		
^{103}Ru	σ_{th}	35b		2	D=60b/3/		radioactive; D between 2 evaluations(/5/,/7/)
	RI	1000b			D=500b/3/		
^{103}Rh	σ_{th}	5	S	1	4/2/	1- 4100 eV	met
	RI	10	W		5/2/		
^{105}Rh	σ_{th}	5	W	1	10/1/		radioactive
	RI	20			10/1/		
^{107}Pd	σ_{th}	10b	W	2	D=100b/3/		
	RI	10			6/3/		D between calc. and exp.RI>100%

Table 11 (continued)

FP	Quantity	required accuracy %	source of request	priority	status g) (%)	E-range of resolved resonances (eV)	Comments
^{107}Ag	σ_{th}	10	W	2	3 /1/		met
	RI	10			10 /1/		
^{109}Ag	σ_{th},RI	10	W	2	3 /1/	5eV-2.5 keV	"
^{127m}Te	σ_{th}	900b	W	2			105d isomer; estimate /5/ for σ_{th}=9.4b
	RI	20					
^{132}Te	σ_{th}	250b	W	2			radioactive; estimate /5/ for σ_{th}=2.4mb, RI=7mb
	RI	500b					
^{131}Xe	σ_{th}	15	S	1	11 /1/		met
	RI	10			5 /1/		
^{133}Xe	σ_{th}	3	W	2	50 /1/		radioactive
	RI	3					
^{135}Xe	σ_{th}	8	S	1	3 /2/		" ; met
	RI	100			7 /2/	0.084 eV	
	E-depend.	10	S				
^{133}Cs	σ_{th}	3(-5) c)	BU		3		met (according /1/ accuracy is 5%)
	RI	3(-5)			10	7.14- 3520 eV	139 resonances (according /1/ accuracy is 4%)
^{134}Cs	σ_{th}	3(-5) c)	BU		10		
	RI	10 d)			no data		
^{135}Cs	σ_{th}	10	W	1	8 /1/		
	RI	10			D=20 /3/		D between calcul. and exp. RI

Table 11 (continued)

FP	Quantity	required accuracy %	source of request	priority	status g) (%)	E-range of resolved resonances (eV)	Comments
^{141}Pr	$\sigma_{th,RI}$	3-5 c)	BU		3 /1/	85 eV - 10 keV	σ_{th} and RI lower than 20b, therefore no requirement
^{143}Nd	σ_{th}	3-5 c)	BU	1	3 /2/		met
	RI	10 d)			>factor 2	6 eV - 5.5 keV	112 resonances
^{145}Nd	σ_{th}	3-5 c)	BU	1	5 /1/		met
	RI	10 d)			12 /1/	6 eV - 4.6 keV	192 resonances; nearly met
^{147}Nd	σ_{th}	10	BU b,f)	1	30 /6/		1 measurement with 30% accuracy
	RI	10					
^{147}Pm	σ_{th}	20	BU e)	1	4 /1/		met
	RI	20			30 /1/	1.6-160 eV	42 resonances
^{148g}Pm	σ_{th}	10	W	1	50 /1/		radioactive, $T_{1/2}$ = 5.37d
	RI	10			D=50 /4/		D between evaluations (/5/,/7/)
^{148m}Pm	σ_{th}	30	DH	1	12 /1/		met
	RI	30			70 /1/	0.169eV	1 resonance; $T_{1/2}$ = 41d
^{149}Pm	σ_{th}	20	W	1	20 /1/		met; radioactive
	RI	20					
^{151}Pm	$\sigma_{th,RI}$	10	W	2			radioactive
^{149}Sm	σ_{th}	20	?		3 /1/		met
	E-depend.	10				0.1-249eV	
^{150}Sm	$\sigma_{th,RI}$	3	W	1	5 /1/		

Table 11 (continued)

FP	Quantity	required accuracy %	source of request	priority	status g) (%)	E-range of resolved resonances (eV)	Comments
^{151}Sm	σ_{th}	8	ρ		2 /6/		met
	RI	40	ρ		5	0.45-295.7 eV	121 resonances, met
^{152}Sm	σ_{th}	20	ρ	2	3 /1/		met
	RI	10	ρ	2	5	8- 5000 eV	met
^{153}Sm	σ_{th}	1000b	BU		no data		radioactive
	RI	20	W				radioactive
^{153}Eu	σ_{th}	3	Sg		15 b)		
	RI	10 d)	BU		12 /1/	0.457-97.6 eV	76 resonances
^{154}Eu	σ_{th}	2	Sg		30 /1/		radioactive
	RI	10 d)	BU		no data		radioactive
^{155}Eu	RI	10	W		D=56 /3/	0.19-3.9 eV	radioactive; D for evaluations

a) Sources of requests:

W .... WRENDA 76/77
DH .... decay heat (RP 4)
ρ .... reactivity predictions (RP 3 here and at Bologna Panel)
BU .... burnup determination (RP 6)
Sg .... safeguards (RP 6)

Table 11 (continued)

b) experimental data with ± 15%, evaluation with ± 8% accuracy

c) required to 3.5% if σ_{th} > 20b

d) required to 10% if RI > 50b

e) not in RP 6

f) not for power reactors, but for special high flux irradiations ($5 \cdot 10^{14}$ n/cm^2 s)

g) References:

/1/ BNL-325, 3rd edition (1973)

/2/ 1973 Bologna Panel, P.Ribon: RP 10 (IAEA-169,Vol.I)

/3/ This meeting, RP 7 (E. Fort)

/4/ A.L. Pope, J.S. Story, contribution to RP 10 of 1973 Bologna Meeting, IAEA-169,Vol.III, p.163

/5/ 1971 Cook Library, as quoted in /4/

/6/ G.J. Kirouac and H.M. Eiland, Phys. Rev. C11 (1975) 895

/7/ ENDF/B-III Library (1971), as quoted in /4/

D ... discrepancies

cross sections (>100mb) of all major stable FP to 15%.

As a long term goal, the calculation of the net effect of lumped FP on reactivity should be accurate to ± 7%. Calculations have been carried out in the Netherlands [76Hei] and France [77Lan] which suggest that, with the accuracies of individual cross sections as given in present evaluation, this target is already reached. However, preliminary results of experiments performed in France on irradiated fuel from PHENIX [77Lan] show integral data which are systematically about 15% lower than those calculated. On the other hand, Dutch experiences with samples of irradiated thermal reactor fuel oscillated in STEK (see RP 14) are in satisfactory agreement with the calculations. Before judgement is made, the final analysis of the French experiments must be awaited; only then it can also be decided whether new experiments on bulk FP samples are required or not.

There was some discussion about the fast capture cross section accuracies of individual FP that should be reached in order to safely fulfill the bulk requirements. Finally, the values included in Table 12 were agreed upon, which are mostly much lower than those requested at the Bologna Panel. The main argument for accepting these tight requests is that possible systematic errors in the capture cross sections of individual FP in general do not cancel statistically.

Table 12 gives for each FP the most stringent requirement, the source of the request, the status of differential (σ_γ vs. neutron energy) as well as of integral (σ_γ averaged over fast neutron spectrum) data or measurements, and remarks about planned, ongoing or recommended actions to improve the situation. As far as requests for reactivity calculations are concerned, the required accuracy relates to the capture cross section averaged over a fast breeder reactor spectrum.

(iii) Scattering data

The reactivity effect due to inelastic scattering of lumped FP is 10% to 15% of the capture effect. An accuracy of ± 30% in the bulk FP reactivity effect is wanted.

The data for inelastic scattering cross sections are mainly based on theory. Calculations performed with the data from the various recent evaluations differ by no more than about 15% in the net effect due to scattering, the agreement being probably due to partial cancellation of errors. This suggests that the 30% accuracy requirement has been achieved, but a check of the evaluations by integral measurements is recommended. Possibly, the CFRMF reactivity worth measurements could be used for such a test. If the uncertainty in the scattering effect would turn out to be lower than 20%, this would relax the demands for capture data.

Table 12: Requests and Status for fast capture data

Nuclide	Request [a]	Status [b] microscopic	Status [b] integral	Action
^{93}Zr	20 %	only 1 resonance no keV data not met	only STEK oscill. /13/ probably met	further analysis of STEK data
^{95}Mo	10 %	many resonances new data of Musgrove /1/ <90keV status 15%	STEK oscill. PHENIX irrad. /14/ FRO oscill. /15/ (agreement) met	no action
^{97}Mo	10 %	many resonances new data of Musgrove /1/ <90keV status 15%	STEK oscill. PHENIX irrad. FRO oscill. (agreement) met	no action
^{98}Mo	20 %	many resonances new data of Musgrove /1/ <90keV bad for E >90keV status 15%	STEK oscill. CFRMF activ. /3/ ERMINE activ. (not very good agreement between STEK/CFRMF) met	no action
^{99}Mo	(ϱ(t))	Interpolation by Musgrove /1/		reevaluation is recommended
^{100}Mo	20 %	many resonances new data of Musgrove /1/ <90keV status 15%	STEK oscill. CFRMF activ. (in same direction) ERMINE activ. met	no action
^{99}Tc	10 %	only one set of data for E <50keV /2/ very discrepant calculations for E >100keV not met	STEK oscill. French oscill. /14/ CFRMF activ. FRO oscill. (discrepancies) not met	planned: resolved resonances experiments in Kiel recommended: measurement of average σ for E=1 to 500 keV; $\langle \Gamma_\gamma \rangle$ measurements; irradiation in EBR-2

Table 12 (continued)

Nuclide	Request [a]	Status [b] microscopic	Status [b] integral	Action
^{101}Ru	10 %	many resonances unpublished RPI data /4/ not met	STEK oscill. FRO oscill. PHENIX irrad. (good agreement) probably met	analyse data of Hockenbury /4/ compare with integral data
^{102}Ru	20 %	few resonances; unpublished RPI data /4/ (very low) not met	French oscill. FRO oscill. STEK oscill. CFRMF activ. ERMINE activ. (very good agreement) met	(perhaps more resonances required) compare RPI data with integral data
^{103}Ru	20 %	no data at all very large differences between evaluations not met	no data	evaluation with new microscopic + integral data of $^{101,102,104}Ru$
^{104}Ru	20 %	see ^{102}Ru	see ^{102}Ru (no French oscill.)	see ^{102}Ru
^{106}Ru	low priority; remove from request list			
^{103}Rh	10 %	many data uncertain: 1-10keV status: 10 to 15%	French oscill. FRO oscill. STEK oscill. CFRMF activ. (good agreement) met	no action
^{105}Rh	(for time dependence of reactivity)			reevaluation recommended
^{105}Pd	10 %	resonances to 160 eV recent RPI /5/ and ORELA /6/ data in keV range; discr. near 100 keV no data for $160\ eV \leq E \leq$ few keV status 20%	STEK oscill. French oscill. PHENIX irrad. (30% discrepancies between STEK and PHENIX; irradiations: difficult to obtain pure sample!) not met	planned: resolved resonances in Geel ongoing: resolved resonances in RPI recommended: microscopic data for 160 eV $\leq E \leq$ 10keV; integral irradiation experiments

Table 12 (continued)

Nuclide	Request [a]	Status [b] microscopic	integral	Action
^{107}Pd	10 %	no data; to be published: RPI data in resolved resonance range not met	only STEK oscill. (not a very high accuracy) not met	new evaluation RPI + STEK data
^{109}Ag	10 % to 20 %	many resonances discrepant series of data in keV region data also available for ^{107}Ag, natural Ag not met	CFRMF activ. STEK oscill. French oscill. (reasonably good agreement) met	evaluations can be improved with integral + micr. data of ^{107}Ag, nat. Ag.
^{127}I	10 % (St)	new resonances (Geel /7/) many data; discrepancy between stat. model and keV data; status 20%	STEK oscill. CFRMF activ. (in agreement with most keV data) (status: met for reactor physics purposes)	more microscopic data in keV range, to become a secondary standard
^{129}I	20 %	few resonances, Γ_γ not known no keV data not met	STEK oscill. CFRMF activ. (good agreement) met	no action
^{131}Xe	20 %	no data at all; large discr. between evaluations not met	only STEK oscill. (FP mixture) not yet analyzed	analyse STEK data
^{132}Xe	30 %	no data not met	STEK oscill. (FP mixture) CFRMF activ. not yet analyzed	analyse STEK data
^{133}Cs	10 % (5 to 10% Fh)	many resonances; discrepant series of keV data; to be published: RPI data /8/, Japanese data /16/, /17/ not met	RAPSODIE irrad. /18/ CFRMF activ. STEK, French oscill. PHENIX irrad. (good agreement between STEK/French oscill., CFRMF data lower; transm. and activ. data in agreement) probably 10% met	recommended: evaluate new data

Table 12 (continued)

Nuclide	Request [a]	Status [b] microscopic	Status [b] integral	Action
^{135}Cs	10 %	no data at all planned: Kiel /9/ mixed FP resolved res. not met	only STEK oscill. (sample not very good) not met	recommended: integral activation measurements evaluation with Cs133,136 data
^{139}La	20 %	many resonances many keV data nearly met?	STEK oscill. CFRMF activ. (good agreement) met	no action
^{144}Ce		low priority; remove from request list		
^{141}Pr	20 %	many resonances many keV data discr. at high E not met	STEK oscill. CFRMF activ. French oscill. ERMINE oscill. (good agreement) met	no action
$^{143-150}Nd$	10 % (BU)	resolved res. known recent data of Musgrove et al. E= 1 to 19 keV /10/ status: ≈15%	STEK oscill. (not yet analyzed) Nd145: PHENIX irrad. in progress: stable Nd143-150 EBR-2 irrad. and RAPSODIE (meas'ments completed) planned: Nd143 PHENIX irrad. status: not known	evaluate Musgrove's data; analyse STEK data
^{147}Pm	10 %	many resonances no keV data, evaluations in good agreement, not met	STEK oscill. (not analyzed) CFRMF activ. French oscill. FRO oscill. (good agreement) not met	microscopic keV data required planned: integral activ. ERMINE
^{148m}Pm	Dh	no data at all probably met with ENDF/B-IV	no data	no action
^{149}Pm	(ϱ(t))	no data		reevaluation recommended

Table 12 (continued)

Nuclide	Request [a]	Status [b] microscopic	integral	Action
^{147}Sm		low priority; remove from request list		
^{149}Sm	10 %	many resonances; Russian keV data /11/ to be published: RPI keV data /4/ not met	FRO oscill. STEK oscill. PHENIX irrad. EBR-2 irrad. (to be analyzed) discrepancy between STEK and recent keV data not met	recommended: evaluate new data
^{151}Sm	10 %	many resonances no keV data not met	STEK oscill. (not accurate) PHENIX irrad. (perhaps new PHENIX irrad. in future) not met	keV data required
^{152}Sm	20 %	many resonances few activation data /12/ not met	STEK oscill. CFRMF activ (good agreement) probably met	
^{153}Eu	20 %	resonances up to 100eV discrepant keV data to be published: JAERI data probably met with new data	STEK oscill. (not analyzed) CFRMF activ. French oscill. probably met	analyse STEK, JAERI data
^{155}Eu	20 %	no data at all planned: data from Kiel /9/ not met	no data	
^{151}Eu	5 %	required for control rod materials	for several isotopes there are data from STEK, CFRMF and EBR-2 (to be analyzed)	
^{152}Eu	20 %			
^{153}Eu	5 %			
^{154}Eu	20 %			
Eu nat	?			

Table 12 (continued)

a) Source of requests:

All requests are for reactivity calculations, except where stated otherwise:

$\rho(t)$	...	is a request for the time dependence of reactivity at reactor shutdown (Sect. III.2.2.(iii)
Fh	...	Fuel handling (request made at Bologna Panel)
BU	...	burnup monitors
Dh	...	decay heat calculation
St	...	secondary standard

b) References:

/1/ A.R. Musgrove, Nucl. Phys. A270 (1976)108

/2/ Chou, J. of Nucl. Energy 27 (1973)811

/3/ Y.D. Harker, in "Progress in FPND", INDC(NDS)-86, p. 77-83 (1977)

/4/ Hockenbury; Bull.Am. Phys. Soc. 20 (1976)560 (abstract, no data); see also EXFOR 10552

/5/ Hockenbury, NBS-Spec. Publ.-425 (1975 Washington Conf.) p. 904

/6/ see INDC(NDS)-86 ("Progress in FPND") p.72 (1977)

/7/ G. Rohr et al, Int. Conf. on Interactions of Neutrons with Nuclei; Lowell, Massachusetts, 6-9 July 1976; p.1249

/8/ Hockenbury, Bull. Am. Phys. Soc. 21 (1976)537 (abstract no data)

/9/ see INDC(NDS)-86 ("Progress in FPND") p.10 (1977)

/10/ A.R. Musgrove, to be published in Nucl. Phys. See also EXFOR 30360

/11/ Kononov et al, YK-22(1976)29

/12/ F. Bensch, H. Ledermann, INDC(AUS)-2/G, p.1 (1971)

/13/ J.J. Veenema, A.J. Janssen, "Small sample reactivity worths of FP isotopes and some other meterials measured in STEK", ECN-10(1976)

Table 12 (continued)

/14/ Langlet and Martin-Deidier, contribution to RP 14 of this meeting. Published in INDC(NDS)-87 (1978). ("French oscill." means: ERMINE and MASURCA oscillation experiments)

/15/ T.L. Anderson, AE-428 (1971)

/16/ N. Yamamuro et al., Conf. on Nuclear Cross Sections and Technology, Washington D.C. (1975), NBS-SP-425, p.802.

/17/ N. Yamamuro, private communication 1977

/18/ L. Koch, private communication 1977

IV.5.2. Recommendations

(i) - New measurements of differential fast capture cross sections are recommended for the following FP (see also Table 12, "actions"):

Tc99, (Ru102,104), Pd105, I127, Pm147, Sm151;

- Additional integral irradiation measurements of fast neutron capture cross sections would be of value for:

Tc99, Ru101, Pd105, Pd107, Cs135 and Sm151;

- New evaluations are recommended for all FP whose differential or integral capture cross sections do not meet the required accuracies. Some nuclides like Ru103 and Cs135 have isotopic neighbours whose capture cross sections have been measured recently. In these cases the required data may be deduced from systematics; nevertheless the determination of some data (e.g. resolved resonances) of the nuclides themselves would improve the quality and reliability of the systematics and the evaluated data.

(ii) Because evaluations of fast neutron cross sections are partly based on nuclear models, the following recommendations are considered as important:

- The methods of determining average parameters from resolved resonance parameters should be improved. This could for instance be done through an intercomparison of available methods by computer simulation, preferably on an international basis. It was suggested that P. Ribon could act as coordinator of such an international project, with the support of IAEA/NDS.

- Strong support should be given to the evaluators of level scheme data.

- It is recommended that IAEA/NDS organize a specialist meeting on the systematics of all parameters needed in model calculations of 'neutron cross sections'.

- Evaluators should make use of the recent developments in nuclear theory, in close cooperation with fundamental physicists. Important developments are e.g.: recent statistical model improvements, SPRT method for optical model parametrization [75Del] and inclusion of direct collective effects to calculate inelastic scattering cross sections (see also the recommendations of the Consultants Meeting on Nuclear Theory in Neutron Nuclear Data Evaluation, Trieste 1975 [75Tri]).

(iii) There is a large number of recent microscopic capture cross section data which have not yet been included in the present evaluations. Moreover many experiments on differential and integral data are ongoing. It is therefore recommended that:

-A specialist meeting on the status of capture cross sections for FP should be organized in a few years time. Both experimentalists and evaluators should re-examine the cross section status.

(iv) With respect to the role of integral data the following recommendations are made:

- It is recommended to use various integral data obtained at different facilities to derive adjusted capture cross sections.

- For the convenience of the cross section data users, the results of integral measurements should be incorporated in evaluated point cross section libraries, preferably in one of the well-known formats.

- It is recommended that further integral measurements, in particular irradiation measurements in fast power reactors (or prototypes) are performed for a number of important unstable FP nuclides (see Table 12).

- For the estimate of the bulk FP effect on sodium void reactivity, integral experiments would be of help; the necessity of such experiments must however be confirmed by feasibility studies.

- As "standard" for integral measurements the nuclide Rh^{103} is suggested. Also I^{127} could be used but the microscopic data for this nuclide have to be improved first.

References

61Shu K. Shure, WAPD-BT-24 (1961)

74Bec F. Becvar et al., Nucl. Phys. A236 (1974) 198

74Hec D. Heck et al., Atomkernenergie 24 (1974) 141

75Del J.P. Delaroche et al., IAEA-190 vol.I, p.251 (1976) (Consultants meeting on the Use of Nuclear Theory in Neutron Nuclear Data Evaluation, Trieste, December 1975)

75Hoc R.W. Hockenbury et al., Bull. American Phys. Soc. 20 (1975) 560

75Kir G.J. Kirouac and H.M. Eiland, Phys. Rec. C 11 (1975) 895

75Pet First ASTM-Euratom Symposium on Reactor Dosimetry, Petten 1975

75Tri Consultants meeting on the use of Nuclear Theory in Neutron Nuclear Data Evaluation, Trieste, December 1975: Summary Report (IAEA-190 vol.I., p.1)

76But A.T.D. Butland, contribution to RP 3, private communication

76Hei R.J. Heijboer et al., "Pseudo fission product cross sections for a fast breeder reactor", ECN-11 (1976), and RP 14

76IAE IAEA Consultants Meeting on Integral Cross Section Measurements in Standard Neutron Fields, Vienna, November 1976: Summary Report (INDC(NDS)-81, 1977)

76Mae W.J. Maeck et al., USERDA-report ICP-1092 (1976)

76Ree P.L. Reeder, J.F. Wright, J.L. Alquist, Battelle Pacific Northwest Laboratories Report BNWL-SA-5890 Rev (1976)

77Cro E.A.C. Crouch, Atomic Data and Nuclear Data Tables 19, No. 5 (1977)

77Mee M.E. Meek and B.F. Rider, USERDA-report NEDO 12154-2 (1977)

77Lan G. Langlet, L. Martin-Deidier, "The French programme for the determination of the fission product effect in fast reactors", contribution to RP 14 of this meeting. Published in INDC(NDS)-87 (1978).

APPENDIX A: LIST OF PARTICIPANTS

AUSTRIA

Lammer, M.	Österreichische Studienges. für Atomenergie Forschungszentrum Seibersdorf A-2444 Seibersdorf

BELGIUM

Bemelmans, P.	Centre d'Etude de l'Energie Nucléaire B-2400 Mol
Del Marmol, P.	"

CANADA

Walker, W.H.	Atomic Energy of Canada Limited Chalk River, Ontario

FRANCE

Delaroche, J.P.	Centre d'Etudes de Bruyères-le-Châtel B.P. No. 61 F-92120 Montrouge
Barrê, J.Y.	Centre d'Etudes Nucléaires de Cadarache C.E.A. B.P. No. 1 F-13115 Saint Paul Lez Durance
Fort, E.	"
Langlet, G.	"
Robin, M.	"
Blachot, J.	Centre d'Etudes Nucléaires de Grenoble Cedex No. 85 F-38041 Grenoble Gare
Devillers, C.	Centre d'Etudes Nucléaires de Saclay B.P. No. 2 F-91190 Gif-sur-Yvette

GERMANY, FED. REP.

Debertin, K.	Physikalisch-Technische Bundesanstalt Abteilung 6 Bundesallee 100 D-3300 Braunschweig

Denschlag, J.O.	Institut für Kernchemie Universität Mainz Friedrich v. Pfefferweg 14 Postfach 3980 D-6500 Mainz
Kratz, K.L.	"
Priesmeyer, H.G.	Institut für Reine und Angewandte Kernphysik Reaktorstation D-2054 Geesthacht

ISRAEL

Amiel, S.	Soreq Nuclear Research Centre Atomic Energy Commission Yavne 70600
Nir-El, Y.	"

ITALY

Fabbri, F.	Centro di Calcolo del C.N.E.N. Via Mazzini 2 I-40138 Bologna
Menapace, E.	"
Reffo, G.	"

JAPAN

Iijima, Shungo	NAIG Nuclear Research Laboratory NAIG Co., Ltd. 4-1 Ukishima-Cho, Kawasaki-Ku Kawasaki 210

NETHERLANDS

Aten, A.H.W.	IKO, Institute for Nuclear Research 18 Oosterringdijk P.O. Box 4395 Amsterdam-1006
Bustraan, M.	Energy Research Foundation (ECN) Petten
Dekker, J.W.M.	"
Dragt, J.B.	"

Gruppelaar, H.	Energy Research Foundation (ECN) Petten
Heijboer, R.J.	"
Janssen, A.J.	"

SWEDEN

Lindborg, L.	National Institute of Radiation Protection Fack S-10401 Stockholm
Nilsson, G.	AB Atomenergi Studsvik Fack S-611 01 Nykoeping
Rudstam, G.	The Swedish Research Council's Laboratory Studsvik Fack S-611 01 Nykoeping 1

SWITZERLAND

Von Gunten, H.R.	Institut Fédéral de Recherches en Matières de Réacteurs CH-5303 Würenlingen

UNITED KINGDOM

Crouch, E.A.C.	Chemistry Div., Bldg. 220 Atomic Energy Research Establishment Harwell, Didcot, Oxon. OX11 ORA
McKay, H.A.C.	Chemical Technology Div., Bldg. 220 Atomic Energy Research Establishment Harwell, Didcot, Oxon. OX11 ORA
Cuninghame, J.G.	Chemistry Div., Bldg. 540.1 Atomic Energy Research Establishment Harwell, Didcot, Oxon. OX11 ORA
James, M.F.	Reactor Physics Div., B.21 Atomic Energy Establishment Winfrith, Dorchester, Dorset
Rowlands, J.L.	Room 220, Building B.21 Atomic Energy Establishment Winfrith, Dorchester, Dorset

UNITED STATES OF AMERICA

Dickens, J.K.	Oak Ridge National Laboratory Oak Ridge, Tennessee 37830
England, T.R.	Los Alamos Scientific Laboratory P.O. Box 1663 Los Alamos, New Mexico 87545
Yarnell, J.L.	"
Harker, Y.D.	Nuclear Physics Branch EG and G Idaho, Inc. P.O. Box 1625 Idaho Falls, Idaho 83401
Maeck, W.J.	Allied Chemical Idaho Chemical Programs-Operations Office 550 Second Street Idaho Falls, Idaho 83401
Schenter, R.E.	Hanford Engineering Development Laboratory P.O. Box 1970 Richland, Washington 99352
Stamatelatos, M.G.	Science Applications, Inc. 1200 Prospect Stree P.O. Box 2351 La Jolla, California 92038

C.E.C. - GEEL

Bambynek, W.	Bureau Central de Mesures Nucléaires Steenweg naar Retie B-2440 Geel
Corvi, Mr.	"

C.E.C. - ISPRA

Foggi, C.	Centre Commun de Recherche C.C.E. I-21020 Ispra (Varese)
Sola, A.	"

C.E.C. - KARLSRUHE

Koch, L.	Europäisches Institut für Transurane Postfach 2266 D-7500 Karlsruhe

I.A.E.A. - NDS (Scientific Secretaries)

Lammer, G.	Nucelar Data Section International Atomic Energy Agency Vienna
Schmidt, J.J.	"

N.E.A. - NDCC

Osterhage, W.	NEA Neutron Data Compilation Centre B.P. No. 9 F-91190 Gif-sur-Yvette

APPENDIX B: MEETING AGENDA

Monday, 5 September

Morning

INTRODUCTION

Welcome addresses, introduction

RP 1

SESSION I: User requirements (Chairman: J.L. Rowlands)

RP 2, 3, 5 and 6

Afternoon

RP 4 and 15

Contributed paper by J.K. Dickens

Contributed paper by J.L. Yarnell

Nomination of working groups, their chairmen and secretaries

Tueday, 6 September

Morning

SESSION II: Status of FPND (Chairman: S. Amiel)

RP 11 and 10

Contributed paper by S. Amiel

Contributed paper by L. Koch

Afternoon

RP 7

Contributed paper by G. Reffo

RP 9

Wednesday, 7 September

Morning

SESSION II (continued)

RP 14

Contributed paper by G. Langlet

RP 8, 12, 13

Contributed paper by K.L. Kratz

Afternoon

WORKING GROUP (WG) Meetings (all simultaneously):

WG on bulk properties of fission products (Chairman: M. Lammer)

WG on fission product yields (Chairman: J.G. Cuninghame)

WG on fission product decay data (Chairman: J. Blachot)

WG on delayed neutron data of fission products (Chairman: G. Rudstam)

WG on neutron reaction cross-sections of fission products (Chairman: M. Bustraan)

Thursday, 8 September

Morning and Afternoon

WORKING GROUP Meetings continued

Friday, 9 September

Morning

FINAL PLENARY SESSION (Chairman: J.J. Schmidt)

Presentation of the general recommendations to the IAEA and of the conclusions and recommendations drafted by the working groups, and their discussion.

APPENDIX C

WORKING GROUPS (WG) AND THEIR MEMBERS

(S .. Secretary, C .. Chairman)

WG on FP bulk properties

Lammer, M. (C, S)
Lindborg, L.
McKay, H.A.C.
Rowlands, J.L.
Sola, A.

WG on FP yield data

Amiel, S.
Bemelmans, B.
Crouch, E.A.C.
Cuninghame, J.G. (C)
Debertin, K.
Denschlag, J.O. (S)
Koch, L.
Lammer, M.
Lammer, G.
Lindborg, L.
Maeck, W.J.
McKay, H.A.C.
Nir-El, Y.
Robin, M.
von Gunten, H.R.
Walker, W.H.

WG on FP decay data

Bambynek, W.
Bemelmans, P.
Blachot, J. (C)
DelMarmol, P.
Devillers, C.
Dickens, J.K.
James, M.F. (S)
Kratz, K.L.
Nilsson, G.
Rudstam, G.
Schenter, R.E.
Schmidt, J.J.
Stamatelatos, M.G.
Yarnell, J.L.

WG on FP delayed neutron data

DelMarmol, P.
England, T.R. (S)
Kratz, K.L.
Nir-El, Y.
Rudstam, G. (C)

WG on FP cross section data

Bustraan, M. (C)
Dekker, J.W.M.
Delaroche, J.P.
Fabbri, F.
Fort, E.
Gruppelaar, H. (S)
Harker, Y.D.
Heijboer, R.J.
Iijima, S.
Janssen, A.J.
Langlet, G.
Menapace, E.
Osterhage, W.
Priesmeyer, H.G.
Reffo, G.
Rowlands, J.L.
Schmidt, J.J.